Physics Reports 494 (2010) 1–196

Contents lists available at ScienceDirect

Physics Reports

journal homepage: www.elsevier.com/locate/physrep

Two-component spinor techniques and Feynman rules for quantum field theory and supersymmetry

Herbi K. Dreiner [a,*], Howard E. Haber [b], Stephen P. Martin [c,d]

[a] Bethe Center for Theoretical Physics and Physikalisches Institut der Universität Bonn, Nußallee 12, 53115 Bonn, Germany

[b] Santa Cruz Institute for Particle Physics, University of California, Santa Cruz, CA 95064, United States

[c] Department of Physics, Northern Illinois University, DeKalb, IL 60115, United States

[d] Fermi National Accelerator Laboratory, P.O. Box 500, Batavia, IL 60510, United States

ARTICLE INFO

Article history:
Accepted 18 April 2010
Available online 12 May 2010
editor: J.A. Bagger

ABSTRACT

Two-component spinors are the basic ingredients for describing fermions in quantum field theory in $3+1$ spacetime dimensions. We develop and review the techniques of the two-component spinor formalism and provide a complete set of Feynman rules for fermions using two-component spinor notation. These rules are suitable for practical calculations of cross-sections, decay rates, and radiative corrections in the Standard Model and its extensions, including supersymmetry, and many explicit examples are provided. The unified treatment presented in this review applies to massless Weyl fermions and massive Dirac and Majorana fermions. We exhibit the relation between the two-component spinor formalism and the more traditional four-component spinor formalism, and indicate their connections to the spinor helicity method and techniques for the computation of helicity amplitudes.

Contents

* Corresponding author.
E-mail address: dreiner@th.physik.uni-bonn.de (H.K. Dreiner).

0370-1573/$ – see front matter © 2010 Published by Elsevier B.V.
doi:10.1016/j.physrep.2010.05.002

1. Introduction

A crucial feature of the Standard Model of particle physics is the chiral nature of fermion quantum numbers and interactions. According to the modern understanding of the electroweak interactions, the fundamental degrees of freedom for quarks and leptons are two-component Weyl–van der Waerden fermions [1], i.e. two-component Lorentz spinors that transform as irreducible representations under the gauge group $SU(2)_L \times U(1)_Y$. Furthermore, within the context of supersymmetric field theories, two-component spinors enter naturally, due to the spinorial nature of the symmetry generators themselves, and the holomorphic structure of the superpotential. Despite this, most pedagogical treatments and practical calculations in high energy physics continue to use the four-component Dirac spinor notation, which combines distinct irreducible representations of the Lorentz symmetry algebra. Parity-conserving theories such as QED and QCD are well suited to the four-component fermion methods. There is also a certain perceived advantage to familiarity. However, as we progress to phenomena at and above the scale of electroweak symmetry breaking, it seems increasingly natural to employ two-component fermion notation, in harmony with the irreducible transformation properties dictated by the physics.

One occasionally encounters the misconception that two-component fermion notations are somehow inherently ill-suited or unwieldy for practical use. Perhaps this is due in part to a lack of examples of calculations using two-component language in the pedagogical literature. In this review, we seek to dispel this idea by presenting Feynman rules for fermions using two-component spinor notation, intended for practical calculations of cross-sections, decays, and radiative corrections. This formalism employs a unified framework that applies equally well to Dirac fermions [2] such as the Standard Model quarks and charged leptons, and to Majorana fermions [3] such as the light neutrinos of the seesaw extension of the Standard Model [4,5] or the neutralinos of the minimal supersymmetric extension of the Standard Model (MSSM) [6–10].

Spinors were introduced by Cartan in 1913 as projective representations of the rotation group [11,12], and entered into physics via the Dirac equation in 1928 [2]. In the same year, Weyl discussed the representations of the Lorentz group [13], including the two-component spinor representations, in terms of stereographic projective coordinates [14]. The extension of the tensor calculus (or tensor analysis) to spinor calculus (or spinor analysis) was given by van der Waerden [1], upon the instigation of Ehrenfest. It is in this paper that van der Waerden (not Weyl as often claimed in the literature) first introduced the notation of dotted and undotted indices for the irreducible $(\frac{1}{2}, 0)$ and $(0, \frac{1}{2})$ representations of the Lorentz group. Both Weyl [15] and van der Waerden independently considered the decomposition of the Dirac equation into two coupled differential equations for two-component spinors. In the 1930s, more pedagogical presentations of two-component spinors were given in Refs. [16–18]. In particular, Ref. [16] was the first paper in English to employ the dotted and undotted index notation. Ref. [17] also presents the first two-component spinor analysis for general relativity. In the early 1950s, comprehensive reviews of two-component spinor techniques were published in English by Bade and Jehle [19] and in German by Cap [20]. Shortly thereafter, Bergmann reintroduced two-component spinors into the formalism of general relativity [21], which was followed by significant developments by Penrose [22].[1] Two-component spinor techniques in curved space are reviewed in Refs. [23,24], with an extensive bibliography given in Ref. [25]. A recent mathematical treatment of two-component spinors and their geometry can be found in Ref. [26]. Two-component spinors also play a central role in the covariant formulation of relativistic wave equations [27].

The formalism of two-component spinors has also been discussed in many textbooks on relativistic quantum mechanics, quantum field theory, elementary particle physics, group theoretical methods in physics, general relativity, and supersymmetry. For a guide to the non-supersymmetric literature, see for example, Refs. [14,28–67]. Among the early books, we would like to draw attention to Ref. [28], which has an extensive discussion of two-component spinor methods. Scheck [41] includes a short discussion of the field theory of two-component spinors, including the propagator. A more extensive field theoretic treatment, including Feynman rules and applications, is given by Ticciati [49]. A modern textbook on quantum field theory by Srednicki [65] includes a comprehensive treatment of two-component fermions

[1] For typographical reasons, Penrose replaced the dotted indices with primed indices, a notation still employed by most general relativists today.

and their quantization. Most textbooks and introductory reviews of supersymmetry [6–9,68–89] include a discussion of two-component spinors on some level, with a treatment of dotted and undotted indices and a collection of identities involving two-component spinors and the sigma matrices. Particularly extensive and useful sets of identities can be found in Refs. [68,72,74,77,83,85]. Finally, some mathematically sophisticated textbook treatments of spinors can be found in Refs. [90–92].

The standard technique for computing scattering cross-sections with initial and final state fermions involves squaring the quantum S-matrix amplitude, summing over the spin states and then computing the traces of products of gamma matrices (in the four-component spinor formalism), or products of sigma matrices (in the two-component spinor formalism). We employ this latter technique throughout this paper (with a translation to the four-component formalism provided in an appendix). However, the computational effort rises rapidly as the number of interfering diagrams increases. The standard techniques typically become impractical with four or more particles in the final state. One approach to make such extensive calculations manageable is the helicity amplitude technique. Here the scattering process is decomposed into the scattering of helicity eigenstates. Then the individual amplitudes are computed analytically in terms of Lorentz scalar invariants, i.e. a complex number that can be readily computed. It is then a simple numerical task to sum all the contributing amplitudes and compute the square of the complex magnitude of the resulting sum. Such methods were first explored in Refs. [93–96], using four-component spinors (see also Refs. [97–101]). Spinor techniques in the helicity formalism were also developed in Ref. [102]. In fact, the natural spinor formalism for the helicity amplitude techniques makes use of the two-component Weyl–van der Waerden spinors, which we discuss in detail in this review. They were implemented in the helicity amplitude technique in Refs. [103–109]. Recently, the two-component formalism has been implemented in a computer program for the numerical computation of amplitudes and cross-sections for event generators multi-particle processes [110].

This review is outlined as follows. In Section 2, we present our conventions and notation (with some additional discussion of our conventions in Appendix A). We also establish numerous identities involving sigma matrices, epsilon symbols and two-component spinors. In Section 3, we derive the basic properties of the quantized two-component fermion fields. For a generic collection of N two-component fermion fields with identical conserved quantum numbers, the corresponding mass matrix is an $N \times N$ complex symmetric matrix. To identify the corresponding mass eigenstates, one must perform a fermion mass diagonalization that differs from the usual unitary similarity transformation of an hermitian matrix that is employed for a collection of scalar fields. In Section 4, we derive the Feynman rules for two-component spinors and describe how to write down amplitudes in our formalism. We demonstrate how to employ the two-component formalism for both tree-level and loop-level processes. In Section 5, we establish a naming convention for fermion and antifermion particle states and the corresponding fields. This is important as it provides an unambiguous procedure for obtaining the amplitudes for a given physical process, and for comparing these computations in the two-component and four-component spinor formalisms. In Section 6 we provide an extensive number of examples of computations using the two-component spinor formalism. This is the central part of our review.

We have relegated many details to a set of twelve appendices. In Appendix A, we summarize our metric and sigma matrix conventions and indicate how to translate between conventions with opposite metric signature. With our definition of the sigma matrices, one can switch easily between the two conventions by computing one overall sign factor. In Appendix B, we provide a comprehensive list of sigma matrix identities, and indicate which of these identities can be generalized to $d \neq 4$ dimensions required for loop computations that employ dimensional regularization. Explicit forms for the two-component spinor wave functions are given in Appendix C (where we exhibit two of the most common phase conventions employed in the literature). The mathematics of fermion mass diagonalization is discussed in Appendix D. In contrast to the unitary similarity transformation of the scalar squared-mass matrix, fermion mass diagonalization involves the Takagi diagonalization [111] of a complex symmetric matrix (for neutral fermions) or the singular value decomposition of a complex matrix (for charged fermions). In Appendix E, we review some of the basic facts of Lie groups and Lie algebras needed in the treatment of gauge theories. The two-component fermion propagators (derived in Section 4 using canonical field theory techniques) can also be obtained by path integral methods, as exhibited in Appendix F.

As most textbooks on quantum field theory and elementary particle physics employ the four-component spinor formalism for fermions, we provide in Appendix G a dictionary that allows one to translate between the two-component and four-component spinor techniques. We use the two-component spinor methods developed in this review to establish a generalization of the standard four-component spinor Feynman rules that incorporate Majorana fermions in a natural way. In Appendix H, we develop a method for computing helicity amplitudes in terms of Lorentz-invariant scalar quantities. This method, which makes use of the Bouchiat–Michel formulae [112] (originally established in the four-component spinor formalism) is developed in the language of two-component spinors. However, these methods are somewhat limited in scope and must be generalized in the case of multi-particle final states. This was accomplished by Hagiwara and Zeppenfeld (HZ) based on a two-component spinor treatment [105]. In Appendix I, we provide a translation between the HZ formalism and the two-component spinor formalism of this review. We also demonstrate that the spinor helicity method that is now commonly used in obtaining compact expressions for helicity amplitudes of multi-particle processed has a very simple development within the two-component spinor formalism. Finally, the two-component spinor Feynman rules for the Standard Model, the seesaw-extended Standard Model (which incorporates massive neutrinos), the minimal supersymmetric extension of the Standard Model (MSSM), and the R-parity-violating extension of the MSSM are given in Appendices J–L.

2. Essential conventions, notations and two-component spinor identities

We begin with a discussion of necessary conventions. The metric tensor is taken to be[2]:

$$g_{\mu\nu} = g^{\mu\nu} = \mathrm{diag}(+1, -1, -1, -1), \tag{2.1}$$

where $\mu, \nu = 0, 1, 2, 3$ are spacetime vector indices. Contravariant four-vectors (e.g. positions and momenta) are defined with raised indices, and covariant four-vectors (e.g. derivatives) with lowered indices:

$$x^\mu = (t; \vec{\boldsymbol{x}}), \tag{2.2}$$

$$p^\mu = (E; \vec{\boldsymbol{p}}), \tag{2.3}$$

$$\partial_\mu \equiv \frac{\partial}{\partial x^\mu} = (\partial/\partial t; \vec{\boldsymbol{\nabla}}), \tag{2.4}$$

in units with $c = 1$. The totally antisymmetric pseudo-tensor $\epsilon^{\mu\nu\rho\sigma}$ is defined such that

$$\epsilon^{0123} = -\epsilon_{0123} = +1. \tag{2.5}$$

More details on our conventions can be found in Appendix A.

The irreducible building blocks for spin-1/2 fermions are fields that transform either under the left-handed $(\frac{1}{2}, 0)$ or the right-handed $(0, \frac{1}{2})$ representation of the Lorentz group. Hermitian conjugation interchanges these two representations. A Majorana fermion field can be constructed from either representation; this is the spin-1/2 analogue of a real scalar field. A Dirac fermion field combines two equal mass two-component fields into a reducible representation of the form $(\frac{1}{2}, 0) \oplus (0, \frac{1}{2})$; this is the spin-1/2 analogue of a complex scalar field. It is also possible to use four-component notation to describe a Majorana fermion by imposing a reality condition on the spinor in order to reduce the number of degrees of freedom in half. Details of this construction are given in Appendix G.1. However, in this review, we shall focus primarily on two-component spinor notation for all fermions. In the following, $(\frac{1}{2}, 0)$ spinors carry undotted indices $\alpha, \beta, \ldots = 1, 2$, and $(0, \frac{1}{2})$ spinors carry dotted indices $\dot{\alpha}, \dot{\beta}, \ldots = 1, 2$.

We first provide a brief introduction to the Lorentz group and its two-dimensional spinor representations. Under a Lorentz transformation, a contravariant four-vector x^μ transforms as

$$x^\mu \to x'^\mu = \Lambda^\mu{}_\nu x^\nu, \tag{2.6}$$

where $\Lambda \in \mathrm{SO}(3, 1)$ satisfies $\Lambda^\mu{}_\nu g_{\mu\rho} \Lambda^\rho{}_\lambda = g_{\nu\lambda}$. It then follows that the transformation of the corresponding covariant four-vector $x_\mu \equiv g_{\mu\nu} x^\nu$ satisfies:

$$x_\nu = x'_\mu \Lambda^\mu{}_\nu. \tag{2.7}$$

The most general proper orthochronous Lorentz transformation (which is continuously connected to the identity), corresponding to a rotation by an angle θ about an axis $\widehat{\boldsymbol{n}}$ [$\vec{\boldsymbol{\theta}} \equiv \theta\widehat{\boldsymbol{n}}$] and a boost vector $\vec{\boldsymbol{\zeta}} \equiv \hat{\boldsymbol{v}} \tanh^{-1}\beta$ [where $\hat{\boldsymbol{v}} \equiv \vec{\boldsymbol{v}}/|\vec{\boldsymbol{v}}|$ and $\beta \equiv |\vec{\boldsymbol{v}}|$], is a 4×4 matrix given by:

$$\Lambda = \exp\left(-\frac{i}{2}\theta^{\rho\sigma}\mathcal{J}_{\rho\sigma}\right) = \exp\left(-i\vec{\boldsymbol{\theta}}\cdot\vec{\boldsymbol{\mathcal{J}}} - i\vec{\boldsymbol{\zeta}}\cdot\vec{\boldsymbol{\mathcal{K}}}\right), \tag{2.8}$$

where $\theta^i \equiv \frac{1}{2}\epsilon^{ijk}\theta_{jk}$, $\zeta^i \equiv \theta^{i0} = -\theta^{0i}$, $\mathcal{J}^i \equiv \frac{1}{2}\epsilon^{ijk}\mathcal{J}_{jk}$, $\mathcal{K}^i \equiv \mathcal{J}^{0i} = -\mathcal{J}^{i0}$ and

$$(\mathcal{J}_{\rho\sigma})^\mu{}_\nu = i(g_\rho{}^\mu g_{\sigma\nu} - g_\sigma{}^\mu g_{\rho\nu}). \tag{2.9}$$

Here, the indices $i, j, k = 1, 2, 3$ and $\epsilon^{123} = +1$.

It follows from Eqs. (2.8) and (2.9) that an infinitesimal orthochronous Lorentz transformation is given by $\Lambda^\mu{}_\nu \simeq \delta^\mu_\nu + \theta^\mu{}_\nu$ (after noting that $\theta^\mu{}_\nu = -\theta_\nu{}^\mu$). Moreover, the infinitesimal boost parameter is $\vec{\boldsymbol{\zeta}} \equiv \hat{\boldsymbol{v}} \tanh^{-1}\beta \simeq \beta\hat{\boldsymbol{v}} \equiv \vec{\boldsymbol{\beta}}$, since $\beta \ll 1$ for an infinitesimal boost. Hence, the actions of the infinitesimal boosts and rotations on the spacetime coordinates are

$$\text{Rotations:} \quad \begin{cases} \vec{\boldsymbol{x}} \to \vec{\boldsymbol{x}}' \simeq \vec{\boldsymbol{x}} + (\vec{\boldsymbol{\theta}} \times \vec{\boldsymbol{x}}), \\ t \to t' \simeq t, \end{cases} \tag{2.10}$$

$$\text{Boosts:} \quad \begin{cases} \vec{\boldsymbol{x}} \to \vec{\boldsymbol{x}}' \simeq \vec{\boldsymbol{x}} + \vec{\boldsymbol{\beta}}\, t, \\ t \to t' \simeq t + \vec{\boldsymbol{\beta}}\cdot\vec{\boldsymbol{x}}, \end{cases} \tag{2.11}$$

with exactly analogous transformations for any contravariant four-vector.

[2] The published version of this paper employs the $(+, -, -, -)$ Minkowski space metric. An otherwise identical version, using the $(-, +, +, +)$ metric favored by one of the authors (SPM), may be found at http://zippy.physics.niu.edu/spinors.html. It can also be constructed by changing a single macro at the beginning of the LaTeX source file [113], in an obvious way. You can tell which version you are presently reading from Eq. (2.1). See Appendix A for further details and rules for translating between metric conventions.

With respect to the Lorentz transformation Λ, a general n-component field Φ transforms according to a representation R of the Lorentz group as $\Phi(x^\mu) \to \Phi'(x'^\mu) = M_R(\Lambda)\,\Phi(x^\mu)$, where $M_R(\Lambda)$ is the corresponding (finite) d_R-dimensional matrix representation. Equivalently, the functional form of the transformed field Φ obeys

$$\Phi'(x^\mu) = M_R(\Lambda)\Phi([\Lambda^{-1}]^\mu{}_\nu x^\nu), \tag{2.12}$$

after using Eq. (2.6). For proper orthochronous Lorentz transformations,

$$M_R = \exp\left(-\frac{i}{2}\theta_{\mu\nu}J^{\mu\nu}\right) \simeq \mathbb{1}_{d_R\times d_R} - i\vec{\boldsymbol{\theta}}\cdot\vec{\boldsymbol{J}} - i\vec{\boldsymbol{\zeta}}\cdot\vec{\boldsymbol{K}}, \tag{2.13}$$

where $\mathbb{1}_{d_R\times d_R}$ is the $d_R \times d_R$ identity matrix and $\theta_{\mu\nu}$ parameterizes the Lorentz transformation Λ [Eq. (2.8)]. The six independent components of the matrix-valued antisymmetric tensor $J^{\mu\nu}$ are the d_R-dimensional generators of the Lorentz group and satisfy the commutation relations:

$$[J^{\mu\nu}, J^{\lambda\kappa}] = i(g^{\mu\kappa}J^{\nu\lambda} + g^{\nu\lambda}J^{\mu\kappa} - g^{\mu\lambda}J^{\nu\kappa} - g^{\nu\kappa}J^{\mu\lambda}). \tag{2.14}$$

We identify $\vec{\boldsymbol{J}}$ and $\vec{\boldsymbol{K}}$ as the generators of rotations parameterized by $\vec{\boldsymbol{\theta}}$ and boosts parameterized by $\vec{\boldsymbol{\zeta}}$, respectively, where

$$J^i \equiv \tfrac{1}{2}\epsilon^{ijk}J_{jk}, \qquad K^i \equiv J^{0i}. \tag{2.15}$$

Here we focus on the simplest non-trivial irreducible representations of the Lorentz algebra. These are the two-dimensional (inequivalent) representations: $(\frac{1}{2}, 0)$ and $(0, \frac{1}{2})$. In the $(\frac{1}{2}, 0)$ representation, $\vec{\boldsymbol{J}} = \vec{\boldsymbol{\sigma}}/2$ and $\vec{\boldsymbol{K}} = -i\vec{\boldsymbol{\sigma}}/2$ in Eq. (2.13), which yields

$$M_{(\frac{1}{2},0)} \equiv M \simeq \mathbb{1}_{2\times2} - i\vec{\boldsymbol{\theta}}\cdot\vec{\boldsymbol{\sigma}}/2 - \vec{\boldsymbol{\zeta}}\cdot\vec{\boldsymbol{\sigma}}/2, \tag{2.16}$$

where $\vec{\boldsymbol{\sigma}} \equiv (\sigma^1, \sigma^2, \sigma^3)$ are the Pauli matrices [cf. Eq. (2.27)]. By definition M carries undotted spinor indices, as indicated by $M_\alpha{}^\beta$. A two-component $(\frac{1}{2}, 0)$ spinor is denoted by ψ_α and transforms as $\psi_\alpha \to M_\alpha{}^\beta\psi_\beta$, omitting the coordinate arguments of the fields, which are as in Eq. (2.12). In our conventions for the location of the spinor indices, we sum implicitly over a repeated index pair in which one index is lowered and one index is raised.

In the $(0, \frac{1}{2})$ representation, $\vec{\boldsymbol{J}} = -\vec{\boldsymbol{\sigma}}^*/2$ and $\vec{\boldsymbol{K}} = -i\vec{\boldsymbol{\sigma}}^*/2$ in Eq. (2.13), so that its representation matrix is M^*, the complex conjugate of Eq. (2.16). By definition, the indices carried by M^* are dotted, as indicated by $(M^*)_{\dot\alpha}{}^{\dot\beta}$. A two-component $(0, \frac{1}{2})$ spinor is denoted by $\psi^\dagger_{\dot\alpha}$ and transforms as $\psi^\dagger_{\dot\alpha} \to (M^*)_{\dot\alpha}{}^{\dot\beta}\psi^\dagger_{\dot\beta}$, again suppressing the coordinate arguments of the fields, which are as in Eq. (2.12). We distinguish between the undotted and dotted spinor index types because they cannot be directly contracted with each other to form a Lorentz invariant quantity.

It follows that the $(\frac{1}{2}, 0)$ and $(0, \frac{1}{2})$ representations are related by hermitian conjugation. That is, if ψ_α is a $(\frac{1}{2}, 0)$ fermion, then $(\psi_\alpha)^\dagger$ transforms as a $(0, \frac{1}{2})$ fermion. This means that we can, and will, describe all fermion degrees of freedom using only fields defined as left-handed $(\frac{1}{2}, 0)$ fermions ψ_α, and their conjugates. In combining spinors to make Lorentz tensors [as in Eq. (2.39)], it is useful to regard $\psi^\dagger_{\dot\alpha}$ as a row vector, and ψ_α as a column vector, with[3]:

$$\psi^\dagger_{\dot\alpha} \equiv (\psi_\alpha)^\dagger. \tag{2.17}$$

The Lorentz transformation property of $\psi^\dagger_{\dot\alpha}$ then follows from $(\psi_\alpha)^\dagger \to (\psi_\beta)^\dagger(M^\dagger)^{\dot\beta}{}_{\dot\alpha}$ [with coordinate arguments of the fields again suppressed], where $(M^\dagger)^{\dot\beta}{}_{\dot\alpha} = (M^*)_{\dot\alpha}{}^{\dot\beta}$ reflects the definition of the hermitian adjoint matrix as the complex conjugate transpose of the matrix. Again the coordinate arguments of the fields have been suppressed, and are as in Eq. (2.12).

In this review, we shall employ the dotted-index notation in association with the dagger to denote hermitian conjugation, as specified in Eq. (2.17). This is the notation for hermitian conjugation of spinors found in most field theory textbooks (e.g., see Refs. [65,88,114]). However, it should be noted that many references in the supersymmetry literature (e.g., see Refs. [68–87]) employ the bar notation made popular by Wess and Bagger [68] where $\overline{\psi}_{\dot\alpha} \equiv \psi^\dagger_{\dot\alpha} \equiv (\psi_\alpha)^\dagger$.

Spinors labeled with one undotted or one dotted index are sometimes called spinors of rank one [or more precisely, spinors of rank $(1, 0)$ or $(0, 1)$, respectively]. One can also define spinors of higher rank, which possess more than one spinor index, with Lorentz transformation properties that depend on the number of undotted and dotted spinor indices [16,19,20,23,27–39,50,52,60,78,115]. In particular, for a spinor of rank (m, n) denoted by $S_{\alpha_1\alpha_2\cdots\alpha_m\dot\beta_1\dot\beta_2\cdots\dot\beta_n}$, each lowered undotted α-index transforms separately according to $M_{\alpha'_i}{}^{\alpha_i}$ in Eq. (2.16) and each lowered dotted $\dot\beta$-index transforms according to $(M^*)_{\dot\beta'_i}{}^{\dot\beta_i}$.

[3] In the early literature that employed the van der Waerden spinor index notation (surveyed in Section 1), no dagger was used in conjunction with the dotted index. The advantage to attaching the dagger to the dotted spinor field is that it permits the development of a spinor-index-free notation for Lorentz-covariant spinor products [see Eqs. (2.36)–(2.40) and the accompanying text].

There are two additional spin-1/2 irreducible representations of the Lorentz group, $(M^{-1})^{\mathsf{T}}$ and $(M^{-1})^{\dagger}$, but these are equivalent representations to the $(\frac{1}{2}, 0)$ and the $(0, \frac{1}{2})$ representations, respectively. The spinors that transform under these representations have raised spinor indices, ψ^{α} and $\psi^{\dagger\dot{\alpha}}$, with transformation laws $\psi^{\alpha} \to [(M^{-1})^{\mathsf{T}}]^{\alpha}{}_{\beta}\psi^{\beta}$ and $\psi^{\dagger\dot{\alpha}} \to [(M^{-1})^{\dagger}]^{\dot{\alpha}}{}_{\dot{\beta}}\psi^{\dagger\dot{\beta}}$, respectively (with coordinate arguments of the fields again suppressed). It is convenient to rewrite the transformation law for the undotted spinor as $\psi^{\alpha} \to \psi^{\beta}(M^{-1})_{\beta}{}^{\alpha}$. In combining spinors to make Lorentz tensors [as in Eq. (2.40)], it is useful to regard ψ^{α} as a row vector, and $\psi^{\dagger\dot{\alpha}}$ as a column vector, with:

$$\psi^{\dagger\dot{\alpha}} \equiv (\psi^{\alpha})^{\dagger}. \tag{2.18}$$

The Lorentz transformation property of $\psi^{\dagger\dot{\alpha}}$ then follows from $(\psi^{\alpha})^{\dagger} \to [(M^{-1})^{\dagger}]^{\dot{\alpha}}{}_{\dot{\beta}}(\psi^{\beta})^{\dagger}$.

The spinor indices are raised and lowered with the two-index antisymmetric epsilon symbol with non-zero components,[4]

$$\epsilon^{12} = -\epsilon^{21} = \epsilon_{21} = -\epsilon_{12} = 1, \tag{2.19}$$

and the same set of sign conventions for the corresponding dotted spinor indices. In particular, we formally define $\epsilon^{\dot{\alpha}\dot{\beta}} \equiv (\epsilon^{\alpha\beta})^*$ and $\epsilon_{\dot{\alpha}\dot{\beta}} \equiv (\epsilon_{\alpha\beta})^*$. Viewed as a 2×2 matrix, the epsilon symbol with lowered undotted [dotted] indices is the inverse of the epsilon symbol with raised undotted [dotted] indices. Thus, consistent with Eqs. (2.17) and (2.18), one can write[5,6]:

$$\psi_{\alpha} = \epsilon_{\alpha\beta}\psi^{\beta}, \qquad \psi^{\alpha} = \epsilon^{\alpha\beta}\psi_{\beta}, \qquad \psi^{\dagger}_{\dot{\alpha}} = \epsilon_{\dot{\alpha}\dot{\beta}}\psi^{\dagger\dot{\beta}}, \qquad \psi^{\dagger\dot{\alpha}} = \epsilon^{\dot{\alpha}\dot{\beta}}\psi^{\dagger}_{\dot{\beta}}, \tag{2.20}$$

which respects Lorentz covariance due to the properties of M given in Eqs. (2.102) and (2.103). The epsilon symbols $\epsilon^{\alpha\beta}$ ($\epsilon_{\alpha\beta}$) and $\epsilon^{\dot{\alpha}\dot{\beta}}$ ($\epsilon_{\dot{\alpha}\dot{\beta}}$), first introduced in this context in Ref. [1], are also called the *spinor metric tensors*, as they raise (lower) the undotted and dotted spinor indices, respectively. Note that in raising or lowering an index of a spinor quantity, *adjacent* spinor indices are summed over when multiplied on the *left* by the appropriate epsilon symbol.

The epsilon symbols can also be used to raise or lower undotted or dotted indices of spinors of higher rank. For example, for an object with two undotted indices it is natural to define

$$A^{\gamma\delta} = \epsilon^{\gamma\alpha}\epsilon^{\delta\beta}A_{\alpha\beta}, \qquad A_{\gamma\delta} = \epsilon_{\gamma\alpha}\epsilon_{\delta\beta}A^{\alpha\beta}. \tag{2.21}$$

In the special case that $A^{\alpha\beta} = \psi^{\alpha}\chi^{\beta}$ is a product of rank-one spinors, Eq. (2.21) is not just natural but necessary, as it follows directly from Eq. (2.20). However, in other cases there can be a different sign associated (by convention) with raising and lowering spinor indices, because of the antisymmetry of the epsilon symbols (in contrast to the symmetry of the spacetime metric used to raise and lower spacetime indices). This sign convention can be defined independently for distinct higher-rank spinors (even in the case where the higher-rank spinors possess the same index structure). Indeed, as a consequence of our epsilon symbol conventions of Eq. (2.19), the epsilon symbols themselves satisfy:

$$\epsilon^{\gamma\delta} = -\epsilon^{\gamma\alpha}\epsilon^{\delta\beta}\epsilon_{\alpha\beta}, \qquad \epsilon_{\gamma\delta} = -\epsilon_{\gamma\alpha}\epsilon_{\delta\beta}\epsilon^{\alpha\beta}, \tag{2.22}$$

in contrast to Eq. (2.21). The above results (and similar ones with dotted indices) show that some care is required [33], since the extra overall minus signs of Eq. (2.22) in comparison to Eq. (2.21) might otherwise have been unexpected [e.g., see Eqs. (2.41) and (2.42) below].[7] This reflects an awkwardness imposed by the epsilon symbol conventions of Eq. (2.19), rather than an inconsistency. Practitioners of spinor algebra in the conventions used in this review should be wary of this sign issue

---

[4] For related earlier work on the epsilon symbol and its properties, see Refs. [16,17,19,116]. Various subsets of the subsequent identities in this section involving commuting and anticommuting two-component spinors, as well as the ϵ symbol and the sigma matrices appear in many books and reviews (e.g., see Refs. [18,68–83,85–88]) and in papers (e.g., see Refs. [103–109]).

[5] In the general relativity literature (see e.g., Refs. [22,23,37,42,43,46,52,60,62,64]), the more common convention for the epsilon symbol (also adopted in Refs. [19,28,30,36,45,47,92,109]) is $\epsilon^{\alpha\beta} = \epsilon_{\alpha\beta}$ with $\epsilon^{12} = -\epsilon^{21} = 1$, and similarly for the epsilon symbol with dotted spinor indices. In this convention, one writes $\psi^{\alpha} = \epsilon^{\alpha\beta}\psi_{\beta}$ as above, but in contrast to Eq. (2.20), $\psi_{\alpha} = \psi^{\beta}\epsilon_{\beta\alpha}$, and similarly for the corresponding equations with dotted spinor indices. That is, in raising [lowering] an index of a spinor quantity, *adjacent* spinor indices are summed over when multiplied on the left [right] by the appropriate epsilon symbol. The various identities involving the epsilon symbols given in this review must then be modified by a minus sign for every epsilon symbol with lowered spinor indices. There are some benefits for this alternative convention; e.g., the minus signs appearing in Eq. (2.22) are absent. However, one must keep track of other minus signs that arise because $\epsilon_{\alpha\beta}$ is the *negative* of the inverse of $\epsilon^{\alpha\beta}$. In this review, we have adopted the convention of Eq. (2.19), which is consistent with most of the supersymmetry literature.

[6] In Refs. [50,69], one finds yet another convention in which the spinor indices are raised and lowered by a two-index antisymmetric quantity, $C_{\alpha\beta} = -C^{\alpha\beta} = C_{\dot{\alpha}\dot{\beta}} = -C^{\dot{\alpha}\dot{\beta}} = \begin{pmatrix} 0 & -i \\ i & 0 \end{pmatrix}$, which play the role of the epsilon symbols. As in footnote 5, $C_{\alpha\beta}$ is the negative inverse of $C^{\alpha\beta}$ in which case $\psi^{\alpha} = C^{\alpha\beta}\psi_{\beta}$ whereas $\psi_{\alpha} = \psi^{\beta}C_{\beta\alpha}$, and similarly for the corresponding equations with dotted spinor indices. However, in this convention where C is pure imaginary, if $\psi^{\dagger\dot{\alpha}} \equiv (\psi^{\alpha})^{\dagger}$ as in Eq. (2.18), then $\psi^{\dagger}_{\dot{\alpha}} = -(\psi_{\alpha})^{\dagger}$ in contrast to Eq. (2.17). We choose not to pursue the alternative epsilon symbol conventions of footnotes 5 or 6 in this review.

[7] It would be perhaps more transparent to simply replace the symbol $\epsilon_{\alpha\beta}$ with $\epsilon^{-1}_{\alpha\beta}$, in which case $\epsilon^{\alpha\beta}$ is used to raise spinor indices and $\epsilon^{-1}_{\alpha\beta}$ is used to lower spinor indices (cf. Ref. [38]). Although this convention avoids an apparent conflict between Eqs. (2.21) and (2.22), it doubles the number of distinct epsilon symbols. We shall not adopt such an approach in this review.

when using the epsilon symbols to explicitly raise or lower two or more spinor indices of higher-rank spinors.[8] Fortunately, such manipulations are quite rare in practical calculations.

We also introduce the two-index symmetric Kronecker delta symbol,

$$\delta_1^1 = \delta_2^2 = 1, \qquad \delta_2^1 = \delta_2^1 = 0, \tag{2.23}$$

and $\delta_{\dot\alpha}^{\dot\beta} \equiv (\delta_\alpha^\beta)^*$. Eq. (2.23) implies that the numerical values of the undotted and dotted Kronecker delta symbols coincide. The epsilon symbols with undotted and with dotted indices respectively satisfy:

$$\epsilon_{\alpha\beta}\epsilon^{\gamma\delta} = -\delta_\alpha^\gamma\delta_\beta^\delta + \delta_\alpha^\delta\delta_\beta^\gamma, \qquad \epsilon_{\dot\alpha\dot\beta}\epsilon^{\dot\gamma\dot\delta} = -\delta_{\dot\alpha}^{\dot\gamma}\delta_{\dot\beta}^{\dot\delta} + \delta_{\dot\alpha}^{\dot\delta}\delta_{\dot\beta}^{\dot\gamma}, \tag{2.24}$$

from which it follows that:

$$\epsilon_{\alpha\beta}\epsilon^{\beta\gamma} = \epsilon^{\gamma\beta}\epsilon_{\beta\alpha} = \delta_\alpha^\gamma, \qquad \epsilon_{\dot\alpha\dot\beta}\epsilon^{\dot\beta\dot\gamma} = \epsilon^{\dot\gamma\dot\beta}\epsilon_{\dot\beta\dot\alpha} = \delta_{\dot\alpha}^{\dot\gamma}, \tag{2.25}$$

$$\epsilon_{\alpha\beta}\epsilon_{\gamma\delta} + \epsilon_{\alpha\gamma}\epsilon_{\delta\beta} + \epsilon_{\alpha\delta}\epsilon_{\beta\gamma} = 0, \qquad \epsilon_{\dot\alpha\dot\beta}\epsilon_{\dot\gamma\dot\delta} + \epsilon_{\dot\alpha\dot\gamma}\epsilon_{\dot\delta\dot\beta} + \epsilon_{\dot\alpha\dot\delta}\epsilon_{\dot\beta\dot\gamma} = 0. \tag{2.26}$$

In the literature, Eq. (2.26) is often referred to as the Schouten identities.[9]

To construct Lorentz invariant Lagrangians and observables, one needs to first combine products of spinors to make objects that transform as Lorentz tensors. In particular, Lorentz vectors are obtained by introducing the sigma matrices $\sigma^\mu_{\alpha\dot\beta}$ and $\overline{\sigma}^{\mu\,\dot\alpha\beta}$ defined by [1,14,17,18]

$$\sigma^0 = \overline{\sigma}^0 = \begin{pmatrix} 1 & 0 \\ 0 & 1 \end{pmatrix}, \qquad \sigma^1 = -\overline{\sigma}^1 = \begin{pmatrix} 0 & 1 \\ 1 & 0 \end{pmatrix}, \tag{2.27}$$

$$\sigma^2 = -\overline{\sigma}^2 = \begin{pmatrix} 0 & -i \\ i & 0 \end{pmatrix}, \qquad \sigma^3 = -\overline{\sigma}^3 = \begin{pmatrix} 1 & 0 \\ 0 & -1 \end{pmatrix}. \tag{2.28}$$

The sigma matrices are hermitian, and have been defined above with an upper (contravariant) index. We denote the 2×2 identity matrix by $\mathbb{1}_{2\times2}$ and the three-vector of Pauli matrices by $\vec{\boldsymbol{\sigma}} \equiv (\sigma^1, \sigma^2, \sigma^3)$. Hence, Eq. (2.27) is equivalent to:

$$\sigma^\mu = (\mathbb{1}_{2\times2};\, \vec{\boldsymbol{\sigma}}), \qquad \overline{\sigma}^\mu = (\mathbb{1}_{2\times2};\, -\vec{\boldsymbol{\sigma}}). \tag{2.29}$$

We also define the corresponding quantities with lower (covariant) indices:

$$\sigma_\mu = g_{\mu\nu}\sigma^\nu = (\mathbb{1}_{2\times2};\, -\vec{\boldsymbol{\sigma}}), \qquad \overline{\sigma}_\mu = g_{\mu\nu}\overline{\sigma}^\nu = (\mathbb{1}_{2\times2};\, \vec{\boldsymbol{\sigma}}). \tag{2.30}$$

The relations between σ^μ and $\overline{\sigma}^\mu$ are

$$\sigma^\mu_{\alpha\dot\alpha} = \epsilon_{\alpha\beta}\epsilon_{\dot\alpha\dot\beta}\overline{\sigma}^{\mu\,\dot\beta\beta}, \qquad \overline{\sigma}^{\mu\,\dot\alpha\alpha} = \epsilon^{\alpha\beta}\epsilon^{\dot\alpha\dot\beta}\sigma^\mu_{\beta\dot\beta}, \tag{2.31}$$

$$\epsilon^{\alpha\beta}\sigma^\mu_{\beta\dot\alpha} = \epsilon_{\dot\alpha\dot\beta}\overline{\sigma}^{\mu\dot\beta\alpha}, \qquad \epsilon^{\dot\alpha\dot\beta}\sigma^\mu_{\alpha\dot\beta} = \epsilon_{\alpha\beta}\overline{\sigma}^{\mu\dot\alpha\beta}. \tag{2.32}$$

Consider a spinor of rank (n, n) denoted by $S_{\alpha_1\alpha_2\ldots\alpha_n\dot\beta_1\dot\beta_2\ldots\dot\beta_n}$. The object obtained by multiplying S by $\overline{\sigma}^{\mu_1\,\dot\beta_1\alpha_1}\cdots\overline{\sigma}^{\mu_n\,\dot\beta_n\alpha_n}$ has the transformation properties of an nth rank contravariant Lorentz tensor [29,32,115]. For example, there is a one-to-one correspondence between each bi-spinor $V_{\alpha\dot\beta}$ and the associated Lorentz four-vector V^μ [1,17,19,20,28,29],[10]

$$V^\mu \equiv \tfrac{1}{2}\overline{\sigma}^{\mu\dot\beta\alpha}V_{\alpha\dot\beta}, \qquad V_{\alpha\dot\beta} = V^\mu\sigma_{\mu\alpha\dot\beta}. \tag{2.33}$$

In particular, if V^μ is a real four-vector then $V_{\alpha\dot\beta}$ is hermitian (and vice versa). To clarify this last remark, consider the bi-spinor $V_{\alpha\dot\beta}$ regarded as a 2×2 matrix. Then,[11,12]

$$(V^{\mathsf{T}})_{\alpha\dot\beta} \equiv V_{\beta\dot\alpha}, \qquad (V^*)_{\dot\alpha\beta} \equiv (V_{\alpha\dot\beta})^*, \qquad (V^\dagger)_{\alpha\dot\beta} \equiv (V_{\beta\dot\alpha})^* = (V^*)_{\dot\beta\alpha}. \tag{2.34}$$

An hermitian bi-spinor satisfies $V = V^\dagger$, or equivalently $V_{\alpha\dot\beta} = (V^*)_{\dot\beta\alpha}$.

---

8 In the alternative convention mentioned in footnote 5, this particular awkwardness is absent; the minus signs in the analogue of Eq. (2.22) do not occur, in which case the rules for raising and lowering the spinor indices in Eqs. (2.21) and (2.22) are identical. More generally, in the convention of footnote 5, the indices of all higher-rank spinors can be raised [lowered] via multiplication on the left [right] by the appropriate epsilon symbol, including the epsilon symbols themselves, with no extra signs.

9 The Schouten identities also follow from the observation that a rank-four spinor must vanish if it is antisymmetric with respect to more than two undotted or dotted two-component spinor indices.

10 In the general relativity literature [42,46,60,92], the more common normalization is $V^\mu \equiv \frac{1}{\sqrt{2}}\overline{\sigma}^{\mu\dot\beta\alpha}V_{\alpha\dot\beta}$, which yields $V_{\alpha\dot\beta} = \frac{1}{\sqrt{2}}V^\mu\sigma_{\mu\alpha\dot\beta}$. In this context, the $\frac{1}{\sqrt{2}}\sigma^\mu_{\alpha\dot\beta}$ are often called the Infeld–van der Waerden symbols.

11 As stressed in Ref. [19], taking the transpose of $V_{\alpha\dot\beta}$ interchanges its rows and columns without altering the fact that the first spinor index is undotted and the second spinor index is dotted. Moreover, it is often useful to further simplify the notation by *defining* $V_{\dot\alpha\beta} \equiv (V_{\alpha\dot\beta})^*$ [i.e., omitting the asterisk in $(V^*)_{\dot\alpha\beta}$]. In this notation, an hermitian bi-spinor satisfies $V_{\alpha\dot\beta} = V_{\dot\alpha\beta}$.

12 The reader is cautioned that some authors do not attach a significance to the relative placement of undotted and dotted indices [16], and thus adopt a notational style for higher-rank spinors in which all undotted spinor indices appear *before* the dotted indices (see, e.g., Refs. [50,69]). In this latter convention, one would define $(V^*)_{\dot\beta\dot\alpha} \equiv (V_{\alpha\dot\beta})^*$. However, we choose not to adopt this approach, as it is not particularly convenient for the matrix interpretation of a bi-spinor where the row index traditionally precedes the column index.

Rank-two spinors (with two undotted or with two dotted indices) can also be interpreted as 2×2 matrices. In the case of the rank-two spinor $W_\alpha{}^\beta$, it is convenient to define:

$$(W^{\mathsf{T}})_\alpha{}^\beta \equiv W^\beta{}_\alpha, \qquad (W^*)_{\dot\alpha}{}^{\dot\beta} \equiv (W_\alpha{}^\beta)^*, \qquad (W^\dagger)^{\dot\beta}{}_{\dot\alpha} \equiv (W_\alpha{}^\beta)^* = (W^*)_{\dot\alpha}{}^{\dot\beta}. \tag{2.35}$$

Note that the matrix transposition of $W_\alpha{}^\beta$ interchanges the rows and columns of W without altering the relative heights of the α and β indices. Similar results hold for $W_{\alpha\beta}$ and $W^{\alpha\beta}$ by either lowering or raising the relevant spinor indices with the appropriate epsilon symbol.

When constructing Lorentz tensors from fermion fields, the heights of spinor indices must be consistent in the sense that lowered indices must only be contracted with raised indices. As a convention, *descending* contracted undotted indices and *ascending* contracted dotted indices,

$$^\alpha{}_\alpha \quad \text{and} \quad {}_{\dot\alpha}{}^{\dot\alpha}, \tag{2.36}$$

can be suppressed. In all spinor products given in this paper, contracted indices always have heights that conform to Eq. (2.36). For example, in an index-free notation, we define:

$$\xi\eta \equiv \xi^\alpha \eta_\alpha, \tag{2.37}$$

$$\xi^\dagger \eta^\dagger \equiv \xi^\dagger_{\dot\alpha} \eta^{\dagger\dot\alpha}, \tag{2.38}$$

$$\xi^\dagger \overline{\sigma}^\mu \eta \equiv \xi^\dagger_{\dot\alpha} \overline{\sigma}^{\mu\dot\alpha\beta} \eta_\beta, \tag{2.39}$$

$$\xi \sigma^\mu \eta^\dagger \equiv \xi^\alpha \sigma^\mu_{\alpha\dot\beta} \eta^{\dagger\dot\beta}. \tag{2.40}$$

All the spinor-index-contracted products above have natural interpretations as products of matrices and vectors by regarding η_α and $\eta^{\dagger\dot\alpha}$ as column vectors and $\xi^\dagger_{\dot\alpha}$ and ξ^α as row vectors of the two-dimensional spinor space. However, the reader is cautioned that in the index-free notation (with undotted and dotted indices suppressed), the undaggered and daggered spinors cannot be uniquely identified as column or row vectors until their locations within the spinor product are specified. Nevertheless, the proper identifications are straightforward, as any spinor on the left end of a spinor product can be identified as a row vector and any spinor on the right end of a spinor product can be identified as a column vector.

For an *anticommuting* two-component spinor ψ, the product $\psi^\alpha \psi^\beta$ is antisymmetric with respect to the interchange of the spinor indices α and β. Hence, this product of spinors must be proportional to $\epsilon^{\alpha\beta}$. Similar conclusions hold for the corresponding spinor products with raised undotted indices and with lowered and raised dotted indices, respectively. Thus,

$$\psi^\alpha \psi^\beta = -\tfrac{1}{2}\epsilon^{\alpha\beta}\psi\psi, \qquad \psi_\alpha \psi_\beta = \tfrac{1}{2}\epsilon_{\alpha\beta}\psi\psi, \tag{2.41}$$

$$\psi^{\dagger\dot\alpha}\psi^{\dagger\dot\beta} = \tfrac{1}{2}\epsilon^{\dot\alpha\dot\beta}\psi^\dagger\psi^\dagger, \qquad \psi^\dagger_{\dot\alpha}\psi^\dagger_{\dot\beta} = -\tfrac{1}{2}\epsilon_{\dot\alpha\dot\beta}\psi^\dagger\psi^\dagger, \tag{2.42}$$

where $\psi\psi \equiv \psi^\alpha\psi_\alpha$ and $\psi^\dagger\psi^\dagger \equiv \psi^\dagger_{\dot\alpha}\psi^{\dagger\dot\alpha}$ as in Eqs. (2.37) and (2.38). Note that the minus signs above can be understood to be a consequence of the extra minus sign that arises when the indices of the epsilon symbol are lowered or raised [cf. Eqs. (2.21) and (2.22)].

The behavior of the spinor products under hermitian conjugation (for quantum field operators) or complex conjugation (for classical fields) is as follows:

$$(\xi\eta)^\dagger = \eta^\dagger\xi^\dagger, \tag{2.43}$$

$$(\xi\sigma^\mu\eta^\dagger)^\dagger = \eta\sigma^\mu\xi^\dagger, \tag{2.44}$$

$$(\xi^\dagger\overline{\sigma}^\mu\eta)^\dagger = \eta^\dagger\overline{\sigma}^\mu\xi, \tag{2.45}$$

$$(\xi\sigma^\mu\overline{\sigma}^\nu\eta)^\dagger = \eta^\dagger\overline{\sigma}^\nu\sigma^\mu\xi^\dagger, \tag{2.46}$$

where we have used the hermiticity properties, $(\sigma^\mu)^\dagger = \sigma^\mu$ and $(\overline{\sigma}^\mu)^\dagger = \overline{\sigma}^\mu$. More generally,

$$(\xi\,\Sigma\eta)^\dagger = \eta^\dagger\,\Sigma_r\xi^\dagger, \qquad (\xi\,\Sigma\eta^\dagger)^\dagger = \eta\,\Sigma_r\xi^\dagger, \tag{2.47}$$

where in each case Σ stands for any sequence of alternating σ and $\overline{\sigma}$ matrices, and Σ_r is obtained from Σ by reversing the order of all of the σ and $\overline{\sigma}$ matrices, since the sigma matrices are hermitian. Eqs. (2.43)–(2.47) are applicable both to anticommuting and to commuting spinors.

The properties of the two-component spinor fields under the discrete C, P and T transformations are elucidated in Refs. [39,117]. The corresponding behaviors of the spinor products under C, P and T are easily obtained (and are left as an exercise for the reader).

The following identities can be used to systematically simplify expressions involving products of σ and $\overline{\sigma}$ matrices[13]:

$$\sigma^{\mu}_{\alpha\dot{\alpha}}\overline{\sigma}^{\dot{\beta}\beta}_{\mu} = 2\delta_{\alpha}{}^{\beta}\delta^{\dot{\beta}}{}_{\dot{\alpha}}, \tag{2.48}$$

$$\sigma^{\mu}_{\alpha\dot{\alpha}}\sigma_{\mu\beta\dot{\beta}} = 2\epsilon_{\alpha\beta}\epsilon_{\dot{\alpha}\dot{\beta}}, \tag{2.49}$$

$$\overline{\sigma}^{\mu\dot{\alpha}\alpha}\overline{\sigma}^{\dot{\beta}\beta}_{\mu} = 2\epsilon^{\alpha\beta}\epsilon^{\dot{\alpha}\dot{\beta}}, \tag{2.50}$$

$$[\sigma^{\mu}\overline{\sigma}^{\nu} + \sigma^{\nu}\overline{\sigma}^{\mu}]^{\beta}_{\alpha} = 2g^{\mu\nu}\delta_{\alpha}{}^{\beta}, \tag{2.51}$$

$$[\overline{\sigma}^{\mu}\sigma^{\nu} + \overline{\sigma}^{\nu}\sigma^{\mu}]^{\dot{\alpha}}{}_{\dot{\beta}} = 2g^{\mu\nu}\delta^{\dot{\alpha}}{}_{\dot{\beta}}, \tag{2.52}$$

$$\sigma^{\mu}\overline{\sigma}^{\nu}\sigma^{\rho} = g^{\mu\nu}\sigma^{\rho} - g^{\mu\rho}\sigma^{\nu} + g^{\nu\rho}\sigma^{\mu} + i\epsilon^{\mu\nu\rho\kappa}\sigma_{\kappa}, \tag{2.53}$$

$$\overline{\sigma}^{\mu}\sigma^{\nu}\overline{\sigma}^{\rho} = g^{\mu\nu}\overline{\sigma}^{\rho} - g^{\mu\rho}\overline{\sigma}^{\nu} + g^{\nu\rho}\overline{\sigma}^{\mu} - i\epsilon^{\mu\nu\rho\kappa}\overline{\sigma}_{\kappa}. \tag{2.54}$$

In the literature, one sometimes sees Eqs. (2.49) and (2.50) rewritten using the identity $\epsilon_{ab}\epsilon_{cd} = \delta_{ac}\delta_{bd} - \delta_{ad}\delta_{bc}$. However, as this latter result does not formally respect covariance with respect to the dotted and undotted indices, we shall not employ it here.

Computations of cross-sections and decay rates generally require traces of alternating products of σ and $\overline{\sigma}$ matrices (e.g., see Ref. [104]):

$$\mathrm{Tr}[\sigma^{\mu}\overline{\sigma}^{\nu}] = \mathrm{Tr}[\overline{\sigma}^{\mu}\sigma^{\nu}] = 2g^{\mu\nu}, \tag{2.55}$$

$$\mathrm{Tr}[\sigma^{\mu}\overline{\sigma}^{\nu}\sigma^{\rho}\overline{\sigma}^{\kappa}] = 2\left(g^{\mu\nu}g^{\rho\kappa} - g^{\mu\rho}g^{\nu\kappa} + g^{\mu\kappa}g^{\nu\rho} + i\epsilon^{\mu\nu\rho\kappa}\right), \tag{2.56}$$

$$\mathrm{Tr}[\overline{\sigma}^{\mu}\sigma^{\nu}\overline{\sigma}^{\rho}\sigma^{\kappa}] = 2\left(g^{\mu\nu}g^{\rho\kappa} - g^{\mu\rho}g^{\nu\kappa} + g^{\mu\kappa}g^{\nu\rho} - i\epsilon^{\mu\nu\rho\kappa}\right). \tag{2.57}$$

Traces involving a larger even number of σ and $\overline{\sigma}$ matrices can be systematically obtained from Eqs. (2.55)–(2.57) by repeated use of Eqs. (2.51) and (2.52) and the cyclic property of the trace. Traces involving an odd number of σ and $\overline{\sigma}$ matrices cannot arise, since there is no way to connect the spinor indices consistently.

In addition to manipulating expressions containing anticommuting fermion quantum fields, we often must deal with products of *commuting* spinor wave functions that arise when evaluating the Feynman rules. In the following expressions we denote the generic spinor by z_i. In the various identities listed below, an extra minus sign arises when interchanging the order of two anticommuting fermion fields of a given spinor index height. It is convenient to introduce the notation:

$$(-1)^A \equiv \begin{cases} +1, & \text{commuting spinors,} \\ -1, & \text{anticommuting spinors.} \end{cases} \tag{2.58}$$

The following identities hold for the z_i:

$$z_1 z_2 = -(-1)^A z_2 z_1, \tag{2.59}$$

$$z_1^{\dagger} z_2^{\dagger} = -(-1)^A z_2^{\dagger} z_1^{\dagger}, \tag{2.60}$$

$$z_1 \sigma^{\mu} z_2^{\dagger} = (-1)^A z_2^{\dagger}\overline{\sigma}^{\mu} z_1, \tag{2.61}$$

$$z_1 \sigma^{\mu}\overline{\sigma}^{\nu} z_2 = -(-1)^A z_2 \sigma^{\nu}\overline{\sigma}^{\mu} z_1, \tag{2.62}$$

$$z_1^{\dagger}\overline{\sigma}^{\mu}\sigma^{\nu} z_2^{\dagger} = -(-1)^A z_2^{\dagger}\overline{\sigma}^{\nu}\sigma^{\mu} z_1^{\dagger}, \tag{2.63}$$

$$z_1^{\dagger}\overline{\sigma}^{\mu}\sigma^{\rho}\overline{\sigma}^{\nu} z_2 = (-1)^A z_2 \sigma^{\nu}\overline{\sigma}^{\rho}\sigma^{\mu} z_1^{\dagger}, \tag{2.64}$$

and so on.[14] The hermiticity properties of the spinor products given in Eqs. (2.43)–(2.47) hold for both commuting and anticommuting spinors, with no additional sign factor.

Two-component spinor products can often be simplified by using Fierz identities. Due to the antisymmetry of the suppressed two-index epsilon symbol [or equivalently, using the Schouten identities given in Eq. (2.26)], the following identities are obtained:

$$(z_1 z_2)(z_3 z_4) = -(z_1 z_3)(z_4 z_2) - (z_1 z_4)(z_2 z_3), \tag{2.65}$$

$$(z_1^{\dagger} z_2^{\dagger})(z_3^{\dagger} z_4^{\dagger}) = -(z_1^{\dagger} z_3^{\dagger})(z_4^{\dagger} z_2^{\dagger}) - (z_1^{\dagger} z_4^{\dagger})(z_2^{\dagger} z_3^{\dagger}), \tag{2.66}$$

---

[13] Since the Kronecker delta symbol is symmetric under the interchange of its two indices, naively there is nothing gained in writing $\delta_{\alpha}{}^{\beta}$ and $\delta^{\dot{\beta}}{}_{\dot{\alpha}}$, with the spinor indices staggered as shown, instead of δ^{β}_{α} and $\delta^{\dot{\beta}}_{\dot{\alpha}}$, respectively. Nevertheless, we often prefer to employ the former rather than the latter as it provides some insight into the spinor index structure of the equation. For example, in Eq. (2.51), α labels the row and β labels the column of the product of sigma matrices. Neither $\sigma^{\mu}\overline{\sigma}^{\nu}$ nor $\sigma^{\nu}\overline{\sigma}^{\mu}$ is symmetric under the interchange of the (suppressed) spinor indices (although the sum of the two is symmetric). By writing $\delta_{\alpha}{}^{\beta}$ on the right-hand side of Eq. (2.51), one formally maintains the index structure of each of the separate terms of the equation.

[14] In particular, if z is a *commuting* spinor, then $zz = z^{\dagger}z^{\dagger} = 0$, as emphasized in Refs. [16,19].

where we have used Eqs. (2.59) and (2.60) to eliminate any residual factors of $(-1)^A$. Similarly, Eqs. (2.48)–(2.50) can be used to derive additional Fierz identities,

$$(z_1\sigma^\mu z_2^\dagger)(z_3^\dagger\overline{\sigma}_\mu z_4) = -2(z_1z_4)(z_2^\dagger z_3^\dagger), \tag{2.67}$$

$$(z_1^\dagger\overline{\sigma}^\mu z_2)(z_3^\dagger\overline{\sigma}_\mu z_4) = 2(z_1^\dagger z_3^\dagger)(z_4z_2), \tag{2.68}$$

$$(z_1\sigma^\mu z_2^\dagger)(z_3\sigma_\mu z_4^\dagger) = 2(z_1z_3)(z_4^\dagger z_2^\dagger). \tag{2.69}$$

Having eliminated all factors of $(-1)^A$, Eqs. (2.65)–(2.69) hold for both commuting and anticommuting spinors.

From the sigma matrices, one can construct the antisymmetrized products[15]:

$$(\sigma^{\mu\nu})_\alpha{}^\beta \equiv \frac{i}{4}\left(\sigma^\mu{}_{\alpha\dot\gamma}\overline{\sigma}^{\nu\dot\gamma\beta} - \sigma^\nu{}_{\alpha\dot\gamma}\overline{\sigma}^{\mu\dot\gamma\beta}\right), \tag{2.70}$$

$$(\overline{\sigma}^{\mu\nu})^{\dot\alpha}{}_{\dot\beta} \equiv \frac{i}{4}\left(\overline{\sigma}^{\mu\dot\alpha\gamma}\sigma^\nu_{\gamma\dot\beta} - \overline{\sigma}^{\nu\dot\alpha\gamma}\sigma^\mu_{\gamma\dot\beta}\right). \tag{2.71}$$

Equivalently, we can use Eqs. (2.51) and (2.52) to write:

$$(\sigma^\mu\overline{\sigma}^\nu)_\alpha{}^\beta = g^{\mu\nu}\delta_\alpha{}^\beta - 2i(\sigma^{\mu\nu})_\alpha{}^\beta, \tag{2.72}$$

$$(\overline{\sigma}^\mu\sigma^\nu)^{\dot\alpha}{}_{\dot\beta} = g^{\mu\nu}\delta^{\dot\alpha}{}_{\dot\beta} - 2i(\overline{\sigma}^{\mu\nu})^{\dot\alpha}{}_{\dot\beta}. \tag{2.73}$$

The components of $\sigma^{\mu\nu}$ and $\overline{\sigma}^{\mu\nu}$ are easily evaluated:

$$\sigma^{ij} = \overline{\sigma}^{ij} = \tfrac{1}{2}\epsilon^{ijk}\sigma^k, \qquad \sigma^{i0} = -\sigma^{0i} = -\overline{\sigma}^{i0} = \overline{\sigma}^{0i} = \tfrac{1}{2}i\sigma^i. \tag{2.74}$$

The matrices $\sigma^{\mu\nu}$ and $\overline{\sigma}^{\mu\nu}$ satisfy self-duality relations,

$$\sigma^{\mu\nu} = -\tfrac{1}{2}i\epsilon^{\mu\nu\rho\kappa}\sigma_{\rho\kappa}, \qquad \overline{\sigma}^{\mu\nu} = \tfrac{1}{2}i\epsilon^{\mu\nu\rho\kappa}\overline{\sigma}_{\rho\kappa}. \tag{2.75}$$

The self-duality relations can be used to obtain the following two identities:

$$g^{\kappa\rho}\sigma^{\mu\nu} - g^{\nu\rho}\sigma^{\mu\kappa} + g^{\mu\rho}\sigma^{\nu\kappa} - i\epsilon^{\mu\nu\kappa}{}_\lambda\sigma^{\lambda\rho} = 0, \tag{2.76}$$

$$g^{\kappa\rho}\overline{\sigma}^{\mu\nu} - g^{\nu\rho}\overline{\sigma}^{\mu\kappa} + g^{\mu\rho}\overline{\sigma}^{\nu\kappa} + i\epsilon^{\mu\nu\kappa}{}_\lambda\overline{\sigma}^{\lambda\rho} = 0. \tag{2.77}$$

A number of useful properties and identities involving $\sigma^{\mu\nu}$ and $\overline{\sigma}^{\mu\nu}$ can be derived. For example, Eq. (2.24) implies that:

$$(\sigma^{\mu\nu})_\alpha{}^\beta = \epsilon_{\alpha\tau}\epsilon^{\beta\gamma}(\sigma^{\mu\nu})_\gamma{}^\tau, \qquad (\overline{\sigma}^{\mu\nu})^{\dot\alpha}{}_{\dot\beta} = \epsilon^{\dot\alpha\dot\tau}\epsilon_{\dot\beta\dot\gamma}(\overline{\sigma}^{\mu\nu})^{\dot\gamma}{}_{\dot\tau}, \tag{2.78}$$

$$\epsilon^{\tau\alpha}(\sigma^{\mu\nu})_\alpha{}^\beta = \epsilon^{\beta\gamma}(\sigma^{\mu\nu})_\gamma{}^\tau, \qquad \epsilon_{\dot\tau\dot\alpha}(\overline{\sigma}^{\mu\nu})^{\dot\alpha}{}_{\dot\beta} = \epsilon_{\dot\beta\dot\gamma}(\overline{\sigma}^{\mu\nu})^{\dot\gamma}{}_{\dot\tau}, \tag{2.79}$$

$$\epsilon_{\gamma\beta}(\sigma^{\mu\nu})_\alpha{}^\beta = \epsilon_{\alpha\tau}(\sigma^{\mu\nu})_\gamma{}^\tau, \qquad \epsilon^{\dot\gamma\dot\beta}(\overline{\sigma}^{\mu\nu})^{\dot\alpha}{}_{\dot\beta} = \epsilon^{\dot\alpha\dot\tau}(\overline{\sigma}^{\mu\nu})^{\dot\gamma}{}_{\dot\tau}. \tag{2.80}$$

Using Eqs. (2.48)–(2.54), the following identities can be obtained:

$$(\sigma^{\mu\nu})_\alpha{}^\beta(\sigma_{\mu\nu})_\gamma{}^\tau = \epsilon_{\alpha\gamma}\epsilon^{\beta\tau} + \delta_\alpha{}^\tau\delta_\gamma{}^\beta = 2\delta_\alpha{}^\tau\delta_\gamma{}^\beta - \delta_\alpha{}^\beta\delta_\gamma{}^\tau, \tag{2.81}$$

$$(\overline{\sigma}^{\mu\nu})^{\dot\alpha}{}_{\dot\beta}(\overline{\sigma}_{\mu\nu})^{\dot\gamma}{}_{\dot\tau} = \epsilon^{\dot\alpha\dot\gamma}\epsilon_{\dot\beta\dot\tau} + \delta^{\dot\alpha}{}_{\dot\tau}\delta^{\dot\gamma}{}_{\dot\beta} = 2\delta^{\dot\alpha}{}_{\dot\tau}\delta^{\dot\gamma}{}_{\dot\beta} - \delta^{\dot\alpha}{}_{\dot\beta}\delta^{\dot\gamma}{}_{\dot\tau}, \tag{2.82}$$

$$(\sigma^{\mu\nu})_\alpha{}^\beta(\overline{\sigma}_{\mu\nu})^{\dot\gamma}{}_{\dot\tau} = 0, \tag{2.83}$$

$$\sigma^{\mu\nu}\sigma^\rho = \tfrac{1}{2}i\left(g^{\nu\rho}\sigma^\mu - g^{\mu\rho}\sigma^\nu + i\epsilon^{\mu\nu\rho\kappa}\sigma_\kappa\right), \tag{2.84}$$

$$\overline{\sigma}^{\mu\nu}\overline{\sigma}^\rho = \tfrac{1}{2}i\left(g^{\nu\rho}\overline{\sigma}^\mu - g^{\mu\rho}\overline{\sigma}^\nu - i\epsilon^{\mu\nu\rho\kappa}\overline{\sigma}_\kappa\right), \tag{2.85}$$

$$\overline{\sigma}^\mu\sigma^{\nu\rho} = \tfrac{1}{2}i\left(g^{\mu\nu}\overline{\sigma}^\rho - g^{\mu\rho}\overline{\sigma}^\nu - i\epsilon^{\mu\nu\rho\kappa}\overline{\sigma}_\kappa\right), \tag{2.86}$$

$$\sigma^\mu\overline{\sigma}^{\nu\rho} = \tfrac{1}{2}i\left(g^{\mu\nu}\sigma^\rho - g^{\mu\rho}\sigma^\nu + i\epsilon^{\mu\nu\rho\kappa}\sigma_\kappa\right), \tag{2.87}$$

$$\sigma^{\mu\nu}\sigma^{\rho\kappa} = -\tfrac{1}{4}\left(g^{\nu\rho}g^{\mu\kappa} - g^{\mu\rho}g^{\nu\kappa} + i\epsilon^{\mu\nu\rho\kappa}\right) + \tfrac{1}{2}i\left(g^{\nu\rho}\sigma^{\mu\kappa} + g^{\mu\kappa}\sigma^{\nu\rho} - g^{\mu\rho}\sigma^{\nu\kappa} - g^{\nu\kappa}\sigma^{\mu\rho}\right), \tag{2.88}$$

$$\overline{\sigma}^{\mu\nu}\overline{\sigma}^{\rho\kappa} = -\tfrac{1}{4}\left(g^{\nu\rho}g^{\mu\kappa} - g^{\mu\rho}g^{\nu\kappa} - i\epsilon^{\mu\nu\rho\kappa}\right) + \tfrac{1}{2}i\left(g^{\nu\rho}\overline{\sigma}^{\mu\kappa} + g^{\mu\kappa}\overline{\sigma}^{\nu\rho} - g^{\mu\rho}\overline{\sigma}^{\nu\kappa} - g^{\nu\kappa}\overline{\sigma}^{\mu\rho}\right). \tag{2.89}$$

[15] The reader is cautioned that $\sigma^{\mu\nu}$ and $\overline{\sigma}^{\mu\nu}$ are sometimes defined in the literature without the factor of i in Eqs. (2.70) and (2.71) (as in Ref. [77]), or with an overall factor of $\frac{1}{2}i$ (as in Ref. [71]) instead of $\frac{1}{4}i$.

Eqs. (2.88) and (2.89) and the antisymmetry of $\sigma^{\mu\nu}$ and $\overline{\sigma}^{\mu\nu}$ yield the following trace formulae:

$$\mathrm{Tr}\,\sigma^{\mu\nu} = \mathrm{Tr}\,\overline{\sigma}^{\mu\nu} = 0, \tag{2.90}$$

$$\mathrm{Tr}[\sigma^{\mu\nu}\sigma^{\rho\kappa}] = \tfrac{1}{2}\left[g^{\mu\rho}g^{\nu\kappa} - g^{\mu\kappa}g^{\nu\rho} - i\epsilon^{\mu\nu\rho\kappa}\right], \tag{2.91}$$

$$\mathrm{Tr}[\overline{\sigma}^{\mu\nu}\overline{\sigma}^{\rho\kappa}] = \tfrac{1}{2}\left[g^{\mu\rho}g^{\nu\kappa} - g^{\mu\kappa}g^{\nu\rho} + i\epsilon^{\mu\nu\rho\kappa}\right]. \tag{2.92}$$

The properties of spinor products involving $\sigma^{\mu\nu}$ and $\overline{\sigma}^{\mu\nu}$ are easily derived. Under hermitian conjugation (for quantum field operators) or complex conjugation (for classical fields),

$$(\xi\sigma^{\mu\nu}\eta)^\dagger = \eta^\dagger\overline{\sigma}^{\mu\nu}\xi^\dagger, \tag{2.93}$$

due to the hermiticity relation, $(\sigma^{\mu\nu})^\dagger = \overline{\sigma}^{\mu\nu}$. Next, we use Eqs. (2.62) and (2.63) to obtain:

$$z_1\sigma^{\mu\nu}z_2 = (-1)^A z_2\sigma^{\mu\nu}z_1, \tag{2.94}$$

$$z_1^\dagger\overline{\sigma}^{\mu\nu}z_2^\dagger = (-1)^A z_2^\dagger\overline{\sigma}^{\mu\nu}z_1^\dagger. \tag{2.95}$$

One can also derive additional Fierz identities, which follow from Eqs. (2.81)–(2.83),

$$(z_1\sigma^{\mu\nu}z_2)(z_3\sigma_{\mu\nu}z_4) = -2(z_1z_4)(z_2z_3) - (z_1z_2)(z_3z_4), \tag{2.96}$$

$$(z_1^\dagger\overline{\sigma}^{\mu\nu}z_2^\dagger)(z_3^\dagger\overline{\sigma}_{\mu\nu}z_4^\dagger) = -2(z_1^\dagger z_4^\dagger)(z_2^\dagger z_3^\dagger) - (z_1^\dagger z_2^\dagger)(z_3^\dagger z_4^\dagger), \tag{2.97}$$

$$(z_1\sigma^{\mu\nu}z_2)(z_3^\dagger\overline{\sigma}_{\mu\nu}z_4^\dagger) = 0, \tag{2.98}$$

where we have again used Eqs. (2.59) and (2.60) to eliminate any residual factors of $(-1)^A$. Thus, Eqs. (2.96)–(2.98) hold for both commuting and anticommuting spinors. A more comprehensive list of sigma matrix identities and their associated Fierz identities are given in Appendix B.1 (see also Appendix B of Ref. [77]).

The $\sigma^{\mu\nu}$ and $\overline{\sigma}^{\mu\nu}$ satisfy the commutation relations of the $J^{\mu\nu}$ [cf. Eq. (2.14)], and thus can be identified as the generators of the Lorentz group in the $(\frac{1}{2}, 0)$ and $(0, \frac{1}{2})$ representations, respectively. That is, for the $(\frac{1}{2}, 0)$ representation with a lowered undotted index (e.g. ψ_α), $J^{\mu\nu} = \sigma^{\mu\nu}$, while for the $(0, \frac{1}{2})$ representation with a raised dotted index (e.g. $\psi^{\dagger\dot\alpha}$), $J^{\mu\nu} = \overline{\sigma}^{\mu\nu}$. In particular, the infinitesimal forms for the 4×4 Lorentz transformation matrix Λ and the corresponding matrices M and $(M^{-1})^\dagger$ that transform the $(\frac{1}{2}, 0)$ and $(0, \frac{1}{2})$ spinors, respectively, are given by:

$$\Lambda^\mu{}_\nu \simeq \delta^\mu_\nu + \tfrac{1}{2}\left(\theta_{\alpha\nu}g^{\alpha\mu} - \theta_{\nu\beta}g^{\beta\mu}\right), \tag{2.99}$$

$$M \simeq \mathbb{1}_{2\times 2} - \tfrac{1}{2}i\theta_{\mu\nu}\sigma^{\mu\nu}, \tag{2.100}$$

$$(M^{-1})^\dagger \simeq \mathbb{1}_{2\times 2} - \tfrac{1}{2}i\theta_{\mu\nu}\overline{\sigma}^{\mu\nu}. \tag{2.101}$$

The inverses of these quantities are obtained (to first order in θ) by replacing $\theta \to -\theta$ in the above formulae. Using Eqs. (2.78), (2.100) and (2.101), it follows that:

$$(M^{-1})_\gamma{}^\tau = \epsilon^{\tau\alpha}M_\alpha{}^\beta\epsilon_{\beta\gamma}, \tag{2.102}$$

$$(M^{-1\,\dagger})^{\dot\gamma}{}_{\dot\tau} = \epsilon_{\dot\tau\dot\alpha}\,(M^\dagger)^{\dot\alpha}{}_{\dot\beta}\,\epsilon^{\dot\beta\dot\gamma}. \tag{2.103}$$

These results can be used to demonstrate the covariance (with respect to Lorentz transformations) of the spinor index raising and lowering properties of the epsilon symbols defined in Eq. (2.20). The infinitesimal forms given by Eqs. (2.99)–(2.101) can also be used [with the assistance of Eqs. (2.84)–(2.86)] to establish the following two results:

$$M^\dagger\overline{\sigma}^\mu M = \Lambda^\mu{}_\nu\,\overline{\sigma}^\nu, \tag{2.104}$$

$$M^{-1}\sigma^\mu(M^{-1})^\dagger = \Lambda^\mu{}_\nu\,\sigma^\nu. \tag{2.105}$$

Using the Lorentz transformation properties of the undotted and dotted two-component spinor fields, Eqs. (2.104) and (2.105) can be used, respectively, to prove that the spinor products $\xi^\dagger\overline{\sigma}^\mu\eta$ and $\xi\sigma^\mu\eta^\dagger$ transform as Lorentz four-vectors.

As an example, consider a pure boost from the rest frame to a frame where $p^\mu = (E_{\boldsymbol{p}}, \vec{\boldsymbol{p}})$, which corresponds to $\theta_{ij} = 0$ and $\zeta^i = \theta^{i0} = -\theta^{0i}$. We assume that the mass–shell condition is satisfied, i.e. $p^0 = E_{\vec{\boldsymbol{p}}} \equiv (|\vec{\boldsymbol{p}}|^2 + m^2)^{1/2}$. The matrices $M_\alpha{}^\beta$ and $[(M^{-1})^\dagger]^{\dot\alpha}{}_{\dot\beta}$ that govern the Lorentz transformations of spinor fields with a lowered undotted index and spinor fields with a raised dotted index, respectively, are given by:

$$\exp\left(-\frac{i}{2}\theta_{\mu\nu}J^{\mu\nu}\right) = \begin{cases} M = \exp\left(-\tfrac{1}{2}\vec{\boldsymbol{\zeta}}\cdot\vec{\boldsymbol{\sigma}}\right) = \sqrt{\dfrac{p\cdot\sigma}{m}}, & \text{for } \left(\tfrac{1}{2}, 0\right), \\ (M^{-1})^\dagger = \exp\left(\tfrac{1}{2}\vec{\boldsymbol{\zeta}}\cdot\vec{\boldsymbol{\sigma}}\right) = \sqrt{\dfrac{p\cdot\overline{\sigma}}{m}}, & \text{for } \left(0, \tfrac{1}{2}\right), \end{cases} \tag{2.106}$$

where

$$\sqrt{p\cdot\sigma}\equiv\frac{(E_{\boldsymbol{p}}+m)\,\mathbb{1}_{2\times2}-\vec{\boldsymbol{\sigma}}\cdot\vec{\boldsymbol{p}}}{\sqrt{2(E_{\boldsymbol{p}}+m)}},\tag{2.107}$$

$$\sqrt{p\cdot\overline{\sigma}}\equiv\frac{(E_{\boldsymbol{p}}+m)\,\mathbb{1}_{2\times2}+\vec{\boldsymbol{\sigma}}\cdot\vec{\boldsymbol{p}}}{\sqrt{2(E_{\boldsymbol{p}}+m)}}.\tag{2.108}$$

These matrix square roots are defined to be the unique non-negative definite hermitian matrices (i.e., with non-negative eigenvalues) whose squares are equal to the non-negative definite hermitian matrices $p\cdot\sigma$ and $p\cdot\overline{\sigma}$, respectively.[16]

According to Eq. (2.106), the spinor index structure of $\sqrt{p\cdot\sigma}$ and $\sqrt{p\cdot\overline{\sigma}}$ corresponds to that of $M_\alpha{}^\beta$ and $[(M^{-1})^\dagger]^{\dot\alpha}{}_{\dot\beta}$, respectively. In this case, we can rewrite Eqs. (2.107) and (2.108) as:

$$\left[\sqrt{p\cdot\sigma}\,\right]_\alpha{}^\beta\equiv\left[\sqrt{p\cdot\sigma\,\overline{\sigma}^0}\,\right]_\alpha{}^\beta=\frac{(p\cdot\sigma_{\alpha\dot\alpha})\overline{\sigma}^{0\,\dot\alpha\beta}+m\delta_\alpha^\beta}{\sqrt{2(E_{\boldsymbol{p}}+m)}},\tag{2.109}$$

$$\left[\sqrt{p\cdot\overline{\sigma}}\,\right]^{\dot\alpha}{}_{\dot\beta}\equiv\left[\sqrt{p\cdot\overline{\sigma}\,\sigma^0}\,\right]^{\dot\alpha}{}_{\dot\beta}=\frac{(p\cdot\overline{\sigma}^{\dot\alpha\alpha})\sigma^0_{\alpha\dot\beta}+m\delta^{\dot\alpha}_{\dot\beta}}{\sqrt{2(E_{\boldsymbol{p}}+m)}},\tag{2.110}$$

since $\sigma^0=\overline{\sigma}^0=\mathbb{1}_{2\times2}$. Using Eqs. (2.53) and (2.54), one can easily verify that:

$$\left[\sqrt{p\cdot\sigma}\,\right]_\alpha{}^\gamma\left[\sqrt{p\cdot\sigma}\,\right]_\gamma{}^\beta=(p\cdot\sigma\,\overline{\sigma}^0)_\alpha{}^\beta,\tag{2.111}$$

$$\left[\sqrt{p\cdot\overline{\sigma}}\,\right]^{\dot\alpha}{}_{\dot\gamma}\left[\sqrt{p\cdot\overline{\sigma}}\,\right]^{\dot\gamma}{}_{\dot\beta}=(p\cdot\overline{\sigma}\,\sigma^0)^{\dot\alpha}{}_{\dot\beta},\tag{2.112}$$

where implicit factors of $\overline{\sigma}^0$ and σ^0 inside the square roots of Eq. (2.111) have been suppressed.

Due to the fact that $p\cdot\sigma$ and $p\cdot\overline{\sigma}$ are hermitian, we could have defined their hermitian matrix square roots by the hermitian conjugate of Eq. (2.106). In this case, the spinor index structure of $\sqrt{p\cdot\sigma}$ and $\sqrt{p\cdot\overline{\sigma}}$ would correspond to that of $[M^\dagger]^{\dot\alpha}{}_{\dot\beta}$ and $[M^{-1}]_\alpha{}^\beta$, respectively. That is, instead of Eqs. (2.109) and (2.110), we would now rewrite Eqs. (2.107) and (2.108) in the following form:

$$\left[\sqrt{p\cdot\sigma}\,\right]^{\dot\alpha}{}_{\dot\beta}\equiv\left[\sqrt{\overline{\sigma}^0\,p\cdot\sigma}\,\right]^{\dot\alpha}{}_{\dot\beta}=\frac{\overline{\sigma}^{0\,\dot\alpha\beta}(p\cdot\sigma_{\beta\dot\beta})+m\delta^{\dot\alpha}_{\dot\beta}}{\sqrt{2(E_{\boldsymbol{p}}+m)}},\tag{2.113}$$

$$\left[\sqrt{p\cdot\overline{\sigma}}\,\right]_\alpha{}^\beta\equiv\left[\sqrt{\sigma^0\,p\cdot\overline{\sigma}}\,\right]_\alpha{}^\beta=\frac{\sigma^0_{\alpha\dot\beta}(p\cdot\overline{\sigma}^{\dot\beta\beta})+m\delta_\alpha^\beta}{\sqrt{2(E_{\boldsymbol{p}}+m)}}.\tag{2.114}$$

Using Eqs. (2.53) and (2.54), one can again confirm that:

$$\left[\sqrt{p\cdot\sigma}\,\right]^{\dot\alpha}{}_{\dot\gamma}\left[\sqrt{p\cdot\sigma}\,\right]^{\dot\gamma}{}_{\dot\beta}=(\overline{\sigma}^0\,p\cdot\sigma)^{\dot\alpha}{}_{\dot\beta},\tag{2.115}$$

$$\left[\sqrt{p\cdot\overline{\sigma}}\,\right]_\alpha{}^\gamma\left[\sqrt{p\cdot\overline{\sigma}}\,\right]_\gamma{}^\beta=(\sigma^0\,p\cdot\overline{\sigma})_\alpha{}^\beta,\tag{2.116}$$

where implicit factors of $\overline{\sigma}^0$ and σ^0 inside the square roots of Eq. (2.115) have been suppressed.

The proper choice of the spinor index structure for $\sqrt{p\cdot\sigma}$ and $\sqrt{p\cdot\overline{\sigma}}$ can always be determined for any covariant expression. That is, if we employ the spinor index-free notation (and suppress the factors of σ^0 and $\overline{\sigma}^0$), it will always be clear from the context which spinor index structure for $\sqrt{p\cdot\sigma}$ and $\sqrt{p\cdot\overline{\sigma}}$ is implicit.

As an example that will prove valuable later on, consider an arbitrary four-vector S^μ, defined in a reference frame where $p^\mu=(E;\vec{\boldsymbol{p}})$, whose rest frame value is S_R^μ, i.e.

$$S^\mu=\Lambda^\mu{}_\nu S_R^\nu,\quad\text{with }\Lambda=\begin{pmatrix}E/m & p^j/m\\ p^i/m & \delta_{ij}+\dfrac{p^ip^j}{m(E+m)}\end{pmatrix}.\tag{2.117}$$

Then, using Eqs. (2.7), (2.105) and (2.106), it follows that:

$$\sqrt{p\cdot\sigma}\,S\cdot\overline{\sigma}\,\sqrt{p\cdot\sigma}=mS_R\cdot\overline{\sigma},\tag{2.118}$$

$$\sqrt{p\cdot\overline{\sigma}}\,S\cdot\sigma\,\sqrt{p\cdot\overline{\sigma}}=mS_R\cdot\sigma.\tag{2.119}$$

[16] Note that $p\cdot\sigma$ and $p\cdot\overline{\sigma}$ are non-negative matrices due to the implicit mass–shell condition satisfied by p^μ.

The spinor index structure of Eqs. (2.118) and (2.119) is easily established:

$$\left[\sqrt{p\cdot\sigma}\,\right]^{\dot\beta}{}_{\dot\gamma}\, S\cdot\overline{\sigma}^{\dot\gamma\alpha}\left[\sqrt{p\cdot\sigma}\,\right]_{\alpha}{}^{\beta} = mS_R\cdot\overline{\sigma}^{\dot\beta\beta}, \tag{2.120}$$

$$\left[\sqrt{p\cdot\overline{\sigma}}\,\right]_{\beta}{}^{\gamma}\, S\cdot\sigma_{\gamma\dot\alpha}\left[\sqrt{p\cdot\overline{\sigma}}\,\right]^{\dot\alpha}{}_{\dot\beta} = mS_R\cdot\sigma_{\beta\dot\beta}. \tag{2.121}$$

Using Eqs. (2.109)–(2.117) and (2.53)–(2.54), one can directly verify the above results.

The two-component spinor formalism established in this section will be applied to the quantum field theory of fermions in Minkowski space of one time and three space dimensions in this review. We also direct the reader's attention to Appendices G.1 and G.2, which provide details of the correspondence between the two-component and four-component spinor notation.

For certain applications, the spinor formalism in four-dimensional Minkowski space is not sufficient. For example, in order to obtain instanton solutions [118–120], it is necessary to formulate quantum field theory in Euclidean space. One also needs the Euclidean space formalism for a rigorous definition of the path integral [121,122]. The Green functions derived from the Euclidean path integral can be related to the Green functions of the Minkowski space theory by a Wick rotation [123]. In addition, to evaluate the loop-corrected Green functions of the theory, it is often most convenient to apply a regularization scheme that involves dimensional continuation away from $d = 4$ spacetime dimensions [124]. Thus, we also need to generalize the spinor results of this section to $d \neq 4$.

The treatment of fermions in Euclidean space is subtle [125–127]. Here, we focus briefly on the mathematics of fermions in $d = 4$ Euclidean dimensions, where the relevant spacetime symmetry group is SO(4) rather than SO(3,1). The two-dimensional representations of $\mathrm{SO}(3,1) \cong \mathrm{SL}(2,\mathbb{C})$, denoted in this section by $(\frac{1}{2},0)$ and $(0,\frac{1}{2})$, respectively, are complex representations that are related by hermitian conjugation. In contrast, the two-dimensional representations of $\mathrm{SO}(4) \cong \mathrm{SU}(2)\times\mathrm{SU}(2)$, also denoted by $(\frac{1}{2},0)$ and $(0,\frac{1}{2})$, respectively,[17] are independent pseudo-real representations, i.e. *not* related by hermitian conjugation. A two-component spinor notation can be formulated for fields that transform respectively under the $(\frac{1}{2},0)$ and $(0,\frac{1}{2})$ representations of SO(4). Details can be found in Refs. [119,128,129].

In Feynman diagram calculations, one can adopt the standard procedure for the Wick rotation in order to evaluate the loop integrals in Euclidean space. We shall employ the standard Euclidean metric $\delta^{\mu\nu}$ in computing scalar products of four-vectors. Moreover, one can define Euclidean sigma matrices, $\sigma_E^\mu = (-i\vec{\boldsymbol{\sigma}}, \sigma_E^4)$ and $\overline{\sigma}_E^\mu = (i\vec{\boldsymbol{\sigma}}, \overline{\sigma}_E^4)$, where $\sigma_E^4 = \overline{\sigma}_E^4 \equiv \mathbb{1}_{2\times2}$. In this convention, the Wick-rotated versions of Eqs. (2.51)–(2.57) are preserved [after making the replacements $g^{\mu\nu} \to \delta^{\mu\nu}$ and $i\epsilon^{ijk0} \to \epsilon^{ijk4}$, with $\epsilon^{1234} = \epsilon_{1234} = +1$].[18] Further details of our Euclidean space conventions are provided at the end of Appendix A.

The generalization of the spinor results of this section to $d \neq 4$, useful for dimensional continuation regularization schemes, is discussed in Appendix B.2. In particular, the identities of Appendix B.1 used to derive Fierz identities [cf. Eqs. (2.65)–(2.69) and (2.96)–(2.98)] and any identities involving the four-dimensional Levi-Civita ϵ-tensor are not valid unless μ is a Lorentz vector index in exactly four dimensions. In $d \neq 4$ dimensions, as used for loop amplitudes in dimensional regularization and dimensional.

In our treatment of two-component spinor identities in $d \neq 4$ dimensions given in Appendix B.2, we take the Lorentz vector indices to formally run over d values, whereas the undotted and dotted spinor indices continue to take on two possible values. This is sufficient when used as a regularization procedure for divergent integrals that arise in loop computations. However in generic d-dimensional field theories (where d is a positive integer), where d is an integer greater than 4, the two-component spinor formalism of this review is no longer applicable. Suitable methods for treating spinors in diverse spacetime dimensions and signatures [90,91,130–142] are briefly presented in Appendix G.3.

3. Properties of fermion fields

In this review, we refer to spin-1/2 particles as Majorana or Dirac fermions depending on the nature of the global symmetry[19] that governs the fermion Lagrangian and dictates the form of the fermion mass terms. A *Majorana fermion* is a two-component massive field that is completely neutral (i.e. a singlet with respect to the symmetry group) or transforms as a non-trivial real representation of the symmetry group (cf. footnote 31). A *Dirac fermion* consists of a pair of two-component massive fields that are oppositely charged with respect to a conserved O(2) symmetry. As shown in Section 3.2, Dirac fermions arise when a multiplet of two-component fermions transforms as a complex or pseudo-real representation of the symmetry group.[20]

[17] These SO(4) representations transform as a doublet under one of the SU(2) groups and as a singlet under the other SU(2) group.

[18] In practical computations of one-loop matrix elements, one can carry out all the sigma matrix algebra in Minkowski space *before* Wick-rotating to Euclidean space in order to perform the loop integrals.

[19] A subgroup of the global symmetry group may be gauged (and hence promoted to a local symmetry). Degrees of freedom not associated with the gauged subgroup are typically referred to as flavor degrees of freedom.

[20] Majorana and Dirac fermions can also be described in terms of four-component Majorana and Dirac spinor fields, as in Appendix G. However, keep in mind that the terms *Majorana spinor* and *Dirac spinor* are defined strictly in the context of the four-component spinor formalism as in Appendix G.1, or in the more general context of a d-dimensional spacetime as in Appendix G.3.

The case of a massless fermion is special, as the absence of mass terms leads to an enhanced global symmetry group. Each physical spin-1/2 zero mass eigenstate is fundamentally a two-component spinor. Thus, following the standard nomenclature used for massless neutrinos, it is common to employ the term *massless Weyl fermion* to describe any massless spin-1/2 particle.[21]

3.1. The two-component fermion field and spinor wave functions

We begin by describing the properties of a free neutral massive anticommuting spin-1/2 field, denoted $\xi_\alpha(x)$, which transforms as $(\frac{1}{2}, 0)$ under the Lorentz group. The field ξ_α therefore describes a Majorana fermion [3]. The free-field Lagrangian density is [16]:

$$\mathscr{L} = i\xi^\dagger\overline{\sigma}^\mu\partial_\mu\xi - \tfrac{1}{2}m(\xi\xi + \xi^\dagger\xi^\dagger). \tag{3.1.1}$$

On-shell, ξ satisfies the free-field Dirac equation [1,2,14,143,144],

$$i\,\overline{\sigma}^{\mu\dot\alpha\beta}\partial_\mu\xi_\beta = m\xi^{\dagger\dot\alpha}. \tag{3.1.2}$$

Consequently after quantization, ξ_α can be expanded in a Fourier series [143]:

$$\xi_\alpha(x) = \sum_s \int \frac{\mathrm{d}^3\vec{\boldsymbol{p}}}{(2\pi)^{3/2}(2E_{\boldsymbol{p}})^{1/2}}\left[x_\alpha(\vec{\boldsymbol{p}},s)a(\vec{\boldsymbol{p}},s)e^{-ip\cdot x} + y_\alpha(\vec{\boldsymbol{p}},s)a^\dagger(\vec{\boldsymbol{p}},s)e^{ip\cdot x}\right], \tag{3.1.3}$$

where $E_{\boldsymbol{p}} \equiv (|\vec{\boldsymbol{p}}|^2 + m^2)^{1/2}$, and the creation and annihilation operators $a^\dagger$ and a satisfy anticommutation relations:

$$\{a(\vec{\boldsymbol{p}},s),\, a^\dagger(\vec{\boldsymbol{p}}',\boldsymbol{s}')\} = \delta^3(\vec{\boldsymbol{p}} - \vec{\boldsymbol{p}}')\delta_{ss'}, \tag{3.1.4}$$

and all other anticommutators vanish. It follows that

$$\xi^\dagger_{\dot\alpha}(x) \equiv (\xi_\alpha)^\dagger = \sum_s \int \frac{\mathrm{d}^3\vec{\boldsymbol{p}}}{(2\pi)^{3/2}(2E_{\boldsymbol{p}})^{1/2}}\left[x^\dagger_{\dot\alpha}(\vec{\boldsymbol{p}},s)a^\dagger(\vec{\boldsymbol{p}},s)e^{ip\cdot x} + y^\dagger_{\dot\alpha}(\vec{\boldsymbol{p}},s)a(\vec{\boldsymbol{p}},s)e^{-ip\cdot x}\right]. \tag{3.1.5}$$

We employ covariant normalization of the one-particle states, i.e., we act with one creation operator on the vacuum with the following convention

$$\left|\vec{\boldsymbol{p}},s\right\rangle \equiv (2\pi)^{3/2}(2E_{\boldsymbol{p}})^{1/2}a^\dagger(\vec{\boldsymbol{p}},s)\,|0\rangle\,, \tag{3.1.6}$$

so that $\left\langle\vec{\boldsymbol{p}},s|\vec{\boldsymbol{p}}',s'\right\rangle = (2\pi)^3(2E_{\boldsymbol{p}})\delta^3(\vec{\boldsymbol{p}} - \vec{\boldsymbol{p}}')\delta_{ss'}$. Therefore,

$$\langle 0|\,\xi_\alpha(x)\,\left|\vec{\boldsymbol{p}},s\right\rangle = x_\alpha(\vec{\boldsymbol{p}},s)e^{-ip\cdot x}, \qquad \langle 0|\,\xi^\dagger_{\dot\alpha}(x)\,\left|\vec{\boldsymbol{p}},s\right\rangle = y^\dagger_{\dot\alpha}(\vec{\boldsymbol{p}},s)e^{-ip\cdot x}, \tag{3.1.7}$$

$$\left\langle\vec{\boldsymbol{p}},s\right|\,\xi_\alpha(x)\,|0\rangle = y_\alpha(\vec{\boldsymbol{p}},s)e^{ip\cdot x}, \qquad \left\langle\vec{\boldsymbol{p}},s\right|\,\xi^\dagger_{\dot\alpha}(x)\,|0\rangle = x^\dagger_{\dot\alpha}(\vec{\boldsymbol{p}},s)e^{ip\cdot x}. \tag{3.1.8}$$

It should be emphasized that $\xi_\alpha(x)$ is an anticommuting spinor field, whereas x_α and y_α are *commuting* two-component spinor wave functions. The anticommuting properties of the fields are carried by the creation and annihilation operators.

Applying Eq. (3.1.2) to Eq. (3.1.3), we find that the x_α and y_α satisfy momentum space Dirac equations. These conditions can be written down in a number of equivalent ways:

$$(p\cdot\overline{\sigma})^{\dot\alpha\beta}x_\beta = my^{\dagger\dot\alpha}, \qquad (p\cdot\sigma)_{\alpha\dot\beta}y^{\dagger\dot\beta} = mx_\alpha, \tag{3.1.9}$$

$$(p\cdot\sigma)_{\alpha\dot\beta}x^{\dagger\dot\beta} = -my_\alpha, \qquad (p\cdot\overline{\sigma})^{\dot\alpha\beta}y_\beta = -mx^{\dagger\dot\alpha}, \tag{3.1.10}$$

$$x^\alpha(p\cdot\sigma)_{\alpha\dot\beta} = -my^\dagger_{\dot\beta}, \qquad y^\dagger_{\dot\alpha}(p\cdot\overline{\sigma})^{\dot\alpha\beta} = -mx^\beta, \tag{3.1.11}$$

$$x^\dagger_{\dot\alpha}(p\cdot\overline{\sigma})^{\dot\alpha\beta} = my^\beta, \qquad y^\alpha(p\cdot\sigma)_{\alpha\dot\beta} = mx^\dagger_{\dot\beta}. \tag{3.1.12}$$

Using the identities $[(p\cdot\sigma)(p\cdot\overline{\sigma})]_\alpha{}^\beta = p^2\,\delta_\alpha{}^\beta$ and $[(p\cdot\overline{\sigma})(p\cdot\sigma)]^{\dot\alpha}{}_{\dot\beta} = p^2\,\delta^{\dot\alpha}{}_{\dot\beta}$, one can check that both x_α and y_α must satisfy the mass–shell condition, $p^2 = m^2$ (or equivalently, $p^0 = E_{\boldsymbol{p}}$). We will later see that Eqs. (3.1.9)–(3.1.12) are often useful for simplifying matrix elements.

The quantum number s labels the spin or helicity of the spin-1/2 fermion. We shall examine two approaches for constructing the spin-1/2 states. In the first approach, we consider the particle in its rest frame and quantize the spin along a fixed axis specified by the unit vector $\hat{\boldsymbol{s}} \equiv (\sin\theta\cos\phi, \sin\theta\sin\phi, \cos\theta)$ with polar angle θ and azimuthal angle

[21] Two-component fermions are often called Weyl fermions, due to their association with the two-dimensional spinor representations of the Lorentz group introduced by Weyl in Refs. [14,15]. It is now common practice to define a Weyl spinor as the left- or right-handed projection of a four-component spinor [as in Eq. (G.1.8)]. Of course, there is a one-to-one correspondence between these two definitions.

ϕ with respect to a fixed z-axis.[22] The corresponding spin states will be called fixed-axis spin states. The relevant basis of two-component spinors χ_s are eigenstates of $\frac{1}{2}\vec{\sigma}\cdot\hat{\mathbf{s}}$, i.e.,

$$\tfrac{1}{2}\vec{\sigma}\cdot\hat{\mathbf{s}}\,\chi_s = s\chi_s, \quad s = \pm\tfrac{1}{2}. \tag{3.1.13}$$

Explicit forms for the two-component spinors χ_s and their properties are given in Appendix C.

The fixed-axis spin states described above are not very convenient for particles in relativistic motion. Moreover, these states cannot be employed for massless particles since no rest frame exists. Thus, a second approach is to consider helicity states and the corresponding basis of two-component helicity spinors χ_λ that are eigenstates of $\frac{1}{2}\vec{\sigma}\cdot\hat{\mathbf{p}}$, i.e.,

$$\tfrac{1}{2}\vec{\sigma}\cdot\hat{\mathbf{p}}\,\chi_\lambda = \lambda\chi_\lambda, \quad \lambda = \pm\tfrac{1}{2}. \tag{3.1.14}$$

Here $\hat{\mathbf{p}}$ is the unit vector in the direction of the three-momentum, with polar angle θ and azimuthal angle ϕ with respect to a fixed z-axis. That is, the two-component helicity spinors can be obtained from the fixed-axis spinors by replacing $\hat{\mathbf{s}}$ by $\hat{\mathbf{p}}$ and identifying θ and ϕ as the polar and azimuthal angles of $\hat{\mathbf{p}}$.

For fermions of mass $m \neq 0$, it is possible to define the spin four-vector S^μ, which is specified in the rest frame by $(0;\hat{\mathbf{s}})$. The unit three-vector $\hat{\mathbf{s}}$ corresponds to the axis of spin quantization in the case of fixed-axis spin states. In an arbitrary reference frame, the spin four-vector satisfies $S\cdot p = 0$ and $S\cdot S = -1$. After boosting from the rest frame to a frame in which $p^\mu = (E,\ \vec{\mathbf{p}})$ [cf. Eq. (2.117)], one finds:

$$S^\mu = \left(\frac{\vec{\mathbf{p}}\cdot\hat{\mathbf{s}}}{m};\, \hat{\mathbf{s}} + \frac{(\vec{\mathbf{p}}\cdot\hat{\mathbf{s}})\,\vec{\mathbf{p}}}{m(E+m)}\right). \tag{3.1.15}$$

If necessary, we shall write $S^\mu(\hat{\mathbf{s}})$ to emphasize the dependence of S^μ on $\hat{\mathbf{s}}$.

The spin four-vector for helicity states is defined by taking $\hat{\mathbf{s}} = \hat{\mathbf{p}}$. Eq. (3.1.15) then reduces to

$$S^\mu = \frac{1}{m}\left(|\vec{\mathbf{p}}|;\, E\hat{\mathbf{p}}\right). \tag{3.1.16}$$

In the non-relativistic limit, the spin four-vector for helicity states is $S^\mu \simeq (0;\hat{\mathbf{p}})$, as expected.[23] In the high energy limit ($E \gg m$), $S^\mu = p^\mu/m + \mathcal{O}(m/E)$. For a massless fermion, the spin four-vector does not exist (as there is no rest frame). Nevertheless, one can obtain consistent results by working with massive helicity states and taking the $m \to 0$ limit at the end of the computation. In this case, one can simply use $S^\mu = p^\mu/m + \mathcal{O}(m/E)$; in practical computations the final result will be well defined in the zero mass limit. In contrast, for massive fermions at rest, the helicity state does not exist without reference to some particular boost direction as noted in footnote 23.

Using Eqs. (2.118) and (2.119) with $S^\mu_R = (0;\hat{\mathbf{s}})$, two important formulae are obtained:

$$\sqrt{p\cdot\sigma}\, S\cdot\overline{\sigma}\,\sqrt{p\cdot\sigma} = m\,\vec{\boldsymbol{\sigma}}\cdot\hat{\mathbf{s}}, \tag{3.1.17}$$

$$\sqrt{p\cdot\overline{\sigma}}\, S\cdot\sigma\,\sqrt{p\cdot\overline{\sigma}} = -m\,\vec{\boldsymbol{\sigma}}\cdot\hat{\mathbf{s}}. \tag{3.1.18}$$

These results can also be derived directly by employing the explicit form for the spin vector S^μ [Eq. (3.1.15)] and the results of Eqs. (2.107) and (2.108).

The two-component spinor wave functions x and y can now be given explicitly in terms of the χ_s defined in Eq. (C.1.11). First, we note that Eq. (3.1.9) when evaluated in the rest frame yields $x_1 = y^{\dagger 1}$ and $x_2 = y^{\dagger 2}$. That is, as column vectors, $x_\alpha(\vec{\mathbf{p}}=0) = y^{\dagger\dot{\alpha}}(\vec{\mathbf{p}}=0)$ can be expressed in general as some linear combination of the χ_s ($s = \pm\frac{1}{2}$). Hence, we may choose $x_\alpha(\vec{\mathbf{p}}=0,s) = y^{\dagger\dot{\alpha}}(\vec{\mathbf{p}}=0,s) = \sqrt{m}\chi_s$, where the factor of $\sqrt{m}$ reflects the standard relativistic normalization of the rest frame spin states. These wave functions can be boosted to an arbitrary frame using Eq. (2.106). The resulting undotted spinor wave functions are given by:

$$x_\alpha(\vec{\mathbf{p}},s) = \sqrt{p\cdot\sigma}\,\chi_s, \qquad x^\alpha(\vec{\mathbf{p}},s) = -2s\chi_{-s}^\dagger\sqrt{p\cdot\overline{\sigma}}, \tag{3.1.19}$$

$$y_\alpha(\vec{\mathbf{p}},s) = 2s\sqrt{p\cdot\sigma}\,\chi_{-s}, \qquad y^\alpha(\vec{\mathbf{p}},s) = \chi_s^\dagger\sqrt{p\cdot\overline{\sigma}}, \tag{3.1.20}$$

and the dotted spinor wave functions are given by

$$x^{\dagger\dot{\alpha}}(\vec{\mathbf{p}},s) = -2s\sqrt{p\cdot\overline{\sigma}}\,\chi_{-s}, \qquad x^\dagger_{\dot{\alpha}}(\vec{\mathbf{p}},s) = \chi_s^\dagger\sqrt{p\cdot\sigma}, \tag{3.1.21}$$

$$y^{\dagger\dot{\alpha}}(\vec{\mathbf{p}},s) = \sqrt{p\cdot\overline{\sigma}}\,\chi_s, \qquad y^\dagger_{\dot{\alpha}}(\vec{\mathbf{p}},s) = 2s\chi_{-s}^\dagger\sqrt{p\cdot\sigma}, \tag{3.1.22}$$

[22] In the literature, it is a common practice to choose $\hat{\mathbf{s}} = \hat{\mathbf{z}}$. However in order to be somewhat more general, we shall not assume this convention here.

[23] Strictly speaking, $\hat{\mathbf{p}}$ is not defined in the rest frame. In practice, helicity states are defined in some moving frame with momentum $\vec{\mathbf{p}}$. The rest frame is achieved by boosting in the direction of $-\vec{\mathbf{p}}$.

where $\sqrt{p\cdot\sigma}$ and $\sqrt{p\cdot\overline{\sigma}}$ are defined either by Eqs. (2.109) and (2.110) or by Eqs. (2.113) and (2.114), respectively (as mandated by the spinor index structure).[24] Note that Eqs. (3.1.19)–(3.1.22) imply that the x and y spinors are related:

$$y(\vec{\boldsymbol{p}},s)=2sx(\vec{\boldsymbol{p}},-s),\qquad y^\dagger(\vec{\boldsymbol{p}},s)=2sx^\dagger(\vec{\boldsymbol{p}},-s). \tag{3.1.23}$$

The phase choices in Eqs. (3.1.19)–(3.1.22) are consistent with those employed for four-component spinor wave functions [see Appendix G]. We again emphasize that in Eqs. (3.1.19)–(3.1.22), one may either choose χ_s to be an eigenstate of $\vec{\boldsymbol{\sigma}}\cdot\hat{\boldsymbol{s}}$, where the spin is measured in the rest frame along the quantization axis $\hat{\boldsymbol{s}}$, or choose χ_s to be an eigenstate of $\vec{\boldsymbol{\sigma}}\cdot\hat{\boldsymbol{p}}$ (in this case we shall write $s=\lambda$), which yields the helicity spinor wave functions.

The following equations can now be derived:

$$(S\cdot\overline{\sigma})^{\dot\alpha\beta}x_\beta(\vec{\boldsymbol{p}},s)=2sy^{\dagger\dot\alpha}(\vec{\boldsymbol{p}},s),\qquad (S\cdot\sigma)_{\alpha\dot\beta}y^{\dagger\dot\beta}(\vec{\boldsymbol{p}},s)=-2sx_\alpha(\vec{\boldsymbol{p}},s), \tag{3.1.24}$$

$$(S\cdot\sigma)_{\alpha\dot\beta}x^{\dagger\dot\beta}(\vec{\boldsymbol{p}},s)=-2sy_\alpha(\vec{\boldsymbol{p}},s),\qquad (S\cdot\overline{\sigma})^{\dot\alpha\beta}y_\beta(\vec{\boldsymbol{p}},s)=2sx^{\dagger\dot\alpha}(\vec{\boldsymbol{p}},s), \tag{3.1.25}$$

$$x^\alpha(\vec{\boldsymbol{p}},s)(S\cdot\sigma)_{\alpha\dot\beta}=-2sy^\dagger_{\dot\beta}(\vec{\boldsymbol{p}},s),\qquad y^\dagger_{\dot\alpha}(\vec{\boldsymbol{p}},s)(S\cdot\overline{\sigma})^{\dot\alpha\beta}=2sx^\beta(\vec{\boldsymbol{p}},s), \tag{3.1.26}$$

$$x^\dagger_{\dot\alpha}(\vec{\boldsymbol{p}},s)(S\cdot\overline{\sigma})^{\dot\alpha\beta}=2sy^\beta(\vec{\boldsymbol{p}},s),\qquad y^\alpha(\vec{\boldsymbol{p}},s)(S\cdot\sigma)_{\alpha\dot\beta}=-2sx^\dagger_{\dot\beta}(\vec{\boldsymbol{p}},s). \tag{3.1.27}$$

For example, using Eqs. (3.1.17) and (3.1.18) and the definitions above for $x_\alpha(\vec{\boldsymbol{p}},s)$ and $y^{\dagger\dot\alpha}(\vec{\boldsymbol{p}},s)$, we find (suppressing spinor indices),

$$\sqrt{p\cdot\sigma}\,S\cdot\overline{\sigma}\,x(\vec{\boldsymbol{p}},s)=\sqrt{p\cdot\sigma}\,S\cdot\overline{\sigma}\,\sqrt{p\cdot\sigma}\,\chi_s=m\vec{\boldsymbol{\sigma}}\cdot\hat{\boldsymbol{s}}\,\chi_s=2sm\,\chi_s. \tag{3.1.28}$$

Multiplying both sides of Eq. (3.1.28) by $\sqrt{p\cdot\overline{\sigma}}$ and noting that $\sqrt{p\cdot\overline{\sigma}}\sqrt{p\cdot\sigma}=m$, we end up with

$$S\cdot\overline{\sigma}\,x(\vec{\boldsymbol{p}},s)=2s\sqrt{p\cdot\overline{\sigma}}\,\chi_s=2sy^\dagger(\vec{\boldsymbol{p}},s). \tag{3.1.29}$$

All the results of Eqs. (3.1.24)–(3.1.27) can be derived in this manner.

The consistency of Eqs. (3.1.24)–(3.1.27) can also be checked as follows. First, each of these equations yields

$$(S\cdot\sigma)_{\alpha\dot\alpha}(S\cdot\overline{\sigma})^{\dot\alpha\beta}=-\delta^\beta_\alpha,\qquad (S\cdot\overline{\sigma})^{\dot\alpha\alpha}(S\cdot\sigma)_{\alpha\dot\beta}=-\delta^{\dot\alpha}_{\dot\beta}, \tag{3.1.30}$$

after noting that $4s^2=1$ (for $s=\pm\frac{1}{2}$). From Eqs. (2.51) and (2.52) it follows that $S\cdot S=-1$, as required. Second, if one applies

$$(p\cdot\sigma\,S\cdot\overline{\sigma}+S\cdot\sigma\,p\cdot\overline{\sigma})_\alpha{}^\beta=2p\cdot S\,\delta_\alpha{}^\beta, \tag{3.1.31}$$

$$(p\cdot\overline{\sigma}\,S\cdot\sigma+S\cdot\overline{\sigma}\,p\cdot\sigma)^{\dot\alpha}{}_{\dot\beta}=2p\cdot S\,\delta^{\dot\alpha}{}_{\dot\beta}, \tag{3.1.32}$$

to Eqs. (3.1.9)–(3.1.12) and Eqs. (3.1.24)–(3.1.27), it follows that $p\cdot S=0$.

It is useful to combine the results of Eqs. (3.1.9)–(3.1.12) and Eqs. (3.1.24)–(3.1.27) as follows:

$$(p^\mu-2smS^\mu)\overline{\sigma}^{\dot\alpha\beta}_\mu x_\beta(\vec{\boldsymbol{p}},s)=0,\qquad (p_\mu-2smS_\mu)\sigma^\mu_{\alpha\dot\beta}x^{\dagger\dot\beta}(\vec{\boldsymbol{p}},s)=0, \tag{3.1.33}$$

$$(p^\mu+2smS^\mu)\overline{\sigma}^{\dot\alpha\beta}_\mu y_\beta(\vec{\boldsymbol{p}},s)=0,\qquad (p_\mu+2smS_\mu)\sigma^\mu_{\alpha\dot\beta}y^{\dagger\dot\beta}(\vec{\boldsymbol{p}},s)=0, \tag{3.1.34}$$

$$x^\alpha(\vec{\boldsymbol{p}},s)\sigma^\mu_{\alpha\dot\beta}(p_\mu-2smS_\mu)=0,\qquad x^\dagger_{\dot\alpha}(\vec{\boldsymbol{p}},s)\overline{\sigma}^{\dot\alpha\beta}_\mu(p^\mu-2smS^\mu)=0, \tag{3.1.35}$$

$$y^\alpha(\vec{\boldsymbol{p}},s)\sigma^\mu_{\alpha\dot\beta}(p_\mu+2smS_\mu)=0,\qquad y^\dagger_{\dot\alpha}(\vec{\boldsymbol{p}},s)\overline{\sigma}^{\dot\alpha\beta}_\mu(p^\mu+2smS^\mu)=0. \tag{3.1.36}$$

Eqs. (3.1.19)–(3.1.36) also apply to the helicity wave functions $x(\vec{\boldsymbol{p}},\lambda)$ and $y(\vec{\boldsymbol{p}},\lambda)$ simply by replacing s with λ and $S^\mu(\hat{\boldsymbol{s}})$ [Eq. (3.1.15)] with $S^\mu(\hat{\boldsymbol{p}})$ [Eq. (3.1.16)].

The above results are applicable only for massive fermions (where the spin four-vector S^μ exists). We may treat the case of massless fermions directly by employing helicity spinors in Eqs. (3.1.19)–(3.1.22). Putting $E=|\vec{\boldsymbol{p}}|$ and $m=0$, we easily obtain:

$$x_\alpha(\vec{\boldsymbol{p}},\lambda)=\sqrt{2E}\,\left(\tfrac{1}{2}-\lambda\right)\,\chi_\lambda,\qquad x^\alpha(\vec{\boldsymbol{p}},\lambda)=\sqrt{2E}\,\left(\tfrac{1}{2}-\lambda\right)\,\chi^\dagger_{-\lambda}, \tag{3.1.37}$$

$$y_\alpha(\vec{\boldsymbol{p}},\lambda)=\sqrt{2E}\,\left(\tfrac{1}{2}+\lambda\right)\,\chi_{-\lambda},\qquad y^\alpha(\vec{\boldsymbol{p}},\lambda)=\sqrt{2E}\,\left(\tfrac{1}{2}+\lambda\right)\,\chi^\dagger_\lambda, \tag{3.1.38}$$

[24] Explicit forms for two-component spinor wave functions have been exhibited a number of times in the literature. For example, see Refs. [104,105] and Appendix I.1.

or equivalently,

$$x^{\dagger\dot\alpha}(\vec{\boldsymbol{p}},\lambda)=\sqrt{2E}\,\left(\tfrac{1}{2}-\lambda\right)\,\chi_{-\lambda},\qquad x^{\dagger}_{\dot\alpha}(\vec{\boldsymbol{p}},\lambda)=\sqrt{2E}\,\left(\tfrac{1}{2}-\lambda\right)\,\chi^{\dagger}_{\lambda},\tag{3.1.39}$$

$$y^{\dagger\dot\alpha}(\vec{\boldsymbol{p}},\lambda)=\sqrt{2E}\,\left(\tfrac{1}{2}+\lambda\right)\,\chi_{\lambda},\qquad y^{\dagger}_{\dot\alpha}(\vec{\boldsymbol{p}},\lambda)=\sqrt{2E}\,\left(\tfrac{1}{2}+\lambda\right)\,\chi^{\dagger}_{-\lambda}.\tag{3.1.40}$$

It follows that:

$$\left(\tfrac{1}{2}+\lambda\right)x(\vec{\boldsymbol{p}},\lambda)=0,\qquad \left(\tfrac{1}{2}+\lambda\right)x^{\dagger}(\vec{\boldsymbol{p}},\lambda)=0,\tag{3.1.41}$$

$$\left(\tfrac{1}{2}-\lambda\right)y(\vec{\boldsymbol{p}},\lambda)=0,\qquad \left(\tfrac{1}{2}-\lambda\right)y^{\dagger}(\vec{\boldsymbol{p}},\lambda)=0.\tag{3.1.42}$$

The significance of Eqs. (3.1.41) and (3.1.42) is clear; for massless fermions, only one helicity component of x and y is non-zero. Applying this result to neutrinos, we find that massless neutrinos are left-handed ($\lambda=-1/2$), while antineutrinos are right-handed ($\lambda=+1/2$).

Eqs. (3.1.41) and (3.1.42) can also be derived by carefully taking the $m\to 0$ limit of Eqs. (3.1.33) and (3.1.34) applied to the helicity wave functions $x(\vec{\boldsymbol{p}},\lambda)$ and $y(\vec{\boldsymbol{p}},\lambda)$ [i.e., replacing s with λ]. We then replace mS^{μ} with p^{μ}, which is the leading term in the limit of $E\gg m$. Using the results of Eqs. (3.1.9) and (3.1.10) and dividing out by an overall factor of m (before finally taking the $m\to 0$ limit) reproduces Eqs. (3.1.41) and (3.1.42).

Having defined explicit forms for the two-component spinor wave functions, we can now write down the spin projection matrices. Noting that $\frac{1}{2}(1+2s\,\vec{\boldsymbol{\sigma}}\cdot\hat{\mathbf{s}})\chi_{s'}=\frac{1}{2}(1+4ss')\chi_{s'}=\delta_{ss'}\chi_{s'}$ (since $s,s'=\pm\frac{1}{2}$), one can write:

$$\chi_s\chi_s^{\dagger}=\tfrac{1}{2}\left(1+2s\,\vec{\boldsymbol{\sigma}}\cdot\hat{\mathbf{s}}\right)\sum_{s'}\chi_{s'}\chi_{s'}^{\dagger}=\tfrac{1}{2}\left(1+2s\,\vec{\boldsymbol{\sigma}}\cdot\hat{\mathbf{s}}\right),\tag{3.1.43}$$

where at the second step, we have employed the completeness relation given in Eq. (C.1.21). Making use of Eq. (3.1.17) for $\vec{\boldsymbol{\sigma}}\cdot\hat{\mathbf{s}}$, it follows that

$$\chi_s\chi_s^{\dagger}=\tfrac{1}{2}\left(1+\frac{2s}{m}\sqrt{p\cdot\sigma}\,S\cdot\overline{\sigma}\,\sqrt{p\cdot\sigma}\right).\tag{3.1.44}$$

Hence, with both spinor indices in the lowered position,

$$\begin{aligned}x(\vec{\boldsymbol{p}},s)x^{\dagger}(\vec{\boldsymbol{p}},s)&=\sqrt{p\cdot\sigma}\,\chi_s\chi_s^{\dagger}\,\sqrt{p\cdot\sigma}\\&=\tfrac{1}{2}\sqrt{p\cdot\sigma}\left[1+\frac{2s}{m}\sqrt{p\cdot\sigma}S\cdot\overline{\sigma}\sqrt{p\cdot\sigma}\right]\sqrt{p\cdot\sigma}\\&=\tfrac{1}{2}\left[p\cdot\sigma+\frac{2s}{m}p\cdot\sigma S\cdot\overline{\sigma}p\cdot\sigma\right]\\&=\tfrac{1}{2}\left[p\cdot\sigma-2smS\cdot\sigma\right].\end{aligned}\tag{3.1.45}$$

In the final step above, we simplified the product of three dot products by noting that $p\cdot S=0$ implies that $S\cdot\overline{\sigma}\;p\cdot\sigma=-p\cdot\overline{\sigma}\;S\cdot\sigma$. The other spin projection formulae for massive fermions can be similarly derived. The complete set of such formulae is given below[25]:

$$x_{\alpha}(\vec{\boldsymbol{p}},s)x^{\dagger}_{\dot\beta}(\vec{\boldsymbol{p}},s)=\tfrac{1}{2}(p_{\mu}-2smS_{\mu})\sigma^{\mu}_{\alpha\dot\beta},\tag{3.1.46}$$

$$y^{\dagger\dot\alpha}(\vec{\boldsymbol{p}},s)y^{\beta}(\vec{\boldsymbol{p}},s)=\tfrac{1}{2}(p^{\mu}+2smS^{\mu})\overline{\sigma}^{\dot\alpha\beta}_{\mu},\tag{3.1.47}$$

$$x_{\alpha}(\vec{\boldsymbol{p}},s)y^{\beta}(\vec{\boldsymbol{p}},s)=\tfrac{1}{2}\left(m\delta_{\alpha}{}^{\beta}-2s[S\cdot\sigma\,p\cdot\overline{\sigma}]_{\alpha}{}^{\beta}\right),\tag{3.1.48}$$

$$y^{\dagger\dot\alpha}(\vec{\boldsymbol{p}},s)x^{\dagger}_{\dot\beta}(\vec{\boldsymbol{p}},s)=\tfrac{1}{2}\left(m\delta^{\dot\alpha}{}_{\dot\beta}+2s[S\cdot\overline{\sigma}\,p\cdot\sigma]^{\dot\alpha}{}_{\dot\beta}\right).\tag{3.1.49}$$

By taking the hermitian conjugate of the above results, one obtains an equivalent set of formulae,

$$x^{\dagger\dot\alpha}(\vec{\boldsymbol{p}},s)x^{\beta}(\vec{\boldsymbol{p}},s)=\tfrac{1}{2}(p^{\mu}-2smS^{\mu})\overline{\sigma}^{\dot\alpha\beta}_{\mu},\tag{3.1.50}$$

$$y_{\alpha}(\vec{\boldsymbol{p}},s)y^{\dagger}_{\dot\beta}(\vec{\boldsymbol{p}},s)=\tfrac{1}{2}(p_{\mu}+2smS_{\mu})\sigma^{\mu}_{\alpha\dot\beta},\tag{3.1.51}$$

$$y_{\alpha}(\vec{\boldsymbol{p}},s)x^{\beta}(\vec{\boldsymbol{p}},s)=-\tfrac{1}{2}\left(m\delta_{\alpha}{}^{\beta}+2s[S\cdot\sigma\,p\cdot\overline{\sigma}]_{\alpha}{}^{\beta}\right),\tag{3.1.52}$$

$$x^{\dagger\dot\alpha}(\vec{\boldsymbol{p}},s)y^{\dagger}_{\dot\beta}(\vec{\boldsymbol{p}},s)=-\tfrac{1}{2}\left(m\delta^{\dot\alpha}{}_{\dot\beta}-2s[S\cdot\overline{\sigma}\,p\cdot\sigma]^{\dot\alpha}{}_{\dot\beta}\right).\tag{3.1.53}$$

25 Similar formulae for the products of two-component spinor wave functions are given in Ref. [104].

For the case of massless spin-1/2 fermions, we must use helicity spinor wave functions. The corresponding massless projection operators can be obtained directly from the explicit forms for the two-component spinor wave functions given in Eqs. (3.1.37)–(3.1.40):

$$x_\alpha(\vec{\boldsymbol{p}},\lambda)x^\dagger_{\dot\beta}(\vec{\boldsymbol{p}},\lambda) = \left(\tfrac{1}{2}-\lambda\right)p\cdot\sigma_{\alpha\dot\beta}, \qquad x^{\dagger\dot\alpha}(\vec{\boldsymbol{p}},\lambda)x^\beta(\vec{\boldsymbol{p}},\lambda) = \left(\tfrac{1}{2}-\lambda\right)p\cdot\overline{\sigma}^{\dot\alpha\beta}, \tag{3.1.54}$$

$$y^{\dagger\dot\alpha}(\vec{\boldsymbol{p}},\lambda)y^\beta(\vec{\boldsymbol{p}},\lambda) = \left(\tfrac{1}{2}+\lambda\right)p\cdot\overline{\sigma}^{\dot\alpha\beta}, \qquad y_\alpha(\vec{\boldsymbol{p}},\lambda)y^\dagger_{\dot\beta}(\vec{\boldsymbol{p}},\lambda) = \left(\tfrac{1}{2}+\lambda\right)p\cdot\sigma_{\alpha\dot\beta}, \tag{3.1.55}$$

$$x_\alpha(\vec{\boldsymbol{p}},\lambda)y^\beta(\vec{\boldsymbol{p}},\lambda) = 0, \qquad y_\alpha(\vec{\boldsymbol{p}},\lambda)x^\beta(\vec{\boldsymbol{p}},\lambda) = 0, \tag{3.1.56}$$

$$y^{\dagger\dot\alpha}(\vec{\boldsymbol{p}},\lambda)x^\dagger_{\dot\beta}(\vec{\boldsymbol{p}},\lambda) = 0, \qquad x^{\dagger\dot\alpha}(\vec{\boldsymbol{p}},\lambda)y^\dagger_{\dot\beta}(\vec{\boldsymbol{p}},\lambda) = 0. \tag{3.1.57}$$

As a check, one can verify that the above results follow from Eqs. (3.1.46)–(3.1.53), by replacing s with λ, setting $mS^\mu = p^\mu$, and taking the $m \to 0$ limit at the end of the computation.

Having listed the projection operators for definite spin projection or helicity, we may now sum over spins to derive the spin-sum identities. These arise when computing squared matrix elements for unpolarized scattering and decay. There are only four basic identities, but for convenience we list each of them with the two-index height permutations that can occur in squared amplitudes by following the rules given in this paper. The results can be derived by inspection of the spin projection operators, since summing over $s = \pm\frac{1}{2}$ simply removes all terms linear in the spin four-vector S^μ.

$$\sum_s x_\alpha(\vec{\boldsymbol{p}},s)x^\dagger_{\dot\beta}(\vec{\boldsymbol{p}},s) = p\cdot\sigma_{\alpha\dot\beta}, \qquad \sum_s x^{\dagger\dot\alpha}(\vec{\boldsymbol{p}},s)x^\beta(\vec{\boldsymbol{p}},s) = p\cdot\overline{\sigma}^{\dot\alpha\beta}, \tag{3.1.58}$$

$$\sum_s y^{\dagger\dot\alpha}(\vec{\boldsymbol{p}},s)y^\beta(\vec{\boldsymbol{p}},s) = p\cdot\overline{\sigma}^{\dot\alpha\beta}, \qquad \sum_s y_\alpha(\vec{\boldsymbol{p}},s)y^\dagger_{\dot\beta}(\vec{\boldsymbol{p}},s) = p\cdot\sigma_{\alpha\dot\beta}, \tag{3.1.59}$$

$$\sum_s x_\alpha(\vec{\boldsymbol{p}},s)y^\beta(\vec{\boldsymbol{p}},s) = m\delta_\alpha{}^\beta, \qquad \sum_s y_\alpha(\vec{\boldsymbol{p}},s)x^\beta(\vec{\boldsymbol{p}},s) = -m\delta_\alpha{}^\beta, \tag{3.1.60}$$

$$\sum_s y^{\dagger\dot\alpha}(\vec{\boldsymbol{p}},s)x^\dagger_{\dot\beta}(\vec{\boldsymbol{p}},s) = m\delta^{\dot\alpha}{}_{\dot\beta}, \qquad \sum_s x^{\dagger\dot\alpha}(\vec{\boldsymbol{p}},s)y^\dagger_{\dot\beta}(\vec{\boldsymbol{p}},s) = -m\delta^{\dot\alpha}{}_{\dot\beta}. \tag{3.1.61}$$

These results are applicable both to spin sums and helicity sums, and hold for both massive and massless spin-1/2 fermions.

One can generalize the above massive and massless projection operators by considering products of two-component spinor wave functions, where the spin or helicity of each spinor can be different. These are the Bouchiat–Michel formulae [112], which are derived in Appendix H.3.

3.2. Fermion mass diagonalization in a general theory

Consider a collection of free anticommuting two-component spin-1/2 fields, $\hat\xi_{\alpha i}(x)$, which transform as $(\frac{1}{2},0)$ fields under the Lorentz group. Here, α is the spinor index, and i labels the distinct fields of the collection. The free-field Lagrangian is given by (e.g., see Ref. [5]):

$$\mathscr{L} = i\hat\xi^{\dagger i}\overline{\sigma}^\mu\partial_\mu\hat\xi_i - \tfrac{1}{2}M^{ij}\hat\xi_i\hat\xi_j - \tfrac{1}{2}M_{ij}\hat\xi^{\dagger i}\hat\xi^{\dagger j}, \tag{3.2.1}$$

where

$$M_{ij} \equiv (M^{ij})^*. \tag{3.2.2}$$

Note that M is a complex symmetric matrix, since the product of anticommuting two-component fields satisfies $\hat\xi_i\hat\xi_j = \hat\xi_j\hat\xi_i$ [with the spinor contraction rule according to Eq. (2.36)].

In Eq. (3.2.1), we have employed the U(N)-covariant tensor calculus [44,145] for "flavor-tensors" labeled by the flavor indices i and j. Each left-handed $(\frac{1}{2},0)$ fermion always has an index with the opposite height of the corresponding right-handed $(0,\frac{1}{2})$ fermion. Raised indices can only be contracted with lowered indices and vice versa. Flipping the heights of all flavor indices of an object corresponds to complex conjugation, as in Eq. (3.2.2). In particular, we generalize Eq. (2.17) as follows[26]:

$$\psi^{\dagger i}_{\dot\alpha} \equiv (\psi_{\alpha i})^\dagger. \tag{3.2.3}$$

[26] In the case at hand, we have more specifically chosen all of the left-handed fermions to have lowered flavor indices, which implies that all of the right-handed fermions have raised flavor indices. However, in cases where a subset of left-handed fermions transform according to some representation R of a (global) symmetry and a different subset of left-handed fermions transform according to the conjugate representation R^*, it is often more convenient to employ a raised flavor index for the latter subset of left-handed fields.

If $M = 0$, then the free-field Lagrangian is invariant under a global U(N) symmetry. That is, for a unitary matrix U, with matrix elements $U_i{}^j$, and its hermitian conjugate defined by:

$$(U^\dagger)_i{}^j = (U_j{}^i)^* \equiv U^j{}_i, \tag{3.2.4}$$

with $U_i{}^k(U^\dagger)_k{}^j = \delta_i^j$, the massless free-field Lagrangian is invariant under the transformations:

$$\hat{\xi}_i \longrightarrow U_i{}^j\hat{\xi}_j, \qquad \hat{\xi}^{\dagger i} \longrightarrow U^i{}_j\hat{\xi}^{\dagger j}. \tag{3.2.5}$$

For $M \neq 0$, Eq. (3.2.1) remains formally invariant under the global U(N)-symmetry if M acts as a spurion field [146] with the appropriate tensorial transformation law, $M^{ij} \longrightarrow U^i{}_k U^j{}_\ell M^{k\ell}$.

Expressions consisting of flavor-vectors and second-rank flavor-tensors have natural interpretations as products of vectors and matrices. As a result, the flavor indices can be suppressed, and the resulting expressions can be written in an index-free matrix notation. To accomplish this, one must first assign a particular flavor index structure to the matrices that will appear in the index-free expression. For example, given the second-rank flavor-tensors introduced above, we define the matrix elements of M to be M^{ij} and the matrix elements of U to be $U_i{}^j$. Note that $(U^\dagger)_i{}^j$ has the same flavor index structure as U.[27]

As a simple example, in an index-free notation Eq. (3.2.5) reads: $\hat{\xi} \longrightarrow U\hat{\xi}$ and $\hat{\xi}^\dagger \longrightarrow \hat{\xi}^\dagger U^\dagger$. A slightly more complicated example is exhibited below:

$$U^i{}_k M^{k\ell} = (U^\dagger)_k{}^i M^{k\ell} = (U^* M)^{i\ell}, \tag{3.2.6}$$

where we have used $(U^\dagger)^{\mathsf{T}} = U^*$ in obtaining the final result. That is, in matrix notation with suppressed indices, $U^i{}_k M^{k\ell}$ corresponds to the matrix U^*M. Thus, in an index-free notation, the tensorial transformation law for the spurion field M is given by $M \longrightarrow U^* M U^\dagger$.

We can diagonalize the mass matrix M and rewrite the Lagrangian in terms of mass eigenstates $\xi_{\alpha i}$ and (real non-negative) masses m_i. To do this, we introduce a unitary matrix Ω,

$$\hat{\xi}_i = \Omega_i{}^k \xi_k, \tag{3.2.7}$$

and demand that $M^{ij}\Omega_i{}^k\Omega_j{}^\ell = m_k\delta^{k\ell}$ (no sum over k), where the m_k are real and non-negative. Equivalently, in matrix notation with suppressed indices, $\hat{\xi} = \Omega\xi$ and[28]

$$\Omega^{\mathsf{T}} M\, \Omega = \boldsymbol{m} = \mathrm{diag}(m_1, m_2, \ldots). \tag{3.2.8}$$

This is the Takagi diagonalization [111,147] of an arbitrary complex symmetric matrix, which is discussed in more detail in Appendix D.2. To compute the values of the diagonal elements of $\boldsymbol{m}$, note that

$$\Omega^\dagger M^\dagger M \Omega = \boldsymbol{m}^2. \tag{3.2.9}$$

Indeed $M^\dagger M$ is hermitian and thus it can be diagonalized by a unitary matrix. Hence, the elements of the diagonal matrix $\boldsymbol{m}$ are the non-negative square roots of the corresponding eigenvalues of $M^\dagger M$. However, in cases where $M^\dagger M$ has degenerate eigenvalues, Eq. (3.2.9) *cannot* be employed to determine the unitary matrix Ω that satisfies Eq. (3.2.8). A more general technique for determining Ω that works in all cases is given in Appendix D.2.

In terms of the mass eigenstates,

$$\mathscr{L} = i\xi^{\dagger i}\overline{\sigma}^\mu\partial_\mu\xi_i - \tfrac{1}{2}m_i(\xi_i\xi_i + \xi^{\dagger i}\xi^{\dagger i}), \tag{3.2.10}$$

where the sum over i is implicit. If the $m_i \neq 0$ are non-degenerate, then the corresponding field ξ_i describes a neutral Majorana fermion consisting of two on-shell real degrees of freedom. The case of mass degeneracies will be treated explicitly below. If $m_i = 0$, then we shall denote the corresponding field ξ_i as a massless Weyl fermion [15].

Each $\xi_{\alpha i}$ can now be expanded in a Fourier series, exactly as in Eq. (3.1.3):

$$\xi_{\alpha i}(x) = \sum_s \int \frac{\mathrm{d}^3\vec{\boldsymbol{p}}}{(2\pi)^{3/2}(2E_{i\boldsymbol{p}})^{1/2}}\left[x_\alpha(\vec{\boldsymbol{p}},s)a_i(\vec{\boldsymbol{p}},s)e^{-ip\cdot x} + y_\alpha(\vec{\boldsymbol{p}},s)a_i^\dagger(\vec{\boldsymbol{p}},s)e^{ip\cdot x}\right], \tag{3.2.11}$$

where $E_{i\boldsymbol{p}} \equiv (|\vec{\boldsymbol{p}}|^2 + m_i^2)^{1/2}$, and the creation and annihilation operators, $a_i^\dagger$ and a_i satisfy anticommutation relations:

$$\{a_i(\vec{\boldsymbol{p}},s),\, a_j^\dagger(\vec{\boldsymbol{p}}',s')\} = \delta^3(\vec{\boldsymbol{p}} - \vec{\boldsymbol{p}}')\delta_{ss'}\delta_{ij}. \tag{3.2.12}$$

---

27 The reader should not be tempted to substitute $U^\dagger$ for U in Eq. (3.2.4), as the resulting flavor index structure for U and $U^\dagger$ would then disagree with the original flavor index assignments.

28 In general, the m_i are *not* the eigenvalues of M. Rather, they are the *singular values* of the matrix M, which are defined to be the non-negative square roots of the eigenvalues of $M^\dagger M$. See Appendix D for further details.

We employ covariant normalization of the one-particle states, i.e., we act with one creation operator on the vacuum with the following convention

$$\left|\vec{\boldsymbol{p}}, i, s\right\rangle \equiv (2\pi)^{3/2}(2E_{i\boldsymbol{p}})^{1/2} a_i^\dagger(\vec{\boldsymbol{p}}, s)\,|0\rangle\,, \tag{3.2.13}$$

so that $\left\langle \vec{\boldsymbol{p}}, i, s \mid \vec{\boldsymbol{p}}', j, s'\right\rangle = (2\pi)^3(2E_{i\boldsymbol{p}})\delta^3(\vec{\boldsymbol{p}} - \vec{\boldsymbol{p}}')\delta_{ij}\delta_{ss'}$.

In the case of two mass-degenerate massive fermion fields, $m_1 = m_2 \neq 0$, Eq. (3.2.10) possesses a global internal O(2) flavor symmetry, $\xi_i \to \mathcal{O}_i^j \xi_j$ $(i = 1, 2)$, where $\mathcal{O}^{\mathsf{T}}\mathcal{O} = \mathbb{1}_{2\times 2}$. Corresponding to this symmetry is a conserved hermitian Noether current:

$$J^\mu = i(\xi^{\dagger 1}\overline{\sigma}^\mu \xi_2 - \xi^{\dagger 2}\overline{\sigma}^\mu \xi_1), \tag{3.2.14}$$

with a corresponding conserved charge, $Q = \int J^0 \mathrm{d}^3x$. In the ξ_1–ξ_2 basis, the Noether current is off-diagonal. However, it is convenient to define a new basis of fields:

$$\chi \equiv \frac{1}{\sqrt{2}}(\xi_1 + i\xi_2), \qquad \eta \equiv \frac{1}{\sqrt{2}}(\xi_1 - i\xi_2). \tag{3.2.15}$$

With respect to the χ–η basis, the Noether current is diagonal:

$$J^\mu = \chi^\dagger \overline{\sigma}^\mu \chi - \eta^\dagger \overline{\sigma}^\mu \eta. \tag{3.2.16}$$

That is, the fermions χ and η are eigenstates of the charge operator Q with corresponding eigenvalues ± 1. In terms of the fermion fields of definite charge, the free-field fermion Lagrangian [Eq. (3.2.10) with $i = 1, 2$ and $m_1 = m_2 \equiv m$] is given by [16][29]:

$$\mathscr{L} = i\chi^\dagger \overline{\sigma}^\mu \partial_\mu \chi + i\eta^\dagger \overline{\sigma}^\mu \partial_\mu \eta - m(\chi\eta + \chi^\dagger \eta^\dagger). \tag{3.2.17}$$

On-shell, χ and η satisfy the free-field Dirac equations:

$$i\,\overline{\sigma}^\mu \partial_\mu \chi - m\eta^\dagger = 0, \qquad i\,\overline{\sigma}^\mu \partial_\mu \eta - m\chi^\dagger = 0. \tag{3.2.18}$$

In the χ–η basis, the global internal SO(2) symmetry (which is continuously connected to the identity) is realized as the U(1) symmetry $\chi \to e^{i\theta}\chi$ and $\eta \to e^{-i\theta}\eta$, where θ is the rotation angle that defines the SO(2) rotation matrix.

Together, χ and $\eta^\dagger$ constitute a single Dirac fermion. We can then write:

$$\chi_\alpha(x) = \sum_s \int \frac{\mathrm{d}^3\vec{\boldsymbol{p}}}{(2\pi)^{3/2}(2E_{\boldsymbol{p}})^{1/2}} \left[x_\alpha(\vec{\boldsymbol{p}}, s) a(\vec{\boldsymbol{p}}, s) e^{-ip\cdot x} + y_\alpha(\vec{\boldsymbol{p}}, s) b^\dagger(\vec{\boldsymbol{p}}, s) e^{ip\cdot x}\right], \tag{3.2.19}$$

$$\eta_\alpha(x) = \sum_s \int \frac{\mathrm{d}^3\vec{\boldsymbol{p}}}{(2\pi)^{3/2}(2E_{\boldsymbol{p}})^{1/2}} \left[x_\alpha(\vec{\boldsymbol{p}}, s) b(\vec{\boldsymbol{p}}, s) e^{-ip\cdot x} + y_\alpha(\vec{\boldsymbol{p}}, s) a^\dagger(\vec{\boldsymbol{p}}, s) e^{ip\cdot x}\right], \tag{3.2.20}$$

where $E_{\boldsymbol{p}} \equiv (|\vec{\boldsymbol{p}}|^2 + m^2)^{1/2}$, the creation and annihilation operators, $a^\dagger$, $b^\dagger$, a and b satisfy anticommutation relations:

$$\{a(\vec{\boldsymbol{p}}, s), a^\dagger(\vec{\boldsymbol{p}}', s')\} = \{b(\vec{\boldsymbol{p}}, s), b^\dagger(\vec{\boldsymbol{p}}', s')\} = \delta^3(\vec{\boldsymbol{p}} - \vec{\boldsymbol{p}}')\delta_{s,s'}, \tag{3.2.21}$$

and all other anticommutators vanish. We now must distinguish between two types of one-particle states, which we can call fermion (F) and antifermion ($\overline{F}$):

$$\left|\vec{\boldsymbol{p}}, s; F\right\rangle \equiv (2\pi)^{3/2}(2E_{\boldsymbol{p}})^{1/2} a^\dagger(\vec{\boldsymbol{p}}, s)\,|0\rangle\,, \qquad \left|\vec{\boldsymbol{p}}, s; \overline{F}\right\rangle \equiv (2\pi)^{3/2}(2E_{\boldsymbol{p}})^{1/2} b^\dagger(\vec{\boldsymbol{p}}, s)\,|0\rangle\,. \tag{3.2.22}$$

Note that both $\eta(x)$ and $\chi^\dagger(x)$ can create $\left|\vec{\boldsymbol{p}}, s; F\right\rangle$ from the vacuum, while $\eta^\dagger(x)$ and $\chi(x)$ can create $\left|\vec{\boldsymbol{p}}, s; \overline{F}\right\rangle$. The one-particle wave functions are given by:

$$\langle 0|\,\chi_\alpha(x)\,\left|\vec{\boldsymbol{p}}, s; F\right\rangle = x_\alpha(\vec{\boldsymbol{p}}, s) e^{-ip\cdot x}, \qquad \langle 0|\,\eta^\dagger_{\dot\alpha}(x)\,\left|\vec{\boldsymbol{p}}, s; F\right\rangle = y^\dagger_{\dot\alpha}(\vec{\boldsymbol{p}}, s) e^{-ip\cdot x}, \tag{3.2.23}$$

$$\left\langle F; \vec{\boldsymbol{p}}, s\right|\,\eta_\alpha(x)\,|0\rangle = y_\alpha(\vec{\boldsymbol{p}}, s) e^{ip\cdot x}, \qquad \left\langle F; \vec{\boldsymbol{p}}, s\right|\,\chi^\dagger_{\dot\alpha}(x)\,|0\rangle = x^\dagger_{\dot\alpha}(\vec{\boldsymbol{p}}, s) e^{ip\cdot x}, \tag{3.2.24}$$

$$\langle 0|\,\eta_\alpha(x)\,\left|\vec{\boldsymbol{p}}, s; \overline{F}\right\rangle = x_\alpha(\vec{\boldsymbol{p}}, s) e^{-ip\cdot x}, \qquad \langle 0|\,\chi^\dagger_{\dot\alpha}(x)\,\left|\vec{\boldsymbol{p}}, s; \overline{F}\right\rangle = y^\dagger_{\dot\alpha}(\vec{\boldsymbol{p}}, s) e^{-ip\cdot x}, \tag{3.2.25}$$

$$\left\langle \overline{F}; \vec{\boldsymbol{p}}, s\right|\,\chi_\alpha(x)\,|0\rangle = y_\alpha(\vec{\boldsymbol{p}}, s) e^{ip\cdot x}, \qquad \left\langle \overline{F}; \vec{\boldsymbol{p}}, s\right|\,\eta^\dagger_{\dot\alpha}(x)\,|0\rangle = x^\dagger_{\dot\alpha}(\vec{\boldsymbol{p}}, s) e^{ip\cdot x}, \tag{3.2.26}$$

and the eight other single-particle matrix elements vanish.

---

[29] Although the fermion mass matrix is not diagonal in the χ–η basis, this is not an obstacle to the subsequent analysis, as one only needs a diagonal *squared*-mass matrix, $M^\dagger M$, to ensure that the denominators of propagators are diagonal. Eq. (3.2.15) provides the explicit Takagi diagonalization of the Dirac fermion matrix $\begin{pmatrix} 0 & 1 \\ 1 & 0 \end{pmatrix}$. See Appendix D.3 for the mathematical interpretation of this special case.

More generally, consider a collection of free anticommuting charged Dirac fermions, which can be represented by pairs of two-component fields $\hat{\chi}_{\alpha i}(x)$, $\hat{\eta}^i_\alpha(x)$. These fields transform in (possibly reducible) representations of the unbroken symmetry group that are conjugates of each other. This accounts for the opposite flavor index heights of $\hat{\chi}_i$ and $\hat{\eta}^i$ [cf. footnote 26]. The free-field Lagrangian is given by

$$\mathscr{L} = i\hat{\chi}^{\dagger i}\overline{\sigma}^\mu\partial_\mu\hat{\chi}_i + i\hat{\eta}^\dagger_i\overline{\sigma}^\mu\partial_\mu\hat{\eta}^i - M^i{}_j\hat{\chi}_i\hat{\eta}^j - M_i{}^j\hat{\chi}^{\dagger i}\hat{\eta}^\dagger_j, \tag{3.2.27}$$

where M is an arbitrary complex matrix with matrix elements $M^i{}_j$, and

$$M_i{}^j \equiv (M^i{}_j)^*. \tag{3.2.28}$$

If $M = 0$, then the free-field Lagrangian is invariant under a global U(N)×U(N) symmetry. That is, for a pair of unitary matrices U_L and U_R, with matrix elements given respectively by $(U_L)_i{}^j$ and $(U_R)^i{}_j$, and the corresponding hermitian conjugates defined by:

$$(U_L^\dagger)_j{}^i = [(U_L)_i{}^j]^* \equiv (U_L)^i{}_j, \qquad (U_R^\dagger)^j{}_i = [(U_R)^i{}_j]^* \equiv (U_R)_i{}^j, \tag{3.2.29}$$

the massless free-field Lagrangian is invariant under the transformations:

$$\hat{\chi}_i \longrightarrow (U_L)_i{}^j\hat{\chi}_j, \qquad \hat{\chi}^{\dagger i} \longrightarrow (U_L)^i{}_j\hat{\chi}^{\dagger j}, \qquad \hat{\eta}^i \longrightarrow (U_R)^i{}_j\hat{\eta}^j, \qquad \hat{\eta}^\dagger_i \longrightarrow (U_R)_i{}^j\hat{\eta}^\dagger_j. \tag{3.2.30}$$

For $M \neq 0$, Eq. (3.2.27) remains formally invariant under the U(N)×U(N) symmetry if M acts as a spurion field [146] with the appropriate tensorial transformation law, $M^i{}_j \to (U_L)^i{}_k(U_R)_j{}^\ell M^k{}_\ell$ (or equivalently, in an index-free matrix notation with suppressed flavor indices, $M \longrightarrow U_L^* M U_R^\dagger$).

In order to diagonalize the mass matrix, we introduce the mass eigenstates χ_i and η^i and unitary matrices L and R, with matrix elements given respectively by $L_i{}^k$ and $R^i{}_k$, such that

$$\hat{\chi}_i = L_i{}^k\chi_k, \qquad \hat{\eta}^i = R^i{}_k\eta^k, \tag{3.2.31}$$

and demand that $M^i{}_jL_i{}^kR^j{}_\ell = m_k\delta^k_\ell$ (no sum over k), where the m_k are real and non-negative. Equivalently, in matrix notation with suppressed indices, $\hat{\chi} = L\chi$, $\hat{\eta} = R\eta$ and

$$L^{\mathsf{T}}MR = \boldsymbol{m} = \mathrm{diag}(m_1, m_2, \ldots), \tag{3.2.32}$$

with the m_i real and non-negative (cf. footnote 28). The singular value decomposition of linear algebra, discussed more fully in Appendix D.1, states that for any complex matrix M, unitary matrices L and R exist such that Eq. (3.2.32) is satisfied. It then follows that:

$$L^{\mathsf{T}}(MM^\dagger)L^* = R^\dagger(M^\dagger M)R = \boldsymbol{m}^2. \tag{3.2.33}$$

That is, since $MM^\dagger$ and $M^\dagger M$ are both hermitian, they can be diagonalized by unitary matrices. The diagonal elements of $\boldsymbol{m}$ are therefore the non-negative square roots of the corresponding eigenvalues of $MM^\dagger$ (or equivalently, $M^\dagger M$). In terms of the mass eigenstates,

$$\mathscr{L} = i\chi^{\dagger i}\overline{\sigma}^\mu\partial_\mu\chi_i + i\eta^\dagger_i\,\overline{\sigma}^\mu\partial_\mu\eta^i - m_i(\chi_i\eta^i + \chi^{\dagger i}\eta^\dagger_i). \tag{3.2.34}$$

The mass matrix now consists of 2×2 blocks $\left(\begin{smallmatrix} 0 & m_i \\ m_i & 0 \end{smallmatrix}\right)$ along the diagonal. More importantly, the squared-mass matrix is diagonal with doubly degenerate entries m_i^2 that will appear in the denominators of the propagators of the theory. For $m_i \neq 0$, each χ_i–η^i pair describes a charged Dirac fermion consisting of four on-shell real degrees of freedom.[30] In addition, Eq. (3.2.34) yields an even number of massless Weyl fermions.

Given an arbitrary collection of two-component left-handed $(\frac{1}{2}, 0)$ fermions, the distinction between Majorana and Dirac fermions depends on whether the Lagrangian is invariant under a global (or local) continuous symmetry group G, and the corresponding multiplet structure of the fermion fields [148]. If no such continuous symmetry exist, then the fermion mass eigenstates will consist of Majorana fermions. If the Lagrangian is invariant under a symmetry group G, then the collection of two-component fermions will break up into a sum of multiplets that transform irreducibly under G. As described in Appendix E, a representation R can be either a real, pseudo-real, or complex representation of G. If a multiplet transforms under a real representation of G, then the corresponding fermion mass eigenstates are Majorana fermions.[31] If a multiplet transforms under a complex representation of G, then the corresponding fermion mass eigenstates are Dirac fermions. In

30 Of course, one could always choose instead to treat the Dirac fermions in a non-charge-eigenstate basis with a fully diagonalized mass matrix, as in Eq. (3.2.10). Inverting Eq. (3.2.15) for each Dirac fermion yields $\xi_{2i-1} = (\chi_i + \eta^i)/\sqrt{2}$ and $\xi_{2i} = i(\eta_i - \chi^i)/\sqrt{2}$. However, it is rarely, if ever, convenient to do so; practical calculations only require that the squared-mass matrix $M^\dagger M$ is diagonal, and it is of course more convenient to employ fields that carry well-defined charges.

31 This is a slight generalization of the more restrictive definition that requires Majorana fermions to transform trivially under the group G. Gluinos, which transform under the (real) adjoint representation of the color SU(3) group, are Majorana fermions according to our more general definition.

particular [as noted above Eq. (3.2.27)], if the χ_i transform under the representation R, then the η^i transform under the conjugate representation R^*.

The case where a multiplet of two-component left-handed fermions transform under a pseudo-real representation of G has not been explicitly treated above. The simplest example of this kind is a model of $2n$ multiplets (or "flavors") of two-component SU(2)-doublet[32] fermions, $\hat{\psi}_{ia}$ (where $i = 1, 2, \ldots, 2n$ labels the flavor index and a labels the SU(2) doublet index). The free-field Lagrangian is given by:

$$\mathscr{L} = i\hat{\psi}^{\dagger ia}\overline{\sigma}^{\mu}\partial_{\mu}\hat{\psi}_{ia} - \tfrac{1}{2}\left(M^{ij}\epsilon^{ab}\hat{\psi}_{ia}\hat{\psi}_{jb} + \text{h.c.}\right), \tag{3.2.35}$$

where ϵ^{ab} is the antisymmetric SU(2)-invariant tensor, defined such that $\epsilon^{12} = -\epsilon^{21} = +1$. As $\epsilon^{ab}\hat{\psi}_{ia}\hat{\psi}_{jb}$ is antisymmetric under the interchange of flavor indices i and j, it follows that M is a complex antisymmetric matrix. To identify the fermion mass eigenstates ψ_{ja}, we introduce a unitary matrix U (with matrix elements $U_i^{\ j}$) such that $\hat{\psi}_{ia} = U_i^{\ j}\psi_{ja}$ and demand that:

$$U^{\mathsf{T}}MU = \boldsymbol{N} \equiv \text{diag}\left\{\begin{pmatrix} 0 & m_1 \\ -m_1 & 0 \end{pmatrix}, \begin{pmatrix} 0 & m_2 \\ -m_2 & 0 \end{pmatrix}, \ldots, \begin{pmatrix} 0 & m_n \\ -m_n & 0 \end{pmatrix}\right\}, \tag{3.2.36}$$

where $\boldsymbol{N}$ is written in block diagonal form consisting of 2×2 matrix blocks appearing along the diagonal, and the m_j are real and non-negative. Eq. (3.2.36) corresponds to the reduction of a complex antisymmetric matrix to its real normal form [149], which is discussed in more detail in Appendix D.4. In order to compute the m_k, we first note that

$$U^{\dagger}M^{\dagger}MU = \text{diag}(m_1^2, m_1^2, m_2^2, m_2^2, \ldots, m_n^2, m_n^2). \tag{3.2.37}$$

Hence, the m_j are the non-negative square roots of the corresponding eigenvalues of $M^{\dagger}M$. Since the dimension of the doublet representation of SU(2) provides an additional degeneracy factor of 2, Eq. (3.2.37) implies that the mass spectrum consists of $2n$ pairs of mass-degenerate two-component fermions, which are equivalent to $2n$ Dirac fermions. In particular,

$$\mathscr{L} = \sum_{i=1}^{2n} i\psi^{\dagger ia}\overline{\sigma}^{\mu}\partial_{\mu}\psi_{ia} - \sum_{i=1}^{n}\left(m_i\epsilon^{ab}\psi_{2i-1,a}\psi_{2i,b} + \text{h.c.}\right). \tag{3.2.38}$$

In the general case of a pseudo-real representation R (of dimension d_R), the SU(2)-invariant ϵ-tensor is replaced by a more general $d_R \times d_R$ unitary antisymmetric matrix, C [defined in Eq. (E.1.9)]. Thus, the analysis above can be repeated virtually unchanged. By defining

$$\chi_{ia} \equiv \psi_{2i-1,a}, \qquad \eta^{ia} \equiv C^{ab}\psi_{2i,b}, \quad i = 1, 2, \ldots, n;\ a = 1, 2, \ldots, d_R, \tag{3.2.39}$$

with an implicit sum over the repeated index b, the resulting Lagrangian given by

$$\mathscr{L} = \sum_{i=1}^{n} i\chi^{\dagger ia}\overline{\sigma}^{\mu}\partial_{\mu}\chi_{ia} + i\eta_{ia}^{\dagger}\overline{\sigma}^{\mu}\partial_{\mu}\eta^{ia} - m_i\left(\chi_{ia}\eta^{ia} + \chi^{\dagger ia}\eta_{ia}^{\dagger}\right), \tag{3.2.40}$$

describes a free-field theory of nd_R Dirac fermions [cf. Eq. (3.2.34)]. Therefore, if a multiplet of two-component left-handed fermions transforms under a pseudo-real representation of G, then the corresponding fermion mass eigenstates are Dirac fermions [148]. If Eq. (3.2.35) contains an odd number of pseudo-real fermion multiplets, then the (antisymmetric) mass matrix M is odd dimensional and thus has an odd number of zero eigenvalues [according to Eq. (D.4.1)]. But as d_R must be even, it follows that the pseudo-real fermion multiplet contains an even number of massless Weyl fermions.

In conclusion, the mass diagonalization procedure of an arbitrary field theory of fermions yields (in general) a set of massless Weyl fermions, a set of massive neutral Majorana fermions [as in Eq. (3.2.10)], and a set of massive charged Dirac fermions [as in Eq. (3.2.34)]. The Feynman rules for these mass-eigenstate two-component fermion fields are given in Section 4.

For completeness, we review the squared-mass matrix diagonalization procedure for scalar fields. First, consider a collection of free commuting real spin-0 fields, $\hat{\varphi}_i(x)$, where the flavor index i labels the distinct scalar fields of the collection. The free-field Lagrangian is given by [33]

$$\mathscr{L} = \tfrac{1}{2}\partial_{\mu}\hat{\varphi}_i\partial^{\mu}\hat{\varphi}_i - \tfrac{1}{2}M_{ij}^2\hat{\varphi}_i\hat{\varphi}_j, \tag{3.2.41}$$

where M^2 is a real symmetric matrix. We diagonalize the scalar squared-mass matrix by introducing mass eigenstates φ_i and the orthogonal matrix Q such that $\hat{\varphi}_i = Q_{ij}\varphi_j$, with $M_{ij}^2Q_{ik}Q_{j\ell} = m_k^2\delta_{k\ell}$ (no sum over k). In matrix form,

$$Q^{\mathsf{T}}M^2Q = \boldsymbol{m}^2 = \text{diag}(m_1^2, m_2^2, \ldots), \tag{3.2.42}$$

32 The doublet representation of SU(2) is pseudo-real.

33 Since the scalar fields are real, there is no need to distinguish between raised and lowered flavor indices.

where the squared-mass eigenvalues m_k^2 are real.[34] This is the standard diagonalization problem for a real symmetric matrix.

Next, consider a collection of free commuting complex spin-0 fields, $\hat{\Phi}_i(x)$. For complex fields, we follow the conventions for flavor indices enunciated below Eq. (3.2.2) [e.g. $\hat{\Phi}^i = (\hat{\Phi}_i)^\dagger$]. The free-field Lagrangian is given by

$$\mathscr{L} = \partial_\mu \hat{\Phi}^i \partial^\mu \hat{\Phi}_i - (M^2)^i{}_j \hat{\Phi}_i \hat{\Phi}^j, \tag{3.2.43}$$

where M^2 is an hermitian matrix [i.e., $(M^2)^i{}_j = (M^2)_j{}^i$ in the notation of Eq. (3.2.29)].

We diagonalize the scalar squared-mass matrix by introducing mass eigenstates Φ_i and the unitary matrix W such that $\hat{\Phi}_i = W_i{}^k \Phi_k$ (and $\hat{\Phi}^i = W^i{}_k \Phi^k$), with $(M^2)^i{}_j W_i{}^k W^j{}_\ell = m_k^2 \delta_\ell^k$ (no sum over k). In matrix form,

$$W^\dagger M^2 W = \boldsymbol{m}^2 = \mathrm{diag}(m_1^2, m_2^2, \ldots). \tag{3.2.44}$$

where the squared-mass eigenvalues m_k^2 are real (cf. footnote 34). This is the standard diagonalization problem for an hermitian matrix.

4. Feynman rules with two-component spinors

In order to systematically perform perturbative calculations using two-component spinors, we present the basic Feynman rules. The Feynman rules for the Standard Model (and its seesaw extension) and the MSSM (including possible R-parity-violating interactions) are given in Appendix J, K and L. Feynman rules for two-component spinors have also been treated in Refs. [49,106,109].

4.1. External fermion and boson rules

Consider a general theory, for which we may assume that the mass matrix for fermions has been diagonalized as discussed in Section 3.2. The rules for assigning two-component external state spinors are then as follows:

- For an initial state (incoming) left-handed $(\frac{1}{2}, 0)$ fermion: x
- For an initial state (incoming) right-handed $(0, \frac{1}{2})$ fermion: $y^\dagger$
- For a final state (outgoing) left-handed $(\frac{1}{2}, 0)$ fermion: $x^\dagger$
- For a final state (outgoing) right-handed $(0, \frac{1}{2})$ fermion: y

where we have suppressed the momentum and spin arguments of the spinor wave functions. These rules are summarized in the mnemonic diagram of Fig. 4.1.1.

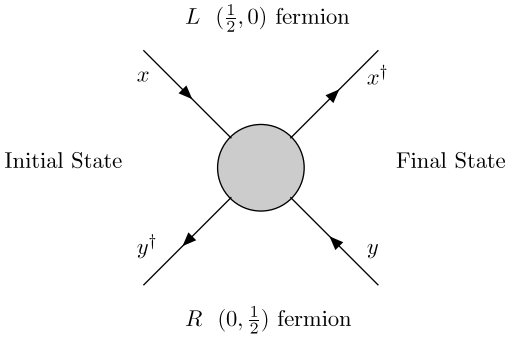

Fig. 4.1.1. The external wave function spinors should be assigned as indicated here, for initial state and final state left-handed $(\frac{1}{2}, 0)$ and right-handed $(0, \frac{1}{2})$ fermions.

In general, the two-component external state fermion wave functions are distinguished by their Lorentz group transformation properties, rather than by their particle or antiparticle status as in four-component Feynman rules. This helps to explain why two-component notation is especially convenient for (i) theories with Majorana particles, in which there is no fundamental distinction between particles and antiparticles, and (ii) theories like the Standard Model and MSSM in which the left- and right-handed fermions transform under different representations of the gauge group and (iii) problems with polarized particle beams.

[34] If the vacuum corresponds to a local minimum (or flat direction) of the scalar potential, then the squared-mass eigenvalues of M^2 are real *and* non-negative.

In contrast to four-component Feynman rules (given in Appendix G.5), the direction of the arrows do *not* correspond to the flow of charge or fermion number. The two-component Feynman rules for external fermion lines simply correspond to the formulae for the one-particle wave functions exhibited in Eqs. (3.1.7) and (3.1.8) [with the convention that $|\vec{p}, s\rangle$ is an initial state fermion and $\langle \vec{p}, s|$ is a final state fermion]. In particular, the arrows indicate the spinor index structure, with fields of undotted indices flowing *into* any vertex and fields of dotted indices flowing *out* of any vertex.

The rules above apply to any mass-eigenstate two-component fermion external wave functions. It is noteworthy that the same rules apply for the two-component fermions governed by the Lagrangians of Eq. (3.2.10) [Majorana] and Eqs. (3.2.34) or (3.2.40) [Dirac].

The corresponding rules for external boson lines are well known (see, e.g. Ref. [114]).

- For an initial state (incoming) or final state (outgoing) spin-0 boson: 1
- For an initial state (incoming) spin-1 boson of momentum $\vec{k}$ and helicity λ: $\varepsilon^{\mu}(\vec{k}, \lambda)$
- For a final state (outgoing) spin-1 boson of momentum $\vec{k}$ and helicity λ: $\varepsilon^{\mu}(\vec{k}, \lambda)^*$.

The explicit form of the helicity ± 1 (massless or massive) spin-1 polarization vector ε^{μ} is given in Eq. (I.2.41). The helicity zero massive spin-1 polarization vector is given in Eq. (I.2.43).

4.2. Propagators

Next we turn to the subject of fermion propagators for two-component fermions. A derivation of the two-component fermion propagators using path integral techniques is given in Appendix F. Here, we will follow the more elementary approach typically given in an initial textbook treatment of quantum field theory.

Fermion propagators are the Fourier transforms of the free-field vacuum expectation values of time-ordered products of two fermion fields. They are obtained by inserting the free-field expansion of the two-component fermion field and evaluating the spin sums using the formulae given in Eqs. (3.1.58) and (3.1.61). For the case of a single neutral two-component fermion field $\xi(x)$ of mass m, Eqs. (3.2.11) and (3.2.12) yield [49,106,108,109,143,150]:

$$\langle 0|\, T\xi_{\alpha}(x)\xi^{\dagger}_{\dot{\beta}}(y)\,|0\rangle_{\rm FT} = \frac{i}{p^2 - m^2 + i\epsilon}\sum_{s} x_{\alpha}(\vec{p}, s)x^{\dagger}_{\dot{\beta}}(\vec{p}, s) = \frac{i}{p^2 - m^2 + i\epsilon}\, p\cdot\sigma_{\alpha\dot{\beta}}, \tag{4.2.1}$$

$$\langle 0|\, T\xi^{\dagger\dot{\alpha}}(x)\xi^{\beta}(y)\,|0\rangle_{\rm FT} = \frac{i}{p^2 - m^2 + i\epsilon}\sum_{s} y^{\dagger\dot{\alpha}}(\vec{p}, s)y^{\beta}(\vec{p}, s) = \frac{i}{p^2 - m^2 + i\epsilon}\, p\cdot\overline{\sigma}^{\dot{\alpha}\beta}, \tag{4.2.2}$$

$$\langle 0|\, T\xi^{\dagger\dot{\alpha}}(x)\xi^{\dagger}_{\dot{\beta}}(y)\,|0\rangle_{\rm FT} = \frac{i}{p^2 - m^2 + i\epsilon}\sum_{s} y^{\dagger\dot{\alpha}}(\vec{p}, s)x^{\dagger}_{\dot{\beta}}(\vec{p}, s) = \frac{i}{p^2 - m^2 + i\epsilon}\, m\delta^{\dot{\alpha}}{}_{\dot{\beta}}, \tag{4.2.3}$$

$$\langle 0|\, T\xi_{\alpha}(x)\xi^{\beta}(y)\,|0\rangle_{\rm FT} = \frac{i}{p^2 - m^2 + i\epsilon}\sum_{s} x_{\alpha}(\vec{p}, s)y^{\beta}(\vec{p}, s) = \frac{i}{p^2 - m^2 + i\epsilon}\, m\delta_{\alpha}{}^{\beta}, \tag{4.2.4}$$

where FT indicates the Fourier transform from position to momentum space.[35] These results have a clear diagrammatic representation, as shown in Fig. 4.2.1. Note that the direction of the momentum flow p^{μ} here is determined by the creation operator that appears in the evaluation of the free-field propagator. Arrows on fermion lines always run away from dotted indices at a vertex and toward undotted indices at a vertex.

There are clearly two types of fermion propagators. The first type preserves the direction of arrows, so it has one dotted and one undotted index. For this type of propagator, it is convenient to establish a convention where p^{μ} in the diagram is defined to be the momentum flowing in the direction of the arrow on the fermion propagator. With this convention, the two rules above for propagators of the first type can be summarized by one rule, as shown in Fig. 4.2.2. Here the choice of the σ or the $\overline{\sigma}$ version of the rule is uniquely determined by the height of the indices on the vertex to which the propagator is connected.[36] These heights should always be chosen so that they are contracted as in Eq. (2.36). It should be noted that in

[35] The Fourier transform of a translationally invariant function $f(x, y) \equiv f(x - y)$ is given by

$$f(x, y) = \int \frac{\mathrm{d}^4 p}{(2\pi)^4}\,\widehat{f}(p)\, e^{-ip\cdot(x-y)}, \quad \text{where}\, \widehat{f}(p) = \int \mathrm{d}^4 x f(x) e^{ip\cdot x}.$$

In the notation of the text above, $f(x, y)_{\rm FT} \equiv \widehat{f}(p)$.

[36] The second form of the rule in Fig. 4.2.2 arises when one flips diagram (b) of Fig. 4.2.1 around by a 180° rotation (about an axis perpendicular to the plane of the diagram), and then relabels $p \to -p, \dot{\alpha} \to \dot{\beta}$ and $\beta \to \alpha$.

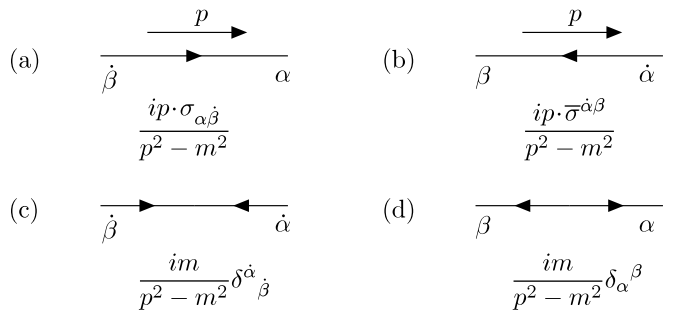

Fig. 4.2.1. Feynman rules for propagator lines of a neutral two-component fermion with mass m. (For simplicity, the $+i\epsilon$ terms in the denominators are omitted in all propagator rules.)

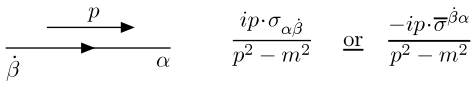

Fig. 4.2.2. This rule summarizes the results of both Fig. 4.2.1(a) and (b) for a neutral two-component fermion with mass m.

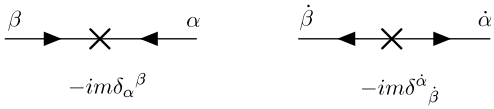

Fig. 4.2.3. Fermion mass insertions (indicated by the crosses) can be treated as a type of interaction vertex, using the Feynman rules shown here.

diagrams (a) and (b) of Fig. 4.2.1 as drawn, the indices on the σ and $\overline\sigma$ read from right to left. In particular, the Feynman rules for the propagator can be employed with the spinor indices suppressed provided that the arrow-preserving propagator lines are traversed in the direction parallel [antiparallel] to the arrowed line segment for the $\overline\sigma$ [σ] version of the rule, respectively.

The second type of propagator shown in diagrams (c) and (d) of Fig. 4.2.1 does not preserve the direction of arrows, and corresponds to an odd number of mass insertions. The indices on $\delta^{\dot\alpha}{}_{\dot\beta}$ and $\delta_\alpha{}^\beta$ are staggered as shown to indicate that $\dot\alpha$ and α are to be contracted with expressions to the left, while $\dot\beta$ and β are to be contracted with expressions to the right, in accord with Eq. (2.36).[37]

Starting with massless fermion propagators, one can also derive the massive fermion propagators by employing mass insertions as interaction vertices, as shown in Fig. 4.2.3. By summing up an infinite chain of such mass insertions between massless fermion propagators, one can reproduce the massive fermion propagators of both types.

The above results for the propagator of a Majorana fermion can be generalized to a multiplet of mass-eigenstate Majorana fermions, $\xi_{\alpha a}(x)$ [such as a color octet of gluinos], which transforms as a real representation R of a (gauge or flavor) group G (where $a = 1, 2, \ldots, d_R$ for a representation of dimension d_R). In this case, the Feynman graphs given in Figs. 4.2.1–4.2.3 are modified simply by specifying a group index a and b at either end of the propagator line. The corresponding Feynman rules then includes an additional Kronecker delta factor in the group indices. In particular, if we associate the index a with the spinor indices $\alpha, \dot\alpha$ and the index b with the spinor indices $\beta, \dot\beta$, then the rules exhibited in Fig. 4.2.1(a) and (b) would include the following Kronecker delta factors:

$$\text{(a)}\quad \delta^b_a, \qquad\qquad \text{(b)}\quad \delta^a_b, \tag{4.2.5}$$

and the factors of m in the rules exhibited in Fig. 4.2.1(c) and (d) would be replaced by

$$\text{(c)}\quad \delta^a_c m^{cd}\delta^b_d = m_a\delta^{ab}, \qquad \text{(d)}\quad \delta^c_a m_{cd}\delta^d_b = m_a\delta_{ab}, \tag{4.2.6}$$

(with no sum over the repeated index a), where m^{cd} and $m_{cd} \equiv m^{cd}$ are diagonal matrices with real non-negative diagonal elements m_c. Here, we have introduced the separate symbol m_{cd} in order to maintain the convention that two repeated group indices are summed when one index is raised and one index is lowered. Of course, if the Lagrangian is invariant under the symmetry group G, then a multiplet of Majorana fermions corresponding to an irreducible representation R has a common mass $m = m_a$.

It is convenient to treat separately the case of charged massive fermions. Consider a charged Dirac fermion of mass m, which is described by a pair of two-component fields $\chi(x)$ and $\eta(x)$ [cf. Eq. (3.2.17)]. Using the free-field expansions

[37] As in Fig. 4.2.2, alternative and equivalent versions of the rules corresponding to diagrams (c) and (d) of Fig. 4.2.1 can be given for which the indices on the Kronecker deltas are staggered as $\delta^{\dot\beta}{}_{\dot\alpha}$ and $\delta_{\beta}{}^{\alpha}$. These versions correspond to flipping the two respective diagrams by 180° and relabeling the indices $\dot\alpha \to \dot\beta$ and $\beta \to \alpha$.

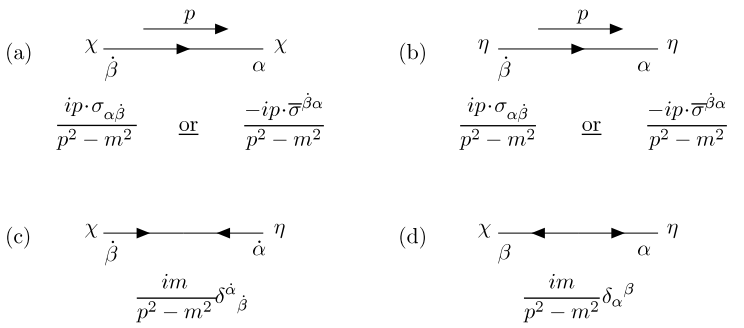

Fig. 4.2.4. Feynman rules for propagator lines of a pair of charged two-component fermions with a Dirac mass m. As in Fig. 4.2.2, the direction of the momentum is taken to flow from the dotted to the undotted index in diagrams (a) and (b).

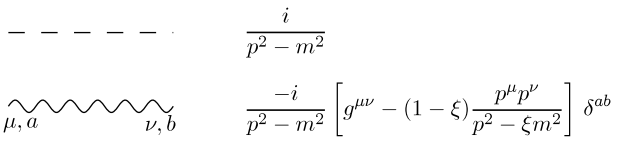

Fig. 4.2.5. Feynman rules for the (neutral or charged) scalar and gauge boson propagators, in the R_ξ gauge, where p^μ is the propagating four-momentum. In the gauge boson propagator, $\xi = 1$ defines the 't Hooft–Feynman gauge, $\xi = 0$ defines the Landau gauge, and $\xi \to \infty$ defines the unitary gauge. For the propagation of a non-abelian gauge boson, one must also specify the adjoint representation indices a, b.

[Eqs. (3.2.19) and (3.2.20)] and the spin sums [Eqs. (3.1.58)–(3.1.61)], the two-component free-field propagators are obtained:

$$\langle 0|\, T\chi_\alpha(x)\chi^\dagger_{\dot\beta}(y)\,|0\rangle_{\rm FT} = \langle 0|\, T\eta_\alpha(x)\eta^\dagger_{\dot\beta}(y)\,|0\rangle_{\rm FT} = \frac{i}{p^2-m^2}\, p\cdot\sigma_{\alpha\dot\beta}, \tag{4.2.7}$$

$$\langle 0|\, T\chi^{\dagger\dot\alpha}(x)\chi^\beta(y)\,|0\rangle_{\rm FT} = \langle 0|\, T\eta^{\dagger\dot\alpha}(x)\eta^\beta(y)\,|0\rangle_{\rm FT} = \frac{i}{p^2-m^2}\, p\cdot\overline{\sigma}^{\dot\alpha\beta}, \tag{4.2.8}$$

$$\langle 0|\, T\chi_\alpha(x)\eta^\beta(y)\,|0\rangle_{\rm FT} = \langle 0|\, T\eta_\alpha(x)\chi^\beta(y)\,|0\rangle_{\rm FT} = \frac{i}{p^2-m^2}\, m\,\delta_\alpha{}^\beta, \tag{4.2.9}$$

$$\langle 0|\, T\chi^{\dagger\dot\alpha}(x)\eta^\dagger_{\dot\beta}(y)\,|0\rangle_{\rm FT} = \langle 0|\, T\eta^{\dagger\dot\alpha}(x)\chi^\dagger_{\dot\beta}(y)\,|0\rangle_{\rm FT} = \frac{i}{p^2-m^2}\, m\,\delta^{\dot\alpha}{}_{\dot\beta}. \tag{4.2.10}$$

For all other combinations of fermion bilinears, the corresponding two-point functions vanish. These results again have a simple diagrammatic representation, as shown in Fig. 4.2.4. Note that for Dirac fermions, the propagators with opposing arrows (proportional to a mass) necessarily change the identity (χ or η) of the two-component fermion, while the single-arrow propagators are diagonal in the fields. In processes involving such a charged fermion, one must of course distinguish between the χ and η fields.

The above results for the propagator of a Dirac fermion can be generalized to a multiplet of mass-eigenstate Dirac fermions, $\chi_{\alpha i}$, η^i_α, which transform under a (gauge or flavor) group G. In this case, the Feynman graphs given in Fig. 4.2.4 are modified simply by specifying a group index i and j at either end of the propagator line. The corresponding Feynman rules then include an additional Kronecker delta factor in the group indices. In particular, if we associate the group index i with the spinor indices α, $\dot\alpha$ and the index j with the spinor indices β, $\dot\beta$, then the rules exhibited in Fig. 4.2.4(a) and (b) would include the following Kronecker delta factors:

$$\text{(a)}\quad \delta^j_i \qquad \text{(b)}\quad \delta^i_j, \tag{4.2.11}$$

and the factors of m in the rules exhibited in Fig. 4.2.4(c) and (d) would be replaced by

$$\text{(c)}\quad \delta^\ell_i m_\ell{}^n \delta^j_n = m_i\delta^j_i, \qquad \text{(d)}\quad \delta^i_\ell m^\ell{}_n \delta^n_j = m_i\delta^i_j, \tag{4.2.12}$$

where $m^\ell{}_n$ and $m_\ell{}^n \equiv m^\ell{}_n$ are diagonal matrices with real non-negative diagonal elements m_ℓ, and there is no sum over the repeated index i. (Here, we have introduced the separate symbol $m_\ell{}^n$ in order to maintain the convention that two repeated group indices are summed when one index is raised and one index is lowered.) As before, if the Lagrangian is invariant under the symmetry group G, then an irreducible multiplet of Dirac fermions has a common mass $m = m_i$.

For completeness, we exhibit in Fig. 4.2.5 the Feynman rules for the propagators of the (neutral or charged) scalar boson and gauge boson in the R_ξ gauge, with gauge parameter ξ [151].

4.3. Fermion interactions with bosons

We next discuss the interaction vertices for fermions with bosons. Renormalizable Lorentz-invariant interactions involving fermions must consist of bilinears in the fermion fields, which transform as a Lorentz scalar or vector, coupled to the appropriate bosonic scalar or vector field to make an overall Lorentz scalar quantity.

Let us write all of the two-component left-handed $(\frac{1}{2}, 0)$ fermions of the theory as $\hat{\psi}_i$, where i runs over all of the gauge group representation and flavor degrees of freedom. In general, the $(\frac{1}{2}, 0)$-fermion fields $\hat{\psi}_i$ consist of Majorana fermions $\hat{\xi}_i$, and Dirac fermion pairs $\hat{\chi}_i$ and $\hat{\eta}^i$ after mass terms (both explicit and coming from spontaneous symmetry breaking) are taken into account. Likewise, consider a multiplet of scalar fields $\hat{\phi}_I$, where I runs over all of the gauge group representation and flavor degrees of freedom. In general, the scalar fields $\hat{\phi}_I$ consist of real scalar fields $\hat{\varphi}_I$ and pairs of complex scalar fields $\hat{\Phi}_I$ and $\hat{\Phi}^I \equiv (\hat{\Phi}_I)^\dagger$. In matrix form,

$$\hat{\psi} \equiv \begin{pmatrix} \hat{\xi} \\ \hat{\chi} \\ \hat{\eta} \end{pmatrix}, \qquad \hat{\phi} \equiv \begin{pmatrix} \hat{\varphi} \\ \hat{\Phi} \\ \hat{\Phi}^\dagger \end{pmatrix}. \tag{4.3.1}$$

By dividing up the fermions into Majorana and Dirac fermions and the spin-zero fields into real and complex scalars, we are assuming implicitly that some of the indices I and i correspond to states of a definite (global) U(1)-charge (denoted in the following by q_I and q_i, respectively).

The most general set of Yukawa interactions of the scalar fields with a pair of fermion fields is then given by:

$$\mathscr{L}_{\rm int} = -\tfrac{1}{2}\hat{Y}^{Ijk}\hat{\phi}_I\hat{\psi}_j\hat{\psi}_k - \tfrac{1}{2}\hat{Y}_{Ijk}\hat{\phi}^I\hat{\psi}^{\dagger j}\hat{\psi}^{\dagger k}, \tag{4.3.2}$$

where $\hat{Y}_{Ijk} = (\hat{Y}^{Ijk})^*$. We have suppressed the spinor indices here; the product of two-component spinors is always performed according to the index convention indicated in Eq. (2.36). The Yukawa Lagrangian [Eq. (4.3.2)] must be invariant under:

$$\hat{\xi}_i \to \hat{\xi}_i, \qquad \hat{\chi}_i \to e^{iq_i\theta}\hat{\chi}_i, \qquad \hat{\eta}^i \to e^{-iq_i\theta}\hat{\eta}^i, \qquad \hat{\varphi}_i \to \hat{\varphi}_i, \qquad \hat{\Phi}_I \to e^{iq_I\theta}\hat{\Phi}_I, \qquad \hat{\Phi}^I \to e^{-iq_I\theta}\hat{\Phi}^I, \tag{4.3.3}$$

where the q_i are the U(1)-charges of the corresponding Dirac fermions and the q_I are the U(1)-charges of the corresponding complex scalars. Consequently, the form of the $\hat{Y}^{Ijk}$ is constrained:

$$\hat{Y}^{Ijk} = 0, \quad \text{unless} \quad q_I + q_j + q_k = 0. \tag{4.3.4}$$

Of course, any other conserved symmetries will impose additional selection rules on the Yukawa couplings Y^{Ijk}.

The hatted fields are the interaction-eigenstate fields. However, in general the mass eigenstates can be different, as discussed in Section 3.2. The computation of matrix elements for physical processes is more conveniently done in terms of the propagating mass-eigenstate fields. The mass-eigenstate basis ψ is related to the interaction-eigenstate basis $\hat{\psi}$ by a unitary rotation $U_i{}^j$ on the flavor indices. In matrix form:

$$\hat{\psi} \equiv \begin{pmatrix} \hat{\xi}_i \\ \hat{\chi}_i \\ \hat{\eta}^i \end{pmatrix} = U\psi \equiv \begin{pmatrix} \Omega_i{}^j & 0 & 0 \\ 0 & L_i{}^j & 0 \\ 0 & 0 & R^i{}_j \end{pmatrix} \begin{pmatrix} \xi_j \\ \chi_j \\ \eta^j \end{pmatrix}, \tag{4.3.5}$$

where Ω, L, and R are constructed as described previously in Section 3.2 [see Eqs. (3.2.8) and (3.2.32)]. Likewise, the mass-eigenstate basis ϕ is related to the interaction-eigenstate basis $\hat{\phi}$ by a unitary rotation $V_I{}^J$ on the flavor indices. In matrix form,

$$\hat{\phi} \equiv \begin{pmatrix} \hat{\varphi}_I \\ \hat{\Phi}_I \\ \hat{\Phi}^I \end{pmatrix} = V\phi \equiv \begin{pmatrix} Q_I{}^J & 0 & 0 \\ 0 & W_I{}^J & 0 \\ 0 & 0 & W^I{}_J \end{pmatrix} \begin{pmatrix} \varphi_J \\ \Phi_J \\ \Phi^J \end{pmatrix}, \tag{4.3.6}$$

where $W^I{}_J = (W_I{}^J)^*$, and Q and W are constructed according to Eqs. (3.2.42) and (3.2.44).

Thus, we may rewrite Eq. (4.3.2) in terms of mass-eigenstate fields:

$$\mathscr{L}_{\rm int} = -\tfrac{1}{2}Y^{Ijk}\phi_I\psi_j\psi_k - \tfrac{1}{2}Y_{Ijk}\phi^I\psi^{\dagger j}\psi^{\dagger k}, \tag{4.3.7}$$

where

$$Y^{Ijk} = V_J{}^I U_m{}^j U_n{}^k \hat{Y}^{Jmn}. \tag{4.3.8}$$

Note that Eq. (4.3.4) implies that $Y^{Ijk} = 0$ unless $q_I + q_j + q_k = 0$. The corresponding Feynman rules that arise from the Yukawa interaction Lagrangian are shown in Fig. 4.3.1. If the scalar ϕ_I is complex, then one can associate an arrow with the

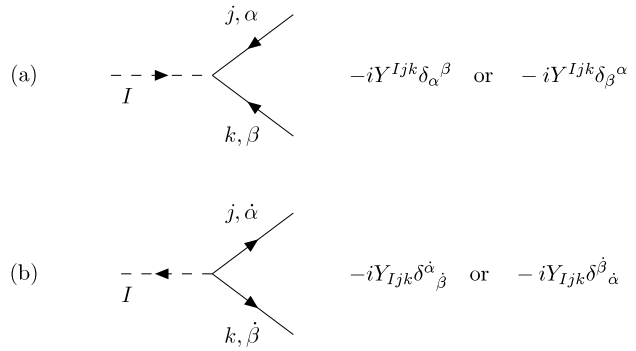

Fig. 4.3.1. Feynman rules for Yukawa couplings of scalars to two-component fermions in a general field theory. The choice of which rule to use depends on how the vertex connects to the rest of the amplitude. When indices are suppressed, the spinor index part is always just proportional to the identity matrix.

flow of analyticity, which would point into the vertex in (a) and would point out of the vertex in (b). That is, the arrow on the scalar line keeps track of the height of the scalar flavor index entering or leaving the vertex.

In Fig. 4.3.1, two versions are given for each Feynman rule. The choice of which rule to use is dictated by the height of the indices on the fermion lines that connect to the vertex. These heights should always be chosen so that they are contracted as in Eq. (2.36). However, when all spinor indices are suppressed, the scalar-fermion–fermion rules will have an identical appearance for both cases, since they are just proportional to the identity matrix of the 2×2 spinor space.

To provide a more concrete example of the above results, consider a real neutral scalar field ϕ and a (possibly) complex charged scalar field Φ (with U(1)-charge q_Φ) that interact with a multiplet of Majorana fermions ξ_i and Dirac fermion pairs χ_j and η^j (with U(1)-charges q_j and $-q_j$, respectively). We assume that all fields are given in the mass-eigenstate basis. The Yukawa interaction Lagrangian is given by:

$$\begin{aligned}\mathscr{L}_{\rm int} &= -\tfrac{1}{2}(\lambda^{ij}\xi_i\xi_j + \lambda_{ij}\xi^{\dagger i}\xi^{\dagger j})\phi - \kappa^i{}_j\chi_i\eta^j\Phi + \kappa_i{}^j\chi^{\dagger i}\eta^\dagger_j\Phi^\dagger \\ &\quad - [(\kappa_1)^i{}_j\xi_i\eta^j + (\kappa_2)_{ij}\xi^{\dagger i}\chi^{\dagger j}]\Phi - [(\kappa_2)^{ij}\xi_i\chi_j + (\kappa_1)_i{}^j\xi^{\dagger i}\eta^\dagger_j]\Phi^\dagger,\end{aligned} \tag{4.3.9}$$

where λ is a complex symmetric matrix, and κ, κ_1 and κ_2 are complex matrices such that $\kappa^i{}_j = 0$ unless $q_\Phi = q_j - q_i$ and $(\kappa_1)^i{}_j = (\kappa_2)_{ij} = 0$ unless $q_\Phi = q_j$ [flavor index conventions are specified in Eqs. (3.2.2) and (3.2.28)]. The corresponding Feynman rules of Fig. 4.3.1(a) are obtained by identifying $Y^{Iij} = \lambda^{ij}$, $\kappa^i{}_j$, $(\kappa_1)^i{}_j$ and $(\kappa_2)^{ij}$ for the undotted fermion vertices $\phi\xi_i\xi_j$, $\Phi\chi_i\eta^j$, $\Phi\xi_i\eta^j$ and $\Phi^\dagger\xi_i\chi_j$, respectively.[38] The corresponding Feynman rules of Fig. 4.3.1(b) for the dotted fermion vertices are governed by the complex-conjugated Yukawa couplings, $Y_{Ijk} \equiv (Y^{Ijk})^*$.

The renormalizable interactions of vector bosons with fermions and scalars arise from gauge interactions. These interaction terms of the Lagrangian derive from the respective kinetic energy terms of the fermions and scalars when the derivative is promoted to the covariant derivative:

$$(D_\mu)_i{}^j \equiv \delta_i{}^j\partial_\mu + ig_aA^a_\mu(\boldsymbol{T^a})_i{}^j, \tag{4.3.10}$$

where the index a labels the real (interaction-eigenstate) vector bosons A^μ_a and is summed over. The index a runs over the adjoint representation of the gauge group,[39] and the $(\boldsymbol{T^a})_i{}^j$ are hermitian representation matrices of the generators of the Lie algebra of the gauge group acting on the left-handed fermions (for further details, see Appendix E). For a $U(1)$ gauge group, the $\boldsymbol{T^a}$ are replaced by real numbers corresponding to the U(1) charges of the left-handed $(\frac{1}{2}, 0)$ fermions. There is a separate coupling g_a for each simple group or U(1) factor of the gauge group G.[40]

In the gauge-interaction basis for the left-handed $(\frac{1}{2}, 0)$ two-component fermions the corresponding interaction Lagrangian is given by

$$\mathscr{L}_{\rm int} = -g_aA^\mu_a\hat\psi^{\dagger i}\overline{\sigma}_\mu(\boldsymbol{T}^a)_i{}^j\hat\psi_j. \tag{4.3.11}$$

In the case of spontaneously broken gauge theories, one must diagonalize the vector boson squared-mass matrix. The form of Eq. (4.3.11) still applies where A^a_μ are gauge boson fields of definite mass, although in this case for a fixed value of a, $g_a\boldsymbol{T}^a$

[38] For the $\Phi^\dagger\xi_i\chi_j$ vertex, we should reverse the direction of the arrow on the scalar line in Fig. 4.3.1(a) [and likewise for the corresponding hermitian-conjugated vertex of Fig. 4.3.1(b)], in which case all arrows on the charged scalar and fermion lines would represent the direction of flow of the conserved U(1)-charge.

[39] Since the adjoint representation is a real representation, the height of the adjoint index a is not significant. The choice of a subscript or superscript adjoint index is based solely on typographical considerations.

[40] That is, the generators $\boldsymbol{T^a}$ separate out into distinct classes, each of which is associated with a simple group or one of the U(1) factors contained in the direct product that defines G. In particular, $g_a = g_b$ if $\boldsymbol{T^a}$ and $\boldsymbol{T^b}$ are in the same class. If G is simple, then $g_a = g$ for all a.

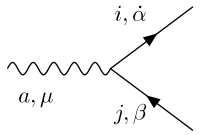

$$-i(G^a)_i{}^j\,\overline{\sigma}_\mu^{\dot{\alpha}\beta} \quad \text{or} \quad i(G^a)_i{}^j\,\sigma_{\mu\beta\dot{\alpha}}$$

Fig. 4.3.2. The Feynman rules for two-component fermion interactions with gauge bosons. The choice of which rule to use depends on how the vertex connects to the rest of the amplitude. The G^a are defined in Eq. (4.3.14). The index a runs over both neutral and charged (mass-eigenstate) gauge bosons, consistent with charge conservation at the vertex.

[which multiplies A^a_μ in Eq. (4.3.11)] is some linear combination of the original $g_a\boldsymbol{T}^a$ of the unbroken theory. That is, the hermitian matrix gauge field $(A_\mu)_i{}^j \equiv A^a_\mu(\boldsymbol{T^a})_i{}^j$ appearing in Eq. (4.3.11) can always be re-expressed in terms of the *physical* mass-eigenstate gauge boson fields.

If an unbroken U(1) (global or local) symmetry exists, then the physical gauge bosons will be eigenstates of the conserved U(1)-charge.[41] If the U(1) symmetry group is orthogonal to the gauge group under which the A^μ_a transform, then all the gauge bosons are neutral with respect to the U(1)-charge. For example, in the case of the interaction of a gluon with a pair of Majorana fermion gluinos, the gluon is a gauge boson that transforms under the SU(3) color group, which is orthogonal to the conserved $\mathrm{U}(1)_{\mathrm{EM}}$. That is, gluinos are color octet, electrically neutral fermions. In contrast, in the case of the interaction of a Z^0 with pair of Majorana neutralinos, $\mathrm{U}(1)_{\mathrm{EM}}$ is not orthogonal to the electroweak SU(2)×U(1) gauge group. Nevertheless, the Z^0-gauge boson interactions of the neutralinos are allowed as they conserve electric charge.

To obtain the desired Feynman rule, we rewrite Eq. (4.3.11) in terms of mass-eigenstate fermion fields. The resulting interaction Lagrangian can be rewritten as

$$\mathscr{L}_{\mathrm{int}} = -A^\mu_a \psi^{\dagger i}\,\overline{\sigma}_\mu (G^a)_i{}^j \psi_j, \tag{4.3.13}$$

where the A^μ_a are the mass-eigenstate gauge fields (of definite U(1)-charge, if relevant), and

$$(G^a)_i{}^j = g_a U^k{}_i (\boldsymbol{T^a})_k{}^m U_m{}^j, \tag{4.3.14}$$

or in matrix form, $G^a = g_a U^\dagger \boldsymbol{T^a} U$ (no sum over a). For values of a corresponding to the neutral gauge fields, the G^a are hermitian matrices. The corresponding Feynman rule is shown in Fig. 4.3.2.

The above treatment of the gauge interactions of (two-component) fermions is general. Nevertheless, it is useful to consider separately three cases where the gauge bosons couple to a pair of Majorana fermions, a pair of Dirac fermions, and a fermion pair consisting of one Majorana and one Dirac fermion.

First, consider the gauge interactions of neutral Majorana fermions. The Majorana fermions consist of left-handed $(\frac{1}{2}, 0)$ interaction-eigenstate fermions $\hat{\xi}_i$ that transform under a real representation of the gauge group. After converting from the interaction eigenstates $\hat{\xi}_i$ to the mass eigenstates ξ_i using Eq. (3.2.7), the Lagrangian for the gauge interactions of Majorana fermions is given by:

$$\mathscr{L}_{\mathrm{int}} = -A^a_\mu \xi^{\dagger i}\,\overline{\sigma}^\mu (G^a)_i{}^j \xi_j, \tag{4.3.15}$$

where the A^a_μ are *neutral* (real) mass-eigenstate gauge fields, and

$$(G^a)_i{}^j = g_a \Omega^k{}_i (\boldsymbol{T^a})_k{}^m \Omega_m{}^j, \tag{4.3.16}$$

or in matrix form, $G^a = g_a \Omega^\dagger \boldsymbol{T^a} \Omega$ (no sum over a). Note that the G^a are hermitian matrices. The corresponding Feynman rule takes the same form as the generalized rule shown in Fig. 4.3.2, with a restricted to values corresponding to the neutral mass-eigenstate gauge bosons.

Next, consider the gauge interactions of charged Dirac fermions. The Dirac fermions consist of pairs of left-handed $(\frac{1}{2}, 0)$ interaction-eigenstate fermions $\hat{\chi}_i$ and $\hat{\eta}^i$ that transform as conjugate representations of the gauge group (hence the opposite flavor index heights). The fermion mass matrix couples χ and η type fields as in Eq. (3.2.27). In the coupling to the interaction-eigenstate gauge fields, if the $(\boldsymbol{T}^a)_i{}^j$ are matrix elements of the hermitian representation matrices of the generators acting on the $\hat{\chi}_i$, then the $\hat{\eta}^i$ transform in the complex conjugate representation with the corresponding generator

41 In terms of the physical gauge boson fields, $A^a_\mu \boldsymbol{T^a}$ consists of a sum over real neutral gauge fields multiplied by hermitian generators, and complex charged gauge fields multiplied by non-hermitian generators. For example, in the electroweak Standard Model, $G = \mathrm{SU}(2) \times \mathrm{U}(1)$ with gauge bosons and generators W^a_μ and $\boldsymbol{T}^a = \frac{1}{2}\tau^a$ for SU(2) and B_μ and $\boldsymbol{Y}$ for U(1), where the τ^a are the usual Pauli matrices. After diagonalizing the gauge boson squared-mass matrix[151]:

$$gW^a_\mu \boldsymbol{T^a} + g' B_\mu \boldsymbol{Y} = \frac{g}{\sqrt{2}}(W^+_\mu \boldsymbol{T}^+ + W^-_\mu \boldsymbol{T}^-) + \frac{g}{\cos\theta_W}\left(\boldsymbol{T^3} - \boldsymbol{Q}\sin^2\theta_W\right) Z_\mu + e\boldsymbol{Q}A_\mu, \tag{4.3.12}$$

where $\boldsymbol{Q} = \boldsymbol{T^3} + \boldsymbol{Y}$ is the generator of the unbroken $\mathrm{U}(1)_{\mathrm{EM}}$, $\boldsymbol{T}^\pm \equiv \boldsymbol{T^1} \pm i\boldsymbol{T^2}$, and $e = g\sin\theta_W = g'\cos\theta_W$. The massive gauge boson charge-eigenstate fields of the broken theory consist of a charged massive gauge boson pair, $W^\pm \equiv (W^1 \mp iW^2)/\sqrt{2}$, a neutral massive gauge boson, $Z \equiv W^3\cos\theta_W - B\sin\theta_W$, and the massless photon, $A \equiv W^3\sin\theta_W + B\cos\theta_W$.

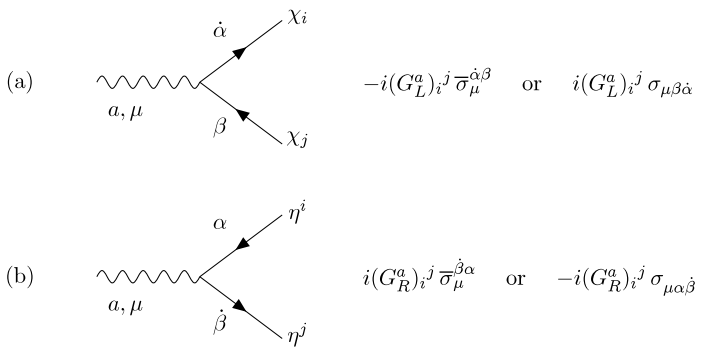

Fig. 4.3.3. The Feynman rules for the interaction of a gauge boson and a pair of Dirac fermions (each formed by χ and η of the appropriate flavor index). The fermion lines are labeled by the corresponding two-component left-handed $(\frac{1}{2}, 0)$ fermion fields. The matrices G_L^a and G_R^a depend on the group generators for the representation carried by the χ_i according to Eqs. (4.3.19) and (4.3.20). The index a runs over both neutral and charged (mass-eigenstate) gauge bosons, consistent with charge conservation at the vertex.

matrices $-(\boldsymbol{T}^a)^* = -(\boldsymbol{T}^a)^{\mathsf{T}}$, i.e. with matrix elements $-(\boldsymbol{T}^a)_j{}^i$. Hence, the Lagrangian for the gauge interactions of Dirac fermions can be written in the form:

$$\mathscr{L}_{\rm int} = -g_a A_a^\mu\, \hat\chi^{\dagger i}\,\overline\sigma_\mu (\boldsymbol{T}^a)_i{}^j \hat\chi_j + g_a A_a^\mu\, \hat\eta_i^\dagger\, \overline\sigma_\mu (\boldsymbol{T}^a)_j{}^i \hat\eta^j. \tag{4.3.17}$$

We now rewrite Eq. (4.3.17) in terms of mass-eigenstate fermion fields using Eq. (3.2.31), and express the hermitian matrix gauge field $A^\mu \equiv A_a^\mu \boldsymbol{T^a}$ in terms of mass-eigenstate gauge fields (of definite U(1)-charge, if relevant). The resulting interaction Lagrangian is then given by:

$$\mathscr{L}_{\rm int} = -A_a^\mu \left[\chi^{\dagger i}\,\overline\sigma_\mu (G_L^a)_i{}^j \chi_j - \eta_i^\dagger\,\overline\sigma_\mu (G_R^a)_j{}^i \eta^j\right], \tag{4.3.18}$$

where $A_a^\mu G_L^a$ and $A_a^\mu G_R^a$ are hermitian matrix-valued gauge fields, with:

$$(G_L^a)_i{}^j = g_a L^k{}_i (\boldsymbol{T^a})_k{}^m L_m{}^j, \tag{4.3.19}$$

$$(G_R^a)_j{}^i = g_a R^m{}_j (\boldsymbol{T^a})_m{}^k R_k{}^i. \tag{4.3.20}$$

In matrix form, Eqs. (4.3.19) and (4.3.20) read: $G_L^a = g_a L^\dagger \boldsymbol{T^a} L$ and $G_R^a = g_a R^\dagger \boldsymbol{T^a} R$ (no sum over a). For values of a corresponding to the neutral gauge fields, G_L^a and G_R^a are hermitian matrices. The corresponding Feynman rules for the gauge interactions of Dirac fermions are shown in Fig. 4.3.3. Note that χ_i with its arrow pointing out of the vertex and η^i with its arrow pointing into the vertex represent the same Dirac fermion.

Finally, consider the interaction of a charged vector boson W (with U(1)-charge q_W) with a fermion pair consisting of one Majorana and one Dirac fermion. As before, we denote the Majorana fermion by ξ_i and the Dirac fermion pair by χ_j and η^j (with U(1)-charges q_j and $-q_j$, respectively). All fields are assumed to be in the mass-eigenstate basis. The interaction Lagrangian is given by[42]:

$$\mathscr{L}_{\rm int} = -W_\mu [(G_1)_j{}^i \chi^{\dagger j} \overline\sigma^\mu \xi_i - (G_2)_{ij} \xi^{\dagger i} \overline\sigma^\mu \eta^j] - W_\mu^\dagger [(G_1)^j{}_i\, \xi^{\dagger i} \overline\sigma^\mu \chi_j - (G_2)^{ij} \eta_j^\dagger \overline\sigma^\mu \xi_i], \tag{4.3.21}$$

where G_1 and G_2 are arbitrary complex matrices, with $(G_1)^i{}_j \equiv [(G_1)_i{}^j]^*$ and $(G_2)^{ij} \equiv [(G_2)_{ij}]^*$, such that $(G_1)_j{}^i = (G_2)_{ij} = 0$ unless $q_W = q_j$. The interactions of Eq. (4.3.21) yield the Feynman rules exhibited in Fig. 4.3.4. Note that rules (c) and (d) are the complex conjugates of rules (a) and (b), respectively, corresponding to a reversal of the flow of the U(1)-charge through the interaction vertex.

In Figs. 4.3.2–4.3.4, two versions are given for each of the boson–fermion–fermion Feynman rules. The correct version to use depends in a unique way on the heights of indices used to connect each fermion line to the rest of the diagram. For example, the way of writing the vector-fermion–fermion interaction rule depends on whether we used $\psi^{\dagger i} \overline\sigma^\mu \psi_j$, or its equivalent form $-\psi_j \sigma^\mu \psi^{\dagger i}$, in Eq. (4.3.11). Note the different heights of the undotted and dotted spinor indices that adorn σ^μ and $\overline\sigma^\mu$. The choice of which rule to use is thus dictated by the height of the indices on the lines that connect to the vertex. These heights should always be chosen so that they are contracted as in Eq. (2.36).

The application of the rules of this subsection will be exhibited in Section 4.5. Many additional examples involving Standard Model and MSSM processes can be found in Section 6.

[42] The sign in front of G_2 is conventionally chosen to match the sign of the term proportional to G_R^a in Eq. (4.3.18).

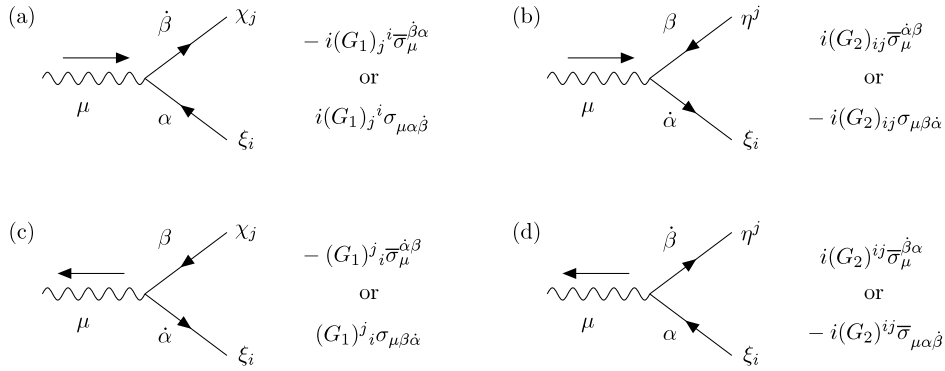

Fig. 4.3.4. The Feynman rules for the interactions of a charged vector boson (with U(1)-charge q_W) with a fermion pair consisting of one Majorana fermion ξ_i and one Dirac fermion formed by χ_j and η^j (with corresponding U(1)-charges q_j and $-q_j$). The fermion lines are labeled by the corresponding two-component left-handed $(\frac{1}{2}, 0)$ fermion fields. The matrix couplings G_1 and G_2 are defined in Eq. (4.3.21). Note that $(G_1)_j{}^i = (G_2)_{ij} = 0$ unless $q_W = q_j$. The arrows indicate the direction of flow of the U(1)-charges of the fermion and boson fields.

4.4. General structure and rules for Feynman graphs

When computing an amplitude for a given process, all possible diagrams should be drawn that conform with the rules given in Sections 4.1–4.3 for external wave functions, propagators, and interactions, respectively. Starting from any external wave function spinor (or from any vertex on a fermion loop), factors corresponding to each propagator and vertex should be written down from left to right, following the line until it ends at another external state wave function (or at the original point on the fermion loop). If one starts a fermion line at an x or y external state spinor, it should have a raised undotted index in accord with Eq. (2.36). Or, if one starts with an $x^\dagger$ or $y^\dagger$, it should have a lowered dotted spinor index. Then, all spinor indices should always be contracted as in Eq. (2.36). If one ends with an x or y external state spinor, it will have a lowered undotted index, while if one ends with an $x^\dagger$ or $y^\dagger$ spinor, it will have a raised dotted index. For arrow-preserving fermion propagators and gauge vertices, the preceding determines whether the σ or $\overline\sigma$ rule should be used.

With only a little practice, one can write down amplitudes immediately with all spinor indices suppressed. In particular, the following must be satisfied:

- For any scattering matrix amplitude, factors of σ and $\overline\sigma$ must alternate. If one or more factors of σ and/or $\overline\sigma$ are present, then x and y must be followed [preceded] by a σ [$\overline\sigma$], and $x^\dagger$ and $y^\dagger$ must be followed [preceded] by a $\overline\sigma$ [σ]. (4.4.1)

These requirements automatically dictate whether the σ or $\overline\sigma$ version of the rule for arrow-preserving fermion propagators and gauge vertices are employed in any tree-level Feynman diagram. In loop diagrams, we must add one further requirement that governs the order of the σ and $\overline\sigma$ factors as one traverses around the loop.

- Arrow-preserving propagator lines must be traversed in a direction parallel [anti-parallel] to the arrowed line segment for the $\overline\sigma$ [σ] version of the propagator rule.[43] (4.4.2)

For fermion lines that are not closed loops, this last requirement is realized automatically provided that the requirements of Eq. (4.4.1) are satisfied. However, for closed fermion loops, one must use the correct fermion propagator corresponding to the direction around the loop one has chosen to follow in writing down the spinor trace with suppressed indices. For example, having employed a σ [$\overline\sigma$] rule at one vertex attached to the loop, one must then traverse the loop from that vertex point in a direction parallel [antiparallel] to the arrow-preserving propagator lines in the loop. Indeed, this rule is crucial for obtaining the correct sign for the triangle anomaly calculation in Section 6.26.

Symmetry factors for identical particles are implemented in the usual way. Fermi–Dirac statistics are implemented by the following rules:

- Each closed fermion loop gets a factor of -1.
- A relative minus sign is imposed between terms contributing to a given amplitude whenever the ordering of external state spinors (written left-to-right in a formula) differs by an odd permutation.

Amplitudes generated according to these rules will contain objects of the form:

$$a = z_1 \Sigma z_2 \tag{4.4.3}$$

[43] This rule is simply a consequence of the order of the spinor indices in Fig. 4.2.2, as noted in Section 4.2.

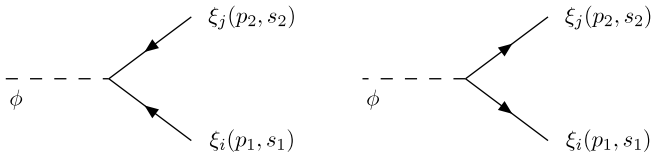

Fig. 4.5.1. The two tree-level Feynman diagrams contributing to the decay of a neutral scalar into a pair of Majorana fermions.

where z_1 and z_2 are each commuting external spinor wave functions x, $x^\dagger$, y, or $y^\dagger$, and Σ is a sequence of alternating σ and $\overline{\sigma}$ matrices. The complex conjugate of this quantity is obtained by applying the results of Eqs. (2.43)–(2.47), and is given by[44]

$$a^* = z_2^\dagger \Sigma_r z_1^\dagger \tag{4.4.4}$$

where Σ_r is obtained from Σ by reversing the order of all the σ and $\overline{\sigma}$ matrices, and using the same rule for suppressed spinor indices. [Notice that this rule for taking complex conjugates has the same form as for anticommuting spinors; cf. Eqs. (2.43)–(2.47).] We emphasize that in principle, it does not matter in what direction a diagram is traversed while applying the rules. However, for each diagram one must include a sign that depends on the ordering of the external fermions. This sign can be fixed by first choosing some canonical ordering of the external fermions. Then for any graph that contributes to the process of interest, the corresponding sign is positive (negative) if the ordering of external fermions is an even (odd) permutation with respect to the canonical ordering. If one chooses a different canonical ordering, then the resulting amplitude changes by an overall phase (is unchanged) if this ordering is an odd (even) permutation of the original canonical ordering.[45] This is consistent with the fact that the S-matrix element is only defined up to an overall sign, which is not physically observable.[46]

Note that different graphs contributing to the same process will often have different external state wave function spinors, with different arrow directions, for the same external fermion. Furthermore, there are no arbitrary choices to be made for arrow directions, as there are in some four-component Feynman rules for Majorana fermions (as discussed in Appendix G). Instead, one must add together *all* Feynman graphs that obey the rules.

4.5. Basic examples of writing down diagrams and amplitudes

Some simple examples will help clarify the rules of Section 4.4. In the tree-level Feynman graphs of this subsection, we label all two-component fermion lines by their corresponding left-handed $(\frac{1}{2}, 0)$ fields. (We shall propose a slightly different labeling convention in Section 5.) A larger number of examples, drawn from practical calculations, are given in Section 6.

4.5.1. Scalar boson decay to fermion pairs

Let us first consider a theory with a multiplet of uncharged, massive $(\frac{1}{2}, 0)$ fermions ξ_i, and a real scalar ϕ, with interaction

$$\mathscr{L}_{\rm int} = -\tfrac{1}{2}\left(\lambda^{ij}\xi_i\xi_j + \lambda_{ij}\xi^{\dagger i}\xi^{\dagger j}\right)\phi, \tag{4.5.1}$$

where $\lambda_{ij} \equiv (\lambda^{ij})^*$ and $\lambda^{ij} = \lambda^{ji}$. Consider the decay $\phi \to \xi_i(\vec{\boldsymbol{p}}_1, s_1)\xi_j(\vec{\boldsymbol{p}}_2, s_2)$ [for a fixed choice of i and j], where by $\xi_i(\vec{\boldsymbol{p}}, s)$ we mean the one-particle state given by Eq. (3.2.13).

Two diagrams contribute to this process, as shown in Fig. 4.5.1. The matrix element is:

$$\begin{aligned} i\mathcal{M} &= y(\vec{\boldsymbol{p}}_1, s_1)^\alpha(-i\lambda^{ij}\delta_\alpha{}^\beta)y(\vec{\boldsymbol{p}}_2, s_2)_\beta + x^\dagger(\vec{\boldsymbol{p}}_1, s_1)_{\dot\alpha}(-i\lambda_{ij}\delta^{\dot\alpha}{}_{\dot\beta})x^\dagger(\vec{\boldsymbol{p}}_2, s_2)^{\dot\beta} \\ &= -i\lambda^{ij}y(\vec{\boldsymbol{p}}_1, s_1)y(\vec{\boldsymbol{p}}_2, s_2) - i\lambda_{ij}x^\dagger(\vec{\boldsymbol{p}}_1, s_1)x^\dagger(\vec{\boldsymbol{p}}_2, s_2). \end{aligned} \tag{4.5.2}$$

The second line could be written down directly by recalling that the sum over suppressed spinor indices is taken according to Eq. (2.36). Note that if we reverse the ordering for the external fermions, the overall sign of the amplitude changes sign. This is easily checked, since for the commuting spinor wave functions (x and y), the spinor products in Eq. (4.5.2) change

---

44 For Lorentz scalar quantities of the form given by Eq. (4.4.3), there is no distinction between complex conjugation and hermitian conjugation.

45 For a process with exactly two external fermions, it is convenient to apply the Feynman rules by starting from the same fermion external state in all diagrams. That way, all terms in the amplitude have the same canonical ordering of fermions and there are no additional minus signs between diagrams. However, if there are four or more external fermions, it often happens that there is no way to choose the same ordering of external state spinors for all graphs when the amplitude is written down. Then the relative signs between different graphs must be chosen according to the relative sign of the permutation of the corresponding external fermion spinors. This guarantees that the total amplitude is antisymmetric under the interchange of any pair of external fermions.

46 The S-matrix element is related to the invariant matrix element $\mathcal{M}_{fi}$ by $S_{fi} = \delta_{fi} + (2\pi)^4\delta^{(4)}(p_f - p_i)\,i\mathcal{M}_{fi}$, where p_f (p_i) is the total four-momentum of the final (initial) state. If $f \neq i$ (i.e. the final and initial states are distinct), then $\delta_{fi} = 0$ in which case the invariant matrix element is only defined up to an overall (unphysical) sign. However, if $f = i$, the most convenient choice for the canonical ordering of external fermions is the one that yields $\langle f|i\rangle = \delta_{fi}$ (with no extra minus sign), which then fixes the absolute sign of the invariant matrix element.

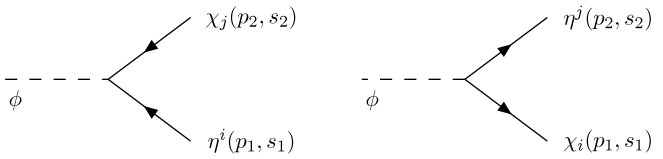

Fig. 4.5.2. The two tree-level Feynman diagrams contributing to the decay of a neutral scalar into a pair of Dirac fermions. The χ_i–η^i and χ_j–η^j pairs, each with oppositely directed arrows, comprise Dirac fermion states with flavor indices i and j, respectively.

sign when the order is reversed [see Eqs. (2.59) and (2.60)]. This overall sign is not significant and depends on the order used in constructing the two-particle state. One could even make the choice of starting the first diagram from fermion 1, and the second diagram from fermion 2:

$$i\mathcal{M} = -i\lambda^{ij}y(\vec{\boldsymbol{p}}_1, s_1)y(\vec{\boldsymbol{p}}_2, s_2) - (-1)i\lambda_{ij}x^\dagger(\vec{\boldsymbol{p}}_2, s_2)x^\dagger(\vec{\boldsymbol{p}}_1, s_1). \tag{4.5.3}$$

Here, the first term establishes the canonical ordering of fermions (12), and the contribution from the second diagram therefore includes the relative minus sign in parentheses. Indeed, Eqs. (4.5.2) and (4.5.3) are equal. In the computation of the total decay rate for the case of $i = j$, one must multiply the integral over the total phase space by $1/2$ to account for the identical particles.

Next, we consider a theory of a massive neutral scalar boson that couples to a multiplet of Dirac fermions. We denote the corresponding two-component fields by χ_i and η^i. For simplicity, we take all the U(1)-charges of the χ_i to be equal (and opposite to the charges of the η^i). The corresponding U(1)-invariant interaction is:

$$\mathscr{L}_{\rm int} = -(\kappa^i{}_j\chi_i\eta^j + \kappa_i{}^j\chi^{\dagger i}\eta_j^\dagger)\phi, \tag{4.5.4}$$

where $\kappa_i{}^j = (\kappa^i{}_j)^*$. Consider the decay $\phi \to f_i(\vec{\boldsymbol{p}}_1, s_1)\overline{f}^j(\vec{\boldsymbol{p}}_2, s_2)$ [for a fixed choice of i and j], where by $f(\vec{\boldsymbol{p}}, s)$ and $\overline{f}(\vec{\boldsymbol{p}}, s)$ we mean the one-particle states given by Eq. (3.2.22). Two diagrams contribute to this process, as shown in Fig. 4.5.2. Note that the outgoing fermion lines are distinguished by their U(1)-charges. The matrix element is then given by

$$i\mathcal{M} = -i\kappa^j{}_i y(\vec{\boldsymbol{p}}_1, s_1)y(\vec{\boldsymbol{p}}_2, s_2) - i\kappa_i{}^j x^\dagger(\vec{\boldsymbol{p}}_1, s_1)x^\dagger(\vec{\boldsymbol{p}}_2, s_2). \tag{4.5.5}$$

The matrix element for $\phi \to f_i(\vec{\boldsymbol{p}}_1, s_1)\overline{f}^j(\vec{\boldsymbol{p}}_2, s_2)$ is identical to that of $\phi \to \xi_i(\vec{\boldsymbol{p}}_1, s_1)\xi_j(\vec{\boldsymbol{p}}_2, s_2)$ after replacing λ^{ij} with $\kappa^i{}_j$. However for fixed $i = j$, the rate for scalar boson decay to $f_i\overline{f}^i$ is twice that of $\xi_i\xi_i$ due to the final state identical particles in the latter case, as noted above. One also arrives at the same conclusion if one treats a single Dirac fermion as a pair of mass-degenerate two-component fields ξ_1 and ξ_2 [cf. Eq. (3.2.15)]. Due to the U(1)-symmetry, the scalar Yukawa interactions are diagonal in the ξ_1–ξ_2 basis, so the rate for scalar decay into the Dirac fermion pair is equal to the incoherent sum of the rate for decay into $\xi_1\xi_1$ and $\xi_2\xi_2$.

4.5.2. Fermion pair annihilation into a scalar boson

It is also instructive to consider the corresponding $2 \to 1$ scattering (annihilation) processes $\xi(\vec{\boldsymbol{p}}_1, s_1)\xi(\vec{\boldsymbol{p}}_2, s_2) \to \phi$ and $f(\vec{\boldsymbol{p}}_1, s_1)\overline{f}(\vec{\boldsymbol{p}}_2, s_2) \to \phi$, respectively. The corresponding amplitudes are given by Eqs. (4.5.2) and (4.5.5) with $y \to x$ and $x^\dagger \to y^\dagger$ (for simplicity, we neglect flavor). In the computation of the cross-sections, there is no extra factor required to account for the case of identical particles in the initial state. That is, the cross-section for $f(\vec{\boldsymbol{p}}_1, s_1)\overline{f}(\vec{\boldsymbol{p}}_2, s_2) \to \phi$ is equal to the cross-section for $\xi(\vec{\boldsymbol{p}}_1, s_1)\xi(\vec{\boldsymbol{p}}_2, s_2) \to \phi$ after replacing λ with κ.

This may at first seem puzzling given that a Dirac fermion can be represented by a pair of mass-degenerate two-component fields χ_1 and χ_2. But, recall the standard procedure for the calculation of decay rates and cross-sections in field theory—*average over unobserved degrees of freedom of the initial state and sum over unobserved degrees of freedom of the final state*. This mantra is well known for dealing with spin and color degrees of freedom, but it is also applicable to degrees of freedom associated with global internal symmetries. Thus, the cross-section for the annihilation of a Dirac fermion pair into a neutral scalar boson can be obtained by computing the *average* of the cross-sections for $\xi_1(\vec{\boldsymbol{p}}_1, s_1)\xi_1(\vec{\boldsymbol{p}}_2, s_2) \to \phi$ and $\xi_2(\vec{\boldsymbol{p}}_1, s_1)\xi_2(\vec{\boldsymbol{p}}_2, s_2) \to \phi$. Since the annihilation cross-sections for $\xi_1\xi_1$ and $\xi_2\xi_2$ are equal, we confirm the annihilation cross-section for the Dirac fermion pair obtained above in the χ–η basis. Since the latter is conceptually simpler, subsequent computations involving Dirac fermions will be performed in the χ–η basis.

The annihilation rate of fermions enters in the analysis of the event flux due to the annihilation of dark matter in the halo of our galaxy. Let us compare the rates in the case that the dark matter is either a Majorana or a Dirac fermion. Suppose the annihilation involves two fermions whose number densities are n_1 and n_2 respectively. Then the observer on Earth who integrates along the line of sight to the annihilation events that are detected sees a flux of events proportional to [152]

$$\frac{{\rm d}N_{\rm events}}{{\rm d}A\,{\rm d}t} \sim \int n_1 n_2 \,\langle\sigma_{\rm ann} v_{\rm rel}\rangle\,{\rm d}\ell, \tag{4.5.6}$$

where $v_{\rm rel}$ is the relative velocity of the annihilating initial state particles, $\sigma_{\rm ann}$ is the annihilation cross-section and $\langle\cdots\rangle$ refers to a thermal average [153] over the velocity distribution of dark matter particles in the halo. We now compare the

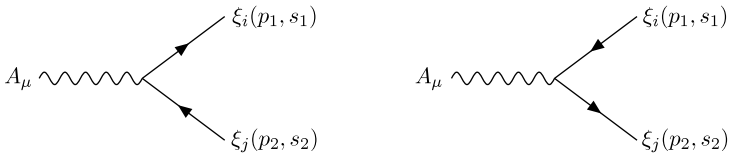

Fig. 4.5.3. The two tree-level Feynman diagrams contributing to the decay of a massive neutral vector boson A_μ into a pair of Majorana fermions.

case of the annihilation of a single species of Majorana particles and the annihilation of a Dirac fermion–antifermion pair (assumed to have the same mass and couplings). We assume that the number density of Dirac fermions and antifermions and the corresponding number density of Majorana fermions are all the same (and denoted by n). Above, we showed that $\sigma_{\rm ann}$ is the same for the annihilation of a single species of Majorana and Dirac fermions. For the Dirac case, $n_1 n_2 = n^2$. For the Majorana case, because the Majorana fermions are identical particles, given N initial state fermions in a volume V, there are $N(N-1)/2$ possible scatterings. In the thermodynamic limit where $N, V \to \infty$ at fixed $n \equiv N/V$, we conclude that $n_1 n_2 = \frac{1}{2}n^2$ for a single species of annihilating Majorana fermions.[47] Hence the event flux rate for the annihilation of a Dirac fermion–antifermion pair is double that of a single species of Majorana fermions.[48] The extra factor of $1/2$ can also be understood by noting that in the case of annihilating dark matter particles (in the large N limit), all possible scattering axes occur and are implicitly integrated over. But, integrating over 4π steradians double counts the annihilation of identical particles (in the same way it does in the computation of the decay rate of a scalar into identical fermions discussed above). Hence, one must include a factor of $\frac{1}{2}$ in this case by replacing $n_1 n_2 = n^2$ by $\frac{1}{2}n^2$ in Eq. (4.5.6).

The relic abundance of primordial dark matter particles in the universe is inversely proportional to $\langle \sigma_{\rm ann} v_{\rm rel} \rangle$ [155]. By similar arguments to the ones just presented, it follows that the relic abundance of a single species of Majorana fermions would be twice that of a single species of Dirac fermions.

4.5.3. Vector boson decay into fermion pairs

Consider next the decay of a massive neutral vector boson A_μ into a pair of Majorana fermions, $A_\mu \to \xi_i(\vec{\boldsymbol{p}}_1, s_1)\xi_j(\vec{\boldsymbol{p}}_2, s_2)$, following from the interaction,

$$\mathscr{L}_{\rm int} = -G_i^j A^\mu \xi^{\dagger i} \overline{\sigma}_\mu \xi_j, \tag{4.5.7}$$

where G is an hermitian coupling matrix. The two diagrams shown in Fig. 4.5.3 contribute.

We start from the fermion with momentum p_1 and spin vector s_1 and end at the fermion with momentum p_2 and spin vector s_2, using the rules of Fig. 4.3.2. The resulting amplitude for the decay is

$$i\mathcal{M} = \varepsilon^\mu \left[-iG_i^j x^\dagger(\vec{\boldsymbol{p}}_1, s_1)\overline{\sigma}_\mu y(\vec{\boldsymbol{p}}_2, s_2) + iG_j{}^i y(\vec{\boldsymbol{p}}_1, s_1)\sigma_\mu x^\dagger(\vec{\boldsymbol{p}}_2, s_2) \right], \tag{4.5.8}$$

where ε^μ is the vector boson polarization vector. We have used the $\overline{\sigma}$-version of the vector-fermion–fermion rule [see Fig. 4.3.2] for the first diagram of Fig. 4.5.3 and the σ-version for the second diagram of Fig. 4.5.3, as dictated by the implicit spinor indices, which we have suppressed. However, we could have chosen to evaluate the second diagram of Fig. 4.5.3 using the $\overline{\sigma}$-version of the vector-fermion–fermion rule by starting from the fermion with momentum p_2 and spin vector s_2. In that case, the term $iG_j{}^i y(\vec{\boldsymbol{p}}_1, s_1)\sigma_\mu x^\dagger(\vec{\boldsymbol{p}}_2, s_2)$ in Eq. (4.5.8) is replaced by

$$(-1)[-iG_j{}^i x^\dagger(\vec{\boldsymbol{p}}_2, s_2)\overline{\sigma}_\mu y(\vec{\boldsymbol{p}}_1, s_1)]. \tag{4.5.9}$$

In Eq. (4.5.9), the factor of $-iG_j{}^i$ arises from the use of the $\overline{\sigma}$-version of the vector-fermion–fermion rule, and the overall factor of -1 appears because the order of the fermion wave functions has been reversed; i.e. (21) is an odd permutation of (12). This is in accord with the ordering rule stated at the end of Section 4.4. Thus, the resulting amplitude for the decay of the vector boson into the pair of Majorana fermions now takes the form:

$$i\mathcal{M} = \varepsilon^\mu \left[-iG_i^j x^\dagger(\vec{\boldsymbol{p}}_1, s_1)\overline{\sigma}_\mu y(\vec{\boldsymbol{p}}_2, s_2) + iG_j{}^i x^\dagger(\vec{\boldsymbol{p}}_2, s_2)\overline{\sigma}_\mu y(\vec{\boldsymbol{p}}_1, s_1) \right], \tag{4.5.10}$$

which coincides with Eq. (4.5.8) after using $y\sigma^\mu x^\dagger = x^\dagger \overline{\sigma}^\mu y$ [cf. Eq. (2.61) with commuting spinors]. Eq. (4.5.10) explicitly exhibits the property that the amplitude is antisymmetric under the interchange of the two external identical fermions. Again, the absolute sign of the total amplitude is not significant and depends on the choice of ordering of the outgoing states.

Next, we consider the decay of a massive neutral vector boson into a pair of Dirac fermions. Each Dirac fermion is described by the two-component fields χ_i and η^i, which possess equal and opposite U(1)-charges, respectively. The corresponding interaction Lagrangian is given by:

$$\mathscr{L}_{\rm int} = -A^\mu [(G_L)_i{}^j \chi^{\dagger i} \overline{\sigma}_\mu \chi_j - (G_R)_j{}^i \eta_i^\dagger \overline{\sigma}_\mu \eta^j], \tag{4.5.11}$$

where G_L and G_R are hermitian. There are two contributing graphs, as shown in Fig. 4.5.4.

47 The factor of $1/2$, which has been erroneously omitted in many papers in the literature, was correctly employed and explained in Ref. [154].

48 This is also consistent with the interpretation of a Dirac fermion as a pair of mass-degenerate Majorana fermions.

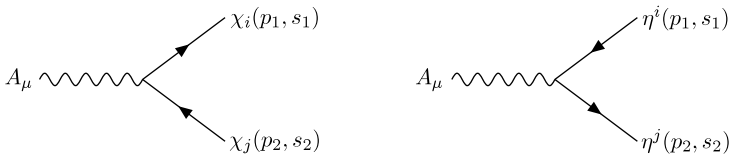

Fig. 4.5.4. The two tree-level Feynman diagrams contributing to the decay of a massive neutral vector boson A_μ into a pair of Dirac fermions. The χ_i–η^i and χ_j–η^j pairs, each with oppositely directed arrows, comprise Dirac fermion states with flavor indices i and j, respectively.

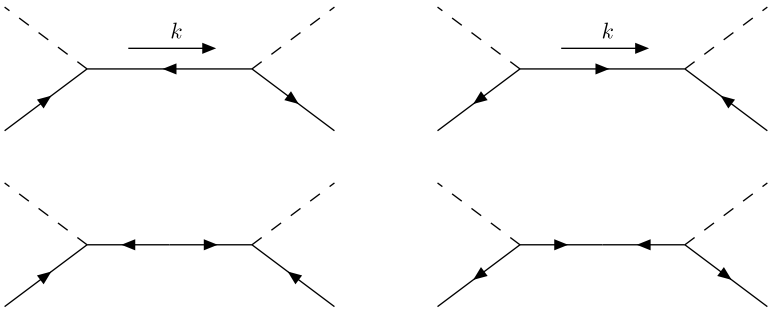

Fig. 4.5.5. Tree-level Feynman diagrams contributing to the elastic scattering of a neutral scalar and a Majorana fermion. There are four more diagrams, obtained from these by crossing the initial and final scalar lines.

To evaluate the amplitude, we start with the fermion of momentum p_1 and spin vector s_1, and end at the fermion with momentum p_2 and spin vector s_2. Note that the outgoing χ_i with the arrow pointing outward from the vertex and the outgoing η^i with the arrow pointing inward to the vertex both correspond to the same outgoing Dirac fermion. The amplitude for the decay is given by:

$$\begin{aligned} i\mathcal{M} &= \varepsilon^\mu \left[-i(G_L)_i{}^j x^\dagger(\vec{\boldsymbol{p}}_1, s_1)\overline{\sigma}_\mu y(\vec{\boldsymbol{p}}_2, s_2) - i(G_R)_i{}^j y(\vec{\boldsymbol{p}}_1, s_1)\sigma_\mu x^\dagger(\vec{\boldsymbol{p}}_2, s_2)\right] \\ &= \varepsilon^\mu \left[-i(G_L)_i{}^j x^\dagger(\vec{\boldsymbol{p}}_1, s_1)\overline{\sigma}_\mu y(\vec{\boldsymbol{p}}_2, s_2) - i(G_R)_i{}^j x^\dagger(\vec{\boldsymbol{p}}_2, s_2)\overline{\sigma}_\mu y(\vec{\boldsymbol{p}}_1, s_1)\right]. \end{aligned} \tag{4.5.12}$$

As in the case of the decay to a pair of Majorana fermions, we have exhibited a second form for the amplitude in Eq. (4.5.12) in which the $\overline{\sigma}$-version of the vertex Feynman rule has been employed in both diagrams. Of course, the resulting amplitude must be the same in each method (up to a possible overall sign of the total amplitude that is not determined).

The computation of the amplitude for the decay of a charged vector boson to a fermion pair consisting of one Majorana fermion and one Dirac fermion, due to the interactions given in Eq. (4.3.21), is straightforward and will not be given explicitly here.

4.5.4. Two-body scattering of a boson and a neutral fermion

The next level of complexity consists of diagrams that involve fermion propagators. In the examples that follow in this and in the next subsection, we shall ignore the flavor index and consider scattering processes that involve a single flavor of Majorana or Dirac fermion. For our first example of this type, consider the tree-level matrix element for the scattering of a neutral scalar and a two-component neutral massive fermion ($\phi\xi \to \phi\xi$), with the interaction Lagrangian given above in Eq. (4.5.1). Using the corresponding Feynman rules, there are eight contributing diagrams. Four are depicted in Fig. 4.5.5; there are another four diagrams (not shown) where the initial and final state scalars are crossed (i.e., the initial state scalar is attached to the same vertex as the final state fermion).

We shall write down the amplitudes for the four diagrams shown in Fig. 4.5.5, starting with the final state fermion line and moving toward the initial state fermion line. Then,

$$\begin{aligned} i\mathcal{M} = \frac{i}{k^2 - m_\xi^2} &\left\{(-i\lambda)(-i\lambda^*)\left[x^\dagger(\vec{\boldsymbol{p}}_2, s_2)\,\overline{\sigma}\cdot k\, x(\vec{\boldsymbol{p}}_1, s_1) + y(\vec{\boldsymbol{p}}_2, s_2)\,\sigma\cdot k\, y^\dagger(\vec{\boldsymbol{p}}_1, s_1)\right]\right. \\ &\left. + m_\xi\left[(-i\lambda)^2 y(\vec{\boldsymbol{p}}_2, s_2)x(\vec{\boldsymbol{p}}_1, s_1) + (-i\lambda^*)^2 x^\dagger(\vec{\boldsymbol{p}}_2, s_2)y^\dagger(\vec{\boldsymbol{p}}_1, s_1)\right]\right\} + (\text{crossed}), \end{aligned} \tag{4.5.13}$$

where k^μ is the sum of the two incoming (or outgoing) four-momenta, (p_1, s_1) are the momentum and spin four-vectors of the incoming fermion, and (p_2, s_2) are those of the outgoing fermion. The notation "(crossed)" refers to the contribution to the amplitude from diagrams which have the initial and final scalars interchanged. Note that we could have evaluated the diagrams above by starting with the initial vertex and moving toward the final vertex. It is easy to check that the resulting amplitude is the negative of the one obtained in Eq. (4.5.13); the overall sign change simply corresponds to swapping the order of the two fermions and has no physical consequence. The overall minus sign is a consequence of Eqs. (2.59)–(2.61) and the minus sign difference between the two ways of evaluating the propagator that preserves the arrow direction.

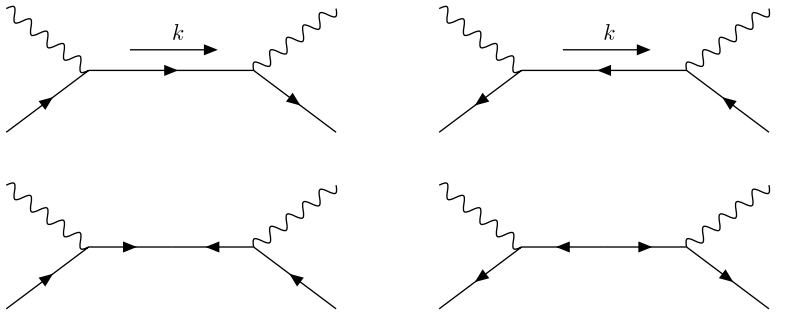

Fig. 4.5.6. Tree-level Feynman diagrams contributing to the elastic scattering of a neutral vector boson and a Majorana fermion. There are four more diagrams, obtained from these by crossing the initial and final scalar lines.

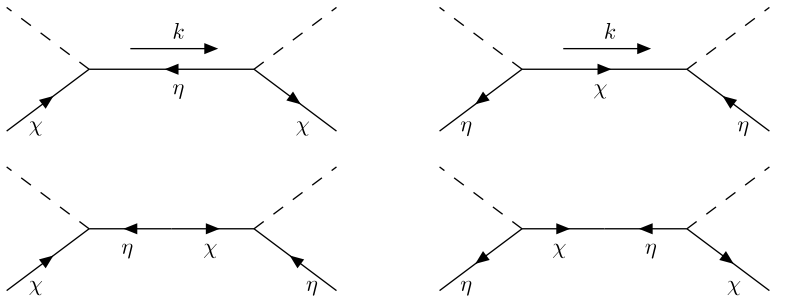

Fig. 4.5.7. Tree-level Feynman diagrams contributing to the elastic scattering of a neutral scalar and a charged fermion. There are four more diagrams, obtained from these by crossing the initial and final scalar lines.

Next, we compute the tree-level matrix element for the scattering of a neutral vector boson and a neutral massive two-component fermion ξ with the interaction Lagrangian of Eq. (4.5.7). Again there are eight diagrams: the four diagrams depicted in Fig. 4.5.6 plus another four (not shown) where the initial and final state vector bosons are crossed.

Starting with the final state fermion line and moving toward the initial state, we obtain

$$i\mathcal{M} = \frac{i}{k^2 - m_\xi^2}\left\{(-iG)^2 x^\dagger(\vec{\boldsymbol{p}}_2, s_2)\,\overline{\sigma}\cdot\varepsilon_2^*\,\sigma\cdot k\,\overline{\sigma}\cdot\varepsilon_1\,x(\vec{\boldsymbol{p}}_1, s_1) + (iG)^2 y(\vec{\boldsymbol{p}}_2, s_2)\,\sigma\cdot\varepsilon_2^*\,\overline{\sigma}\cdot k\,\sigma\cdot\varepsilon_1 y^\dagger(\vec{\boldsymbol{p}}_1, s_1)\right.$$
$$\left. + (-iG)(iG)m_\xi\left[y(\vec{\boldsymbol{p}}_2, s_2)\,\sigma\cdot\varepsilon_2^*\,\overline{\sigma}\cdot\varepsilon_1\,x(\vec{\boldsymbol{p}}_1, s_1) + x^\dagger(\vec{\boldsymbol{p}}_2, s_2)\,\overline{\sigma}\cdot\varepsilon_2^*\,\sigma\cdot\varepsilon_1\,y^\dagger(\vec{\boldsymbol{p}}_1, s_1)\right]\right\} + (\text{crossed}), \tag{4.5.14}$$

where ε_1 and ε_2 are the initial and final vector boson polarization four-vectors, respectively. As before, k^μ is the sum of the two incoming (or outgoing) four-momenta, (p_1, s_1) and (p_2, s_2) are the momentum and spin four-vectors of the incoming and outgoing fermions, respectively, and "(crossed)" indicates the terms from diagrams in which the initial and final vector bosons are interchanged. Alternatively, if one starts with an initial state fermion and moves toward the final state, the resulting amplitude is the negative of the one obtained in Eq. (4.5.14), as expected.

The computation of the amplitude for the scattering of a charged scalar or vector boson and a Majorana fermion is straightforward and will not be given explicitly here.

4.5.5. Two-body scattering of a boson and a charged fermion

We first consider the scattering of a Dirac fermion with a neutral scalar. We denote the Dirac mass of the fermion by m_D. The left-handed fields χ and η have opposite charges (which we take to be $Q = +1$ and -1 respectively), and interact with the scalar ϕ according to

$$\mathscr{L}_{\text{int}} = -\phi[\kappa\,\chi\,\eta + \kappa^*\chi^\dagger\eta^\dagger], \tag{4.5.15}$$

where κ is a coupling parameter. Then, for the elastic scattering of the $Q = +1$ fermion and a scalar, the diagrams of Fig. 4.5.7 contribute at tree level plus another four diagrams (not shown) where the initial and final state scalars are crossed. Now, these diagrams match precisely those of Fig. 4.5.5. Thus, applying the Feynman rules yields the same matrix element, Eq. (4.5.13), previously obtained for the scattering of a neutral scalar and neutral two-component fermion, with the replacement of λ with κ and m_ξ with m_D.

We next examine the scattering of a Dirac fermion and a charged scalar, where both the scalar and fermion have the same absolute value of the charge. As above, we denote the charged $Q = \pm 1$ fermion by the pair of two-component fermions χ and η and the (intermediate state) neutral two-component fermion by ξ. The charged $Q = \pm 1$ scalar is represented by the

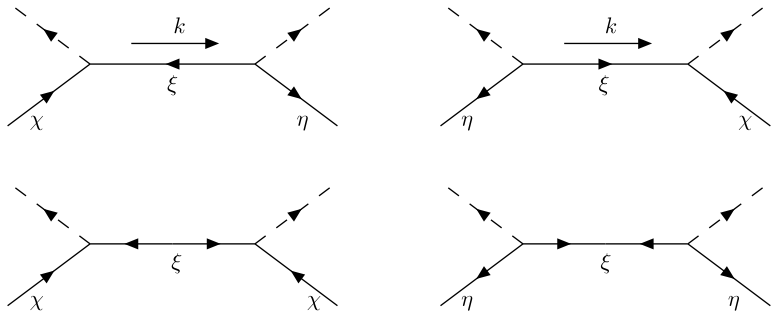

Fig. 4.5.8. Tree-level Feynman diagrams contributing to the scattering of an initial charged scalar and a charged fermion into its charge-conjugated final state. The unlabeled intermediate state is a neutral fermion. There are four more diagrams, obtained from these by crossing the initial and final scalar lines.

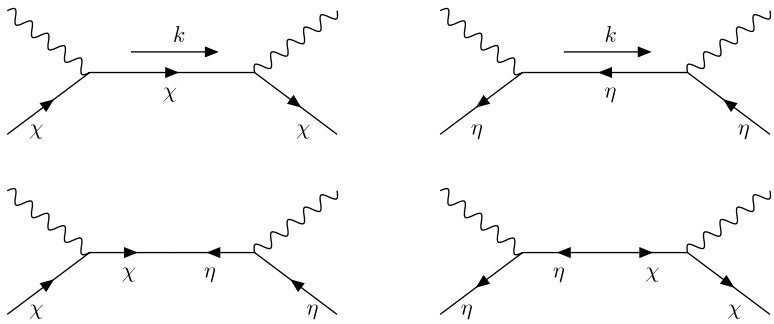

Fig. 4.5.9. Tree-level Feynman diagrams contributing to the elastic scattering of a neutral vector boson and a Dirac fermion. There are four more diagrams, obtained from these by crossing the initial and final vector lines.

complex scalar field Φ and its hermitian conjugate. The interaction Lagrangian takes the form:

$$\mathscr{L}_{\rm int} = -\Phi[\kappa_1\eta\xi + \kappa_2^*\chi^\dagger\xi^\dagger] - \Phi^\dagger[\kappa_2\chi\xi + \kappa_1^*\eta^\dagger\xi^\dagger]. \tag{4.5.16}$$

Consider the scattering of an initial boson–fermion state into its charge-conjugated final state via the exchange of a neutral fermion. The relevant diagrams are shown in Fig. 4.5.8 plus the corresponding diagrams with the initial and final scalars crossed. We define the four-momentum k to be the sum of the two initial state four-momenta as shown in Fig. 4.5.8. The derivation of the amplitude is similar to the ones given previously, and we end up with

$$\begin{aligned} i\mathcal{M} = \frac{-i}{k^2 - m_\xi^2} &\left\{\kappa_1^*\kappa_2[x^\dagger(\vec{\boldsymbol{p}}_2, s_2)\,\overline{\sigma}\cdot k\, x(\vec{\boldsymbol{p}}_1, s_1) + y(\vec{\boldsymbol{p}}_2, s_2)\,\sigma\cdot k\, y^\dagger(\vec{\boldsymbol{p}}_1, s_1)]\right. \\ &\left. + m_\xi\left[\kappa_2^2 y(\vec{\boldsymbol{p}}_2, s_2)x(\vec{\boldsymbol{p}}_1, s_1) + (\kappa_1^*)^2 x^\dagger(\vec{\boldsymbol{p}}_2, s_2)y^\dagger(\vec{\boldsymbol{p}}_1, s_1)\right]\right\} + (\text{crossed}). \end{aligned} \tag{4.5.17}$$

The scattering of a charged fermion and a neutral spin-1 vector boson can be similarly treated. For example, consider the amplitude for the elastic scattering of a charged fermion of mass m_D and a neutral vector boson. Again taking the interactions as given in Eq. (4.5.11), the relevant diagrams are those shown in Fig. 4.5.9, plus four diagrams (not shown) obtained from these by crossing the initial and final state vector bosons. Applying the Feynman rules of Fig. 4.3.3, one obtains the following matrix element:

$$\begin{aligned} i\mathcal{M} = \frac{-i}{k^2 - m_D^2} &\left\{G_L^2 x^\dagger(\vec{\boldsymbol{p}}_2, s_2)\,\overline{\sigma}\cdot\varepsilon_2^*\,\sigma\cdot k\,\overline{\sigma}\cdot\varepsilon_1\, x(\vec{\boldsymbol{p}}_1, s_1) + G_R^2 y(\vec{\boldsymbol{p}}_2, s_2)\,\sigma\cdot\varepsilon_2^*\,\overline{\sigma}\cdot k\,\sigma\cdot\varepsilon_1 y^\dagger(\vec{\boldsymbol{p}}_1, s_1)\right. \\ &\left. + m_D G_L G_R\left[y(\vec{\boldsymbol{p}}_2, s_2)\,\sigma\cdot\varepsilon_2^*\,\overline{\sigma}\cdot\varepsilon_1\, x(\vec{\boldsymbol{p}}_1, s_1) + x^\dagger(\vec{\boldsymbol{p}}_2, s_2)\,\overline{\sigma}\cdot\varepsilon_2^*\,\sigma\cdot\varepsilon_1\, y^\dagger(\vec{\boldsymbol{p}}_1, s_1)\right]\right\} + (\text{crossed}), \end{aligned} \tag{4.5.18}$$

and the assignments of momenta and spins are as before.

The computation of the amplitude for the scattering of a charged fermion and a charged vector boson is straightforward and will not be given explicitly here.

4.5.6. Two-body fermion–fermion scattering

Finally, let us work out an example with four external state fermions. Consider the case of elastic scattering of two identical Majorana fermions due to scalar exchange, governed by the interaction of Eq. (4.5.1). The diagrams for scattering initial fermions labeled 1, 2 into final state fermions labeled 3, 4 are shown in Fig. 4.5.10.

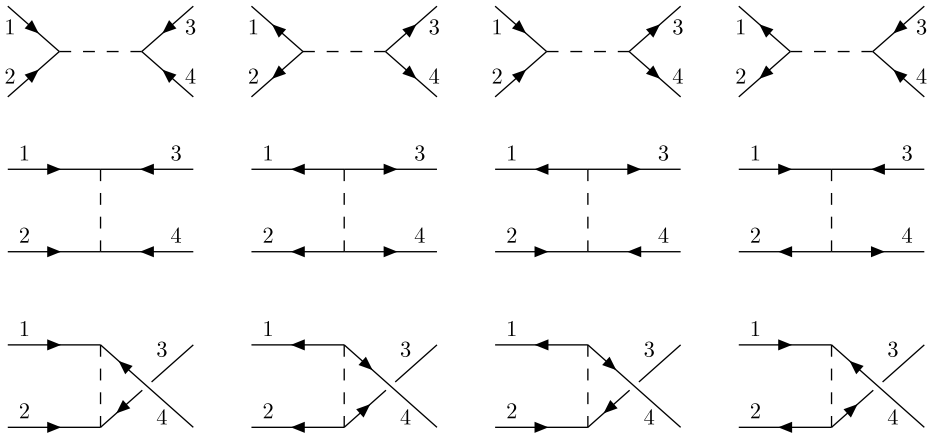

Fig. 4.5.10. Tree-level Feynman diagrams contributing to the elastic scattering of identical Majorana fermions via scalar exchange in the s-channel (top row), t-channel (middle row), and u-channel (bottom row).

The resulting invariant matrix element is:

$$
\begin{aligned}
i\mathcal{M} = {} & (-1)\frac{-i}{s-m_\phi^2}\left\{\lambda^2(x_1x_2)(y_3y_4)+(\lambda^*)^2(y_1^\dagger y_2^\dagger)(x_3^\dagger x_4^\dagger)+|\lambda|^2\left[(x_1x_2)(x_3^\dagger x_4^\dagger)+(y_1^\dagger y_2^\dagger)(y_3y_4)\right]\right\}\\
& +\frac{-i}{t-m_\phi^2}\left\{\lambda^2(y_3x_1)(y_4x_2)+(\lambda^*)^2(x_3^\dagger y_1^\dagger)(x_4^\dagger y_2^\dagger)+|\lambda|^2\left[(x_3^\dagger y_1^\dagger)(y_4x_2)+(y_3x_1)(x_4^\dagger y_2^\dagger)\right]\right\}\\
& +(-1)\frac{-i}{u-m_\phi^2}\left\{\lambda^2(y_4x_1)(y_3x_2)+(\lambda^*)^2(x_4^\dagger y_1^\dagger)(x_3^\dagger y_2^\dagger)+|\lambda|^2\left[(x_4^\dagger y_1^\dagger)(y_3x_2)+(y_4x_1)(x_3^\dagger y_2^\dagger)\right]\right\},
\end{aligned}
\tag{4.5.19}
$$

where $x_i \equiv x(\vec{\boldsymbol{p}}_i, s_i)$, $y_i \equiv y(\vec{\boldsymbol{p}}_i, s_i)$, m_ϕ is the mass of the exchanged scalar, $s=(p_1+p_2)^2$, $t=(p_1-p_3)^2$ and $u=(p_1-p_4)^2$. We have chosen the canonical ordering of external fermions to be 3142 (corresponding to the t-channel contribution). For elastic scattering, this choice of canonical ordering guarantees that if no scattering occurs then the S-matrix is just equal to the unit operator with no extraneous minus sign (cf. footnote 46). The relative minus signs between the t-channel diagram and the s and u-channel diagrams [shown in parentheses in Eq. (4.5.19)] are obtained by observing that both 1234 and 4132 are both odd permutations of 3142. Note that we would have obtained the same relative signs for the u-channel diagrams had we crossed the initial state fermion lines instead of the final state fermion lines.

Eq. (4.5.19) can be factorized with respect to the scalar line:

$$
\begin{aligned}
i\mathcal{M} = {} & \frac{i}{s-m_\phi^2}(\lambda x_1x_2+\lambda^* y_1^\dagger y_2^\dagger)(\lambda y_3y_4+\lambda^* x_3^\dagger x_4^\dagger)+\frac{-i}{t-m_\phi^2}(\lambda y_3x_1+\lambda^* x_3^\dagger y_1^\dagger)(\lambda y_4x_2+\lambda^* x_4^\dagger y_2^\dagger)\\
& +\frac{i}{u-m_\phi^2}(\lambda y_4x_1+\lambda^* x_4^\dagger y_1^\dagger)(\lambda y_3x_2+\lambda^* x_3^\dagger y_2^\dagger).
\end{aligned}
\tag{4.5.20}
$$

This is a common feature of Feynman graphs with a virtual boson. This example also illustrates that in contrast to the four-component fermion formalism, the two-component fermion Feynman rules typically yield many more diagrams, but the contribution of each of the diagrams is correspondingly simpler.

4.5.7. Non-relativistic potential due to scalar or pseudoscalar exchange

Consider two distinguishable fermions, and a scalar-fermion–fermion Yukawa interaction given by Eq. (4.3.9). We can compute the force law that the fermions experience due to exchange of a spinless boson. That is, we shall derive the Yukawa potential as a function of the separation distance of the two fermions in the static limit.

To carry out this computation, we compute the invariant matrix element for two-body fermion–fermion elastic scattering in the non-relativistic limit. The relevant diagrams are shown in Fig. 4.5.10. As our two fermions are distinguishable, only the t-channel graphs (shown in the middle row of Fig. 4.5.10) are relevant. As a result, the matrix element for the elastic scattering of two Majorana fermions is given by the t-channel contribution of Eq. (4.5.20),

$$
i\mathcal{M} = \frac{i}{m_\phi^2-t}(\lambda y_3x_1+\lambda^* x_3^\dagger y_1^\dagger)(\lambda y_4x_2+\lambda^* x_4^\dagger y_2^\dagger).
\tag{4.5.21}
$$

The choice of the overall sign is fixed by the canonical ordering of the external fermions.[49] Although the two fermions are distinguishable, we have assumed for simplicity that their (complex) Yukawa coupling strengths are the same and given by λ. For the scattering of two distinguishable Dirac fermions, the resulting expression for the scattering amplitude is identical to Eq. (4.5.21), with λ replaced by the appropriate complex Yukawa coupling κ.

We denote the masses of the distinguishable fermions by m_1 and m_2. In the non-relativistic limit, $p_1 \simeq (m_1; \vec{\boldsymbol{p}}_1)$ and $p_3 \simeq (m_1; \vec{\boldsymbol{p}}_3)$, so that

$$m_\phi^2 - t \simeq |\vec{\boldsymbol{p}}_1 - \vec{\boldsymbol{p}}_3|^2 + m_\phi^2 \equiv |\vec{\boldsymbol{q}}|^2 + m_\phi^2, \tag{4.5.22}$$

where

$$\vec{\boldsymbol{q}} \equiv \vec{\boldsymbol{p}}_3 - \vec{\boldsymbol{p}}_1 = \vec{\boldsymbol{p}}_2 - \vec{\boldsymbol{p}}_4 \tag{4.5.23}$$

is the momentum-transfer three-vector. Two separate cases will be considered.

In the first case, λ is a real coupling. This corresponds to the exchange of a $J^{PC} = 0^{++}$ scalar. Using the non-relativistic forms of Eqs. (C.2.16) and (C.2.22) for the spinor bilinears, it is only necessary to keep the leading term. We then find:

$$i\mathcal{M} = \frac{4i|\lambda|^2 m_1 m_2}{|\vec{\boldsymbol{q}}|^2 + m_\phi^2} \delta_{s_1 s_3} \delta_{s_2 s_4}, \tag{4.5.24}$$

in agreement with Eq. (4.123) of Ref. [114].

In the second case, λ is purely imaginary, and we will write $\lambda = i|\lambda|$ (the overall sign is not significant). This corresponds to the exchange of a $J^{PC} = 0^{-+}$ pseudoscalar. Again, we use the non-relativistic forms of Eqs. (C.2.16) and (C.2.22) for the spinor bilinears. However, in this case the leading term cancels and we must retain the $\mathcal{O}(|\vec{\boldsymbol{p}}|/m)$ terms appearing in the non-relativistic limit of the spinor bilinears. In this case, we find

$$i\mathcal{M} = \frac{i|\lambda|^2}{|\vec{\boldsymbol{q}}|^2 + m_\phi^2} (\vec{\boldsymbol{q}} \cdot \hat{\boldsymbol{s}}^{\boldsymbol{a}} \tau^a_{s_3 s_1}) (\vec{\boldsymbol{q}} \cdot \hat{\boldsymbol{s}}^{\boldsymbol{b}} \tau^b_{s_4 s_2}). \tag{4.5.25}$$

We choose the spin quantization axis to lie along the z-direction. That is, according to Eq. (C.1.27), we choose

$$(\hat{\boldsymbol{s}}^1, \hat{\boldsymbol{s}}^2, \hat{\boldsymbol{s}}^3) = (\hat{\boldsymbol{x}}, \hat{\boldsymbol{y}}, \hat{\boldsymbol{z}}), \tag{4.5.26}$$

in which case one can rewrite Eq. (4.5.25) in the more traditional way,

$$i\mathcal{M} = \frac{i|\lambda|^2}{|\vec{\boldsymbol{q}}|^2 + m_\phi^2} (\vec{\boldsymbol{q}} \cdot \vec{\boldsymbol{\sigma}}_{s_3 s_1}) (\vec{\boldsymbol{q}} \cdot \vec{\boldsymbol{\sigma}}_{s_4 s_2}), \tag{4.5.27}$$

where $\vec{\boldsymbol{\sigma}} \equiv \hat{\boldsymbol{x}}\tau^1 + \hat{\boldsymbol{y}}\tau^2 + \hat{\boldsymbol{z}}\tau^3$ are the usual spin-1/2 Pauli matrices.[50] Thus, pseudoscalar exchange yields a spin-dependent force law.

The non-relativistic potential that arises from the t-channel scalar or pseudoscalar exchange is obtained by comparing the relativistic scattering amplitude $\mathcal{M}$ with the Born approximation for scattering off a potential $V(\vec{\boldsymbol{x}})$ in non-relativistic quantum mechanics. Taking into account the difference between the conventions for the normalization of relativistic and non-relativistic single-particle states, one finds that the static potential is given by [156]

$$V(\vec{\boldsymbol{x}}) = -\frac{1}{4m_1 m_2} \int \frac{\mathrm{d}^3 q}{(2\pi)^3} \mathcal{M}(\vec{\boldsymbol{q}}) e^{i\vec{\boldsymbol{q}}\cdot\vec{\boldsymbol{x}}}, \tag{4.5.28}$$

in a convention where the invariant amplitude is defined as in footnote 46. Inserting the scattering amplitude for scalar (S) exchange, one obtains the well-known attractive spin-independent Yukawa potential

$$V(\vec{\boldsymbol{x}})_{\mathrm{S}} = -\frac{|\lambda|^2}{4\pi r} e^{-m_\phi r} \delta_{s_1 s_3} \delta_{s_2 s_4}, \tag{4.5.29}$$

where $r \equiv |\vec{\boldsymbol{x}}|$. For the case of pseudoscalar (PS) exchange, one can easily evaluate the integral in Eq. (4.5.28) by writing $q_j q_k e^{i\vec{\boldsymbol{q}}\cdot\vec{\boldsymbol{x}}} = -\nabla_j \nabla_k e^{i\vec{\boldsymbol{q}}\cdot\vec{\boldsymbol{x}}}$. The end result is [157]:

$$\begin{aligned} V(\vec{\boldsymbol{x}})_{\mathrm{PS}} &= \frac{|\lambda|^2}{16\pi m_1 m_2} (\vec{\boldsymbol{\sigma}}_{s_3 s_1} \cdot \vec{\nabla})(\vec{\boldsymbol{\sigma}}_{s_4 s_2} \cdot \vec{\nabla}) \frac{e^{-m_\phi r}}{r} \\ &= \frac{|\lambda|^2 m_\phi^2}{16\pi m_1 m_2} \left\{ \left[-\frac{4\pi}{3m_\phi^2} \delta^{(3)}(\vec{\boldsymbol{x}}) + \frac{e^{-m_\phi r}}{r} \right] \vec{\boldsymbol{\sigma}}_{s_3 s_1} \cdot \vec{\boldsymbol{\sigma}}_{s_4 s_2} \right. \\ &\quad \left. + \left[\frac{1}{(m_\phi r)^2} + \frac{1}{(m_\phi r)} + \frac{1}{3} \right] \left[\frac{3(\vec{\boldsymbol{\sigma}}_{s_3 s_1} \cdot \vec{\boldsymbol{x}})(\vec{\boldsymbol{\sigma}}_{s_4 s_2} \cdot \vec{\boldsymbol{x}})}{r^2} - \vec{\boldsymbol{\sigma}}_{s_3 s_1} \cdot \vec{\boldsymbol{\sigma}}_{s_4 s_2} \right] \frac{e^{-m_\phi r}}{r} \right\}, \end{aligned} \tag{4.5.30}$$

[49] As noted in Section 4.5.6, the canonical ordering of the external fermions in two-body elastic scattering is determined by the requirement that $\langle f|i\rangle = +1$ for $f = i$ (cf. footnote 46).

[50] The subscripted spin labels on $\vec{\boldsymbol{\sigma}}$ should be interpreted in the same way as outlined in footnote 95.

where we have used [158]:

$$\nabla_i\nabla_j\left(\frac{1}{r}\right) = -\frac{4\pi}{3}\delta_{ij}\,\delta^{(3)}(\vec{\boldsymbol{x}}) + \frac{3x_ix_j - r^2\delta_{ij}}{r^5}. \tag{4.5.31}$$

4.6. Self-energy functions and pole masses for two-component fermions

In this section, we discuss the self-energy functions for fermions in two-component notation, taking into account the possibilities of loop-induced mixing and absorptive parts corresponding to decays to intermediate states. This formalism is useful in the computation of loop-corrected physical pole masses.

Consider a theory with left-handed fermion degrees of freedom $\hat{\psi}_i$ labeled by an index $i = 1, 2, \ldots, N$. Associated with each $\hat{\psi}_i$ is a right-handed fermion $\hat{\psi}^{\dagger i}$, where the flavor labels are treated as described below Eq. (3.2.2). The theory is assumed to contain arbitrary interactions, which we will not need to refer to explicitly. As discussed in Section 3.2, we diagonalize the fermion mass matrix and identify the fermion mass eigenstates ψ_i as indicated in Eq. (4.3.5). In general, the mass eigenstates consist of Majorana fermions ξ_k ($k = 1, \ldots N-2n$) and Dirac fermion pairs χ_ℓ and η_ℓ ($\ell = 1, \ldots, n$).[51] With respect to this basis, the symmetric $N \times N$ tree-level fermion mass matrix, $\boldsymbol{m}^{ij}$, is made up of diagonal elements m_k and 2×2 blocks $\left(\begin{smallmatrix} 0 & m_\ell \\ m_\ell & 0 \end{smallmatrix}\right)$ along the diagonal, where the m_k and m_ℓ are real and non-negative. Since $\boldsymbol{m}^{ij}$ is real, the height of the flavor indices is not significant. Nevertheless, it is useful to define $\overline{\boldsymbol{m}}_{ij} \equiv \boldsymbol{m}^{ij}$ in order to maintain the convention that two repeated flavor indices are summed when one index is raised and the other is lowered.[52] Note that $\overline{\boldsymbol{m}}_{ik}\boldsymbol{m}^{kj} = \boldsymbol{m}^{ik}\overline{\boldsymbol{m}}_{kj} = m_i^2\delta_i^j$ is a diagonal matrix.

The full, loop-corrected Feynman propagators with four-momentum p^μ are defined by the Fourier transforms of vacuum expectation values of time-ordered products of bilinears of the fully interacting two-component fermion fields [cf. footnote 35]. Following Eqs. (4.2.1)–(4.2.4), we define:

$$\langle 0|\, T\psi_{\alpha i}(x)\psi^{\dagger j}_{\dot\beta}(y)\,|0\rangle_{\rm FT} = ip\cdot\sigma_{\alpha\dot\beta}\,\boldsymbol{C}_i{}^j(s), \tag{4.6.1}$$

$$\langle 0|\, T\psi^{\dagger\dot\alpha i}(x)\psi_j^{\beta}(y)\,|0\rangle_{\rm FT} = ip\cdot\overline{\sigma}^{\dot\alpha\beta}\,(\boldsymbol{C}^{\mathsf T})^i{}_j(s), \tag{4.6.2}$$

$$\langle 0|\, T\psi^{\dagger\dot\alpha i}(x)\psi^{\dagger j}_{\dot\beta}(y)\,|0\rangle_{\rm FT} = i\delta^{\dot\alpha}{}_{\dot\beta}\,\boldsymbol{D}^{ij}(s), \tag{4.6.3}$$

$$\langle 0|\, T\psi_{\alpha i}(x)\psi_j^{\beta}(y)\,|0\rangle_{\rm FT} = i\delta_\alpha{}^\beta\,\overline{\boldsymbol{D}}_{ij}(s), \tag{4.6.4}$$

where $s \equiv p^2$ and

$$(\boldsymbol{C}^{\mathsf T})^i{}_j \equiv \boldsymbol{C}_j{}^i. \tag{4.6.5}$$

One can derive Eq. (4.6.2) from Eq. (4.6.1) by first writing

$$\psi^{\dagger\dot\alpha i}(x)\psi_j^{\beta}(y) = -\epsilon^{\beta\alpha}\,\epsilon^{\dot\alpha\dot\beta}\psi_{\alpha j}(y)\psi^{\dagger i}_{\dot\beta}(x), \tag{4.6.6}$$

where the minus sign arises due to the anticommutativity of the fields, and then using Eq. (2.31); the interchange of x and y (after FT) simply changes p^μ to $-p^\mu$.

In general, $\boldsymbol{D}$ and $\overline{\boldsymbol{D}}$ are complex symmetric matrices, and $\overline{\boldsymbol{D}} = \boldsymbol{D}^\star$. The matrix $\boldsymbol{C}$ satisfies the hermiticity condition $[\boldsymbol{C}^{\mathsf T}]^\star = \boldsymbol{C}$. Here, we have introduced the star symbol to mean that a quantity $Q^\star$ is obtained from Q by taking the complex conjugate of all Lagrangian parameters appearing in its calculation, but not taking the complex conjugates of Euclideanized loop integral functions, whose imaginary (absorptive) parts correspond to fermion decay widths to multi-particle intermediate states. That is, the dispersive part of $\boldsymbol{C}$ is hermitian and the absorptive part of $\boldsymbol{C}$ is anti-hermitian.

The diagrammatic representations of the full propagators are displayed in Fig. 4.6.1, where $\boldsymbol{C}_i{}^j$, $\boldsymbol{D}^{ij}$, and $\overline{\boldsymbol{D}}_{ij}$ defined above are each $N\times N$ matrix functions. Note that the second diagram of Fig. 4.6.1, when flipped by 180° about the axis that bisects the diagram, is equivalent to the first diagram of Fig. 4.6.1 (with $p \to -p$, $\alpha \to \beta$, $\dot\beta \to \dot\alpha$ and $i \leftrightarrow j$). In analogy with Fig. 4.2.2, one could replace the first two diagrammatic rules of Fig. 4.6.1 with a single rule shown in Fig. 4.6.2, where we have used Eq. (4.6.5) to rewrite the second version of the rule in terms of $\boldsymbol{C}^{\mathsf T}$. Indeed, by using the $\overline{\sigma}$-version of the rule shown in Fig. 4.6.2 and flipping the corresponding diagram by 180° as described above, one reproduces the rule of the second diagram of Fig. 4.6.1.

In what follows, we prefer to keep the first two rules of Fig. 4.6.1 as separate entities. This will permit us to conveniently assemble the four diagrams of Fig. 4.6.1 into a 2×2 block matrix of two-component propagators [cf. Eq. (G.5.2)]. In addition,

51 In order to have a unified description, we shall take the flavor index of all left-handed fields (including η_k) in the lowered position in this subsection, in contrast to the convention adopted in Sections 3.2 and 4.3.

52 We will soon be suppressing the indices, so it is convenient to employ the bar on $\overline{\boldsymbol{m}}_{ij}$ to indicate its lowered index structure.

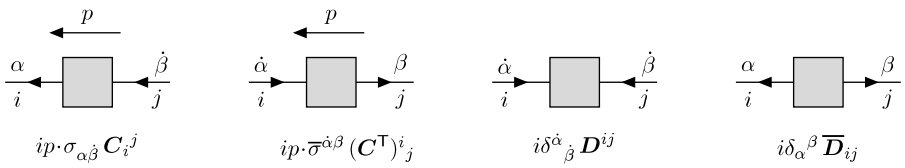

Fig. 4.6.1. The full, loop-corrected propagators for two-component fermions are associated with functions $\boldsymbol{C}(p^2)_i{}^j$ [and its matrix transpose], $\boldsymbol{D}(p^2)^{ij}$, and $\overline{\boldsymbol{D}}(p^2)_{ij}$, as shown. The shaded boxes represent the sum of all connected Feynman diagrams, with external legs included. The four-momentum p flows from right to left.

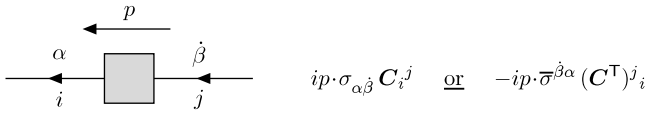

Fig. 4.6.2. The first two diagrammatic rules of Fig. 4.6.1 can be summarized by a single diagram. Here, the choice of the σ or $\overline{\sigma}$ version of the rule is uniquely determined by the height of the spinor indices on the vertex to which the full loop-corrected propagator is connected (cf. Fig. 4.2.2 and the accompanying text).

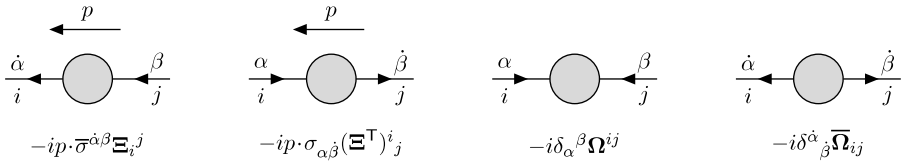

Fig. 4.6.3. The self-energy functions for two-component fermions are associated with functions $\boldsymbol{\Xi}(s)_i{}^j$ [and its matrix transpose], $\boldsymbol{\Omega}(s)^{ij}$, and $\overline{\boldsymbol{\Omega}}(s)_{ij}$, as shown. The shaded circles represent the sum of all one-particle irreducible, connected Feynman diagrams, and the external legs are amputated. The four-momentum p flows from right to left.

by choosing the momentum flow in the two-component propagators from right to left, the left-to-right orderings of the spinor labels of the diagrams coincide with the ordering of spinor indices that appear in the corresponding algebraic representations. Thus, we can multiply diagrams together and interpret them as the product of the respective algebraic quantities taken from left to right in the normal fashion.

Given the tree-level propagators of Fig. 4.2.1, the full propagator functions are given by:

$$\boldsymbol{C}_i{}^j = \delta_i{}^j/(s - m_i^2) + \cdots \tag{4.6.7}$$

$$\boldsymbol{D}^{ij} = \boldsymbol{m}^{ij}/(s - m_i^2) + \cdots \tag{4.6.8}$$

$$\overline{\boldsymbol{D}}_{ij} = \overline{\boldsymbol{m}}_{ij}/(s - m_i^2) + \cdots\,, \tag{4.6.9}$$

with no sum on i in each case. They are functions of the external momentum invariant s and of the masses and couplings of the theory. Inserting the leading terms [Eqs. (4.6.7)–(4.6.9)] into Fig. 4.6.1 and organizing the result in a 2×2 block matrix of two-component propagators reproduces the usual four-component fermion tree-level propagator given in Eq. (G.5.2).

The computation of the full propagators can be organized, as usual in quantum field theory, in terms of one-particle irreducible (1PI) self-energy functions. These are formally defined to be the sum of Feynman diagrams to all orders in perturbation theory (with the corresponding tree-level graph *excluded*) that contribute to the 1PI two-point Green function. Diagrammatically, the 1PI self-energy functions are defined in Fig. 4.6.3. As in the case of the full loop-corrected propagators, $[\boldsymbol{\Xi}^{\mathsf T}]^\star = \boldsymbol{\Xi}$ and $\overline{\boldsymbol{\Omega}} = \boldsymbol{\Omega}^\star$, where the star symbol was defined in the paragraph following Eq. (4.6.6), and $(\boldsymbol{\Xi}^{\mathsf T})^i{}_j \equiv \boldsymbol{\Xi}_j{}^i$.

We illustrate the computation of the full propagator by considering first the following diagrammatic identity (with momentum p flowing from right to left):

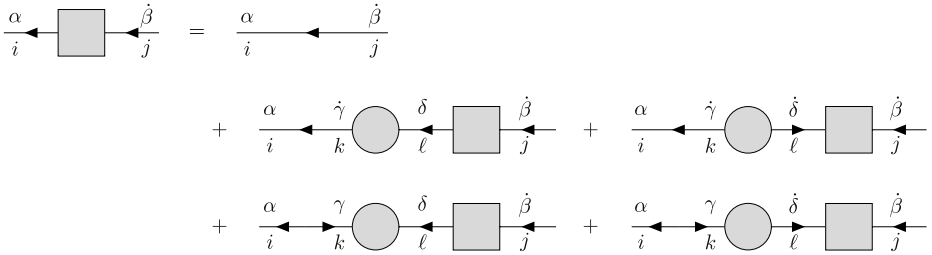

(4.6.10)

Similar diagrammatic identities can be constructed for the three other full loop-corrected propagators of Fig. 4.6.1. The resulting four equations can be neatly summarized by:

$$F = T + TSF, \tag{4.6.11}$$

where F is the matrix of full loop-corrected propagators, T is the matrix of tree-level propagators and S is the matrix of self-energy functions. Expressing Eq. (4.6.11) in terms of diagrams,

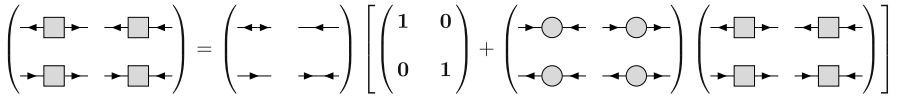

(4.6.12)

which, when expanded out, yields Eq. (4.6.10) and the corresponding identities for the three other full loop-corrected propagators of Fig. 4.6.1. Note that we have chosen the labeling and momentum flow in Figs. 4.6.1 and 4.6.3 such that the spinor and flavor labels of the diagrams appear in the appropriate left-to-right order to permit the interpretation of Eq. (4.6.12) as a matrix equation. To solve for F,[53] we multiply Eq. (4.6.11) on the left by T^{-1} and on the right by F^{-1} to obtain $T^{-1} = F^{-1} + S$. Thus, $F = [T^{-1} - S]^{-1}$. In pictures:

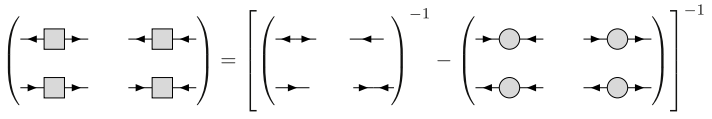

(4.6.13)

We evaluate the tree-level propagator matrix and its inverse using Eqs. (4.6.7)–(4.6.9), keeping in mind that the direction of momentum flow is from right to left:

$$\begin{pmatrix} \rightarrow & \leftarrow \\ \rightarrow & \rightarrow \end{pmatrix} = \frac{1}{s - m_i^2} \begin{pmatrix} i\,\overline{\boldsymbol{m}}_{ij}\,\delta_\alpha{}^\beta & ip\cdot\sigma_{\alpha\dot\beta}\,\delta_i{}^j \\ ip\cdot\overline{\sigma}^{\dot\alpha\beta}\,\delta^i{}_j & i\,\boldsymbol{m}^{ij}\,\delta^{\dot\alpha}{}_{\dot\beta} \end{pmatrix}, \tag{4.6.14}$$

$$\begin{pmatrix} \rightarrow & \leftarrow \\ \rightarrow & \rightarrow \end{pmatrix}^{-1} = \begin{pmatrix} i\,\boldsymbol{m}^{ij}\,\delta_\alpha{}^\beta & -ip\cdot\sigma_{\alpha\dot\beta}\,\delta^i{}_j \\ -ip\cdot\overline{\sigma}^{\dot\alpha\beta}\,\delta_i{}^j & i\,\overline{\boldsymbol{m}}_{ij}\,\delta^{\dot\alpha}{}_{\dot\beta} \end{pmatrix}, \tag{4.6.15}$$

where we follow the index structure defined in Figs. 4.6.1 and 4.6.3. Inserting Eq. (4.6.15) into Eq. (4.6.13), one obtains a $4N \times 4N$ matrix equation for the full propagator functions:

$$\begin{pmatrix} i\overline{\boldsymbol{D}} & ip\cdot\sigma\,\boldsymbol{C} \\ ip\cdot\overline{\sigma}\,\boldsymbol{C}^{\mathsf T} & i\boldsymbol{D} \end{pmatrix} = \begin{pmatrix} i(\boldsymbol{m}+\boldsymbol{\Omega}) & -ip\cdot\sigma\,(\mathbf{1}-\boldsymbol{\Xi}^{\mathsf T}) \\ -ip\cdot\overline{\sigma}\,(\mathbf{1}-\boldsymbol{\Xi}) & i(\overline{\boldsymbol{m}}+\overline{\boldsymbol{\Omega}}) \end{pmatrix}^{-1}, \tag{4.6.16}$$

where $\mathbf{1}$ is the $N\times N$ identity matrix. The right-hand side of Eq. (4.6.16) can be evaluated by employing the following identity for the inverse of a block-partitioned matrix [159]:

$$\begin{pmatrix} P & Q \\ R & S \end{pmatrix}^{-1} = \begin{pmatrix} (P - QS^{-1}R)^{-1} & (R - SQ^{-1}P)^{-1} \\ (Q - PR^{-1}S)^{-1} & (S - RP^{-1}Q)^{-1} \end{pmatrix}, \tag{4.6.17}$$

under the assumption that all inverses appearing in Eq. (4.6.17) exist. Applying this result to Eq. (4.6.16), we obtain

$$\boldsymbol{C}^{-1} = s(\mathbf{1}-\boldsymbol{\Xi}) - (\overline{\boldsymbol{m}}+\overline{\boldsymbol{\Omega}})(\mathbf{1}-\boldsymbol{\Xi}^{\mathsf T})^{-1}(\boldsymbol{m}+\boldsymbol{\Omega}), \tag{4.6.18}$$

$$\boldsymbol{D}^{-1} = s(\mathbf{1}-\boldsymbol{\Xi})(\boldsymbol{m}+\boldsymbol{\Omega})^{-1}(\mathbf{1}-\boldsymbol{\Xi}^{\mathsf T}) - (\overline{\boldsymbol{m}}+\overline{\boldsymbol{\Omega}}), \tag{4.6.19}$$

$$\overline{\boldsymbol{D}}^{-1} = s(\mathbf{1}-\boldsymbol{\Xi}^{\mathsf T})(\overline{\boldsymbol{m}}+\overline{\boldsymbol{\Omega}})^{-1}(\mathbf{1}-\boldsymbol{\Xi}) - (\boldsymbol{m}+\boldsymbol{\Omega}). \tag{4.6.20}$$

Note that Eq. (4.6.20) is consistent with Eq. (4.6.19) as $\boldsymbol{\Xi}^\star = \boldsymbol{\Xi}^{\mathsf T}$.

The pole mass can be found most easily by considering the rest frame of the (off-shell) fermion, in which the space components of p^μ vanish. This reduces the spinor index dependence to a triviality. Setting $p^\mu = (\sqrt{s};\mathbf{0})$, we search for values of s where the inverse of the full propagator has a zero eigenvalue. This is equivalent to setting the determinant of the inverse of the full propagator to zero. Here we shall use the well-known formula for the determinant of a block-partitioned

[53] Alternatively, one can solve Eq. (4.6.12) by iteration and summing the resulting geometric series. This yields:

$$\begin{aligned} F &= T + TS(T + TS(T + TS(\cdots))) = T + TST + TSTST + \cdots = T[1 + ST + (ST)^2 + \cdots] \\ &= T[1 - ST]^{-1} = (T^{-1})^{-1}[1 - ST]^{-1} = [(1 - ST)T^{-1}]^{-1} = [T^{-1} - S]^{-1}, \end{aligned}$$

which is equivalent to Eq. (4.6.13).

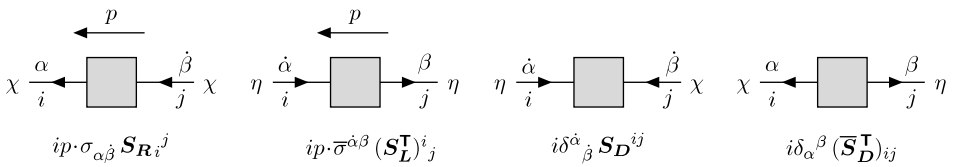

Fig. 4.6.4. The full, loop-corrected propagators for Dirac fermions, represented by pairs of two-component (oppositely charged) fermion fields χ_i and η_i, are associated with functions $\boldsymbol{S_R}(s)_i{}^j$, $\boldsymbol{S_L^T}(s)^i{}_j$, $\boldsymbol{S_D}(s)^{ij}$, and $\overline{\boldsymbol{S}}_{\boldsymbol{D}}^{\boldsymbol{T}}(s)_{ij}$, as shown. The shaded boxes represent the sum of all connected Feynman diagrams, with external legs included. The four-momentum p and the charge of χ flow from right to left.

matrix [159]:

$$\det\begin{pmatrix} P & Q \\ R & S \end{pmatrix} = \det P\ \det\,(S - RP^{-1}Q). \tag{4.6.21}$$

The end result is that the poles of the full propagator (which are in general complex),

$$s_{\text{pole},j} \equiv M_j^2 - i\Gamma_j M_j, \tag{4.6.22}$$

are formally the solutions to the non-linear equation[54]

$$\det\left[s\mathbf{1} - (\mathbf{1} - \boldsymbol{\Xi}^{\mathsf T})^{-1}(\boldsymbol{m} + \boldsymbol{\Omega})(\mathbf{1} - \boldsymbol{\Xi})^{-1}(\overline{\boldsymbol{m}} + \overline{\boldsymbol{\Omega}})\right] = 0. \tag{4.6.23}$$

Some care is required in using Eq. (4.6.23), since the pole squared mass always has a *non-positive* imaginary part, while the loop integrals used to find the self-energy functions are complex functions of a real variable s that is given an infinitesimal *positive* imaginary part. Therefore, Eq. (4.6.23) should be solved iteratively by first expanding the self-energy function matrices $\boldsymbol{\Xi}$, $\boldsymbol{\Omega}$ and $\overline{\boldsymbol{\Omega}}$ in a series in s about either $m_j^2 + i\epsilon$ or $M_j^2 + i\epsilon$. The complex quantities $s_{\text{pole},j}$, which can be identified as the complex pole squared masses, are renormalization group and gauge invariant physical observables. Examples are given in Sections 6.24 and 6.25.

The results of this section can be applied to an arbitrary collection of fermions (both Majorana or Dirac). However, it is convenient to treat separately the case where all fermions are Dirac fermions (consisting of pairs of two-component fields χ_i and η^i). As discussed in Section 3.2, the Dirac fermion mass eigenstates are defined in Eq. (3.2.31) and are determined by the singular value decomposition of the Dirac fermion mass matrix. With respect to the mass basis, we denote the diagonal Dirac fermion mass matrix by $\boldsymbol{M}^{ij}$. The elements of this matrix are real and non-negative. Nevertheless, it will be convenient as before to define $\overline{\boldsymbol{M}}_{ij} \equiv \boldsymbol{M}^{ij}$ to maintain covariance when manipulating tensors with flavor indices.

At tree level, there are four propagators for each pair of χ and η fields as shown in Fig. 4.2.4. The corresponding full, loop-corrected propagators are shown in Fig. 4.6.4. The naming and sign conventions employed for the full, loop-corrected Dirac fermion propagator functions in Fig. 4.6.4 derives from the corresponding functions used in the more traditional four-component treatment presented in Appendix G [cf. Eq. (G.7.2)].

In general, the complex matrices $\boldsymbol{S_R}$ and $\boldsymbol{S_L}$ satisfy hermiticity conditions $[\boldsymbol{S_R^T}]^\star = \boldsymbol{S_R}$ and $[\boldsymbol{S_L^T}]^\star = \boldsymbol{S_L}$, whereas the complex matrices $\boldsymbol{S_D}$ and $\overline{\boldsymbol{S}}_{\boldsymbol{D}}$ are related by $\overline{\boldsymbol{S}}_{\boldsymbol{D}} = \boldsymbol{S_D^\star}$, where the star symbol is defined in the paragraph below Eq. (4.6.6). In contrast to the general case of an arbitrary collection of fermions treated earlier, $\boldsymbol{S_R}$ and $\boldsymbol{S_L}$ are unrelated and $\boldsymbol{S}_D$ is a complex matrix (not necessarily symmetric).

Instead of working in a χ–η basis for the two-component Dirac fermion fields, one can Takagi diagonalize the fermion mass matrix. In the new ψ-basis, the loop-corrected propagators of Fig. 4.6.1 are applicable. It is easy to check that the number of independent functions is the same in both methods for treating Dirac fermions. In particular, the loop-corrected propagator functions in the ψ-basis are given in terms of the corresponding functions in the χ–η basis by[55]:

$$\boldsymbol{C} = \begin{pmatrix} \boldsymbol{S_R} & 0 \\ 0 & \boldsymbol{S_L} \end{pmatrix}, \qquad \boldsymbol{D} = \begin{pmatrix} 0 & \boldsymbol{S}_D^{\mathsf T} \\ \boldsymbol{S}_D & 0 \end{pmatrix}, \qquad \overline{\boldsymbol{D}} = \begin{pmatrix} 0 & \overline{\boldsymbol{S}}_{\boldsymbol{D}}^{\mathsf T} \\ \overline{\boldsymbol{S}}_{\boldsymbol{D}} & 0 \end{pmatrix}. \tag{4.6.24}$$

We similarly introduce the 1PI self-energy matrix functions for the Dirac fermions in the χ–η basis, where the corresponding self-energy functions are defined in Fig. 4.6.5. As before, the naming and sign conventions employed for the Dirac fermion self-energy functions above derives from the corresponding functions used in the more traditional four-component treatment of Appendix G [cf. Eq. (G.7.3)].

Once again, the complex matrices $\boldsymbol{\Sigma_L}$ and $\boldsymbol{\Sigma_R}$ satisfy hermiticity conditions $[\boldsymbol{\Sigma_L^T}]^\star = \boldsymbol{\Sigma_L}$ and $[\boldsymbol{\Sigma_R^T}]^\star = \boldsymbol{\Sigma_R}$, whereas the complex matrices $\boldsymbol{\Sigma_D}$ and $\overline{\boldsymbol{\Sigma}}_{\boldsymbol{D}}$ are related by $\overline{\boldsymbol{\Sigma}}_{\boldsymbol{D}} = \boldsymbol{\Sigma_D^\star}$, where the star symbol is defined in the paragraph below Eq. (4.6.6). Likewise, $\boldsymbol{\Sigma_L}$ and $\boldsymbol{\Sigma_R}$ are unrelated and $\boldsymbol{\Sigma_D}$ is a complex matrix (not necessarily symmetric). The self-energy functions in

54 The determinant of the inverse of the full propagator [the inverse of Eq. (4.6.16)] is equal to Eq. (4.6.23) multiplied by $\det[-(\mathbf{1} - \boldsymbol{\Xi})(\mathbf{1} - \boldsymbol{\Xi}^{\mathsf T})]$. We assume that the latter does not vanish. This must be true perturbatively since the eigenvalues of $\boldsymbol{\Xi}$ are one-loop (or higher) quantities, which one assumes cannot be as large as 1.

55 The simple forms of $\boldsymbol{C}$ in Eq. (4.6.24) and $\boldsymbol{\Xi}$ in Eq. (4.6.25) motivate our definitions of $\boldsymbol{S_L}$ and $\boldsymbol{\Sigma_R}$ with the transpose as indicated in Figs. 4.6.4 and 4.6.5, respectively.

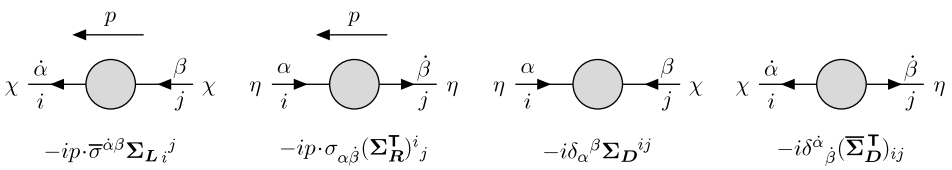

Fig. 4.6.5. The self-energy functions for two-component Dirac fermions, represented by pairs of two-component (oppositely charged) fermion fields χ_i and η_i, are associated with functions $\boldsymbol{\Sigma_L}(s)_i{}^j$, $\boldsymbol{\Sigma_R^\mathsf{T}}(s)^i{}_j$, $\boldsymbol{\Sigma_D}(s)^{ij}$, and $\overline{\boldsymbol{\Sigma}}_{\boldsymbol{D}}^\mathsf{T}(s)_{ij}$, as shown. The shaded circles represent the sum of all one-particle irreducible, connected Feynman diagrams, and the external legs are amputated. The four-momentum p flows from right to left.

the ψ-basis are given in terms of the corresponding functions in the χ–η basis by:[55]

$$\boldsymbol{\Xi}=\begin{pmatrix}\boldsymbol{\Sigma_L} & 0\\ 0 & \boldsymbol{\Sigma_R}\end{pmatrix},\qquad \boldsymbol{\Omega}=\begin{pmatrix}0 & \boldsymbol{\Sigma_D^\mathsf{T}}\\ \boldsymbol{\Sigma_D} & 0\end{pmatrix},\qquad \overline{\boldsymbol{\Omega}}=\begin{pmatrix}0 & \overline{\boldsymbol{\Sigma}}_{\boldsymbol{D}}^\mathsf{T}\\ \overline{\boldsymbol{\Sigma}}_{\boldsymbol{D}} & 0\end{pmatrix}. \tag{4.6.25}$$

In the case of Dirac fermions fields, Eq. (4.6.13) still holds in the χ–η basis, which yields:

$$\begin{pmatrix}i\overline{\boldsymbol{S}}_{\boldsymbol{D}}^\mathsf{T} & ip\cdot\sigma\,\boldsymbol{S_R}\\ ip\cdot\overline{\sigma}\,\boldsymbol{S_L^\mathsf{T}} & i\boldsymbol{S}_D\end{pmatrix}=\begin{pmatrix}i(\boldsymbol{M}+\boldsymbol{\Sigma_D}) & -ip\cdot\sigma\,(\mathbf{1}-\boldsymbol{\Sigma_R^\mathsf{T}})\\ -ip\cdot\overline{\sigma}\,(\mathbf{1}-\boldsymbol{\Sigma_L}) & i(\overline{\boldsymbol{M}}+\overline{\boldsymbol{\Sigma}}_{\boldsymbol{D}}^\mathsf{T})\end{pmatrix}^{-1}. \tag{4.6.26}$$

Using Eq. (4.6.17), it follows that:

$$\boldsymbol{S_L}^{-1}=s(\mathbf{1}-\boldsymbol{\Sigma_R})-(\overline{\boldsymbol{M}}+\overline{\boldsymbol{\Sigma}}_{\boldsymbol{D}})(\mathbf{1}-\boldsymbol{\Sigma_L^\mathsf{T}})^{-1}(\boldsymbol{M}+\boldsymbol{\Sigma_D^\mathsf{T}}), \tag{4.6.27}$$

$$\boldsymbol{S_R}^{-1}=s(\mathbf{1}-\boldsymbol{\Sigma_L})-(\overline{\boldsymbol{M}}+\overline{\boldsymbol{\Sigma}}_{\boldsymbol{D}}^\mathsf{T})(\mathbf{1}-\boldsymbol{\Sigma_R^\mathsf{T}})^{-1}(\boldsymbol{M}+\boldsymbol{\Sigma_D}), \tag{4.6.28}$$

$$\boldsymbol{S_D}^{-1}=s(\mathbf{1}-\boldsymbol{\Sigma_L})(\boldsymbol{M}+\boldsymbol{\Sigma_D})^{-1}(\mathbf{1}-\boldsymbol{\Sigma_R^\mathsf{T}})-(\overline{\boldsymbol{M}}+\overline{\boldsymbol{\Sigma}}_{\boldsymbol{D}}^\mathsf{T}), \tag{4.6.29}$$

$$\overline{\boldsymbol{S}}_{\boldsymbol{D}}^{-1}=s(\mathbf{1}-\boldsymbol{\Sigma_L^\mathsf{T}})(\overline{\boldsymbol{M}}+\overline{\boldsymbol{\Sigma}}_{\boldsymbol{D}})^{-1}(\mathbf{1}-\boldsymbol{\Sigma_R})-(\boldsymbol{M}+\boldsymbol{\Sigma_D^\mathsf{T}}). \tag{4.6.30}$$

Note that Eq. (4.6.30) is consistent with Eq. (4.6.29) as $\boldsymbol{\Sigma}^\star_{\boldsymbol{L},\boldsymbol{R}}=\boldsymbol{\Sigma}^\mathsf{T}_{\boldsymbol{L},\boldsymbol{R}}$.

The pole mass is now easily computed using the technique previously outlined. In particular, Eq. (4.6.23) becomes:

$$\det\left[s\mathbf{1}-(\mathbf{1}-\boldsymbol{\Sigma_R^\mathsf{T}})^{-1}(\boldsymbol{M}+\boldsymbol{\Sigma_D})(\mathbf{1}-\boldsymbol{\Sigma_L})^{-1}(\overline{\boldsymbol{M}}+\overline{\boldsymbol{\Sigma}}_{\boldsymbol{D}}^\mathsf{T})\right]=0, \tag{4.6.31}$$

which determines the complex pole squared masses, $s_{\rm pole}$, of the corresponding Dirac fermions. Again, the self-energy functions should be expanded in a series in s about a point with an infinitesimal positive imaginary part.

Finally, we examine the special case of a parity-conserving vectorlike theory of Dirac fermions (such as QED or QCD). In this case, the following relations hold among the loop-corrected propagator functions and self-energy functions, respectively[56]:

$$\boldsymbol{S_R}_i{}^j=(\boldsymbol{S_L^\mathsf{T}})^i{}_j,\qquad \boldsymbol{S_D}^{ij}=(\overline{\boldsymbol{S}}_{\boldsymbol{D}}^\mathsf{T})_{ij}, \tag{4.6.32}$$

$$\boldsymbol{\Sigma_L}_i{}^j=(\boldsymbol{\Sigma_R^\mathsf{T}})^i{}_j,\qquad \boldsymbol{\Sigma_D}^{ij}=(\overline{\boldsymbol{\Sigma}}_{\boldsymbol{D}}^\mathsf{T})_{ij}. \tag{4.6.33}$$

By imposing Eq. (4.6.33) on Eqs. (4.6.27)–(4.6.30) and recalling that $\overline{\boldsymbol{M}}_{ij}=\boldsymbol{M}^{ij}$, it is straightforward to verify that Eq. (4.6.32) is satisfied.

5. Conventions for fermion and antifermion names and fields

In this section, we establish conventions for labeling Feynman diagrams that contain two-component fermion fields of the Standard Model (SM) and its minimal supersymmetric extension (MSSM). In the case of Majorana fermions, there is a one-to-one correspondence between the particle names and the undaggered $(\frac{1}{2},0)$ [left-handed] fields. In contrast, for Dirac fermions there are always two distinct two-component fields that correspond to each particle name. For a quark or lepton generically denoted by f, we employ the two-component undaggered $(\frac{1}{2},0)$ [left-handed] fields f and $\bar f$ (where the bar is part of the field name and does *not* refer to complex conjugation of any kind). This is illustrated in Table 5.1, which lists the SM and MSSM fermion particle names together with the corresponding two-component fields. For each particle, we list the two-component field with the same quantum numbers, i.e., the field that contains the annihilation operator for that one-particle state (which creates the one-particle state when acting to the *left* on the vacuum $\langle 0|$).

There is an option of labeling fermion lines in Feynman diagrams by particle names or by field names; each choice has advantages and disadvantages.[57] In all of the examples that follow, we have chosen to eliminate the possibility of ambiguity

[56] These relations are derived using four-component spinor methods in Appendix G [cf. Eqs. (G.7.10) and (G.7.11)].

[57] Unfortunately, the notation for fermion names can be ambiguous because some of the symbols used also appear as names for one of the two-component fermion fields. In practice, it should be clear from the context which set of names are being employed.

Table 5.1
Fermion and antifermion names and two-component fields in the Standard Model and the MSSM. In the listing of two-component fields, the first is an undaggered $(\frac{1}{2}, 0)$ [left-handed] field and the second is a daggered $(0, \frac{1}{2})$ [right-handed] field. The bars on the two-component (antifermion) fields are part of their names, and do not denote some form of complex conjugation. (In this table, neutrinos are considered to be exactly massless and the left-handed antineutrino $\bar{\nu}$ is absent from the spectrum.)

Fermion name	Two-component fields
ℓ^- (lepton)	$\ell, \bar{\ell}^\dagger$
ℓ^+ (anti-lepton)	$\bar{\ell}, \ell^\dagger$
ν (neutrino)	$\nu, -$
$\bar{\nu}$ (antineutrino)	$-, \nu^\dagger$
q (quark)	$q, \bar{q}^\dagger$
$\bar{q}$ (anti-quark)	$\bar{q}, q^\dagger$
f (quark or lepton)	$f, \bar{f}^\dagger$
$\bar{f}$ (anti-quark or anti-lepton)	$\bar{f}, f^\dagger$
$\widetilde{N}_i$ (neutralino)	$\chi_i^0, \chi_i^{0\dagger}$
$\widetilde{C}_i^+$ (chargino)	$\chi_i^+, \chi_i^{-\dagger}$
$\widetilde{C}_i^-$ (anti-chargino)	$\chi_i^-, \chi_i^{+\dagger}$
$\widetilde{g}$ (gluino)	$\widetilde{g}, \widetilde{g}^\dagger$

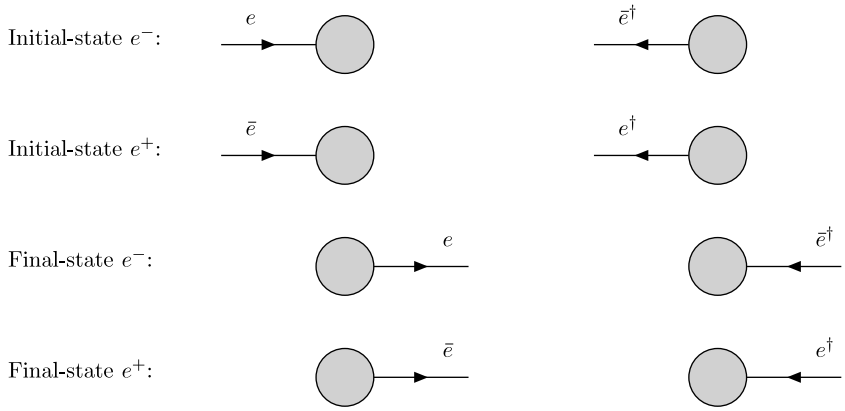

Fig. 5.1. The two-component field labeling conventions for external Dirac fermion lines in a Feynman diagram for a physical process. The top row corresponds to an initial state electron, the second row to an initial state positron, the third row to a final state electron, and the fourth row to a final state positron. The labels above each line are the two-component field names. The corresponding conventions for a massless neutrino are obtained by deleting the diagrams with $\bar{e}$ or $\bar{e}^\dagger$, and changing e and $e^\dagger$ to ν and $\nu^\dagger$, respectively.

as follows. We always label fermion lines with two-component fields (rather than particle names), and adopt the following conventions:

• In the Feynman rules for interaction vertices, the external lines are always labeled by the undaggered $(\frac{1}{2}, 0)$ [left-handed] field, regardless of whether the corresponding arrow is pointed in or out of the vertex. Two-component fermion lines with arrows pointing away from the vertex correspond to dotted indices, and two-component fermion lines with arrows pointing toward the vertex always correspond to undotted indices. This also applies to Feynman diagrams where the roles of the initial state and the final state are ambiguous (such as self-energy diagrams).

• Internal fermion lines in Feynman diagrams are also always labeled by the undaggered $(\frac{1}{2}, 0)$ [left-handed] field(s). Internal fermion lines containing a propagator with opposing arrows can carry two labels (e.g., see Fig. 4.5.7).

• Initial state external fermion lines (which always have physical three-momenta pointing into the vertex) in Feynman diagrams for complete processes are labeled by the corresponding undaggered $(\frac{1}{2}, 0)$ [left-handed] field if the arrow is into the vertex, and by the daggered $(0, \frac{1}{2})$ [right-handed] field if the arrow is away from the vertex.

• Final state external fermion lines (which always have physical three-momenta pointing out of the vertex) in Feynman diagrams for complete processes are labeled by the corresponding daggered $(0, \frac{1}{2})$ [right-handed] field if the arrow is into the vertex, and by the undaggered $(\frac{1}{2}, 0)$ [left-handed] field if the arrow is away from the vertex.

The rules for labeling external Dirac fermions are summarized in Fig. 5.1. These labeling conventions differ slightly from the ones employed in Section 4.5, where *all* internal and external initial state and final state fermion lines were labeled by the corresponding *undaggered* $(\frac{1}{2}, 0)$ left-handed fields. In this latter convention, the conserved quantities (charges, lepton numbers, baryon numbers, etc.) of the labeled fields follow the direction of the arrow that adorns the corresponding fermion line in the diagram. In contrast, in the convention of Fig. 5.1, the field labels used for external fermion lines always correspond to the physical particle, and the corresponding conserved quantities of the labeled fields follow the direction

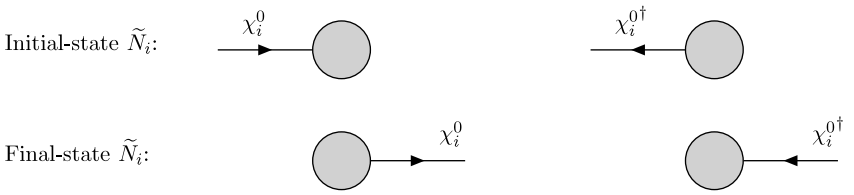

Fig. 5.2. The two-component field labeling conventions for external Majorana fermion lines in a Feynman diagram for a physical process. The top row corresponds to an initial state neutralino, and the second row to a final state neutralino. The labels above each line are the two-component field names. (The neutralino is its own antiparticle.)

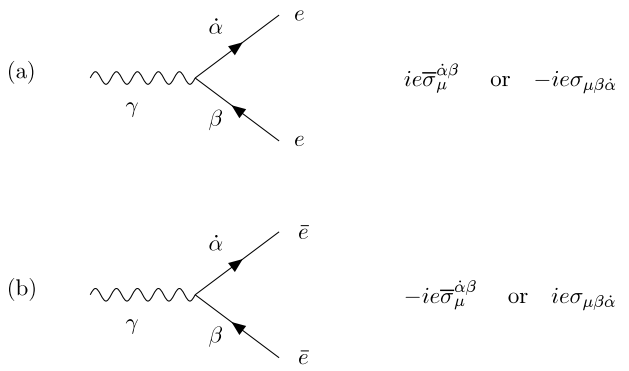

Fig. 5.3. The two-component Feynman rules for the QED vertex. Following the conventions outlined in Section 5, we label these rules with the $(\frac{1}{2}, 0)$ [left-handed] fields e and $\bar{e}$, which comprise the Dirac electron. Note that $Q_e = -1$, and the electromagnetic coupling constant e (not to be confused with the two-component electron field that is denoted by the same letter) is conventionally defined such that $e > 0$ [cf. Fig. J.1.2].

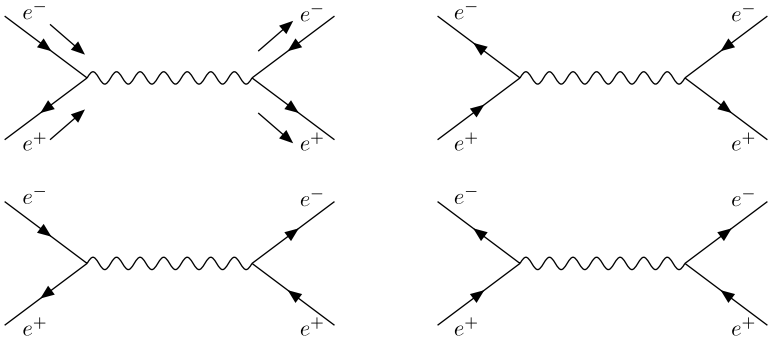

Fig. 5.4. Tree-level s-channel Feynman diagrams for $e^-e^+ \to e^-e^+$, with the external lines labeled according to the particle names. The initial state is on the left, and the final state is on the right. Thus, the physical momentum flow of the external particles, as well as the flow of the labeled charges, are indicated by the arrows adjacent to the corresponding fermion lines in the upper left diagram.

of the particle three-momentum. As an example, for either initial or final states, the two-component fields e and $\bar{e}^\dagger$ both represent a negatively charged electron, conventionally denoted by e^-, whereas both $\bar{e}$ and $e^\dagger$ represent a positively charged positron, conventionally denoted by e^+ (cf. Table 5.1).

The application of our labeling conventions to processes involving Majorana fermions is completely straightforward. For example, the conventions for employing the neutralino states as external particles are summarized in Fig. 5.2.

As a simple example, consider Bhabha scattering ($e^-e^+ \to e^-e^+$) [160]. We require the two-component Feynman rules for the QED coupling of electrons and positrons to the photon, which are exhibited in Fig. 5.3. Consider the s-channel tree-level Feynman diagrams that contribute to the invariant amplitude for $e^-e^+ \to e^-e^+$. If we were to label the external fermion lines according to the corresponding particle names (which does *not* conform to the conventions introduced above), the result is shown in Fig. 5.4. One can find the identity of the external two-component fermion fields by carefully observing the direction of the arrow of each fermion line. For contrast, the same diagrams, relabeled with two-component fields following the conventions established in this section (cf. Fig. 5.1), are shown in Fig. 5.5. An explicit computation of the invariant amplitude is given in Section 6.3.

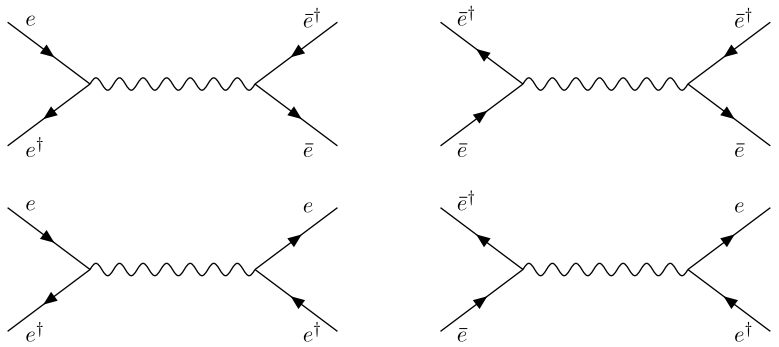

Fig. 5.5. Tree-level s-channel Feynman diagrams for $e^+e^- \to e^+e^-$. These diagrams are the same as in Fig. 5.4, but with the external lines relabeled by the two-component fermion fields according to the conventions of Fig. 5.1.

6. Practical examples from the Standard Model and its supersymmetric extension

In this section we will present some examples to illustrate the use of the rules presented in this paper. These examples are chosen from the Standard Model [161] and the MSSM [6–10], in order to provide an unambiguous point of reference. In all cases, the fermion lines in Feynman diagrams are labeled by two-component field names, rather than the particle names, as explained in Section 5.

6.1. Top quark decay: $t \to bW^+$

We begin by calculating the decay width of a top quark into a bottom quark and W^+ vector boson. For simplicity, we treat this as a one-generation problem and ignore Cabibbo–Kobayashi–Maskawa (CKM) [162] mixing among the three quark generations [see Eq. (J.1.16) and the surrounding text]. Let the four-momenta and helicities of these particle be (p_t, λ_t), (k_b, λ_b) and (k_W, λ_W), respectively. Then $p_t^2 = m_t^2$, $k_b^2 = m_b^2$ and $k_W^2 = m_W^2$ and

$$2p_t \cdot k_W = m_t^2 - m_b^2 + m_W^2, \tag{6.1.1}$$

$$2p_t \cdot k_b = m_t^2 + m_b^2 - m_W^2, \tag{6.1.2}$$

$$2k_W \cdot k_b = m_t^2 - m_b^2 - m_W^2. \tag{6.1.3}$$

Because only left-handed top quarks couple to the W boson, the only Feynman diagram for $t \to bW^+$ is the one shown in Fig. 6.1.1. The corresponding amplitude can be read off of the Feynman rule of Fig. J.1.2 in Appendix J. Here the initial state top quark is a two-component field t going into the vertex and the final state bottom quark is created by a two-component field $b^\dagger$. Therefore the amplitude is given by:

$$i\mathcal{M} = -i\frac{g}{\sqrt{2}}\varepsilon_\mu^* x_b^\dagger \overline{\sigma}^\mu x_t, \tag{6.1.4}$$

where $\varepsilon_\mu^* \equiv \varepsilon_\mu(k_W, \lambda_W)^*$ is the polarization vector of the W^+, and $x_b^\dagger \equiv x^\dagger(\vec{\boldsymbol{k}}_b, \lambda_b)$ and $x_t \equiv x(\vec{\boldsymbol{p}}_t, \lambda_t)$ are the external state wave function factors for the bottom and top quark. Squaring this amplitude using Eq. (2.45) yields:

$$|\mathcal{M}|^2 = \frac{g^2}{2}\varepsilon_\mu^* \varepsilon_\nu (x_b^\dagger \overline{\sigma}^\mu x_t)\,(x_t^\dagger \overline{\sigma}^\nu x_b). \tag{6.1.5}$$

Next, we can average over the top quark spin polarizations using Eq. (3.1.58):

$$\frac{1}{2}\sum_{\lambda_t} |\mathcal{M}|^2 = \frac{g^2}{4}\varepsilon_\mu^* \varepsilon_\nu x_b^\dagger \overline{\sigma}^\mu\, p_t \cdot \sigma\, \overline{\sigma}^\nu x_b. \tag{6.1.6}$$

Summing over the bottom quark spin polarizations in the same way yields a trace over spinor indices:

$$\begin{aligned}\frac{1}{2}\sum_{\lambda_t,\lambda_b} |\mathcal{M}|^2 &= \frac{g^2}{4}\varepsilon_\mu^* \varepsilon_\nu \,\mathrm{Tr}[\overline{\sigma}^\mu p_t \cdot \sigma\, \overline{\sigma}^\nu k_b \cdot \sigma] \\ &= \frac{g^2}{2}\varepsilon_\mu^* \varepsilon_\nu \left(p_t^\mu k_b^\nu + k_b^\mu p_t^\nu - g^{\mu\nu} p_t \cdot k_b - i\epsilon^{\mu\rho\nu\kappa} p_{t\rho} k_{b\kappa}\right),\end{aligned} \tag{6.1.7}$$

where we have used Eq. (2.57). Finally we can sum over the W^+ polarizations according to:

$$\sum_{\lambda_W} \varepsilon_\mu^* \varepsilon_\nu = -g_{\mu\nu} + (k_W)_\mu (k_W)_\nu / m_W^2. \tag{6.1.8}$$

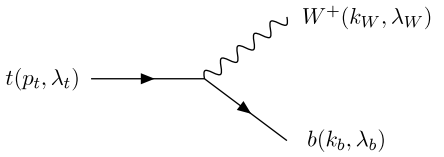

Fig. 6.1.1. The Feynman diagram for $t \to bW^+$ at tree level.

The end result is:

$$\frac{1}{2}\sum_{\text{spins}}|\mathcal{M}|^2 = \frac{g^2}{2}\left[p_t\cdot k_b + 2(p_t\cdot k_W)(k_b\cdot k_W)/m_W^2\right]. \tag{6.1.9}$$

After performing the phase space integration, one obtains:

$$\begin{aligned}\Gamma(t\to bW^+) &= \frac{1}{16\pi m_t^3}\lambda^{1/2}(m_t^2, m_W^2, m_b^2)\left(\frac{1}{2}\sum_{\text{spins}}|\mathcal{M}|^2\right)\\ &= \frac{g^2}{64\pi m_W^2 m_t^3}\lambda^{1/2}(m_t^2, m_W^2, m_b^2)\left[(m_t^2+2m_W^2)(m_t^2-m_W^2)+m_b^2(m_W^2-2m_t^2)+m_b^4\right],\end{aligned} \tag{6.1.10}$$

where the kinematical triangle function $\lambda^{1/2}$ is defined by [163]:

$$\lambda(x,y,z) \equiv x^2+y^2+z^2-2xy-2xz-2yz. \tag{6.1.11}$$

In the approximation $m_b \ll m_W, m_t$, one ends up with the well-known result [164]

$$\Gamma(t\to bW^+) = \frac{g^2 m_t}{64\pi}\left(2+\frac{m_t^2}{m_W^2}\right)\left(1-\frac{m_W^2}{m_t^2}\right)^2, \tag{6.1.12}$$

which exhibits the Nambu–Goldstone enhancement factor (m_t^2/m_W^2) for the longitudinal W contribution compared to the two transverse W contributions [164].

6.2. Z^0 vector boson decay: $Z^0 \to f\bar{f}$

Consider the partial decay width of the Z^0 boson into a Standard Model fermion–antifermion pair. As in the generic example of Fig. 4.5.4, there are two contributing Feynman diagrams, shown in Fig. 6.2.1. In diagram (a), the fermion particle f in the final state is created by a two-component field f in the Feynman rule, and the antifermion particle $\bar{f}$ by a two-component field $f^\dagger$. In diagram (b), the fermion particle f in the final state is created by a two-component field $\bar{f}$, and the antifermion particle $\bar{f}$ by a two-component field $\bar{f}^\dagger$. Denote the initial Z^0 four-momentum and helicity (p, λ_Z) and the final state fermion (f) and antifermion $(\bar{f})$ momentum and helicities (k_f, λ_f) and $(k_{\bar{f}}, \lambda_{\bar{f}})$, respectively. Then, $k_f^2 = k_{\bar{f}}^2 = m_f^2$ and $p^2 = m_Z^2$, and

$$k_f\cdot k_{\bar{f}} = \frac{1}{2}m_Z^2 - m_f^2, \tag{6.2.1}$$

$$p\cdot k_f = p\cdot k_{\bar{f}} = \tfrac{1}{2}m_Z^2. \tag{6.2.2}$$

According to the rules of Fig. J.1.2, the matrix elements for the two Feynman graphs are:

$$i\mathcal{M}_a = -i\frac{g}{c_W}(T_3^f - s_W^2 Q_f)\,\varepsilon_\mu x_f^\dagger \overline{\sigma}^\mu y_{\bar{f}}, \tag{6.2.3}$$

$$i\mathcal{M}_b = ig\frac{s_W^2}{c_W}Q_f\,\varepsilon_\mu y_f \sigma^\mu x_{\bar{f}}^\dagger, \tag{6.2.4}$$

where $x_i \equiv x(\vec{\boldsymbol{k}}_i, \lambda_i)$ and $y_i \equiv y(\vec{\boldsymbol{k}}_i, \lambda_i)$, for $i = f, \bar{f}$, and $\varepsilon_\mu \equiv \varepsilon_\mu(p, \lambda_Z)$.

Using the Bouchiat–Michel formulae developed in Appendix H.3, one can explicitly evaluate $\mathcal{M}_a$ and $\mathcal{M}_b$ as a function of the final state fermion helicities. The result of this computation is given in Eqs. (H.3.40) and (H.3.41). If the final state helicities are not measured, then it is simpler to square the amplitude and sum over the final state spins.

It is convenient to define:

$$a_f \equiv T_3^f - Q_f s_W^2, \qquad b_f \equiv -Q_f s_W^2. \tag{6.2.5}$$

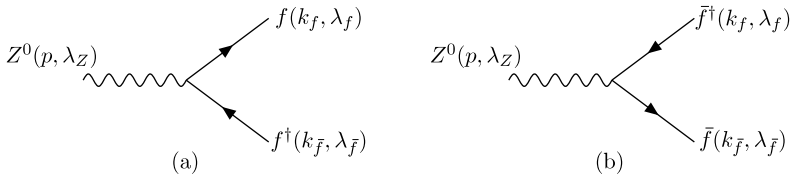

Fig. 6.2.1. The Feynman diagrams for Z^0 decay into a fermion–antifermion pair. Fermion lines are labeled according to the two-component fermion field labeling convention established in Section 5.

Then the squared matrix element for the decay is, using Eqs. (2.44) and (2.45),

$$|\mathcal{M}|^2 = \frac{g^2}{c_W^2}\varepsilon_\mu\varepsilon_\nu^*\left(a_f x_f^\dagger\overline{\sigma}^\mu y_{\bar f} + b_f y_f\sigma^\mu x_{\bar f}^\dagger\right)\left(a_f y_{\bar f}^\dagger\overline{\sigma}^\nu x_f + b_f x_{\bar f}\sigma^\nu y_f^\dagger\right). \tag{6.2.6}$$

Summing over the antifermion helicity using Eqs. (3.1.58)–(3.1.61) gives:

$$\sum_{\lambda_{\bar f}}|\mathcal{M}|^2 = \frac{g^2}{c_W^2}\varepsilon_\mu\varepsilon_\nu^*\Big(a_f^2 x_f^\dagger\overline{\sigma}^\mu k_{\bar f}\cdot\sigma\overline{\sigma}^\nu x_f + b_f^2 y_f\sigma^\mu k_{\bar f}\cdot\overline{\sigma}\sigma^\nu y_f^\dagger - m_f a_f b_f x_f^\dagger\overline{\sigma}^\mu\sigma^\nu y_f^\dagger - m_f a_f b_f y_f\sigma^\mu\overline{\sigma}^\nu x_f\Big). \tag{6.2.7}$$

Next, we sum over the fermion helicity:

$$\begin{aligned}\sum_{\lambda_f,\lambda_{\bar f}}|\mathcal{M}|^2 &= \frac{g^2}{c_W^2}\varepsilon_\mu\varepsilon_\nu^*\Big(a_f^2\mathrm{Tr}[\overline{\sigma}^\mu k_{\bar f}\cdot\sigma\overline{\sigma}^\nu k_f\cdot\sigma] + b_f^2\mathrm{Tr}[\sigma^\mu k_{\bar f}\cdot\overline{\sigma}\sigma^\nu k_f\cdot\overline{\sigma}]\\ &\quad - m_f^2 a_f b_f\mathrm{Tr}[\overline{\sigma}^\mu\sigma^\nu] - m_f^2 a_f b_f\mathrm{Tr}[\sigma^\mu\overline{\sigma}^\nu]\Big).\end{aligned} \tag{6.2.8}$$

Averaging over the Z^0 polarization using

$$\frac{1}{3}\sum_{\lambda_Z}\varepsilon_\mu\varepsilon_\nu^* = \frac{1}{3}\left(-g_{\mu\nu} + \frac{p_\mu p_\nu}{m_Z^2}\right), \tag{6.2.9}$$

and applying Eqs. (2.55)–(2.57), one gets:

$$\begin{aligned}\frac{1}{3}\sum_{\text{spins}}|\mathcal{M}|^2 &= \frac{g^2}{3c_W^2}\left[(a_f^2+b_f^2)\left(2k_f\cdot k_{\bar f} + 4\,k_f\cdot p\,k_{\bar f}\cdot p/m_Z^2\right) + 12a_f b_f m_f^2\right]\\ &= \frac{2g^2}{3c_W^2}\left[(a_f^2+b_f^2)(m_Z^2 - m_f^2) + 6a_f b_f m_f^2\right],\end{aligned} \tag{6.2.10}$$

where we have used Eqs. (6.2.1) and (6.2.2). After the standard phase space integration, we obtain the well-known result for the partial width of the Z^0:

$$\begin{aligned}\Gamma(Z^0\to f\bar f) &= \frac{N_c^f}{16\pi m_Z}\left(1-\frac{4m_f^2}{m_Z^2}\right)^{1/2}\left(\frac{1}{3}\sum_{\text{spins}}|\mathcal{M}|^2\right)\\ &= \frac{N_c^f g^2 m_Z}{24\pi c_W^2}\left(1-\frac{4m_f^2}{m_Z^2}\right)^{1/2}\left[(a_f^2+b_f^2)\left(1-\frac{m_f^2}{m_Z^2}\right) + 6a_f b_f\frac{m_f^2}{m_Z^2}\right].\end{aligned} \tag{6.2.11}$$

Here we have also included a factor of N_c^f (equal to 1 for leptons and 3 for quarks) for the sum over colors. Since the Z^0 is a color singlet, the color factor is simply equal to the dimension of the color representation of the outgoing fermions.

6.3. Bhabha scattering: $e^-e^+\to e^-e^+$

In our next example, we consider the computation of Bhabha scattering in QED (that is, we consider photon exchange but neglect Z^0-exchange) [160]. Bhabha scattering has also been computed using two-component spinors in [104]. We denote the initial state electron and positron momenta and helicities by (p_1,λ_1) and (p_2,λ_2) and the final state electron and positron momenta and helicities by (p_3,λ_3) and (p_4,λ_4), respectively. Neglecting the electron mass, we have in terms of the usual Mandelstam variables s, t, u:

$$p_1\cdot p_2 = p_3\cdot p_4 \equiv \tfrac{1}{2}s, \tag{6.3.1}$$

$$p_1\cdot p_3 = p_2\cdot p_4 \equiv -\tfrac{1}{2}t, \tag{6.3.2}$$

$$p_1\cdot p_4 = p_2\cdot p_3 \equiv -\tfrac{1}{2}u, \tag{6.3.3}$$

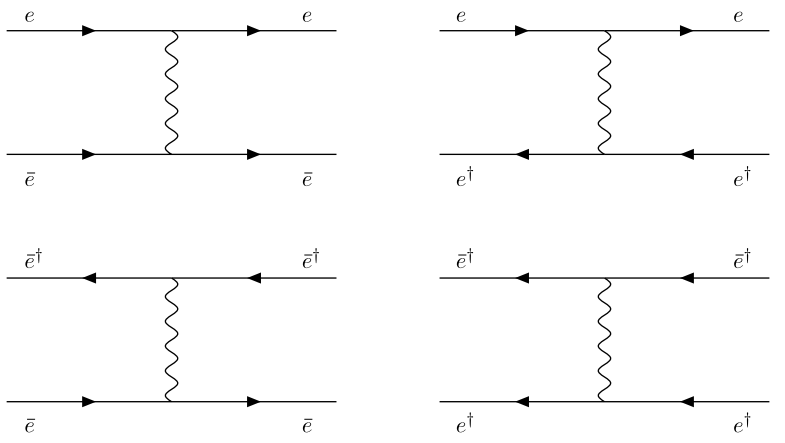

Fig. 6.3.1. Tree-level t-channel Feynman diagrams for $e^-e^+ \to e^-e^+$, with the external lines labeled according to the two-component field names. The momentum flow of the external particles is from left to right.

and $p_i^2 = 0$ for $i = 1, \ldots, 4$. There are eight distinct Feynman diagrams. First, there are four s-channel diagrams, as shown in Fig. 5.5 with amplitudes that follow from the Feynman rules of Fig. 5.3 (more generally, see Fig. J.1.2 in Appendix J):

$$i\mathcal{M}_s = \left(\frac{-ig^{\mu\nu}}{s}\right)\Big[(-ie\,x_1\sigma_\mu y_2^\dagger)(ie\,y_3\sigma_\nu x_4^\dagger) + (-ie\,y_1^\dagger\overline{\sigma}_\mu x_2)(ie\,y_3\sigma_\nu x_4^\dagger) + (-ie\,x_1\sigma_\mu y_2^\dagger)(ie\,x_3^\dagger\overline{\sigma}_\nu y_4) + (-ie\,y_1^\dagger\overline{\sigma}_\mu x_2)(ie\,x_3^\dagger\overline{\sigma}_\nu y_4)\Big], \tag{6.3.4}$$

where $x_i \equiv x(\vec{\boldsymbol{p}}_i, \lambda_i)$ and $y_i \equiv y(\vec{\boldsymbol{p}}_i, \lambda_i)$, for $i = 1, 4$. The photon propagator in Feynman gauge is $-ig^{\mu\nu}/(p_1+p_2)^2 = -ig^{\mu\nu}/s$. Here, we have chosen to write the external fermion spinors in the order 1, 2, 3, 4. This dictates in each term the use of either the $\overline{\sigma}$ or σ forms of the Feynman rules of Fig. 5.3. One can group the terms of Eq. (6.3.4) together more compactly:

$$i\mathcal{M}_s = e^2\left(\frac{-ig^{\mu\nu}}{s}\right)\left(x_1\sigma_\mu y_2^\dagger + y_1^\dagger\overline{\sigma}_\mu x_2\right)\left(y_3\sigma_\nu x_4^\dagger + x_3^\dagger\overline{\sigma}_\nu y_4\right). \tag{6.3.5}$$

There are also four t-channel diagrams, as shown in Fig. 6.3.1. The corresponding amplitudes for these four diagrams can be written:

$$i\mathcal{M}_t = (-1)e^2\left(\frac{-ig^{\mu\nu}}{t}\right)\left(x_1\sigma_\mu x_3^\dagger + y_1^\dagger\overline{\sigma}_\mu y_3\right)\left(x_2\sigma_\nu x_4^\dagger + y_2^\dagger\overline{\sigma}_\nu y_4\right). \tag{6.3.6}$$

Here, the overall factor of (-1) comes from Fermi–Dirac statistics, since the external fermion wave functions are written in an odd permutation (1, 3, 2, 4) of the original order (1, 2, 3, 4) established by the first term in Eq. (6.3.4).

Fierzing each term using Eqs. (2.67)–(2.69), and using Eqs. (2.59) and (2.60), the total amplitude can be written as:

$$\mathcal{M} = \mathcal{M}_s + \mathcal{M}_t = 2e^2\Big[\frac{1}{s}(x_1y_3)(y_2^\dagger x_4^\dagger) + \frac{1}{s}(y_1^\dagger x_3^\dagger)(x_2y_4) + \left(\frac{1}{s}+\frac{1}{t}\right)(y_1^\dagger x_4^\dagger)(x_2y_3) + \left(\frac{1}{s}+\frac{1}{t}\right)(x_1y_4)(y_2^\dagger x_3^\dagger) - \frac{1}{t}(x_1x_2)(x_3^\dagger x_4^\dagger) - \frac{1}{t}(y_1^\dagger y_2^\dagger)(y_3y_4)\Big]. \tag{6.3.7}$$

Squaring this amplitude and summing over spins, all of the cross terms will vanish in the $m_e \to 0$ limit. This is because each cross term will have an x or an $x^\dagger$ for some electron or positron combined with a y or a $y^\dagger$ for the same particle, and the corresponding spin sum is proportional to m_e [see Eqs. (3.1.60) and (3.1.61)]. Hence, summing over final state spins and averaging over initial state spins, the end result contains only the sum of the squares of the six terms in Eq. (6.3.7):

$$\frac{1}{4}\sum_{\text{spins}}|\mathcal{M}|^2 = e^4\sum_{\lambda_1,\lambda_2,\lambda_3,\lambda_4}\Big\{\frac{1}{s^2}\Big[(x_1y_3)(y_3^\dagger x_1^\dagger)(y_2^\dagger x_4^\dagger)(x_4y_2) + (y_1^\dagger x_3^\dagger)(x_3y_1)(x_2y_4)(y_4^\dagger x_2^\dagger)\Big] + \left(\frac{1}{s}+\frac{1}{t}\right)^2\Big[(y_1^\dagger x_4^\dagger)(x_4y_1)(x_2y_3)(y_3^\dagger x_2^\dagger) + (x_1y_4)(y_4^\dagger x_1^\dagger)(y_2^\dagger x_3^\dagger)(x_3y_2)\Big] + \frac{1}{t^2}\Big[(x_1x_2)(x_2^\dagger x_1^\dagger)(x_3^\dagger x_4^\dagger)(x_4x_3) + (y_1^\dagger y_2^\dagger)(y_2y_1)(y_3y_4)(y_4^\dagger y_3^\dagger)\Big]\Big\}. \tag{6.3.8}$$

Here we have used Eq. (2.43) to get the complex square of the fermion bilinears. Performing these spin sums using Eqs. (3.1.58) and (3.1.59) and using the trace identities Eq. (B.2.5):

$$\begin{aligned}\frac{1}{4}\sum_{\text{spins}}|\mathcal{M}|^2 &= 8e^4\left[\frac{p_2\cdot p_4\, p_1\cdot p_3}{s^2}+\frac{p_1\cdot p_2\, p_3\cdot p_4}{t^2}+\left(\frac{1}{s}+\frac{1}{t}\right)^2 p_1\cdot p_4\, p_2\cdot p_3\right]\\ &= 2e^4\left[\frac{t^2}{s^2}+\frac{s^2}{t^2}+\left(\frac{u}{s}+\frac{u}{t}\right)^2\right].\end{aligned} \tag{6.3.9}$$

Thus, the differential cross-section for Bhabha scattering is given by:

$$\frac{\mathrm{d}\sigma}{\mathrm{d}t}=\frac{1}{16\pi s^2}\left(\frac{1}{4}\sum_{\text{spins}}|\mathcal{M}|^2\right)=\frac{2\pi\alpha^2}{s^2}\left[\frac{t^2}{s^2}+\frac{s^2}{t^2}+\left(\frac{u}{s}+\frac{u}{t}\right)^2\right]. \tag{6.3.10}$$

This agrees with the result given in problem 5.2 of Ref. [114].

6.4. Polarized muon decay

So far we have only treated cases where the initial state fermion spins are averaged and the final state spins are summed. In the case of the polarized decay of a particle or polarized scattering we must project out the appropriate polarization of the particles in the spin sums. This is achieved by replacing the spin sums given in Eqs. (3.1.58)–(3.1.61) by the corresponding polarized spin projections Eqs. (3.1.33)–(3.1.36). As an example, we consider the decay of a polarized muon. Polarized muon decay has also been computed using two-component spinors in Ref. [104], however with an effective four-fermion interaction.

In Fig. 6.4.1, we show the single leading order Feynman diagram for muon decay, including the definition of the momenta. We denote the mass of the muon by m_μ, and neglect the electron mass. We shall measure the spin of the muon in its rest frame with respect to a fixed z-axis. Assume that the muon at rest is polarized such that its spin component along the $\hat{\boldsymbol{z}}$-direction is $s=+\frac{1}{2}$.

The decay amplitude is given by[58]

$$i\mathcal{M}=\left(\frac{-ig}{\sqrt{2}}\right)^2\left(x^\dagger_{\nu_\mu}\overline{\sigma}_\rho x_\mu\right)\left(x^\dagger_e\overline{\sigma}_\tau y_{\bar{\nu}_e}\right)\left(\frac{-ig^{\rho\tau}}{D_W}\right), \tag{6.4.1}$$

where $D_W=(p-k_{\nu_\mu})^2-m_W^2$ is the denominator of the W-boson propagator. In Eq. (6.4.1), $x_\mu\equiv x(\vec{\boldsymbol{p}},s=\frac{1}{2})$ for the spin-polarized initial state muon, and $x^\dagger_{\nu_\mu}\equiv x(\vec{\boldsymbol{k}}_{\nu_\mu},\lambda_{\nu_\mu})$, $x^\dagger_e\equiv x^\dagger(\vec{\boldsymbol{k}}_e,\lambda_e)$, and $y_{\bar{\nu}_e}\equiv y(\vec{\boldsymbol{k}}_{\bar{\nu}_e},\lambda_{\bar{\nu}_e})$. Squaring the amplitude using Eq. (2.45), we obtain

$$|\mathcal{M}|^2=\frac{g^4}{4D_W^2}\left(x^\dagger_{\nu_\mu}\overline{\sigma}^\rho x_\mu\right)\left(x^\dagger_\mu\overline{\sigma}^\tau x_{\nu_\mu}\right)\left(x^\dagger_e\overline{\sigma}_\rho y_{\bar{\nu}_e}\right)\left(y^\dagger_{\bar{\nu}_e}\overline{\sigma}_\tau x_e\right). \tag{6.4.2}$$

Summing over the neutrino and electron spins using Eqs. (3.1.58)–(3.1.59), and using Eq. (3.1.46) for the muon spin (with $s=\frac{1}{2}$) yields:

$$\begin{aligned}\sum_{\lambda_{\nu_\mu}\lambda_e\lambda_{\bar{\nu}_e}}|\mathcal{M}|^2 &= \frac{g^4}{8D_W^2}\mathrm{Tr}[k_{\nu_\mu}\cdot\sigma\,\overline{\sigma}^\rho(p\cdot\sigma-m_\mu S\cdot\sigma)\,\overline{\sigma}^\tau]\,\mathrm{Tr}[k_e\cdot\sigma\,\overline{\sigma}_\rho k_{\bar{\nu}_e}\cdot\sigma\,\overline{\sigma}_\tau]\\ &= \frac{2g^4}{D_W^2}\,k_e\cdot k_{\nu_\mu}\,k_{\bar{\nu}_e}\cdot(p-m_\mu S),\end{aligned} \tag{6.4.3}$$

where S^μ in an arbitrary frame is given by Eq. (3.1.15) [with $\hat{\boldsymbol{s}}=\hat{\boldsymbol{z}}$]. To obtain the second line we have used the trace identity Eq. (2.56) twice; note that the resulting terms linear in the antisymmetric tensor do not contribute, but the term quadratic in the antisymmetric tensor does.

The differential decay amplitude is now given by

$$\mathrm{d}\Gamma=\frac{1}{2m_\mu}|\mathcal{M}|^2\frac{\mathrm{d}^3\vec{\boldsymbol{k}}_e}{(2\pi)^3 2E_e}\frac{\mathrm{d}^3\vec{\boldsymbol{k}}_{\bar{\nu}_e}}{(2\pi)^3 2E_{\bar{\nu}_e}}\frac{\mathrm{d}^3\vec{\boldsymbol{k}}_{\nu_\mu}}{(2\pi)^3 2E_{\nu_\mu}}(2\pi)^4\delta^4(p-k_e-k_{\bar{\nu}_e}-k_{\nu_\mu}), \tag{6.4.4}$$

[58] Throughout this subsection μ and ν are particle labels. Hence, we employ ρ and τ as Lorentz vector indices.

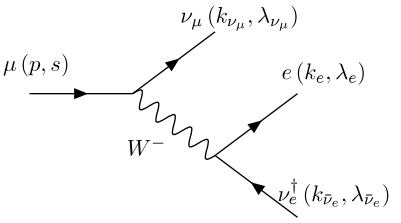

Fig. 6.4.1. Feynman diagram for electroweak muon decay.

where E_i, $i = e, \bar\nu_e, \nu_\mu$ are the energies of the final state particles in the muon rest frame. In the following we shall neglect both the electron mass and the momentum in the W-propagator compared to the W-boson mass, so $D_W^2 \to m_W^4$. We can now use the following identity to integrate over the neutrino momenta [165]

$$\int \frac{\mathrm{d}^3\vec{\boldsymbol{k}}_{\bar\nu_e}}{(2\pi)^3 2E_{\bar\nu_e}} \frac{\mathrm{d}^3\vec{\boldsymbol{k}}_{\nu_\mu}}{(2\pi)^3 2E_{\nu_\mu}} (2\pi)^4\delta^4(q - k_{\bar\nu_e} - k_{\nu_\mu}) k^\rho_{\bar\nu_e} k^\tau_{\nu_\mu} = \frac{1}{96\pi}(q^2 g^{\rho\tau} + 2q^\rho q^\tau), \tag{6.4.5}$$

where $q = p - k_e$. It follows that

$$\mathrm{d}\Gamma = \frac{g^4}{1536\pi^4 m_\mu m_W^4}\left[q^2\, k_e\cdot(p - m_\mu S) \,+\, 2q\cdot k_e\, q\cdot(p - m_\mu S)\right]\frac{\mathrm{d}^3\vec{\boldsymbol{k}}_e}{E_e}. \tag{6.4.6}$$

In the muon rest frame, $k_e = E_e(1; \cos\phi\sin\theta, \sin\phi\sin\theta, \cos\theta)$ and $S = (0; 0, 0, 1)$, so that $q^2 = m_\mu^2 - 2E_e m_\mu$ and $k_e\cdot(p - m_\mu S) = m_\mu E_e(1 + \cos\theta)$ and $q\cdot k_e = m_\mu E_e$ and $q\cdot(p - m_\mu S) = m_\mu(m_\mu - E_e - E_e\cos\theta)$. Noting that the maximum energy of the electron is $m_\mu/2$ (when the neutrino and antineutrino both recoil in the opposite direction), we obtain

$$\begin{aligned}\frac{\mathrm{d}\Gamma}{\mathrm{d}(\cos\theta)} &= \frac{g^4 m_\mu^2}{768\pi^3 m_W^4}\int_0^{m_\mu/2}\mathrm{d}E_e E_e^2\left[3 - \frac{4E_e}{m_\mu} + \left(1 - \frac{4E_e}{m_\mu}\right)\cos\theta\right]\\ &= \frac{g^4 m_\mu^5}{3\cdot 2^{12}\pi^3 m_W^4}\left(1 - \tfrac{1}{3}\cos\theta\right),\end{aligned} \tag{6.4.7}$$

in agreement with Ref. [165]. Introducing the Fermi constant, $G_F \equiv \sqrt{2}g^2/(8m_W^2)$, we can rewrite Eq. (6.4.7) as:

$$\frac{\mathrm{d}\Gamma}{\mathrm{d}(\cos\theta)} = \frac{G_F^2 m_\mu^5}{384\pi^3}\left(1 - \tfrac{1}{3}\cos\theta\right). \tag{6.4.8}$$

Integrating over $\cos\theta$ reproduces the well-known total muon decay width,

$$\Gamma = \frac{G_F^2 m_\mu^5}{192\pi^3}. \tag{6.4.9}$$

6.5. Neutral MSSM Higgs boson decays $\phi^0 \to f\bar f$, for $\phi^0 = h^0, H^0, A^0$

In this subsection, we consider the decays of the neutral Higgs scalar bosons $\phi^0 = h^0, H^0$, and A^0 of the MSSM into Standard Model fermion–antifermion pairs. The relevant tree-level Feynman diagrams are shown in Fig. 6.5.1. The final state fermion is assigned four-momentum p_1 and polarization λ_1, and the antifermion is assigned four-momentum p_2 and polarization λ_2. We will first work out the case that f is a charge $-1/3$ quark or a charged lepton, and later note the simple change needed for charge $+2/3$ quarks. The Feynman rules of Fig. K.1.1 of Appendix K tell us that the amplitudes are:

$$i\mathcal{M}_a = -\frac{i}{\sqrt{2}}\, Y_f\, k^*_{d\phi^0}\, x_1^\dagger x_2^\dagger, \tag{6.5.1}$$

$$i\mathcal{M}_b = -\frac{i}{\sqrt{2}}\, Y_f\, k_{d\phi^0}\, y_1 y_2. \tag{6.5.2}$$

Here Y_f is the Yukawa coupling of the fermion, $k_{d\phi^0}$ is the Higgs mixing parameter from Eq. (K.1.8), and the external wave functions are denoted $x_1 \equiv x(\vec{\boldsymbol{p}}_1, \lambda_1), y_1 \equiv y(\vec{\boldsymbol{p}}_1, \lambda_1)$ for the fermion and $x_2 \equiv x(\vec{\boldsymbol{p}}_2, \lambda_2), y_2 \equiv y(\vec{\boldsymbol{p}}_2, \lambda_2)$ for the antifermion. Squaring the total amplitude $i\mathcal{M} = i\mathcal{M}_a + i\mathcal{M}_b$ using Eq. (2.43) results in:

$$|\mathcal{M}|^2 = \frac{1}{2}|Y_f|^2\left[|k_{d\phi^0}|^2(y_1 y_2\, y_2^\dagger y_1^\dagger + x_1^\dagger x_2^\dagger\, x_2 x_1) + (k^*_{d\phi^0})^2 x_1^\dagger x_2^\dagger\, y_2^\dagger y_1^\dagger + (k_{d\phi^0})^2 y_1 y_2\, x_2 x_1\right]. \tag{6.5.3}$$

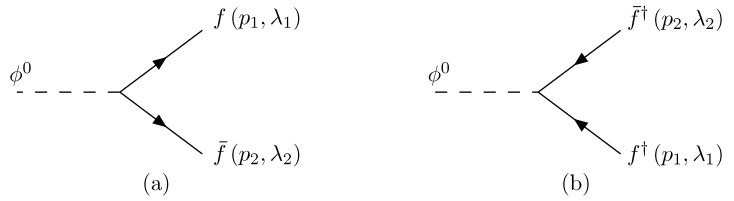

Fig. 6.5.1. The Feynman diagrams for the decays $\phi^0 \to f\bar{f}$, where $\phi^0 = h^0, H^0, A^0$ are the neutral Higgs scalar bosons of the MSSM, and f is a Standard Model quark or lepton, and $\bar{f}$ is the corresponding antiparticle. We have labeled the external fermions according to the two-component field names.

Summing over the final state antifermion spin using Eqs. (3.1.58)–(3.1.61) gives:

$$\sum_{\lambda_2} |\mathcal{M}|^2 = \frac{1}{2}|Y_f|^2 \left[|k_{d\phi^0}|^2 (y_1 p_2 \cdot \sigma y_1^\dagger + x_1^\dagger p_2 \cdot \overline{\sigma} x_1) - (k^*_{d\phi^0})^2 m_f x_1^\dagger y_1^\dagger - (k_{d\phi^0})^2 m_f y_1 x_1 \right]. \tag{6.5.4}$$

Summing over the fermion spins in the same way yields:

$$\begin{aligned} \sum_{\lambda_1,\lambda_2} |\mathcal{M}|^2 &= \frac{1}{2}|Y_f|^2 \left\{ |k_{d\phi^0}|^2 (\mathrm{Tr}[p_2 \cdot \sigma p_1 \cdot \overline{\sigma}] + \mathrm{Tr}[p_2 \cdot \overline{\sigma} p_1 \cdot \sigma]) - 2(k^*_{d\phi^0})^2 m_f^2 - 2(k_{d\phi^0})^2 m_f^2 \right\} \\ &= |Y_f|^2 \left\{ 2|k_{d\phi^0}|^2 p_1 \cdot p_2 - 2\mathrm{Re}[(k_{d\phi^0})^2] m_f^2 \right\} \\ &= |Y_f|^2 \left\{ |k_{d\phi^0}|^2 (m^2_{\phi^0} - 2m_f^2) - 2\mathrm{Re}[(k_{d\phi^0})^2] m_f^2 \right\}, \end{aligned} \tag{6.5.5}$$

where we have used the trace identity Eq. (2.55) to obtain the second equality. The corresponding expression for charge $+2/3$ quarks can be obtained by simply replacing $k_{d\phi^0}$ with $k_{u\phi^0}$. The total decay rates now follow from integration over phase space [166]

$$\Gamma(\phi^0 \to f\bar{f}) = \frac{N_c^f}{16\pi m_{\phi^0}} \left(1 - 4m_f^2/m^2_{\phi^0}\right)^{1/2} \sum_{\lambda_1,\lambda_2} |\mathcal{M}|^2. \tag{6.5.6}$$

The factor of $N_c^f = 3$ for quarks and 1 for leptons comes from the sum over colors.

Results for special cases are obtained by putting in the relevant values for the couplings and the mixing parameters from Eqs. (K.1.7) and (K.1.8). In particular, for the CP-even Higgs bosons h^0 and H^0, $k_{d\phi^0}$ and $k_{u\phi^0}$ are real, so one obtains:

$$\Gamma(h^0 \to b\bar{b}) = \frac{3}{16\pi} Y_b^2 \sin^2\alpha\, m_{h^0} \left(1 - 4m_b^2/m^2_{h^0}\right)^{3/2}, \tag{6.5.7}$$

$$\Gamma(h^0 \to c\bar{c}) = \frac{3}{16\pi} Y_c^2 \cos^2\alpha\, m_{h^0} \left(1 - 4m_c^2/m^2_{h^0}\right)^{3/2}, \tag{6.5.8}$$

$$\Gamma(h^0 \to \tau^+\tau^-) = \frac{1}{16\pi} Y_\tau^2 \sin^2\alpha\, m_{h^0} \left(1 - 4m_\tau^2/m^2_{h^0}\right)^{3/2}, \tag{6.5.9}$$

$$\Gamma(H^0 \to t\bar{t}) = \frac{3}{16\pi} Y_t^2 \sin^2\alpha\, m_{H^0} \left(1 - 4m_t^2/m^2_{H^0}\right)^{3/2}, \tag{6.5.10}$$

$$\Gamma(H^0 \to b\bar{b}) = \frac{3}{16\pi} Y_b^2 \cos^2\alpha\, m_{H^0} \left(1 - 4m_b^2/m^2_{H^0}\right)^{3/2}, \tag{6.5.11}$$

etc., which check with the expressions in Appendix C of Ref. [167]. For the CP-odd Higgs boson A^0, the mixing parameters $k_{uA^0} = i\cos\beta_0$ and $k_{dA^0} = i\sin\beta_0$ are purely imaginary, so

$$\Gamma(A^0 \to t\bar{t}) = \frac{3}{16\pi} Y_t^2 \cos^2\beta_0\, m_{A^0} \left(1 - 4m_t^2/m^2_{A^0}\right)^{1/2}, \tag{6.5.12}$$

$$\Gamma(A^0 \to b\bar{b}) = \frac{3}{16\pi} Y_b^2 \sin^2\beta_0\, m_{A^0} \left(1 - 4m_b^2/m^2_{A^0}\right)^{1/2}, \tag{6.5.13}$$

$$\Gamma(A^0 \to \tau^+\tau^-) = \frac{1}{16\pi} Y_\tau^2 \sin^2\beta_0\, m_{A^0} \left(1 - 4m_\tau^2/m^2_{A^0}\right)^{1/2}. \tag{6.5.14}$$

Note that the differing kinematic factors for the CP-odd Higgs decays came about because of the different relative sign between the two Feynman diagrams. For example, in the case of $h^0 \to b\bar{b}$, the matrix element is

$$i\mathcal{M} = \frac{i}{\sqrt{2}} Y_b \sin\alpha\, (y_1 y_2 + x_1^\dagger x_2^\dagger), \tag{6.5.15}$$

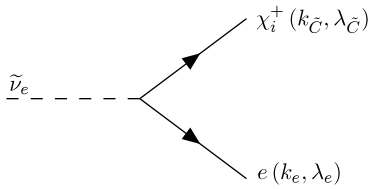

Fig. 6.6.1. The Feynman diagram for $\widetilde{\nu}_e \to \widetilde{C}_i^+ e^-$ in the MSSM.

while for $A^0 \to b\bar{b}$, it is

$$i\mathcal{M} = \frac{1}{\sqrt{2}} Y_b \sin\beta_0\,(y_1 y_2 - x_1^\dagger x_2^\dagger). \tag{6.5.16}$$

The differing relative sign between $y_1 y_2$ and $x_1^\dagger x_2^\dagger$ follows from the imaginary pseudoscalar Lagrangian coupling, which is complex conjugated in the second diagram.

6.6. Sneutrino decay $\widetilde{\nu}_e \to \widetilde{C}_i^+ e^-$

Next we consider the process of sneutrino decay $\widetilde{\nu}_e \to \widetilde{C}_i^+ e^-$ in the MSSM. Because only the left-handed electron can couple to the chargino and sneutrino (with the excellent approximation that the electron Yukawa coupling vanishes), there is just one Feynman diagram, shown in Fig. 6.6.1. The external wave functions of the electron and chargino are denoted as $x_e \equiv x(\vec{\boldsymbol{k}}_e, \lambda_e)$, and $x_{\tilde{C}} \equiv x(\vec{\boldsymbol{k}}_{\tilde{C}}, \lambda_{\tilde{C}})$, respectively. From the corresponding Feynman rule given in Fig. K.4.1 of Appendix K, the amplitude is:

$$i\mathcal{M} = -igV_{i1}\, x_{\tilde{C}}^\dagger x_e^\dagger, \tag{6.6.1}$$

where V_{ij} is one of the two matrices used to diagonalize the chargino masses [cf. Eq. (K.2.6)]. Squaring this using Eq. (2.43) yields:

$$|\mathcal{M}|^2 = g^2 |V_{i1}|^2\,(x_{\tilde{C}}^\dagger x_e^\dagger)(x_e x_{\tilde{C}}). \tag{6.6.2}$$

Summing over the electron and chargino spin polarizations using Eq. (3.1.58) yields

$$\sum_{\lambda_e,\lambda_{\tilde{C}}} |\mathcal{M}|^2 = g^2 |V_{i1}|^2 \mathrm{Tr}[k_e \cdot \overline{\sigma}\, k_{\tilde{C}} \cdot \sigma] = 2g^2 |V_{i1}|^2\, k_e \cdot k_{\tilde{C}} = g^2 |V_{i1}|^2 (m_{\tilde{\nu}_e}^2 - m_{\tilde{C}_i}^2), \tag{6.6.3}$$

where we have used $2k_e \cdot k_{\tilde{C}} = m_{\tilde{\nu}_e}^2 - m_{\tilde{C}_i}^2$, neglecting the electron mass. Therefore, after integrating over phase space in the standard way, the decay width is:

$$\Gamma(\widetilde{\nu}_e \to \widetilde{C}_i^+ e^-) = \frac{1}{16\pi m_{\tilde{\nu}_e}} \left(1 - \frac{m_{\tilde{C}_i}^2}{m_{\tilde{\nu}_e}^2}\right) \left[\sum_{\lambda_e,\lambda_{\tilde{C}}} |\mathcal{M}|^2\right] = \frac{g^2}{16\pi} |V_{i1}|^2 m_{\tilde{\nu}_e} \left(1 - \frac{m_{\tilde{C}_i}^2}{m_{\tilde{\nu}_e}^2}\right)^2, \tag{6.6.4}$$

which agrees with Ref. [168] and Eq. (3.8) in Ref. [7].

6.7. Chargino decay $\widetilde{C}_i^+ \to \widetilde{\nu}_e e^+$

Here again, there is just one Feynman diagram (neglecting the electron mass in the Yukawa coupling) shown in Fig. 6.7.1. The external wave functions for the chargino and the positron are denoted by $x_{\tilde{C}} \equiv x(\vec{\boldsymbol{p}}_{\tilde{C}}, \lambda_{\tilde{C}})$ and $y_e \equiv y(\vec{\boldsymbol{k}}_e, \lambda_e)$, respectively. The fermion momenta and helicities are denoted as in Fig. 6.7.1. As in the previous example, the amplitude can be directly determined using the Feynman rule given in Fig. K.4.1 in Appendix K:

$$\mathcal{M} = -igV_{i1}^*\, x_{\tilde{C}}\, y_e. \tag{6.7.1}$$

Squaring this using Eq. (2.43) yields:

$$|\mathcal{M}|^2 = g^2 |V_{i1}|^2\,(x_{\tilde{C}} y_e)\,(y_e^\dagger x_{\tilde{C}}^\dagger). \tag{6.7.2}$$

Summing over the electron helicity and averaging over the chargino helicity using Eqs. (3.1.58) and (3.1.59) we obtain:

$$\tfrac{1}{2} \sum_{\lambda_e,\lambda_{\tilde{C}}} |\mathcal{M}|^2 = \tfrac{1}{2} g^2 |V_{i1}|^2 \mathrm{Tr}[k_e \cdot \sigma\, p_{\tilde{C}} \cdot \overline{\sigma}] = g^2 |V_{i1}|^2 k_e \cdot p_{\tilde{C}} = \frac{g^2}{2} |V_{i1}|^2 (m_{\tilde{C}_i}^2 - m_{\tilde{\nu}_e}^2). \tag{6.7.3}$$

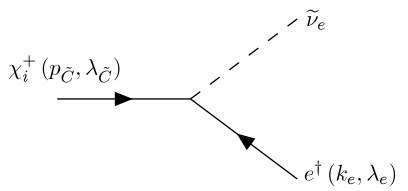

Fig. 6.7.1. The Feynman diagram for $\widetilde{C}_i^+ \to \widetilde{\nu}_e e^+$ in the MSSM.

So the decay width is, neglecting the electron mass:

$$\Gamma(\widetilde{C}_i^+ \to \widetilde{\nu} e^+) = \frac{1}{16\pi m_{\widetilde{C}_i}} \left(1 - \frac{m_{\widetilde{\nu}_e}^2}{m_{\widetilde{C}_i}^2}\right) \left(\frac{1}{2} \sum_{\lambda_e, \lambda_{\widetilde{C}}} |\mathcal{M}|^2\right) = \frac{g^2}{32\pi} |V_{i1}|^2 m_{\widetilde{C}_i} \left(1 - \frac{m_{\widetilde{\nu}_e}^2}{m_{\widetilde{C}_i}^2}\right)^2, \tag{6.7.4}$$

which agrees with Ref. [168].

6.8. Neutralino decays $\widetilde{N}_i \to \phi^0 \widetilde{N}_j$, for $\phi^0 = h^0, H^0, A^0$

Next we consider the decay of a neutralino to a lighter neutralino and neutral Higgs boson $\phi^0 = h^0, H^0$, or A^0. The two tree-level Feynman graphs are shown in Fig. 6.8.1, where we have also labeled the momenta and helicities. We denote the masses for the neutralinos and the Higgs boson as $m_{\widetilde{N}_i}$, $m_{\widetilde{N}_j}$, and m_{ϕ^0}. Using the Feynman rules of Fig. K.3.1, the amplitudes are respectively given by

$$i\mathcal{M}_1 = -iY\, x_i y_j, \tag{6.8.1}$$

$$i\mathcal{M}_2 = -iY^*\, y_i^\dagger x_j^\dagger, \tag{6.8.2}$$

where the coupling $Y \equiv Y^{\phi^0 \chi_i^0 \chi_j^0}$ is defined in Eq. (K.3.1), and the external wave functions are $x_i \equiv x(\vec{\boldsymbol{p}}_i, \lambda_i)$, $y_i^\dagger \equiv y^\dagger(\vec{\boldsymbol{p}}_i, \lambda_i)$, $y_j \equiv y(\vec{\boldsymbol{k}}_j, \lambda_j)$, and $x_j^\dagger \equiv x^\dagger(\vec{\boldsymbol{k}}_j, \lambda_j)$.

Taking the square of the total matrix element using Eq. (2.43) gives:

$$|\mathcal{M}|^2 = |Y|^2 (x_i y_j y_j^\dagger x_i^\dagger + y_i^\dagger x_j^\dagger x_j y_i) + Y^2 x_i y_j x_j y_i + Y^{*2} y_i^\dagger x_j^\dagger y_j^\dagger x_i^\dagger. \tag{6.8.3}$$

Summing over the final state neutralino spins using Eqs. (3.1.58)–(3.1.61) yields

$$\sum_{\lambda_j} |\mathcal{M}|^2 = |Y|^2 (x_i k_j \cdot \sigma x_i^\dagger + y_i^\dagger k_j \cdot \overline{\sigma} y_i) - Y^2 m_{\widetilde{N}_j} x_i y_i - Y^{*2} m_{\widetilde{N}_j} y_i^\dagger x_i^\dagger. \tag{6.8.4}$$

Averaging over the initial state neutralino spins in the same way gives

$$\begin{aligned} \frac{1}{2} \sum_{\lambda_i, \lambda_j} |\mathcal{M}|^2 &= \frac{1}{2} |Y|^2 (\mathrm{Tr}[k_j \cdot \sigma p_i \cdot \overline{\sigma}] + \mathrm{Tr}[k_j \cdot \overline{\sigma} p_i \cdot \sigma]) + \mathrm{Re}[Y^2] m_{\widetilde{N}_i} m_{\widetilde{N}_j} \mathrm{Tr}[\mathbb{1}_{2\times 2}] \\ &= 2|Y|^2 p_i \cdot k_j + 2\mathrm{Re}[Y^2] m_{\widetilde{N}_i} m_{\widetilde{N}_j} \\ &= |Y|^2 (m_{\widetilde{N}_i}^2 + m_{\widetilde{N}_j}^2 - m_{\phi^0}^2) + 2\mathrm{Re}[Y^2] m_{\widetilde{N}_i} m_{\widetilde{N}_j}, \end{aligned} \tag{6.8.5}$$

where we have used Eq. (2.55) to obtain the second equality. The total decay rate is therefore

$$\begin{aligned} \Gamma(\widetilde{N}_i \to \phi^0 \widetilde{N}_j) &= \frac{1}{16\pi m_{\widetilde{N}_i}^3} \lambda^{1/2}(m_{\widetilde{N}_i}^2, m_{\phi^0}^2, m_{\widetilde{N}_j}^2) \left(\frac{1}{2} \sum_{\lambda_i, \lambda_j} |\mathcal{M}|^2\right) \\ &= \frac{m_{\widetilde{N}_i}}{16\pi} \lambda^{1/2}(1, r_\phi, r_j) \left[|Y^{\phi^0 \chi_i^0 \chi_j^0}|^2 (1 + r_j - r_\phi) + 2\mathrm{Re}\left[\left(Y^{\phi^0 \chi_i^0 \chi_j^0}\right)^2\right] \sqrt{r_j}\right], \end{aligned} \tag{6.8.6}$$

where the triangle function $\lambda^{1/2}$ is defined in Eq. (6.1.11), $r_j \equiv m_{\widetilde{N}_j}^2 / m_{\widetilde{N}_i}^2$ and $r_\phi \equiv m_{\phi^0}^2 / m_{\widetilde{N}_i}^2$. The results for $\phi^0 = h^0, H^0, A^0$ can now be obtained by using Eqs. (K.1.7) and (K.1.8) in Eq. (K.3.1). In comparing Eq. (6.8.6) with the original calculation in Ref. [169], it is helpful to employ Eqs. (4.51) and (4.53) of [170]. The results agree.

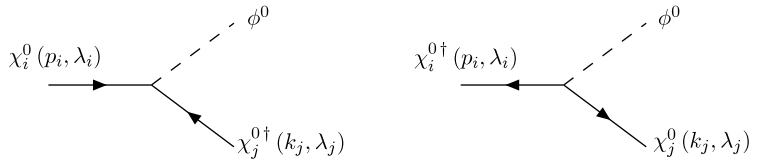

Fig. 6.8.1. The Feynman diagrams for $\widetilde{N}_i \to \widetilde{N}_j\phi^0$ in the MSSM.

6.9. $\widetilde{N}_i \to Z^0 N_j$

For this two-body decay there are two tree-level Feynman diagrams, shown in Fig. 6.9.1 with the definitions of the helicities and the momenta. Using the Feynman rules of Fig. K.2.1, the two amplitudes are given by[59]

$$i\mathcal{M}_1 = -i\frac{g}{c_W}\mathcal{O}''^L_{ji}x_i\sigma^\mu x_j^\dagger\varepsilon_\mu^*, \tag{6.9.1}$$

$$i\mathcal{M}_2 = i\frac{g}{c_W}\mathcal{O}''^L_{ij}y_i^\dagger\,\overline{\sigma}^\mu y_j\varepsilon_\mu^*, \tag{6.9.2}$$

where the external wave functions are $x_i = x(\vec{\boldsymbol{p}}_i,\lambda_i)$, $y_i^\dagger = y^\dagger(\vec{\boldsymbol{p}}_i,\lambda_i)$, $x_j^\dagger = x^\dagger(\vec{\boldsymbol{k}}_j,\lambda_j)$, $y_j = y(\vec{\boldsymbol{k}}_j,\lambda_j)$, and $\varepsilon_\mu^* = \varepsilon_\mu(\vec{\boldsymbol{k}}_Z,\lambda_Z)^*$. Noting that $\mathcal{O}''^L_{ji} = \mathcal{O}''^{L*}_{ij}$ [see Eq. (K.2.5)], and applying Eqs. (2.44) and (2.45), we find that the squared matrix element is:

$$|\mathcal{M}|^2 = \frac{g^2}{c_W^2}\varepsilon_\mu^*\varepsilon_\nu\left[|\mathcal{O}''^L_{ij}|^2(x_i\sigma^\mu x_j^\dagger x_j\sigma^\nu x_i^\dagger + y_i^\dagger\,\overline{\sigma}^\mu y_j y_j^\dagger\overline{\sigma}^\nu y_i) - \left(\mathcal{O}''^L_{ij}\right)^2 y_i^\dagger\,\overline{\sigma}^\mu y_j x_j\sigma^\nu x_i^\dagger - \left(\mathcal{O}''^{L*}_{ij}\right)^2 x_i\sigma^\mu x_j^\dagger y_j^\dagger\overline{\sigma}^\nu y_i\right]. \tag{6.9.3}$$

Summing over the final state neutralino spin using Eqs. (3.1.58)–(3.1.61) yields:

$$\begin{aligned}\sum_{\lambda_j}|\mathcal{M}|^2 \;=\; &\frac{g^2}{c_W^2}\varepsilon_\mu^*\varepsilon_\nu\Big[|\mathcal{O}''^L_{ij}|^2(x_i\sigma^\mu k_j\cdot\overline{\sigma}\sigma^\nu x_i^\dagger + y_i^\dagger\,\overline{\sigma}^\mu k_j\cdot\sigma\overline{\sigma}^\nu y_i)\\ &+ \left(\mathcal{O}''^L_{ij}\right)^2 m_{\widetilde{N}_j}y_i^\dagger\,\overline{\sigma}^\mu\sigma^\nu x_i^\dagger + \left(\mathcal{O}''^{L*}_{ij}\right)^2 m_{\widetilde{N}_j}x_i\sigma^\mu\overline{\sigma}^\nu y_i\Big].\end{aligned} \tag{6.9.4}$$

Averaging over the initial state neutralino spins in the same way gives

$$\begin{aligned}\frac{1}{2}\sum_{\lambda_i,\lambda_j}|\mathcal{M}|^2 \;&=\; \frac{g^2}{2c_W^2}\varepsilon_\mu^*\varepsilon_\nu\Big[|\mathcal{O}''^L_{ij}|^2\Big(\mathrm{Tr}[\sigma^\mu k_j\cdot\overline{\sigma}\sigma^\nu p_i\cdot\overline{\sigma}] + \mathrm{Tr}[\overline{\sigma}^\mu k_j\cdot\sigma\overline{\sigma}^\nu p_i\cdot\sigma]\Big)\\ &\quad - \left(\mathcal{O}''^L_{ij}\right)^2 m_{\widetilde{N}_i}m_{\widetilde{N}_j}\mathrm{Tr}[\overline{\sigma}^\mu\sigma^\nu] - \left(\mathcal{O}''^{L*}_{ij}\right)^2 m_{\widetilde{N}_i}m_{\widetilde{N}_j}\mathrm{Tr}[\sigma^\mu\overline{\sigma}^\nu]\Big]\\ &=\; \frac{2g^2}{c_W^2}\varepsilon_\mu^*\varepsilon_\nu\Big\{|\mathcal{O}''^L_{ij}|^2\left(k_j^\mu p_i^\nu + p_i^\mu k_j^\nu - p_i\cdot k_j g^{\mu\nu}\right) - \mathrm{Re}\Big[\left(\mathcal{O}''^L_{ij}\right)^2\Big]m_{\widetilde{N}_i}m_{\widetilde{N}_j}g^{\mu\nu}\Big\},\end{aligned} \tag{6.9.5}$$

where in the last equality we have applied Eqs. (2.55)–(2.57). Using

$$\sum_{\lambda_Z}\varepsilon^{\mu*}\varepsilon^\nu = -g^{\mu\nu} + k_Z^\mu k_Z^\nu/m_Z^2, \tag{6.9.6}$$

we obtain

$$\frac{1}{2}\sum_{\lambda_i,\lambda_j,\lambda_Z}|\mathcal{M}|^2 \;=\; \frac{2g^2}{c_W^2}\left\{|\mathcal{O}''^L_{ij}|^2\left(p_i\cdot k_j + 2p_i\cdot k_Z k_j\cdot k_Z/m_Z^2\right) + 3m_{\widetilde{N}_i}m_{\widetilde{N}_j}\mathrm{Re}\Big[\left(\mathcal{O}''^L_{ij}\right)^2\Big]\right\}. \tag{6.9.7}$$

Using $2k_j\cdot k_Z = m_{\widetilde{N}_i}^2 - m_{\widetilde{N}_j}^2 - m_Z^2$, $2p_i\cdot k_j = m_{\widetilde{N}_i}^2 + m_{\widetilde{N}_j}^2 - m_Z^2$, and $2p_i\cdot k_Z = m_{\widetilde{N}_i}^2 - m_{\widetilde{N}_j}^2 + m_Z^2$, we obtain the total decay width:

$$\Gamma(\widetilde{N}_i\to Z^0\widetilde{N}_j) \;=\; \frac{1}{16\pi m_{\widetilde{N}_i}^3}\lambda^{1/2}\left(m_{\widetilde{N}_i}^2, m_Z^2, m_{\widetilde{N}_j}^2\right)\left(\frac{1}{2}\sum_{\lambda_i,\lambda_j,\lambda_Z}|\mathcal{M}|^2\right) \tag{6.9.8}$$

$$\;=\; \frac{g^2 m_{\widetilde{N}_i}}{16\pi c_W^2}\lambda^{1/2}(1,r_Z,r_j)\Big[|\mathcal{O}''^L_{ij}|^2\left(1 + r_j - 2r_Z + (1-r_j)^2/r_Z\right) + 6\mathrm{Re}\Big[\left(\mathcal{O}''^L_{ij}\right)^2\Big]\sqrt{r_j}\Big], \tag{6.9.9}$$

[59] When comparing with the four-component Feynman rule in Ref. [7] note that $\mathcal{O}''^L_{ij} = -\mathcal{O}''^{R*}_{ij}$ [cf. Eq. (K.2.5)].

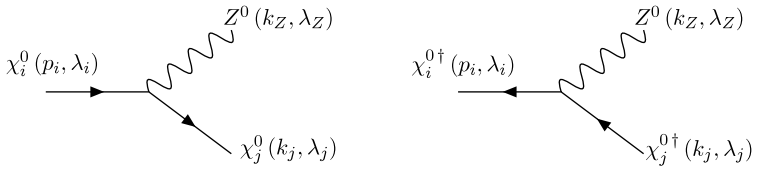

Fig. 6.9.1. The Feynman diagrams for $\widetilde{N}_i \to \widetilde{N}_j Z^0$ in the MSSM.

where

$$r_j \equiv m^2_{\widetilde{N}_j}/m^2_{\widetilde{N}_i}, \qquad r_Z \equiv m^2_Z/m^2_{\widetilde{N}_i}, \tag{6.9.10}$$

and the triangle function $\lambda^{1/2}$ is defined in Eq. (6.1.11). The result obtained in Eq. (6.9.9) agrees with the original calculation in Ref. [169].

6.10. Selectron pair production in electron–electron collisions

6.10.1. $e^-e^- \to \widetilde{e}_L^-\widetilde{e}_R^-$

Here there are two Feynman graphs (neglecting the electron mass and Yukawa couplings), shown in Fig. 6.10.1. Note that these two graphs are related by interchange of the identical initial state electrons. Let the electrons have momenta p_1 and p_2 and the selectrons have momenta $k_{\widetilde{e}_L}$ and $k_{\widetilde{e}_R}$, so that $p_1^2 = p_2^2 = 0$; $k_1^2 = m^2_{\widetilde{e}_L}$; $k_2^2 = m^2_{\widetilde{e}_R}$; $s = (p_1 + p_2)^2 = (k_1 + k_2)^2$; $t = (k_1 - p_1)^2 = (k_2 - p_2)^2$; $u = (k_1 - p_2)^2 = (k_2 - p_1)^2$.

Using the Feynman rules of Fig. K.4.2, the matrix element for the first graph, for each neutralino $\widetilde{N}_i$ exchanged in the t channel, is:

$$i\mathcal{M}_t = \left[i\frac{g}{\sqrt{2}}\left(N^*_{i2} + \frac{s_W}{c_W}N^*_{i1}\right)\right]\left[-i\sqrt{2}g\frac{s_W}{c_W}N_{i1}\right]x_1\left[\frac{i(k_1 - p_1)\cdot\sigma}{(k_1 - p_1)^2 - m^2_{\widetilde{N}_i}}\right]y_2^\dagger. \tag{6.10.1}$$

We employ the notation for the external wave functions $x_i = (\vec{\boldsymbol{p}}_i, \lambda_i)$, $i = 1, 2$ and analogously for $y_i, x_i^\dagger, y_i^\dagger$. The matrix elements for the second (u-channel) graph are the same with the two incoming electrons exchanged, $e_1 \leftrightarrow e_2$:

$$i\mathcal{M}_u = (-1)\left[i\frac{g}{\sqrt{2}}\left(N^*_{i2} + \frac{s_W}{c_W}N^*_{i1}\right)\right]\left[-i\sqrt{2}g\frac{s_W}{c_W}N_{i1}\right]x_2\left[\frac{i(k_1 - p_2)\cdot\sigma}{(k_1 - p_2)^2 - m^2_{\widetilde{N}_i}}\right]y_1^\dagger. \tag{6.10.2}$$

Note that since we have written the fermion wave function spinors in the opposite order in $\mathcal{M}_2$ compared to $\mathcal{M}_1$, there is a factor (-1) for Fermi–Dirac statistics. Alternatively, starting at the electron with momentum p_1 and using the Feynman rules as above, we can directly write:

$$i\mathcal{M}_u = \left[i\frac{g}{\sqrt{2}}\left(N^*_{i2} + \frac{s_W}{c_W}N^*_{i1}\right)\right]\left[-i\sqrt{2}g\frac{s_W}{c_W}N_{i1}\right]y_1^\dagger\left[\frac{-i(k_1 - p_2)\cdot\overline{\sigma}}{(k_1 - p_2)^2 - m^2_{\widetilde{N}_i}}\right]x_2. \tag{6.10.3}$$

This has no Fermi–Dirac factor (-1) because the wave function spinors are written in the same order as in $\mathcal{M}_t$. However, now the Feynman rule for the propagator has an extra minus sign, as can be seen in Fig. 4.2.2. We can also obtain Eq. (6.10.3) from Eq. (6.10.2) by using Eq. (2.61). So we can write for the total amplitude:

$$\mathcal{M} = \mathcal{M}_t + \mathcal{M}_u = x_1 a\cdot\sigma y_2^\dagger + y_1^\dagger b\cdot\overline{\sigma}x_2, \tag{6.10.4}$$

where

$$a^\mu \equiv \frac{g^2 s_W}{c_W}(k_1^\mu - p_1^\mu)\sum_{i=1}^4 N_{i1}\left(N^*_{i2} + \frac{s_W}{c_W}N^*_{i1}\right)\frac{1}{t - m^2_{\widetilde{N}_i}}, \tag{6.10.5}$$

$$b^\mu \equiv -\frac{g^2 s_W}{c_W}(k_1^\mu - p_2^\mu)\sum_{i=1}^4 N_{i1}\left(N^*_{i2} + \frac{s_W}{c_W}N^*_{i1}\right)\frac{1}{u - m^2_{\widetilde{N}_i}}. \tag{6.10.6}$$

Hence, using Eqs. (2.44) and (2.45):

$$\begin{aligned}|\mathcal{M}|^2 = {} & \left(x_1 a\cdot\sigma y_2^\dagger\right)\left(y_2 a^*\cdot\sigma x_1^\dagger\right) + \left(y_1^\dagger b\cdot\overline{\sigma}x_2\right)\left(x_2^\dagger b^*\cdot\overline{\sigma}y_1\right)\\ & + \left(x_1 a\cdot\sigma y_2^\dagger\right)\left(x_2^\dagger b^*\cdot\overline{\sigma}y_1\right) + \left(y_1^\dagger b\cdot\overline{\sigma}x_2\right)\left(y_2 a^*\cdot\sigma x_1^\dagger\right).\end{aligned} \tag{6.10.7}$$

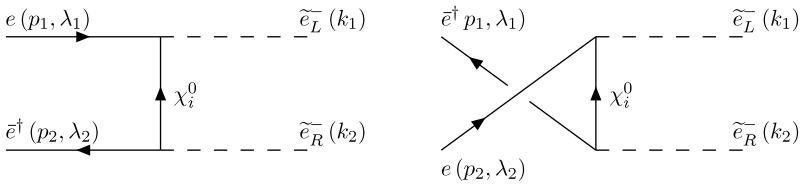

Fig. 6.10.1. Feynman diagrams for $e^-e^- \to \widetilde{e}_L^-\widetilde{e}_R^-$.

Averaging over the initial state electron spins using Eqs. (3.1.58)–(3.1.61), the a, b^* and a^*, b cross terms are proportional to m_e and can thus be neglected in our approximation. We get:

$$\frac{1}{4}\sum_{\lambda_1,\lambda_2}|\mathcal{M}|^2 = \frac{1}{4}\mathrm{Tr}[a\cdot\sigma\ p_2\cdot\overline{\sigma}\ a^*\cdot\sigma\ p_1\cdot\overline{\sigma}] + \frac{1}{4}\mathrm{Tr}[b\cdot\overline{\sigma}\ p_2\cdot\sigma\ b^*\cdot\overline{\sigma}\ p_1\cdot\sigma]. \tag{6.10.8}$$

These terms can be simplified using the identities:

$$\begin{aligned}\mathrm{Tr}[(k_1-p_1)\cdot\sigma\ p_2\cdot\overline{\sigma}\ (k_1-p_1)\cdot\sigma\ p_1\cdot\overline{\sigma}] &= \mathrm{Tr}[(k_1-p_2)\cdot\overline{\sigma}\ p_2\cdot\sigma\ (k_1-p_2)\cdot\overline{\sigma}\ p_1\cdot\sigma]\\ &= tu - m^2_{\widetilde{e}_L}m^2_{\widetilde{e}_R},\end{aligned} \tag{6.10.9}$$

which follow from Eqs. (2.56) and (2.57), resulting in:

$$\begin{aligned}\frac{1}{4}\sum_{\lambda_1,\lambda_2}|\mathcal{M}|^2 = \frac{g^4 s_W^2}{4c_W^2}(tu - m^2_{\widetilde{e}_L}m^2_{\widetilde{e}_R})\sum_{i,j=1}^{4}N_{j1}N_{i1}^*\left(N_{j2}^* + \frac{s_W}{c_W}N_{j1}^*\right)\left(N_{i2} + \frac{s_W}{c_W}N_{i1}\right)\\ \times\left[\frac{1}{(t-m^2_{\widetilde{N}_i})(t-m^2_{\widetilde{N}_j})} + \frac{1}{(u-m^2_{\widetilde{N}_i})(u-m^2_{\widetilde{N}_j})}\right].\end{aligned} \tag{6.10.10}$$

To get the differential cross-section $\mathrm{d}\sigma/\mathrm{d}t$, multiply this by $1/(16\pi s^2)$:

$$\begin{aligned}\frac{\mathrm{d}\sigma}{\mathrm{d}t} = \frac{\pi\alpha^2}{4s_W^2c_W^2}\left(\frac{tu - m^2_{\widetilde{e}_L}m^2_{\widetilde{e}_R}}{s^2}\right)\sum_{i,j=1}^{4}N_{j1}N_{i1}^*\left(N_{j2}^* + \frac{s_W}{c_W}N_{j1}^*\right)\left(N_{i2} + \frac{s_W}{c_W}N_{i1}\right)\\ \times\left[\frac{1}{(t-m^2_{\widetilde{N}_i})(t-m^2_{\widetilde{N}_j})} + \frac{1}{(u-m^2_{\widetilde{N}_i})(u-m^2_{\widetilde{N}_j})}\right].\end{aligned} \tag{6.10.11}$$

To compare with the original calculation in Ref. [171] and with Eq. (E26), p. 244 in Ref. [7], note that for a pure photino exchange, $N_{i1} \to c_W\delta_{i1}$ and $N_{i2} \to s_W\delta_{i1}$, so that

$$\frac{1}{4s_W^2c_W^2}|N_{i1}|^2|N_{i2} + \frac{s_W}{c_W}N_{i1}|^2 \to 1. \tag{6.10.12}$$

Also note that in Ref. [171] polarized electron beams are assumed. The result checks.

6.10.2. $e^-e^- \to \widetilde{e}_R^-\widetilde{e}_R^-$

For this process, there are again two Feynman graphs, which are related by the exchange of identical electrons in the initial state or equivalently by exchange of the identical selectrons in the final state, as shown in Fig. 6.10.2. (We again neglect the electron mass and thus the higgsino coupling to the electron.) Let the electrons have momenta p_1 and p_2 and the selectrons have momenta k_1 and k_2, so that $p_1^2 = p_2^2 = 0$; $k_1^2 = k_2^2 = m^2_{\widetilde{e}_R}$; $s = (p_1+p_2)^2$; $t = (k_1-p_1)^2$; $u = (k_1-p_2)^2$.

Using the Feynman rules of Fig. K.4.2, the amplitude for the first graph is:

$$i\mathcal{M}_t = \left(-i\sqrt{2}g\frac{s_W}{c_W}N_{i1}\right)^2\left[\frac{i\,m_{\widetilde{N}_i}}{(k_1-p_1)^2 - m^2_{\widetilde{N}_i}}\right]y_1^\dagger y_2^\dagger, \tag{6.10.13}$$

for each exchanged neutralino. The amplitudes for the second graph are the same, but with the electrons interchanged:

$$i\mathcal{M}_u = \left(-i\sqrt{2}g\frac{s_W}{c_W}N_{i1}\right)^2\left[\frac{i\,m_{\widetilde{N}_i}}{(k_1-p_2)^2 - m^2_{\widetilde{N}_i}}\right]y_1^\dagger y_2^\dagger. \tag{6.10.14}$$

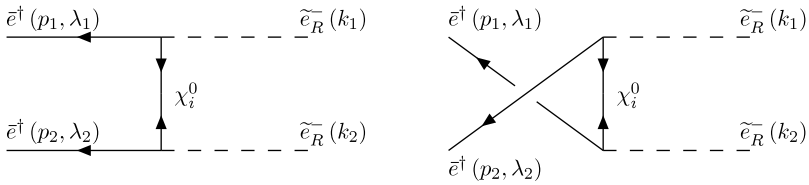

Fig. 6.10.2. The two Feynman diagrams for $e^-e^- \to \widetilde{e}_R^-\widetilde{e}_R^-$ in the limit where $m_e \to 0$.

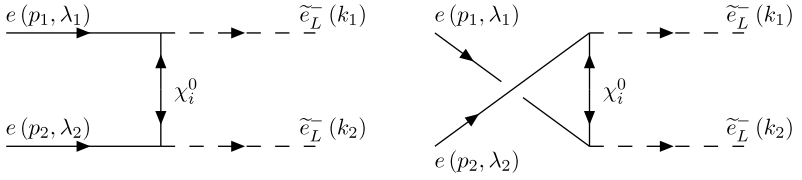

Fig. 6.10.3. The two Feynman diagrams for $e^-e^- \to \widetilde{e}_L^-\widetilde{e}_L^-$ in the limit of vanishing electron mass.

Since we have chosen to write the external state wave function spinors in the same order in $\mathcal{M}_t$ and $\mathcal{M}_u$, there is no factor of (-1) for Fermi–Dirac statistics. So, applying Eq. (2.43), the total amplitude squared is:

$$|\mathcal{M}|^2 = \frac{4g^4 s_W^4}{c_W^4}(y_1^\dagger y_2^\dagger)(y_2 y_1)\left|\sum_{i=1}^{4}(N_{i1})^2 m_{\widetilde{N}_i}\left(\frac{1}{t-m^2_{\widetilde{N}_i}}+\frac{1}{u-m^2_{\widetilde{N}_i}}\right)\right|^2. \tag{6.10.15}$$

The sum over the electron spins is obtained from

$$\sum_{\lambda_1,\lambda_2}(y_1^\dagger y_2^\dagger)(y_2 y_1) = \mathrm{Tr}[p_2\cdot\overline{\sigma}p_1\cdot\sigma] = 2p_2\cdot p_1 = s. \tag{6.10.16}$$

So, using Eq. (3.1.59), the spin-averaged differential cross-section is:

$$\begin{aligned}\frac{\mathrm{d}\sigma}{\mathrm{d}t} &= \left(\frac{1}{2}\right)\frac{1}{16\pi s^2}\left(\frac{1}{4}\sum_{\lambda_1,\lambda_2}|\mathcal{M}|^2\right)\\ &= \frac{\pi\alpha^2}{2c_W^4 s}\left|\sum_{i=1}^{4}(N_{i1})^2 m_{\widetilde{N}_i}\left(\frac{1}{t-m^2_{\widetilde{N}_i}}+\frac{1}{u-m^2_{\widetilde{N}_i}}\right)\right|^2.\end{aligned} \tag{6.10.17}$$

The first factor of $(1/2)$ in Eq. (6.10.17) comes from the fact that there are identical sleptons in the final state and thus the phase space is degenerate.

To compare with [171] and also with Eq. (E27) of Ref. [7], note that for a pure photino exchange, $N_{i1} \to c_W\delta_{i1}$, so it checks.

6.10.3. $e^-e^- \to \widetilde{e}_L^-\widetilde{e}_L^-$

Again, in the limit of vanishing electron mass, there are two Feynman graphs, which are related by the exchange of identical electrons in the initial state or equivalently by exchange of the identical selectrons in the final state. As shown in Fig. 6.10.3, they are exactly like the previous example, but with all arrows reversed.

Using the Feynman rules of Fig. K.4.2, the amplitude for the first graph is:

$$\mathcal{M}_t = \left(i\frac{g}{\sqrt{2}}\left[N_{i2}^* + \frac{s_W}{c_W}N_{i1}^*\right]\right)^2\left[\frac{i\,m_{\widetilde{N}_i}}{(p_1-k_1)^2-m^2_{\widetilde{N}_i}}\right]x_1x_2, \tag{6.10.18}$$

for each exchanged neutralino. The amplitudes for the second graph are the same, but with $p_1 \leftrightarrow p_2$:

$$\mathcal{M}_u = \left(i\frac{g}{\sqrt{2}}\left[N_{i2}^* + \frac{s_W}{c_W}N_{i1}^*\right]\right)^2\left[\frac{i\,m_{\widetilde{N}_i}}{(p_2-k_1)^2-m^2_{\widetilde{N}_i}}\right]x_1x_2. \tag{6.10.19}$$

Since we have chosen to write the external state wave function spinors in the same order in $\mathcal{M}_1$ and $\mathcal{M}_2$, there is no factor of (-1) for Fermi–Dirac statistics. The total amplitude squared is:

$$|\mathcal{M}|^2 = \frac{g^4}{4}(x_1x_2)(x_2^\dagger x_1^\dagger)\left|\sum_{i=1}^{4}\left(N_{i2}^* + \frac{s_W}{c_W}N_{i1}^*\right)^2 m_{\widetilde{N}_i}\left(\frac{1}{t-m^2_{\widetilde{N}_i}}+\frac{1}{u-m^2_{\widetilde{N}_i}}\right)\right|^2. \tag{6.10.20}$$

The average over the electron spins follows from Eq. (3.1.58):

$$\sum_{\lambda_1,\lambda_2}(x_1x_2)(x_2^\dagger x_1^\dagger) = \mathrm{Tr}[p_2\cdot\sigma\, p_1\cdot\overline{\sigma}] = 2p_2\cdot p_1 = s. \tag{6.10.21}$$

So the spin-averaged differential cross-section is:

$$\begin{aligned}\frac{\mathrm{d}\sigma}{\mathrm{d}t} &= \left(\frac{1}{2}\right)\frac{1}{16\pi s^2}\left(\frac{1}{4}\sum_{\lambda_1,\lambda_2}|\mathcal{M}|^2\right)\\ &= \frac{\pi\alpha^2}{32 s_W^4 s}\left|\sum_{i=1}^{4}\left(N_{i2}^* + \frac{s_W}{c_W}N_{i1}^*\right)^2 m_{\widetilde{N}_i}\left(\frac{1}{t-m^2_{\widetilde{N}_i}}+\frac{1}{u-m^2_{\widetilde{N}_i}}\right)\right|^2,\end{aligned} \tag{6.10.22}$$

where the first factor of (1/2) in Eq. (6.10.22) comes from the fact that there are identical sleptons in the final state. To compare with [171] and also with Eq. (E27) of Ref. [7], note that for a pure photino exchange, $N_{i1}\to c_W\delta_{i1}$ and $N_{i2}\to s_W\delta_{i1}$, so it checks.

6.11. $e^-e^+\to\widetilde{\nu}\widetilde{\nu}^*$

Consider now the pair production of sneutrinos in electron–positron collisions. There are two graphs featuring the s-channel exchange of the Z^0. We will neglect the electron mass and Yukawa coupling, so there is only one graph involving the t-channel exchange of the charginos. These three Feynman diagrams are shown in Fig. 6.11.1, where we have also defined the helicities and momenta of the particles. The Mandelstam variables can be expressed in terms of the external momenta and the sneutrino mass:

$$2p_1\cdot p_2 = s, \qquad 2k_1\cdot k_2 = s - 2m^2_{\tilde{\nu}}, \tag{6.11.1}$$

$$2p_1\cdot k_1 = 2p_2\cdot k_2 = m^2_{\tilde{\nu}} - t, \qquad 2p_1\cdot k_2 = 2p_2\cdot k_1 = m^2_{\tilde{\nu}} - u. \tag{6.11.2}$$

Using the Feynman rules of Fig. J.1.2, the amplitudes for the two s-channel Z boson exchange diagrams are[60]:

$$i\mathcal{M}_1 = \left[-i\frac{g}{2c_W}(k_1-k_2)_\mu\right]\left[\frac{-ig^{\mu\nu}}{D_Z}\right]\left[i\frac{g}{c_W}\left(s_W^2-\tfrac{1}{2}\right)\right]x_1\sigma_\nu y_2^\dagger, \tag{6.11.3}$$

$$i\mathcal{M}_2 = \left[-i\frac{g}{2c_W}(k_1-k_2)_\mu\right]\left[\frac{-ig^{\mu\nu}}{D_Z}\right]\left[i\frac{g s_W^2}{c_W}\right]y_1^\dagger\overline{\sigma}_\nu x_2, \tag{6.11.4}$$

where the first factor in each case is the Feynman rule from the Z boson coupling to the sneutrinos (see Fig. 72c, Ref. [7]), and $D_Z \equiv s - m_Z^2 + i\Gamma_Z m_Z$ is the denominator of the Z boson propagator.[61] The t-channel diagram due to each chargino gives a contribution

$$i\mathcal{M}_3 = \left(-igV_{i1}^*\right)\left(-igV_{i1}\right)x_1\left[\frac{i(k_1-p_1)\cdot\sigma}{(k_1-p_1)^2-m^2_{\tilde{C}_i}}\right]y_2^\dagger, \tag{6.11.5}$$

using the rules of Fig. K.4.1. Therefore, the total amplitude can be rewritten as:

$$\mathcal{M} = c_1 x_1(k_1-k_2)\cdot\sigma y_2^\dagger + c_2 y_1^\dagger(k_1-k_2)\cdot\overline{\sigma}x_2 + c_3 x_1(k_1-p_1)\cdot\sigma y_2^\dagger, \tag{6.11.6}$$

where

$$c_1 \equiv \frac{g^2(1-2s_W^2)}{4c_W^2 D_Z}, \qquad c_2 \equiv -\frac{g^2 s_W^2}{2c_W^2 D_Z}, \qquad c_3 \equiv g^2\sum_{i=1}^{2}\frac{|V_{i1}|^2}{m^2_{\tilde{C}_j}-t}. \tag{6.11.7}$$

---

60 Because we neglect the electron mass, we may drop the $Q^\mu Q^\nu$ term of the Z propagator, where $Q \equiv p_1 + p_2$ is the propagating four-momentum in the s-channel [cf. Fig. 4.2.5].

61 The explicit inclusion of the finite decay width in the propagator of an unstable particle involves subtle issues of gauge invariance and unitarity, particularly in higher loop computations. The authors of Ref. [172] recommend the complex-mass scheme for perturbative calculations with unstable particles, first introduced in Ref. [173].

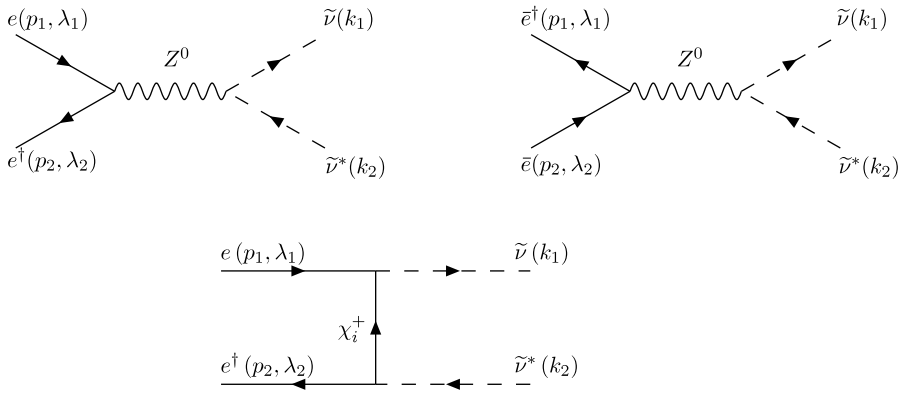

Fig. 6.11.1. The Feynman diagrams for $e^-e^+ \to \widetilde{\nu}\widetilde{\nu}^*$.

Squaring the amplitude and summing over the electron and positron spins, the interference terms involving c_2 will vanish in the massless electron limit due to Eqs. (3.1.60) and (3.1.61). Therefore, we obtain

$$\begin{aligned}\sum_{\lambda_1,\lambda_2}|\mathcal{M}|^2 &= \sum_{\lambda_1,\lambda_2}\Big\{|c_1|^2\,x_1(k_1-k_2)\cdot\sigma y_2^\dagger\,y_2(k_1-k_2)\cdot\sigma x_1^\dagger + |c_2|^2\,y_1^\dagger(k_1-k_2)\cdot\overline{\sigma}x_2\,x_2^\dagger(k_1-k_2)\cdot\overline{\sigma}y_1\\ &\quad + c_3^2\,x_1(k_1-p_1)\cdot\sigma y_2^\dagger\,y_2(k_1-p_1)\cdot\sigma x_1^\dagger + 2\mathrm{Re}[c_1c_3\,x_1(k_1-k_2)\cdot\sigma y_2^\dagger\,y_2(k_1-p_1)\cdot\sigma x_1^\dagger]\Big\}\\ &= |c_1|^2\,\mathrm{Tr}[(k_1-k_2)\cdot\sigma p_2\cdot\overline{\sigma}(k_1-k_2)\cdot\sigma p_1\cdot\overline{\sigma}] + |c_2|^2\,\mathrm{Tr}[(k_1-k_2)\cdot\overline{\sigma}p_2\cdot\sigma(k_1-k_2)\cdot\overline{\sigma}p_1\cdot\sigma]\\ &\quad + c_3^2\,\mathrm{Tr}[(k_1-p_1)\cdot\sigma p_2\cdot\overline{\sigma}(k_1-p_1)\cdot\sigma p_1\cdot\overline{\sigma}] + 2\mathrm{Re}[c_1]c_3\,\mathrm{Tr}[(k_1-k_2)\cdot\sigma p_2\cdot\overline{\sigma}(k_1-p_1)\cdot\sigma p_1\cdot\overline{\sigma}],\end{aligned}\tag{6.11.8}$$

where we have used Eqs. (3.1.58) and (3.1.59) to perform the spin sums. Applying the trace identities Eqs. (2.56) and (2.57) and simplifying the results using Eqs. (6.11.1)–(6.11.2) and $u = 2m_{\tilde{\nu}}^2 - s - t$, we get

$$\sum_{\lambda_1,\lambda_2}|\mathcal{M}|^2 = -[st + (t-m_{\tilde{\nu}}^2)^2]\left(4|c_1|^2 + 4|c_2|^2 + c_3^2 + 4\mathrm{Re}[c_1]c_3\right).\tag{6.11.9}$$

When $m_{\tilde{C}_1} = m_{\tilde{C}_2}$, this agrees with Eqs. (E46)–(E48) of Ref. [7][62] and with Ref. [174]. The differential cross-section follows in the standard way by averaging over the initial state spins:

$$\frac{\mathrm{d}\sigma}{\mathrm{d}t} = \frac{1}{16\pi s^2}\left(\frac{1}{4}\sum_{\lambda_1,\lambda_2}|\mathcal{M}|^2\right).\tag{6.11.10}$$

Note that

$$t = m_{\tilde{\nu}}^2 - \tfrac{1}{2}(1-\beta\cos\theta)s, \qquad \beta \equiv \left(1-\frac{4m_{\tilde{\nu}}^2}{s}\right)^{1/2},\tag{6.11.11}$$

where θ is the angle between the initial state electron and the final state sneutrino in the center-of-momentum frame. The upper and lower limits t_+ and t_- are obtained by inserting $\cos\theta = \pm 1$ above, respectively.

Performing the integration over t to obtain the total cross-section, one obtains

$$\sigma = \int_{t_-}^{t_+}\frac{\mathrm{d}\sigma}{\mathrm{d}t}\mathrm{d}t = \frac{g^4}{64\pi s}\left(S_Z + \sum_{i,j=1}^{2}S_{ij} + \sum_{i=1}^{2}S_{Zi}\right),\tag{6.11.12}$$

where

$$S_Z = \frac{\beta^3}{24c_W^4}(8s_W^4 - 4s_W^2 + 1)\frac{s^2}{|D_Z|^2},\tag{6.11.13}$$

$$S_{ii} = |V_{i1}|^4\left[(1-2\gamma_i)L_i - 2\beta\right],\tag{6.11.14}$$

$$S_{12} = S_{21} = |V_{11}V_{12}|^2\left\{\frac{(m_{\tilde{C}_2}^2 + s\gamma_2^2)L_2 - (m_{\tilde{C}_1}^2 + s\gamma_1^2)L_1}{m_{\tilde{C}_2}^2 - m_{\tilde{C}_1}^2} - \beta\right\},\tag{6.11.15}$$

$$S_{Zi} = \frac{(2s_W^2-1)}{c_W^2}|V_{i1}|^2\left[(m_{\tilde{C}_i}^2 + s\gamma_i^2)L_i + s\beta(\gamma_i - 1/2)\right]\frac{(s-m_Z^2)}{|D_Z|^2},\tag{6.11.16}$$

62 There is a typographical error in Eq. (E48) of [7]; the right-hand side should be multiplied by $1/\cos^2\theta_W$.

with

$$\gamma_i \equiv \frac{m_{\tilde{\nu}}^2 - m_{\tilde{C}_i}^2}{s}, \qquad L_i \equiv \ln\left(\frac{m_{\tilde{C}_i}^2 - t_-}{m_{\tilde{C}_i}^2 - t_+}\right). \tag{6.11.17}$$

This agrees with Eqs. (E49)–(E52) of Ref. [7] in the limit of degenerate charginos, or of a single wino chargino with $|V_{11}| = 1$ and $V_{12} = 0$. It also agrees with [174].

6.12. $e^-e^+ \to \widetilde{N}_i\widetilde{N}_j$

Next we consider the pair production of neutralinos via e^-e^+ annihilation. There are four Feynman graphs for s-channel Z^0 exchange, shown in Fig. 6.12.1, and four for t/u-channel selectron exchange, shown in Fig. 6.12.2. The momenta and polarizations are as labeled in the graphs. We denote the neutralino masses as $m_{\widetilde{N}_i}$, $m_{\widetilde{N}_j}$ and the selectron masses as $m_{\tilde{e}_L}$ and $m_{\tilde{e}_R}$. The electron mass will again be neglected. The kinematic variables are then given by

$$s = 2p_1 \cdot p_2 = m_{\widetilde{N}_i}^2 + m_{\widetilde{N}_j}^2 + 2k_i \cdot k_j, \tag{6.12.1}$$

$$t = m_{\widetilde{N}_i}^2 - 2p_1 \cdot k_i = m_{\widetilde{N}_j}^2 - 2p_2 \cdot k_j, \tag{6.12.2}$$

$$u = m_{\widetilde{N}_i}^2 - 2p_2 \cdot k_i = m_{\widetilde{N}_j}^2 - 2p_1 \cdot k_j. \tag{6.12.3}$$

By applying the Feynman rules of Figs. J.1.2 and K.2.1, we obtain for the sum of the s-channel diagrams in Fig. 6.12.1 [cf. footnote 60],

$$i\mathcal{M}_Z = \frac{-ig^{\mu\nu}}{D_Z}\left[\frac{ig(s_W^2 - \frac{1}{2})}{c_W}x_1\sigma_\mu y_2^\dagger + \frac{igs_W^2}{c_W}y_1^\dagger\overline{\sigma}_\mu x_2\right]\left[\frac{ig}{c_W}O''^L_{ij}x_i^\dagger\,\overline{\sigma}_\nu y_j - \frac{ig}{c_W}O''^L_{ji}y_i\sigma_\nu x_j^\dagger\right], \tag{6.12.4}$$

where O''_{ij} is given in Eq. (K.2.5), and $D_Z \equiv s - m_Z^2 + i\Gamma_Z m_Z$. The fermion spinors are denoted by $x_1 \equiv x(\vec{\boldsymbol{p}}_1, \lambda_1), y_2^\dagger \equiv y^\dagger(\vec{\boldsymbol{p}}_2, \lambda_2)$, $x_i^\dagger \equiv x^\dagger(\vec{\boldsymbol{k}}_i, \lambda_i), y_j \equiv y(\vec{\boldsymbol{k}}_j, \lambda_j)$, etc. Note that we have combined the matrix elements of the four diagrams by factorizing with respect to the common boson propagator. For the four t/u-channel diagrams, we obtain, by applying the rules of Fig. K.4.2:

$$i\mathcal{M}^{(t)}_{\tilde{e}_L} = (-1)\left[\frac{i}{t - m_{\tilde{e}_L}^2}\right]\left[\frac{ig}{\sqrt{2}}\left(N_{i2}^* + \frac{s_W}{c_W}N_{i1}^*\right)\right]\left[\frac{ig}{\sqrt{2}}\left(N_{j2} + \frac{s_W}{c_W}N_{j1}\right)\right]x_1y_iy_2^\dagger x_j^\dagger, \tag{6.12.5}$$

$$i\mathcal{M}^{(u)}_{\tilde{e}_L} = \left[\frac{i}{u - m_{\tilde{e}_L}^2}\right]\left[\frac{ig}{\sqrt{2}}\left(N_{j2}^* + \frac{s_W}{c_W}N_{j1}^*\right)\right]\left[\frac{ig}{\sqrt{2}}\left(N_{i2} + \frac{s_W}{c_W}N_{i1}\right)\right]x_1y_jy_2^\dagger x_i^\dagger, \tag{6.12.6}$$

$$i\mathcal{M}^{(t)}_{\tilde{e}_R} = (-1)\left[\frac{i}{t - m_{\tilde{e}_R}^2}\right]\left(-i\sqrt{2}g\frac{s_W}{c_W}N_{i1}\right)\left(-i\sqrt{2}g\frac{s_W}{c_W}N_{j1}^*\right)y_1^\dagger x_i^\dagger x_2y_j, \tag{6.12.7}$$

$$i\mathcal{M}^{(u)}_{\tilde{e}_R} = \left[\frac{i}{u - m_{\tilde{e}_R}^2}\right]\left(-i\sqrt{2}g\frac{s_W}{c_W}N_{j1}\right)\left(-i\sqrt{2}g\frac{s_W}{c_W}N_{i1}^*\right)y_1^\dagger x_j^\dagger x_2y_i. \tag{6.12.8}$$

The first factors of (-1) in each of Eqs. (6.12.5) and (6.12.7) are present because the order of the spinors in each case is an odd permutation of the ordering $(1, 2, i, j)$ established by the s-channel contribution. The other contributions have spinors in an even permutation of that ordering.

The s-channel diagram contribution of Eq. (6.12.4) can be profitably rearranged using the Fierz identities of Eqs. (2.67) and (2.68). Then, combining the result with the t/u-channel and s-channel contributions, we have for the total:

$$\mathcal{M} = c_1x_1y_jy_2^\dagger x_i^\dagger + c_2x_1y_iy_2^\dagger x_j^\dagger + c_3y_1^\dagger x_i^\dagger x_2y_j + c_4y_1^\dagger x_j^\dagger x_2y_i, \tag{6.12.9}$$

where

$$c_1 = \frac{g^2}{c_W^2}\left[(1 - 2s_W^2)O''^L_{ij}/D_Z - \tfrac{1}{2}(c_WN_{i2} + s_WN_{i1})(c_WN_{j2}^* + s_WN_{j1}^*)/(u - m_{\tilde{e}_L}^2)\right], \tag{6.12.10}$$

$$c_2 = \frac{g^2}{c_W^2}\left[(2s_W^2 - 1)O''^L_{ji}/D_Z + \tfrac{1}{2}(c_WN_{i2}^* + s_WN_{i1}^*)(c_WN_{j2} + s_WN_{j1})/(t - m_{\tilde{e}_L}^2)\right], \tag{6.12.11}$$

$$c_3 = \frac{2g^2s_W^2}{c_W^2}\left[-O''^L_{ij}/D_Z + N_{i1}N_{j1}^*/(t - m_{\tilde{e}_R}^2)\right], \tag{6.12.12}$$

$$c_4 = \frac{2g^2s_W^2}{c_W^2}\left[O''^L_{ji}/D_Z - N_{i1}^*N_{j1}/(u - m_{\tilde{e}_R}^2)\right]. \tag{6.12.13}$$

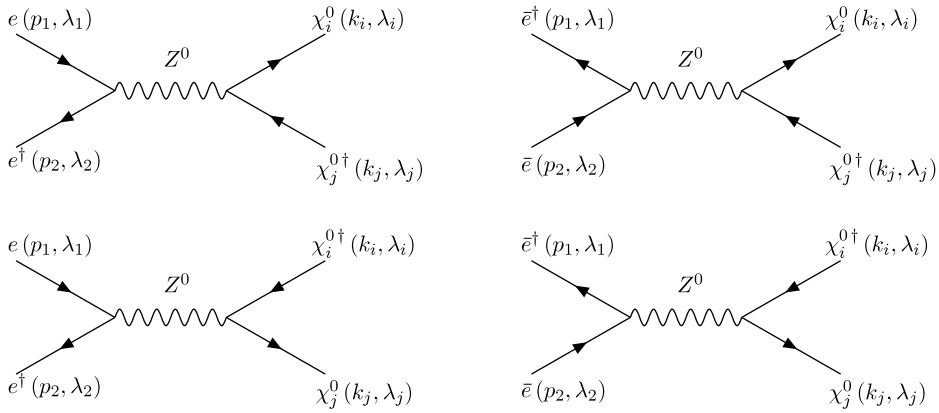

Fig. 6.12.1. The four Feynman diagrams for $e^-e^+ \to \widetilde{N}_i\widetilde{N}_j$ via s-channel Z^0 exchange.

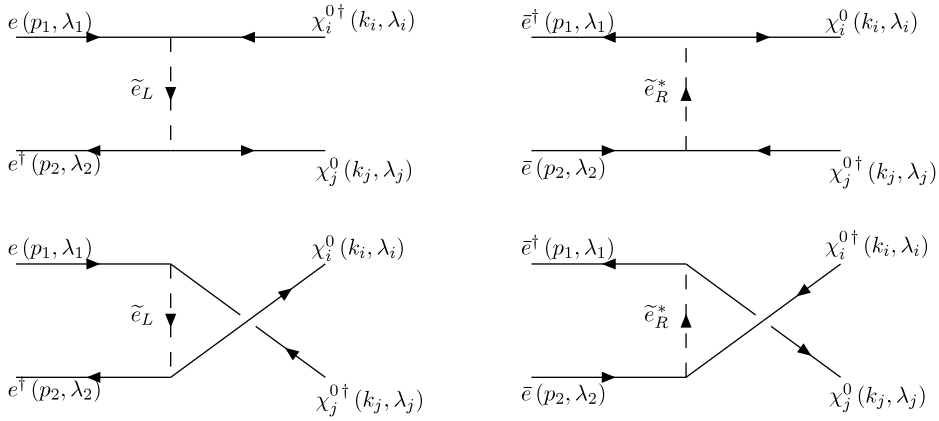

Fig. 6.12.2. The four Feynman diagrams for $e^-e^+ \to \widetilde{N}_i\widetilde{N}_j$ via t/u-channel selectron exchange.

Squaring the amplitude and averaging over electron and positron spins, only terms involving $x_1x_1^\dagger$ or $y_1y_1^\dagger$, and $x_2x_2^\dagger$ or $y_2y_2^\dagger$ survive in the massless electron limit. Thus,

$$\begin{aligned}\sum_{\lambda_1,\lambda_2}|\mathcal{M}|^2 &= \sum_{\lambda_1,\lambda_2}\Big(|c_1|^2y_j^\dagger x_1^\dagger x_1y_jx_iy_2y_2^\dagger x_i^\dagger + |c_2|^2y_i^\dagger x_1^\dagger x_1y_ix_jy_2y_2^\dagger x_j^\dagger \\ &\quad + |c_3|^2x_iy_1y_1^\dagger x_i^\dagger y_j^\dagger x_2^\dagger x_2y_j + |c_4|^2x_jy_1y_1^\dagger x_j^\dagger y_i^\dagger x_2^\dagger x_2y_i \\ &\quad + 2\mathrm{Re}\big[c_1c_2^*y_i^\dagger x_1^\dagger x_1y_jx_jy_2y_2^\dagger x_i^\dagger\big] + 2\mathrm{Re}\big[c_3c_4^*x_jy_1y_1^\dagger x_i^\dagger y_i^\dagger x_2^\dagger x_2y_j\big]\Big) \\ &= |c_1|^2y_j^\dagger p_1\cdot\overline{\sigma}y_j\,x_ip_2\cdot\sigma x_i^\dagger + |c_2|^2y_i^\dagger p_1\cdot\overline{\sigma}y_i\,x_jp_2\cdot\sigma x_j^\dagger \\ &\quad + |c_3|^2x_ip_1\cdot\sigma x_i^\dagger\,y_j^\dagger p_2\cdot\overline{\sigma}y_j + |c_4|^2x_jp_1\cdot\sigma x_j^\dagger\,y_i^\dagger p_2\cdot\overline{\sigma}y_i \\ &\quad + 2\mathrm{Re}\big[c_1c_2^*y_i^\dagger p_1\cdot\overline{\sigma}y_j\,x_jp_2\cdot\sigma x_i^\dagger\big] + 2\mathrm{Re}\big[c_3c_4^*x_jp_1\cdot\sigma x_i^\dagger\,y_i^\dagger p_2\cdot\overline{\sigma}y_j\big],\end{aligned} \tag{6.12.14}$$

after employing the results of Eqs. (3.1.58)–(3.1.61).

We now perform the remaining spin sums using Eqs. (3.1.58)–(3.1.61) again, obtaining:

$$\begin{aligned}\sum_{\lambda_1,\lambda_2,\lambda_i,\lambda_j}|\mathcal{M}|^2 &= |c_1|^2\mathrm{Tr}[p_1\cdot\overline{\sigma}k_j\cdot\sigma]\mathrm{Tr}[p_2\cdot\sigma k_i\cdot\overline{\sigma}] + |c_2|^2\mathrm{Tr}[p_1\cdot\overline{\sigma}k_i\cdot\sigma]\mathrm{Tr}[p_2\cdot\sigma k_j\cdot\overline{\sigma}] \\ &\quad + |c_3|^2\mathrm{Tr}[p_1\cdot\sigma k_i\cdot\overline{\sigma}]\mathrm{Tr}[p_2\cdot\overline{\sigma}k_j\cdot\sigma] + |c_4|^2\mathrm{Tr}[p_1\cdot\sigma k_j\cdot\overline{\sigma}]\mathrm{Tr}[p_2\cdot\overline{\sigma}k_i\cdot\sigma] \\ &\quad + 2\mathrm{Re}[c_1c_2^*]m_{\widetilde{N}_i}m_{\widetilde{N}_j}\mathrm{Tr}[p_2\cdot\sigma p_1\cdot\overline{\sigma}] + 2\mathrm{Re}[c_3c_4^*]m_{\widetilde{N}_i}m_{\widetilde{N}_j}\mathrm{Tr}[p_1\cdot\sigma p_2\cdot\overline{\sigma}].\end{aligned} \tag{6.12.15}$$

Applying the trace identity of Eq. (2.55) to this yields

$$\begin{aligned}\sum_{\text{spins}}|\mathcal{M}|^2 &= (|c_1|^2+|c_4|^2)4p_1\cdot k_j p_2\cdot k_i + (|c_2|^2+|c_3|^2)4p_1\cdot k_i p_2\cdot k_j + 4\text{Re}[c_1c_2^*+c_3c_4^*]m_{\widetilde{N}_i}m_{\widetilde{N}_j}p_1\cdot p_2\\ &= (|c_1|^2+|c_4|^2)(u-m^2_{\widetilde{N}_i})(u-m^2_{\widetilde{N}_j}) + (|c_2|^2+|c_3|^2)(t-m^2_{\widetilde{N}_i})(t-m^2_{\widetilde{N}_j})\\ &\quad + 2\text{Re}[c_1c_2^*+c_3c_4^*]m_{\widetilde{N}_i}m_{\widetilde{N}_j}s. \end{aligned} \tag{6.12.16}$$

The differential cross-section then follows:

$$\frac{\mathrm{d}\sigma}{\mathrm{d}t} = \frac{1}{16\pi s^2}\left(\frac{1}{4}\sum_{\text{spins}}|\mathcal{M}|^2\right). \tag{6.12.17}$$

This agrees with the first complete calculation presented in Ref. [175]. For the case of pure photino pair production, i.e. $N_{i1}\to c_W\delta_{i1}$ and $N_{i2}\to s_W\delta_{i1}$ and for degenerate selectron masses this also agrees with Eq. (E9) of the erratum of [7]. Other earlier calculations with some simplifications are given in Refs. [176,177].

Defining $\cos\theta = \hat{\boldsymbol{p}}_{\boldsymbol{1}}\cdot\hat{\boldsymbol{k}}_{\boldsymbol{i}}$ (the cosine of the angle between the initial state electron and one of the neutralinos in the center-of-momentum frame), the Mandelstam variables t, u are given by

$$t = \frac{1}{2}\left[m^2_{\widetilde{N}_i}+m^2_{\widetilde{N}_j}-s+\lambda^{1/2}(s,m^2_{\widetilde{N}_i},m^2_{\widetilde{N}_j})\cos\theta\right], \tag{6.12.18}$$

$$u = \frac{1}{2}\left[m^2_{\widetilde{N}_i}+m^2_{\widetilde{N}_j}-s-\lambda^{1/2}(s,m^2_{\widetilde{N}_i},m^2_{\widetilde{N}_j})\cos\theta\right], \tag{6.12.19}$$

where the triangle function $\lambda^{1/2}$ is defined in Eq. (6.1.11). Taking into account the identical fermions in the final state when $i=j$, the total cross-section is

$$\sigma = \frac{1}{1+\delta_{ij}}\int_{t_-}^{t_+}\frac{\mathrm{d}\sigma}{\mathrm{d}t}\mathrm{d}t, \tag{6.12.20}$$

where t_- and t_+ are obtained by inserting $\cos\theta = \mp 1$ in Eq. (6.12.18), respectively.

6.13. $\widetilde{N}_1\widetilde{N}_1\to f\bar{f}$

In this section, we compute the annihilation rate for $\widetilde{N}_1\widetilde{N}_1\to f\bar{f}$, where f is any kinematically allowed quark, charged lepton or neutrino. The case of $f=e^-$ is the reversed reaction of the process examined in Section 6.12 (with $i=j=1$). In R-parity-conserving supersymmetric models in which $\widetilde{N}_1$ is the lightest supersymmetric particle (and hence is stable), the $\widetilde{N}_1\widetilde{N}_1$ annihilation process is relevant for the computation of the neutralino relic density [178]. In particular, $\widetilde{N}_1\widetilde{N}_1\to f\bar{f}$ can be an important contribution to cold dark matter annihilation [178–181]. Neutralino dark matter is typically heavier than about 6 GeV [182]; for lighter neutralinos see Ref. [183].

In the computation of the relic density, one computes $v_{\text{rel}}\sigma_{\text{ann}}$, where σ_{ann} is the $\widetilde{N}_1\widetilde{N}_1$ annihilation cross-section and v_{rel} is the relative velocity of the two neutralinos in the center-of-momentum frame. The square of the relative velocity is taken to be its thermal average, $v^2_{\text{rel}}\simeq 6k_BT/m_{\widetilde{N}_1}$ [178], which is typically non-relativistic when the temperature is of order the freeze-out temperature [180] (where the neutralino falls out of thermal equilibrium). Hence, it is sufficient to compute the annihilation cross-section for $\widetilde{N}_1\widetilde{N}_1\to f\bar{f}$ in the non-relativistic limit.

As in Section 6.12, there are four Feynman graphs for s-channel Z^0 exchange, shown in Fig. 6.13.1. In addition, there are s-channel neutral Higgs exchange graphs, shown in Fig. 6.13.2, that yield contributions to the annihilation amplitude proportional to the fermion mass, m_f.[63] Likewise, as in Section 6.12, there are four Feynman graphs for t/u-channel $\widetilde{f}_L$ and $\widetilde{f}_R$ exchange, shown in Fig. 6.13.3. However, because we do not set m_f to zero, four additional t/u-channel graphs contribute, shown in Fig. 6.13.4, that are sensitive to the higgsino components of the neutralino.

The neutralino and the final state fermion four-momenta and polarizations are as labeled in the Feynman graphs. In the center-of-momentum (CM) frame, the four-momenta are

$$p_1^\mu = (E;\vec{\boldsymbol{p}}),\qquad p_2^\mu = (E;-\vec{\boldsymbol{p}}),\qquad k_1^\mu = E(1;\beta\hat{\boldsymbol{k}}),\qquad k_2^\mu = E(1;-\beta\hat{\boldsymbol{k}}), \tag{6.13.1}$$

where

$$\beta\equiv\sqrt{1-\frac{m_f^2}{E^2}}. \tag{6.13.2}$$

[63] In regions of parameter space where $m_{\widetilde{N}_1}\simeq\frac{1}{2}m_Z$ or $m_{\widetilde{N}_1}\simeq\frac{1}{2}m_{\phi^0}$ (where $\phi^0=h^0$, H^0 or A^0), the resonant $2\to 1$ annihilation $\widetilde{N}_1\widetilde{N}_1\to Z^0$ or $\widetilde{N}_1\widetilde{N}_1\to\phi^0$ dominates the $2\to 2$ annihilation processes considered here.

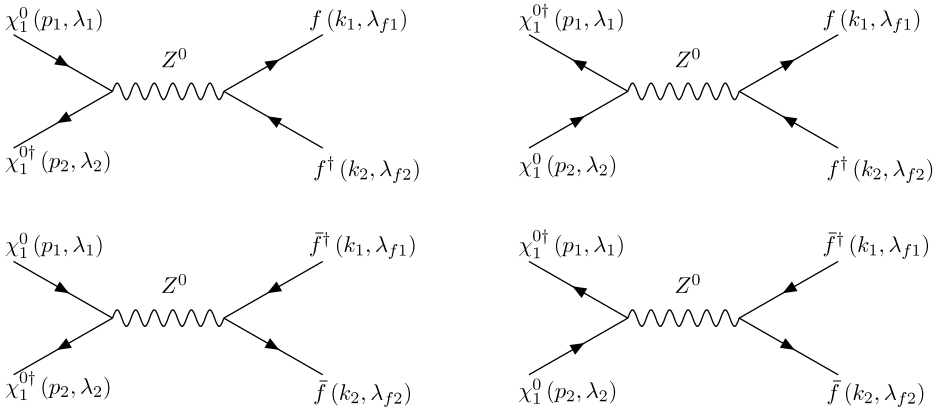

Fig. 6.13.1. The four Feynman diagrams for $\widetilde{N}_1\widetilde{N}_1 \to f\bar{f}$ via s-channel Z^0 exchange, where f is a quark or lepton.

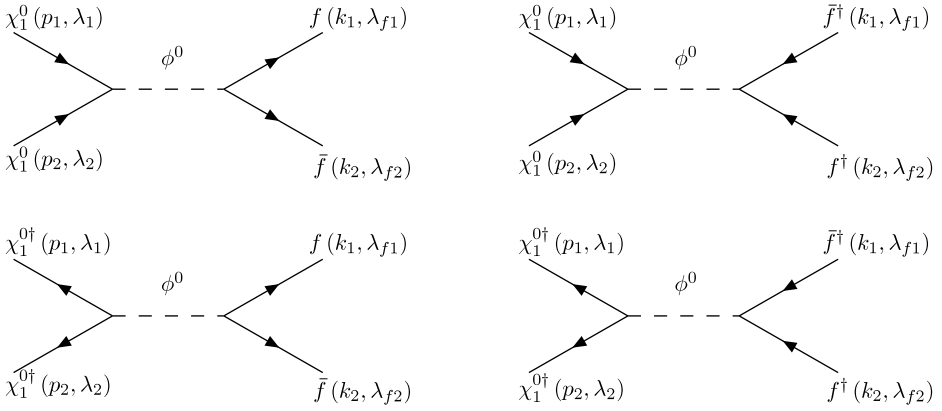

Fig. 6.13.2. Feynman diagrams for $\widetilde{N}_1\widetilde{N}_1 \to f\bar{f}$ via s-channel Higgs exchange. There are four diagrams for each possible neutral Higgs state $\phi^0 = h^0, H^0$ and A^0.

In the non-relativistic limit where $|\vec{\boldsymbol{p}}| \ll m_{\widetilde{N}_1}$,

$$E \simeq m_{\widetilde{N}_1} + \frac{|\vec{\boldsymbol{p}}|^2}{2m_{\widetilde{N}_1}}, \tag{6.13.3}$$

and the kinematic invariants are given by

$$s = (p_1+p_2)^2 = 4E^2 = 4m_{\widetilde{N}_1}^2 + 4|\vec{\boldsymbol{p}}|^2, \tag{6.13.4}$$

$$t = (p_1-k_1)^2 = m_{\widetilde{N}_1}^2 + m_f^2 - 2p_1\cdot k_1 \simeq -m_{\widetilde{N}_1}^2 + m_f^2 + 2\beta m_{\widetilde{N}_1}|\vec{\boldsymbol{p}}|\cos\theta - 2|\vec{\boldsymbol{p}}|^2, \tag{6.13.5}$$

$$u = (p_1-k_2)^2 = m_{\widetilde{N}_1}^2 + m_f^2 - 2p_1\cdot k_2 \simeq -m_{\widetilde{N}_1}^2 + m_f^2 - 2\beta m_{\widetilde{N}_1}|\vec{\boldsymbol{p}}|\cos\theta - 2|\vec{\boldsymbol{p}}|^2, \tag{6.13.6}$$

where θ is the CM scattering angle. Subsequently, we shall neglect the subdominant $\mathcal{O}(|\vec{\boldsymbol{p}}|)$ terms in the t and u-channel propagator denominators by setting $t \simeq u \simeq -m_{\widetilde{N}_1}^2 + m_f^2$.

By applying the Feynman rules of Figs. J.1.2 and K.2.1, and using the unitary gauge for the Z-boson propagator, we obtain for the sum of the s-channel Z-exchange diagrams of Fig. 6.13.1,

$$i\mathcal{M}_Z = \frac{i\left(-g^{\mu\nu} + Q^\mu Q^\nu/m_Z^2\right)}{D_Z}\left(\frac{-ig}{c_W}\right)^2 O''^L_{11}\Big[x_1\sigma_\mu y_2^\dagger - y_1^\dagger\overline{\sigma}_\mu x_2\Big]\Big[(T_3^f - s_W^2 Q_f)x_{f1}^\dagger\overline{\sigma}_\nu y_{f2} - s_W^2 Q_f y_{f1}\sigma_\nu x_{f2}^\dagger\Big], \tag{6.13.7}$$

where O''^L_{11} is given in Eq. (K.2.5), $D_Z \equiv s - m_Z^2 + i\Gamma_Z m_Z$, and $Q \equiv p_1 + p_2 = k_1 + k_2$. The spinor wave functions are denoted by $x_1 \equiv x(\vec{\boldsymbol{p}}_1,\lambda_1)$, $y_2^\dagger \equiv y^\dagger(\vec{\boldsymbol{p}}_2,\lambda_2)$, $x_{f1}^\dagger \equiv x^\dagger(\vec{\boldsymbol{k}}_1,\lambda_{f1})$, $y_{f2} \equiv y(\vec{\boldsymbol{k}}_2,\lambda_{f2})$, etc. In obtaining Eq. (6.13.7), we have combined the matrix elements of the four diagrams by factorizing with respect to the common Z-boson propagator. Note that all four

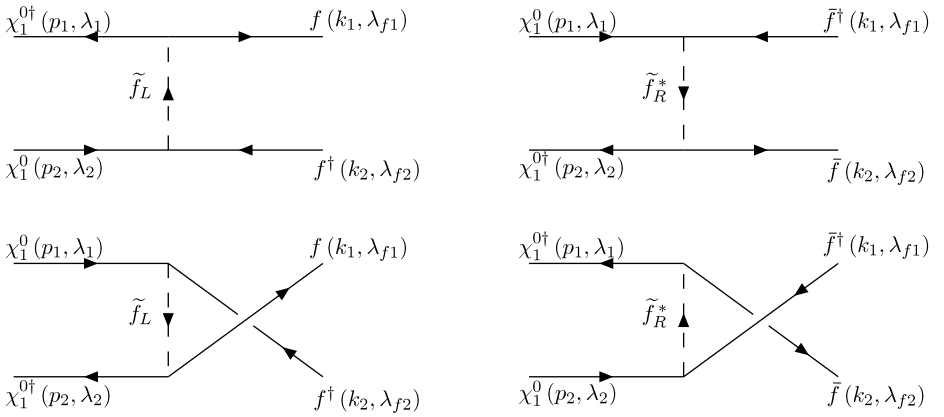

Fig. 6.13.3. The four Feynman diagrams for $\widetilde{N}_i\widetilde{N}_j \to f\bar{f}$ via t/u-channel $\widetilde{f}_L$ and $\widetilde{f}_R$ exchange, where $\widetilde{f}_L$ and $\widetilde{f}_R$ couple to the gaugino components of the neutralino.

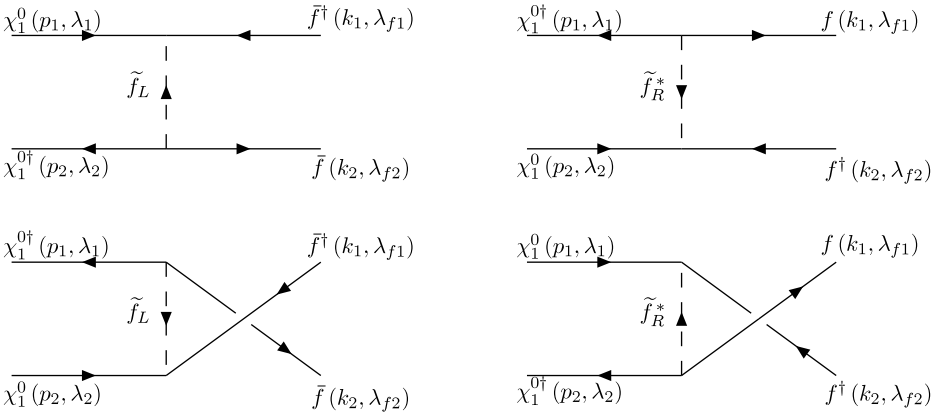

Fig. 6.13.4. The four Feynman diagrams for $\widetilde{N}_i\widetilde{N}_j \to f\bar{f}$ via t/u-channel $\widetilde{f}_L$ and $\widetilde{f}_R$ exchange, where $\widetilde{f}_L$ and $\widetilde{f}_R$ couple to the higgsino components of the neutralino.

terms in Eq. (6.13.7) have the same order of spinor wave functions (1, 2, $f1$, $f2$). Thus, no additional relative signs arise (beyond the sign associated with the choice of the σ or $\overline{\sigma}$ version of the vertex Feynman rules). One can simplify the terms that originate from the $Q^\mu Q^\nu$ part of the Z-boson propagator by writing $Q^\mu = (p_1+p_2)^\mu$ and $Q^\nu = (k_1+k_2)^\nu$. Contracting the μ and ν indices with the help of Eqs. (3.1.9)–(3.1.12) yields:

$$(p_1+p_2)^\mu\left[x_1\sigma_\mu y_2^\dagger - y_1^\dagger\overline{\sigma}_\mu x_2\right] = 2m_{\widetilde{N}_1}\left(x_1x_2 - y_1^\dagger y_2^\dagger\right), \tag{6.13.8}$$

$$(k_1+k_2)^\nu\left[(T_3^f - s_W^2Q_f)x_{f1}^\dagger\overline{\sigma}_\nu y_{f2} - s_W^2Q_f y_{f1}\sigma_\nu x_{f2}^\dagger\right] = T_3^f m_f\left(y_{f1}y_{f2} - x_{f1}^\dagger x_{f2}^\dagger\right). \tag{6.13.9}$$

Hence, we shall write

$$\mathcal{M}_Z \equiv \mathcal{M}_Z^{(1)} + \mathcal{M}_Z^{(2)}, \tag{6.13.10}$$

where

$$i\mathcal{M}_Z^{(1)} = \frac{-ig^{\mu\nu}}{D_Z}\left(\frac{-ig}{c_W}\right)^2 O_{11}''^L\left[x_1\sigma_\mu y_2^\dagger - y_1^\dagger\overline{\sigma}_\mu x_2\right]\left[(T_3^f - s_W^2Q_f)x_{f1}^\dagger\overline{\sigma}_\nu y_{f2} - s_W^2Q_f y_{f1}\sigma_\nu x_{f2}^\dagger\right], \tag{6.13.11}$$

$$i\mathcal{M}_Z^{(2)} = \frac{im_f m_{\widetilde{N}_1}}{m_Z^2 D_Z}\left(\frac{-ig}{c_W}\right)^2 O_{11}''^L(2T_3^f)\left(x_1x_2 - y_1^\dagger y_2^\dagger\right)\left(y_{f1}y_{f2} - x_{f1}^\dagger x_{f2}^\dagger\right). \tag{6.13.12}$$

Next, we apply the Feynman rules of Figs. K.1.1 and K.3.1 to obtain the sum of the four s-channel Higgs exchange diagrams (for $\phi^0 = h^0, H^0$ and A^0) of Fig. 6.13.2,

$$i\mathcal{M}_H = \sum_{\phi^0=h^0,H^0,A^0}\frac{i}{D_{\phi^0}}\left(\frac{-m_f}{\sqrt{2}\,v_f}\right)\left[(Y^{\phi^0\chi_1^0\chi_1^0})x_1x_2 + (Y^{\phi^0\chi_1^0\chi_1^0})^* y_1^\dagger y_2^\dagger\right]\left[k_{f\phi^0}y_{f1}y_{f2} + k_{f\phi^0}^* x_{f1}^\dagger x_{f2}^\dagger\right], \tag{6.13.13}$$

where $Y^{\phi^0\chi_1^0\chi_1^0}$ is given by Eq. (K.3.1), and $D_{\phi^0} \equiv s - m^2_{\phi^0} + i\Gamma_{\phi^0} m_{\phi^0}$. In addition, we have introduced the following notation

$$k_{f\phi^0} \equiv \begin{cases} k_{d\phi^0}, & \text{for } f = d,\ e^-, \\ k_{u\phi^0}, & \text{for } f = u, \\ 0, & \text{for } f = \nu, \end{cases} \qquad v_f \equiv \begin{cases} v_d, & \text{for } f = d,\ e^-, \\ v_u, & \text{for } f = u,\ \nu, \end{cases} \tag{6.13.14}$$

where v_u, v_d are the neutral Higgs vacuum expectation values [cf. Eq. (K.1.9)] and $k_{u\phi^0}$ and $k_{d\phi^0}$ are defined in Eqs. (K.1.7) and (K.1.8). As the order of the spinor wave functions is $(1, 2, f1, f2)$ for all four terms of $\mathcal{M}_H$, no extra minus signs appear.

A good check of the above calculations is to repeat the analysis in the 't Hooft–Feynman gauge (where the gauge parameter $\xi = 1$). In this gauge, $\mathcal{M}_Z = \mathcal{M}_Z^{(1)}$, since the term proportional to $Q^\mu Q^\nu$ is absent from the gauge boson propagator. However, we must now include the diagrams of Fig. 6.13.2 with $\phi^0 = G^0$. In the 't Hooft–Feynman gauge, $m_{G^0} = m_Z$ and $D_{G^0} = D_Z$. Moreover, using Eqs. (K.1.7) and (K.1.8),

$$\frac{k_{fG^0}}{v_f} = \frac{2iT_f}{v}. \tag{6.13.15}$$

Hence, using Eq. (6.13.13) with $\phi^0 = G^0$,

$$i\mathcal{M}_G = \frac{m_f}{\sqrt{2}\, v D_Z} (2T_f)\, Y^{G^0\chi_1^0\chi_1^0} \left(x_1 x_2 - y_1^\dagger y_2^\dagger\right) \left(y_{f1} y_{f2} - x_{f1}^\dagger x_{f2}^\dagger\right), \tag{6.13.16}$$

where we have noted that $iY^{G^0\chi_1^0\chi_1^0}$ is real. In particular, using Eq. (K.3.14) and recalling that $m_W^2 = m_Z^2 c_W^2 = \frac{1}{2} g^2 v^2$, we confirm that $\mathcal{M}_G = \mathcal{M}_Z^{(2)}$ as expected from gauge invariance.

We next evaluate the t/u-channel exchange diagrams shown in Figs. 6.13.3 and 6.13.4. We neglect $\widetilde{f}_L$–$\widetilde{f}_R$ mixing. Eight Feynman graphs contribute, and we denote the total invariant amplitude by:

$$\mathcal{M}_{\tilde{f}} = \sum_{j=1}^{2} (\mathcal{M}_{\tilde{f}_L}^{(tj)} + \mathcal{M}_{\tilde{f}_L}^{(uj)} + \mathcal{M}_{\tilde{f}_R}^{(tj)} + \mathcal{M}_{\tilde{f}_R}^{(uj)}), \tag{6.13.17}$$

where $j = 1, 2$ labels the contributions of Figs. 6.13.3 and 6.13.4, respectively, and the other superscripts (t or u) and subscripts ($\widetilde{f}_L$ or $\widetilde{f}_R$) indicate the exchange channel and the exchanged particle, respectively. These matrix elements are evaluated by applying the rules of Fig. K.4.2.

The graphs of Fig. 6.13.3 are sensitive to the gaugino components of $\widetilde{N}_1$, and yield

$$i\mathcal{M}_{\tilde{f}_L}^{(t1)} = (-1) \left(-ig\sqrt{2}\right)^2 \left(\frac{i}{t - m^2_{\tilde{f}_L}}\right) \left| T_3^f N_{12} + \frac{s_W}{c_W}(Q_f - T_3^f) N_{11} \right|^2 (y_1^\dagger x_{f1}^\dagger)(x_2 y_{f2}), \tag{6.13.18}$$

$$i\mathcal{M}_{\tilde{f}_L}^{(u1)} = \left(-ig\sqrt{2}\right)^2 \left| T_3^f N_{12} + \frac{s_W}{c_W}(Q_f - T_3^f) N_{11} \right|^2 \left(\frac{i}{u - m^2_{\tilde{f}_L}}\right) (x_1 y_{f2})(y_2^\dagger x_{f1}^\dagger), \tag{6.13.19}$$

$$i\mathcal{M}_{\tilde{f}_R}^{(t1)} = (-1) \left(i\sqrt{2} g \frac{s_W}{c_W} Q_f\right)^2 \left(\frac{i}{t - m^2_{\tilde{f}_R}}\right) |N_{11}|^2 (x_1 y_{f1})(y_2^\dagger x_{f2}^\dagger), \tag{6.13.20}$$

$$i\mathcal{M}_{\tilde{f}_R}^{(u1)} = \left(i\sqrt{2} g \frac{s_W}{c_W} Q_f\right)^2 \left(\frac{i}{u - m^2_{\tilde{f}_R}}\right) |N_{11}|^2 (y_1^\dagger x_{f2}^\dagger)(x_2 y_{f1}). \tag{6.13.21}$$

The explicit factors of (-1) in Eqs. (6.13.18) and (6.13.20) are present because the order of the spinor wave functions in these cases is an odd permutation of the ordering $(1, 2, f1, f2)$ established in the computation of the s-channel amplitudes.

The graphs of Fig. 6.13.4 are sensitive to the higgsino components of $\widetilde{N}_1$, and yield

$$i\mathcal{M}_{\tilde{f}_L}^{(t2)} = (-1) \left(\frac{-im_f}{v_f}\right)^2 \left(\frac{i}{t - m^2_{\tilde{f}_L}}\right) |N_{1f}|^2 (x_1 y_{f1})(y_2^\dagger x_{f2}^\dagger), \tag{6.13.22}$$

$$i\mathcal{M}_{\tilde{f}_L}^{(u2)} = \left(\frac{-im_f}{v_f}\right)^2 \left(\frac{i}{u - m^2_{\tilde{f}_L}}\right) |N_{1f}|^2 (y_1^\dagger x_{f2}^\dagger)(x_2 y_{f1}), \tag{6.13.23}$$

$$i\mathcal{M}_{\tilde{f}_R}^{(t2)} = (-1) \left(\frac{-im_f}{v_f}\right)^2 \left(\frac{i}{t - m^2_{\tilde{f}_R}}\right) |N_{1f}|^2 (y_1^\dagger x_{f1}^\dagger)(x_2 y_{f2}), \tag{6.13.24}$$

$$i\mathcal{M}_{\tilde{f}_R}^{(u2)} = \left(\frac{-im_f}{v_f}\right)^2 \left(\frac{i}{u - m^2_{\tilde{f}_R}}\right) |N_{1f}|^2 (x_1 y_{f2})(y_2^\dagger x_{f1}^\dagger), \tag{6.13.25}$$

where v_f is defined in Eq. (6.13.14), and

$$N_{1f} \equiv \begin{cases} N_{13}, & \text{for } f = d,\ e^-, \\ N_{14}, & \text{for } f = u, \\ 0, & \text{for } f = \nu. \end{cases} \tag{6.13.26}$$

As before, the explicit factors of (-1) are due to the ordering of the spinor wave functions.

It is convenient to write the total matrix element for $\widetilde{N}_1\widetilde{N}_1 \to f\bar{f}$ as the sum of products of separate neutralino and final state fermionic currents. The contributions of the s-channel diagrams are already in this form. The contributions of the t- and u-channel diagrams given in Eqs. (6.13.18)–(6.13.25) can be rearranged using the Fierz identities of Eqs. (2.67)–(2.69),

$$y_1^\dagger x_{f1}^\dagger x_2 y_{f2} = -\tfrac{1}{2}(y_1^\dagger \overline{\sigma}^\mu x_2)(x_{f1}^\dagger \overline{\sigma}_\mu y_{f2}), \tag{6.13.27}$$

$$x_1 y_{f2} y_2^\dagger x_{f1}^\dagger = -\tfrac{1}{2}(x_1 \sigma^\mu y_2^\dagger)(x_{f1}^\dagger \overline{\sigma}_\mu y_{f2}), \tag{6.13.28}$$

$$x_1 y_{f1} y_2^\dagger x_{f2}^\dagger = -\tfrac{1}{2}(x_1 \sigma^\mu y_2^\dagger)(y_{f1} \sigma_\mu x_{f2}^\dagger), \tag{6.13.29}$$

$$y_1^\dagger x_{f2}^\dagger x_2 y_{f1} = -\tfrac{1}{2}(y_1^\dagger \overline{\sigma}^\mu x_2)(y_{f1} \sigma_\mu x_{f2}^\dagger). \tag{6.13.30}$$

Combining the result of the s, t, and u-channel contributions, we have for the total amplitude:

$$\begin{aligned} \mathcal{M} = {} & \frac{m_f m_{\widetilde{N}_1}}{m_Z^2} c_0 \left(x_1 x_2 - y_1^\dagger y_2^\dagger\right)\left(y_{f1} y_{f2} - x_{f1}^\dagger x_{f2}^\dagger\right) \\ & + c_1 (y_1^\dagger \overline{\sigma}^\mu x_2)(x_{f1}^\dagger \overline{\sigma}_\mu y_{f2}) + c_2 (x_1 \sigma^\mu y_2^\dagger)(x_{f1}^\dagger \overline{\sigma}_\mu y_{f2}) + c_3 (x_1 \sigma^\mu y_2^\dagger)(y_{f1} \sigma_\mu x_{f2}^\dagger) + c_4 (y_1^\dagger \overline{\sigma}^\mu x_2)(y_{f1} \sigma_\mu x_{f2}^\dagger) \\ & + m_f \left[c_5 (x_1 x_2)(y_{f1} y_{f2}) + c_6 (x_1 x_2)(x_{f1}^\dagger x_{f2}^\dagger) + c_7 (y_1^\dagger y_2^\dagger)(y_{f1} y_{f2}) + c_8 (y_1^\dagger y_2^\dagger)(x_{f1}^\dagger x_{f2}^\dagger)\right], \end{aligned} \tag{6.13.31}$$

where the coefficients $c_0,\ c_1,\ \ldots,\ c_4$ are given by

$$c_0 = -g^2 \frac{2 T_3^f O_{11}''^L}{c_W^2 D_Z}, \tag{6.13.32}$$

$$c_1 = -g^2 \left[\frac{(T_3^f - s_W^2 Q_f) O_{11}''^L}{c_W^2 D_Z} + \frac{|T_3^f N_{12} + \frac{s_W}{c_W}(Q_f - T_3^f) N_{11}|^2}{t - m_{\tilde{f}_L}^2}\right] - \frac{m_f^2}{2 v_f^2}\left(\frac{|N_{1f}|^2}{t - m_{\tilde{f}_R}^2}\right), \tag{6.13.33}$$

$$c_2 = g^2 \left[\frac{(T_3^f - s_W^2 Q_f) O_{11}''^L}{c_W^2 D_Z} + \frac{|T_3^f N_{12} + \frac{s_W}{c_W}(Q_f - T_3^f) N_{11}|^2}{u - m_{\tilde{f}_L}^2}\right] + \frac{m_f^2}{2 v_f^2}\left(\frac{|N_{1f}|^2}{u - m_{\tilde{f}_R}^2}\right), \tag{6.13.34}$$

$$c_3 = -g^2 \frac{s_W^2}{c_W^2} Q_f \left[\frac{O_{11}''^L}{D_Z} + \frac{Q_f |N_{11}|^2}{t - m_{\tilde{f}_R}^2}\right] - \frac{m_f^2}{2 v_f^2}\left(\frac{|N_{1f}|^2}{t - m_{\tilde{f}_L}^2}\right), \tag{6.13.35}$$

$$c_4 = g^2 \frac{s_W^2}{c_W^2} Q_f \left[\frac{O_{11}''^L}{D_Z} + \frac{Q_f |N_{11}|^2}{u - m_{\tilde{f}_R}^2}\right] + \frac{m_f^2}{2 v_f^2}\left(\frac{|N_{1f}|^2}{u - m_{\tilde{f}_L}^2}\right). \tag{6.13.36}$$

The coefficients $c_5, \ldots, c_8$ are obtained from Eq. (6.13.13) and represent the s-channel Higgs exchange contributions to the annihilation matrix element.

In the non-relativistic limit, $|\vec{\boldsymbol{p}}| \ll m_{\widetilde{N}_1}$. Then $t \simeq u \simeq -m_{\widetilde{N}_1}^2 + m_f^2$, and we can approximate[64] $c_1 = -c_2$ and $c_3 = -c_4$. Hence, the total amplitude, Eq. (6.13.31), can be written as

$$\begin{aligned} \mathcal{M} = {} & \frac{m_f m_{\widetilde{N}_1}}{m_Z^2} c_0 \left(x_1 x_2 - y_1^\dagger y_2^\dagger\right)\left(y_{f1} y_{f2} - x_{f1}^\dagger x_{f2}^\dagger\right) \\ & + \left[y_1^\dagger \overline{\sigma}^\mu x_2 - x_1 \sigma^\mu y_2^\dagger\right]\left[c_1 (x_{f1}^\dagger \overline{\sigma}_\mu y_{f2}) - c_3 (y_{f1} \sigma_\mu x_{f2}^\dagger)\right] + \mathcal{M}_H, \end{aligned} \tag{6.13.37}$$

[64] In particular, we assume that $\widetilde{f}_L$ and $\widetilde{f}_R$ are significantly heavier than all other particles in the annihilation process. Consequently, we can ignore all $\mathcal{O}(|\vec{\boldsymbol{p}}|/m_{\widetilde{f}_{L,R}})$ terms in $c_1 + c_2$ and $c_3 + c_4$.

where the s-channel Higgs exchange contributions, $\mathcal{M}_H$, will be neglected for simplicity in the subsequent analysis. The spin-averaged squared matrix element for $\widetilde{N}_1\widetilde{N}_1 \to f\bar{f}$ then takes the following form:

$$\frac{1}{4}\sum_{s_1,s_2,s_{f1},s_{f2}}|\mathcal{M}_Z+\mathcal{M}_{\tilde{f}}|^2 = N_{\mu\nu}\left[|c_1|^2F_1^{\mu\nu}+|c_3|^2F_2^{\mu\nu}-2\mathrm{Re}(c_1c_3^*)F_{12}^{\mu\nu}\right]+\frac{m_f^2m_{\widetilde{N}_1}^2}{m_Z^4}|c_0|^2NF$$
$$+\frac{2m_fm_{\widetilde{N}_1}}{m_Z^2}\mathrm{Re}[c_0^*(c_1+c_3)]N_\mu F^\mu, \tag{6.13.38}$$

where $N_{\mu\nu}$, N_μ and N are spin-averaged tensor, vector and scalar quantities that depend on the initial state neutralino kinematics and $F_{1,2,12}^{\mu\nu}$, F^μ and F are spin-summed tensor, vector and scalar quantities that depend on the final state fermion kinematics. These quantities are easily computed using the projection operators of Eqs. (3.1.58)–(3.1.61) and the standard trace techniques to perform the spin averages and sums. Explicitly, the spin-averaged neutralino quantities are

$$N \equiv \frac{1}{4}\sum_{s_1,s_2}(x_1x_2-y_1^\dagger y_2^\dagger)(x_2^\dagger x_1^\dagger-y_2y_1) = p_1\cdot p_2+m_{\widetilde{N}_1}^2 = 2E^2, \tag{6.13.39}$$

$$N^\mu \equiv \frac{1}{4}\sum_{s_1,s_2}(y_1^\dagger\bar{\sigma}^\mu x_2-x_1\sigma^\mu y_2^\dagger)(x_2^\dagger x_1^\dagger-y_2y_1) = -m_{\widetilde{N}_1}(p_1+p_2)^\mu = \begin{cases}-2m_{\widetilde{N}_1}E, & \mu=0,\\ 0, & \mu=i,\end{cases} \tag{6.13.40}$$

and a symmetric second-rank tensor,

$$N^{\mu\nu} \equiv \frac{1}{4}\sum_{s_1,s_2}(y_1^\dagger\bar{\sigma}^\mu x_2-x_1\sigma^\mu y_2^\dagger)(x_2^\dagger\bar{\sigma}^\nu y_1-y_2\sigma^\nu x_1^\dagger) = p_1^\mu p_2^\nu+p_2^\mu p_1^\nu-g^{\mu\nu}(p_1\cdot p_2-m_{\widetilde{N}_1}^2)$$
$$= \begin{cases}2m_{\widetilde{N}_1}^2, & \mu=\nu=0,\\ 0, & \mu=0,\ \nu=j \text{ or } \mu=i,\ \nu=0,\\ 2\left[|\vec{\boldsymbol{p}}|^2\,\delta^{ij}-p^ip^j\right], & \mu=i,\ \nu=j,\end{cases} \tag{6.13.41}$$

where the final results given in Eqs. (6.13.39)–(6.13.41) have been evaluated in the CM frame. Similarly, the spin-summed final state fermion quantities are

$$F \equiv \sum_{s_{f1},s_{f2}}(y_{f1}y_{f2}-x_{f1}^\dagger x_{f2}^\dagger)(y_{f2}^\dagger y_{f1}^\dagger-x_{f2}x_{f1}) = 4(k_1\cdot k_2+m_f^2) = 8E^2, \tag{6.13.42}$$

$$F^\mu \equiv \sum_{s_{f1},s_{f2}}(x_{f1}^\dagger\bar{\sigma}^\mu y_{f2})(y_{f2}^\dagger y_{f1}^\dagger-x_{f2}x_{f1}) = -\sum_{s_{f1},s_{f2}}(y_{f1}\sigma^\mu x_{f2}^\dagger)(y_{f2}^\dagger y_{f1}^\dagger-x_{f2}x_{f1})$$
$$= 2m_f(k_1+k_2)^\mu = \begin{cases}4m_fE, & \mu=0,\\ 0, & \mu=i,\end{cases} \tag{6.13.43}$$

after evaluating the above quantities in the CM frame, and

$$F_1^{\mu\nu} \equiv \sum_{s_{f1},s_{f2}}(x_{f1}^\dagger\bar{\sigma}^\mu y_{f2})(y_{f2}^\dagger\bar{\sigma}^\nu x_{f1}) = k_{1\rho}k_{2\lambda}\mathrm{Tr}(\sigma^\rho\bar{\sigma}^\mu\sigma^\lambda\bar{\sigma}^\nu), \tag{6.13.44}$$

$$F_2^{\mu\nu} \equiv \sum_{s_{f1},s_{f2}}(y_{f1}\sigma^\mu x_{f2}^\dagger)(x_{f2}\sigma^\nu y_{f1}^\dagger) = k_{1\rho}k_{2\lambda}\mathrm{Tr}(\bar{\sigma}^\rho\sigma^\mu\bar{\sigma}^\lambda\sigma^\nu), \tag{6.13.45}$$

$$F_{12}^{\mu\nu} \equiv \sum_{s_{f1},s_{f2}}(y_{f1}\sigma^\mu x_{f2}^\dagger)(y_{f2}^\dagger\bar{\sigma}^\nu x_{f1}) = \sum_{s_{f1},s_{f2}}(x_{f1}^\dagger\bar{\sigma}^\mu y_{f2})(x_{f2}\sigma^\nu y_{f1}^\dagger) = -m_f^2\mathrm{Tr}(\sigma^\mu\bar{\sigma}^\nu). \tag{6.13.46}$$

Since $N^{\mu\nu}$ is symmetric, the antisymmetric parts of $F_1^{\mu\nu}$ and $F_2^{\mu\nu}$ do not contribute in Eq. (6.13.38). The symmetric parts of $F_1^{\mu\nu}$ and $F_2^{\mu\nu}$ are equal and given by:

$$[F_1^{\mu\nu}]_{\mathrm{symm}} = [F_2^{\mu\nu}]_{\mathrm{symm}} = 2(k_1^\mu k_2^\nu+k_1^\nu k_2^\mu-k_1\cdot k_2g^{\mu\nu})$$
$$= \begin{cases}2m_f^2, & \mu=\nu=0,\\ 0, & \mu=0,\ \nu=j \text{ or } \mu=i,\ \nu=0,\\ 2m_f^2(2\hat{\boldsymbol{k}}^i\hat{\boldsymbol{k}}^j-\delta^{ij})-4E^2(\hat{\boldsymbol{k}}^i\hat{\boldsymbol{k}}^j-\delta^{ij}), & \mu=i,\ \nu=j,\end{cases} \tag{6.13.47}$$

and $F_{12}^{\mu\nu} = -2m_f^2 g^{\mu\nu}$. The spin-averaged squared matrix element for $\widetilde{N}_1\widetilde{N}_1 \to f\bar{f}$ given by Eq. (6.13.38) can now be fully evaluated, resulting in

$$\frac{1}{4}\sum_{s_1,s_2,s_{f1},s_{f2}} |\mathcal{M}_Z + \mathcal{M}_{\tilde{f}}|^2 = 4(|c_1|^2+|c_3|^2)\left[m_{\widetilde{N}_1}^2 m_f^2 + 2|\vec{\boldsymbol{p}}|^2(E^2(1+\cos^2\theta) - m_f^2\cos^2\theta)\right]$$
$$+ 8m_f^2\,\mathrm{Re}(c_1c_3^*)\left[m_{\widetilde{N}_1}^2 - 2|\vec{\boldsymbol{p}}|^2\right] + \frac{16m_f^2 m_{\widetilde{N}_1}^2}{m_Z^4}E^2\left[E^2|c_0|^2 - m_Z^2\mathrm{Re}[c_0^*(c_1+c_3)]\right], \quad (6.13.48)$$

where $\cos\theta = \vec{\boldsymbol{p}}\cdot\hat{\boldsymbol{k}}/|\vec{\boldsymbol{p}}|$. In the non-relativistic limit, we use Eq. (6.13.3) and drop terms of $\mathcal{O}(|\vec{\boldsymbol{p}}|^4)$.

To compute $v_{\rm rel}\sigma_{\rm ann}$, we make use of the following result for the differential annihilation cross-section in the CM frame:

$$v_{\rm rel}\left(\frac{\mathrm{d}\sigma}{\mathrm{d}\Omega}\right)_{\rm CM} = \frac{1}{32\pi^2 s}\left(1-\frac{4m_f^2}{s}\right)^{1/2}|\mathcal{M}|^2_{\rm ave}, \quad (6.13.49)$$

where $|\mathcal{M}|^2_{\rm ave}$ is the squared matrix element for the annihilation process, averaged over initial spins and summed over final spins, and the relative velocity of the initial state neutralinos in the CM frame is given by $v_{\rm rel} = 4|\vec{\boldsymbol{p}}|/\sqrt{s} \simeq 2|\vec{\boldsymbol{p}}|/m_{\widetilde{N}_1}$, after noting that $\sqrt{s} \simeq 2m_{\widetilde{N}_1}$ in the non-relativistic limit. Inserting the squared matrix element obtained above into Eq. (6.13.49) and integrating over solid angles, we end up with:

$$v_{\rm rel}\sigma_{\rm ann} = \frac{1}{8\pi E^2}\left(1-\frac{m_f^2}{E^2}\right)^{1/2}\left\{(|c_1|^2+|c_3|^2)\left[m_{\widetilde{N}_1}^2 m_f^2 + \frac{2|\vec{\boldsymbol{p}}|^2}{3}\left(4m_{\widetilde{N}_1}^2 - m_f^2\right)\right]\right.$$
$$+ \frac{4m_f^2 m_{\widetilde{N}_1}^2}{m_Z^4}\left[m_{\widetilde{N}_1}^2(m_{\widetilde{N}_1}^2 + 2|\vec{\boldsymbol{p}}|^2)|c_0|^2 - m_Z^2(m_{\widetilde{N}_1}^2 + |\vec{\boldsymbol{p}}|^2)\mathrm{Re}[c_0^*(c_1+c_3)]\right]$$
$$\left. + 2m_f^2\,\mathrm{Re}(c_1c_3^*)\left[m_{\widetilde{N}_1}^2 - 2|\vec{\boldsymbol{p}}|^2\right] + \mathcal{O}(|\vec{\boldsymbol{p}}|^4)\right\}, \quad (6.13.50)$$

where the effects of the s-channel Higgs boson exchanges have been omitted.

The momentum dependence of Eq. (6.13.50) reflects the famous p-wave suppression of the annihilation cross-section in the $m_f = 0$ limit noted in Ref. [178].[65] In general, the annihilation cross-section in the non-relativistic limit behaves as $v_{\rm rel}\,\sigma_{\rm ann} \propto |\vec{\boldsymbol{p}}|^{2\ell}$. Applying this result to Eq. (6.13.50) in the $m_f = 0$ limit implies that $\ell = 1$. This is a consequence of the Majorana nature of the neutralino. In particular, in the limit of $m_f = 0$, the $f\bar{f}$ pair is in a $J = 1$ angular momentum state. However, Fermi statistics dictates that at threshold, a pair of identical Majorana fermions in a $J = 1$ state must have relative orbital angular momentum $\ell = 1$ (corresponding to p-wave annihilation). The s-wave annihilation (corresponding to the Majorana fermion pair in a $J = 0$ state) is suppressed by a factor of m_f^2, as is evident from Eq. (6.13.50).

We have checked that Eq. (6.13.50) corresponds to a result first obtained in Ref. [179] (although the latter reference omits the terms in Eq. (6.13.50) proportional to c_0). However, we emphasize that this formula neglects the effects of s-channel Higgs boson exchanges. We invite the reader to complete the computation of the annihilation cross-section by including these terms (along with the effects of interference between the neglected contributions and the ones computed above).

The annihilation of $\widetilde{N}_1\widetilde{N}_1$ into heavy quarks (c, b and t), followed by the decay of the heavy quarks, can yield observable signatures suitable for indirect dark matter detection. For example, the annihilation of neutralinos in the galaxy provides a possible source of indirect dark matter detection via the observation of positrons in cosmic rays [184]. Neutralino dark matter can also be captured in the sun [185]. The neutrinos that arise (either directly or indirectly) from the neutralino annihilation in the sun can be detected on Earth (see, e.g., Ref. [186]).

6.14. $e^-e^+ \to \widetilde{C}_i^-\widetilde{C}_j^+$

Next we consider the pair production of charginos in electron–positron collisions. The s-channel Feynman diagrams are shown in Fig. 6.14.1, where we have also introduced the notation for the fermion momenta and polarizations. The Mandelstam variables are given by

$$s = 2p_1\cdot p_2 = m_{\widetilde{C}_i}^2 + m_{\widetilde{C}_j}^2 + 2k_i\cdot k_j, \quad (6.14.1)$$

$$t = m_{\widetilde{C}_i}^2 - 2p_1\cdot k_i = m_{\widetilde{C}_j}^2 - 2p_2\cdot k_j, \quad (6.14.2)$$

$$u = m_{\widetilde{C}_i}^2 - 2p_2\cdot k_i = m_{\widetilde{C}_j}^2 - 2p_1\cdot k_j. \quad (6.14.3)$$

[65] In Ref. [178], the annihilation rate for photinos is computed, corresponding to $N_{11} = c_W$, $N_{12} = s_W$ and $N_{13} = N_{14} = 0$. In this case, the Z boson and Higgs boson s-channel exchange diagrams are absent. The result presented in Ref. [178] should be multiplied by a factor of two (H. Goldberg, private communication)—the corrected expression then agrees with Eq. (6.13.50).

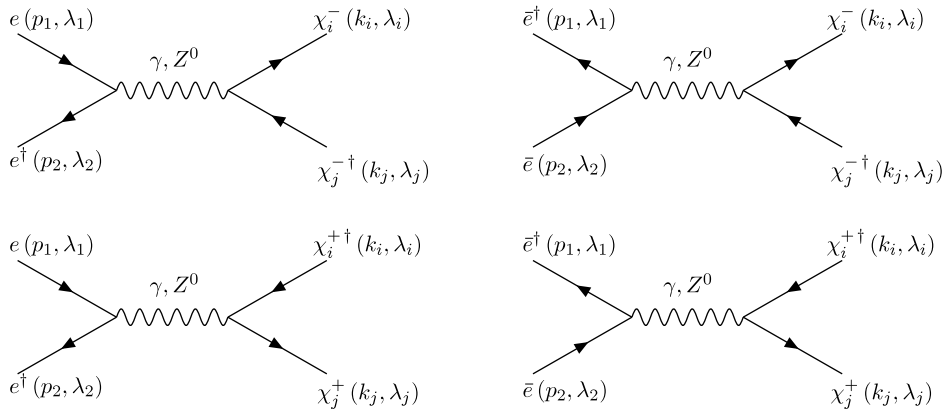

Fig. 6.14.1. Feynman diagrams for $e^-e^+ \to \widetilde{C}_i^-\widetilde{C}_j^+$ via s-channel γ and Z^0 exchange.

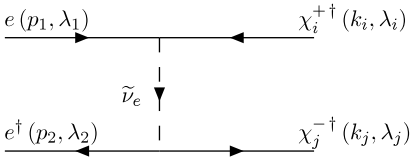

Fig. 6.14.2. The Feynman diagram for $e^-e^+ \to \widetilde{C}_i^-\widetilde{C}_j^+$ via the t-channel exchange of a sneutrino.

Note that the negatively charged chargino carries momentum and polarization (k_i, λ_i), while the positively charged one carries (k_j, λ_j).

Using the Feynman rules of Figs. J.1.2 and K.2.1, the sum of the photon-exchange diagrams is given by:

$$i\mathcal{M}_\gamma = \frac{-ig^{\mu\nu}}{s}\left(-ie\,x_1\sigma_\mu y_2^\dagger - ie\,y_1^\dagger\overline{\sigma}_\mu x_2\right)\left(ie\,\delta_{ij}y_i\sigma_\nu x_j^\dagger + ie\,\delta_{ij}x_i^\dagger\,\overline{\sigma}_\nu y_j\right). \tag{6.14.4}$$

The Z-exchange diagrams yields [cf. footnote 60]:

$$i\mathcal{M}_Z = \frac{-ig^{\mu\nu}}{D_Z}\left[\frac{ig}{c_W}\left(s_W^2 - \tfrac{1}{2}\right)x_1\sigma_\mu y_2^\dagger + \frac{igs_W^2}{c_W}\,y_1^\dagger\overline{\sigma}_\mu x_2\right]\left[-\frac{ig}{c_W}O'^L_{ji}\,y_i\sigma_\nu x_j^\dagger - \frac{ig}{c_W}O'^R_{ji}\,x_i^\dagger\,\overline{\sigma}_\nu y_j\right], \tag{6.14.5}$$

where $D_Z \equiv s - m_Z^2 + i\Gamma_Z m_Z$. The t-channel Feynman diagram via sneutrino exchange is shown in Fig. 6.14.2. Applying the rules of Fig. K.4.1, we find:

$$i\mathcal{M}_{\tilde{\nu}_e} = (-1)\frac{i}{t - m_{\tilde{\nu}_e}^2}\left(-igV_{i1}^*x_1y_i\right)\left(-igV_{j1}y_2^\dagger x_j^\dagger\right). \tag{6.14.6}$$

The Fermi–Dirac factor (-1) in this equation arises because the spinors appear an order which is an odd permutation of the order used in all of the s-channel diagram results.

One can now apply the Fierz transformation identities Eqs. (2.67)–(2.69) to Eqs. (6.14.4) and (6.14.5) to remove the σ and $\overline{\sigma}$ matrices. The result can be combined with the t-channel contribution to obtain a total matrix element $\mathcal{M}$ with exactly the same form as Eq. (6.12.9), but now with:

$$c_1 = 2\frac{e^2\delta_{ij}}{s} - \frac{g^2}{c_W^2 D_Z}(1 - 2s_W^2)O'^R_{ji}, \tag{6.14.7}$$

$$c_2 = \frac{2e^2\delta_{ij}}{s} - \frac{g^2}{c_W^2 D_Z}(1 - 2s_W^2)O'^L_{ji} + \frac{g^2V_{i1}^*V_{j1}}{t - m_{\tilde{\nu}_e}^2}, \tag{6.14.8}$$

$$c_3 = \frac{2e^2\delta_{ij}}{s} + \frac{2g^2s_W^2}{c_W^2 D_Z}O'^R_{ji}, \tag{6.14.9}$$

$$c_4 = \frac{2e^2\delta_{ij}}{s} + \frac{2g^2s_W^2}{c_W^2 D_Z}O'^L_{ji}. \tag{6.14.10}$$

The rest of this calculation is identical in form to Eqs. (6.12.9)–(6.12.16), so that the result is:

$$\sum_{\text{spins}} |\mathcal{M}|^2 = (|c_1|^2 + |c_4|^2)(u - m^2_{\widetilde{C}_i})(u - m^2_{\widetilde{C}_j}) + (|c_2|^2 + |c_3|^2)(t - m^2_{\widetilde{C}_i})(t - m^2_{\widetilde{C}_j}) + 2\text{Re}[c_1 c_2^* + c_3 c_4^*] m_{\widetilde{C}_i} m_{\widetilde{C}_j} s. \tag{6.14.11}$$

The differential cross-section then follows:

$$\frac{\mathrm{d}\sigma}{\mathrm{d}t} = \frac{1}{16\pi s^2}\left(\frac{1}{4}\sum_{\text{spins}} |\mathcal{M}|^2\right). \tag{6.14.12}$$

As in the previous subsection, we define $\cos\theta = \hat{\boldsymbol{p}}_1 \cdot \hat{\boldsymbol{k}}_{\boldsymbol{i}}$ (where θ is the angle between the initial state electron and $\tilde{C}_i^-$ in the center-of-momentum frame). The Mandelstam variables t, u are given by

$$t = \frac{1}{2}\left[m^2_{\widetilde{C}_i} + m^2_{\widetilde{C}_j} - s + \lambda^{1/2}(s, m^2_{\widetilde{C}_i}, m^2_{\widetilde{C}_j})\cos\theta\right], \tag{6.14.13}$$

$$u = \frac{1}{2}\left[m^2_{\widetilde{C}_i} + m^2_{\widetilde{C}_j} - s - \lambda^{1/2}(s, m^2_{\widetilde{C}_i}, m^2_{\widetilde{C}_j})\cos\theta\right]. \tag{6.14.14}$$

The total cross-section can now be computed as

$$\sigma = \int_{t_-}^{t_+} \frac{\mathrm{d}\sigma}{\mathrm{d}t}\mathrm{d}t, \tag{6.14.15}$$

where t_- and t_+ are obtained with $\cos\theta = -1$ and $+1$ in Eq. (6.14.13), respectively. Our results agree with the original first complete calculation in Ref. [187]. Earlier work with simplifying assumptions is given in Ref. [188]. An extended calculation for the production of polarized charginos is given in [189].

6.15. $u\bar{d} \to \widetilde{C}_i^+ \widetilde{N}_j$

Next we consider the associated production of a chargino and a neutralino in quark, anti-quark collisions. The leading order Feynman diagrams are shown in Fig. 6.15.1, where we have also defined the momenta and the helicities. The corresponding Mandelstam variables are

$$s = 2p_1 \cdot p_2 = m^2_{\widetilde{C}_i} + m^2_{\widetilde{N}_j} + 2k_i \cdot k_j, \tag{6.15.1}$$

$$t = m^2_{\widetilde{C}_i} - 2p_1 \cdot k_i = m^2_{\widetilde{N}_j} - 2p_2 \cdot k_j, \tag{6.15.2}$$

$$u = m^2_{\widetilde{C}_i} - 2p_2 \cdot k_i = m^2_{\widetilde{N}_j} - 2p_1 \cdot k_j. \tag{6.15.3}$$

The matrix elements for the s-channel diagrams are obtained by applying the Feynman rules of Figs. J.1.2 and K.2.2:

$$i\mathcal{M}_s = \frac{-ig^{\mu\nu}}{s - m_W^2}\left(\frac{ig}{\sqrt{2}} x_1 \sigma_\mu y_2^\dagger\right)\left(igO^{L*}_{ji} x_i^\dagger \overline{\sigma}_\nu y_j + igO^{R*}_{ji} y_i \sigma_\nu x_j^\dagger\right). \tag{6.15.4}$$

The external spinors are denoted by $x_1 \equiv x(\vec{\boldsymbol{p}}_1, \lambda_1), y_2^\dagger \equiv y^\dagger(\vec{\boldsymbol{p}}_2, \lambda_2), x_i^\dagger \equiv x^\dagger(\vec{\boldsymbol{k}}_i, \lambda_i), y_j \equiv y(\vec{\boldsymbol{k}}_j, \lambda_j)$, etc. The matrix elements for the t and u channel graphs follow from the rules of Figs. K.4.1 and K.4.2:

$$i\mathcal{M}_t = (-1)\frac{i}{t - m^2_{\tilde{d}_L}}\left(-igU^*_{i1}\right)\left(\frac{ig}{\sqrt{2}}\left[N_{j2} - \frac{s_W}{3c_W}N_{j1}\right]\right) x_1 y_i y_2^\dagger x_j^\dagger, \tag{6.15.5}$$

$$i\mathcal{M}_u = \frac{i}{u - m^2_{\tilde{u}_L}}\left(-igV_{i1}\right)\left(\frac{ig}{\sqrt{2}}\left[-N^*_{j2} - \frac{s_W}{3c_W}N^*_{j1}\right]\right) x_1 y_j y_2^\dagger x_i^\dagger. \tag{6.15.6}$$

The first factor of (-1) in Eq. (6.15.5) is required because the order of the spinors $(1, i, 2, j)$ is in an odd permutation of the order $(1, 2, i, j)$ used in the s-channel and u-channel results.

Now we can use the Fierz relations Eqs. (2.67) and (2.69) to rewrite the s-channel amplitude in a form without σ or $\overline{\sigma}$ matrices. Combining the result with the t-channel and u-channel contributions yields a total $\mathcal{M}$ with exactly the same form as Eq. (6.12.9), but now with

$$c_1 = -\sqrt{2}g^2\left[\frac{O^{L*}_{ji}}{s - m_W^2} + \left(\frac{1}{2}N^*_{j2} + \frac{s_W}{6c_W}N^*_{j1}\right)\frac{V_{i1}}{u - m_{\tilde{u}_L}}\right], \tag{6.15.7}$$

$$c_2 = -\sqrt{2}g^2\left[\frac{O^{R*}_{ji}}{s - m_W^2} + \left(\frac{1}{2}N^*_{j2} - \frac{s_W}{6c_W}N^*_{j1}\right)\frac{U^*_{i1}}{t - m_{\tilde{d}_L}}\right], \tag{6.15.8}$$

$$c_3 = c_4 = 0. \tag{6.15.9}$$

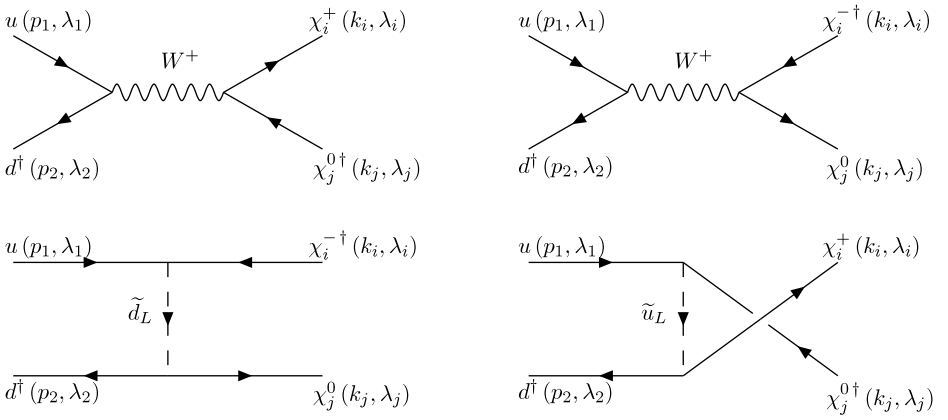

Fig. 6.15.1. The four tree-level Feynman diagrams for $u\bar{d} \to \widetilde{C}_i^+ \widetilde{N}_j$.

The rest of this calculation is identical in form to that of Eqs. (6.12.9)–(6.12.16), leading to:

$$\sum_{\text{spins}} |\mathcal{M}|^2 = |c_1|^2(u - m^2_{\widetilde{C}_i})(u - m^2_{\widetilde{N}_j}) + |c_2|^2(t - m^2_{\widetilde{C}_i})(t - m^2_{\widetilde{N}_j}) + 2\text{Re}[c_1 c_2^*] m_{\widetilde{C}_i} m_{\widetilde{N}_j} s. \tag{6.15.10}$$

From this, one can obtain:

$$\frac{\mathrm{d}\sigma}{\mathrm{d}t} = \frac{1}{16\pi s^2}\left(\frac{1}{3\cdot 4}\sum_{\text{spins}} |\mathcal{M}|^2\right), \tag{6.15.11}$$

where we have included a factor of 1/3 from the color average for the incoming quarks. As in the previous two subsections, Eq. (6.15.11) can be expressed in terms of the angle between the u quark and the chargino in the center-of-momentum frame, using

$$t = \frac{1}{2}\left[m^2_{\widetilde{C}_i} + m^2_{\widetilde{N}_j} - s + \lambda^{1/2}(s, m^2_{\widetilde{C}_i}, m^2_{\widetilde{N}_j})\cos\theta\right], \tag{6.15.12}$$

$$u = \frac{1}{2}\left[m^2_{\widetilde{C}_i} + m^2_{\widetilde{N}_j} - s - \lambda^{1/2}(s, m^2_{\widetilde{C}_i}, m^2_{\widetilde{N}_j})\cos\theta\right]. \tag{6.15.13}$$

This process occurs in proton–antiproton and proton–proton collisions, where $\sqrt{s}$ is not fixed, and the angle θ is different than the lab frame angle. The observable cross-section depends crucially on experimental cuts. Our result in Eq. (6.15.11) agrees with the complete computation in Ref. [190]. Earlier calculations in special supersymmetric scenarios, e.g. with photino mass eigenstates, are given in Refs. [177,191].

6.16. $\widetilde{N}_i \to \widetilde{N}_j \widetilde{N}_k \widetilde{N}_\ell$

Next we consider the decay of a neutralino $\widetilde{N}_i$ to three lighter neutralinos: $\widetilde{N}_j$, $\widetilde{N}_k$, $\widetilde{N}_\ell$. To the best of our knowledge, this process has not been computed in the literature. This decay is not likely to be phenomenologically relevant, because a variety of two-body decay modes will always be available. Furthermore, the calculation itself is quite complicated because of the large number of Feynman diagrams involved. Therefore, we consider this only as a matter-of-principle example of a process with four external state Majorana fermions, and will restrict ourselves to writing down the contributing matrix element amplitudes.

At tree level, the decay can proceed via a virtual Z^0 boson; the Feynman graphs are shown in Fig. 6.16.1. In addition, it can proceed via the exchange of any of the neutral scalar Higgs bosons of the MSSM, $\phi^0 = h^0, H^0, A^0$, as shown in Fig. 6.16.2. Since any of the final state neutralinos can directly couple to the initial state neutralino there are two more diagrams for each one shown in Figs. 6.16.1 and 6.16.2, for a total of 48 tree-level diagrams (counting each intermediate Higgs boson state as distinct). In all cases, the four-momenta of the neutralinos $\widetilde{N}_i$, $\widetilde{N}_j$, $\widetilde{N}_k$, $\widetilde{N}_\ell$ are denoted p_i, k_j, k_k, k_ℓ respectively.

We obtain the sum of the four diagrams in Fig. 6.16.1 by implementing the rules of Fig. K.2.1, and using the 't Hooft–Feynman gauge :

$$i\mathcal{M}_Z^{(1)} = \frac{-ig^2/c_W^2}{(p_i - k_j)^2 - m_Z^2}\left(O''^L_{ji} x_i \sigma_\mu x_j^\dagger - O''^L_{ij} y_i^\dagger \overline{\sigma}_\mu y_j\right)\left(O''^L_{k\ell} x_k^\dagger \overline{\sigma}^\mu y_\ell - O''^L_{\ell k} y_k \sigma^\mu x_\ell^\dagger\right). \tag{6.16.1}$$

The external wave functions are $x_i \equiv x(\vec{\boldsymbol{p}}_i, \lambda_i)$, $x_{j,k,\ell} \equiv x(\vec{\boldsymbol{k}}_{j,k,\ell}, \lambda_{j,k,\ell})$, and analogously for $x^\dagger_{i,j,k,\ell}$, and $y_{i,j,k,\ell}$ and $y^\dagger_{i,j,k,\ell}$. Note that we have factorized the sum of the four diagrams, taking advantage of the common virtual boson line propagator. By a

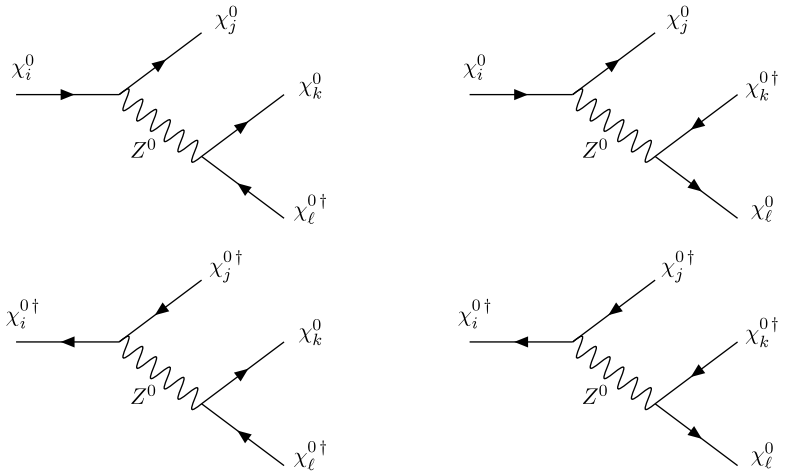

Fig. 6.16.1. Four Feynman diagrams for $\widetilde{N}_i \to \widetilde{N}_j\widetilde{N}_k\widetilde{N}_\ell$ in the MSSM via Z^0 exchange. There are four more where $\widetilde{N}_j \leftrightarrow \widetilde{N}_k$ and another four where $\widetilde{N}_j \leftrightarrow \widetilde{N}_\ell$.

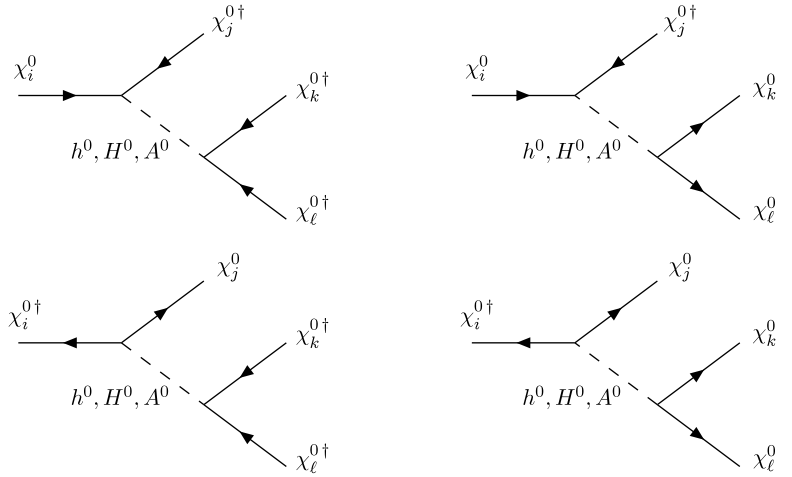

Fig. 6.16.2. Four Feynman diagrams for $\widetilde{N}_i \to \widetilde{N}_j\widetilde{N}_k\widetilde{N}_\ell$ in the MSSM via $\phi^0 = h^0,\ H^0,\ A^0$ exchange. There are four more where $\widetilde{N}_j \leftrightarrow \widetilde{N}_k$ and another four where $\widetilde{N}_j \leftrightarrow \widetilde{N}_\ell$.

judicious use of the σ or $\overline{\sigma}$ version of the vertex rule, we have ensured that the order of the four spinor wave functions is the same for each of the four diagrams. Hence, no additional relative minus signs are required.

The contributions from the diagrams related to these by permutations can now be obtained from the appropriate substitutions ($j \leftrightarrow k$) and ($j \leftrightarrow \ell$):

$$i\mathcal{M}_Z^{(2)} = (-1)\frac{-ig^2/c_W^2}{(p_i - k_k)^2 - m_Z^2}\Big(O''^L_{ki}x_i\sigma_\mu x_k^\dagger - O''^L_{ik}y_i^\dagger\,\overline{\sigma}_\mu y_k\Big)\Big(O''^L_{j\ell}x_j^\dagger\overline{\sigma}^\mu y_\ell - O''^L_{\ell j}y_j\sigma^\mu x_\ell^\dagger\Big), \tag{6.16.2}$$

$$i\mathcal{M}_Z^{(3)} = (-1)\frac{-ig^2/c_W^2}{(p_i - k_\ell)^2 - m_Z^2}\Big(O''^L_{\ell i}x_i\sigma_\mu x_\ell^\dagger - O''^L_{i\ell}y_i^\dagger\,\overline{\sigma}_\mu y_\ell\Big)\Big(O''^L_{kj}x_k^\dagger\overline{\sigma}^\mu y_j - O''^L_{jk}y_k\sigma^\mu x_j^\dagger\Big). \tag{6.16.3}$$

The first factors of (-1) in $i\mathcal{M}_Z^{(2)}$ and $i\mathcal{M}_Z^{(3)}$ are present because the order of the spinors in each case appear in an odd permutation of the canonical order set by $i\mathcal{M}_Z^{(1)}$. Note that if we were to proceed to a computation of the decay rate, the very first step would be to apply the Fierz relations of Eqs. (2.67)–(2.69) to eliminate all of the σ and $\overline{\sigma}$ matrices in the above amplitudes.

The diagrams in Fig. 6.16.2 combine to give a contribution:

$$i\mathcal{M}_{\phi^0}^{(1)} = \frac{-i}{(p_i - k_j)^2 - m_{\phi^0}^2}(Y^{ij}x_iy_j + Y_{ij}y_i^\dagger x_j^\dagger)(Y^{k\ell}y_ky_\ell + Y_{k\ell}x_k^\dagger x_\ell^\dagger), \tag{6.16.4}$$

where we have used the Feynman rules of Fig. K.3.1, and adopted the shorthand notation $Y^{ij} = (Y_{ij})^* = Y^{\phi^0\chi_i^0\chi_j^0}$. Again we have factored the amplitude using the common virtual boson propagator. As in the Z-exchange diagrams, the other contributions can be obtained by the appropriate substitutions:

$$i\mathcal{M}^{(2)}_{\phi^0} = (-1)\frac{-i}{(p_i - k_k)^2 - m^2_{\phi^0}}(Y^{ik}x_i y_k + Y_{ik}y_i^\dagger x_k^\dagger)(Y^{j\ell}y_j y_\ell + Y_{j\ell}x_j^\dagger x_\ell^\dagger), \tag{6.16.5}$$

$$i\mathcal{M}^{(3)}_{\phi^0} = (-1)\frac{-i}{(p_i - k_\ell)^2 - m^2_{\phi^0}}(Y^{i\ell}x_i y_\ell + Y_{i\ell}y_i^\dagger x_\ell^\dagger)(Y^{kj}y_k y_j + Y_{kj}x_k^\dagger x_j^\dagger). \tag{6.16.6}$$

The first factors of (-1) in $i\mathcal{M}^{(2)}_{\phi^0}$ and $i\mathcal{M}^{(3)}_{\phi^0}$ are needed because the spinors in each case are in an odd permutation of the canonical order established earlier.

The total matrix element is obtained by adding all the contributing diagrams:

$$\mathcal{M} = \sum_{n=1}^{3}\mathcal{M}_Z^{(n)} + \sum_{\phi^0}\sum_{n=1}^{3}\mathcal{M}^{(n)}_{\phi^0}. \tag{6.16.7}$$

Squaring the matrix element, dividing by $2M_{\tilde{N}_i}$, and integrating over phase space yields the total decay rate. Note that final states differing by the interchange of identical particles must be considered as a single state, counted once [38]. Given an N-body final state made up of ν_r particles of type r (where $r \leq N$), we define a statistical factor S,

$$S = \prod_r \nu_r!, \quad \text{where } \sum_r \nu_r = N. \tag{6.16.8}$$

Then, in computing the total decay rate, the integration over the total phase space must be divided by S to avoid over-counting. In the present example, $N = 3$ with $S = 2$ [or $S = 6$] in the case of two [or three] identical neutralinos in the final state, respectively

6.17. Three-body slepton decays $\widetilde{\ell}_R^- \to \ell^-\tau^\pm\widetilde{\tau}_1^\mp$ for $\ell = e, \mu$

We next consider the three-body decays of sleptons through a virtual neutralino. The usual assumption in supersymmetric phenomenology is that these decays will have a very small branching fraction, because a two-body decay to a lighter neutralino and lepton is always open. However, in Gauge Mediated Supersymmetry Breaking models with a non-minimal messenger sector, the sleptons can be lighter than the lightest neutralino [192,193]. In that case, the mostly R-type smuon and selectron, $\widetilde{\mu}_R$ and $\tilde{e}_R$, will decay by $\widetilde{\ell}_R^- \to \ell^-\tau^\pm\widetilde{\tau}_1^\mp$. The lightest stau mass eigenstate, $\widetilde{\tau}_1^\pm$, is a mixture of the weak eigenstates $\widetilde{\tau}_L^\pm$ and $\widetilde{\tau}_R^\pm$, as described in Appendix K.4:

$$\widetilde{\tau}_1^- = R^*_{\tilde{\tau}_1}\widetilde{\tau}_R^- + L^*_{\tilde{\tau}_1}\widetilde{\tau}_L^-, \tag{6.17.1}$$

and $\widetilde{\tau}_1^+ = (\widetilde{\tau}_1^-)^*$, while the $\widetilde{\mu}_R$ and $\tilde{e}_R$ are taken to be unmixed.

First consider the decay $\widetilde{\ell}_R^- \to \ell^-\tau^+\widetilde{\tau}_1^-$, which proceed by the diagrams in the top row of Fig. 6.17.1. The momenta and polarizations of the particles are also indicated on the diagram. Using the Feynman rules of Fig. K.4.4, we find that the amplitudes of these two diagrams, for each neutralino $\tilde{N}_j$ exchanged, are:

$$i\mathcal{M}_1 = (-ia_j^{\tilde{\ell}*})(-ia_j^{\tilde{\tau}})\,y_1\left[\frac{-i(p - k_1)\cdot\sigma}{(p - k_1)^2 - m^2_{\tilde{N}_j}}\right]x_2^\dagger, \tag{6.17.2}$$

$$i\mathcal{M}_2 = (-ia_j^{\tilde{\ell}*})(-ib_j^{\tilde{\tau}})\,y_1\left[\frac{im_{\tilde{N}_j}}{(p - k_1)^2 - m^2_{\tilde{N}_j}}\right]y_2 \tag{6.17.3}$$

where

$$a_j^{\tilde{\ell}} = \sqrt{2}g'N_{j1}, \tag{6.17.4}$$

$$a_j^{\tilde{\tau}} = Y_\tau N_{j3}L^*_{\tilde{\tau}_1} + \sqrt{2}g'N_{j1}R^*_{\tilde{\tau}_1}, \tag{6.17.5}$$

$$b_j^{\tilde{\tau}} = Y_\tau N^*_{j3}R^*_{\tilde{\tau}_1} - \frac{1}{\sqrt{2}}(gN^*_{j2} + g'N^*_{j1})L^*_{\tilde{\tau}_1}. \tag{6.17.6}$$

The spinor wave function factors are $y_1 = y(\vec{\boldsymbol{k}}_1, \lambda_1)$, $y_2 = y(\vec{\boldsymbol{k}}_2, \lambda_2)$, and $x_2^\dagger = x^\dagger(\vec{\boldsymbol{k}}_2, \lambda_2)$.

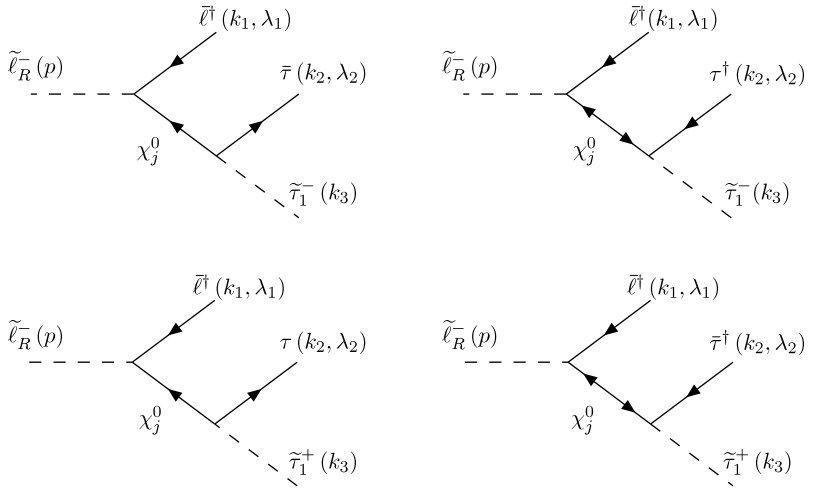

Fig. 6.17.1. Feynman diagrams for the three-body slepton decays $\widetilde{\ell}_R^- \to \ell^-\tau^+\widetilde{\tau}_1^-$ (top row) and $\widetilde{\ell}_R^- \to \ell^-\tau^-\widetilde{\tau}_1^+$ (bottom row) in the MSSM.

In the following, we will use the kinematic variables

$$z_\ell \equiv 2p\cdot k_1/m^2_{\tilde{\ell}_R} = 2E_\ell/m_{\tilde{\ell}_R}, \qquad z_\tau \equiv 2p\cdot k_2/m^2_{\tilde{\ell}_R} = 2E_\tau/m_{\tilde{\ell}_R}, \tag{6.17.7}$$

$$r_{\tilde{N}_j} \equiv m_{\tilde{N}_j}/m_{\tilde{\ell}_R}, \qquad r_{\tilde{\tau}} \equiv m_{\tilde{\tau}_1}/m_{\tilde{\ell}_R}, \tag{6.17.8}$$

$$r_\tau \equiv m_\tau/m_{\tilde{\ell}_R}, \qquad r_\ell \equiv m_\ell/m_{\tilde{\ell}_R}. \tag{6.17.9}$$

The total amplitude then can be written as

$$\mathcal{M} = \sum_{j=1}^{4}\Big[c_j y_1(p-k_1)\cdot\sigma x_2^\dagger + d_j y_1 y_2\Big], \tag{6.17.10}$$

where

$$c_j = -a_j^{\tilde{\ell}*}a_j^{\tilde{\tau}}/[m^2_{\tilde{\ell}_R}(r^2_{\tilde{N}_j} - 1 + z_\ell)], \tag{6.17.11}$$

$$d_j = a_j^{\tilde{\ell}*}b_j^{\tilde{\tau}}m_{\tilde{N}_j}/[m^2_{\tilde{\ell}_R}(r^2_{\tilde{N}_j} - 1 + z_\ell)]. \tag{6.17.12}$$

We consistently neglect the electron and muon masses and Yukawa couplings (so $r_\ell = 0$) in the matrix elements, but not below in the kinematic integration over phase space, where the muon mass can be important.

Using Eqs. (2.43) and (2.44), we find

$$\begin{aligned}|\mathcal{M}|^2 = \sum_{j,k}\Big[&c_j c_k^*\, y_1(p-k_1)\cdot\sigma x_2^\dagger x_2(p-k_1)\cdot\sigma y_1^\dagger + d_j d_k^* y_1 y_2\, y_2^\dagger y_1^\dagger \\ &+ c_j d_k^* y_1(p-k_1)\cdot\sigma x_2^\dagger y_2^\dagger y_1^\dagger + c_j^* d_k x_2(p-k_1)\cdot\sigma y_1^\dagger y_1 y_2\Big].\end{aligned} \tag{6.17.13}$$

Summing over the lepton spins using Eqs. (3.1.58)–(3.1.61) gives

$$\begin{aligned}\sum_{\lambda_1,\lambda_2}|\mathcal{M}|^2 = \sum_{j,k}\Big[&c_j c_k^*\mathrm{Tr}[(p-k_1)\cdot\sigma k_2\cdot\overline{\sigma}(p-k_1)\cdot\sigma k_1\cdot\overline{\sigma}] + d_j d_k^*\mathrm{Tr}[k_2\cdot\sigma k_1\cdot\overline{\sigma}] \\ &- c_j d_k^* m_\tau\mathrm{Tr}[(p-k_1)\cdot\sigma k_1\cdot\overline{\sigma}] - c_j^* d_k m_\tau\mathrm{Tr}[(p-k_1)\cdot\sigma k_1\cdot\overline{\sigma}]\Big].\end{aligned} \tag{6.17.14}$$

Taking the traces using Eqs. (2.55) and (2.56) yields

$$\begin{aligned}\sum_{\text{spins}}|\mathcal{M}|^2 &= \sum_{j,k}\Big\{c_j c_k^*[4k_1\cdot(p-k_1)k_2\cdot(p-k_1) - 2k_1\cdot k_2(p-k_1)^2] + 2d_j d_k^* k_1\cdot k_2 \\ &\quad - 4\mathrm{Re}[c_j d_k^*]m_\tau k_1\cdot(p-k_1)\Big\} \\ &= \sum_{j,k}\Big\{c_j c_k^* m^4_{\tilde{\ell}_R}[(1-z_\ell)(1-z_\tau) - r_{\tilde{\tau}}^2 + r_\tau^2] \\ &\quad + d_j d_k^* m^2_{\tilde{\ell}_R}(z_\ell + z_\tau - 1 + r_{\tilde{\tau}}^2 - r_\tau^2) - 2\mathrm{Re}[c_j d_k^*]m_\tau m^2_{\tilde{\ell}_R} z_\ell\Big\}.\end{aligned} \tag{6.17.15}$$

The differential decay rate for $\widetilde{\ell}_R^- \to \ell^- \tau^+ \widetilde{\tau}_1^-$ then follows:

$$\frac{\mathrm{d}^2\Gamma}{\mathrm{d}z_\ell \mathrm{d}z_\tau} = \frac{m_{\tilde{\ell}_R}}{256\pi^3}\left(\sum_{\text{spins}} |\mathcal{M}|^2\right). \tag{6.17.16}$$

The total decay rate in that channel can be found by integrating over z_ℓ, z_τ, with the limits (see for example Ref. [164]):

$$2r_\ell < z_\ell < 1 + r_\ell^2 - (r_\tau + r_{\tilde{\tau}})^2, \tag{6.17.17}$$

$$(z_\tau)_{\min} < z_\tau < (z_\tau)_{\max}, \tag{6.17.18}$$

where

$$(z_\tau)_{\min,\,\max} = \frac{1}{2(1 - z_\ell + r_\ell^2)}\Big[(2 - z_\ell)(1 + r_\ell^2 + r_\tau^2 - r_{\tilde{\tau}}^2 - z_\ell) \mp (z_\ell^2 - 4r_\ell^2)^{1/2}\lambda^{1/2}(1 + r_\ell^2 - z_\ell, r_\tau^2, r_{\tilde{\tau}}^2)\Big], \tag{6.17.19}$$

and the triangle function $\lambda^{1/2}$ is defined in Eq. (6.1.11).

Now we turn to the competing decay $\widetilde{\ell}_R^- \to \ell^- \tau^- \widetilde{\tau}_1^+$, with diagrams appearing in the bottom row of Fig. 6.17.1. By appealing again to the Feynman rules of Fig. K.4.3, we find that the amplitude has exactly the same form as in Eqs. (6.17.2) and (6.17.3), except now with $a_j^{\tilde{\tau}} \leftrightarrow b_j^{\tilde{\tau}*}$. Therefore, the entire previous calculation goes through precisely as before, but now with

$$c_j = \frac{-a_j^{\tilde{\ell}*} b_j^{\tilde{\tau}*}}{m_{\tilde{\ell}_R}^2 (r_{\tilde{N}_j}^2 - 1 + z_\ell)}, \tag{6.17.20}$$

$$d_j = \frac{a_j^{\tilde{\ell}*} a_j^{\tilde{\tau}*} m_{\tilde{N}_j}}{m_{\tilde{\ell}_R}^2 (r_{\tilde{N}_j}^2 - 1 + z_\ell)}. \tag{6.17.21}$$

The differential decay widths found above can be integrated to find the total decay widths. The results agree with Ref. [194], except that the signs of the coefficient $c_{ij}^{(3)}$ and $c_{ij}^{(4)}$ in the published version of that paper are incorrect; the arXiv eprint version has been corrected. (Also, the notations for the sfermion mixing angle are different in that paper.) If $m_{\tilde{\ell}_R} - m_{\tilde{\tau}_1} - m_\tau$ is not too large, the resulting decays can have a macroscopic length in a detector, and the ratio of the two decay modes can provide an interesting probe of the supersymmetric Lagrangian.

6.18. *Neutralino decay to photon and Goldstino:* $\widetilde{N}_i \to \gamma \widetilde{G}$

The Goldstino $\widetilde{G}$ is a massless Weyl fermion that couples to the neutralino and photon fields according to the non-renormalizable Lagrangian term [195]:

$$\mathscr{L} = -\frac{a_i}{2}(\chi_i^0 \sigma^\mu \overline{\sigma}^\rho \sigma^\nu \partial_\mu \widetilde{G}^\dagger)\,(\partial_\nu A_\rho - \partial_\rho A_\nu) + \text{h.c.} \tag{6.18.1}$$

Here χ_i^0 is the left-handed two-component fermion field that corresponds to the neutralino $\widetilde{N}_i$ particle, $\widetilde{G}$ is the two-component fermion field corresponding to the (nearly) massless Goldstino, and the effective coupling is

$$a_i \equiv \frac{1}{\sqrt{2}\langle F\rangle}(N_{i1}^* \cos\theta_W + N_{i2}^* \sin\theta_W), \tag{6.18.2}$$

where N_{ij} the mixing matrix for the neutralinos [see Eq. (K.2.8)], and $\langle F\rangle$ is the F-term expectation value associated with supersymmetry breaking. Therefore $\widetilde{N}_i$ can decay to γ plus $\widetilde{G}$ through the diagrams shown in Fig. 6.18.1, with amplitudes:

$$i\mathcal{M}_1 = i\frac{a_i}{2} x_{\tilde{N}} k_{\tilde{G}} \cdot \sigma \left(\varepsilon^* \cdot \overline{\sigma}\, k_\gamma \cdot \sigma - k_\gamma \cdot \overline{\sigma}\, \varepsilon^* \cdot \sigma\right) x_{\tilde{G}}^\dagger, \tag{6.18.3}$$

$$i\mathcal{M}_2 = -i\frac{a_i^*}{2} y_{\tilde{N}}^\dagger k_{\tilde{G}} \cdot \overline{\sigma} \left(\varepsilon^* \cdot \sigma\, k_\gamma \cdot \overline{\sigma} - k_\gamma \cdot \sigma\, \varepsilon^* \cdot \overline{\sigma}\right) y_{\tilde{G}}\,. \tag{6.18.4}$$

Here $x_{\tilde{N}} \equiv x(\vec{\boldsymbol{p}}, \lambda_{\tilde{N}})$, $y_{\tilde{N}}^\dagger \equiv y^\dagger(\vec{\boldsymbol{p}}, \lambda_{\tilde{N}})$, and $x_{\tilde{G}}^\dagger \equiv x^\dagger(\vec{\boldsymbol{k}}_{\tilde{G}}, \lambda_{\tilde{G}})$, $y_{\tilde{G}} \equiv y(\vec{\boldsymbol{k}}_{\tilde{G}}, \lambda_{\tilde{G}})$, and $\varepsilon^* = \varepsilon^*(\vec{\boldsymbol{k}}_\gamma, \lambda_\gamma)$ are the external wave function factors for the neutralino, Goldstino, and photon, respectively. Using the on-shell condition $k_\gamma \cdot \varepsilon^* = 0$, we have $k_\gamma \cdot \sigma \varepsilon^* \cdot \overline{\sigma} = -\varepsilon^* \cdot \sigma k_\gamma \cdot \overline{\sigma}$ and $k_\gamma \cdot \overline{\sigma} \varepsilon^* \cdot \sigma = -\varepsilon^* \cdot \overline{\sigma} k_\gamma \cdot \sigma$ from Eqs. (2.51) and (2.52). So we can rewrite the total amplitude as

$$\mathcal{M} = \mathcal{M}_1 + \mathcal{M}_2 = x_{\tilde{N}} A x_{\tilde{G}}^\dagger + y_{\tilde{N}}^\dagger B y_{\tilde{G}}, \tag{6.18.5}$$

where

$$A = a_i\, k_{\tilde{G}} \cdot \sigma\, \varepsilon^* \cdot \overline{\sigma}\, k_\gamma \cdot \sigma, \tag{6.18.6}$$

$$B = -a_i^*\, k_{\tilde{G}} \cdot \overline{\sigma}\, \varepsilon^* \cdot \sigma\, k_\gamma \cdot \overline{\sigma}. \tag{6.18.7}$$

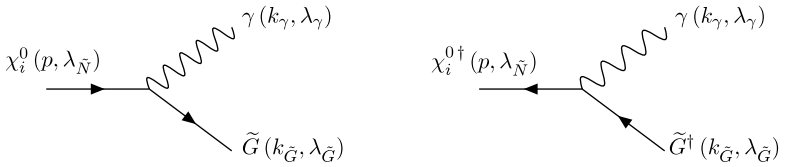

Fig. 6.18.1. The two Feynman diagrams for $\widetilde N_i \to \gamma\widetilde G$ in supersymmetric models with a light Goldstino.

The complex square of the matrix element is therefore

$$|\mathcal{M}|^2 = x_{\tilde N} A x^\dagger_{\tilde G} x_{\tilde G} \hat A x^\dagger_{\tilde N} + y^\dagger_{\tilde N} B y_{\tilde G} y^\dagger_{\tilde G} \hat B y_{\tilde N} + x_{\tilde N} A x^\dagger_{\tilde G} y^\dagger_{\tilde G} \hat B y_{\tilde N} + y^\dagger_{\tilde N} B y_{\tilde G} x_{\tilde G} \hat A x^\dagger_{\tilde N}, \tag{6.18.8}$$

where $\hat A$ and $\hat B$ are obtained from A and B by reversing the order of the σ and $\overline\sigma$ matrices and taking the complex conjugates of a_i and ε [cf. Eq. (4.4.4) and the associated text].

Summing over the Goldstino spins using Eqs. (3.1.58)–(3.1.61) now yields:

$$\sum_{\lambda_{\tilde G}} |\mathcal{M}|^2 = x_{\tilde N} A k_{\tilde G}\cdot\overline\sigma \hat A x^\dagger_{\tilde N} + y^\dagger_{\tilde N} B k_{\tilde G}\cdot\sigma \hat B y_{\tilde N}. \tag{6.18.9}$$

(The A, $\hat B$ and $\hat A$, B cross terms vanish because of $m_{\tilde G} = 0$.) Averaging over the neutralino spins using Eqs. (3.1.58) and (3.1.59), we find

$$\begin{aligned}\frac{1}{2}\sum_{\lambda_{\tilde N},\lambda_{\tilde G}} |\mathcal{M}|^2 &= \frac{1}{2}\mathrm{Tr}[A k_{\tilde G}\cdot\overline\sigma \hat A p\cdot\overline\sigma] + \frac{1}{2}\mathrm{Tr}[B k_{\tilde G}\cdot\sigma \hat B p\cdot\sigma]\\ &= \frac{1}{2}|a_i|^2\mathrm{Tr}[\varepsilon^*\cdot\overline\sigma\, k_\gamma\cdot\sigma\, k_{\tilde G}\cdot\overline\sigma\, k_\gamma\cdot\sigma\,\varepsilon\cdot\overline\sigma\, k_{\tilde G}\cdot\sigma\, p\cdot\overline\sigma\, k_{\tilde G}\cdot\sigma] + (\sigma\leftrightarrow\overline\sigma).\end{aligned} \tag{6.18.10}$$

We now use

$$k_\gamma\cdot\sigma\, k_{\tilde G}\cdot\overline\sigma\, k_\gamma\cdot\sigma = 2k_{\tilde G}\cdot k_\gamma\, k_\gamma\cdot\sigma, \tag{6.18.11}$$

$$k_{\tilde G}\cdot\sigma\, p\cdot\overline\sigma\, k_{\tilde G}\cdot\sigma = 2k_{\tilde G}\cdot p\, k_{\tilde G}\cdot\sigma, \tag{6.18.12}$$

which follow from Eq. (2.53), and the corresponding identities with $\sigma\leftrightarrow\overline\sigma$, to obtain:

$$\frac{1}{2}\sum_{\lambda_{\tilde N},\lambda_{\tilde G}} |\mathcal{M}|^2 = 2|a_i|^2(k_{\tilde G}\cdot k_\gamma)(k_{\tilde G}\cdot p)\mathrm{Tr}[\varepsilon^*\cdot\overline\sigma\, k_\gamma\cdot\sigma\,\varepsilon\cdot\overline\sigma\, k_{\tilde G}\cdot\sigma] + (\sigma\leftrightarrow\overline\sigma). \tag{6.18.13}$$

Applying the photon spin-sum identity

$$\sum_{\lambda_\gamma}\varepsilon^\mu\varepsilon^{\nu *} = -g^{\mu\nu}, \tag{6.18.14}$$

and the trace identities Eqs. (2.56) and (2.57), we get

$$\frac{1}{2}\sum_{\lambda_\gamma,\lambda_{\tilde N},\lambda_{\tilde G}} |\mathcal{M}|^2 = 16|a_i|^2(k_{\tilde G}\cdot k_\gamma)^2(k_{\tilde G}\cdot p) = 2|a_i|^2 m^6_{\widetilde N_i}. \tag{6.18.15}$$

So, the decay rate is [192,196]:

$$\Gamma(\widetilde N_i\to\gamma\widetilde G) = \frac{1}{16\pi\, m_{\widetilde N_i}}\left(\frac{1}{2}\sum_{\lambda_\gamma,\lambda_{\tilde N},\lambda_{\tilde G}}|\mathcal{M}|^2\right) = |N_{i1}\cos\theta_W + N_{i2}\sin\theta_W|^2\frac{m^5_{\widetilde N_i}}{16\pi\,|\langle F\rangle|^2}. \tag{6.18.16}$$

6.19. Gluino pair production from gluon fusion: $gg\to\widetilde g\widetilde g$

In this subsection we will compute the cross-section for the process $gg\to\widetilde g\widetilde g$. The relevant Feynman diagrams are shown in Fig. 6.19.1. The initial state gluons have $SU(3)_c$ adjoint representation indices a and b, with momenta p_1 and p_2 and polarization vectors $\varepsilon_1^\mu = \varepsilon^\mu(\vec{\boldsymbol{p}}_1,\lambda_1)$ and $\varepsilon_2^\mu = \varepsilon^\mu(\vec{\boldsymbol{p}}_2,\lambda_2)$, respectively. The final state gluinos carry adjoint representation indices c and d, with momenta k_1 and k_2 and wave function spinors $x_1^\dagger = x^\dagger(\vec{\boldsymbol{k}}_1,\lambda_1')$ or $y_1 = y(\vec{\boldsymbol{k}}_1,\lambda_1')$ and $x_2^\dagger = x^\dagger(\vec{\boldsymbol{k}}_2,\lambda_2')$ or $y_2 = y(\vec{\boldsymbol{k}}_2,\lambda_2')$, respectively.

The Feynman rules for the gluino couplings in the supersymmetric extension of QCD are given in Fig. K.5.1. For the two s-channel amplitudes, we obtain:

$$\begin{aligned}i\mathcal{M}_s = &\left(-g_s f^{abe}[g_{\mu\nu}(p_1-p_2)_\rho + g_{\nu\rho}(p_1+2p_2)_\mu - g_{\mu\rho}(2p_1+p_2)_\nu]\right)\left(\frac{-ig^{\rho\kappa}}{s}\right)\varepsilon_1^\mu\varepsilon_2^\nu\\ &\times\left[(-g_s f^{cde})\, x_1^\dagger\overline\sigma_\kappa y_2 + (g_s f^{dce})\, y_1\sigma_\kappa x_2^\dagger\right].\end{aligned} \tag{6.19.1}$$

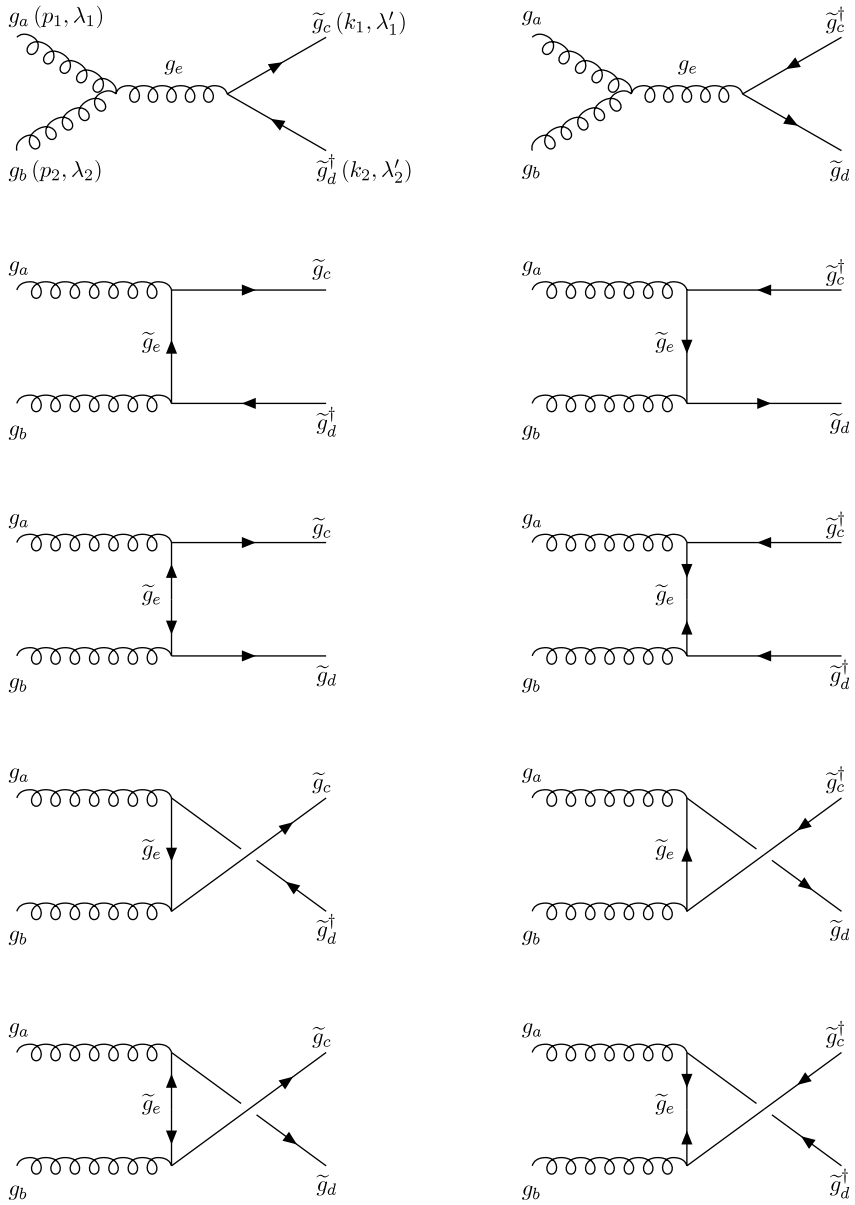

Fig. 6.19.1. The ten Feynman diagrams for $gg \to \widetilde{g}\,\widetilde{g}$. The momentum and spin polarization assignments are indicated on the first diagram.

The first factor is the Feynman rule for the three-gluon interaction of standard QCD, and the second factor is the gluon propagator. The next four (t-channel) diagrams have a total amplitude:

$$
\begin{aligned}
i\mathcal{M}_t = {} & \left(-g_s f^{cea}\varepsilon_1^\mu\right)\left(-g_s f^{edb}\varepsilon_2^\nu\right) x_1^\dagger \overline{\sigma}_\mu \left[\frac{i(k_1-p_1)\cdot\sigma}{(k_1-p_1)^2-m_{\tilde{g}}^2}\right]\overline{\sigma}_\nu y_2 + \left(g_s f^{eca}\varepsilon_1^\mu\right)\left(g_s f^{deb}\varepsilon_2^\nu\right) y_1 \sigma_\mu \left[\frac{i(k_1-p_1)\cdot\overline{\sigma}}{(k_1-p_1)^2-m_{\tilde{g}}^2}\right]\sigma_\nu x_2^\dagger \\
& + \left(-g_s f^{cea}\varepsilon_1^\mu\right)\left(g_s f^{deb}\varepsilon_2^\nu\right) x_1^\dagger \overline{\sigma}_\mu \left[\frac{i m_{\tilde{g}}}{(k_1-p_1)^2-m_{\tilde{g}}^2}\right]\sigma_\nu x_2^\dagger \\
& + \left(g_s f^{eca}\varepsilon_1^\mu\right)\left(-g_s f^{edb}\varepsilon_2^\nu\right) y_1 \sigma_\mu \left[\frac{i m_{\tilde{g}}}{(k_1-p_1)^2-m_{\tilde{g}}^2}\right]\overline{\sigma}_\nu y_2. \qquad (6.19.2)
\end{aligned}
$$

Finally, the u-channel Feynman diagrams result in:

$$\begin{aligned} i\mathcal{M}_u \;=\; & \left(-g_s f^{eda}\varepsilon_1^\mu\right)\left(-g_s f^{ceb}\varepsilon_2^\nu\right) x_1^\dagger \overline{\sigma}_\nu \left[\frac{i(k_1-p_2)\cdot\sigma}{(k_1-p_2)^2-m_{\tilde g}^2}\right]\overline{\sigma}_\mu y_2 \\ & + \left(g_s f^{dea}\varepsilon_1^\mu\right)\left(g_s f^{ecb}\varepsilon_2^\nu\right) y_1 \sigma_\nu \left[\frac{i(k_1-p_2)\cdot\overline{\sigma}}{(k_1-p_2)^2-m_{\tilde g}^2}\right]\sigma_\mu x_2^\dagger \\ & + \left(g_s f^{dea}\varepsilon_1^\mu\right)\left(-g_s f^{ceb}\varepsilon_2^\nu\right) x_1^\dagger \overline{\sigma}_\nu \left[\frac{im_{\tilde g}}{(k_1-p_2)^2-m_{\tilde g}^2}\right]\sigma_\mu x_2^\dagger \\ & + \left(-g_s f^{eda}\varepsilon_1^\mu\right)\left(g_s f^{ecb}\varepsilon_2^\nu\right) y_1 \sigma_\nu \left[\frac{im_{\tilde g}}{(k_1-p_2)^2-m_{\tilde g}^2}\right]\overline{\sigma}_\mu y_2. \end{aligned} \tag{6.19.3}$$

We choose to work with *real* transverse polarization vectors ε_1, ε_2. These vectors must both be orthogonal to the initial state collision axis in the center-of-momentum frame. Hence,

$$\varepsilon_1\cdot\varepsilon_1 = \varepsilon_2\cdot\varepsilon_2 = -1, \tag{6.19.4}$$

$$\varepsilon_1\cdot p_1 = \varepsilon_2\cdot p_1 = \varepsilon_1\cdot p_2 = \varepsilon_2\cdot p_2 = 0, \tag{6.19.5}$$

$$\varepsilon_1\cdot k_2 = -\varepsilon_1\cdot k_1, \tag{6.19.6}$$

$$\varepsilon_2\cdot k_2 = -\varepsilon_2\cdot k_1, \tag{6.19.7}$$

for each choice of λ_1, λ_2. The sums over gluon polarizations will be performed using [cf. Eq. (I.2.61)]:

$$\sum_{\lambda_1}\varepsilon_1^\mu\varepsilon_1^\nu = \sum_{\lambda_2}\varepsilon_2^\mu\varepsilon_2^\nu = -g^{\mu\nu} + \frac{2\left(p_1^\mu p_2^\nu + p_2^\mu p_1^\nu\right)}{s}. \tag{6.19.8}$$

Note that in QCD processes with two or more external gluons, the term $2\left(p_1^\mu p_2^\nu + p_2^\mu p_1^\nu\right)/s$ in Eq. (6.19.8) cannot in general be dropped [197]. This is to be contrasted to the photon polarization sum [cf. Eq. (6.18.14)], where this latter term can always be neglected (due to a Ward identity of quantum electrodynamics).

Before taking the complex square of the amplitude, it is convenient to rewrite the last two terms in each of Eqs. (6.19.2) and (6.19.3) by using the identities [see Eq. (3.1.12)]:

$$m_{\tilde g}x_1^\dagger = y_1(k_1\cdot\sigma), \qquad m_{\tilde g}y_1 = x_1^\dagger(k_1\cdot\overline{\sigma}). \tag{6.19.9}$$

Using Eqs. (2.53) and (2.54), the resulting total matrix element is then reduced to a sum of terms that each contain exactly one σ or $\overline{\sigma}$ matrix. We define convenient factors:

$$G_s \equiv g_s^2 f^{abe}f^{cde}/s, \tag{6.19.10}$$

$$G_t \equiv g_s^2 f^{ace}f^{bde}/(t-m_{\tilde g}^2), \tag{6.19.11}$$

$$G_u \equiv g_s^2 f^{ade}f^{bce}/(u-m_{\tilde g}^2) \tag{6.19.12}$$

where the usual Mandelstam variables are:

$$s = (p_1+p_2)^2 = (k_1+k_2)^2, \tag{6.19.13}$$

$$t = (k_1-p_1)^2 = (k_2-p_2)^2, \tag{6.19.14}$$

$$u = (k_1-p_2)^2 = (k_2-p_1)^2. \tag{6.19.15}$$

Then the total amplitude is (noting that the gluon polarizations ε_1, ε_2 were chosen real):

$$\mathcal{M} = \mathcal{M}_s + \mathcal{M}_t + \mathcal{M}_u = x_1^\dagger a\cdot\overline{\sigma}y_2 + y_1 a^*\cdot\sigma x_2^\dagger, \tag{6.19.16}$$

where

$$\begin{aligned} a^\mu \;\equiv\; & -(G_t+G_s)\varepsilon_1\cdot\varepsilon_2\, p_1^\mu - (G_u-G_s)\varepsilon_1\cdot\varepsilon_2\, p_2^\mu - 2G_t k_1\cdot\varepsilon_1\,\varepsilon_2^\mu - 2G_u k_1\cdot\varepsilon_2\,\varepsilon_1^\mu \\ & - i\epsilon^{\mu\nu\rho\kappa}\varepsilon_{1\nu}\varepsilon_{2\rho}(G_t p_1 - G_u p_2)_\kappa. \end{aligned} \tag{6.19.17}$$

Squaring the amplitude using Eqs. (2.44) and (2.45), we get:

$$|\mathcal{M}|^2 = x_1^\dagger a\cdot\overline{\sigma}y_2 y_2^\dagger a^*\cdot\overline{\sigma}x_1 + y_1 a^*\cdot\sigma x_2^\dagger x_2 a\cdot\sigma y_1^\dagger + x_1^\dagger a\cdot\overline{\sigma}y_2 x_2 a\cdot\sigma y_1^\dagger + y_1 a^*\cdot\sigma x_2^\dagger y_2^\dagger a^*\cdot\overline{\sigma}x_1. \tag{6.19.18}$$

Summing over the gluino spins using Eqs. (3.1.58)–(3.1.61), we find:

$$\begin{aligned} \sum_{\lambda_1',\lambda_2'}|\mathcal{M}|^2 \;=\; & \mathrm{Tr}[a\cdot\overline{\sigma}k_2\cdot\sigma a^*\cdot\overline{\sigma}k_1\cdot\sigma] + \mathrm{Tr}[a^*\cdot\sigma k_2\cdot\overline{\sigma}a\cdot\sigma k_1\cdot\overline{\sigma}] \\ & - m_{\tilde g}^2\mathrm{Tr}[a\cdot\overline{\sigma}a\cdot\sigma] - m_{\tilde g}^2\mathrm{Tr}[a^*\cdot\sigma a^*\cdot\overline{\sigma}]. \end{aligned} \tag{6.19.19}$$

Performing the traces with Eqs. (2.55)–(2.57) then yields:

$$\sum_{\lambda_1',\lambda_2'} |\mathcal{M}|^2 = 8\,\mathrm{Re}[a\cdot k_1 a^*\cdot k_2] - 4a\cdot a^*\, k_1\cdot k_2 - 4i\epsilon^{\mu\nu\rho\kappa} k_{1\mu} k_{2\nu} a_\rho a_\kappa^* - 4m_{\tilde g}^2 \mathrm{Re}[a^2]. \tag{6.19.20}$$

Inserting the explicit form for a^μ [Eq. (6.19.17)] into the above result, we obtain:

$$\begin{aligned}\sum_{\lambda_1',\lambda_2'} |\mathcal{M}|^2 &= 2(t-m_{\tilde g}^2)(u-m_{\tilde g}^2)[(G_t+G_u)^2 + 4(G_s+G_t)(G_s-G_u)(\varepsilon_1\cdot\varepsilon_2)^2] \\ &\quad + 16(G_t+G_u)[G_s(t-u) + G_t(t-m_{\tilde g}^2) + G_u(u-m_{\tilde g}^2)](\varepsilon_1\cdot\varepsilon_2)(k_1\cdot\varepsilon_1)(k_1\cdot\varepsilon_2) \\ &\quad - 32(G_t+G_u)^2(k_1\cdot\varepsilon_1)^2(k_1\cdot\varepsilon_2)^2. \end{aligned}\tag{6.19.21}$$

The sums over gluon polarizations can be done using Eq. (6.19.8), which implies:

$$\sum_{\lambda_1,\lambda_2} 1 = 4, \qquad \sum_{\lambda_1,\lambda_2} (\varepsilon_1\cdot\varepsilon_2)^2 = 2, \tag{6.19.22}$$

$$\sum_{\lambda_1,\lambda_2} (\varepsilon_1\cdot\varepsilon_2)(k_1\cdot\varepsilon_1)(k_1\cdot\varepsilon_2) = m_{\tilde g}^2 - (t-m_{\tilde g}^2)(u-m_{\tilde g}^2)/s, \tag{6.19.23}$$

$$\sum_{\lambda_1,\lambda_2} (k_1\cdot\varepsilon_1)^2(k_1\cdot\varepsilon_2)^2 = \left(m_{\tilde g}^2 - (t-m_{\tilde g}^2)(u-m_{\tilde g}^2)/s\right)^2. \tag{6.19.24}$$

Summing over colors using $f^{abe}f^{cde}f^{abe'}f^{cde'} = 2f^{abe}f^{cde}f^{ace'}f^{bde'} = N_c^2(N_c^2-1) = 72$,

$$\sum_{\text{colors}} G_s^2 = \frac{72g_s^4}{s^2}, \qquad \sum_{\text{colors}} G_t^2 = \frac{72g_s^4}{(t-m_{\tilde g}^2)^2}, \tag{6.19.25}$$

$$\sum_{\text{colors}} G_u^2 = \frac{72g_s^4}{(u-m_{\tilde g}^2)^2}, \qquad \sum_{\text{colors}} G_sG_t = \frac{36g_s^4}{s(t-m_{\tilde g}^2)}, \tag{6.19.26}$$

$$\sum_{\text{colors}} G_sG_u = -\frac{36g_s^4}{s(u-m_{\tilde g}^2)}, \qquad \sum_{\text{colors}} G_tG_u = \frac{36g_s^4}{(t-m_{\tilde g}^2)(u-m_{\tilde g}^2)}. \tag{6.19.27}$$

Putting all the factors together, and averaging over the initial state colors and spins, we have:

$$\begin{aligned}\frac{\mathrm{d}\sigma}{\mathrm{d}t} &= \frac{1}{16\pi s^2}\left(\frac{1}{64}\sum_{\text{colors}}\frac{1}{4}\sum_{\text{spins}}|\mathcal{M}|^2\right) \\ &= \frac{9\pi\alpha_s^2}{4s^4}\left[2(t-m_{\tilde g}^2)(u-m_{\tilde g}^2) - 3s^2 - 4m_{\tilde g}^2 s + \frac{s^2(s+2m_{\tilde g}^2)^2}{(t-m_{\tilde g}^2)(u-m_{\tilde g}^2)} - \frac{4m_{\tilde g}^4 s^4}{(t-m_{\tilde g}^2)^2(u-m_{\tilde g}^2)^2}\right],\end{aligned}\tag{6.19.28}$$

which agrees with the result of [177,198] (after some rearrangement). Note that in the center-of-momentum frame, the Mandelstam variable t is related to the scattering angle θ between an initial state gluon and a final state gluino by:

$$t = m_{\tilde g}^2 + \frac{s}{2}\left(\cos\theta\sqrt{1-4m_{\tilde g}^2/s} - 1\right). \tag{6.19.29}$$

Since the final state has identical particles, the total cross-section can now be obtained by:

$$\sigma = \frac{1}{2}\int_{t_-}^{t_+}\frac{\mathrm{d}\sigma}{\mathrm{d}t}\mathrm{d}t, \tag{6.19.30}$$

where $t_\pm$ are obtained by inserting $\cos\theta = \pm 1$ into Eq. (6.19.29).

6.20. R-parity-violating stau decay: $\widetilde{\tau}_R^+ \to e^+\bar\nu_\mu$

In an R-parity-violating extension of the MSSM (denoted henceforth by RPV-MSSM), new Yukawa couplings can arise [see Eqs. (L.1)–(L.3)] that violate either a global U(1) lepton number L or baryon number B. The corresponding Feynman rules are derived in Appendix L. Consider the decay of a right-handed scalar tau via an L-violating $LL\bar e$ coupling governed by Eq. (L.1). This is particularly relevant when the scalar tau is the lightest supersymmetric particle (LSP) [199,200] and in the case of resonant slepton production [201,202]. Note that in R-parity violation the LSP need not be the lightest neutralino and in a minimal supergravity embedding often it is not [203,204]. The Feynman diagram is shown in Fig. 6.20.1, where we have also defined the momenta and the helicities of the fermions.

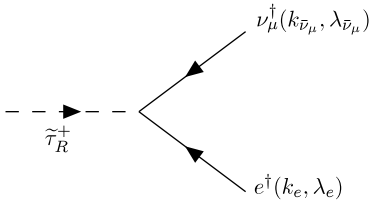

Fig. 6.20.1. Feynman diagram for the R-parity-violating decay $\widetilde{\tau}_R^+ \to e^+\bar\nu_\mu$.

The amplitude for the R-parity-violating $\tilde\tau_R^+$ decay is given by:

$$i\mathcal{M} = -i\lambda y_e y_{\bar\nu_\mu}. \tag{6.20.1}$$

Here we have defined $\lambda \equiv \lambda_{123}$, and the external wave functions are denoted by $y_e \equiv y(\vec{\boldsymbol{k}}_e, \lambda_e)$, and $y_{\bar\nu_\mu} \equiv y(\vec{\boldsymbol{k}}_{\bar\nu_\mu}, \lambda_{\bar\nu_\mu})$, respectively. Using Eq. (2.43), the amplitude squared is

$$|\mathcal{M}|^2 = |\lambda|^2 y_e y_{\bar\nu_\mu} y_{\bar\nu_\mu}^\dagger y_e^\dagger. \tag{6.20.2}$$

Summing over the fermion spins using Eq. (3.1.59) gives:

$$\sum_{\lambda_e,\lambda_{\bar\nu_\mu}} |\mathcal{M}|^2 = |\lambda|^2 \mathrm{Tr}[k_e \cdot \sigma\, k_{\bar\nu_\mu} \cdot \overline{\sigma}] = |\lambda|^2 m_{\tilde\tau_R}^2, \tag{6.20.3}$$

where in the last step we have used the trace formula Eq. (2.55), and neglected the mass of the electron and the neutrino. The total decay rate is then given by

$$\Gamma = \frac{1}{16\pi m_{\tilde\tau_R}} \left(\sum_{\lambda_e,\lambda_{\bar\nu_\mu}} |\mathcal{M}|^2 \right) = \frac{|\lambda|^2}{16\pi} m_{\tilde\tau_R}, \tag{6.20.4}$$

which agrees with the computation in Refs. [205–207]. Completely analogously we can obtain the total rate for the decays $\widetilde{\nu}_\mu \to \tau^- e^+$ and $\widetilde{e}_L^- \to \tau^-\bar\nu_\mu$, which proceed via the same operator, by replacing $m_{\tilde\tau_R} \to (m_{\tilde e_L}, m_{\tilde\nu_\mu})$, respectively.

In general the two-body decay rate of a sfermion $\widetilde{f}$ via the L-violating $LQ\bar d$ coupling governed by Eq. (L.2) or the B-violating $\bar u\bar d\bar d$ coupling governed by Eq. (L.3) is given by:

$$\Gamma(\tilde f \to f_1 f_2) = \frac{C|\lambda|^2}{16\pi} m_{\tilde f}, \tag{6.20.5}$$

where we have neglected the masses $m_{1,2}$ of the final state fermions. The factor C denotes the color factor. For the slepton decays via the $LQ\bar d$ coupling which are summed over the final state quark colors, $C = \delta^{ij}\delta_{ij} = 3$, where $i, j = 1, 2, 3$ and δ_{ij} is the symmetric invariant tensor of color SU(3). For the squark decays via the $LQ\bar d$ where the initial state color is averaged over and the final state color is summed, $C = 1$. For the squark decays via the $\bar u\bar d\bar d$ coupling, $C = \frac{1}{3}\epsilon^{ijk}\epsilon_{ijk} = 2$, where the Levi-Civita tensor, $\epsilon^{ijk} = \epsilon_{ijk}$, is the antisymmetric invariant tensor of color SU(3). In realistic cases, one must also include the effects of mixing for the third-family sfermions, which we have omitted here for simplicity.

6.21. *R-parity-violating neutralino decay: $\widetilde{N}_i \to \mu^- u\bar d$*

Next we consider the R-parity-violating three-body decay of a neutralino $\widetilde{N}_i \to \mu^- u\bar d$, which arises due to the L-violating $LQ\bar d$ coupling governed by Eq. (L.2). This is of particular interest when the neutralino is the LSP, since it determines the final state signatures [208–210]. The three Feynman diagrams are shown in Fig. 6.21.1, including the definitions of the momenta and helicities. We have neglected sfermion mixing, i.e. we assume $\widetilde{\mu}_L$, $\widetilde{u}_L$, and $\widetilde{d}_R$ are mass eigenstates. Using the Feynman rules given in Figs. L.2 and K.4.2 (or K.4.4), we obtain the corresponding contributions to the decay amplitude,

$$i\mathcal{M}_1 = \left(i\lambda'^*\right)\left[\frac{i}{\sqrt{2}}(gN_{i2} + g'N_{i1})\right]\left[\frac{i}{(p_i - k_\mu)^2 - m_{\tilde\mu_L}^2}\right] y_i^\dagger x_\mu^\dagger x_u^\dagger x_d^\dagger, \tag{6.21.1}$$

$$i\mathcal{M}_2 = \left(i\lambda'^*\right)\left[-\frac{i\sqrt{2}}{3}g'N_{i1}\right]\left[\frac{i}{(p_i - k_d)^2 - m_{\tilde d_R}^2}\right] y_i^\dagger x_d^\dagger x_\mu^\dagger x_u^\dagger, \tag{6.21.2}$$

$$i\mathcal{M}_3 = \left(i\lambda'^*\right)\left[-\frac{i}{\sqrt{2}}(gN_{i2} + g'N_{i1}/3)\right]\left[\frac{i}{(p_i - k_u)^2 - m_{\tilde u_L}^2}\right] y_i^\dagger x_u^\dagger x_d^\dagger x_\mu^\dagger. \tag{6.21.3}$$

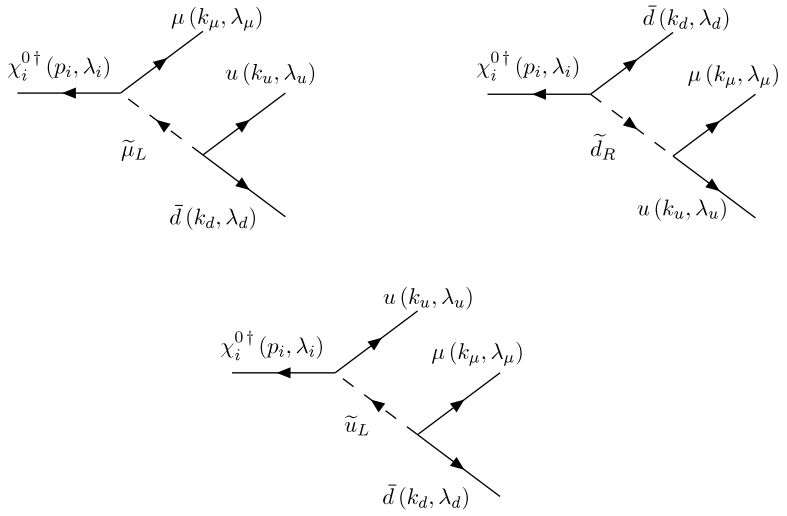

Fig. 6.21.1. Feynman diagrams for the R-parity-violating decay $\widetilde{N}_i \to \mu^- u\bar{d}$.

Here we have defined $\lambda' \equiv \lambda'_{211}$, and the external wave functions are denoted by $y_i^\dagger \equiv y^\dagger(\vec{\boldsymbol{p}}_i, \lambda_i)$, $x_\mu^\dagger \equiv x^\dagger(\vec{\boldsymbol{k}}_\mu, \lambda_\mu)$, $x_u^\dagger \equiv x^\dagger(\vec{\boldsymbol{k}}_u, \lambda_u)$, and $x_d^\dagger \equiv x^\dagger(\vec{\boldsymbol{k}}_d, \lambda_d)$, respectively. In the following, we will neglect all of the final state fermion masses. The results will be expressed in terms of the kinematic variables

$$z_\mu \equiv 2p_i \cdot k_\mu / m^2_{\tilde{N}_i} = 2E_\mu / m_{\tilde{N}_i}, \tag{6.21.4}$$

$$z_d \equiv 2p_i \cdot k_d / m^2_{\tilde{N}_i} = 2E_d / m_{\tilde{N}_i}, \tag{6.21.5}$$

$$z_u \equiv 2p_i \cdot k_u / m^2_{\tilde{N}_i} = 2E_u / m_{\tilde{N}_i}, \tag{6.21.6}$$

which satisfy $z_\mu + z_d + z_u = 2$. Then we can rewrite the total matrix element as:

$$\mathcal{M} = c_1 y_i^\dagger x_\mu^\dagger x_u^\dagger x_d^\dagger + c_2 y_i^\dagger x_d^\dagger x_\mu^\dagger x_u^\dagger + c_3 y_i^\dagger x_u^\dagger x_d^\dagger x_\mu^\dagger, \tag{6.21.7}$$

where

$$c_1 \equiv \frac{1}{\sqrt{2}} \lambda'^* (g N_{i2} + g' N_{i1}) / [m^2_{\tilde{\mu}_L} - m^2_{\tilde{N}_i}(1 - z_\mu)], \tag{6.21.8}$$

$$c_2 \equiv -\frac{\sqrt{2}}{3} \lambda'^* g' N_{i1} / [m^2_{\tilde{d}_R} - m^2_{\tilde{N}_i}(1 - z_d)], \tag{6.21.9}$$

$$c_3 \equiv -\frac{1}{\sqrt{2}} \lambda'^* (g N_{i2} + g' N_{i1}/3) / [m^2_{\tilde{u}_L} - m^2_{\tilde{N}_i}(1 - z_u)]. \tag{6.21.10}$$

Before squaring the amplitude, it is convenient to use the Fierz identity [Eq. (2.66)] to reduce the number of terms:

$$\mathcal{M} = (c_1 - c_3) y_i^\dagger x_\mu^\dagger x_u^\dagger x_d^\dagger + (c_2 - c_3) y_i^\dagger x_d^\dagger x_\mu^\dagger x_u^\dagger. \tag{6.21.11}$$

Using Eq. (2.43), we obtain

$$\begin{aligned} |\mathcal{M}|^2 \;=\; & |c_1 - c_3|^2 y_i^\dagger x_\mu^\dagger x_\mu y_i x_u^\dagger x_d^\dagger x_d x_u + |c_2 - c_3|^2 y_i^\dagger x_d^\dagger x_d y_i x_\mu^\dagger x_u^\dagger x_u x_\mu \\ & - 2\mathrm{Re}[(c_1 - c_3)(c_2^* - c_3^*) y_i^\dagger x_\mu^\dagger x_\mu x_u x_u^\dagger x_d^\dagger x_d y_i], \end{aligned} \tag{6.21.12}$$

where Eq. (2.59) was used on the last term. Summing over the fermion spins using Eqs. (3.1.58)–(3.1.61), we obtain:

$$\begin{aligned} \sum_{\text{spins}} |\mathcal{M}|^2 \;=\; & |c_1 - c_3|^2 \mathrm{Tr}[k_\mu \cdot \overline{\sigma} p_i \cdot \sigma] \mathrm{Tr}[k_d \cdot \overline{\sigma} k_u \cdot \sigma] + |c_2 - c_3|^2 \mathrm{Tr}[k_d \cdot \overline{\sigma} p_i \cdot \sigma] \mathrm{Tr}[k_u \cdot \overline{\sigma} k_\mu \cdot \sigma] \\ & - 2\mathrm{Re}\big[(c_1 - c_3)(c_2^* - c_3^*) \mathrm{Tr}[k_\mu \cdot \overline{\sigma} k_u \cdot \sigma k_d \cdot \overline{\sigma} p_i \cdot \sigma]\big]. \end{aligned} \tag{6.21.13}$$

Applying the trace formulae, Eqs. (2.55) and (2.57), we obtain

$$\begin{aligned}\sum_{\text{spins}}|\mathcal{M}|^2 &= 4|c_1-c_3|^2 p_i\cdot k_\mu\, k_d\cdot k_u + 4|c_2-c_3|^2 p_i\cdot k_d\, k_\mu\cdot k_u \\ &\quad - 4\text{Re}\big[(c_1-c_3)(c_2^*-c_3^*)\big](k_\mu\cdot k_u\, p_i\cdot k_d + p_i\cdot k_\mu\, k_d\cdot k_u - k_\mu\cdot k_d\, p_i\cdot k_u) \\ &= m_{\tilde N_i}^4\Big[|c_1|^2 z_\mu(1-z_\mu) + |c_2|^2 z_d(1-z_d) + |c_3|^2 z_u(1-z_u) \\ &\quad - 2\text{Re}[c_1c_2^*](1-z_\mu)(1-z_d) - 2\text{Re}[c_1c_3^*](1-z_\mu)(1-z_u) - 2\text{Re}[c_2c_3^*](1-z_d)(1-z_u)\Big], \end{aligned} \tag{6.21.14}$$

where in the last equality we have used Eqs. (6.21.4)–(6.21.6) and

$$2k_\mu\cdot k_d = (1-z_u)m_{\tilde N_i}^2, \qquad 2k_\mu\cdot k_u = (1-z_d)m_{\tilde N_i}^2, \qquad 2k_d\cdot k_u = (1-z_\mu)m_{\tilde N_i}^2. \tag{6.21.15}$$

The differential decay rate follows:

$$\frac{\mathrm{d}^2\Gamma}{\mathrm{d}z_\mu \mathrm{d}z_d} = \frac{N_c m_{\tilde N_i}}{2^8\pi^3}\left(\frac{1}{2}\sum_{\text{spins}}|\mathcal{M}|^2\right), \tag{6.21.16}$$

where a factor of $N_c = 3$ has been included for the sum over colors, a factor of $1/2$ to average over the neutralino spin, and the kinematic limits are

$$0 < z_\mu < 1, \tag{6.21.17}$$

$$1 - z_\mu < z_d < 1. \tag{6.21.18}$$

In the limit of heavy sfermions, the integrations over z_d and then z_μ are simple, with the result for the total decay width:

$$\Gamma = \frac{N_c m_{\tilde N_i}^5}{2^{11}\cdot 3\pi^3}\left(|c_1'|^2 + |c_2'|^2 + |c_3'|^2 - \text{Re}[c_1'c_2'^* + c_1'c_3'^* + c_2'c_3'^*]\right), \tag{6.21.19}$$

where the c_i' are obtained from c_i of Eqs. (6.21.8)–(6.21.10) by neglecting $m_{\tilde N_i}^2$ in the denominators. Our results agree with the complete computation (which includes mixing) given in Refs. [206,207,211]. Earlier calculations with some simplifications are given in Refs. [209,212].

6.22. Top quark condensation from a Nambu–Jona–Lasinio model gap equation

The previous examples have involved renormalizable field theories. However, there are cases in which it is preferable to use effective four-fermion interactions. The obvious historical example is the four-fermion Fermi theory of weak decays. This has been superseded by a more complete and accurate theory of the weak interactions but is still useful for leading order calculations of low energy processes. Another case of some interest is the use of strong coupling four-fermion interactions to drive symmetry breaking via a Nambu–Jona–Lasinio model [213], as in the top quark condensate approach [214–218] to electroweak symmetry breaking.

Consider an effective four-fermion Lagrangian involving the top quark [216], written in two-component fermion form as:

$$\mathscr{L} = it^\dagger\bar\sigma^\mu\partial_\mu t + i\bar t^\dagger\bar\sigma^\mu\partial_\mu\bar t + \frac{G}{\Lambda^2}(t\bar t)(t^\dagger\bar t^\dagger). \tag{6.22.1}$$

Here the Standard Model gauge interactions have been suppressed; the quantities within parentheses are color singlets. Note also that there is no top quark Yukawa coupling to a Higgs scalar boson, nor a top quark mass term, which would normally appear in the form $-m_t(t\bar t + t^\dagger\bar t^\dagger)$. Instead, the effective top quark mass is supposed to be driven by a non-perturbatively large and positive dimensionless coupling G, with Λ the cutoff scale at which G arises from some more fundamental physics such as topcolor [218].

The Feynman rule for the four-fermion interaction can be derived from the mode expansion results of Section 3, and is given in Fig. 6.22.1. The resulting gap equation for the dynamically generated top quark mass is shown in Fig. 6.22.2. Evaluating this using the Feynman rules of Figs. 4.2.3 and 4.2.4, one finds:

$$-im_t\delta_i^j\delta_\alpha^\beta = (-1)\int^\Lambda \frac{\mathrm{d}^4k}{(2\pi)^4}\left(i\frac{G}{\Lambda^2}\delta_i^j\delta_n^k\delta_\alpha^\beta\delta_{\dot\alpha}^{\dot\beta}\right)\left(\delta_k^n\delta_{\dot\beta}^{\dot\alpha}\frac{im_t}{k^2-m_t^2+i\epsilon}\right). \tag{6.22.2}$$

Here i, j, k, n are color indices of the fundamental representation of $SU(3)$, and $\alpha, \beta, \dot\alpha, \dot\beta$ are two-component spinor indices. The factor of (-1) on the right-hand side is due to the presence of a fermion loop.

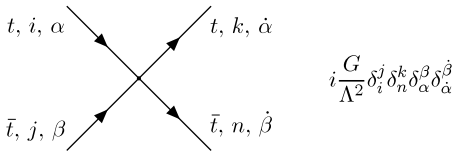

Fig. 6.22.1. Feynman rule for the four-fermion interaction in the top quark condensate model. The indices $i, j, k, n = 1, 2, 3$ are for color in the fundamental representation of $SU(3)$, and the indices $\alpha, \beta, \dot\alpha, \dot\beta$ are two-component spinor indices.

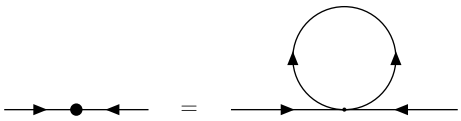

Fig. 6.22.2. The Nambu–Jona–Lasinio gap equation for a possible dynamically generated top quark mass m_t.

Euclideanizing the loop integration over k^μ by $k^2 \to -k_E^2$ and $\int \mathrm{d}^4k \to i\int \mathrm{d}^4k_E$, and then rewriting the integration in terms of $x = k_E^2$, this amounts to [216]:

$$\begin{aligned} m_t &= \frac{2N_c G m_t}{16\pi^2\Lambda^2}\int_0^{\Lambda^2} \mathrm{d}x/(1+m_t^2/x) \\ &= \frac{3Gm_t}{8\pi^2}[1-(m_t^2/\Lambda^2)\ln(\Lambda^2/m_t^2)+\ldots], \end{aligned} \tag{6.22.3}$$

where $N_c = 3$ is the number of colors, and a factor of two arises from the sum over dotted spinor indices of $\delta_{\dot\alpha}^{\dot\beta}\delta_{\dot\beta}^{\dot\alpha}$.

For small or negative G, only the trivial solution $m_t = 0$ is possible. However, for $G \geq G_{\text{critical}} = 8\pi^2/3 \approx 26$, there is a positive solution for m_t^2/Λ^2 [216]. It is now known that this minimal version of the model cannot explain the top quark mass and the observed features of electroweak symmetry breaking, but extensions of it may be viable [219].

6.23. Electroweak vector boson self-energies from fermion loops

In this subsection, we consider the contributions to the self-energy functions of the Standard Model electroweak vector bosons coming from quark and lepton loops. (For a derivation of equivalent results in the four-component fermion formalism, see for example Section 21.3 of [114].) The independent self-energies are given by $\Pi_{\mu\nu}^{WW}$, $\Pi_{\mu\nu}^{ZZ}$, $\Pi_{\mu\nu}^{\gamma Z} = \Pi_{\mu\nu}^{Z\gamma}$, and $\Pi_{\mu\nu}^{\gamma\gamma}$, as shown in Figs. 6.23.1 and 6.23.2. In each case, $i\Pi_{\mu\nu}$ is equal to the sum of Feynman diagrams for two-point functions with amputated external legs, and is implicitly a function of the external momentum p^μ.

First consider the self-energy function for the W boson, shown in Fig. 6.23.1. The W boson only couples to left-handed fermions, so there is only one Feynman diagram for each Standard model weak isodoublet. Taking the external momentum flowing from left to right to be p, and the loop momentum flowing counterclockwise in the upper fermion line (f) to be k, we have from the Feynman rules of Fig. J.1.2:

$$i\Pi_{\mu\nu}^{WW} = (-1)\,\mu^{2\epsilon}\int\frac{\mathrm{d}^dk}{(2\pi)^d}\sum_{(f,f')}N_c^f\mathrm{Tr}\left[\left(-i\frac{g}{\sqrt{2}}\overline{\sigma}_\mu\right)\left(\frac{ik\cdot\sigma}{k^2-m_f^2}\right)\left(-i\frac{g}{\sqrt{2}}\overline{\sigma}_\nu\right)\left(\frac{i(k+p)\cdot\sigma}{(k+p)^2-m_{f'}^2}\right)\right]. \tag{6.23.1}$$

Here μ is a regularization scale for dimensional regularization in $d \equiv 4-2\epsilon$ dimensions. The sum in Eq. (6.23.1) is over the six isodoublet pairs $(f, f') = (e, \nu_e)$, (μ, ν_μ), (τ, ν_τ), (d, u), (s, c), and (b, t) with CKM mixing neglected, and

$$N_c^f = \begin{cases} 3, & f = \text{quarks}, \\ 1, & f = \text{leptons}. \end{cases} \tag{6.23.2}$$

The first factor of (-1) in Eq. (6.23.1) is due to the presence of a closed fermion loop. The trace is taken over the two-component dotted spinor indices. Using Eq. (B.2.27), it follows that

$$\Pi_{\mu\nu}^{WW} = \frac{g^2}{32\pi^2}\sum_f N_c^f I_{\mu\nu}(m_f^2, m_{f'}^2), \tag{6.23.3}$$

where we have defined

$$I_{\mu\nu}(x,y) = i(16\pi^2)\,\mu^{2\epsilon}\int\frac{\mathrm{d}^dk}{(2\pi)^d}\frac{4k_\mu k_\nu + 2k_\mu p_\nu + 2k_\nu p_\mu - 2k\cdot(k+p)\,g_{\mu\nu}}{(k^2-x)[(k+p)^2-y]}. \tag{6.23.4}$$

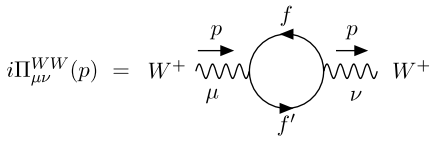

Fig. 6.23.1. Contributions to the self-energy function for the W boson in the Standard Model, from loops involving the left-handed quark and lepton pairs $(f, f') = (e, \nu_e)$, (μ, ν_μ), (τ, ν_τ), (d, u), (s, c), and (b, t). The momentum of the positively charged W^+ flows from left to right.

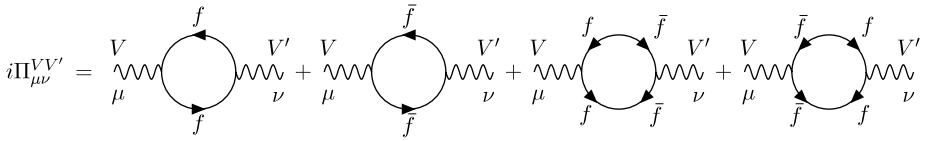

Fig. 6.23.2. Contributions to the diagonal and off-diagonal self-energy functions for the neutral vector bosons $V, V' = \gamma, Z$ in the Standard Model, from loops involving the three generations of leptons and quarks: $f = e, \nu_e, \mu, \nu_\mu, \tau, \nu_\tau, d, u, s, c, b, t$.

This integral can be evaluated by the standard dimensional regularization methods [114,220]:

$$I_{\mu\nu}(x, y) = (p^2 g_{\mu\nu} - p_\mu p_\nu) I_1(p^2; x, y) + g_{\mu\nu} I_2(p^2; x, y), \tag{6.23.5}$$

where, after neglecting terms that vanish as $\epsilon \to 0$,

$$\begin{aligned} I_1(s; x, y) \;=\; & -\frac{2}{3\epsilon} + \frac{2}{3s^2}\Big\{(2x - 2y - s)A(x) + (2y - 2x - s)A(y) \\ & + \Big[2(x - y)^2 - s(x + y) - s^2\Big]B(s; x, y) - s(x + y) + s^2/3\Big\}, \end{aligned} \tag{6.23.6}$$

$$I_2(s; x, y) = \frac{x + y}{\epsilon} - \frac{1}{s}\Big\{(x - y)\big[A(x) - A(y)\big] + \Big[(x - y)^2 - s(x + y)\Big]B(s; x, y)\Big\}. \tag{6.23.7}$$

The functions

$$A(x) \equiv x \ln(x/Q^2) - x, \tag{6.23.8}$$

$$B(s; x, y) \equiv -\int_0^1 \mathrm{d}t\, \ln\left(\frac{tx + (1 - t)y - t(1 - t)s - i\varepsilon}{Q^2}\right), \tag{6.23.9}$$

are the finite parts of one-loop Passarino–Veltman functions [221], with the renormalization scale Q related to the regularization scale μ by the modified minimal subtraction relation

$$\mu^2 = Q^2 e^\gamma / 4\pi, \tag{6.23.10}$$

where $\gamma = 0.577216\ldots$ is Euler's constant.

The photon and Z boson have mixed self-energy functions, defined in Fig. 6.23.2. Applying the pertinent Feynman rules from Fig. J.1.2, we obtain:

$$\begin{aligned} i\Pi^{VV'}_{\mu\nu} \;=\; & (-1)\mu^{2\epsilon} \int \frac{\mathrm{d}^d k}{(2\pi)^d} \sum_f N_c^f \mathrm{Tr}\Big\{\big(-iG^f_V \overline{\sigma}_\mu\big)\left(\frac{ik \cdot \sigma}{k^2 - m_f^2}\right)\big(-iG^f_{V'} \overline{\sigma}_\nu\big)\left(\frac{i(k + p) \cdot \sigma}{(k + p)^2 - m_f^2}\right) \\ & + \big(-iG^{\bar{f}}_V \overline{\sigma}_\mu\big)\left(\frac{ik \cdot \sigma}{k^2 - m_f^2}\right)\big(-iG^{\bar{f}}_{V'} \overline{\sigma}_\nu\big)\left(\frac{i(k + p) \cdot \sigma}{(k + p)^2 - m_f^2}\right) \\ & + \big(-iG^f_V \overline{\sigma}_\mu\big)\left(\frac{im_f}{k^2 - m_f^2}\right)\big(iG^{\bar{f}}_{V'} \sigma_\nu\big)\left(\frac{im_f}{(k + p)^2 - m_f^2}\right) \\ & + \big(-iG^{\bar{f}}_V \overline{\sigma}_\mu\big)\left(\frac{im_f}{k^2 - m_f^2}\right)\big(iG^f_{V'} \sigma_\nu\big)\left(\frac{im_f}{(k + p)^2 - m_f^2}\right)\Big\}, \end{aligned} \tag{6.23.11}$$

where V and V' can each be either γ or Z, and $\sum_f$ is taken over the 12 Standard Model fermions. The corresponding Vff and $V\bar{f}\bar{f}$ couplings are[66]:

$$G^f_\gamma = -G^{\bar{f}}_\gamma = eQ_f, \tag{6.23.12}$$

$$G^f_Z = \frac{g}{c_W}(T^f_3 - s^2_W Q_f), \qquad G^{\bar{f}}_Z = \frac{g}{c_W} s^2_W Q_f. \tag{6.23.13}$$

66 Note that there is no contribution from the left-handed two-component antineutrino fields, $\bar{\nu}_e, \bar{\nu}_\mu, \bar{\nu}_\tau$, which do not exist in the Standard Model.

The four terms in Eq. (6.23.11) correspond to the four diagrams in Fig. 6.23.2, in the same order.

The first two terms in Eq. (6.23.11) are computed exactly as for $\Pi^{WW}_{\mu\nu}$, while in the last two terms we use Eq. (B.2.5) to compute the trace. It follows that the neutral electroweak vector boson self-energy function matrix, after dropping terms that vanish as $\epsilon \to 0$, is given by

$$\Pi^{VV'}_{\mu\nu} = \frac{1}{16\pi^2}\sum_f N_c^f\Big[(G_V^f G_{V'}^f + G_V^{\bar f} G_{V'}^{\bar f})I_{\mu\nu}(m_f^2, m_f^2) + g_{\mu\nu}(G_V^f G_{V'}^{\bar f} + G_V^{\bar f} G_{V'}^f)m_f^2 I_3(m_f^2, m_f^2)\Big], \tag{6.23.14}$$

where $I_{\mu\nu}(x, y)$ was defined in Eqs. (6.23.5)–(6.23.7), and we have defined the function

$$I_3(x, y) = -i(16\pi^2)\mu^{2\epsilon}\int \frac{\mathrm{d}^d k}{(2\pi)^d}\frac{2}{(k^2 - x)[(k + p)^2 - y]} = \frac{2}{\epsilon} + 2B(p^2; x, y). \tag{6.23.15}$$

The photon self-energy function is a simple special case of Eq. (6.23.14):

$$\Pi^{\gamma\gamma}_{\mu\nu} = \frac{1}{16\pi^2}\sum_f 2N_c^f(eQ_f)^2\big[I_{\mu\nu}(m_f^2, m_f^2) - g_{\mu\nu}m_f^2 I_3(m_f^2, m_f^2)\big]. \tag{6.23.16}$$

Evaluating the integrals $I_{\mu\nu}$ and I_3 yields

$$\Pi^{\gamma\gamma}_{\mu\nu} = \frac{\alpha}{3\pi}\sum_f N_c^f Q_f^2\left(p^2 g_{\mu\nu} - p_\mu p_\nu\right)\left\{-\frac{1}{\epsilon} + \frac{1}{3} - \frac{2}{p^2}\left[A(m_f^2) + m_f^2\right] - \left(1 + \frac{2m_f^2}{p^2}\right)B(p^2; m_f^2, m_f^2)\right\}, \tag{6.23.17}$$

in agreement with the result given in, for example, Eq. (7.90) of [114]. This formula satisfies $p^\mu \Pi^{\gamma\gamma}_{\mu\nu} = p^\nu \Pi^{\gamma\gamma}_{\mu\nu} = 0$ as required by the Ward identity of QED, and is regular in the limit $p^2 \to 0$.

In each of Eqs. (6.23.3), (6.23.14) and (6.23.17), there are $1/\epsilon$ poles, contained in the loop integral functions. In the $\overline{\text{MS}}$ renormalization scheme, these poles are simply removed by counterterms, which have no other effect.

In Eqs. (6.23.1) and (6.23.11), we chose to write a $\overline{\sigma}_\mu$ for the left vertex in the Feynman diagram in each case. This is an arbitrary choice; we could also have chosen to use instead $-\sigma_\mu$ for the left vertex in any given diagram, as mentioned in the caption for Fig. J.1.2. This would have dictated the replacements $\overline{\sigma} \leftrightarrow -\sigma$ throughout the expression for the diagram, including for the fermion propagators, as was indicated in Fig. 4.2.4. It is not hard to check that the result after computing the spinor index traces is unaffected. Note that the contribution proportional to $\epsilon_{\mu\nu\rho\kappa}$ from Eq. (B.2.26) or Eq. (B.2.27) vanishes; this is clear because the self-energy function is symmetric under interchange of vector indices, and there is only one independent momentum in the problem.

6.24. Self-energy and pole mass of the top quark

We next consider the one-loop calculation of the self-energy and the pole mass of the top quark in the Standard Model, including the effects of the gauge interactions and the top and bottom quark Yukawa couplings. As in Section 6.1, we treat this as a one-generation problem, neglecting CKM mixing. Consequently, the corresponding Yukawa couplings Y_t and Y_b are real and positive (by a suitable phase redefinition of the Higgs field[67]). Using the formalism of Section 4.6 for Dirac fermions, the independent 1PI self-energy functions are given by[68] Σ_{Lt}, Σ_{Rt} and Σ_{Dt} (defined in Fig. 4.6.5) as shown in Fig. 6.24.1. Note that in these diagrams, the physical top quark moves from right to left, carrying momentum p^μ. Then according to the general formula obtained in Eq. (4.6.31), the complex pole squared mass of the top quark is given by:

$$M_t^2 - i\Gamma_t M_t = \frac{(m_t + \Sigma_{Dt})^2}{(1 - \Sigma_{Lt})(1 - \Sigma_{Rt})}, \tag{6.24.1}$$

where m_t is the tree-level mass. Working consistently to one-loop order, this yields

$$M_t^2 - i\Gamma_t M_t = \left[m_t^2(1 + \Sigma_{Lt} + \Sigma_{Rt}) + 2m_t\Sigma_{Dt}\right]\Big|_{s = m_t^2 + i\varepsilon}. \tag{6.24.2}$$

(It would be just as valid to substitute in $s = M_t^2 + i\varepsilon$ here, as two-loop order effects are being neglected.)

It remains to calculate the self-energy functions Σ_{Lt}, Σ_{Rt} and Σ_{Dt}. Two regularization procedures will be used simultaneously—the $\overline{\text{MS}}$ scheme [222] based on dimensional regularization [124] and the $\overline{\text{DR}}$ scheme based on dimensional reduction [223]. This is accomplished by integrating over the loop momentum in

$$d \equiv 4 - 2\epsilon \tag{6.24.3}$$

---

67 As shown in Section 3.2, after the fermion mass matrix diagonalization procedure, the tree-level fermion masses are real and non-negative. If CKM mixing is neglected, it follows from Eq. (J.1.9) that the corresponding diagonal Yukawa couplings are real and positive if the phase of the Higgs field is chosen such that the neutral Higgs vacuum expectation value $v > 0$.

68 Since the Yukawa couplings can be chosen real (in the one-generation model), $\overline{\Sigma}_{Lt} = \Sigma_{Lt}$. Note that after suppressing the color degrees of freedom, Σ_{Lt}, Σ_{Rt} and Σ_{Dt} are one-dimensional matrices, so we do not employ boldface letters in this case.

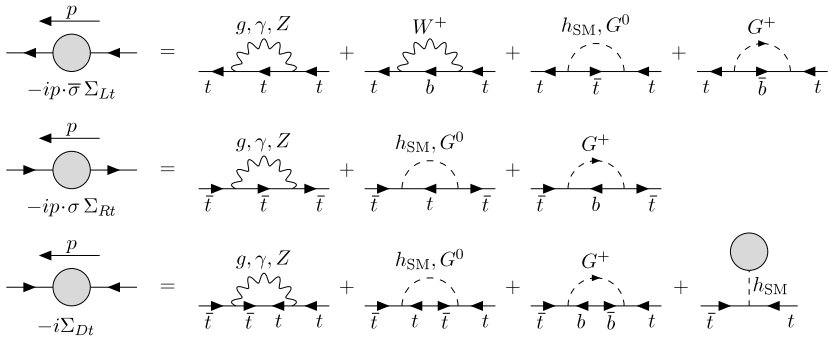

Fig. 6.24.1. One-loop contributions to the 1PI self-energy functions for the top quark in the Standard Model. The external momentum of the physical top quark, p^μ, flows from the right to the left. The loop momentum k^μ in the text is taken to flow clockwise. Spinor and color indices are suppressed. The external legs are amputated. The last diagram contains one-loop tadpole contributions.

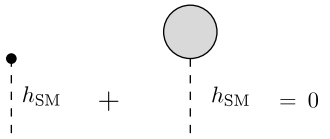

Fig. 6.24.2. The tree-level Higgs tadpole cancels against the one-loop Higgs tadpole, provided that one expands around a Higgs vacuum expectation value that minimizes the one-loop effective potential (rather than the tree-level Higgs potential, which would yield no tree-level tadpole).

dimensions, but with the vector bosons possessing

$$D \equiv 4 - 2\epsilon\delta_{\overline{\rm MS}} \tag{6.24.4}$$

components, where

$$\delta_{\overline{\rm MS}} \equiv \begin{cases} 1 & \text{for } \overline{\rm MS}, \\ 0 & \text{for } \overline{\rm DR}. \end{cases} \tag{6.24.5}$$

In other words, the metric $g^{\mu\nu}$ appearing explicitly in the vector propagator is treated as four dimensional in $\overline{\rm DR}$, but as d-dimensional in $\overline{\rm MS}$. The renormalization scale Q is related to the regularization scale μ in both cases by the modified minimal subtraction relation of Eq. (6.23.10).

The calculation of the non-tadpole contributions to the self-energy functions will be performed below in a general R_ξ gauge, with a vector boson propagator as in Fig. 4.2.5. There are different ways to treat the tadpole contributions, corresponding to different choices for the Higgs vacuum expectation value around which the tree-level Lagrangian is expanded. If one chooses to expand around the minimum of the tree-level Higgs potential, then there are no tree-level tadpoles, but there will be non-zero contributions from the last diagram shown in Fig. 6.24.1. (This corresponds to the treatment given, for example, in Ref. [224].) Alternatively, one can choose to expand around the Higgs vacuum expectation value v that minimizes the one-loop Landau gauge[69] effective potential. In that case, the one-loop tadpole contribution is precisely canceled by the tree-level Higgs tadpole, as shown in Fig. 6.24.2. Here, we have in mind the latter prescription; the calculation for the pole mass is therefore complete without tadpole contributions provided that the tree-level top quark mass is taken to be

$$m_t = Y_t v, \tag{6.24.6}$$

where Y_t is the $\overline{\rm MS}$ or $\overline{\rm DR}$ Yukawa coupling, and v is the Higgs vacuum expectation value at the minimum of the one-loop effective potential in Landau gauge. To be consistent with this choice, $\xi = 0$ should be taken in all formulae below that involve electroweak gauge bosons or Goldstone bosons. (The gluon contribution is naturally independent of ξ because the gauge symmetry is unbroken, providing a check of gauge-fixing invariance.) Nevertheless, for the sake of generality we will keep the dependence on ξ in the computation of the individual non-tadpole self-energy diagrams below.

Consider the one-loop calculation of the self-energy Σ_{Lt}, which is the sum of individual diagram contributions $\Sigma_{Lt} = [\Sigma_{Lt}]_g + [\Sigma_{Lt}]_\gamma + [\Sigma_{Lt}]_Z + [\Sigma_{Lt}]_W + [\Sigma_{Lt}]_{h_{\rm SM}} + [\Sigma_{Lt}]_{G^0} + [\Sigma_{Lt}]_{G^+}$. First, consider the diagrams involving exchanges of the scalars $\phi = h_{\rm SM}, G^0, G^\pm$. These contributions all have the same form

$$-ip\cdot\overline{\sigma}\,[\Sigma_{Lt}]_\phi = \mu^{2\epsilon}\int\frac{{\rm d}^dk}{(2\pi)^d}(-iY^*)\left(\frac{i(k+p)\cdot\overline{\sigma}}{(k+p)^2-m_f^2}\right)(-iY)\left(\frac{i}{k^2-m_\phi^2}\right), \tag{6.24.7}$$

[69] This procedure is considerably more involved outside of Landau gauge, because the propagators mix the longitudinal components of the vector boson with the Nambu–Goldstone bosons for $\xi \neq 0$ if one expands around a Higgs vacuum expectation value that does not minimize the tree-level potential. This is the same reason the effective potential is traditionally calculated specifically in Landau gauge.

where the loop momentum k^μ flows clockwise, and the couplings and propagator masses are, using the Feynman rules of Figs. J.1.3 and J.1.4,

$$\text{for } \phi = h_{\rm SM}: \qquad Y = Y_t/\sqrt{2}; \qquad m_f = m_t; \qquad m_\phi^2 = m_{h_{\rm SM}}^2, \tag{6.24.8}$$

$$\text{for } \phi = G^0: \qquad Y = iY_t/\sqrt{2}; \qquad m_f = m_t; \qquad m_\phi^2 = \xi m_Z^2, \tag{6.24.9}$$

$$\text{for } \phi = G^\pm: \qquad Y = Y_b; \qquad m_f = m_b; \qquad m_\phi^2 = \xi m_W^2. \tag{6.24.10}$$

Multiplying both sides by $p\cdot\sigma$ and taking the trace over spinor indices using Eq. (B.2.5), one finds

$$[\Sigma_{Lt}]_\phi = i|Y|^2 \frac{\mu^{2\epsilon}}{p^2}\int \frac{\mathrm{d}^d k}{(2\pi)^d}\frac{p\cdot(k+p)}{[(k+p)^2-m_f^2][k^2-m_\phi^2]}. \tag{6.24.11}$$

Performing the loop momentum integration in the standard way [114,220], and expanding in ϵ up to constant terms, one finds that in each case

$$[\Sigma_{Lt}]_\phi = -\frac{1}{16\pi^2}|Y|^2\, I_{FS}(s; m_f^2, m_\phi^2). \tag{6.24.12}$$

Here we have introduced some notation for the loop integral:

$$I_{FS}(s;x,y) \equiv \frac{1}{2\epsilon} + \frac{(s+x-y)B(s;x,y)+A(x)-A(y)}{2s}, \tag{6.24.13}$$

where the Passarino–Veltman functions $A(x)$ and $B(s;x,y)$ were defined in Eqs. (6.23.8) and (6.23.9). These functions depend on the renormalization scale Q, which is related to μ via Eq. (6.23.10). It can be checked that $I_{FS}(s;x,y)$ has a smooth limit as $s\to 0$.

Next, let us consider the contributions to Σ_{Lt} involving the vector bosons $V = g, \gamma, Z, W$. These have the common form:

$$\begin{aligned} -ip\cdot\overline{\sigma}[\Sigma_{Lt}]_V = \mu^{2\epsilon}\int \frac{\mathrm{d}^d k}{(2\pi)^d}\left(-iG\overline{\sigma}_\mu\right)\left(\frac{i(k+p)\cdot\sigma}{(k+p)^2-m_f^2}\right)\left(-iG\overline{\sigma}_\nu\right) \\ \times\left(\frac{-i}{k^2-m_V^2}\right)\left(g^{\mu\nu}+\frac{(\xi-1)k^\mu k^\nu}{k^2-\xi m_V^2}\right), \end{aligned} \tag{6.24.14}$$

where again the loop momentum k flows clockwise, and, using the rules of Figs. J.1.2 and K.5.1:

$$\text{for } V = g: \qquad G = g_s T^a, \qquad m_f = m_t, \tag{6.24.15}$$

$$\text{for } V = \gamma: \qquad G = eQ_t, \qquad m_f = m_t, \tag{6.24.16}$$

$$\text{for } V = Z: \qquad G = g(T_3^t - s_W^2 Q_t)/c_W, \qquad m_f = m_t, \tag{6.24.17}$$

$$\text{for } V = W: \qquad G = g/\sqrt{2}, \qquad m_f = m_b. \tag{6.24.18}$$

In the case of gluon exchange ($V = g$), the T^a are the $SU(3)_C$ generators (with color indices suppressed). The adjoint representation index a is summed over, producing a factor of the Casimir invariant $(T^aT^a)_{ij} = C_F\delta_{ij} = \frac{4}{3}\delta_{ij}$. We now use $\overline{\sigma}_\mu\,\sigma_\rho\,\overline{\sigma}_\nu\, g^{\mu\nu} = -(D-2)\,\overline{\sigma}_\rho$ [see Eq. (B.2.11)]; note that this introduces a difference between the $\overline{\rm MS}$ and $\overline{\rm DR}$ schemes. Also, we use $k\cdot\overline{\sigma}(k+p)\cdot\sigma k\cdot\overline{\sigma} = (k^2+2k\cdot p)k\cdot\overline{\sigma} - k^2 p\cdot\overline{\sigma}$, which follows from Eq. (2.54). One therefore obtains, after multiplying by $p\cdot\sigma$ and taking the trace over spinor indices:

$$\begin{aligned} [\Sigma_{Lt}]_V = -iG^2\frac{\mu^{2\epsilon}}{p^2}\int\frac{\mathrm{d}^d k}{(2\pi)^d}\frac{1}{[(k+p)^2-m_f^2][k^2-m_V^2]} \\ \times\left[(2-D)p\cdot(k+p) + \left(k^2 k\cdot p + 2(k\cdot p)^2 - k^2p^2\right)\frac{(\xi-1)}{k^2-\xi m_V^2}\right]. \end{aligned} \tag{6.24.19}$$

Performing the loop momentum integration, one finds that

$$[\Sigma_{Lt}]_V = -\frac{1}{16\pi^2}G^2 I_{FV}(s; m_f^2, m_V^2), \tag{6.24.20}$$

where we have introduced the notation

$$\begin{aligned} I_{FV}(s;x,y) = \frac{\xi}{\epsilon} + [(s+x-y)B(s;x,y)+A(x)-A(y)]/s - \delta_{\overline{\rm MS}} + \big\{(s-x)[A(y)-A(\xi y)] \\ + [(s-x)^2 - y(s+x)]B(s;x,y) - [(s-x)^2 - \xi y(s+x)]B(s;x,\xi y)\big\}/2ys, \end{aligned} \tag{6.24.21}$$

after dropping terms that vanish as $\epsilon \to 0$. Combining the results of Eqs. (6.24.12) and (6.24.20):

$$\Sigma_{Lt} = -\frac{1}{16\pi^2}\Big[\Big(g_s^2 C_F + e^2 Q_t^2\Big) I_{FV}(m_t^2; m_t^2, 0) + [g(T_3^t - s_W^2 Q_t)/c_W]^2 I_{FV}(m_t^2; m_t^2, m_Z^2) + \frac{1}{2} g^2 I_{FV}(m_t^2; m_b^2, m_W^2) + \frac{1}{2} Y_t^2 I_{FS}(m_t^2; m_t^2, m_{h_{\rm SM}}^2) + \frac{1}{2} Y_t^2 I_{FS}(m_t^2; m_t^2, \xi m_Z^2) + Y_b^2 I_{FS}(m_t^2; m_b^2, \xi m_W^2)\Big], \quad (6.24.22)$$

where we have now substituted $s = m_t^2$. It is useful to note that for massless gauge bosons,

$$I_{FV}(x; x, 0) = \xi\left[\frac{1}{\epsilon} - \ln(x/Q^2) + 2\right] + 1 - \delta_{\overline{\rm MS}}. \quad (6.24.23)$$

The contributions to $\Sigma_{Rt} = [\Sigma_{Rt}]_g + [\Sigma_{Rt}]_\gamma + [\Sigma_{Rt}]_Z + [\Sigma_{Rt}]_{h_{\rm SM}} + [\Sigma_{Rt}]_{G^0} + [\Sigma_{Rt}]_{G^\pm}$ are obtained similarly. [Note that there is no W boson contribution, since the right-handed top quark is an $SU(2)_L$ singlet.] For the scalar exchange diagrams with $\phi = h_{\rm SM}, G^0, G^\pm$, the general form is:

$$-ip\cdot\sigma[\Sigma_{Rt}]_\phi = \mu^{2\epsilon}\int\frac{d^dk}{(2\pi)^d}(-iY)\left(\frac{i(k+p)\cdot\sigma}{(k+p)^2 - m_f^2}\right)(-iY^*)\left(\frac{i}{k^2 - m_\phi^2}\right), \quad (6.24.24)$$

which yields

$$[\Sigma_{Rt}]_\phi = -\frac{1}{16\pi^2}|Y|^2 I_{FS}(s; m_f^2, m_\phi^2). \quad (6.24.25)$$

Here the couplings and propagator masses for $h_{\rm SM}$ and G^0 are the same as in Eqs. (6.24.8), (6.24.9), but now instead of Eq. (6.24.10),

$$\text{for } \phi = G^\pm: \qquad Y = -Y_t, \qquad m_f = m_b, \qquad m_\phi^2 = \xi m_W^2, \quad (6.24.26)$$

from Fig. J.1.4. For the contributions due to exchanges of vectors $v = g, \gamma, Z$, the general form is given by

$$-ip\cdot\sigma[\Sigma_{Rt}]_V = \mu^{2\epsilon}\int\frac{d^dk}{(2\pi)^d}(iG\sigma_\mu)\left(\frac{i(k+p)\cdot\overline{\sigma}}{(k+p)^2 - m_f^2}\right)(iG\sigma_\nu)\left(\frac{-i}{k^2 - m_V^2}\right)\left(g^{\mu\nu} + \frac{(\xi-1)k^\mu k^\nu}{k^2 - \xi m_V^2}\right), \quad (6.24.27)$$

where

$$\text{for } V = g: \qquad G = -g_s \boldsymbol{T^a}, \quad (6.24.28)$$

$$\text{for } V = \gamma: \qquad G = -eQ_t, \quad (6.24.29)$$

$$\text{for } V = Z: \qquad G = g s_W^2 Q_t / c_W, \quad (6.24.30)$$

after using the rules of Figs. J.1.2 and K.5.1 with $m_f = m_t$ in each case. We then make use of $\sigma_\mu\,\overline{\sigma}_\rho\,\sigma_\nu\,g^{\mu\nu} = -(D-2)\,\sigma_\rho$ [cf. Eq. (B.2.10)] and $k\cdot\sigma(k+p)\cdot\overline{\sigma}k\cdot\sigma = (k^2 + 2k\cdot p)k\cdot\sigma - k^2 p\cdot\sigma$ [cf. Eq. (2.53)]. After multiplying by $p\cdot\overline{\sigma}$ and taking the trace over spinor indices [using Eq. (B.2.5)], we obtain

$$[\Sigma_{Rt}]_V = -\frac{1}{16\pi^2}G^2 I_{FV}(s; m_t^2, m_V^2), \quad (6.24.31)$$

in terms of the same function appearing in Eqs. (6.24.21) and (6.24.23). Adding up these contributions and taking $s = m_t^2$ yields

$$\Sigma_{Rt} = -\frac{1}{16\pi^2}\Big[\Big(g_s^2 C_F + e^2 Q_t^2\Big) I_{FV}(m_t^2; m_t^2, 0) + (g^2 Q_t^2 s_W^4/c_W^2) I_{FV}(m_t^2; m_t^2, m_Z^2) + \frac{1}{2} Y_t^2 I_{FS}(m_t^2; m_t^2, m_{h_{\rm SM}}^2) + \frac{1}{2} Y_t^2 I_{FS}(m_t^2; m_t^2, \xi m_Z^2) + Y_t^2 I_{FS}(m_t^2; m_b^2, \xi m_W^2)\Big]. \quad (6.24.32)$$

Next, consider the contributions to $\Sigma_{Dt} = [\Sigma_{Dt}]_g + [\Sigma_{Dt}]_\gamma + [\Sigma_{Dt}]_Z + [\Sigma_{Dt}]_{h_{\rm SM}} + [\Sigma_{Dt}]_{G^0} + [\Sigma_{Dt}]_{G^\pm}$, ignoring the tadpole contribution for now. The diagrams involving the exchange of scalars $\phi = h_{\rm SM}, G^0, G^\pm$ have the form:

$$-i[\Sigma_{Dt}]_\phi = \mu^{2\epsilon}\int\frac{d^dk}{(2\pi)^d}(-iY_1)\left(\frac{im_f}{(k+p)^2 - m_f^2}\right)(-iY_2)\left(\frac{i}{k^2 - m_\phi^2}\right), \quad (6.24.33)$$

so that

$$[\Sigma_{Dt}]_\phi = im_f Y_1 Y_2 \mu^{2\epsilon}\int\frac{d^dk}{(2\pi)^d}\frac{1}{[(k+p)^2 - m_f^2][k^2 - m_\phi^2]} = \frac{1}{16\pi^2}m_f Y_1 Y_2 I_{\widetilde{FS}}(s; m_f^2, m_\phi^2), \quad (6.24.34)$$

where we have introduced the notation:

$$I_{\overline{FS}}(s;x,y) \equiv -\frac{1}{\epsilon} - B(s;x,y), \tag{6.24.35}$$

after dropping terms that vanish as $\epsilon \to 0$. The relevant couplings and masses are, from Figs. J.1.3 and J.1.4:

$$\text{for } \phi = h_{\rm SM}: \qquad Y_1 = Y_2 = Y_t/\sqrt{2}, \qquad m_f = m_t, \qquad m_\phi^2 = m_{h_{\rm SM}}^2, \tag{6.24.36}$$

$$\text{for } \phi = G^0: \qquad Y_1 = Y_2 = iY_t/\sqrt{2}, \qquad m_f = m_t, \qquad m_\phi^2 = \xi m_Z^2, \tag{6.24.37}$$

$$\text{for } \phi = G^\pm: \qquad Y_1 = Y_b, Y_2 = -Y_t, \qquad m_f = m_b, \qquad m_\phi^2 = \xi m_W^2. \tag{6.24.38}$$

The contributions from vector boson exchanges are of the form

$$-i[\Sigma_{Dt}]_V = \mu^{2\epsilon}\int \frac{\mathrm{d}^d k}{(2\pi)^d}\left(iG_1\sigma_\mu\right)\left(\frac{im_f}{(k+p)^2-m_f^2}\right)\left(-iG_2\overline{\sigma}_\nu\right)\left(\frac{-i}{k^2-m_V^2}\right)\left(g^{\mu\nu}+\frac{(\xi-1)k^\mu k^\nu}{k^2-\xi m_V^2}\right). \tag{6.24.39}$$

Using $\sigma_\mu\overline{\sigma}_\nu g^{\mu\nu} = D$ [see Eq. (B.2.8)] and $k\cdot\sigma\, k\cdot\overline{\sigma} = k^2$ [from Eq. (2.51)] yields

$$\begin{aligned}[\Sigma_{Dt}]_V &= im_f G_1 G_2 \mu^{2\epsilon}\int \frac{\mathrm{d}^d k}{(2\pi)^d}\frac{1}{[(k+p)^2-m_f^2][k^2-m_V^2]}\left[D+\frac{(\xi-1)k^2}{k^2-\xi m_V^2}\right]\\ &= \frac{1}{16\pi^2}m_f G_1 G_2 I_{\overline{FV}}(s;m_f^2,m_V^2),\end{aligned} \tag{6.24.40}$$

where

$$I_{\overline{FV}}(s;x,y) \equiv -\frac{3+\xi}{\epsilon} - 3B(s;x,y) - \xi B(s;x,\xi y) + 2\delta_{\overline{\rm MS}}, \tag{6.24.41}$$

after dropping terms that vanish as $\epsilon \to 0$. It is useful to note that for massless gauge bosons

$$I_{\overline{FV}}(x;x,0) \equiv -\frac{3+\xi}{\epsilon} + (3+\xi)[\ln(x/Q^2) - 2] + 2\delta_{\overline{\rm MS}}. \tag{6.24.42}$$

The relevant couplings are obtained from the rules of Figs. J.1.2 and K.5.1:

$$\text{for } V = g: \qquad G_1 = -G_2 = g_s T^a, \tag{6.24.43}$$

$$\text{for } V = \gamma: \qquad G_1 = -G_2 = eQ_t, \tag{6.24.44}$$

$$\text{for } V = Z: \qquad G_1 = g(T_3^t - s_W^2 Q_t)/c_W, \qquad G_2 = g s_W^2 Q_t/c_W, \tag{6.24.45}$$

and $m_f = m_t$ in each case. Adding up these contributions and taking $s = m_t^2$, we have:

$$\begin{aligned}\Sigma_{Dt} = \frac{m_t}{16\pi^2}\Big\{& g^2\left[(T_3^t - s_W^2 Q_t)s_W^2 Q_t/c_W^2\right] I_{\overline{FV}}(m_t^2;m_t^2,m_Z^2) - (g_s^2 C_F + e^2 Q_t^2) I_{\overline{FV}}(m_t^2;m_t^2,0)\\ &+ \tfrac{1}{2}Y_t^2 I_{\overline{FS}}(m_t^2;m_t^2,m_{h_{\rm SM}}^2) - \tfrac{1}{2}Y_t^2 I_{\overline{FS}}(m_t^2;m_t^2,\xi m_Z^2) - Y_b^2 I_{\overline{FS}}(m_t^2;m_b^2,\xi m_W^2)\Big\},\end{aligned} \tag{6.24.46}$$

where $Y_t = m_t Y_b/m_b$ was used on the last term.

In each of the self-energy functions above, there are poles in $1/\epsilon$, contained within the functions I_{FV}, I_{FS}, $I_{\overline{FV}}$ and $I_{\overline{FS}}$. In the $\overline{\rm MS}$ or $\overline{\rm DR}$ schemes, these poles are simply canceled by counterterms, which have no other effect at one-loop order. The one-loop top quark pole mass can now be obtained by plugging Eq. (6.24.22), (6.24.32), and (6.24.46) into Eq. (6.24.2) with $\xi = 0$, as discussed earlier. It is not hard to check that the terms from massless Nambu–Goldstone boson exchange just cancel against the terms from the vector exchange diagrams that came from ξm_W^2 and ξm_Z^2.

As a simple example, consider the one-loop pole mass with only QCD effects included. Then the result of Eq. (6.24.2) has no imaginary part. Taking the square root (and dropping a two-loop order part) yields the well-known result [225]:

$$\begin{aligned}M_{t,\rm pole} &= m_t(1 + \tfrac{1}{2}\Sigma_{Lt} + \tfrac{1}{2}\Sigma_{Rt}) + \Sigma_{Dt}\\ &= m_t\left(1 - \frac{C_F g_s^2}{16\pi^2}\left[I_{FV}(m_t^2;m_t^2,0) + I_{\overline{FV}}(m_t^2;m_t^2,0)\right]\right)\\ &= m_t\left(1 + \frac{\alpha_s}{4\pi}C_F\left[5 - \delta_{\overline{\rm MS}} - 3\ln(m_t^2/Q^2)\right]\right).\end{aligned} \tag{6.24.47}$$

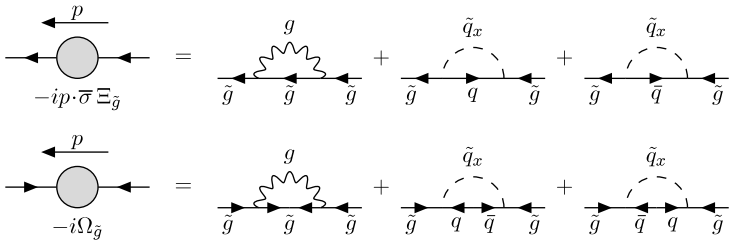

Fig. 6.25.1. Self-energy functions for the gluino in supersymmetry. The external momentum p^μ flows from the right to the left. The loop momentum k^μ in the text is taken to flow clockwise. Spinor and color indices are suppressed. The index $x = 1, 2$ labels the two squark mass eigenstates of a given flavor $q = u, d, s, c, b, t$. Both x and q must be summed over. The external legs are amputated.

As another check, consider the imaginary part of the pole squared mass of the top quark. At leading order, Eq. (6.24.2) implies:

$$\begin{aligned}\Gamma_t &= -\mathrm{Im}[m_t(\Sigma_{Lt} + \Sigma_{Rt}) + 2\Sigma_{Dt}] \\ &= \frac{m_t}{16\pi^2}\mathrm{Im}\Big[\frac{g^2}{2}I_{FV}(m_t^2; m_b^2, m_W^2) + (Y_t^2 + Y_b^2)I_{F\bar{S}}(m_t^2; m_b^2, \xi m_W^2) + 2Y_b^2 I_{\bar{F}S}(m_t^2; m_b^2, \xi m_W^2)\Big] \\ &= \frac{1}{32\pi^2 m_t}\left\{(g^2 + Y_t^2 + Y_b^2)(m_t^2 + m_b^2 - m_W^2) - 4Y_b^2 m_t^2\right\}\mathrm{Im}[B(m_t^2; m_b^2, m_W^2)]. \end{aligned} \tag{6.24.48}$$

The fact that the ξ dependence canceled here is a successful check of gauge-fixing invariance, since the tadpole diagram in Fig. 6.24.1 does not contribute to the absorptive part of the self-energy. One can express $\mathrm{Im}[B(s; x, y)]$ in terms of the triangle function [cf. Eq. (6.1.11)],

$$\mathrm{Im}[B(s; x, y)] = \begin{cases} 0 & \text{for } s \le (\sqrt{x} + \sqrt{y})^2, \\ \pi\lambda^{1/2}(s, x, y)/s & \text{for } s > (\sqrt{x} + \sqrt{y})^2. \end{cases} \tag{6.24.49}$$

Eq. (6.24.48) then reproduces the result of Eq. (6.1.10) for the top quark width at leading order.

6.25. *Self-energy and pole mass of the gluino*

The Feynman diagrams for the gluino self-energy are shown in Fig. 6.25.1. Since the gluino is a Majorana fermion, we can use the general formalism of Section 4.6. We will compute the self-energy functions $\Xi_{\tilde{g}} \equiv \Xi_{\tilde{g}}^{\tilde{g}}$ and $\Omega_{\tilde{g}} \equiv \Omega^{\tilde{g}\tilde{g}}$ defined in Fig. 4.6.3, and infer $\overline{\Omega}_{\tilde{g}} \equiv \overline{\Omega}_{\tilde{g}\tilde{g}}$ from the latter by replacing all Lagrangian parameters by their complex conjugates.[70] At one-loop order, it follows from the general result of Eq. (4.6.23) that the complex pole squared mass of the gluino is related to the tree-level mass $m_{\tilde{g}}$ by

$$M_{\tilde{g}}^2 - iM_{\tilde{g}}\Gamma_{\tilde{g}} = \left[m_{\tilde{g}}^2(1 + 2\Xi_{\tilde{g}}) + m_{\tilde{g}}(\Omega_{\tilde{g}} + \overline{\Omega}_{\tilde{g}})\right]\Big|_{s=m_{\tilde{g}}^2+i\varepsilon}. \tag{6.25.1}$$

It is convenient to split the self-energy functions into gluon/gluino loop and squark/quark loop contributions, as

$$\Xi_{\tilde{g}} = [\Xi_{\tilde{g}}]_g + \sum_q \sum_{x=1,2} [\Xi_{\tilde{g}}]_{\tilde{q}_x}, \quad \text{and} \quad \Omega_{\tilde{g}} = [\Omega_{\tilde{g}}]_g + \sum_q \sum_{x=1,2} [\Omega_{\tilde{g}}]_{\tilde{q}_x}, \tag{6.25.2}$$

where the sum over q runs over the six squark flavors u, d, s, c, b, t, and $x = 1, 2$ corresponds to the two squark mass eigenstates [i.e., the two appropriate linear combinations (for fixed squark flavor) of $\widetilde{q}_L$ and $\widetilde{q}_R$]. The gluon exchange contributions, following from the Feynman rules of Fig. K.5.1, are:

$$\begin{aligned} -ip\cdot\overline{\sigma}\,[\Xi_{\tilde{g}}]_g\,\delta^{ab} &= \mu^{2\epsilon}\int\frac{\mathrm{d}^d k}{(2\pi)^d}\left(-g_s f^{aec}\overline{\sigma}_\mu\right)\left(\frac{i(k+p)\cdot\sigma}{(k+p)^2 - m_{\tilde{g}}^2}\right)\left(-g_s f^{ebc}\overline{\sigma}_\nu\right) \\ &\quad\times\left(\frac{-i}{k^2}\right)\left(g^{\mu\nu} + (\xi - 1)\frac{k^\mu k^\nu}{k^2}\right), \end{aligned} \tag{6.25.3}$$

$$-i\,[\Omega_{\tilde{g}}]_g\,\delta^{ab} = \mu^{2\epsilon}\int\frac{\mathrm{d}^d k}{(2\pi)^d}\left(g_s f^{eac}\sigma_\mu\right)\left(\frac{im_{\tilde{g}}}{(k+p)^2 - m_{\tilde{g}}^2}\right)\left(-g_s f^{ebc}\overline{\sigma}_\nu\right)\left(\frac{-i}{k^2}\right)\left(g^{\mu\nu} + (\xi - 1)\frac{k^\mu k^\nu}{k^2}\right). \tag{6.25.4}$$

70 Suppressing the color degrees of freedom, Ξ, Ω and $\overline{\Omega}$ are one-dimensional matrices, so we do not employ boldface letters in this case.

The internal gluon and gluino lines carry $SU(3)_c$ adjoint representation index indices c and e respectively, while the external gluinos on the left and right carry indices a and b respectively. The gluino external momentum p^μ flows from right to left, and the loop momentum k^μ flows clockwise. Comparing with the derivations of Eqs. (6.24.20) and (6.24.40) in the previous subsection, and using $-f^{aec}f^{ebc} = f^{eac}f^{ebc} = \delta^{ab}C_A$ [with $C_A = 3$ for $SU(3)_c$], we can immediately conclude that

$$[\Xi_{\tilde g}]_g = -\frac{\alpha_s}{4\pi} C_A I_{FV}(s; m_{\tilde g}^2, 0), \tag{6.25.5}$$

$$[\Omega_{\tilde g}]_g = -\frac{\alpha_s}{4\pi} C_A m_{\tilde g} I_{\overline{F}V}(s; m_{\tilde g}^2, 0), \tag{6.25.6}$$

where the loop integral functions I_{FV} and $I_{\overline{F}V}$ were defined in Eqs. (6.24.21) and (6.24.41).

Next consider the virtual squark exchange diagrams contributing to $\Xi_{\tilde g}$. Labeling the quark and squark with color indices j, k respectively, we have for each squark mass eigenstate:

$$\begin{aligned} -ip\cdot\overline{\sigma}\,[\Xi_{\tilde g}]_{\tilde q_x}\,\delta^{ab} = {} & \mu^{2\epsilon}\int \frac{\mathrm{d}^d k}{(2\pi)^d}\left(-i\sqrt{2}g_s T_j^{ak} L_{\tilde q_x}\right)\left(\frac{i(k+p)\cdot\overline{\sigma}}{(k+p)^2 - m_q^2}\right)\left(-i\sqrt{2}g_s T_k^{bj} L_{\tilde q_x}^*\right)\left(\frac{i}{k^2 - m_{\tilde q_x}^2}\right) \\ & + \mu^{2\epsilon}\int \frac{\mathrm{d}^d k}{(2\pi)^d}\left(i\sqrt{2}g_s T_k^{aj} R_{\tilde q_x}^*\right)\left(\frac{i(k+p)\cdot\overline{\sigma}}{(k+p)^2 - m_q^2}\right)\left(i\sqrt{2}g_s T_j^{bk} R_{\tilde q_x}\right)\left(\frac{i}{k^2 - m_{\tilde q_x}^2}\right). \end{aligned} \tag{6.25.7}$$

This uses the Feynman rules shown in Fig. K.5.3, given in terms of the squark mixing parameters $L_{\tilde q_x}$ and $R_{\tilde q_x}$ defined in Eq. (K.4.1). Using $\mathrm{Tr}[T^a T^b] = \frac{1}{2}\delta^{ab}$ and $|L_{\tilde q_x}|^2 + |R_{\tilde q_x}|^2 = 1$, and comparing to the derivation of Eq. (6.24.12) of the previous subsection, we obtain:

$$[\Xi_{\tilde g}]_{\tilde q_x} = -\frac{\alpha_s}{4\pi} I_{FS}(s; m_q^2, m_{\tilde q_x}^2). \tag{6.25.8}$$

Similarly, for the last two diagrams of Fig. 6.25.1, we obtain:

$$\begin{aligned} -i[\Omega_{\tilde g}]_{\tilde q_x}\,\delta^{ab} = {} & \mu^{2\epsilon}\int \frac{\mathrm{d}^d k}{(2\pi)^d}\left(-i\sqrt{2}g_s T_k^{aj} L_{\tilde q_x}^*\right)\left(\frac{i m_q}{(k+p)^2 - m_q^2}\right)\left(i\sqrt{2}g_s T_j^{bk} R_{\tilde q_x}\right)\left(\frac{i}{k^2 - m_{\tilde q_x}^2}\right) \\ & + \mu^{2\epsilon}\int \frac{\mathrm{d}^d k}{(2\pi)^d}\left(i\sqrt{2}g_s T_j^{ak} R_{\tilde q_x}\right)\left(\frac{i m_q}{(k+p)^2 - m_q^2}\right)\left(-i\sqrt{2}g_s T_k^{bj} L_{\tilde q_x}^*\right)\left(\frac{i}{k^2 - m_{\tilde q_x}^2}\right), \end{aligned} \tag{6.25.9}$$

again using the Feynman rules shown in Fig. K.5.3. As before, j and k are the color indices for the quark and the squark, respectively. Comparing to the derivation of Eq. (6.24.34) of the previous subsection, we obtain:

$$[\Omega_{\tilde g}]_{\tilde q_x} = -\frac{\alpha_s}{2\pi} L_{\tilde q_x}^* R_{\tilde q_x} m_q I_{\overline{F}S}(s; m_q^2, m_{\tilde q_x}^2). \tag{6.25.10}$$

Summing up the results obtained above, and taking $s = m_{\tilde g}^2$, we have:

$$\Xi_{\tilde g} = -\frac{\alpha_s}{4\pi}\left[C_A I_{FV}(m_{\tilde g}^2; m_{\tilde g}^2, 0) + \sum_q \sum_{x=1,2} I_{FS}(m_{\tilde g}^2; m_q^2, m_{\tilde q_x}^2)\right], \tag{6.25.11}$$

$$\Omega_{\tilde g} = -\frac{\alpha_s}{4\pi}\left[C_A m_{\tilde g} I_{\overline{F}V}(m_{\tilde g}^2; m_{\tilde g}^2, 0) + 2\sum_q \sum_{x=1,2} L_{\tilde q_x}^* R_{\tilde q_x} m_q I_{\overline{F}S}(m_{\tilde g}^2; m_q^2, m_{\tilde q_x}^2)\right]. \tag{6.25.12}$$

As previously noted, we can now write down $\overline{\Omega}_{\tilde g}$ by replacing the Lagrangian parameters of Eq. (6.25.12) by their complex conjugates:

$$\overline{\Omega}_{\tilde g} = -\frac{\alpha_s}{4\pi}\left[C_A m_{\tilde g} I_{\overline{F}V}(m_{\tilde g}^2; m_{\tilde g}^2, 0) + 2\sum_q \sum_{x=1,2} L_{\tilde q_x} R_{\tilde q_x}^* m_q I_{\overline{F}S}(m_{\tilde g}^2; m_q^2, m_{\tilde q_x}^2)\right]. \tag{6.25.13}$$

Inserting the results of Eqs. (6.25.11)–(6.25.13) into Eq. (6.25.1), one obtains the result [226,227]:

$$\begin{aligned} M_{\tilde g}^2 - iM_{\tilde g}\Gamma_{\tilde g} = {} & m_{\tilde g}^2\Bigg[1 + \frac{\alpha_s}{2\pi}\Bigg\{C_A\left[5 - \delta_{\overline{\mathrm{MS}}} - 3\ln\left(m_{\tilde g}^2/Q^2\right)\right] \\ & - \sum_q \sum_{x=1,2}\left[I_{FS}(m_{\tilde g}^2; m_q^2, m_{\tilde q_x}^2) + 2\mathrm{Re}[L_{\tilde q_x}^* R_{\tilde q_x}]\frac{m_q}{m_{\tilde g}} I_{\overline{F}S}(m_{\tilde g}^2; m_q^2, m_{\tilde q_x}^2)\right]\Bigg\}\Bigg], \end{aligned} \tag{6.25.14}$$

with $\delta_{\overline{\mathrm{MS}}}$ defined in Eq. (6.24.5).

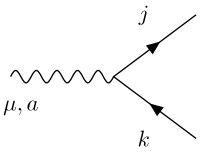

$$-i(\boldsymbol{T^a})_j{}^k\,\overline{\sigma}_\mu \quad \text{or} \quad i(\boldsymbol{T^a})_j{}^k\,\sigma_\mu$$

Fig. 6.26.1. Feynman rule for the coupling of a current carrying vector index μ and corresponding to the symmetry generator $\boldsymbol{T^a}$ acting on $(\frac{1}{2}, 0)$ [left-handed] fermions. Spinor indices are suppressed.

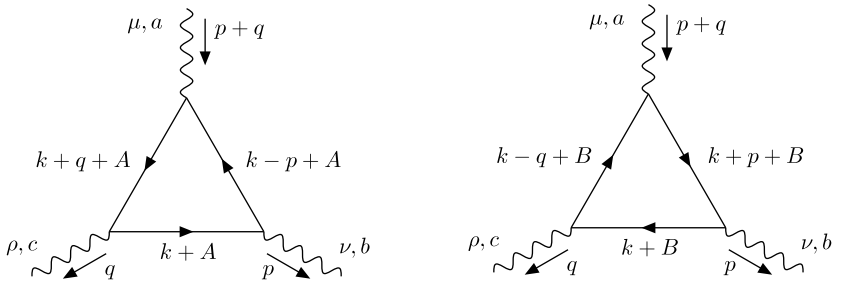

Fig. 6.26.2. Triangle Feynman diagrams leading to the chiral fermion anomaly. Fermion spinor and flavor indices are suppressed. The fermion momenta, as labeled, flow in the arrow directions.

6.26. Triangle anomaly from chiral fermion loops

As our final example, we consider the anomaly in chiral symmetries for fermions, arising from the triangle diagram involving three currents carrying vector indices.[71] Since the anomaly is independent of the fermion masses, we simplify the computation by setting all fermion masses to zero. In four-component notation,[72] the treatment of the anomaly requires care because of the difficulty in defining a consistent and unambiguous γ_5 and the epsilon tensor in dimensional regularization [230,231]. The same subtleties arise in two-component language, of course, but in a slightly different form since γ_5 does not appear explicitly.

We shall assemble all the $(\frac{1}{2}, 0)$ [left-handed] two-component fermion fields of the theory into a multiplet ψ_j. For example, the fermions of the Standard Model are: $\psi_j = (\ell_k,\ \bar{\ell}_k,\ \nu_k,\ q_{i\ell},\ \bar{q}_{i\ell})$, where $k = 1, 2, 3$ and $i = 1, 2, \ldots, 6$ are flavor labels and $\ell = 1, 2, 3$ are color labels [see Table 5.1]. The two-component spinor indices are suppressed here. Let the symmetry generators be given by hermitian matrices T^a, so that the ψ_j transform as:

$$\delta\psi_j = i\theta^a(\boldsymbol{T^a})_j{}^k\psi_k, \tag{6.26.1}$$

for infinitesimal parameters θ^a. The matrices $\boldsymbol{T^a}$ form a representation R of the generators of the Lie algebra of the symmetry group. In general R will be reducible, in which case the $\boldsymbol{T^a}$ have a block diagonal structure, where each block separately transforms (irreducibly) the corresponding field of ψ_j according to its symmetry transformation properties. Some or all of these symmetries may be gauged. The Feynman rule for the corresponding currents is the same as for external gauge bosons, as in Fig. 4.3.2 (but without the gauge couplings), and is shown in Fig. 6.26.1.

Fig. 6.26.2 exhibits the two Feynman diagrams that contribute at one-loop to the three-point function of the symmetry currents. Applying the $\overline{\sigma}$-version of the Feynman rule for the currents given in Fig. 6.26.1, and employing the Feynman rules of Fig. 4.2.1 (with $m = 0$) for the propagators [traversing the loop in the direction dictated by Eq. (4.4.2)], the sum of the two triangle diagrams shown in Fig. 6.26.2 can be evaluated.

The resulting sum of loop integrals is

$$\begin{aligned} i\Gamma^{abc}_{\mu\nu\rho} = (-1)\int \frac{\mathrm{d}^4k}{(2\pi)^4}\mathrm{Tr}\Big\{ &(-i\overline{\sigma}_\mu\boldsymbol{T}^a)\frac{i(k-p+A)\cdot\sigma}{(k-p+A)^2}(-i\overline{\sigma}_\nu\boldsymbol{T}^b)\frac{i(k+A)\cdot\sigma}{(k+A)^2}(-i\overline{\sigma}_\rho\boldsymbol{T}^c)\frac{i(k+q+A)\cdot\sigma}{(k+q+A)^2} \\ &+(-i\overline{\sigma}_\mu\boldsymbol{T}^a)\frac{i(k-q+B)\cdot\sigma}{(k-q+B)^2}(-i\overline{\sigma}_\rho\boldsymbol{T}^c)\frac{i(k+B)\cdot\sigma}{(k+B)^2}(-i\overline{\sigma}_\nu\boldsymbol{T}^b)\frac{i(k+p+B)\cdot\sigma}{(k+p+B)^2}\Big\}, \end{aligned} \tag{6.26.2}$$

where the overall factor of (-1) is due to the presence of a closed fermion loop. The trace is taken over fermion flavor/group and spinor indices, both of which are suppressed. Because the individual integrals are linearly divergent, we must allow for arbitrary constant four-vectors A^μ and B^μ as offsets for the loop momentum when defining the loop integrations for the two diagrams [232,233].

71 The discussion here parallels that given in Ref. [228], Section 22.3.

72 For an excellent review of the computation of the chiral anomaly via four-component massless and massive spinor triangle loops, see Ref. [229].

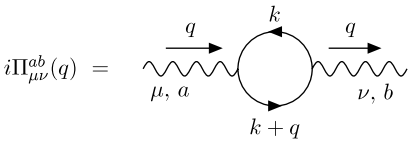

Fig. 6.26.3. The one-loop contribution to the current–current two-point function. The fermion momenta, as labeled, flow along the corresponding arrow directions.

The persistence of the symmetry in the quantum theory for the currents labeled by μ, a and ν, b and ρ, c implies the naive Ward identities[73]:

$$(p+q)^\mu\, i\Gamma^{abc}_{\mu\nu\rho}(-p-q,p,q) = f^{abd}\Pi^{dc}_{\nu\rho}(q) + f^{acd}\Pi^{bd}_{\nu\rho}(p), \tag{6.26.3}$$

$$-p^\nu\, i\Gamma^{abc}_{\mu\nu\rho}(-p-q,p,q) = f^{bcd}\Pi^{da}_{\rho\mu}(p+q) + f^{bad}\Pi^{cd}_{\rho\mu}(q), \tag{6.26.4}$$

$$-q^\rho\, i\Gamma^{abc}_{\mu\nu\rho}(-p-q,p,q) = f^{cad}\Pi^{db}_{\mu\nu}(p) + f^{cbd}\Pi^{ad}_{\mu\nu}(p+q), \tag{6.26.5}$$

where $i\Pi^{ab}_{\mu\nu}(p)$ is the one-loop current–current two-point function shown in Fig. 6.26.3.

By Lorentz covariance, $\Pi^{ab}_{\mu\nu}(p)$ is a rank-two symmetric tensor that is an even function of the four-momentum p [cf. Eq. (6.26.41)]. In Eqs. (6.26.3)–(6.26.5), we have employed a convention in which the arguments of $i\Gamma$ correspond to the *outgoing* momentum of the external legs of the corresponding one-loop Feynman diagrams, and the order of the momentum arguments matches the order of the indices.

It is convenient to define the *symmetrized* three-point function by symmetrizing over the indices a, b and c:

$$\mathcal{A}^{abc}_{\mu\nu\rho} = \frac{1}{6} i\Gamma^{abc}_{\mu\nu\rho} + [\text{five permutations of } a, b, c]. \tag{6.26.6}$$

In terms of the symmetrized three-point function, the naive Ward identities imply

$$(p+q)^\mu \mathcal{A}^{abc}_{\mu\nu\rho} = 0, \qquad -p^\nu \mathcal{A}^{abc}_{\mu\nu\rho} = 0, \quad \text{and} \quad -q^\rho \mathcal{A}^{abc}_{\mu\nu\rho} = 0. \tag{6.26.7}$$

We now perform the explicit diagrammatic computation to show that the naive Ward identities exhibited in Eq. (6.26.7) are violated due to a quantum anomaly. Although the symmetrized three-point function is ultraviolet finite, the individual loop momentum integrals are divergent, and must be defined with care. We do not regularize them by the usual procedure of continuing to $d = 4 - 2\epsilon$ dimensions, because the trace over sigma matrices crucially involves the antisymmetric tensor with four indices, brought in by Eqs. (B.2.26) and (B.2.27), for which there is no consistent and unambiguous generalization outside of four dimensions. (This is related to the difficulty of defining γ_5 in the four-component spinor formalism.) The existence of the vectors A and B corresponds to an ambiguity in the regulation procedure, which can be fixed to preserve some of the symmetries, as we will see below.

Starting from Eq. (6.26.2), it follows from Eq. (E.2.8) that the symmetrized three-point function is proportional to the group theory factor (often called the anomaly coefficient),

$$D^{abc} = \tfrac{1}{2}\mathrm{Tr}[\{\boldsymbol{T^a}, \boldsymbol{T^b}\}\boldsymbol{T^c}], \tag{6.26.8}$$

where the numerical values of the D^{abc} depend on the representation R. As discussed in Appendix E, D^{abc} vanishes for all simple Lie groups, with the exception of SU(N) for $N \geq 3$. The D^{abc} are also non-vanishing in general for any non-semisimple compact Lie group, which contains at least one U(1) factor.

First, consider the result for $(p+q)^\mu \mathcal{A}^{abc}_{\mu\nu\rho}$. This can be simplified by rewriting

$$(p+q)^\mu = (k+q+A)^\mu - (k-p+A)^\mu, \tag{6.26.9}$$

$$(p+q)^\mu = (k+p+B)^\mu - (k-q+B)^\mu, \tag{6.26.10}$$

in the first and second diagram terms, respectively, and then applying the formulae

$$v\cdot\sigma\, v\cdot\overline{\sigma} = v^2, \qquad v\cdot\overline{\sigma}\, v\cdot\sigma = v^2, \tag{6.26.11}$$

which follow from Eqs. (B.2.1) and (B.2.2). After rearranging the terms using the cyclic property of the trace, we obtain:

$$\begin{aligned}(p+q)^\mu \mathcal{A}^{abc}_{\mu\nu\rho} &= -D^{abc}\,\mathrm{Tr}[\sigma_\kappa\overline{\sigma}_\nu\sigma_\lambda\overline{\sigma}_\rho]\,X^{\kappa\lambda},\\ &= -2D^{abc}\left[X_{\nu\rho} + X_{\rho\nu} - g_{\nu\rho}X_\lambda{}^\lambda + i\epsilon_{\kappa\nu\lambda\rho}X^{\kappa\lambda}\right],\end{aligned} \tag{6.26.12}$$

[73] The derivation of the Ward identities is most easily achieved by writing the three-point function in position space as a vacuum expectation value of the time-ordered product of three currents. After taking the divergence (with respect to the position of any one of the three currents) of the time-ordered product and using the fact that the currents are conserved ($\partial_\mu j^{a\mu} = 0$), the surviving terms can be evaluated using the equal-time commutation relations, $\delta(x^0 - y^0)[j^{a0}(x), j^{bv}(y)] = if^{abc}j^{cv}(x)\delta^4(x-y)$. Fourier transforming the result yields the terms on the right-hand side of Eqs. (6.26.3)–(6.26.5). See Refs. [234,235] for further details.

after applying Eq. (B.2.26). (In our conventions, $\epsilon_{0123} = -1$.) The integral $X^{\kappa\lambda}$ is given by:

$$X^{\kappa\lambda} = \int \frac{d^4k}{(2\pi)^4}\left[\frac{(k-p+A)^\kappa}{(k-p+A)^2}\frac{(k+A)^\lambda}{(k+A)^2} - \frac{(k+q+A)^\kappa}{(k+q+A)^2}\frac{(k+A)^\lambda}{(k+A)^2} + \frac{(k+B)^\kappa}{(k+B)^2}\frac{(k-q+B)^\lambda}{(k-q+B)^2} - \frac{(k+B)^\kappa}{(k+B)^2}\frac{(k+p+B)^\lambda}{(k+p+B)^2}\right]. \tag{6.26.13}$$

Naively, this integral appears to vanish, because the first term is equal to the negative of the fourth term after a momentum shift $k \to k-p+A-B$, and the second term is equal to the negative of the third term after $k \to k+q+A-B$. However, these momentum shifts are not valid for the individually divergent integrals. Instead, $X^{\kappa\lambda}$ can be evaluated by a Wick rotation to Euclidean space, followed by isolating the terms that contribute for large k^2 and are responsible for the integral not vanishing, and then employing the divergence (Gauss') theorem in four dimensions to rewrite $X^{\kappa\lambda}$ as an angular integral over a three-sphere with radius tending to infinity. This integral is initially evaluated at large but finite Euclidean k, with the limit $k \to \infty$ taken at the end of the computation. For example, consider a smooth function $f(k)$ of the four-momentum k with the property that the integral

$$\int d^4k f(k) \tag{6.26.14}$$

is at worst quadratically divergent. We define the even and odd parts of $f(k)$, respectively, by:

$$f_e(k) \equiv \tfrac{1}{2}\left[f(k)+f(-k)\right], \qquad f_o(k) \equiv \tfrac{1}{2}\left[f(k)-f(-k)\right]. \tag{6.26.15}$$

It then follows that [234,236,237]

$$\int \frac{d^4k}{(2\pi)^4}\left[f(k+a)-f(k)\right] = \frac{i}{(2\pi)^4}\left[2\pi^2 a_\mu \lim_{k\to\infty} k^\mu k^2 f_o(k) + \pi^2 a_\mu a_\nu \lim_{k\to\infty} k^\mu k^2 \frac{\partial}{\partial k_\nu} f_e(k)\right] \tag{6.26.16}$$

has a finite limit.[74] In deriving this result, we have expanded $f(k+a)$ in a Taylor expansion and follow the procedure outlined above Eq. (6.26.14). Note that the angular integration removes the even parts of $f(k)$ and $\partial f/\partial k^\nu \equiv 2k_\nu\, \partial f/\partial k^2$ from the right-hand side of Eq. (6.26.16). The "limits" in Eq. (6.26.16) actually correspond to an average over the three-sphere at large Euclidean k, and thus should be interpreted by the use of:

$$\lim_{k\to\infty} \frac{k^\mu k^\nu}{k^2} = \tfrac{1}{4} g^{\mu\nu}, \tag{6.26.17}$$

$$\lim_{k\to\infty} \frac{k^\mu k^\nu k^\rho k^\lambda}{(k^2)^2} = \frac{1}{24}\left(g^{\mu\nu}g^{\rho\lambda} + g^{\mu\rho}g^{\nu\lambda} + g^{\mu\lambda}g^{\nu\rho}\right). \tag{6.26.18}$$

For example, if

$$f(k) = \frac{(k-p+A)^\kappa (k+A)^\lambda}{(k-p+A)^2 (k+A)^2}, \tag{6.26.19}$$

then in evaluating Eq. (6.26.16), it is sufficient to write:

$$\begin{aligned} f_o(k) &\simeq \tfrac{1}{2}(k-p+A)^\kappa (k+A)^\lambda \left[\frac{1}{(k^2)^2} + \frac{2k\cdot(p-2A)}{(k^2)^3}\right] - (k \to -k) \\ &\simeq \frac{k^\kappa A^\lambda - k^\lambda (p-A)^\kappa}{(k^2)^2} + \frac{2k^\kappa k^\lambda\, k\cdot(p-2A)}{(k^2)^3}, \end{aligned} \tag{6.26.20}$$

where we have dropped terms that do not contribute to Eq. (6.26.16) in the limit of $k \to \infty$. Similarly,

$$\frac{\partial f_e}{\partial k_\nu} \simeq \frac{g^{\kappa\nu}k^\lambda + g^{\lambda\nu}k^\kappa}{(k^2)^2} - \frac{4k^\kappa k^\lambda k^\nu}{(k^2)^3}. \tag{6.26.21}$$

The evaluation of $X^{\kappa\lambda}$ is now straightforward [after using Eqs. (6.26.17) and (6.26.18)]:

$$X^{\kappa\lambda} = \frac{i}{96\pi^2}\left[g^{\kappa\lambda}(p+q)\cdot(A+B) + (A-2B)^\kappa (p+q)^\lambda + (p+q)^\kappa (B-2A)^\lambda\right]. \tag{6.26.22}$$

74 If Eq. (6.26.14) is linearly divergent, then the second term on the right-hand side of Eq. (6.26.16) is zero. If Eq. (6.26.14) is logarithmically divergent or finite, then the right-hand side of Eq. (6.26.16) vanishes.

Hence, Eq. (6.26.12) yields the result for the anomaly in the current labeled by μ, a:

$$(p+q)^\mu \mathcal{A}^{abc}_{\mu\nu\rho} = \frac{i}{48\pi^2} D^{abc}\Big[(p+q)_\nu (A+B)_\rho + (A+B)_\nu (p+q)_\rho + g_{\nu\rho}(p+q)\cdot(A+B) - 3i\epsilon_{\nu\rho\kappa\lambda}(p+q)^\kappa (A-B)^\lambda\Big]. \tag{6.26.23}$$

Repeating all of the steps starting with Eq. (6.26.9), we similarly obtain[75]:

$$-p^\nu \mathcal{A}^{abc}_{\mu\nu\rho} = -\frac{i}{48\pi^2} D^{abc}\Big[p_\rho (A+B)_\mu + p_\mu (A+B)_\rho + g_{\mu\rho} p\cdot(A+B) - 3i\epsilon_{\rho\mu\kappa\lambda} p^\kappa (A-B+2q)^\lambda\Big], \tag{6.26.24}$$

$$-q^\rho \mathcal{A}^{abc}_{\mu\nu\rho} = -\frac{i}{48\pi^2} D^{abc}\Big[q_\mu (A+B)_\nu + q_\nu (A+B)_\mu + g_{\mu\nu} q\cdot(A+B) - 3i\epsilon_{\mu\nu\kappa\lambda} q^\kappa (A-B-2p)^\lambda\Big]. \tag{6.26.25}$$

Non-chiral anomalies will arise for all three of the currents (assuming D^{abc} is non-vanishing), unless we choose the arbitrary constant vectors A and B such that

$$A+B=0, \tag{6.26.26}$$

with the result:

$$(p+q)^\mu \mathcal{A}^{abc}_{\mu\nu\rho} = \frac{1}{8\pi^2} D^{abc}\epsilon_{\nu\rho\kappa\lambda}(p+q)^\kappa A^\lambda, \tag{6.26.27}$$

$$-p^\nu \mathcal{A}^{abc}_{\mu\nu\rho} = -\frac{1}{8\pi^2} D^{abc}\epsilon_{\rho\mu\kappa\lambda} p^\kappa (A+q)^\lambda, \tag{6.26.28}$$

$$-q^\rho \mathcal{A}^{abc}_{\mu\nu\rho} = -\frac{1}{8\pi^2} D^{abc}\epsilon_{\mu\nu\kappa\lambda} q^\kappa (A-p)^\lambda. \tag{6.26.29}$$

If D^{abc} is non-vanishing, it is not possible to avoid an anomaly simultaneously in all three symmetries, but one can still arrange for two of the symmetries to be non-anomalous. If one wants an anomaly to arise only in the current labeled by μ, a (for example, if the symmetries labeled by b, c are gauged), one must now choose $A = p - q$. The standard result follows:

$$(p+q)^\mu \mathcal{A}^{abc}_{\mu\nu\rho} = -\frac{1}{4\pi^2} D^{abc}\epsilon_{\nu\rho\kappa\lambda} p^\kappa q^\lambda, \tag{6.26.30}$$

$$-p^\nu \mathcal{A}^{abc}_{\mu\nu\rho} = 0, \tag{6.26.31}$$

$$-q^\rho \mathcal{A}^{abc}_{\mu\nu\rho} = 0. \tag{6.26.32}$$

In particular, one cannot gauge all three symmetries labeled by a, b, c unless $D^{abc} = 0$.

If all three currents are identical, then by Bose symmetry the anomalies of the three currents must coincide. This can be achieved by choosing $A = \frac{1}{3}(p-q)$, in which case,

$$(p+q)^\mu \mathcal{A}^{abc}_{\mu\nu\rho} = -\frac{1}{12\pi^2} D^{abc}\epsilon_{\nu\rho\kappa\lambda} p^\kappa q^\lambda, \tag{6.26.33}$$

$$-p^\nu \mathcal{A}^{abc}_{\mu\nu\rho} = -\frac{1}{12\pi^2} D^{abc}\epsilon_{\rho\mu\kappa\lambda} p^\kappa q^\lambda, \tag{6.26.34}$$

$$-q^\rho \mathcal{A}^{abc}_{\mu\nu\rho} = -\frac{1}{12\pi^2} D^{abc}\epsilon_{\mu\nu\kappa\lambda} p^\kappa q^\lambda. \tag{6.26.35}$$

Returning briefly to the original naive Ward identities given in Eqs. (6.26.3)–(6.26.5), the analysis above shows that these identities must be modified by an additional additive contribution given by the right-hand side of Eqs. (6.26.27)–(6.26.29). In particular, there is no anomalous contribution proportional to f^{abc}. This can be checked explicitly by a diagrammatic computation of the two-point and three-point functions that appear in Eqs. (6.26.3) and (6.26.5). We use Eqs. (E.2.12) and (E.2.16) to write

$$\mathrm{Tr}(\boldsymbol{T^a T^b T^c}) = D^{abc}(R) + \frac{i}{2} I_2(R) f^{abc}, \tag{6.26.36}$$

where $I_2(R)$ is the index defined in Eq. (E.2.1) and R is the representation of the generators $\boldsymbol{T^a}$. For example, inserting this result in Eq. (6.26.2), it follows that:

$$(p+q)^\mu\, iI^{abc}_{\mu\nu\rho} = -\left[D^{abc} X^{\kappa\lambda} + \frac{i}{2} I_2(R) f^{abc} Y^{\kappa\lambda}\right] \mathrm{Tr}[\sigma_\kappa \overline{\sigma}_\nu \sigma_\lambda \overline{\sigma}_\rho], \tag{6.26.37}$$

[75] Alternatively, one can simply note that Eq. (6.26.24) follows from Eq. (6.26.23) by making the replacements $\mu \to \nu$, $\nu \to \rho$, $\rho \to \mu$, $A \to A+q$, $B \to B-q$, $p \to q$, and $q \to -p-q$, while Eq. (6.26.25) follows from Eq. (6.26.23) by making the replacements $\mu \to \rho$, $\nu \to \mu$, $\rho \to \nu$, $A \to A-p$, $B \to B+p$, $p \to -p-q$, and $q \to p$.

where the integral $Y^{\kappa\lambda}$ is given by[76]:

$$Y^{\kappa\lambda} = \int \frac{\mathrm{d}^4k}{(2\pi)^4}\left[\frac{(k-p)^\kappa}{(k-p)^2}\frac{k^\lambda}{k^2} - \frac{(k+q)^\kappa}{(k+q)^2}\frac{k^\lambda}{k^2} - \frac{k^\kappa}{k^2}\frac{(k-q)^\lambda}{(k-q)^2} + \frac{k^\kappa}{k^2}\frac{(k+p)^\lambda}{(k+p)^2}\right]. \tag{6.26.38}$$

By letting $k \to -k$ in the third and fourth term in the integrand of Eq. (6.26.38), we see that $Y^{\kappa\lambda} = Y^{\lambda\kappa}$, and hence by Eq. (B.2.26),

$$-\frac{i}{2}I_2(R)f^{abc}\,Y^{\kappa\lambda}\mathrm{Tr}[\sigma_\kappa\overline{\sigma}_\nu\sigma_\lambda\overline{\sigma}_\rho] = -iI_2(R)f^{abc}\left[2Y_{\nu\rho} - g_{\nu\rho}Y_\lambda{}^\lambda\right]. \tag{6.26.39}$$

Since no ϵ-tensor appears, we can evaluate this integral in $d \neq 4$ dimensions using the standard techniques of dimensional regularization.

One can check that this result matches the diagrammatic calculation of the right-hand side of Eq. (6.26.27). In particular, Fig. 6.26.3 yields

$$\begin{aligned} i\Pi^{ab}_{\mu\nu}(q) &= (-1)\int \frac{\mathrm{d}^4k}{(2\pi)^4}\mathrm{Tr}\left[(-i\overline{\sigma}_\mu \boldsymbol{T^a})\frac{ik\cdot\sigma}{k^2}(-i\overline{\sigma}_\nu \boldsymbol{T^b})\frac{i(k+q)\cdot\sigma}{(k+q)^2}\right] \\ &= -I_2(R)\delta^{ab}\mathrm{Tr}(\overline{\sigma}_\mu\sigma_\rho\overline{\sigma}_\nu\sigma_\lambda)\int\frac{\mathrm{d}^4k}{(2\pi)^4}\frac{k^\rho(k+q)^\lambda}{k^2(k+q)^2}, \end{aligned} \tag{6.26.40}$$

where we have used Eq. (E.2.1). Lorentz covariance implies that

$$i\Pi^{ab}_{\mu\nu}(q) = \delta^{ab}\left[C_1(q^2)g_{\mu\nu} + C_2(q^2)q_\mu q_\nu\right], \tag{6.26.41}$$

for some scalar functions C_1 and C_2. It follows that $\Pi^{ab}_{\mu\nu}(q) = \Pi^{ab}_{\mu\nu}(-q)$ and $\Pi^{ab}_{\mu\nu}(q) = \Pi^{ab}_{\nu\mu}(q)$. Consequently, we can write:

$$\Pi^{ab}_{\mu\nu}(q) = \frac{i}{2}I_2(R)\delta^{ab}\mathrm{Tr}(\overline{\sigma}_\mu\sigma_\rho\overline{\sigma}_\nu\sigma_\lambda + \overline{\sigma}_\nu\sigma_\rho\overline{\sigma}_\mu\sigma_\lambda)\int\frac{\mathrm{d}^4k}{(2\pi)^4}\frac{k^\rho(k+q)^\lambda}{k^2(k+q)^2}, \tag{6.26.42}$$

and so no ϵ-tensor appears in the evaluation of the trace. As above, we are now free to evaluate the integral in $d \neq 4$ dimensions. Comparing Eqs. (6.26.37) and (6.26.38) to Eq. (6.26.42), and using Eq. (6.26.27), the end result is

$$(p+q)^\mu\, i\Gamma^{abc}_{\mu\nu\rho}(-p-q,p,q) = I_2(R)f^{abc}\left[\Pi_{\nu\rho}(q) - \Pi_{\nu\rho}(p)\right] + \frac{1}{8\pi^2}D^{abc}(R)\epsilon_{\nu\rho\kappa\lambda}(p+q)^\kappa A^\lambda, \tag{6.26.43}$$

where we have written $\Pi^{ab}_{\nu\rho} \equiv I_2(R)\delta^{ab}\Pi_{\nu\rho}$. Indeed the terms on the right-hand side proportional to f^{abc} match those of the naive Ward identity given in Eq. (6.26.3). As previously asserted, the anomaly only resides in the contributions to the Ward identity proportional to D^{abc}.

In writing down Eq. (6.26.2), we chose to use the rules with $\overline{\sigma}$ matrices for the current vertices and σ matrices for the massless fermion propagators. If we had chosen the opposite prescription (i.e., σ matrices for the current vertices and $\overline{\sigma}$ matrices for the massless fermion propagators), then the order of the factors inside the trace of Eq. (6.26.2) would have been reversed.[77] Instead of Eq. (6.26.12), we would have obtained

$$(p+q)^\mu \mathcal{A}^{abc}_{\mu\nu\rho} = -D^{abc}\,\mathrm{Tr}[\overline{\sigma}_\kappa\sigma_\nu\overline{\sigma}_\lambda\sigma_\rho]\bar{X}^{\kappa\lambda} = -2D^{abc}\left[\bar{X}_{\nu\rho} + \bar{X}_{\rho\nu} - g_{\nu\rho}\bar{X}_\lambda{}^\lambda - i\epsilon_{\kappa\nu\lambda\rho}\bar{X}^{\kappa\lambda}\right], \tag{6.26.44}$$

after applying Eq. (B.2.27). The integral $\bar{X}^{\kappa\lambda}$ is simply related to $X^{\kappa\lambda}$ by:

$$\bar{X}^{\kappa\lambda} = X^{\lambda\kappa}. \tag{6.26.45}$$

Inserting Eq. (6.26.45) into Eq. (6.26.44), we immediately reproduce the result of Eq. (6.26.12), as expected.

It is instructive to examine the case of massless QED. The terms of the Lagrangian involving the electron fields is given by

$$\mathscr{L} = i\chi^\dagger\overline{\sigma}^\mu D_\mu\chi + i\eta^\dagger\overline{\sigma}^\mu D_\mu\eta, \tag{6.26.46}$$

where $D_\mu \equiv \partial_\mu + iQA_\mu$ is the covariant derivative, and Q is the charge operator. Here, we identify χ as the two-component (left-handed) electron field and η as the two-component (left-handed) positron field. The corresponding eigenvalues of

---

76 Here $Y^{\kappa\lambda}$ is obtained from $X^{\kappa\lambda}$ by setting $A = B = 0$, since we can use dimensional regularization for this part of the computation as explained below Eq. (6.26.38).

77 The arrowed fermion lines in the loop must be traversed in the direction parallel [antiparallel] to the arrow directions when the $\overline{\sigma}$ [σ] versions of the propagator rule are employed, as indicated in Eq. (4.4.2) [and in the discussion that follows]. This rule determines the order of the factors inside the spinor trace.

the charge operator are: $Q\chi = -e\chi$ and $Q\eta = +e\eta$ (where $e > 0$ is the electromagnetic gauge coupling constant, or equivalently the electric charge of the positron).

At the classical level, the massless QED Lagrangian [Eq. (6.26.46)] is invariant under a $\mathrm{U}(1)_V \times \mathrm{U}(1)_A$ global symmetry. Under a $\mathrm{U}(1)_V \times \mathrm{U}(1)_A$ transformation specified by the infinitesimal parameters θ_V and θ_A,

$$\mathrm{U}(1)_V: \qquad \delta\chi = ie\theta_V\chi, \qquad \delta\eta = -ie\theta_V\eta, \tag{6.26.47}$$

$$\mathrm{U}(1)_A: \qquad \delta\chi = i\theta_A\chi, \qquad \delta\eta = i\theta_A\eta. \tag{6.26.48}$$

We can combine these equations into a two-dimensional matrix equation,

$$\delta\psi_j = -i\theta_a(\boldsymbol{T_a})_j{}^k\psi_k, \quad \text{where } \psi = \begin{pmatrix}\chi\\ \eta\end{pmatrix}, \tag{6.26.49}$$

and the index a takes on two values, $a = V, A$. It follows that the $\mathrm{U}(1)_V \times \mathrm{U}(1)_A$ generators are given by

$$T_V = e\begin{pmatrix}-1 & 0\\ 0 & 1\end{pmatrix}, \quad \text{for } \mathrm{U}(1)_V, \tag{6.26.50}$$

$$T_A = \begin{pmatrix}-1 & 0\\ 0 & -1\end{pmatrix}, \quad \text{for } \mathrm{U}(1)_A. \tag{6.26.51}$$

The classically conserved Noether currents corresponding to the $\mathrm{U}(1)_V \times \mathrm{U}(1)_A$ global symmetry are the vector and axial currents[78]:

$$J_V^\mu = -e(\chi^\dagger\overline{\sigma}^\mu\chi - \eta^\dagger\overline{\sigma}^\mu\eta), \tag{6.26.52}$$

$$J_A^\mu = -\chi^\dagger\overline{\sigma}^\mu\chi - \eta^\dagger\overline{\sigma}^\mu\eta. \tag{6.26.53}$$

Since the $\mathrm{U}(1)_V$ symmetry is gauged, we demand that this symmetry should be anomaly free. Thus, we make use of Eqs. (6.26.30)–(6.26.32), where we identify the index pair μ, a with the axial vector current and the index pairs ν, b and ρ, c with the vector current. Thus, we compute:

$$D^{AVV} = \mathrm{Tr}\,(T_AT_VT_V) = -2e^2. \tag{6.26.54}$$

Moreover, for an abelian symmetry group, $f^{abc} = 0$. Hence, using Eq. (6.26.30) [which also applies in this case to the unsymmetrized three-point function], the U(1) axial vector anomaly equation reads:

$$(p+q)^\mu\, i\Gamma^{AVV}_{\mu\nu\rho} = \frac{e^2}{2\pi^2}\epsilon_{\nu\rho\kappa\lambda}p^\kappa q^\lambda, \tag{6.26.55}$$

in agreement with the well-known result.[79]

We now convert Eq. (6.26.55) into an operator equation. Consider the process of two photon production by an axial vector current source [239]. First, we note that $\partial_\mu J_A^\mu(x) = i[P^\mu, J_{A\mu}(x)]$, where P^μ is the momentum operator. It follows that:

$$\langle p,\ q|\partial_\mu J_A^\mu(0)|0\rangle = i\langle p,\ q|[P^\mu,\ J_{A\mu}(0)]|0\rangle = i(p+q)^\mu\langle p,\ q|J_{A\mu}(0)|\,0\rangle. \tag{6.26.56}$$

We identify the S-matrix amplitude for the two photon production as:

$$i\Gamma^{AVV}_{\mu\nu\rho}\,\varepsilon^{\nu\,*}(p)\varepsilon^{\rho\,*}(q) = \langle p,\ q| - iJ_{A\mu}(0)|\,0\rangle, \tag{6.26.57}$$

where $\varepsilon(p)$ and $\varepsilon(q)$ are the polarization vectors for the final state photons. Note that the factor of $-i$ on the right-hand side of Eq. (6.26.57) has been inserted to be consistent with the Feynman rule for the axial vector current insertion given in Fig. 6.26.1. Thus, using Eqs. (6.26.55)–(6.26.57), we end up with [114]:

$$\begin{aligned}\langle p,\ q|\partial_\mu J_A^\mu(0)|0\rangle &= -\frac{e^2}{2\pi^2}\epsilon_{\nu\rho\kappa\lambda}\varepsilon^{\nu\,*}(p)\varepsilon^{\rho\,*}(q)p^\kappa q^\lambda\\ &= -\frac{e^2}{16\pi^2}\langle p,\ q|\epsilon_{\kappa\nu\lambda\rho}F^{\kappa\nu}F^{\lambda\rho}(0)\,|0\rangle,\end{aligned} \tag{6.26.58}$$

78 Note that the interaction Lagrangian for massless QED is $\mathscr{L}_{\rm int} = -J_V^\mu A_\mu$, as expected. This accounts for the factor of e in the definition of the vector current. The axial vector current does not couple to the photon field; hence no coupling constant is included in its definition.

79 This result was first obtained by Adler [238]. In comparing Eq. (6.26.55) with Adler's result, note that the normalization of the triangle amplitude in Ref. [238] differs by a factor of $(2\pi)^4$ and the opposite sign convention for ϵ_{0123} is employed.

where $\epsilon_{\kappa\nu\lambda\rho}F^{\kappa\nu}F^{\lambda\rho} = 4\epsilon_{\kappa\nu\lambda\rho}(\partial^\kappa A^\nu)(\partial^\lambda A^\rho)$ has been used to eliminate the photon fields in favor of a product of electromagnetic field strength tensors. In deriving Eq. (6.26.58), an additional factor of two arises due to two possible contractions of the photon fields with the external states. We thus obtain the operator form for the axial vector anomaly[80]:

$$\partial_\mu J_A^\mu = -\frac{e^2}{8\pi^2}F^{\lambda\rho}\widetilde{F}_{\lambda\rho}, \tag{6.26.59}$$

where the dual electromagnetic field strength tensor is defined by $\widetilde{F}_{\lambda\rho} \equiv \frac{1}{2}\epsilon_{\kappa\nu\lambda\rho}F^{\kappa\nu}$.

As a final example, we examine the anomalous baryon number and lepton number currents in the theory of electroweak interactions [240–242]. For simplicity of notation, we consider a one-generation model. The baryon number current is a vector current given by:

$$J_B^\mu = \frac{1}{3}\left[u^\dagger\overline{\sigma}^\mu u + d^\dagger\overline{\sigma}^\mu d - \bar{u}^\dagger\overline{\sigma}^\mu\bar{u} - \bar{d}^\dagger\overline{\sigma}^\mu\bar{d}\right], \tag{6.26.60}$$

following the particle naming conventions of Table 5.1. Consider the process of gauge boson pair production by a baryon number current source. It is convenient to work in the interaction basis of gauge fields, $\{W^{\mu a}, B^\mu\}$, where $W^{\mu a}$ is an SU(2)-triplet of gauge fields and B^μ is a $U(1)_Y$ hypercharge gauge field. We consider triangle diagrams where one generation of quarks runs in the loop. The external vertices consist of the baryon number current source and the two gauge bosons.

The generators corresponding to the SU(2) gauge boson vertices are given in block diagonal form by:

$$\boldsymbol{T^b} = g\,\mathrm{diag}\left(\frac{\tau^b}{2}\otimes\mathbb{1}_{3\times3},\ 0,\ 0\right), \tag{6.26.61}$$

where the τ^b are the Pauli matrices, $\mathbb{1}_{3\times3}$ is the identity matrix in color space, and $\otimes$ is the Kronecker product.[81] We have included a factor of the weak SU(2) coupling g in the definition of $\boldsymbol{T^b}$, since the Feynman rule given by Fig. 6.26.1 does not explicitly include the gauge coupling. Likewise, the generators corresponding to the $U(1)_Y$ gauge boson vertices are given in block diagonal form by (cf. Table J.1):

$$\boldsymbol{Y} = g'\,\mathrm{diag}\left(\frac{1}{6}\mathbb{1}_{2\times2}\otimes\mathbb{1}_{3\times3},\ -\frac{2}{3}\mathbb{1}_{3\times3},\ \frac{1}{3}\mathbb{1}_{3\times3}\right), \tag{6.26.62}$$

where $\mathbb{1}_{2\times2}$ is the identity matrix in weak isospin space, and g' is the $U(1)_Y$ hypercharge gauge coupling. Finally, the generator corresponding to the baryon number current source is given in block diagonal form by:

$$\boldsymbol{B} = \tfrac{1}{3}\mathrm{diag}\left(\mathbb{1}_{2\times2}\otimes\mathbb{1}_{3\times3},\ -\mathbb{1}_{3\times3},\ -\mathbb{1}_{3\times3}\right). \tag{6.26.63}$$

Consider first the production of two SU(2)-triplet gauge fields. We put $\boldsymbol{T^a} = \boldsymbol{B}$ and associate the indices b and c with the SU(2)-triplet gauge bosons. A simple calculation yields

$$D^{Bbc} = g^2\mathrm{Tr}(\boldsymbol{B}\boldsymbol{T^b}\boldsymbol{T^c}) = \tfrac{1}{2}g^2\delta^{bc}, \tag{6.26.64}$$

where the superscript index B refers to the baryon number current. Since the gauged weak SU(2) and hypercharge $U(1)_Y$ currents must be anomaly free for the mathematical consistency of the electroweak theory, it follows that Eqs. (6.26.30)–(6.26.32) apply. That is, the symmetrized amplitude for the production of SU(2) gauge boson pairs by a baryon number source is anomalous:

$$(p+q)^\mu\mathcal{A}^{Bbc}_{\mu\nu\rho} = -\frac{g^2}{8\pi^2}\delta^{bc}\epsilon_{\nu\rho\kappa\lambda}p^\kappa q^\lambda. \tag{6.26.65}$$

Next, consider the production of two $U(1)_Y$ hypercharge gauge fields. A simple calculation yields

$$D^{BYY} = g'^2\mathrm{Tr}(\boldsymbol{B}\boldsymbol{Y}^2) = -\tfrac{1}{2}g'^2. \tag{6.26.66}$$

That is, the symmetrized amplitude for the production of $U(1)_Y$ gauge boson pairs by a baryon number source is anomalous:

$$(p+q)^\mu\mathcal{A}^{BYY}_{\mu\nu\rho} = \frac{g'^2}{8\pi^2}\epsilon_{\nu\rho\kappa\lambda}p^\kappa q^\lambda. \tag{6.26.67}$$

Finally, the symmetrized amplitude for the associated production of an SU(2)-triplet and $U(1)_Y$ hypercharge gauge field exhibits no anomaly as the corresponding $D^{BYc} = gg'\mathrm{Tr}(\boldsymbol{B}\boldsymbol{Y}\boldsymbol{T^c}) = 0$.

---

80 In the literature, Eq. (6.26.59) often occurs with the opposite sign due to a sign convention for the Levi-Civita ϵ-tensor that is opposite to the one employed in this review. Here, we have reproduced the form given in Ref. [114].

81 The Kronecker product of an $n\times n$ matrix and an $m\times m$ matrix is an $nm\times nm$ matrix. In addition, the following two properties of the Kronecker product are noteworthy [159,243]: (i) $(A\otimes B)(C\otimes D) = AC\otimes BD$, and (ii) $\mathrm{Tr}(A\otimes B) = \mathrm{Tr}\,A\,\mathrm{Tr}\,B$.

The symmetrized amplitudes of the triangle diagrams involving a baryon number current source and a pair of SU(2) or $U(1)_Y$ gauge bosons are anomalous. Since the baryon number current is a vector current, we conclude that the source of the anomaly is a VVA triangle diagram in which one of the gauge boson currents is vector (V) and the other gauge boson current is axial vector (A). Nevertheless, the gauge boson axial vector current must be conserved, as noted above. Hence, the baryon number vector current must be anomalous [240]. In Eqs. (6.26.55)–(6.26.58), we showed how to derive the operator form of the anomaly equation from the anomalous non-conservation of the symmetrized triangle amplitude. Following the same set of steps starting with Eqs. (6.26.65) and (6.26.67), one obtains the anomalous non-conservation of the baryon number vector current, in a model with N_g quark generations [55,241,242]:

$$\partial_\mu J_B^\mu = \frac{g^2 N_g}{32\pi^2} W^{\lambda\rho b} \widetilde{W}^b_{\lambda\rho} - \frac{g'^2 N_g}{32\pi^2} B^{\lambda\rho} \widetilde{B}_{\lambda\rho}, \tag{6.26.68}$$

where $B_{\lambda\rho}$ and

$$W^b_{\lambda\rho} = \partial_\lambda W^b_\rho - \partial_\rho W^b_\lambda - g\epsilon^{bca} W^c_\lambda W^a_\rho, \tag{6.26.69}$$

are the field strength tensors for the hypercharge $U(1)_Y$ gauge boson and SU(2) gauge boson fields, respectively.[82] Note that for the non-abelian SU(2) gauge fields W^a_μ,

$$\begin{aligned} W^{\lambda\rho b}\, \widetilde{W}^b_{\lambda\rho} &= 2\epsilon^{\kappa\nu\lambda\rho} \left[(\partial_\kappa W^b_\nu)(\partial_\lambda W^b_\rho) - g\epsilon^{abc} (\partial_\kappa W^a_\nu) W^b_\lambda W^c_\rho \right] \\ &= 2\epsilon^{\kappa\nu\lambda\rho} \partial_\kappa \left[W^b_\nu (\partial_\lambda W^b_\rho) - \tfrac{1}{3} g\epsilon^{abc} W^a_\nu W^b_\lambda W^c_\rho \right]. \end{aligned} \tag{6.26.70}$$

Strictly speaking, the triangle graphs yield only the terms on the right-hand side of Eq. (6.26.68) that are quadratic in the gauge fields. To obtain the corresponding terms that are cubic in the gauge terms, one must compute the anomalies that arise from VVVA and VAAA box diagrams [234,244].

For completeness, we re-express the anomalous non-conservation of the baryon number current in terms of the mass-eigenstate SU(2) × $U(1)_Y$ gauge fields:

$$\partial_\mu J_B^\mu = \frac{g^2 N_g}{16\pi^2} W^{\lambda\rho +} \widetilde{W}^-_{\lambda\rho} - \frac{g^2 N_g}{32\pi^2 c_W^2} Z^{\lambda\rho} \widetilde{Z}_{\lambda\rho} - \frac{egN_g}{32\pi^2 c_W} \left[Z^{\lambda\rho} \widetilde{F}_{\lambda\rho} + F^{\lambda\rho} \widetilde{Z}_{\lambda\rho} \right], \tag{6.26.71}$$

where $c_W \equiv \cos\theta_W$, and $W^\pm_{\lambda\rho}$, $Z_{\lambda\rho}$ and $F_{\lambda\rho}$ are the $W^\pm$, Z and the electromagnetic field strength tensors, respectively.

By a similar analysis, one can also compute the anomalous non-conservation of the lepton number vector current,

$$J_L^\mu = \ell^\dagger \overline{\sigma}^\mu \ell + \nu^\dagger \overline{\sigma}^\mu \nu - \bar{\ell}^\dagger \overline{\sigma}^\mu \bar{\ell}, \tag{6.26.72}$$

due to triangle diagrams with N_g generations of leptons running in the loop. In the one-generation calculation, the relevant generators are:

$$\boldsymbol{T^b} = g\, \mathrm{diag}\left(\frac{\tau^b}{2}, 0 \right), \qquad \boldsymbol{Y} = g'\, \mathrm{diag}\left(-\tfrac{1}{2} \mathbb{1}_{2\times 2},\ 1 \right), \qquad \boldsymbol{L} = \mathrm{diag}\left(\mathbb{1}_{2\times 2},\ -1 \right). \tag{6.26.73}$$

Thus, we end up with:

$$D^{Lbc} = \tfrac{1}{2} g^2 \delta^{bc}, \qquad D^{LYY} = -\tfrac{1}{2} g'^2, \qquad D^{LYc} = 0. \tag{6.26.74}$$

Thus, in the Standard Model with N_g generations of quarks and leptons,

$$\partial_\mu J_L^\mu = \partial_\mu J_B^\mu. \tag{6.26.75}$$

In particular, the $B - L$ current is conserved and anomaly free.

Acknowledgements

H.K.D. would like to thank the Santa Cruz Institute for Particle Physics and the Stanford Linear Accelerator Center for their hospitality during numerous visits to collaborate on this review. H.E.H. would also like to thank the Physikalisches Institut der Universität Bonn and Northern Illinois University for their hospitality during his visits to collaborate on this review. H.K.D. and H.E.H gratefully acknowledge the support and hospitality of the Aspen Center for Physics, the CERN Theory group, the Institute for Particle Physics Phenomenology at the University of Durham, and the Kavli Institute for Theoretical Physics at the University of California, Santa Barbara, where parts of this review were written. H.E.H. and S.P.M. appreciate the support and hospitality of Fermi National Accelerator Laboratory at various stages of this work.

82 We again caution the reader that a different overall sign in Eq. (6.26.68) often appears in the literature due to a sign convention for the Levi-Civita ϵ-tensor that is opposite to the one employed in this review. Here, we have chosen $\epsilon^{0123} = +1$.

We greatly appreciate many valuable conversations with our colleagues, Jonathan Bagger, Thomas Banks, Andrew Cohen, Athanasios (Sakis) Dedes, Michael Dine, Lance Dixon, Manuel Drees, Rainald Flume, Paul Langacker, Christopher Hill, Daniel Maitre, Hans Peter Nilles, Michael Peskin, Stefano Profumo, Janusz Rosiek, Mark Srednicki, Lorenzo Ubaldi, Pascal Vaudrevange, Carlos Wagner, and Dieter Zeppenfeld. We are also grateful for e-mail comments and suggestions received from Garrett Lisi, Chris Oakley, Nicholas Setzer, José Valle, and the anonymous referee. We thank Michaela Mühl (Physikalisches Institut, Bonn) and Antje Daum (DESY, Hamburg) for their efforts in helping us locate some of the relevant earliest references.

Finally, we would like to acknowledge the funding agencies that supported this work. H.K.D. is supported in part by SFB Transregio 33 ("The Dark Universe"), by BMBF grant 05 HT6PDA, and by the Helmholtz Alliance HA-101 ("Physics at the Terascale"). H.E.H. is supported in part by U.S. Department of Energy grant number DE-FG02-04ER41268 and in part by a Humboldt Research Award sponsored by the Alexander von Humboldt Foundation. The work of S.P.M. is supported in part by the National Science Foundation grants PHY-0140129, PHY-0456635, and PHY-0757325.

Appendix A. Metric and sigma matrix conventions

In this review, the metric tensor of four-dimensional Minkowski space is taken to be[83]:

$$g_{\mu\nu} = g^{\mu\nu} = \text{diag}(+1, -1, -1, -1)\,, \tag{A.1}$$

where $\mu, \nu = 0, 1, 2, 3$ are spacetime vector indices. Contravariant four-vectors (e.g. positions, momenta, gauge fields and currents) are defined with raised indices, and covariant four-vectors (e.g. derivatives) with lowered indices:

$$x^\mu = (t; \vec{\boldsymbol{x}}), \tag{A.2}$$

$$p^\mu = (E; \vec{\boldsymbol{p}}), \tag{A.3}$$

$$A^\mu(x) = (\Phi(\vec{\boldsymbol{x}}, t); \vec{\boldsymbol{A}}(\vec{\boldsymbol{x}}, t)), \tag{A.4}$$

$$J^\mu(x) = (\rho(\vec{\boldsymbol{x}}, t); \vec{\boldsymbol{J}}(\vec{\boldsymbol{x}}, t)), \tag{A.5}$$

$$\partial_\mu \equiv \frac{\partial}{\partial x^\mu} = (\partial/\partial t; \vec{\boldsymbol{\nabla}}), \tag{A.6}$$

in units with $c = 1$. The totally antisymmetric pseudo-tensor $\epsilon^{\mu\nu\rho\sigma}$ is defined such that

$$\epsilon^{0123} = -\epsilon_{0123} = +1. \tag{A.7}$$

Eqs. (A.2)–(A.7) are taken to be independent of the metric signature convention.

The sigma matrices are defined with a raised (contravariant) index to be independent of the metric signature convention,

$$\sigma^\mu = (\mathbb{1}_{2\times2}; \vec{\boldsymbol{\sigma}}), \qquad \overline{\sigma}^\mu = (\mathbb{1}_{2\times2}; -\vec{\boldsymbol{\sigma}}), \tag{A.8}$$

where the three-vector of Pauli matrices is given by $\vec{\boldsymbol{\sigma}} \equiv (\sigma^1, \sigma^2, \sigma^3)$ [cf. Eq. (2.27)] and $\mathbb{1}_{2\times2}$ is the 2×2 identity matrix. The corresponding quantities with lower (covariant) index are:

$$\sigma_\mu = g_{\mu\nu}\sigma^\nu = (\mathbb{1}_{2\times2}; -\vec{\boldsymbol{\sigma}}), \qquad \overline{\sigma}_\mu = g_{\mu\nu}\overline{\sigma}^\nu = (\mathbb{1}_{2\times2}; \vec{\boldsymbol{\sigma}}). \tag{A.9}$$

Various identities involving products of sigma matrices are given in Appendix B. The generators of the $(\frac{1}{2}, 0)$ and $(0, \frac{1}{2})$ representations of the Lorentz group are, respectively, given by:

$$\sigma^{\mu\nu} \equiv \frac{i}{4}(\sigma^\mu\overline{\sigma}^\nu - \sigma^\nu\overline{\sigma}^\mu), \qquad \overline{\sigma}^{\mu\nu} \equiv \frac{i}{4}(\overline{\sigma}^\mu\sigma^\nu - \overline{\sigma}^\nu\sigma^\mu). \tag{A.10}$$

In adopting the above definition of the sigma matrices, we differ from the corresponding conventions of Wess and Bagger [68] and Bilal [82]. The Wess/Bagger and Bilal (WBB) definition of the sigma matrices can be written (with lowered index μ) as[84]:

$$(\sigma^{\text{WBB}})_{\mu\,\alpha\dot{\beta}} = \sigma_{0\alpha\dot{\gamma}}\overline{\sigma}_\mu^{\dot{\gamma}\delta}\sigma_{0\delta\dot{\beta}} = (\mathbb{1}_{2\times2}; \vec{\boldsymbol{\sigma}}), \tag{A.11}$$

$$(\overline{\sigma}^{\text{WBB}})_\mu^{\dot{\alpha}\beta} = \overline{\sigma}_0^{\dot{\alpha}\gamma}\sigma_{\mu\gamma\dot{\delta}}\overline{\sigma}_0^{\dot{\delta}\beta} = (\mathbb{1}_{2\times2}; -\vec{\boldsymbol{\sigma}}). \tag{A.12}$$

One consequence of the WBB definition of σ and $\overline{\sigma}$ is that $\gamma_5 = \text{diag}(\mathbb{1}_{2\times2}, -\mathbb{1}_{2\times2})$ in the chiral representation [cf. Eq. (G.1.2)]. This associates a lowered undotted [raised dotted] two-component spinor with a right-handed [left-

83 An otherwise identical version of this paper with the opposite metric signature is also available; see footnote 2.

84 Although Wess/Bagger and Bilal employ opposite metric signatures of $g_{00} = -1$ and $g_{00} = +1$, respectively, their definitions of σ_μ and $\overline{\sigma}_\mu$ (with covariant index μ) coincide. Note that the spinor structure of the σ and $\overline{\sigma}$ matrices and the definitions of the various (two-index and four-index) epsilon tensors [cf. Eqs. (2.19) and (A.7)] are identical in both the WBB conventions and in our conventions.

handed] four-component spinor [cf. Eqs. (G.1.6) and (G.1.8)]. Indeed, this was the common convention in the older literature (e.g., see Refs. [35,36,38,39,41,58]).[85] However, in the modern formulation of electroweak theory in terms of left-handed fermions, it is now more common to associate a lower undotted [raised dotted] two-component spinor with a left-handed [right-handed] four-component spinor. This is the motivation for our conventions for the sigma matrices given in Eqs. (A.8) and (A.9).

In order to facilitate the comparison with the metric signature with $g_{00} = -1$, we provide the key ingredients needed for translating between Minkowski metrics of opposite signature. In our conventions [cf. Eqs. (A.2)–(A.9)], each of the following objects (with the Lorentz index heights as shown) is defined *independently* of the metric signature:

$$x^\mu,\ p^\mu,\ \partial_\mu,\ \sigma^\mu,\ \overline{\sigma}^\mu,\ S^\mu,\ J^\mu,\ A^\mu,\ D_\mu,\ G^\mu{}_\nu,\ \gamma^\mu,\ \gamma_5,\ \delta^\mu_\nu,\ \epsilon^{\mu\nu\rho\sigma},\ \epsilon_{\mu\nu\rho\sigma}, \qquad \text{[no sign change]}, \tag{A.13}$$

but the following objects change sign when the Minkowski metric signature is reversed:

$$g_{\mu\nu},\ g^{\mu\nu},\ x_\mu,\ p_\mu,\ \partial^\mu,\ \sigma_\mu,\ \overline{\sigma}_\mu,\ S_\mu,\ J_\mu,\ A_\mu,\ D^\mu,\ G^{\mu\nu},\ G_{\mu\nu},\ \gamma_\mu, \quad \text{[sign change]}. \tag{A.14}$$

Here, the spin four-vector S^μ is defined in Eq. (3.1.15), J^μ is any conserved current, A^μ is any gauge vector potential, and D_μ and $G_{\mu\nu}$ are the corresponding covariant derivative and antisymmetric tensor field strength, respectively. The Dirac gamma matrices are defined in Eq. (G.1.2). The list of Eq. (A.14) can be deduced from Eq. (A.13) by using the metric tensor and its inverse to lower and raise Lorentz indices, simply because each metric or inverse metric changes sign when the metric signature is reversed. Given any other object not included in Eqs. (A.13) and (A.14), it is straightforward to make the appropriate assignment by considering how the object is defined. For example, we must assign $\sigma_{\mu\nu}$, $\overline{\sigma}_{\mu\nu}$, $\sigma^{\mu\nu}$ and $\overline{\sigma}^{\mu\nu}$ to the list of Eq. (A.13), based on the definitions given in Eqs. (2.70) and (2.71). In general, objects that do not carry Lorentz vector indices (including all fermion spinor fields and spinor wave functions) are defined to be the same in the two metric signatures, with the obvious exception of scalar quantities formed from an odd number of objects from the list of Eq. (A.14). For example, the dot product of two four-vectors may or may not change sign when the Minkowski metric signature is reversed. By writing out the dot product explicitly using the metric tensor to contract the indices, one can use Eqs. (A.13) and (A.14) to determine the behavior of a dot product under the reversal of the metric signature. In particular, $p \cdot A$ changes sign whereas $p \cdot \sigma$ does not change sign, when the Minkowski metric signature is reversed.

The translation between Minkowski metrics of opposite signatures is now straightforward. Given any relativistic covariant quantity or equation in the convention where $g_{00} = +1$, one need only employ Eqs. (A.13) and (A.14) to obtain the same quantity or equation in the convention where $g_{00} = -1$, and vice versa.[86]

As an example, let us verify that under the reversal of the Minkowski metric signature the gauge covariant derivative D_μ does not change sign and the gauge field strength tensor $G^{\mu\nu}$ changes sign. In the metric signature with $g_{00} = +1$, we define

$$D_\mu \equiv \boldsymbol{I}_{d_R}\partial_\mu + igA_\mu, \quad (g_{00} = +1), \tag{A.15}$$

where $A_\mu \equiv A^a_\mu \boldsymbol{T^a}$ is the matrix gauge field for a representation R of dimension d_R, and $\boldsymbol{I}_{d_R}$ is the $d_R \times d_R$ identity matrix. Since under the reversal of the metric signature, ∂_μ does not change sign [according to Eq. (A.13)] whereas A_μ changes sign [according to Eq. (A.14)], it follows that the quantity defined in the metric signature where $g_{00} = -1$,

$$D_\mu \equiv \boldsymbol{I}_{d_R}\partial_\mu - igA_\mu, \quad (g_{00} = -1) \tag{A.16}$$

has the same overall sign as Eq. (A.15). It follows that when the metric signature is reversed, D_μ does not change sign whereas $D^\mu \equiv g^{\mu\nu}D_\nu$ does change sign, as indicated in Eqs. (A.13) and (A.14). Next, consider the matrix gauge field strength tensor $G_{\mu\nu} \equiv G^a_{\mu\nu}\boldsymbol{T^a}$, defined by

$$G^{\mu\nu} \equiv \frac{-i}{g}[D^\mu, D^\nu] = \partial^\mu A^\nu - \partial^\nu A^\mu + ig[A^\mu, A^\nu], \quad (g_{00} = +1), \tag{A.17}$$

where the commutator $[D^\mu, D^\nu]$ is an operator that acts on fields that transform with respect to an arbitrary representation R. In the metric signature with $g_{00} = -1$, we define the gauge field strength tensor as a commutator of covariant derivatives with the *opposite* overall sign:

$$G^{\mu\nu} \equiv \frac{i}{g}[D^\mu, D^\nu] = \partial^\mu A^\nu - \partial^\nu A^\mu - ig[A^\mu, A^\nu], \quad (g_{00} = -1). \tag{A.18}$$

where D^μ is now defined as in Eq. (A.16). Since under a reversal of the metric signature, A^μ does not change sign [according to Eq. (A.13)] whereas ∂^μ changes sign [according to Eq. (A.14)], it follows that $G^{\mu\nu}$ and $G_{\mu\nu} \equiv g_{\mu\rho}g_{\nu\sigma}G^{\rho\sigma}$ do indeed change sign when the metric signature is reversed, as stated in Eq. (A.14).

---

85 This convention persists in the literature of the spinor helicity method (cf. footnote 156 in Appendix I.2).

86 Note that for any relativistic covariant term appearing additively in a valid equation, the *relative* sign that results from changing between Minkowski metrics of opposite signature is simply given by $\mathcal{S} = (-1)^{\mathcal{N}}$, where $\mathcal{N} \equiv N_m + N_d + N_G + \cdots$. Here N_m is the number of metric tensors appearing either explicitly or implicitly through contracted upper and lower indices, N_d is the number of spacetime and/or covariant derivatives, N_G is the number of gauge field strength tensors, and the ellipsis (. . .) accounts for any additional quantities whose contravariant forms (with all Lorentz indices raised) appear in the list of Eq. (A.14).

As another simple illustration, consider the σ-matrix identity,

$$\overline{\sigma}^{\mu}\sigma^{\nu}\overline{\sigma}^{\rho} = g^{\mu\nu}\overline{\sigma}^{\rho} - g^{\mu\rho}\overline{\sigma}^{\nu} + g^{\nu\rho}\overline{\sigma}^{\mu} - i\epsilon^{\mu\nu\rho\kappa}\overline{\sigma}_{\kappa}, \quad (g_{00} = +1), \tag{A.19}$$

In the opposite metric signature with $g_{00} = -1$, we apply the results of Eqs. (A.13) and (A.14) and then multiply both sides of the equation by -1 to obtain:

$$\overline{\sigma}^{\mu}\sigma^{\nu}\overline{\sigma}^{\rho} = -g^{\mu\nu}\overline{\sigma}^{\rho} + g^{\mu\rho}\overline{\sigma}^{\nu} - g^{\nu\rho}\overline{\sigma}^{\mu} + i\epsilon^{\mu\nu\rho\kappa}\overline{\sigma}_{\kappa}, \quad (g_{00} = -1). \tag{A.20}$$

Finally, in the sigma matrix conventions of Wess/Bagger [68] and Bilal [82], both Eqs. (A.19) and (A.20) are modified by changing the overall sign of $i\epsilon^{\mu\nu\rho\kappa}\overline{\sigma}_{\kappa}$. In general, to convert the identities of Appendix B to the conventions of WBB, one must first convert (if necessary) to the appropriate metric signature, and then interchange $\sigma \leftrightarrow \overline{\sigma}$ [cf. Eqs. (A.11) and (A.12)].

We end this appendix with a brief summary of our conventions for four-dimensional Euclidean space. The Euclidean components of the coordinates [represented in Minkowski space by the contravariant four-vector, $x^{\mu} = (x^0; \vec{\boldsymbol{x}})$, for $\mu = 0, 1, 2, 3$], are defined as

$$x_E^{\mu} = x_{E\,\mu} = (\vec{\boldsymbol{x}}, x_E^4), \qquad x_E^4 = x_{E4} \equiv ix^0, \quad (\mu = 1, 2, 3, 4). \tag{A.21}$$

The four-momentum operator in Minkowski space is $p^{\mu} = i\partial^{\mu} = i(\partial/\partial t, -\vec{\nabla})$. Following the conventions of Ref. [245], the Euclidean counterpart of the momentum operator is

$$p_E^{\mu} = p_{E\mu} = (\vec{\boldsymbol{p}}, p_E^4) = -i\partial_E^{\mu} = -i(\vec{\nabla}, \partial/\partial x_E^4), \qquad p_E^4 = p_{E4} = ip^0. \tag{A.22}$$

The Minkowski space Green functions are obtained from Euclidean space Green functions by means of a Wick rotation [123,245,246] of $x_E^4 \equiv ix^0$ in a counterclockwise sense.[87] Scalar products of Euclidean four-vectors are carried out by employing the Euclidean metric tensor $\delta_{\mu\nu} = \delta^{\mu\nu} = \mathrm{diag}(1, 1, 1, 1)$. For example, the Euclidean counterpart of $-p \cdot x = -p^0x^0 + \vec{\boldsymbol{p}} \cdot \vec{\boldsymbol{x}}$ is $p_E^{\mu}x_E^{\mu} = \vec{\boldsymbol{p}} \cdot \vec{\boldsymbol{x}} + p_E^4x_E^4$, etc. Given any tensorial equation in Euclidean space, the heights of the indices is irrelevant. Consequently, one can simply place all indices at the same height (either all raised or all lowered), with an implied sum over a pair of repeated indices.

One can also introduce Euclidean sigma matrices [247]:

$$\sigma_E^{\mu} \equiv (-i\vec{\boldsymbol{\sigma}}, \sigma_E{}^4), \qquad \overline{\sigma}_E^{\mu} \equiv (i\vec{\boldsymbol{\sigma}}, \overline{\sigma}_E^4), \quad \text{where } \sigma_E{}^4 = \overline{\sigma}_E^4 \equiv \mathbb{1}_{2\times2}, \tag{A.23}$$

which satisfy[88]:

$$\sigma_E^{\mu}\overline{\sigma}_E^{\nu} + \sigma_E^{\nu}\overline{\sigma}_E^{\mu} = 2\delta^{\mu\nu}, \qquad \overline{\sigma}_E^{\mu}\sigma_E^{\nu} + \overline{\sigma}_E^{\nu}\sigma_E^{\mu} = 2\delta^{\mu\nu}. \tag{A.24}$$

The four-dimensional rotation group in Euclidean space is SO(4), which is locally equivalent to SU(2)×SU(2). It possesses two independent pseudo-real two-dimensional spinor representations $(\frac{1}{2}, 0)$ and $(0, \frac{1}{2})$ [not related by hermitian conjugation in contrast to the Lorentz group], with corresponding hermitian generators $\sigma_E^{\mu\nu}$ and $\overline{\sigma}_E^{\mu\nu}$, respectively:

$$\sigma_E^{\mu\nu} = \frac{i}{4}\left(\sigma_E^{\mu}\overline{\sigma}_E^{\nu} - \sigma_E^{\nu}\overline{\sigma}_E^{\mu}\right), \qquad \overline{\sigma}_E^{\mu\nu} = \frac{i}{4}\left(\overline{\sigma}_E^{\mu}\sigma_E^{\nu} - \overline{\sigma}_E^{\nu}\sigma_E^{\mu}\right). \tag{A.25}$$

These tensors are anti-self-dual and self-dual, respectively [120],

$$\sigma_E^{\mu\nu} = -\tfrac{1}{2}\epsilon^{\mu\nu\rho\tau}\sigma_E^{\rho\tau}, \qquad \overline{\sigma}_E^{\mu\nu} = \tfrac{1}{2}\epsilon^{\mu\nu\rho\tau}\overline{\sigma}_E^{\rho\tau}, \tag{A.26}$$

where the totally antisymmetric Levi-Civita tensor is defined in Euclidean space such that $\epsilon^{1234} = \epsilon_{1234} = +1$. One can express $\sigma_E^{\mu\nu}$ and $\overline{\sigma}_E^{\mu\nu}$ in terms of the 't Hooft eta symbols [248],

$$\sigma_E^{\mu\nu} = -\tfrac{1}{2}\overline{\eta}^{k\mu\nu}\sigma^k, \qquad \overline{\sigma}_E^{\mu\nu} = -\tfrac{1}{2}\eta^{k\mu\nu}\sigma^k, \tag{A.27}$$

where $\mu, \nu = 1, 2, 3, 4$ and there is an implicit sum over $k = 1, 2, 3$. Equivalently,

$$\sigma_E^{\mu}\overline{\sigma}_E^{\nu} = \delta^{\mu\nu} + i\overline{\eta}^{k\mu\nu}\sigma^k, \qquad \overline{\sigma}_E^{\mu}\sigma_E^{\nu} = \delta^{\mu\nu} + i\eta^{k\mu\nu}\sigma^k. \tag{A.28}$$

The 't Hooft symbols η and $\overline{\eta}$ satisfy self-duality and anti-self-duality properties, respectively:

$$\eta^{k\mu\nu} = \tfrac{1}{2}\epsilon^{\mu\nu\rho\lambda}\eta^{k\rho\lambda}, \qquad \overline{\eta}^{k\mu\nu} = -\tfrac{1}{2}\epsilon^{\mu\nu\rho\lambda}\overline{\eta}^{k\rho\lambda}, \tag{A.29}$$

and are explicitly given by:

$$\eta^{kij} = \overline{\eta}^{kij} = \epsilon^{ijk}, \qquad \eta^{kj4} = -\eta^{k4j} = \overline{\eta}^{k4j} = -\overline{\eta}^{kj4} = \delta^{kj}, \qquad \eta^{k44} = \overline{\eta}^{k44} = 0. \tag{A.30}$$

For a more comprehensive treatment of two-component spinors in Euclidean space, see Ref. [128].

---

87 Expressing the corresponding Green functions as Fourier transforms of momentum space Green functions, one must simultaneously Wick-rotate $p_E^4 \equiv ip^0$ in a clockwise sense to avoid singularities in the complex p^0-plane.

88 It is seemingly more natural to define $\sigma_E^{\mu} \equiv (\vec{\boldsymbol{\sigma}}, \sigma_E^4)$ and $\overline{\sigma}_E^{\mu} \equiv (-\vec{\boldsymbol{\sigma}}, \overline{\sigma}_E^4)$ where $\sigma_E^4 = \overline{\sigma}_E^4 \equiv i\mathbb{1}_{2\times2}$, in which case one must replace $\delta^{\mu\nu}$ with $-\delta^{\mu\nu}$ in Eq. (A.24). Nevertheless we prefer Eq. (A.23), which avoids an overall minus sign in the respective anticommutation relations of the Euclidean sigma and gamma matrices [cf. footnote 133].

Appendix B. Sigma matrix identities and Fierz identities

In Section 2, we derived a number of identities involving σ^μ, $\overline{\sigma}^\mu$, $\sigma^{\mu\nu}$ and $\overline{\sigma}^{\mu\nu}$. When considering a theory regularized by dimensional continuation [124], one must give meaning to the sigma matrices and their respective identities in $d \neq 4$ dimensions. In many cases, it is possible to reinterpret the sigma matrix identities for $d \neq 4$. However, the Fierz identities, which depend on the completeness of $\{\mathbb{1}_{2\times2}, \sigma^i\}$ in the vector space of 2×2 matrices, do not have a consistent, unambiguous meaning outside of four dimensions (e.g., see Refs. [249–252] and references therein). In Appendix B.1, we exhibit a comprehensive list of identities from which many generalized Fierz identities can be derived. In Appendix B.2, we examine the class of sigma matrix identities that can unambiguously be extended to $d \neq 4$ dimension and thus can be employed in the context of dimensional regularization.

B.1. Two-component spinor Fierz identities

We begin with the basic identity for 2×2 matrices [77],

$$\delta_{ab}\delta_{cd} = \tfrac{1}{2}\left[\delta_{ad}\delta_{cb} + \sigma^i_{ad}\sigma^i_{cb}\right], \tag{B.1.1}$$

where there is an implicit sum over the repeated superscript $i = 1, 2, 3$. Eq. (B.1.1) is a consequence of the completeness of $\{\mathbb{1}_{2\times2}, \sigma^i\}$ in the four-dimensional vector space of 2×2 matrices. In particular, we denote the four-dimensional vector spaces of 2×2 matrices labeled by undotted and dotted spinor indices, respectively, by $\mathcal{V}$ and $\overline{\mathcal{V}}$. It is also useful to consider matrices with one undotted and one dotted index. Hence, we construct the Kronecker product $\mathcal{V} \otimes \overline{\mathcal{V}}$, which is a sixteen-dimensional vector space. The sixteen linearly independent matrices taken from the set,[89]

$$\Gamma \equiv \left\{\delta_\alpha{}^\beta,\ \sigma^\mu_{\alpha\dot\beta},\ \sigma^{\mu\nu}{}_\alpha{}^\beta,\ \delta^{\dot\alpha\dot\beta},\ \sigma^{\mu\,\dot\alpha\beta},\ \overline{\sigma}^{\mu\nu\,\dot\alpha}{}_{\dot\beta}\right\}, \tag{B.1.2}$$

serve as a complete basis set for $\mathcal{V} \otimes \overline{\mathcal{V}}$. Elements of Γ will be denoted by $\Gamma^{(n)}$ $(n = 1, 2, \ldots, 6)$.

Starting from Eq. (B.1.1), one can establish a set of 21 identities of the following form:

$$(\Gamma^{(k)})^I_{AB}(\Gamma^{(n)})^J_{CD} = \sum_{p,q,K,L} (C^{kn}_{pq})^{IJ}_{KL}\,(\Gamma^{(p)})^K_{AD}(\Gamma^{(q)})^L_{CB}, \tag{B.1.3}$$

where each label I, J, K and L can represent zero, one or two Lorentz spacetime indices, and A, B, C and D represent two-component spinor indices, each of which may be undotted or dotted and in the lowered or raised position as appropriate. The sum in Eq. (B.1.3) is taken over the matrices specified in Eq. (B.1.2), and the C^{kn}_{pq} are numerical coefficients [cf. Eqs. (B.1.5)–(B.1.25)].

Let us multiply Eq. (B.1.3) by four (commuting or anticommuting) two-component spinors $Z_{1A}Z_{2B}Z_{3C}Z_{4D}$, where Z_i stands for either the undaggered or daggered spinor z_i or $z_i^\dagger$, depending on whether the corresponding spinor index is undotted or dotted. This procedure yields generalized Fierz identities of the form [74,77,85,88]:

$$(Z_1\Gamma^{(k)I}Z_2)(Z_3\Gamma^{(n)J}Z_4) = (-1)^A \sum_{p,q,K,L} (C^{kn}_{pq})^{IJ}_{KL}(Z_1\Gamma^{(p)K}Z_4)(Z_3\Gamma^{(q)L}Z_2), \tag{B.1.4}$$

where $(-1)^A = +1\,[-1]$ for commuting [anticommuting] spinors.[90]

The explicit expressions for the 21 identities represented by Eq. (B.1.3) are as follows

$$\delta_\alpha{}^\beta\delta^{\dot\beta}{}_{\dot\alpha} = \tfrac{1}{2}\sigma^\mu_{\alpha\dot\alpha}\overline{\sigma}^{\dot\beta\beta}_\mu, \tag{B.1.5}$$

$$\delta_\alpha{}^\beta\delta_\gamma{}^\tau = \tfrac{1}{2}\left[\delta_\alpha{}^\tau\delta_\gamma{}^\beta + (\sigma^{\mu\nu})_\alpha{}^\tau(\sigma_{\mu\nu})_\gamma{}^\beta\right], \tag{B.1.6}$$

$$\delta^{\dot\alpha}{}_{\dot\beta}\delta^{\dot\gamma}{}_{\dot\tau} = \tfrac{1}{2}\left[\delta^{\dot\alpha}{}_{\dot\tau}\delta^{\dot\gamma}{}_{\dot\beta} + (\overline{\sigma}^{\mu\nu})^{\dot\alpha}{}_{\dot\tau}(\overline{\sigma}_{\mu\nu})^{\dot\gamma}{}_{\dot\beta}\right], \tag{B.1.7}$$

$$\delta_\alpha{}^\beta\sigma^\mu_{\gamma\dot\alpha} = \tfrac{1}{2}\sigma^\mu_{\alpha\dot\alpha}\delta_\gamma{}^\beta - i\sigma_{\nu\,\alpha\dot\alpha}(\sigma^{\mu\nu})_\gamma{}^\beta, \tag{B.1.8}$$

$$\delta_\alpha{}^\beta\overline{\sigma}^{\mu\,\dot\beta\gamma} = \tfrac{1}{2}\delta_\alpha{}^\gamma\overline{\sigma}^{\mu\,\dot\beta\beta} + i(\sigma^{\mu\nu})_\alpha{}^\gamma\overline{\sigma}^{\dot\beta\beta}_\nu, \tag{B.1.9}$$

89 Due to the self-duality relations of Eq. (2.75), $\sigma^{\mu\nu}$ and $\overline{\sigma}^{\mu\nu}$ are completely determined by the six matrices σ^{0i} and $\overline{\sigma}^{0i}$ $(i = 1, 2, 3)$. However, for convenience we keep all $\sigma^{\mu\nu}$ and $\overline{\sigma}^{\mu\nu}$ matrices in the set Γ.

90 It is often convenient to reverse the order of the spinors Z_2 and Z_3 on the right-hand side of Eq. (B.1.4) by using Eqs. (2.59)–(2.61) and (2.94)–(2.95) to eliminate the factor of $(-1)^A$ [cf. Eq. (2.67)].

$$\delta^{\dot\alpha}{}_{\dot\beta}\sigma^{\mu}_{\beta\dot\gamma} = \tfrac{1}{2}\delta^{\dot\alpha}{}_{\dot\gamma}\sigma^{\mu}_{\beta\dot\beta} + i(\overline{\sigma}^{\mu\nu})^{\dot\alpha}{}_{\dot\gamma}\sigma_{\nu\,\beta\dot\beta}, \tag{B.1.10}$$

$$\delta^{\dot\alpha}{}_{\dot\beta}\overline{\sigma}^{\mu\,\dot\gamma\alpha} = \tfrac{1}{2}\overline{\sigma}^{\mu\,\dot\alpha\alpha}\delta^{\dot\gamma}{}_{\dot\beta} - i\overline{\sigma}^{\dot\alpha\alpha}_{\nu}(\overline{\sigma}^{\mu\nu})^{\dot\gamma}{}_{\dot\beta}, \tag{B.1.11}$$

$$\delta_{\alpha}{}^{\beta}(\sigma^{\mu\nu})_{\gamma}{}^{\tau} = \tfrac{1}{2}\left\{(\sigma^{\mu\nu})_{\alpha}{}^{\tau}\delta_{\gamma}{}^{\beta} + \delta_{\alpha}{}^{\tau}(\sigma^{\mu\nu})_{\gamma}{}^{\beta} - ig_{\rho\kappa}\left[(\sigma^{\mu\kappa})_{\alpha}{}^{\tau}(\sigma^{\nu\rho})_{\gamma}{}^{\beta} - (\sigma^{\nu\kappa})_{\alpha}{}^{\tau}(\sigma^{\mu\rho})_{\gamma}{}^{\beta}\right]\right\}, \tag{B.1.12}$$

$$\delta_{\alpha}{}^{\beta}(\overline{\sigma}^{\mu\nu})^{\dot\beta}{}_{\dot\alpha} = -\tfrac{1}{4}i\left[\sigma^{\mu}_{\alpha\dot\alpha}\overline{\sigma}^{\nu\,\dot\beta\beta} - \sigma^{\nu}_{\alpha\dot\alpha}\overline{\sigma}^{\mu\,\dot\beta\beta} + i\epsilon^{\mu\nu\rho\kappa}\sigma_{\rho\,\alpha\dot\alpha}\overline{\sigma}^{\dot\beta\beta}_{\kappa}\right], \tag{B.1.13}$$

$$\delta^{\dot\alpha}{}_{\dot\beta}(\sigma^{\mu\nu})_{\beta}{}^{\alpha} = -\tfrac{1}{4}i\left[\overline{\sigma}^{\mu\,\dot\alpha\alpha}\sigma^{\nu}_{\beta\dot\beta} - \overline{\sigma}^{\nu\,\dot\alpha\alpha}\sigma^{\mu}_{\beta\dot\beta} - i\epsilon^{\mu\nu\rho\kappa}\overline{\sigma}^{\dot\alpha\alpha}_{\rho}\sigma_{\kappa\,\beta\dot\beta}\right], \tag{B.1.14}$$

$$\delta^{\dot\alpha}{}_{\dot\beta}(\overline{\sigma}^{\mu\nu})^{\dot\gamma}{}_{\dot\tau} = \tfrac{1}{2}\left\{(\overline{\sigma}^{\mu\nu})^{\dot\alpha}{}_{\dot\tau}\delta^{\dot\gamma}{}_{\dot\beta} + \delta^{\dot\alpha}{}_{\dot\tau}(\overline{\sigma}^{\mu\nu})^{\dot\gamma}{}_{\dot\beta} - ig_{\rho\kappa}\left[(\overline{\sigma}^{\mu\kappa})^{\dot\alpha}{}_{\dot\tau}(\overline{\sigma}^{\nu\rho})^{\dot\gamma}{}_{\dot\beta} - (\overline{\sigma}^{\nu\kappa})^{\dot\alpha}{}_{\dot\tau}(\overline{\sigma}^{\mu\rho})^{\dot\gamma}{}_{\dot\beta}\right]\right\}, \tag{B.1.15}$$

$$\sigma^{\mu}_{\alpha\dot\alpha}\sigma^{\nu}_{\beta\dot\beta} = \tfrac{1}{2}\left[\sigma^{\mu}_{\alpha\dot\beta}\sigma^{\nu}_{\beta\dot\alpha} + \sigma^{\nu}_{\alpha\dot\beta}\sigma^{\mu}_{\beta\dot\alpha} - g^{\mu\nu}\sigma^{\lambda}_{\alpha\dot\beta}\sigma_{\lambda\,\beta\dot\alpha} + i\epsilon^{\mu\nu\rho\kappa}\sigma_{\rho\,\alpha\dot\beta}\,\sigma_{\kappa\,\beta\dot\alpha}\right], \tag{B.1.16}$$

$$\overline{\sigma}^{\mu\dot\alpha\alpha}\overline{\sigma}^{\nu\dot\beta\beta} = \tfrac{1}{2}\left[\overline{\sigma}^{\mu\dot\alpha\beta}\overline{\sigma}^{\nu\dot\beta\alpha} + \overline{\sigma}^{\nu\dot\alpha\beta}\overline{\sigma}^{\mu\dot\beta\alpha} - g^{\mu\nu}\overline{\sigma}^{\lambda\,\dot\alpha\beta}\overline{\sigma}^{\dot\beta\alpha}_{\lambda} - i\epsilon^{\mu\nu\rho\kappa}\overline{\sigma}^{\dot\alpha\beta}_{\rho}\,\overline{\sigma}^{\dot\beta\alpha}_{\kappa}\right], \tag{B.1.17}$$

$$\sigma^{\mu}_{\alpha\dot\alpha}\overline{\sigma}^{\nu\dot\beta\beta} = \tfrac{1}{2}\left[g^{\mu\nu}\delta_{\alpha}{}^{\beta}\delta^{\dot\beta}{}_{\dot\alpha} - 2i(\sigma^{\mu\nu})_{\alpha}{}^{\beta}\delta^{\dot\beta}{}_{\dot\alpha} + 2i\delta_{\alpha}{}^{\beta}(\overline{\sigma}^{\mu\nu})^{\dot\beta}{}_{\dot\alpha} - 4g_{\rho\kappa}(\sigma^{\mu\kappa})_{\alpha}{}^{\beta}(\overline{\sigma}^{\nu\rho})^{\dot\beta}{}_{\dot\alpha}\right], \tag{B.1.18}$$

$$\begin{aligned}(\sigma^{\mu\nu})_{\alpha}{}^{\beta}\sigma^{\rho}_{\gamma\dot\alpha} = \tfrac{1}{2}\Big[&\sigma^{\nu}_{\alpha\dot\alpha}(\sigma^{\mu\rho})_{\gamma}{}^{\beta} - \sigma^{\mu}_{\alpha\dot\alpha}(\sigma^{\nu\rho})_{\gamma}{}^{\beta} + i\epsilon^{\mu\nu\kappa}{}_{\lambda}\sigma_{\kappa\,\alpha\dot\alpha}(\sigma^{\lambda\rho})_{\gamma}{}^{\beta}\\ &- \tfrac{1}{2}i\left(g^{\mu\rho}\sigma^{\nu}_{\alpha\dot\alpha} - g^{\nu\rho}\sigma^{\mu}_{\alpha\dot\alpha} - i\epsilon^{\mu\nu\rho\kappa}\sigma_{\kappa\,\alpha\dot\alpha}\right)\delta_{\gamma}{}^{\beta}\Big],\end{aligned} \tag{B.1.19}$$

$$\begin{aligned}\overline{\sigma}^{\rho\,\dot\alpha\beta}(\sigma^{\mu\nu})_{\gamma}{}^{\alpha} = \tfrac{1}{2}\Big[&\overline{\sigma}^{\nu\,\dot\alpha\alpha}(\sigma^{\mu\rho})_{\gamma}{}^{\beta} - \overline{\sigma}^{\mu\,\dot\alpha\alpha}(\sigma^{\nu\rho})_{\gamma}{}^{\beta} + i\epsilon^{\mu\nu\kappa}{}_{\lambda}\overline{\sigma}^{\dot\alpha\alpha}_{\kappa}(\sigma^{\lambda\rho})_{\gamma}{}^{\beta}\\ &+ \tfrac{1}{2}i\left(g^{\mu\rho}\overline{\sigma}^{\nu\,\dot\alpha\alpha} - g^{\nu\rho}\overline{\sigma}^{\mu\,\dot\alpha\alpha} - i\epsilon^{\mu\nu\rho\kappa}\overline{\sigma}^{\dot\alpha\alpha}_{\kappa}\right)\delta_{\gamma}{}^{\beta}\Big],\end{aligned} \tag{B.1.20}$$

$$\begin{aligned}\sigma^{\rho}_{\alpha\dot\beta}(\overline{\sigma}^{\mu\nu})^{\dot\gamma}{}_{\dot\alpha} = \tfrac{1}{2}\Big[&\sigma^{\nu}_{\alpha\dot\alpha}(\overline{\sigma}^{\mu\rho})^{\dot\gamma}{}_{\dot\beta} - \sigma^{\mu}_{\alpha\dot\alpha}(\overline{\sigma}^{\nu\rho})^{\dot\gamma}{}_{\dot\beta} - i\epsilon^{\mu\nu\kappa}{}_{\lambda}\sigma_{\kappa\,\alpha\dot\alpha}(\overline{\sigma}^{\lambda\rho})^{\dot\gamma}{}_{\dot\beta}\\ &+ \tfrac{1}{2}i\left(g^{\mu\rho}\sigma^{\nu}_{\alpha\dot\alpha} - g^{\nu\rho}\sigma^{\mu}_{\alpha\dot\alpha} + i\epsilon^{\mu\nu\rho\kappa}\sigma_{\kappa\,\alpha\dot\alpha}\right)\delta^{\dot\gamma}{}_{\dot\beta}\Big],\end{aligned} \tag{B.1.21}$$

$$\begin{aligned}(\overline{\sigma}^{\mu\nu})^{\dot\alpha}{}_{\dot\beta}\overline{\sigma}^{\rho\,\dot\gamma\alpha} = \tfrac{1}{2}\Big[&\overline{\sigma}^{\nu\,\dot\alpha\alpha}(\overline{\sigma}^{\mu\rho})^{\dot\gamma}{}_{\dot\beta} - \overline{\sigma}^{\mu\,\dot\alpha\alpha}(\overline{\sigma}^{\nu\rho})^{\dot\gamma}{}_{\dot\beta} - i\epsilon^{\mu\nu\kappa}{}_{\lambda}\overline{\sigma}^{\dot\alpha\alpha}_{\kappa}(\overline{\sigma}^{\lambda\rho})^{\dot\gamma}{}_{\dot\beta}\\ &- \tfrac{1}{2}i\left(g^{\mu\rho}\overline{\sigma}^{\nu\,\dot\alpha\alpha} - g^{\nu\rho}\overline{\sigma}^{\mu\,\dot\alpha\alpha} + i\epsilon^{\mu\nu\rho\kappa}\overline{\sigma}^{\dot\alpha\alpha}_{\kappa}\right)\delta^{\dot\gamma}{}_{\dot\beta}\Big],\end{aligned} \tag{B.1.22}$$

$$\begin{aligned}(\sigma^{\mu\nu})_{\alpha}{}^{\beta}(\sigma^{\rho\kappa})_{\gamma}{}^{\tau} = {}&\tfrac{1}{2}(\sigma^{\mu\nu})_{\alpha}{}^{\tau}(\sigma^{\rho\kappa})_{\gamma}{}^{\beta} + \tfrac{1}{8}\delta_{\alpha}{}^{\tau}\delta_{\gamma}{}^{\beta}(g^{\mu\rho}g^{\nu\kappa} - g^{\mu\kappa}g^{\nu\rho} - i\epsilon^{\mu\nu\rho\kappa})\\ &+ \tfrac{1}{4}i\delta_{\alpha}{}^{\tau}\left(g^{\mu\rho}\sigma^{\nu\kappa} + g^{\nu\kappa}\sigma^{\mu\rho} - g^{\nu\rho}\sigma^{\mu\kappa} - g^{\mu\kappa}\sigma^{\nu\rho}\right)_{\gamma}{}^{\beta}\\ &- \tfrac{1}{4}i\delta_{\gamma}{}^{\beta}\left(g^{\mu\rho}\sigma^{\nu\kappa} + g^{\nu\kappa}\sigma^{\mu\rho} - g^{\nu\rho}\sigma^{\mu\kappa} - g^{\mu\kappa}\sigma^{\nu\rho}\right)_{\alpha}{}^{\tau}\\ &+ \tfrac{1}{4}\left[(\sigma^{\mu\rho})_{\alpha}{}^{\tau}(\sigma^{\nu\kappa})_{\gamma}{}^{\beta} + (\sigma^{\nu\kappa})_{\alpha}{}^{\tau}(\sigma^{\mu\rho})_{\gamma}{}^{\beta} - (\sigma^{\nu\rho})_{\alpha}{}^{\tau}(\sigma^{\mu\kappa})_{\gamma}{}^{\beta} - (\sigma^{\mu\kappa})_{\alpha}{}^{\tau}(\sigma^{\nu\rho})_{\gamma}{}^{\beta}\right]\\ &+ \tfrac{1}{4}g_{\lambda\sigma}\left[g^{\mu\kappa}(\sigma^{\rho\sigma})_{\alpha}{}^{\tau}(\sigma^{\nu\lambda})_{\gamma}{}^{\beta} + g^{\nu\rho}(\sigma^{\kappa\sigma})_{\alpha}{}^{\tau}(\sigma^{\mu\lambda})_{\gamma}{}^{\beta}\right.\\ &\left. - g^{\nu\kappa}(\sigma^{\rho\sigma})_{\alpha}{}^{\tau}(\sigma^{\mu\lambda})_{\gamma}{}^{\beta} - g^{\mu\rho}(\sigma^{\kappa\sigma})_{\alpha}{}^{\tau}(\sigma^{\nu\lambda})_{\gamma}{}^{\beta}\right],\end{aligned} \tag{B.1.23}$$

$$
\begin{aligned}
(\overline{\sigma}^{\mu\nu})^{\dot\alpha}{}_{\dot\beta}(\overline{\sigma}^{\rho\kappa})^{\dot\gamma}{}_{\dot\tau} &= \tfrac{1}{2}(\overline{\sigma}^{\mu\nu})^{\dot\alpha}{}_{\dot\tau}(\overline{\sigma}^{\rho\kappa})^{\dot\gamma}{}_{\dot\beta} + \tfrac{1}{8}\delta^{\dot\alpha}{}_{\dot\tau}\delta^{\dot\gamma}{}_{\dot\beta}\,(g^{\mu\rho}g^{\nu\kappa} - g^{\mu\kappa}g^{\nu\rho} + i\epsilon^{\mu\nu\rho\kappa}) \\
&\quad + \tfrac{1}{4}i\delta^{\dot\alpha}{}_{\dot\tau}\,(g^{\mu\rho}\overline{\sigma}^{\nu\kappa} + g^{\nu\kappa}\overline{\sigma}^{\mu\rho} - g^{\nu\rho}\overline{\sigma}^{\mu\kappa} - g^{\mu\kappa}\overline{\sigma}^{\nu\rho})^{\dot\gamma}{}_{\dot\beta} \\
&\quad - \tfrac{1}{4}i\delta^{\dot\gamma}{}_{\dot\beta}\,(g^{\mu\rho}\overline{\sigma}^{\nu\kappa} + g^{\nu\kappa}\overline{\sigma}^{\mu\rho} - g^{\nu\rho}\overline{\sigma}^{\mu\kappa} - g^{\mu\kappa}\overline{\sigma}^{\nu\rho})^{\dot\alpha}{}_{\dot\tau} \\
&\quad + \tfrac{1}{4}\left[(\overline{\sigma}^{\mu\rho})^{\dot\alpha}{}_{\dot\tau}(\overline{\sigma}^{\nu\kappa})^{\dot\gamma}{}_{\dot\beta} + (\overline{\sigma}^{\nu\kappa})^{\dot\alpha}{}_{\dot\tau}(\overline{\sigma}^{\mu\rho})^{\dot\gamma}{}_{\dot\beta} - (\overline{\sigma}^{\nu\rho})^{\dot\alpha}{}_{\dot\tau}(\overline{\sigma}^{\mu\kappa})^{\dot\gamma}{}_{\dot\beta} - (\overline{\sigma}^{\mu\kappa})^{\dot\alpha}{}_{\dot\tau}(\overline{\sigma}^{\nu\rho})^{\dot\gamma}{}_{\dot\beta}\right] \\
&\quad + \tfrac{1}{4}g_{\lambda\sigma}\left[g^{\mu\kappa}(\overline{\sigma}^{\rho\sigma})^{\dot\alpha}{}_{\dot\tau}(\overline{\sigma}^{\nu\lambda})^{\dot\gamma}{}_{\dot\beta} + g^{\nu\rho}(\overline{\sigma}^{\kappa\sigma})^{\dot\alpha}{}_{\dot\tau}(\overline{\sigma}^{\mu\lambda})^{\dot\gamma}{}_{\dot\beta}\right. \\
&\quad \left. - g^{\nu\kappa}(\overline{\sigma}^{\rho\sigma})^{\dot\alpha}{}_{\dot\tau}(\overline{\sigma}^{\mu\lambda})^{\dot\gamma}{}_{\dot\beta} - g^{\mu\rho}(\overline{\sigma}^{\kappa\sigma})^{\dot\alpha}{}_{\dot\tau}(\overline{\sigma}^{\nu\lambda})^{\dot\gamma}{}_{\dot\beta}\right], \qquad \text{(B.1.24)} \\
(\sigma^{\mu\nu})_{\alpha}{}^{\beta}(\overline{\sigma}^{\rho\kappa})^{\dot\beta}{}_{\dot\alpha} &= \tfrac{1}{8}\left[(g^{\mu\rho}g^{\nu\kappa} - g^{\mu\kappa}g^{\nu\rho})\sigma^{\lambda}_{\alpha\dot\alpha}\overline{\sigma}^{\dot\beta\beta}_{\lambda}\right. \\
&\quad + i\epsilon^{\mu\nu\rho\lambda}\sigma_{\lambda\,\alpha\dot\alpha}\overline{\sigma}^{\kappa\,\dot\beta\beta} - i\epsilon^{\mu\nu\kappa\lambda}\sigma_{\lambda\,\alpha\dot\alpha}\overline{\sigma}^{\rho\,\dot\beta\beta} - i\epsilon^{\mu\rho\kappa\lambda}\sigma^{\nu}_{\alpha\dot\alpha}\overline{\sigma}^{\dot\beta\beta}_{\lambda} + i\epsilon^{\nu\rho\kappa\lambda}\sigma^{\mu}_{\alpha\dot\alpha}\overline{\sigma}^{\dot\beta\beta}_{\lambda} \\
&\quad - g^{\mu\rho}(\sigma^{\kappa}_{\alpha\dot\alpha}\overline{\sigma}^{\nu\,\dot\beta\beta} + \sigma^{\nu}_{\alpha\dot\alpha}\overline{\sigma}^{\kappa\,\dot\beta\beta}) + g^{\nu\rho}(\sigma^{\kappa}_{\alpha\dot\alpha}\overline{\sigma}^{\mu\,\dot\beta\beta} + \sigma^{\mu}_{\alpha\dot\alpha}\overline{\sigma}^{\kappa\,\dot\beta\beta}) \\
&\quad \left. + g^{\mu\kappa}(\sigma^{\rho}_{\alpha\dot\alpha}\overline{\sigma}^{\nu\,\dot\beta\beta} + \sigma^{\nu}_{\alpha\dot\alpha}\overline{\sigma}^{\rho\,\dot\beta\beta}) - g^{\nu\kappa}(\sigma^{\rho}_{\alpha\dot\alpha}\overline{\sigma}^{\mu\,\dot\beta\beta} + \sigma^{\mu}_{\alpha\dot\alpha}\overline{\sigma}^{\rho\,\dot\beta\beta})\right]. \qquad \text{(B.1.25)}
\end{aligned}
$$

From Eqs. (B.1.5)–(B.1.25), one immediately obtains the corresponding 21 Fierz identities represented by Eq. (B.1.4). Eleven of these identities also appear in Appendix B of Ref. [77].[91]

The derivation of the 21 identities listed above is straightforward. Eqs. (B.1.5)–(B.1.7) are equivalent to the completeness relation of Eq. (B.1.1). The next eight identities [Eqs. (B.1.8)–(B.1.15)] are easily derived starting from Eqs. (B.1.5)–(B.1.7). As a simple example, using the results of Eqs. (B.1.6) and (B.2.20), it follows that

$$
\begin{aligned}
\delta_{\alpha}{}^{\beta}\sigma^{\mu}_{\gamma\dot\alpha} &= \delta_{\alpha}{}^{\beta}\delta_{\gamma}{}^{\tau}\sigma^{\mu}_{\tau\dot\alpha} = \tfrac{1}{2}\left[\delta_{\alpha}{}^{\tau}\delta_{\gamma}{}^{\beta} + (\sigma^{\rho\kappa})_{\alpha}{}^{\tau}(\sigma_{\rho\kappa})_{\gamma}{}^{\beta}\right]\sigma^{\mu}_{\tau\dot\alpha} \\
&= \tfrac{1}{2}\left[\sigma^{\mu}_{\alpha\dot\alpha}\delta_{\gamma}{}^{\beta} + (\sigma^{\rho\kappa}\sigma^{\mu})_{\alpha\dot\alpha}(\sigma_{\rho\kappa})_{\gamma}{}^{\beta}\right] \\
&= \tfrac{1}{2}\left[\sigma^{\mu}_{\alpha\dot\alpha}\delta_{\gamma}{}^{\beta} + \tfrac{1}{2}i(g^{\kappa\mu}\sigma^{\rho} - g^{\rho\mu}\sigma^{\kappa} + i\epsilon^{\rho\kappa\mu\nu}\sigma_{\nu})_{\alpha\dot\alpha}(\sigma_{\rho\kappa})_{\gamma}{}^{\beta}\right] \\
&= \tfrac{1}{2}\delta_{\alpha}{}^{\gamma}\overline{\sigma}^{\mu\,\dot\beta\beta} + i(\sigma^{\mu\nu})_{\alpha}{}^{\gamma}\overline{\sigma}^{\dot\beta\beta}_{\nu}, \qquad \text{(B.1.26)}
\end{aligned}
$$

where Eq. (2.75) was employed in the final step. We can now use Eqs. (B.1.8)–(B.1.11) to derive Eqs. (B.1.16)–(B.1.22) by a similar technique. Finally, starting from Eqs. (B.1.12)–(B.1.15) we may employ the same technique once more to derive Eqs. (B.1.23)–(B.1.25).[92] A useful check of the last three identities can be carried out by multiplying these results by $g_{\mu\rho}g_{\nu\kappa}$ and summing over the two repeated Lorentz index pairs. We then find:

$$
\begin{aligned}
(\sigma^{\mu\nu})_{\alpha}{}^{\beta}(\sigma_{\mu\nu})_{\gamma}{}^{\tau} &= -\tfrac{1}{2}(\sigma^{\mu\nu})_{\alpha}{}^{\tau}(\sigma_{\mu\nu})_{\gamma}{}^{\beta} + \tfrac{3}{2}\delta_{\alpha}{}^{\tau}\delta_{\gamma}{}^{\beta}, \qquad \text{(B.1.27)} \\
(\overline{\sigma}^{\mu\nu})^{\dot\alpha}{}_{\dot\beta}(\overline{\sigma}_{\mu\nu})^{\dot\gamma}{}_{\dot\tau} &= -\tfrac{1}{2}(\overline{\sigma}^{\mu\nu})^{\dot\alpha}{}_{\dot\tau}(\overline{\sigma}_{\mu\nu})^{\dot\gamma}{}_{\dot\beta} + \tfrac{3}{2}\delta^{\dot\alpha}{}_{\dot\tau}\delta^{\dot\gamma}{}_{\dot\beta}, \qquad \text{(B.1.28)} \\
(\sigma^{\mu\nu})_{\alpha}{}^{\beta}(\overline{\sigma}_{\mu\nu})^{\dot\gamma}{}_{\dot\tau} &= 0. \qquad \text{(B.1.29)}
\end{aligned}
$$

Eq. (B.1.29) has already been recorded in Eq. (2.83). To verify Eqs. (B.1.27) and (B.1.28), we first rewrite these equations with the interchange of $\beta \leftrightarrow \tau$ and $\dot\beta \leftrightarrow \dot\tau$. Inserting the resulting equations back into Eqs. (B.1.27) and (B.1.28) then yields the previously obtained Eqs. (2.81) and (2.82) [or equivalently, Eqs. (B.1.6) and (B.1.7)].

A similar check can be performed on Eqs. (B.1.16)–(B.1.18) by multiplying these results by $g_{\mu\nu}$ and summing over the repeated Lorentz index pair [with assistance from Eq. (B.1.29)]:

$$
\begin{aligned}
\sigma^{\mu}_{\alpha\dot\alpha}\sigma_{\mu\,\beta\dot\beta} &= -\sigma^{\mu}_{\alpha\dot\beta}\sigma_{\mu\,\beta\dot\alpha}, \qquad \text{(B.1.30)} \\
\overline{\sigma}^{\mu\,\dot\alpha\alpha}\overline{\sigma}^{\dot\beta\beta}_{\mu} &= -\sigma^{\mu\,\dot\alpha\beta}\sigma^{\dot\beta\alpha}_{\mu}, \qquad \text{(B.1.31)} \\
\sigma^{\mu}_{\alpha\dot\alpha}\overline{\sigma}^{\dot\beta\beta}_{\mu} &= 2\,\delta_{\alpha}{}^{\beta}\delta^{\dot\beta}{}_{\dot\alpha}. \qquad \text{(B.1.32)}
\end{aligned}
$$

It follows that:

$$
\begin{aligned}
\sigma^{\mu}_{\alpha\dot\alpha}\sigma_{\mu\,\beta\dot\beta} &= 2\,\epsilon_{\alpha\beta}\epsilon_{\dot\alpha\dot\beta}, \qquad \text{(B.1.33)} \\
\overline{\sigma}^{\mu\,\dot\alpha\alpha}\overline{\sigma}^{\dot\beta\beta}_{\mu} &= 2\,\epsilon^{\alpha\beta}\epsilon^{\dot\alpha\dot\beta}, \qquad \text{(B.1.34)}
\end{aligned}
$$

91 Note that in Ref. [77], $\epsilon^{\mu\nu\rho\kappa}$ has the opposite sign with respect to our conventions, and $\sigma^{\mu\nu}$ is defined without an overall factor of i. Taking these differences into account, we have confirmed that the results of Appendix B of Ref. [77] match the corresponding results obtained here.

92 In particular, the identities given in Eqs. (B.2.18) and (B.2.19) are especially useful in the evaluation of Eqs. (B.1.19)–(B.1.24).

since Eqs. (B.1.30) and (B.1.31) are antisymmetric under the separate interchanges of $\alpha \leftrightarrow \beta$ and $\dot\alpha \leftrightarrow \dot\beta$. The coefficients in Eqs. (B.1.33) and (B.1.34) are determined by substituting $\alpha = \dot\alpha = 1$ and $\beta = \dot\beta = 2$. Thus, we have confirmed the results previously obtained in Eqs. (2.48)–(2.50).

Eqs. (B.1.5)–(B.1.7) can also be used to derive four additional identities, which yield Fierz identities of a different form. Simply multiply each of these equations by two ϵ symbols (with appropriately chosen undotted and/or dotted spinor indices), and use Eqs. (2.31) and (2.78). Two of the resulting identities coincide with Eqs. (B.1.33) and (B.1.34), while the other two are:

$$\epsilon_{\alpha\beta}\epsilon^{\gamma\tau} = -\tfrac{1}{2}\big[\delta_\alpha{}^\gamma\delta_\beta{}^\tau - (\sigma^{\mu\nu})_\alpha{}^\gamma(\sigma_{\mu\nu})_\beta{}^\tau\big], \tag{B.1.35}$$

$$\epsilon^{\dot\alpha\dot\beta}\epsilon_{\dot\gamma\dot\tau} = -\tfrac{1}{2}\left[\delta^{\dot\alpha}{}_{\dot\gamma}\delta^{\dot\beta}{}_{\dot\tau} - (\overline\sigma^{\mu\nu})^{\dot\alpha}{}_{\dot\gamma}(\overline\sigma_{\mu\nu})^{\dot\beta}{}_{\dot\tau}\right]. \tag{B.1.36}$$

One can check that Eqs. (B.1.35) and (B.1.36) are equivalent to the previously obtained Eqs. (2.81) and (2.82). Multiplying Eqs. (B.1.33)–(B.1.36) by four (commuting or anticommuting) two-component spinors $Z_{1A}Z_{2B}Z_{3C}Z_{4D}$ yields the corresponding Fierz identities of the form:

$$(Z_1\Gamma^{(k)I}Z_2)(Z_3\Gamma^{(n)J}Z_4) = (-1)^A\sum_{p,q,K,L}(C^{kn}_{pq})^{IJ}_{KL}(Z_1\Gamma^{(p)K}Z_3)(Z_2\Gamma^{(q)L}Z_4), \tag{B.1.37}$$

which differs from Eq. (B.1.4) in the ordering of the spinors on the right-hand side.

Finally, we note that the Schouten identities,

$$\epsilon_{\alpha\beta}\epsilon_{\gamma\delta} + \epsilon_{\alpha\gamma}\epsilon_{\delta\beta} + \epsilon_{\alpha\delta}\epsilon_{\beta\gamma} = 0, \qquad \epsilon_{\dot\alpha\dot\beta}\epsilon_{\dot\gamma\dot\delta} + \epsilon_{\dot\alpha\dot\gamma}\epsilon_{\dot\delta\dot\beta} + \epsilon_{\dot\alpha\dot\delta}\epsilon_{\dot\beta\dot\gamma} = 0, \tag{B.1.38}$$

are the basis for Fierz identities given by Eqs. (2.65) and (2.66), which do not assume the simple forms of either Eqs. (B.1.4) or (B.1.37).

B.2. Sigma matrix identities in $d \neq 4$ dimensions

When considering a theory regularized by dimensional continuation [124], one must be careful in treating cases with contracted spacetime vector indices $\mu, \nu, \kappa, \rho, \ldots$. Instead of taking on four possible values, these vector indices formally run over d values, where d is infinitesimally different from 4. This means that some identities that would hold in unregularized four-dimensional theories are inconsistent and must not be used; other identities remain valid if d replaces 4 in the appropriate spots; and still other identities hold without modification.

Two important identities that do hold in $d \neq 4$ dimensions are:

$$[\sigma^\mu\overline\sigma^\nu + \sigma^\nu\overline\sigma^\mu]_\alpha{}^\beta = 2g^{\mu\nu}\delta_\alpha{}^\beta, \tag{B.2.1}$$

$$[\overline\sigma^\mu\sigma^\nu + \overline\sigma^\nu\sigma^\mu]^{\dot\alpha}{}_{\dot\beta} = 2g^{\mu\nu}\delta^{\dot\alpha}{}_{\dot\beta}. \tag{B.2.2}$$

Equivalently,

$$(\sigma^\mu\overline\sigma^\nu)_\alpha{}^\beta = g^{\mu\nu}\delta_\alpha{}^\beta - 2i(\sigma^{\mu\nu})_\alpha{}^\beta, \tag{B.2.3}$$

$$(\overline\sigma^\mu\sigma^\nu)^{\dot\alpha}{}_{\dot\beta} = g^{\mu\nu}\delta^{\dot\alpha}{}_{\dot\beta} - 2i(\overline\sigma^{\mu\nu})^{\dot\alpha}{}_{\dot\beta}, \tag{B.2.4}$$

where $\sigma^{\mu\nu}$ and $\overline\sigma^{\mu\nu}$ are defined in Eq. (A.10). The trace identities,

$$\mathrm{Tr}[\sigma^\mu\overline\sigma^\nu] = \mathrm{Tr}[\overline\sigma^\mu\sigma^\nu] = 2g^{\mu\nu}, \tag{B.2.5}$$

$$\mathrm{Tr}\sigma^{\mu\nu} = \mathrm{Tr}\overline\sigma^{\mu\nu} = 0, \tag{B.2.6}$$

then follow. We also note that the spinor index trace identity,

$$\mathrm{Tr}[\mathbb{1}] = \delta^\alpha_\alpha = \delta^{\dot\alpha}_{\dot\alpha} = 2, \tag{B.2.7}$$

continues to hold in dimensional continuation regularization methods. In contrast, the Fierz identities of Appendix B.1 do not have a consistent, unambiguous meaning outside of four dimensions [249–252]. However, the following identities that are implied by Eq. (B.1.5) do consistently generalize to $d \neq 4$ spacetime dimensions:

$$[\sigma^\mu\overline\sigma_\mu]_\alpha{}^\beta = d\delta^\beta_\alpha, \tag{B.2.8}$$

$$[\overline\sigma^\mu\sigma_\mu]^{\dot\alpha}{}_{\dot\beta} = d\delta^{\dot\alpha}_{\dot\beta}. \tag{B.2.9}$$

Using Eqs. (B.2.8) and (B.2.9) along with the repeated use of Eqs. (B.2.1) and (B.2.2) then yields:

$$[\sigma^\mu\overline{\sigma}^\nu\sigma_\mu]_{\alpha\dot\beta} = -(d-2)\sigma^\nu_{\alpha\dot\beta}, \tag{B.2.10}$$

$$[\overline{\sigma}^\mu\sigma_\nu\overline{\sigma}_\mu]^{\dot\alpha\beta} = -(d-2)\overline{\sigma}_\nu^{\dot\alpha\beta}, \tag{B.2.11}$$

$$[\sigma^\mu\overline{\sigma}^\nu\sigma^\rho\overline{\sigma}_\mu]_\alpha{}^\beta = 4g^{\nu\rho}\delta^\beta_\alpha - (4-d)[\sigma^\nu\overline{\sigma}^\rho]_\alpha{}^\beta, \tag{B.2.12}$$

$$[\overline{\sigma}^\mu\sigma^\nu\overline{\sigma}^\rho\sigma_\mu]^{\dot\alpha}{}_{\dot\beta} = 4g^{\nu\rho}\delta^{\dot\alpha}_{\dot\beta} - (4-d)[\overline{\sigma}^\nu\sigma^\rho]^{\dot\alpha}{}_{\dot\beta}, \tag{B.2.13}$$

$$[\sigma^\mu\overline{\sigma}^\nu\sigma^\rho\overline{\sigma}^\kappa\sigma_\mu]_{\alpha\dot\beta} = -2[\sigma^\kappa\overline{\sigma}^\rho\sigma^\nu]_{\alpha\dot\beta} + (4-d)[\sigma^\nu\overline{\sigma}^\rho\sigma^\kappa]_{\alpha\dot\beta}, \tag{B.2.14}$$

$$[\overline{\sigma}^\mu\sigma^\nu\overline{\sigma}^\rho\sigma^\kappa\overline{\sigma}_\mu]^{\dot\alpha\beta} = -2[\overline{\sigma}^\kappa\sigma^\rho\overline{\sigma}^\nu]^{\dot\alpha\beta} + (4-d)[\overline{\sigma}^\nu\sigma^\rho\overline{\sigma}^\kappa]^{\dot\alpha\beta}. \tag{B.2.15}$$

Identities that involve the (explicitly and inextricably four-dimensional) $\epsilon^{\mu\nu\rho\kappa}$ symbol

$$\overline{\sigma}^\mu\sigma^\nu\overline{\sigma}^\rho = g^{\mu\nu}\overline{\sigma}^\rho - g^{\mu\rho}\overline{\sigma}^\nu + g^{\nu\rho}\overline{\sigma}^\mu - i\epsilon^{\mu\nu\rho\kappa}\overline{\sigma}_\kappa, \tag{B.2.16}$$

$$\sigma^\mu\overline{\sigma}^\nu\sigma^\rho = g^{\mu\nu}\sigma^\rho - g^{\mu\rho}\sigma^\nu + g^{\nu\rho}\sigma^\mu + i\epsilon^{\mu\nu\rho\kappa}\sigma_\kappa, \tag{B.2.17}$$

$$\epsilon^{\mu\nu\kappa}{}_\lambda\sigma^{\lambda\rho} = -i\left(g^{\kappa\rho}\sigma^{\mu\nu} - g^{\nu\rho}\sigma^{\mu\kappa} + g^{\mu\rho}\sigma^{\nu\kappa}\right), \tag{B.2.18}$$

$$\epsilon^{\mu\nu\kappa}{}_\lambda\overline{\sigma}^{\lambda\rho} = i\left(g^{\kappa\rho}\overline{\sigma}^{\mu\nu} - g^{\nu\rho}\overline{\sigma}^{\mu\kappa} + g^{\mu\rho}\overline{\sigma}^{\nu\kappa}\right), \tag{B.2.19}$$

$$\sigma^{\mu\nu}\sigma^\rho = \tfrac{1}{2}i\left(g^{\nu\rho}\sigma^\mu - g^{\mu\rho}\sigma^\nu + i\epsilon^{\mu\nu\rho\kappa}\sigma_\kappa\right), \tag{B.2.20}$$

$$\overline{\sigma}^{\mu\nu}\overline{\sigma}^\rho = \tfrac{1}{2}i\left(g^{\nu\rho}\overline{\sigma}^\mu - g^{\mu\rho}\overline{\sigma}^\nu - i\epsilon^{\mu\nu\rho\kappa}\overline{\sigma}_\kappa\right), \tag{B.2.21}$$

$$\overline{\sigma}^\mu\sigma^{\nu\rho} = \tfrac{1}{2}i\left(g^{\mu\nu}\overline{\sigma}^\rho - g^{\mu\rho}\overline{\sigma}^\nu - i\epsilon^{\mu\nu\rho\kappa}\overline{\sigma}_\kappa\right), \tag{B.2.22}$$

$$\sigma^\mu\overline{\sigma}^{\nu\rho} = \tfrac{1}{2}i\left(g^{\mu\nu}\sigma^\rho - g^{\mu\rho}\sigma^\nu + i\epsilon^{\mu\nu\rho\kappa}\sigma_\kappa\right), \tag{B.2.23}$$

$$\sigma^{\mu\nu}\sigma^{\rho\kappa} = -\tfrac{1}{4}(g^{\nu\rho}g^{\mu\kappa} - g^{\mu\rho}g^{\nu\kappa} + i\epsilon^{\mu\nu\rho\kappa}) + \tfrac{1}{2}i(g^{\nu\rho}\sigma^{\mu\kappa} + g^{\mu\kappa}\sigma^{\nu\rho} - g^{\mu\rho}\sigma^{\nu\kappa} - g^{\nu\kappa}\sigma^{\mu\rho}), \tag{B.2.24}$$

$$\overline{\sigma}^{\mu\nu}\overline{\sigma}^{\rho\kappa} = -\tfrac{1}{4}(g^{\nu\rho}g^{\mu\kappa} - g^{\mu\rho}g^{\nu\kappa} - i\epsilon^{\mu\nu\rho\kappa}) + \tfrac{1}{2}i(g^{\nu\rho}\overline{\sigma}^{\mu\kappa} + g^{\mu\kappa}\overline{\sigma}^{\nu\rho} - g^{\mu\rho}\overline{\sigma}^{\nu\kappa} - g^{\nu\kappa}\overline{\sigma}^{\mu\rho}), \tag{B.2.25}$$

are also only meaningful in exactly four dimensions. This applies as well to the trace identities which follow from them.[93] For example,

$$\mathrm{Tr}[\sigma^\mu\overline{\sigma}^\nu\sigma^\rho\overline{\sigma}^\kappa] = 2\left(g^{\mu\nu}g^{\rho\kappa} - g^{\mu\rho}g^{\nu\kappa} + g^{\mu\kappa}g^{\nu\rho} + i\epsilon^{\mu\nu\rho\kappa}\right), \tag{B.2.26}$$

$$\mathrm{Tr}[\overline{\sigma}^\mu\sigma^\nu\overline{\sigma}^\rho\sigma^\kappa] = 2\left(g^{\mu\nu}g^{\rho\kappa} - g^{\mu\rho}g^{\nu\kappa} + g^{\mu\kappa}g^{\nu\rho} - i\epsilon^{\mu\nu\rho\kappa}\right). \tag{B.2.27}$$

This could lead to ambiguities in loop computations where it is necessary to perform the computation in $d \neq 4$ dimensions (until the end of the calculation where the limit $d \to 4$ is taken). However, in practice one typically finds that the above expressions appear multiplied by the metric and/or other external tensors (such as four-momenta appropriate to the problem at hand). In almost all such cases, two of the indices appearing in Eqs. (B.2.26) and (B.2.27) are symmetrized which eliminates the $\epsilon^{\mu\nu\rho\kappa}$ term, rendering the resulting expressions unambiguous. Similarly, the sum of the above trace identities can be assigned an unambiguous meaning in $d \neq 4$ dimensions:

$$\mathrm{Tr}[\sigma^\mu\overline{\sigma}^\nu\sigma^\rho\overline{\sigma}^\kappa] + \mathrm{Tr}[\overline{\sigma}^\mu\sigma^\nu\overline{\sigma}^\rho\sigma^\kappa] = 4\left(g^{\mu\nu}g^{\rho\kappa} - g^{\mu\rho}g^{\nu\kappa} + g^{\mu\kappa}g^{\nu\rho}\right). \tag{B.2.28}$$

One can recursively derive trace formulae for products of six or more $\sigma/\overline{\sigma}$ matrices by using the results of Eqs. (B.2.16) and (B.2.17) to reduce the number of $\sigma/\overline{\sigma}$ matrices by two. For example,

$$\begin{aligned}\mathrm{Tr}[\sigma^\mu\overline{\sigma}^\nu\sigma^\rho\overline{\sigma}^\kappa\sigma^\lambda\overline{\sigma}^\delta] &= g^{\mu\nu}\mathrm{Tr}[\sigma^\rho\overline{\sigma}^\kappa\sigma^\lambda\overline{\sigma}^\delta] - g^{\mu\rho}\mathrm{Tr}[\sigma^\nu\overline{\sigma}^\kappa\sigma^\lambda\overline{\sigma}^\delta] + g^{\nu\rho}\mathrm{Tr}[\sigma^\mu\overline{\sigma}^\kappa\sigma^\lambda\overline{\sigma}^\delta]\\ &\quad + i\epsilon^{\mu\nu\rho\epsilon}\mathrm{Tr}[\sigma_\epsilon\overline{\sigma}^\kappa\sigma^\lambda\overline{\sigma}^\delta],\end{aligned} \tag{B.2.29}$$

$$\begin{aligned}\mathrm{Tr}[\overline{\sigma}^\mu\sigma^\nu\overline{\sigma}^\rho\sigma^\kappa\overline{\sigma}^\lambda\sigma^\delta] &= g^{\mu\nu}\mathrm{Tr}[\overline{\sigma}^\rho\sigma^\kappa\overline{\sigma}^\lambda\sigma^\delta] - g^{\mu\rho}\mathrm{Tr}[\overline{\sigma}^\nu\sigma^\kappa\overline{\sigma}^\lambda\sigma^\delta] + g^{\nu\rho}\mathrm{Tr}[\overline{\sigma}^\mu\sigma^\kappa\overline{\sigma}^\lambda\sigma^\delta]\\ &\quad - i\epsilon^{\mu\nu\rho\epsilon}\mathrm{Tr}[\overline{\sigma}_\epsilon\sigma^\kappa\overline{\sigma}^\lambda\sigma^\delta].\end{aligned} \tag{B.2.30}$$

We then use Eqs. (B.2.26) and (B.2.27) to evaluate the remaining traces over four $\sigma/\overline{\sigma}$ matrices.

---

93 This is analogous to the statement that $\mathrm{Tr}\,(\gamma_5\gamma^\mu\gamma^\nu\gamma^\rho\gamma^\kappa) = -4i\epsilon^{\mu\nu\rho\kappa}$ [in our convention where $\epsilon^{0123} = +1$, and γ_5 is defined by Eq. (G.1.2)] is only meaningful in $d = 4$ dimensions. In two-component notation, the equivalent result is $\mathrm{Tr}[\sigma^\mu\overline{\sigma}^\nu\sigma^\rho\overline{\sigma}^\kappa - \overline{\sigma}^\mu\sigma^\nu\overline{\sigma}^\rho\sigma^\kappa] = 4i\epsilon^{\mu\nu\rho\kappa}$. In the literature various schemes have been proposed for defining the properties of γ_5 in $d \neq 4$ dimensions [231,252]. In two-component notation, this would translate into a procedure for dealing with general traces involving four or more $\sigma/\overline{\sigma}$ matrices.

Appendix C. Explicit forms for the two-component spinor wave functions

In this Appendix, we construct the explicit forms for the eigenstates of the spin operator $\frac{1}{2}\vec{\sigma}\cdot\hat{\mathbf{s}}$, and examine their properties. For massive fermions, it is possible to transform to the rest frame, and quantize the spin along a fixed axis in space. The corresponding spinor wave functions will be called fixed-axis spinors. For either massive or massive fermions, one can quantize the spin along the direction of momentum. The corresponding spinor wave functions are helicity spinors. Helicity spinor wave functions are most conveniently applied to massless fermions or fermions in the relativistic limit of high energy $E \gg m$. Fixed-axis spinors are most conveniently applied to massive fermions in the non-relativistic limit.

C.1. Fixed-axis spinor wave functions

Consider a spin-1/2 fermion in its rest frame and quantize the spin along a fixed axis specified by the unit vector

$$\hat{\mathbf{s}} \equiv (\sin\theta\cos\phi, \sin\theta\sin\phi, \cos\theta), \tag{C.1.1}$$

with polar angle θ and azimuthal angle ϕ with respect to a fixed z-axis. The relevant basis of two-component fixed-axis spinors χ_s are eigenstates of $\frac{1}{2}\vec{\sigma}\cdot\hat{\mathbf{s}}$, i.e.,

$$\tfrac{1}{2}\vec{\sigma}\cdot\hat{\mathbf{s}}\,\chi_s = s\chi_s, \quad s = \pm\tfrac{1}{2}. \tag{C.1.2}$$

In order to construct the eigenstates of $\frac{1}{2}\vec{\sigma}\cdot\hat{\mathbf{s}}$, we first consider the case where $\hat{\mathbf{s}} = \hat{\boldsymbol{z}}$. In this case, we define the eigenstates of $\frac{1}{2}\sigma^3$ to be:

$$\chi_{1/2}(\hat{\boldsymbol{z}}) = \begin{pmatrix}1\\0\end{pmatrix}, \qquad \chi_{-1/2}(\hat{\boldsymbol{z}}) = \begin{pmatrix}0\\1\end{pmatrix}. \tag{C.1.3}$$

By convention, we have set an arbitrary overall multiplicative phase factor for each spinor of Eq. (C.1.3) to unity. We then determine $\chi_s(\hat{\mathbf{s}})$ from $\chi_s(\hat{\boldsymbol{z}})$ by employing the spin-1/2 rotation operator that corresponds to a rotation from $\hat{\boldsymbol{z}}$ to $\hat{\mathbf{s}}$. This rotation is represented by a 3×3 matrix $\mathcal{R}$ such that $\hat{\mathbf{s}} = \mathcal{R}\hat{\boldsymbol{z}}$. However, this rotation operator is not unique. In its most general form, the rotation operator can be parameterized in terms of three Euler angles (e.g., see Refs. [44,45]):

$$\mathcal{R}(\phi,\theta,\gamma) \equiv R(\hat{\boldsymbol{z}},\phi)\,R(\hat{\boldsymbol{y}},\theta)\,R(\hat{\boldsymbol{z}},\gamma). \tag{C.1.4}$$

The Euler angles can be chosen to lie in the range $0 \le \theta \le \pi$ and $0 \le \phi, \gamma < 2\pi$. Here, $R(\hat{\mathbf{n}},\theta)$ is a 3×3 orthogonal matrix that represents a rotation by an angle θ about a fixed axis $\hat{\mathbf{n}}$,

$$R^{ij}(\hat{\mathbf{n}},\theta) = \exp(-i\theta\hat{\mathbf{n}}\cdot\vec{\mathcal{J}}) = n^i n^j + (\delta^{ij} - n^i n^j)\cos\theta - \epsilon^{ijk}n^k\sin\theta, \tag{C.1.5}$$

where the $\vec{\mathcal{J}} = (\mathcal{J}^1, \mathcal{J}^2, \mathcal{J}^3)$ are three 3×3 matrices whose matrix elements are given by $(\mathcal{J}^i)^{jk} = -i\epsilon^{ijk}$ [cf. Eq. (2.9)].

However, the angle γ is arbitrary, since $R(\hat{\boldsymbol{z}},\gamma)\hat{\boldsymbol{z}} = \hat{\boldsymbol{z}}$. Thus,

$$\hat{\mathbf{s}} = \mathcal{R}\hat{\boldsymbol{z}} = (\sin\theta\cos\phi, \sin\theta\sin\phi, \cos\theta), \tag{C.1.6}$$

independently of the choice of γ. For $\theta = 0$ or $\theta = \pi$, where $\hat{\mathbf{s}}$ is parallel to the z-axis, the azimuthal angle ϕ is undefined. Since $\hat{\mathbf{s}} \to -\hat{\mathbf{s}}$ corresponds in general to $\theta \to \pi - \theta$ and $\phi \to \phi + \pi \pmod{2\pi}$, we shall adopt a convention whereby:

$$\phi = \begin{cases} 0, & \text{for } \hat{\mathbf{s}} = \hat{\boldsymbol{z}}, \quad (\theta = 0),\\ \pi, & \text{for } \hat{\mathbf{s}} = -\hat{\boldsymbol{z}}, \quad (\theta = \pi). \end{cases} \tag{C.1.7}$$

Using the spin-1/2 rotation operator corresponding to $\mathcal{R}(\phi,\theta,\gamma)$, one can compute $\chi_s(\hat{\mathbf{s}})$,

$$\chi_s(\hat{\mathbf{s}}) = \mathcal{D}(\phi,\theta,\gamma)\,\chi_s(\hat{\boldsymbol{z}}), \tag{C.1.8}$$

where $\mathcal{D}$ is the spin-1/2 unitary representation matrix [253]

$$\mathcal{D}(\phi,\theta,\gamma) \equiv D(\hat{\boldsymbol{z}},\phi)\,D(\hat{\boldsymbol{y}},\theta)\,D(\hat{\boldsymbol{z}},\gamma), \tag{C.1.9}$$

and D is the 2×2 unitary matrix

$$D(\hat{\mathbf{n}},\theta) \equiv \exp\left(-i\theta\hat{\mathbf{n}}\cdot\vec{\sigma}/2\right) = \cos\frac{\theta}{2} - i\hat{\mathbf{n}}\cdot\vec{\sigma}\sin\frac{\theta}{2}. \tag{C.1.10}$$

Eq. (C.1.8) yields explicit forms for the eigenstates of $\frac{1}{2}\vec{\sigma}\cdot\hat{\mathbf{s}}$:

$$\chi_{1/2}(\hat{\mathbf{s}}) = \begin{pmatrix} e^{-i(\phi+\gamma)/2}\cos\dfrac{\theta}{2}\\[2ex] e^{i(\phi-\gamma)/2}\sin\dfrac{\theta}{2}\end{pmatrix}, \qquad \chi_{-1/2}(\hat{\mathbf{s}}) = \begin{pmatrix} -e^{-i(\phi-\gamma)/2}\sin\dfrac{\theta}{2}\\[2ex] e^{i(\phi+\gamma)/2}\cos\dfrac{\theta}{2}\end{pmatrix}. \tag{C.1.11}$$

The well-known two-to-one mapping between SU(2) and SO(3) implies that for a given rotation matrix $\mathcal{R}$ there are two corresponding spin-1/2 rotation matrices $\mathcal{D}$. In particular,

$$\mathcal{D}(\phi + 2\pi, \theta, \gamma) = -\mathcal{D}(\phi, \theta, \gamma), \tag{C.1.12}$$

which implies that a rotation of a spinor by 2π yields an overall change of sign in the spinor wave function (an effect that can be observed in quantum interference experiments!). Strictly speaking, we should take the range of the Euler angles to be $0 \leq \phi < 4\pi$, $0 \leq \theta \leq \pi$ and $0 \leq \gamma < 2\pi$. However, when constructing the spinor wave function of a spin-1/2 particle whose spin quantization axis is given by Eq. (C.1.6), we will fix the overall sign of the spinor wave function by convention.

More generally, the overall phase of the spinor wave function is unphysical. Noting that $D(\hat{\boldsymbol{z}}, \gamma)\, \chi_s(\hat{\boldsymbol{z}}) = e^{-is\gamma}\chi_s(\hat{\boldsymbol{z}})$, the choice of γ is also a matter of convention. First, we will require that when $\hat{\boldsymbol{s}} = \hat{\boldsymbol{z}}$, Eq. (C.1.8) should reproduce the spinor wave functions given in Eq. (C.1.3). This implies that:

$$\gamma = 0, \quad \text{for } \hat{\boldsymbol{s}} = \hat{\boldsymbol{z}}, \quad (\theta = \phi = 0). \tag{C.1.13}$$

For $\hat{\boldsymbol{s}} = -\hat{\boldsymbol{z}}$, we use Eq. (C.1.7) to obtain:

$$\chi_s(-\hat{\boldsymbol{z}}) = ie^{-is\gamma(-\hat{\boldsymbol{z}})}\, \chi_{-s}(\hat{\boldsymbol{z}}), \quad s = \pm\tfrac{1}{2}, \tag{C.1.14}$$

where the notation $\gamma(-\hat{\boldsymbol{z}})$ has been employed to allow the possibility that the convention for γ depends on the direction indicated by its argument.

Two different conventions are commonly employed in the literature. In the first convention, one chooses $\gamma = -\phi$. This choice has the good feature that $\mathcal{R}(\phi, 0, -\phi) = \mathbb{1}_{3\times 3}$, independently of the angle ϕ, which is undefined when $\theta = 0$.[94] Moreover, the rotation matrix $\mathcal{R}(\phi, \theta, -\phi)$ and the corresponding spin-1/2 rotation matrix $\mathcal{D}(\phi, \theta, -\phi)$ can be expressed simply as a single rotation by an angle θ about a fixed axis that points along a unit vector in the azimuthal direction:

$$\hat{\boldsymbol{\varphi}} \equiv (-\sin\phi, \cos\phi, 0). \tag{C.1.15}$$

In particular,

$$R(\hat{\boldsymbol{\varphi}}, \theta) = R(\hat{\boldsymbol{z}}, \phi)\, R(\hat{\boldsymbol{y}}, \theta)\, R(\hat{\boldsymbol{z}}, -\phi), \tag{C.1.16}$$

$$D(\hat{\boldsymbol{\varphi}}, \theta) = \mathcal{D}(\phi, \theta, -\phi). \tag{C.1.17}$$

Hence, in this convention $\chi_s(\hat{\boldsymbol{s}}) = D(\hat{\boldsymbol{\varphi}}, \theta)\chi_s(\hat{\boldsymbol{z}})$, which is the most common choice for the spinor wave function [36,254,255].

In the second convention, one chooses $\gamma = 0$. One motivation for this choice is that the corresponding rotation matrix is somewhat simpler:

$$\mathcal{R}(\phi, \theta, 0) = R(\hat{\boldsymbol{z}}, \phi)\, R(\hat{\boldsymbol{y}}, \theta) = \begin{pmatrix} \cos\theta\cos\phi & -\sin\phi & \sin\theta\cos\phi \\ \cos\theta\sin\phi & \cos\phi & \sin\theta\sin\phi \\ -\sin\theta & 0 & \cos\theta \end{pmatrix}. \tag{C.1.18}$$

Employing the corresponding spin-1/2 rotation operator $\mathcal{D}(\phi, \theta, 0)$ in Eq. (C.1.8) yields a slightly more symmetrical form for the spinor wave function [256].

Explicit forms for the spinor wave functions in the two conventions are obtained from Eq. (C.1.11) by taking $\gamma(\hat{\boldsymbol{s}}) = -\phi$ and $\gamma(\hat{\boldsymbol{s}}) = 0$, respectively. For example, Eq. (C.1.14) reduces to:

$$\chi_s(-\hat{\boldsymbol{z}}) = \begin{cases} -2s\chi_{-s}(\hat{\boldsymbol{z}}) & \text{for } \gamma(-\hat{\boldsymbol{z}}) = -\phi = -\pi, \\ i\chi_{-s}(\hat{\boldsymbol{z}}) & \text{for } \gamma(-\hat{\boldsymbol{z}}) = 0, \end{cases} \quad s = \pm\tfrac{1}{2}, \tag{C.1.19}$$

in the convention specified by Eq. (C.1.7).

Many of the properties of the spinor wave functions are independent of the choice of the Euler angle γ. The spinor wave functions χ_s defined by Eq. (C.1.8) are normalized such that

$$\chi_s^\dagger(\hat{\boldsymbol{s}})\chi_{s'}(\hat{\boldsymbol{s}}) = \delta_{ss'}, \tag{C.1.20}$$

and satisfy the following completeness relation:

$$\sum_s \chi_s(\hat{\boldsymbol{s}})\chi_s^\dagger(\hat{\boldsymbol{s}}) = \begin{pmatrix} 1 & 0 \\ 0 & 1 \end{pmatrix}. \tag{C.1.21}$$

The spinor wave functions $\chi_s(\hat{\boldsymbol{s}})$ and $\chi_{-s}(\hat{\boldsymbol{s}})$ are connected by the following relation:

$$\chi_{-s}(\hat{\boldsymbol{s}}) = -2si\sigma^2\, \chi_s^*(\hat{\boldsymbol{s}}). \tag{C.1.22}$$

Consider a spin-1/2 fermion with four-momentum $p^\mu = (E, \vec{\boldsymbol{p}})$, with $E = (|\vec{\boldsymbol{p}}|^2 + m^2)^{1/2}$, and the direction of $\vec{\boldsymbol{p}}$ given by

$$\hat{\boldsymbol{p}} = (\sin\theta_p\cos\phi_p, \sin\theta_p\sin\phi_p, \cos\theta_p). \tag{C.1.23}$$

Using Eqs. (2.107) and (2.108), one can employ Eqs. (3.1.19)–(3.1.22) to obtain explicit expressions for the two-component spinor wave functions $x(\vec{\boldsymbol{p}}, s)$, $y(\vec{\boldsymbol{p}}, s)$, $x^\dagger(\vec{\boldsymbol{p}}, s)$ and $y^\dagger(\vec{\boldsymbol{p}}, s)$.

[94] However, $\mathcal{R}(\phi, \pi, -\phi) \neq \mathbb{1}_{3\times 3}$ even though ϕ is also undefined when $\theta = \pi$.

Additional properties of the χ_s can be derived by introducing an orthonormal set of unit three-vectors $\hat{\boldsymbol{s}}^a$ that provide a basis for a right-handed coordinate system. Explicitly,

$$\hat{\boldsymbol{s}}^{\boldsymbol{a}} \cdot \hat{\boldsymbol{s}}^{\boldsymbol{b}} = \delta^{ab}, \tag{C.1.24}$$

$$\hat{\boldsymbol{s}}^{\boldsymbol{a}} \times \hat{\boldsymbol{s}}^{\boldsymbol{b}} = \epsilon^{abc}\hat{\boldsymbol{s}}^{\boldsymbol{c}}. \tag{C.1.25}$$

We shall identify

$$\hat{\boldsymbol{s}}^{\boldsymbol{3}} \equiv \hat{\boldsymbol{s}} \tag{C.1.26}$$

as the quantization axis used in defining the third component of the spin of the fermion in its rest frame. The unit vectors $\hat{\boldsymbol{s}}^{\boldsymbol{1}}$ and $\hat{\boldsymbol{s}}^{\boldsymbol{2}}$ are then chosen such that Eqs. (C.1.24) and (C.1.25) are satisfied. To explicitly construct the $\hat{\boldsymbol{s}}^{\boldsymbol{a}}$, we begin with the orthonormal set $\{\hat{\boldsymbol{x}}, \hat{\boldsymbol{y}}, \hat{\boldsymbol{z}}\}$, and employ the *same* rotation operator $\mathcal{R}$ used to define $\chi_s(\hat{\boldsymbol{s}})$. That is,

$$(\hat{\boldsymbol{s}}^{\boldsymbol{1}}, \hat{\boldsymbol{s}}^{\boldsymbol{2}}, \hat{\boldsymbol{s}}^{\boldsymbol{3}}) = (\mathcal{R}\hat{\boldsymbol{x}}, \mathcal{R}\hat{\boldsymbol{y}}, \mathcal{R}\hat{\boldsymbol{z}}), \qquad \text{where } \mathcal{R} \equiv \mathcal{R}(\phi, \theta, \gamma), \tag{C.1.27}$$

and ϕ, θ and γ are the Euler angles used to define the spinor wave function in Eq. (C.1.8). From Eq. (C.1.27), one can immediately derive the completeness relation (as a consequence of $\mathcal{R}\mathcal{R}^{\mathsf{T}} = \mathbb{1}$),

$$\hat{\boldsymbol{s}}^{\boldsymbol{a}i}\hat{\boldsymbol{s}}^{\boldsymbol{a}j} = \delta^{ij}, \tag{C.1.28}$$

where i and j label the space components of the three-vector $\hat{\boldsymbol{s}}^{\boldsymbol{a}}$.

We can use the $\hat{\boldsymbol{s}}^{\boldsymbol{a}}$ to extend the defining equation of χ_s [Eq. (C.1.2)]:

$$\tfrac{1}{2}\,\vec{\boldsymbol{\sigma}} \cdot \hat{\boldsymbol{s}}^{\boldsymbol{a}}\chi_{s'}(\hat{\boldsymbol{s}}) = \tfrac{1}{2}\tau^a_{ss'}\chi_s(\hat{\boldsymbol{s}}), \tag{C.1.29}$$

where the $\tau^a_{ss'}$ are the matrix elements of the Pauli matrices.[95] That is, $\frac{1}{2}\vec{\boldsymbol{\sigma}} \cdot (\boldsymbol{s}^1 \pm i\boldsymbol{s}^2)$ serve as ladder operators that connect the spinor wave functions $\chi_{1/2}$ and $\chi_{-1/2}$. Using Eq. (C.1.20), it follows that Eq. (C.1.29) is equivalent to:

$$\chi_s^\dagger(\hat{\boldsymbol{s}})\,\vec{\boldsymbol{\sigma}} \cdot \hat{\boldsymbol{s}}^{\boldsymbol{a}}\chi_{s'}(\hat{\boldsymbol{s}}) = \tau^a_{ss'}. \tag{C.1.30}$$

It is instructive to prove Eq. (C.1.30) directly. Employing Eq. (C.1.8) and using the fact that $\mathcal{D}$ is a unitary matrix,

$$\chi_s^\dagger(\hat{\boldsymbol{s}})\,\vec{\boldsymbol{\sigma}} \cdot \hat{\boldsymbol{s}}^{\boldsymbol{a}}\chi_{s'}(\hat{\boldsymbol{s}}) = \chi_s^\dagger(\hat{\boldsymbol{z}})\,[\mathcal{D}(\phi, \theta, \gamma)]^{-1}\vec{\boldsymbol{\sigma}} \cdot \hat{\boldsymbol{s}}^{\boldsymbol{a}}\,\mathcal{D}(\phi, \theta, \gamma)\chi_{s'}(\hat{\boldsymbol{z}}). \tag{C.1.31}$$

The above result can be simplified by a repeated use of the following identity,

$$e^{i\theta\hat{\boldsymbol{n}}\cdot\vec{\boldsymbol{\sigma}}/2}\,\sigma^j\,e^{-i\theta\hat{\boldsymbol{n}}\cdot\vec{\boldsymbol{\sigma}}/2} = R^{jk}(\hat{\boldsymbol{n}}, \theta)\sigma^k, \tag{C.1.32}$$

which is valid for any fixed-axis $\hat{\boldsymbol{n}}$, where $R(\hat{\boldsymbol{n}}, \theta)$ is the rotation matrix defined in Eq. (C.1.5). It follows that

$$[\mathcal{D}(\phi, \theta, \gamma)]^{-1}\,\sigma^j\,\mathcal{D}(\phi, \theta, \gamma) = \mathcal{R}^{jk}(\phi, \theta, \gamma)\,\sigma^k, \tag{C.1.33}$$

where $\mathcal{R}(\phi, \theta, \gamma)$ is defined in Eq. (C.1.4). Since $\mathcal{R}^{\mathsf{T}} = \mathcal{R}^{-1}$,

$$\chi_s^\dagger(\hat{\boldsymbol{s}})\,\vec{\boldsymbol{\sigma}} \cdot \hat{\boldsymbol{s}}^{\boldsymbol{a}}\chi_{s'}(\hat{\boldsymbol{s}}) = \chi_s^\dagger(\hat{\boldsymbol{z}})\,\vec{\boldsymbol{\sigma}} \cdot \left[\mathcal{R}^{-1}\hat{\boldsymbol{s}}^{\boldsymbol{a}}\right]\,\chi_{s'}(\hat{\boldsymbol{z}}). \tag{C.1.34}$$

Eq. (C.1.27) implies that $(\mathcal{R}^{-1}\hat{\boldsymbol{s}}^{\boldsymbol{1}}, \mathcal{R}^{-1}\hat{\boldsymbol{s}}^{\boldsymbol{2}}, \mathcal{R}^{-1}\hat{\boldsymbol{s}}^{\boldsymbol{3}}) = (\hat{\boldsymbol{x}}, \hat{\boldsymbol{y}}, \hat{\boldsymbol{z}})$, and it follows that

$$\vec{\boldsymbol{\sigma}} \cdot \left[\mathcal{R}^{-1}\hat{\boldsymbol{s}}^{\boldsymbol{a}}\right] = \sigma^a. \tag{C.1.35}$$

Consequently, we end up with

$$\chi_s^\dagger(\hat{\boldsymbol{s}})\,\vec{\boldsymbol{\sigma}} \cdot \hat{\boldsymbol{s}}^{\boldsymbol{a}}\chi_{s'}(\hat{\boldsymbol{s}}) = \chi_s^\dagger(\hat{\boldsymbol{z}})\sigma^a\chi_{s'}(\hat{\boldsymbol{z}}) \equiv \tau^a_{ss'}, \tag{C.1.36}$$

which defines the matrix elements of the Pauli matrices, and our proof of Eq. (C.1.30) is complete.

Using the completeness relation given by Eq. (C.1.28), we can rewrite Eq. (C.1.30) as

$$\chi_s^\dagger(\hat{\boldsymbol{s}})\,\sigma^i\chi_{s'}(\hat{\boldsymbol{s}}) = \tau^a_{ss'}\hat{\boldsymbol{s}}^{\boldsymbol{a}i}. \tag{C.1.37}$$

Taking the hermitian conjugate of Eq. (C.1.37) is equivalent to interchanging $s \leftrightarrow s'$, since the σ^i are hermitian matrices and $(\tau^a_{ss'})^* = \tau^a_{s's}$. To evaluate expressions similar to Eq. (C.1.37) that contain products of σ-matrices, it is sufficient to use

[95] We use the symbol τ rather than σ to emphasize that the indices of the Pauli matrices τ^a are spin labels s, s' and *not* spinor indices α, $\dot{\alpha}$. The first (second) row and column of the τ-matrices correspond to $s = 1/2$ $(-1/2)$. For example, $\tau^3_{ss'} = 2s\delta_{ss'}$ (no sum over s).

the relation $\sigma^i\sigma^j = \delta^{ij}\mathbb{1} + i\epsilon^{ijk}\sigma^k$ as many times as needed to reduce the final expression to terms containing at most one σ-matrix. For example, using Eqs. (C.1.20) and (C.1.37), it follows that

$$\chi_s^\dagger(\hat{\mathbf{s}})\,\sigma^i\sigma^j\chi_{s'}(\hat{\mathbf{s}}) = \delta_{ss'}\delta^{ij} + i\epsilon^{ijk}\tau^a_{ss'}\hat{\mathbf{s}}^{\boldsymbol{a}k}. \tag{C.1.38}$$

It is sometimes useful to have a more explicit representation of the $\hat{\mathbf{s}}^{\boldsymbol{a}}$. In the convention where $\gamma = -\phi$, Eq. (C.1.27) yields:

$$\begin{aligned}
\hat{\mathbf{s}}^{\mathbf{1}} &= \left(1 - 2\cos^2\phi\,\sin^2\frac{\theta}{2}, -\sin 2\phi\,\sin^2\frac{\theta}{2}, -\sin\theta\cos\phi\right),\\
\hat{\mathbf{s}}^{\mathbf{2}} &= \left(-\sin 2\phi\,\sin^2\frac{\theta}{2}, 1 - 2\sin^2\phi\,\sin^2\frac{\theta}{2}, -\sin\theta\sin\phi\right),\\
\hat{\mathbf{s}}^{\mathbf{3}} &= (\sin\theta\cos\phi, \sin\theta\sin\phi, \cos\theta).
\end{aligned} \tag{C.1.39}$$

The explicit forms for the $\hat{\mathbf{s}}^{\boldsymbol{a}}$ are somewhat simpler in the convention where $\gamma = 0$. In this case, Eqs. (C.1.18) and (C.1.27) yield:

$$\begin{aligned}
\hat{\mathbf{s}}^{\mathbf{1}} &= (\cos\theta\cos\phi, \cos\theta\sin\phi, -\sin\theta),\\
\hat{\mathbf{s}}^{\mathbf{2}} &= (-\sin\phi, \cos\phi, 0),\\
\hat{\mathbf{s}}^{\mathbf{3}} &= (\sin\theta\cos\phi, \sin\theta\sin\phi, \cos\theta).
\end{aligned} \tag{C.1.40}$$

C.2. Fixed-axis spinors in the non-relativistic limit

Consider an on-shell massive fermion of three-momentum $\vec{\boldsymbol{p}}$, mass m and spin quantum number s, where $s = \pm\frac{1}{2}$ are the possible projections of the spin vector (in units of $\hbar$) along the fixed $\hat{\mathbf{s}}$ direction [cf. Eq. (C.1.2)]. The spinor wave functions, x, y, and their hermitian conjugates are given by Eqs. (3.1.19)–(3.1.22). In the non-relativistic limit,

$$\sqrt{p\cdot\sigma} \simeq \sqrt{m}\left(\mathbb{1} - \frac{\vec{\boldsymbol{\sigma}}\cdot\vec{\boldsymbol{p}}}{2m}\right), \qquad \sqrt{p\cdot\overline{\sigma}} \simeq \sqrt{m}\left(\mathbb{1} + \frac{\vec{\boldsymbol{\sigma}}\cdot\vec{\boldsymbol{p}}}{2m}\right), \tag{C.2.1}$$

where we keep terms only up to $\mathcal{O}(|\vec{\boldsymbol{p}}|/m)$. Inserting the above results into Eqs. (3.1.19)–(3.1.22) yields:

$$x_\alpha(\vec{p}, s) \simeq \sqrt{m}\left(\mathbb{1} - \frac{\vec{\boldsymbol{\sigma}}\cdot\vec{\boldsymbol{p}}}{2m}\right)\chi_s(\hat{\mathbf{s}}), \tag{C.2.2}$$

$$x^\alpha(\vec{p}, s) \simeq -2s\sqrt{m}\,\chi_{-s}^\dagger(\hat{\mathbf{s}})\left(\mathbb{1} + \frac{\vec{\boldsymbol{\sigma}}\cdot\vec{\boldsymbol{p}}}{2m}\right), \tag{C.2.3}$$

$$y_\alpha(\vec{p}, s) \simeq 2s\sqrt{m}\left(\mathbb{1} - \frac{\vec{\boldsymbol{\sigma}}\cdot\vec{\boldsymbol{p}}}{2m}\right)\chi_{-s}(\hat{\mathbf{s}}), \tag{C.2.4}$$

$$y^\alpha(\vec{p}, s) \simeq \sqrt{m}\,\chi_s^\dagger(\hat{\mathbf{s}})\left(\mathbb{1} + \frac{\vec{\boldsymbol{\sigma}}\cdot\vec{\boldsymbol{p}}}{2m}\right), \tag{C.2.5}$$

for the undotted spinor wave functions and

$$x^{\dagger\dot{\alpha}}(\vec{p}, s) \simeq -2s\sqrt{m}\left(\mathbb{1} + \frac{\vec{\boldsymbol{\sigma}}\cdot\vec{\boldsymbol{p}}}{2m}\right)\chi_{-s}(\hat{\mathbf{s}}), \tag{C.2.6}$$

$$x^\dagger_{\dot{\alpha}}(\vec{p}, s) \simeq \sqrt{m}\,\chi_s^\dagger(\hat{\mathbf{s}})\left(\mathbb{1} - \frac{\vec{\boldsymbol{\sigma}}\cdot\vec{\boldsymbol{p}}}{2m}\right), \tag{C.2.7}$$

$$y^{\dagger\dot{\alpha}}(\vec{p}, s) \simeq \sqrt{m}\left(\mathbb{1} + \frac{\vec{\boldsymbol{\sigma}}\cdot\vec{\boldsymbol{p}}}{2m}\right)\chi_s(\hat{\mathbf{s}}), \tag{C.2.8}$$

$$y^\dagger_{\dot{\alpha}}(\vec{p}, s) \simeq 2s\sqrt{m}\,\chi_{-s}^\dagger(\hat{\mathbf{s}})\left(\mathbb{1} - \frac{\vec{\boldsymbol{\sigma}}\cdot\vec{\boldsymbol{p}}}{2m}\right), \tag{C.2.9}$$

for the dotted spinor wave functions.

In the computation of the S-matrix amplitudes for scattering and decay processes, one typically must evaluate a bilinear product of spinors, i.e. quantities of the form

$$z_1(\vec{\boldsymbol{p}}_1, s_1)\,\Gamma\,z_2(\vec{\boldsymbol{p}}_2, s_2), \tag{C.2.10}$$

where z_1 and z_2 represent one of the two-component spinor wave functions x, y, $x^\dagger$ or $y^\dagger$, and Γ is a 2×2 matrix (in spinor space) that is either the identity matrix, or is made up of alternating products of σ and $\overline{\sigma}$. In the non-relativistic limit, these bilinears take on rather simple forms. In what follows, we work to first order in $|\vec{\boldsymbol{p}}_i|/m_i$. For example,

$$y^\alpha(\vec{\boldsymbol{p}}_1,s_1)x_\alpha(\vec{\boldsymbol{p}}_2,s_2) \simeq \sqrt{m_1m_2}\,\chi^\dagger_{s_1}(\hat{\boldsymbol{s}})\left(\mathbb{1}+\frac{\vec{\boldsymbol{\sigma}}\cdot\vec{\boldsymbol{p}}}{2m_1}-\frac{\vec{\boldsymbol{\sigma}}\cdot\vec{\boldsymbol{p}}}{2m_2}\right)\chi_{s_2}(\hat{\boldsymbol{s}})$$
$$\simeq \sqrt{m_1m_2}\left[\delta_{s_1,s_2}+\left(\frac{\vec{\boldsymbol{p}}_1}{2m_1}-\frac{\vec{\boldsymbol{p}}_2}{2m_2}\right)\cdot\hat{\boldsymbol{s}}^{\boldsymbol{a}}\tau^a_{s_1,s_2}\right], \tag{C.2.11}$$

where we have used the results of Eqs. (C.1.20) and (C.1.37). Similarly,

$$y^\alpha(\boldsymbol{p}_1,s_1)\sigma^\mu_{\alpha\dot\beta}y^{\dagger\dot\beta}(\boldsymbol{p}_2,s_2) \simeq \sqrt{m_1m_2}\,\chi^\dagger_{s_1}(\hat{\boldsymbol{s}})\left[\sigma^\mu+\frac{\vec{\boldsymbol{\sigma}}\cdot\vec{\boldsymbol{p}}_1}{2m_1}\sigma^\mu+\sigma^\mu\frac{\vec{\boldsymbol{\sigma}}\cdot\vec{\boldsymbol{p}}_2}{2m_2}\right]\chi_{s_2}(\hat{\boldsymbol{s}})$$
$$\simeq \sqrt{m_1m_2}\,Z^\mu_{s_1,s_2}(\vec{\boldsymbol{p}}_1,\vec{\boldsymbol{p}}_2), \tag{C.2.12}$$

where[96]

$$Z^\mu_{ss'}(\vec{\boldsymbol{p}}_1,\vec{\boldsymbol{p}}_2)\equiv\begin{cases}\delta_{ss'}+\left(\dfrac{\vec{\boldsymbol{p}}_1}{2m_1}+\dfrac{\vec{\boldsymbol{p}}_2}{2m_2}\right)\cdot\hat{\boldsymbol{s}}^{\boldsymbol{a}}\tau^a_{ss'}, & \text{for } \mu=0,\\ \hat{\boldsymbol{s}}^{\boldsymbol{a}i}\tau^a_{ss'}+\left(\dfrac{p_1^i}{2m_1}+\dfrac{p_2^i}{2m_2}\right)\delta_{ss'}+\left(\dfrac{p_2^j}{2m_2}-\dfrac{p_1^j}{2m_1}\right)i\epsilon^{ijk}\hat{\boldsymbol{s}}^{\boldsymbol{a}k}\tau^a_{ss'}, & \text{for } \mu=i=1,2,3,\end{cases} \tag{C.2.13}$$

is obtained after using the results of Eqs. (C.1.37) and (C.1.38).

In summary, we list the non-relativistic forms of the spinor bilinears. Referring to Eq. (C.2.10), if $\Gamma=\mathbb{1}$, then

$$x^\alpha(\vec{\boldsymbol{p}}_1,s_1)x_\alpha(\vec{\boldsymbol{p}}_2,s_2)\simeq 2s_2\sqrt{m_1m_2}\left[\delta_{-s_2,s_1}+\left(\frac{\vec{\boldsymbol{p}}_1}{2m_1}-\frac{\vec{\boldsymbol{p}}_2}{2m_2}\right)\cdot\hat{\boldsymbol{s}}^{\boldsymbol{a}}\tau^a_{-s_2,s_1}\right], \tag{C.2.14}$$

$$y^\alpha(\vec{\boldsymbol{p}}_1,s_1)y_\alpha(\vec{\boldsymbol{p}}_2,s_2)\simeq 2s_2\sqrt{m_1m_2}\left[\delta_{s_1,-s_2}+\left(\frac{\vec{\boldsymbol{p}}_1}{2m_1}-\frac{\vec{\boldsymbol{p}}_2}{2m_2}\right)\cdot\hat{\boldsymbol{s}}^{\boldsymbol{a}}\tau^a_{s_1,-s_2}\right], \tag{C.2.15}$$

$$x^\alpha(\vec{\boldsymbol{p}}_1,s_1)y_\alpha(\vec{\boldsymbol{p}}_2,s_2)\simeq \sqrt{m_1m_2}\left[-\delta_{s_2,s_1}+\left(\frac{\vec{\boldsymbol{p}}_1}{2m_1}-\frac{\vec{\boldsymbol{p}}_2}{2m_2}\right)\cdot\hat{\boldsymbol{s}}^{\boldsymbol{a}}\tau^a_{s_2,s_1}\right], \tag{C.2.16}$$

$$y^\alpha(\vec{\boldsymbol{p}}_1,s_1)x_\alpha(\vec{\boldsymbol{p}}_2,s_2)\simeq \sqrt{m_1m_2}\left[\delta_{s_1,s_2}+\left(\frac{\vec{\boldsymbol{p}}_1}{2m_1}-\frac{\vec{\boldsymbol{p}}_2}{2m_2}\right)\cdot\hat{\boldsymbol{s}}^{\boldsymbol{a}}\tau^a_{s_1,s_2}\right], \tag{C.2.17}$$

where we have used

$$\tau^a_{s's}=-4ss'\tau^a_{-s,-s'},\qquad s,s'=\pm\tfrac{1}{2}, \tag{C.2.18}$$

to arrive at the final forms given in Eqs. (C.2.14) and (C.2.16). However, in using the above results, one must now pay close attention to the ordering of the subscript indices of the τ^a. The corresponding formulae for dotted spinor wave function bilinears are obtained by taking the hermitian conjugates of Eqs. (C.2.14)–(C.2.17), which complex conjugates the τ^a that appear on the right-hand side of these equations. Since $(\tau^a_{ss'})^*=\tau^a_{s's}$, we obtain

$$x^\dagger_{\dot\alpha}(\vec{\boldsymbol{p}}_1,s_1)x^{\dagger\dot\alpha}(\vec{\boldsymbol{p}}_2,s_2)\simeq 2s_1\sqrt{m_1m_2}\left[\delta_{s_2,-s_1}-\left(\frac{\vec{\boldsymbol{p}}_1}{2m_1}-\frac{\vec{\boldsymbol{p}}_2}{2m_2}\right)\cdot\hat{\boldsymbol{s}}^{\boldsymbol{a}}\tau^a_{s_2,-s_1}\right], \tag{C.2.19}$$

$$y^\dagger_{\dot\alpha}(\vec{\boldsymbol{p}}_1,s_1)y^{\dagger\dot\alpha}(\vec{\boldsymbol{p}}_2,s_2)\simeq 2s_1\sqrt{m_1m_2}\left[\delta_{-s_1,s_2}-\left(\frac{\vec{\boldsymbol{p}}_1}{2m_1}-\frac{\vec{\boldsymbol{p}}_2}{2m_2}\right)\cdot\hat{\boldsymbol{s}}^{\boldsymbol{a}}\tau^a_{-s_1,s_2}\right], \tag{C.2.20}$$

$$y^\dagger_{\dot\alpha}(\vec{\boldsymbol{p}}_1,s_1)x^{\dagger\dot\alpha}(\vec{\boldsymbol{p}}_2,s_2)\simeq -\sqrt{m_1m_2}\left[\delta_{s_2,s_1}+\left(\frac{\vec{\boldsymbol{p}}_1}{2m_1}-\frac{\vec{\boldsymbol{p}}_2}{2m_2}\right)\cdot\hat{\boldsymbol{s}}^{\boldsymbol{a}}\tau^a_{s_2,s_1}\right], \tag{C.2.21}$$

$$x^\dagger_{\dot\alpha}(\vec{\boldsymbol{p}}_1,s_1)y^{\dagger\dot\alpha}(\vec{\boldsymbol{p}}_2,s_2)\simeq \sqrt{m_1m_2}\left[\delta_{s_1,s_2}-\left(\frac{\vec{\boldsymbol{p}}_1}{2m_1}-\frac{\vec{\boldsymbol{p}}_2}{2m_2}\right)\cdot\hat{\boldsymbol{s}}^{\boldsymbol{a}}\tau^a_{s_1,s_2}\right]. \tag{C.2.22}$$

[96] We also define $Z^\mu_{s's}(\vec{\boldsymbol{p}}_2,\vec{\boldsymbol{p}}_1)$ as the expression given by Eq. (C.2.13) with the interchange of $\{s,\vec{\boldsymbol{p}}_1,m_1\}$ and $\{s',\vec{\boldsymbol{p}}_2,m_2\}$.

Likewise, if $\Gamma = \sigma^\mu$, then

$$x^\alpha(\boldsymbol{p_1}, s_1)\sigma^\mu_{\alpha\dot\beta}x^{\dagger\dot\beta}(\boldsymbol{p}_2, s_2) \simeq 4s_1s_2\sqrt{m_1m_2}\,Z^\mu_{-s_1,-s_2}(\vec{\boldsymbol{p}}_1, \vec{\boldsymbol{p}}_2), \tag{C.2.23}$$

$$y^\alpha(\boldsymbol{p_1}, s_1)\sigma^\mu_{\alpha\dot\beta}y^{\dagger\dot\beta}(\boldsymbol{p}_2, s_2) \simeq \sqrt{m_1m_2}\,Z^\mu_{s_1,s_2}(\vec{\boldsymbol{p}}_1, \vec{\boldsymbol{p}}_2), \tag{C.2.24}$$

$$x^\alpha(\boldsymbol{p_1}, s_1)\sigma^\mu_{\alpha\dot\beta}y^{\dagger\dot\beta}(\boldsymbol{p}_2, s_2) \simeq -2s_1\sqrt{m_1m_2}\,Z^\mu_{-s_1,s_2}(\vec{\boldsymbol{p}}_1, \vec{\boldsymbol{p}}_2), \tag{C.2.25}$$

$$y^\alpha(\boldsymbol{p_1}, s_1)\sigma^\mu_{\alpha\dot\beta}x^{\dagger\dot\beta}(\boldsymbol{p}_2, s_2) \simeq -2s_2\sqrt{m_1m_2}\,Z^\mu_{s_1,-s_2}(\vec{\boldsymbol{p}}_1, \vec{\boldsymbol{p}}_2), \tag{C.2.26}$$

where $Z^\mu_{ss'}(\vec{\boldsymbol{p}}_1, \vec{\boldsymbol{p}}_2)$ is defined in Eq. (C.2.13). If $\Gamma = \overline{\sigma}^\mu$, one can use $z_1\sigma^\mu z_2^\dagger = z_2^\dagger\overline{\sigma}^\mu z_1$ [i.e. Eq. (2.61) for commuting spinors] to obtain the corresponding formulae for the spinor wave function bilinears (cf. footnote 96):

$$x^\dagger_{\dot\alpha}(\boldsymbol{p_1}, s_1)\overline{\sigma}^{\mu\dot\alpha\beta}x_\beta(\boldsymbol{p}_2, s_2) \simeq 4s_1s_2\sqrt{m_1m_2}\,Z^\mu_{-s_2,-s_1}(\vec{\boldsymbol{p}}_2, \vec{\boldsymbol{p}}_1), \tag{C.2.27}$$

$$y^\dagger_{\dot\alpha}(\boldsymbol{p_1}, s_1)\overline{\sigma}^{\mu\dot\alpha\beta}y_\beta(\boldsymbol{p}_2, s_2) \simeq \sqrt{m_1m_2}\,Z^\mu_{s_2,s_1}(\vec{\boldsymbol{p}}_2, \vec{\boldsymbol{p}}_1), \tag{C.2.28}$$

$$y^\dagger_{\dot\alpha}(\boldsymbol{p_1}, s_1)\overline{\sigma}^{\mu\dot\alpha\beta}x_\beta(\boldsymbol{p}_2, s_2) \simeq -2s_2\sqrt{m_1m_2}\,Z^\mu_{-s_2,s_1}(\vec{\boldsymbol{p}}_2, \vec{\boldsymbol{p}}_1), \tag{C.2.29}$$

$$x^\dagger_{\dot\alpha}(\boldsymbol{p_1}, s_1)\overline{\sigma}^{\mu\dot\alpha\beta}y_\beta(\boldsymbol{p}_2, s_2) \simeq -2s_1\sqrt{m_1m_2}\,Z^\mu_{s_2,-s_1}(\vec{\boldsymbol{p}}_2, \vec{\boldsymbol{p}}_1). \tag{C.2.30}$$

These results can also be derived directly from Eqs. (C.2.2)–(C.2.9), after employing Eq. (C.2.18).

It is straightforward to evaluate the spinor wave function bilinears when Γ is a product of two or more $\sigma/\overline{\sigma}$ matrices. As the corresponding expressions are considerably more complicated, we shall not write them out explicitly here.

C.3. Helicity spinor wave functions

All the results of Appendix C.1 apply to the helicity spinors χ_λ, which are defined to be eigenstates of $\frac{1}{2}\vec{\boldsymbol{\sigma}}\cdot\hat{\boldsymbol{p}}$, i.e.,

$$\tfrac{1}{2}\vec{\boldsymbol{\sigma}}\cdot\hat{\boldsymbol{p}}\,\chi_\lambda(\hat{\boldsymbol{p}}) = \lambda\chi_\lambda(\hat{\boldsymbol{p}}), \quad \lambda = \pm\tfrac{1}{2}, \tag{C.3.1}$$

where $\hat{\boldsymbol{p}} = (\sin\theta_p\cos\phi_p, \sin\theta_p\sin\phi_p, \cos\theta_p)$. It follows that:

$$\sqrt{p\cdot\sigma}\;\chi_\lambda(\hat{\boldsymbol{p}}) = \omega_{-\lambda}(\vec{\boldsymbol{p}})\;\chi_\lambda(\hat{\boldsymbol{p}}), \qquad \sqrt{p\cdot\overline{\sigma}}\;\chi_\lambda(\hat{\boldsymbol{p}}) = \omega_\lambda(\vec{\boldsymbol{p}})\;\chi_\lambda(\hat{\boldsymbol{p}}), \tag{C.3.2}$$

where

$$\omega_\lambda(\vec{\boldsymbol{p}}) \equiv (E + 2\lambda|\vec{\boldsymbol{p}}|\,)^{1/2}, \qquad E = \sqrt{|\vec{\boldsymbol{p}}|^2 + m^2}. \tag{C.3.3}$$

As a result, the explicit forms for the two-component helicity spinor wave functions [cf. Eqs. (3.1.19)–(3.1.22)] simplify:

$$x_\alpha(\vec{\boldsymbol{p}}, \lambda) = \omega_{-\lambda}\,\chi_\lambda(\hat{\boldsymbol{p}}), \qquad x^\alpha(\vec{\boldsymbol{p}}, \lambda) = -2\lambda\,\omega_{-\lambda}\,\chi^\dagger_{-\lambda}(\hat{\boldsymbol{p}}), \tag{C.3.4}$$

$$y_\alpha(\vec{\boldsymbol{p}}, \lambda) = 2\lambda\,\omega_\lambda\,\chi_{-\lambda}(\hat{\boldsymbol{p}}), \qquad y^\alpha(\vec{\boldsymbol{p}}, \lambda) = \omega_\lambda\,\chi^\dagger_\lambda(\hat{\boldsymbol{p}}), \tag{C.3.5}$$

$$x^{\dagger\dot\alpha}(\vec{\boldsymbol{p}}, \lambda) = -2\lambda\,\omega_{-\lambda}\,\chi_{-\lambda}(\hat{\boldsymbol{p}}), \qquad x^\dagger_{\dot\alpha}(\vec{\boldsymbol{p}}, \lambda) = \omega_{-\lambda}\,\chi^\dagger_\lambda(\hat{\boldsymbol{p}}), \tag{C.3.6}$$

$$y^{\dagger\dot\alpha}(\vec{\boldsymbol{p}}, \lambda) = \omega_\lambda\,\chi_\lambda(\hat{\boldsymbol{p}}), \qquad y^\dagger_{\dot\alpha}(\vec{\boldsymbol{p}}, \lambda) = 2\lambda\,\omega_\lambda\,\chi^\dagger_{-\lambda}(\hat{\boldsymbol{p}}), \tag{C.3.7}$$

where $\omega_{\pm\lambda} = \omega_{\pm\lambda}(\vec{\boldsymbol{p}})$.

In analogy with the $\hat{\boldsymbol{s}}^{\boldsymbol{a}}$, it is convenient to introduce an orthonormal set of unit three-vectors $\hat{\boldsymbol{p}}^{\boldsymbol{a}}$ such that $\hat{\boldsymbol{p}}^{\boldsymbol{3}} = \hat{\boldsymbol{p}}$. Then, Eqs. (C.1.24)–(C.1.30) apply as well to the two-component helicity spinors after taking $\hat{\boldsymbol{s}}^{\boldsymbol{a}} = \hat{\boldsymbol{p}}^{\boldsymbol{a}}$.

In scattering processes, it is often convenient to work in the rest frame of the incoming particles, in which the corresponding incoming fermion three-momenta are denoted by $\vec{\boldsymbol{p}}$ and $-\vec{\boldsymbol{p}}$, respectively. The helicity spinor wave function of the second fermion depends on the definition of $\chi_\lambda(-\hat{\boldsymbol{p}})$. In this review, we follow a convention[97] in which $\chi_\lambda(-\hat{\boldsymbol{p}})$ is defined to be the spinor wave function obtained from $\chi_\lambda(\hat{\boldsymbol{z}})$ via a rotation by a polar angle $\pi - \theta_p$ and an azimuthal angle $\phi_p + \pi$ with respect to the $\hat{\boldsymbol{z}}$-direction. Then,

$$\chi_\lambda(-\hat{\boldsymbol{p}}) = \mathcal{D}(\phi_p + \pi, \pi - \theta_p, \gamma(-\hat{\boldsymbol{p}}))\;\chi_\lambda(\hat{\boldsymbol{z}}), \tag{C.3.8}$$

[97] An alternative convention (called the *second-particle convention*) advocated by Jacob and Wick [257] is to define $\chi_\lambda(-\hat{\boldsymbol{p}})$ by starting with $\chi_{-\lambda}(\hat{\boldsymbol{z}})$ and then rotating the spinor by polar and azimuthal angles θ_p and ϕ_p. In this case, $\chi_\lambda(-\hat{\boldsymbol{p}}) = \chi_{-\lambda}(\hat{\boldsymbol{p}})$, and the extra phase factors of Eq. (C.3.11) is absent, i.e. $\xi_\lambda(\hat{\boldsymbol{p}}) = 1$ in Eq. (C.3.11). However, this convention is less suited to scattering processes involving final states with more than two fermions. Hence, we do not adopt the second-particle convention in this review.

where we have exhibited the possible dependence of γ on the direction $-\hat{\boldsymbol{p}}$. Using the properties of the spin-1/2 rotation matrices, one can derive

$$\mathcal{D}(\phi_p+\pi,\pi-\theta_p,\gamma(-\hat{\boldsymbol{p}}))=-\mathcal{D}(\phi_p,\theta_p,\gamma(\hat{\boldsymbol{p}}))\,D(\hat{\boldsymbol{z}},-\gamma(\hat{\boldsymbol{p}})-\gamma(-\hat{\boldsymbol{p}}))\,D(\hat{\boldsymbol{x}},\pi). \tag{C.3.9}$$

Inserting this result in Eq. (C.3.8) and using the relation

$$D(\hat{\boldsymbol{x}},\pi)\chi_\lambda(\hat{\boldsymbol{z}})=-i\sigma^1\chi_\lambda(\hat{\boldsymbol{z}})=-i\chi_{-\lambda}(\hat{\boldsymbol{z}}), \tag{C.3.10}$$

we obtain

$$\chi_\lambda(-\hat{\boldsymbol{p}})=\xi_{-\lambda}(\hat{\boldsymbol{p}})\chi_{-\lambda}(\hat{\boldsymbol{p}}), \tag{C.3.11}$$

where the phase factor $\xi_\lambda(\hat{\boldsymbol{p}})$ is given by

$$\xi_\lambda(\hat{\boldsymbol{p}})=ie^{i\lambda[\gamma(\hat{\boldsymbol{p}})+\gamma(-\hat{\boldsymbol{p}})]},\quad \lambda=\pm\tfrac{1}{2}. \tag{C.3.12}$$

Since γ is a real angle, it follows that:

$$\xi^*_\lambda(\hat{\boldsymbol{p}})=\frac{1}{\xi_\lambda(\hat{\boldsymbol{p}})}=-\xi_{-\lambda}(\hat{\boldsymbol{p}}). \tag{C.3.13}$$

Using Eq. (C.3.12), we note that $\chi_\lambda(\hat{\boldsymbol{p}})$ possesses the peculiar property that:

$$\chi_\lambda(-(-\hat{\boldsymbol{p}}))=-\chi_\lambda(\hat{\boldsymbol{p}}). \tag{C.3.14}$$

This is a consequence of the fact that the result of two successive inversions is equivalent to $\phi_p\to\phi_p+2\pi$, which yields an overall change of sign of a spinor wave function [cf. Eq. (C.1.12)].[98]

For example, corresponding to the two conventional choices for γ,

$$\xi_\lambda(\hat{\boldsymbol{p}})=\begin{cases}(-1)^{\frac{1}{2}-\lambda}\,e^{-2i\lambda\phi_p} & \text{for } \gamma(\hat{\boldsymbol{p}})=-\phi_p,\quad \gamma(-\hat{\boldsymbol{p}})=-\pi+\phi_p,\\ i & \text{for } \gamma(\hat{\boldsymbol{p}})=\gamma(-\hat{\boldsymbol{p}})=0,\end{cases} \tag{C.3.15}$$

with the proviso that for $\hat{\boldsymbol{p}}=\pm\hat{\boldsymbol{z}}$, we define ϕ_p according to Eq. (C.1.7).

Suppose that the two fermions considered above have equal mass. In the center-of-mass frame, if the four-momentum of one of the fermions is $p^\mu=(E,\vec{\boldsymbol{p}})$, then the four-momentum of the other fermion is

$$\widetilde{p}^{\,\mu}\equiv(E,-\vec{\boldsymbol{p}}). \tag{C.3.16}$$

The following *numerical* identities are then satisfied: $\sigma\cdot\widetilde{p}=\overline{\sigma}\cdot p$ and $\overline{\sigma}\cdot\widetilde{p}=\sigma\cdot p$. However, in order to maintain covariance with respect to the undotted and dotted spinor indices, we shall write these identities as:

$$\widetilde{p}\cdot\sigma_{\alpha\dot\beta}=\sigma^0_{\alpha\dot\alpha}(p\cdot\overline{\sigma}^{\dot\alpha\beta})\,\sigma^0_{\beta\dot\beta}, \tag{C.3.17}$$

$$\widetilde{p}\cdot\overline{\sigma}^{\dot\alpha\beta}=\overline{\sigma}^{0\dot\alpha\alpha}(p\cdot\sigma_{\alpha\dot\beta})\,\overline{\sigma}^{0\dot\beta\beta}. \tag{C.3.18}$$

Taking the matrix square root of both sides of Eqs. (C.3.17) and (C.3.18) removes one of the factors of σ^0 and $\overline{\sigma}^0$, respectively [cf. Eqs. (2.109)–(2.115)]. Thus, using Eqs. (3.1.19) and (C.3.11),

$$x_\alpha(-\vec{\boldsymbol{p}},-\lambda)=\sqrt{\widetilde{p}\cdot\sigma}\,\chi_{-\lambda}(-\hat{\boldsymbol{p}})=\sigma^0\sqrt{p\cdot\overline{\sigma}}\,\xi_\lambda(\hat{\boldsymbol{p}})\,\chi_\lambda(\vec{\boldsymbol{p}})=\sigma^0_{\alpha\dot\beta}\,\xi_\lambda(\hat{\boldsymbol{p}})\,y^{\dagger\dot\beta}(\vec{\boldsymbol{p}},\lambda). \tag{C.3.19}$$

In this way, we can derive all relations of this kind for the helicity spinor wave functions:

$$x_\alpha(-\vec{\boldsymbol{p}},-\lambda)=\xi_\lambda\sigma^0_{\alpha\dot\beta}\,y^{\dagger\dot\beta}(\vec{\boldsymbol{p}},\lambda)=\omega_\lambda\xi_\lambda\,\chi_\lambda(\hat{\boldsymbol{p}}), \tag{C.3.20}$$

$$y_\alpha(-\vec{\boldsymbol{p}},-\lambda)=\xi_{-\lambda}\sigma^0_{\alpha\dot\beta}\,x^{\dagger\dot\beta}(\vec{\boldsymbol{p}},\lambda)=-2\lambda\,\omega_{-\lambda}\xi_{-\lambda}\,\chi_{-\lambda}(\hat{\boldsymbol{p}}), \tag{C.3.21}$$

$$x^{\dagger\dot\alpha}(-\vec{\boldsymbol{p}},-\lambda)=\xi_{-\lambda}\overline{\sigma}^{0\dot\alpha\beta}\,y_\beta(\vec{\boldsymbol{p}},\lambda)=2\lambda\,\omega_\lambda\xi_{-\lambda}\,\chi_{-\lambda}(\hat{\boldsymbol{p}}), \tag{C.3.22}$$

$$y^{\dagger\dot\alpha}(-\vec{\boldsymbol{p}},-\lambda)=\xi_\lambda\overline{\sigma}^{0\dot\alpha\beta}\,x_\beta(\vec{\boldsymbol{p}},\lambda)=\omega_{-\lambda}\xi_\lambda\,\chi_\lambda(\hat{\boldsymbol{p}}), \tag{C.3.23}$$

where $\omega_{\pm\lambda}\equiv\omega_{\pm\lambda}(\vec{\boldsymbol{p}})$ and $\xi_\lambda\equiv\xi_\lambda(\hat{\boldsymbol{p}})$. Raising the undotted index and lowering the dotted index yields:

$$x^\alpha(-\vec{\boldsymbol{p}},-\lambda)=y^\dagger_\beta(\vec{\boldsymbol{p}},\lambda)\,\xi_{-\lambda}\overline{\sigma}^{0\dot\beta\alpha}=2\lambda\,\omega_\lambda\xi_{-\lambda}\chi^\dagger_{-\lambda}(\hat{\boldsymbol{p}}), \tag{C.3.24}$$

$$y^\alpha(-\vec{\boldsymbol{p}},-\lambda)=x^\dagger_\beta(\vec{\boldsymbol{p}},\lambda)\,\xi_\lambda\overline{\sigma}^{0\dot\beta\alpha}=\omega_{-\lambda}\xi_\lambda\,\chi^\dagger_\lambda(\hat{\boldsymbol{p}}), \tag{C.3.25}$$

$$x^\dagger_{\dot\alpha}(-\vec{\boldsymbol{p}},-\lambda)=y^\beta(\vec{\boldsymbol{p}},\lambda)\,\xi_\lambda\sigma^0_{\beta\dot\alpha}=\omega_\lambda\xi_\lambda\,\chi^\dagger_\lambda(\hat{\boldsymbol{p}}), \tag{C.3.26}$$

$$y^\dagger_{\dot\alpha}(-\vec{\boldsymbol{p}},-\lambda)=x^\beta(\vec{\boldsymbol{p}},\lambda)\,\xi_{-\lambda}\sigma^0_{\beta\dot\alpha}=-2\lambda\,\omega_{-\lambda}\xi_{-\lambda}\,\chi^\dagger_{-\lambda}(\hat{\boldsymbol{p}}). \tag{C.3.27}$$

Eqs. (C.3.20)–(C.3.27) can also be obtained directly from Eqs. (C.3.4)–(C.3.7).

[98] A slightly modified procedure (not adopted in this review) is to take the azimuthal angle of $-\hat{\boldsymbol{p}}$ to be $\phi_p\pm\pi$, where the $\pm$ sign is chosen according to which of the two conditions $0\le\phi_p\pm\pi<2\pi$ is true. This procedure would yield an extra minus sign in the definition of $\xi_\lambda(\hat{\boldsymbol{p}})$ when $\pi\le\phi_p<2\pi$. In this convention, two successive inversions are equivalent to the identity rotation so that $\chi_\lambda(-(-\hat{\boldsymbol{p}}))=\chi_\lambda(\hat{\boldsymbol{p}})$.

Appendix D. Matrix decompositions for mass matrix diagonalization

In scalar field theory, the diagonalization of the scalar squared-mass matrix M^2 is straightforward. For a theory of n complex scalar fields, M^2 is an hermitian $n \times n$ matrix, which can be diagonalized by a unitary matrix W:

$$W^\dagger M^2 W = m^2 = \mathrm{diag}(m_1^2, m_2^2, \ldots, m_n^2). \tag{D.1}$$

For a theory of n real scalar fields, M^2 is a real symmetric $n \times n$ matrix, which can be diagonalized by an orthogonal matrix Q:

$$Q^\mathsf{T} M^2 Q = m^2 = \mathrm{diag}(m_1^2, m_2^2, \ldots, m_n^2). \tag{D.2}$$

In both cases, the eigenvalues m_k^2 of M^2 are real. These are the standard matrix diagonalization problems that are treated in all elementary linear algebra textbooks.

In spin-1/2 fermion field theory, the most general fermion mass matrix, obtained from the Lagrangian, written in terms of two-component spinors, is complex and symmetric [cf. Section 3.2]. If the Lagrangian exhibits a U(1) symmetry, then a basis can be found such that fields that are charged under the U(1) pair up into Dirac fermions. The fermion mass matrix then decomposes into the direct sum of a complex Dirac fermion mass matrix and a complex symmetric neutral fermion mass matrix. In this Appendix, we review the linear algebra theory relevant for the matrix decompositions associated with the general charged and neutral spin-1/2 fermion mass matrix diagonalizations. The diagonalization of the Dirac fermion mass matrix is governed by the singular value decomposition of a complex matrix, as shown in Appendix D.1. In contrast, the diagonalization of a neutral fermion mass matrix is governed by the Takagi diagonalization of a complex symmetric matrix, which is treated in Appendix D.2.[99] These two techniques are compared and contrasted in Appendix D.3. Dirac fermions can also arise in the case of a pseudo-real representation of fermion fields. As shown in Section 3.2, this latter case requires the reduction of a complex antisymmetric fermion mass matrix to real normal form. The relevant theorem and its proof are given in Appendix D.4.

D.1. Singular value decomposition

The diagonalization of the charged (Dirac) fermion mass matrix requires the singular value decomposition of an arbitrary complex matrix M.

Theorem. *For any complex [or real] $n \times n$ matrix M, unitary [or real orthogonal] matrices L and R exist such that*

$$L^\mathsf{T} M R = M_D = \mathrm{diag}(m_1, m_2, \ldots, m_n), \tag{D.1.1}$$

where the m_k are real and non-negative. This is called the singular value decomposition of the matrix M (e.g., see Refs. [147,258]).

In general, the m_k are *not* the eigenvalues of M. Rather, the m_k are the *singular values* of the general complex matrix M, which are defined to be the non-negative square roots of the eigenvalues of $M^\dagger M$ (or equivalently of $MM^\dagger$). An equivalent definition of the singular values can be established as follows. Since $M^\dagger M$ is an hermitian non-negative matrix, its eigenvalues are real and non-negative and its eigenvectors, v_k, defined by $M^\dagger M v_k = m_k^2 v_k$, can be chosen to be orthonormal.[100] Consider first the eigenvectors corresponding to the non-zero eigenvalues of $M^\dagger M$. Then, we define the vectors w_k such that $M v_k = m_k w_k^*$. It follows that $m_k^2 v_k = M^\dagger M v_k = m_k M^\dagger w_k^*$, which yields: $M^\dagger w_k^* = m_k v_k$. Note that these equations also imply that $MM^\dagger w_k^* = m_k^2 w_k^*$. The orthonormality of the v_k implies the orthonormality of the w_k, and vice versa. For example,

$$\delta_{jk} = \langle v_j | v_k \rangle = \frac{1}{m_j m_k} \langle M^\dagger w_j^* | M^\dagger w_k^* \rangle = \frac{1}{m_j m_k} \langle w_j | M M^\dagger w_k^* \rangle = \frac{m_k}{m_j} \langle w_j^* | w_k^* \rangle, \tag{D.1.2}$$

which yields $\langle w_k | w_j \rangle = \delta_{jk}$. If M is a real matrix, then the eigenvectors v_k can be chosen to be real, in which case the corresponding w_k are also real.

If v_i is an eigenvector of $M^\dagger M$ with zero eigenvalue, then $0 = v_i^\dagger M^\dagger M v_i = \langle M v_i | M v_i \rangle$, which implies that $M v_i = 0$. Likewise, if w_i^* is an eigenvector of $MM^\dagger$ with zero eigenvalue, then $0 = w_i^\mathsf{T} M M^\dagger w_i^* = \langle M^\mathsf{T} w_i | M^\mathsf{T} w_i \rangle^*$, which implies that $M^\mathsf{T} w_i = 0$. Because the eigenvectors of $M^\dagger M$ [$MM^\dagger$] can be chosen orthonormal, the eigenvectors corresponding to the zero eigenvalues of M [$M^\dagger$] can be taken to be orthonormal.[101] Finally, these eigenvectors are also orthogonal to the

---

99 One may choose not to work in a basis where the fermion fields are eigenstates of the U(1) charge operator. In this case, all fermions are governed by a complex symmetric mass matrix, which can be Takagi diagonalized according to the procedure described in Appendix D.2.

100 We define the inner product of two vectors to be $\langle v | w \rangle \equiv v^\dagger w$. Then, v and w are orthonormal if $\langle v | w \rangle = 0$. The norm of a vector is defined by $\| v \| = \langle v | v \rangle^{1/2}$.

101 This analysis shows that the number of linearly independent zero eigenvectors of $M^\dagger M$ [$MM^\dagger$] with zero eigenvalue, coincides with the number of linearly independent eigenvectors of M [$M^\dagger$] with zero eigenvalue.

eigenvectors corresponding to the non-zero eigenvalues of $M^\dagger M$ [$MM^\dagger$]. That is, if the indices i and j run over the eigenvectors corresponding to the zero and non-zero eigenvalues of $M^\dagger M$ [$MM^\dagger$], respectively, then

$$\langle v_j|v_i\rangle = \frac{1}{m_j}\langle M^\dagger w_j^*|v_i\rangle = \frac{1}{m_j}\langle w_j^*|Mv_i\rangle = 0, \tag{D.1.3}$$

and similarly $\langle w_j|w_i\rangle = 0$.

Thus, we can define the singular values of a general complex $n \times n$ matrix M to be the simultaneous solutions (with real non-negative m_k) of[102]:

$$Mv_k = m_k w_k^*, \qquad w_k^{\mathsf{T}} M = m_k v_k^\dagger. \tag{D.1.4}$$

The corresponding v_k (w_k), normalized to have unit norm, are called the right (left) singular vectors of M. In particular, the number of linearly independent v_k coincides with the number of linearly independent w_k and is equal to n.

Proof of the singular value decomposition theorem. Eqs. (D.1.2) and (D.1.3) imply that the right [left] singular vectors can be chosen to be orthonormal. Consequently, the unitary matrix R [L] can be constructed such that its kth column is given by the right [left] singular vector v_k [w_k]. It then follows from Eq. (D.1.4) that:

$$w_k^{\mathsf{T}} M v_\ell = m_k \delta_{k\ell}, \quad \text{(no sum over } k\text{)}. \tag{D.1.5}$$

In matrix form, Eq. (D.1.5) coincides with Eq. (D.1.1), and the singular value decomposition is established. If M is real, then the right and left singular vectors, v_k and w_k, can be chosen to be real, in which case Eq. (D.1.1) holds for real orthogonal matrices L and R.

The singular values of a complex matrix M are unique (up to ordering), as they correspond to the eigenvalues of $M^\dagger M$ (or equivalently the eigenvalues of $MM^\dagger$). The unitary matrices L and R are not unique. The matrix R must satisfy

$$R^\dagger M^\dagger M R = M_D^2, \tag{D.1.6}$$

which follows directly from Eq. (D.1.1) by computing $M_D^\dagger M_D = M_D^2$. That is, R is a unitary matrix that diagonalizes the non-negative definite matrix $M^\dagger M$. Since the eigenvectors of $M^\dagger M$ are orthonormal, each v_k corresponding to a non-degenerate eigenvalue of $M^\dagger M$ can be multiplied by an arbitrary phase $e^{i\theta_k}$. For the case of degenerate eigenvalues, any orthonormal linear combination of the corresponding eigenvectors is also an eigenvector of $M^\dagger M$. It follows that within the subspace spanned by the eigenvectors corresponding to non-degenerate eigenvalues, R is uniquely determined up to multiplication on the right by an arbitrary diagonal unitary matrix. Within the subspace spanned by the eigenvectors of $M^\dagger M$ corresponding to a degenerate eigenvalue, R is determined up to multiplication on the right by an arbitrary unitary matrix.

Once R is fixed, L is obtained from Eq. (D.1.1):

$$L = (M^{\mathsf{T}})^{-1} R^* M_D. \tag{D.1.7}$$

However, if some of the diagonal elements of M_D are zero, then L is not uniquely defined. Writing M_D in 2×2 block form such that the upper left block is a diagonal matrix with positive diagonal elements and the other three blocks are equal to the zero matrix of the appropriate dimensions, it follows that, $M_D = M_D W$, where

$$W = \begin{pmatrix} \mathbb{1} & \mathbb{O} \\ \mathbb{O} & W_0 \end{pmatrix} \tag{D.1.8}$$

W_0 is an arbitrary unitary matrix whose dimension is equal to the number of zeros that appear in the diagonal elements of M_D, and $\mathbb{1}$ and $\mathbb{O}$ are respectively the identity matrix and zero matrix of the appropriate size. Hence, we can multiply both sides of Eq. (D.1.7) on the right by W, which means that L is only determined up to multiplication on the right by an arbitrary unitary matrix whose form is given by Eq. (D.1.8).[103]

If M is a real matrix, then the derivation of the singular value decomposition of M is given by Eq. (D.1.1), where L and R are real orthogonal matrices. This result is easily established by replacing "phase" with "sign" and replacing "unitary" by "real orthogonal" in the above proof.

[102] One can always find a solution to Eq. (D.1.4) such that the m_k are real and non-negative. Given a solution where m_k is complex, we simply write $m_k = |m_k|e^{i\theta}$ and redefine $w_k \to w_k e^{i\theta}$ to remove the phase θ.

[103] Of course, one can reverse the above procedure by first determining the unitary matrix L. Eq. (D.1.1) implies that $L^{\mathsf{T}} M M^\dagger L^* = M_D^2$, in which case L is determined up to multiplication on the right by an arbitrary [diagonal] unitary matrix within the subspace spanned by the eigenvectors corresponding to the degenerate [non-degenerate] eigenvalues of $MM^\dagger$. Having fixed L, one can obtain $R = M^{-1} L^* M_D$ from Eq. (D.1.1). As above, R is only determined up to multiplication on the right by a unitary matrix whose form is given by Eq. (D.1.8).

D.2. Takagi diagonalization

The mass matrix of neutral fermions (or a system of two-component fermions in a generic basis) is complex and symmetric. This mass matrix must be diagonalized in order to identify the physical fermion mass eigenstates and to compute their masses. However, the fermion mass matrix is *not* diagonalized by the standard unitary similarity transformation. Instead a different diagonalization equation is employed that was discovered by Takagi [111], and rediscovered many times since [147].[104]

Theorem. *For any complex symmetric $n \times n$ matrix M, there exists a unitary matrix Ω such that:*

$$\Omega^{\mathsf{T}} M\, \Omega = M_D = \mathrm{diag}(m_1, m_2, \ldots, m_n), \tag{D.2.1}$$

where the m_k are real and non-negative. This is the Takagi diagonalization[105] *of the complex symmetric matrix M.*

In general, the m_k are *not* the eigenvalues of M. Rather, the m_k are the singular values of the symmetric matrix M. From Eq. (D.2.1) it follows that:

$$\Omega^{\dagger} M^{\dagger} M \Omega = M_D^2 = \mathrm{diag}(m_1^2, m_2^2, \ldots, m_n^2). \tag{D.2.2}$$

If all of the singular values m_k are non-degenerate, then one can find a solution to Eq. (D.2.1) for Ω from Eq. (D.2.2). This is no longer true if some of the singular values are degenerate. For example, if $M = \left(\begin{smallmatrix} 0 & m \\ m & 0 \end{smallmatrix}\right)$, then the singular value $|m|$ is doubly degenerate, but Eq. (D.2.2) yields $\Omega^{\dagger}\Omega = \mathbb{1}_{2\times 2}$, which does not specify Ω. That is, in the degenerate case, the physical fermion states *cannot* be determined by the diagonalization of $M^{\dagger}M$. Instead, one must make direct use of Eq. (D.2.1). Below, we shall present a constructive method for determining Ω that is applicable in both the non-degenerate and the degenerate cases.

Eq. (D.2.1) can be rewritten as $M\Omega = \Omega^* M_D$, where the columns of Ω are orthonormal. If we denote the kth column of Ω by v_k, then,

$$M v_k = m_k v_k^*, \tag{D.2.3}$$

where the m_k are the singular values and the vectors v_k are normalized to have unit norm. Following Ref. [261], the v_k are called the *Takagi vectors* of the complex symmetric $n \times n$ matrix M. The Takagi vectors corresponding to non-degenerate non-zero [zero] singular values are unique up to an overall sign [phase]. Any orthogonal [unitary] linear combination of Takagi vectors corresponding to a set of degenerate non-zero [zero] singular values is also a Takagi vector corresponding to the same singular value. Using these results, one can determine the degree of non-uniqueness of the matrix Ω. For definiteness, we fix an ordering of the diagonal elements of M_D.[106] If the singular values of M are distinct, then the matrix Ω is uniquely determined up to multiplication by a diagonal matrix whose entries are either ± 1 (i.e., a diagonal orthogonal matrix). If there are degeneracies corresponding to non-zero singular values, then within the degenerate subspace, Ω is unique up to multiplication on the right by an arbitrary orthogonal matrix. Finally, in the subspace corresponding to zero singular values, Ω is unique up to multiplication on the right by an arbitrary unitary matrix.

For a real symmetric matrix M, the Takagi diagonalization [Eq. (D.2.1)] still holds for a unitary matrix Ω, which is easily determined as follows. Any real symmetric matrix M can be diagonalized by a real orthogonal matrix Z,

$$Z^{\mathsf{T}} M Z = \mathrm{diag}(\varepsilon_1 m_1, \varepsilon_2 m_2, \ldots, \varepsilon_n m_n), \tag{D.2.4}$$

where the m_k are real and non-negative and the $\varepsilon_k m_k$ are the real eigenvalues of M with corresponding signs $\varepsilon_k = \pm 1$.[107] Then, the Takagi diagonalization of M is achieved by taking:

$$\Omega_{ij} = \varepsilon_i^{1/2} Z_{ij}, \quad \text{no sum over } i. \tag{D.2.5}$$

Proof of the Takagi diagonalization. To prove the existence of the Takagi diagonalization of a complex symmetric matrix, it is sufficient to provide an algorithm for constructing the orthonormal Takagi vectors v_k that make up the columns of Ω.

---

104 Subsequently, it was recognized in Ref. [258] that the Takagi diagonalization was first established for nonsingular complex symmetric matrices by Autonne [259]. In the physics literature, the first proof of Eq. (D.2.1) was given in Ref. [149]. Applications of Takagi diagonalization to the study of neutrino mass matrices can be found in Refs. [5,260].

105 In Ref. [147], Eq. (D.2.1) is called the Takagi factorization of a complex symmetric matrix. We choose to refer to this as Takagi *diagonalization* to emphasize and contrast this with the more standard diagonalization of normal matrices by a unitary similarity transformation. In particular, not all *complex* symmetric matrices are diagonalizable by a similarity transformation, whereas complex symmetric matrices are *always* Takagi diagonalizable.

106 Permuting the order of the singular values is equivalent to permuting the order of the columns of Ω.

107 In the case of $m_k = 0$, we conventionally choose the corresponding $\varepsilon_k = +1$.

This is achieved by rewriting the $n \times n$ complex matrix equation $Mv = mv^*$ [with m real and non-negative] as a $2n \times 2n$ real matrix equation [262,263]:

$$M_R \begin{pmatrix} \mathrm{Re}\, v \\ \mathrm{Im}\, v \end{pmatrix} \equiv \begin{pmatrix} \mathrm{Re}\, M & -\mathrm{Im}\, M \\ -\mathrm{Im}\, M & -\mathrm{Re}\, M \end{pmatrix} \begin{pmatrix} \mathrm{Re}\, v \\ \mathrm{Im}\, v \end{pmatrix} = m \begin{pmatrix} \mathrm{Re}\, v \\ \mathrm{Im}\, v \end{pmatrix}, \quad \text{where } m \geq 0. \tag{D.2.6}$$

Since $M = M^{\mathsf{T}}$, the $2n \times 2n$ matrix $M_R \equiv \left(\begin{smallmatrix} \mathrm{Re}\, M & -\mathrm{Im}\, M \\ -\mathrm{Im}\, M & -\mathrm{Re}\, M \end{smallmatrix}\right)$ is a real symmetric matrix.[108] In particular, M_R is diagonalizable by a real orthogonal similarity transformation, and its eigenvalues are real. Moreover, if m is an eigenvalue of M_R with eigenvector $(\mathrm{Re}\, v, \mathrm{Im}\, v)$, then $-m$ is an eigenvalue of M_R with (orthogonal) eigenvector $(-\mathrm{Im}\, v, \mathrm{Re}\, v)$. This observation implies that M_R has an equal number of positive and negative eigenvalues and an even number of zero eigenvalues.[109] Thus, Eq. (D.2.3) has been converted into an ordinary eigenvalue problem for a real symmetric matrix. Since $m \geq 0$, we solve the eigenvalue problem $M_R u = mu$ for the real eigenvectors $u \equiv (\mathrm{Re}\, v, \mathrm{Im}\, v)$ corresponding to the non-negative eigenvalues of M_R,[110] which then immediately yields the complex Takagi vectors, v. It is straightforward to prove that the total number of linearly independent Takagi vectors is equal to n. Simply note that the orthogonality of $(\mathrm{Re}\, v_1, \mathrm{Im}\, v_1)$ and $(-\mathrm{Im}\, v_1, \mathrm{Re}\, v_1)$ with $(\mathrm{Re}\, v_2, \mathrm{Im}\, v_2)$ implies that $v_1^\dagger v_2 = 0$.

Thus, we have derived a constructive method for obtaining the Takagi vectors v_k. If there are degeneracies, one can always choose the v_k in the degenerate subspace to be orthonormal. The Takagi vectors then make up the columns of the matrix Ω in Eq. (D.2.1). A numerical package for performing the Takagi diagonalization of a complex symmetric matrix has recently been presented in Ref. [264] (see also Refs. [261,265] for previous numerical approaches to Takagi diagonalization).

D.3. Relation between Takagi diagonalization and singular value decomposition

The Takagi diagonalization is a special case of the singular value decomposition. If the complex matrix M in Eq. (D.1.1) is symmetric, $M = M^{\mathsf{T}}$, then the Takagi diagonalization corresponds to $\Omega = L = R$. In this case, the right and left singular vectors coincide ($v_k = w_k$) and are identified with the Takagi vectors defined in Eq. (D.2.3). However as previously noted, the matrix Ω cannot be determined from Eq. (D.2.2) in cases where there is a degeneracy among the singular values.[111] For example, one possible singular value decomposition of the matrix $M = \left(\begin{smallmatrix} 0 & m \\ m & 0 \end{smallmatrix}\right)$ [with m assumed real and positive] can be obtained by choosing $R = \left(\begin{smallmatrix} 1 & 0 \\ 0 & 1 \end{smallmatrix}\right)$ and $L = \left(\begin{smallmatrix} 0 & 1 \\ 1 & 0 \end{smallmatrix}\right)$, in which case $L^{\mathsf{T}} M R = \left(\begin{smallmatrix} m & 0 \\ 0 & m \end{smallmatrix}\right) = M_D$. Of course, this is not a Takagi diagonalization because $L \neq R$. Since R is only defined modulo the multiplication on the right by an arbitrary 2×2 unitary matrix $\mathcal{O}$, then at least one singular value decomposition exists that is also a Takagi diagonalization. For the example under consideration, it is not difficult to deduce the Takagi diagonalization: $\Omega^{\mathsf{T}} M \Omega = M_D$, where

$$\Omega = \frac{1}{\sqrt{2}} \begin{pmatrix} 1 & i \\ 1 & -i \end{pmatrix} \mathcal{O}, \tag{D.3.1}$$

and $\mathcal{O}$ is any 2×2 orthogonal matrix.

Since the Takagi diagonalization is a special case of the singular value decomposition, it seems plausible that one can prove the former from the latter. This turns out to be correct; for completeness, we provide the proof below. Our second proof depends on the following lemma:

Lemma. *For any symmetric unitary matrix V, there exists a unitary matrix U such that $V = U^{\mathsf{T}} U$.*

Proof of the Lemma: For any $n \times n$ unitary matrix V, there exists an hermitian matrix H such that $V = \exp(iH)$ (this is the polar decomposition of V). If $V = V^{\mathsf{T}}$ then $H = H^{\mathsf{T}} = H^*$ (since H is hermitian); therefore H is real symmetric. But, any real symmetric matrix can be diagonalized by an orthogonal transformation. It follows that V can also be diagonalized by an orthogonal transformation. Since the eigenvalues of any unitary matrix are pure phases, there exists a real orthogonal matrix Q such that $Q^{\mathsf{T}} V Q = \mathrm{diag}\,(e^{i\theta_1}, e^{i\theta_2}, \ldots, e^{i\theta_n})$. Thus, the unitary matrix,

$$U = \mathrm{diag}\,(e^{i\theta_1/2}, e^{i\theta_2/2}, \ldots, e^{i\theta_n/2})\, Q^{\mathsf{T}}, \tag{D.3.2}$$

satisfies $V = U^{\mathsf{T}} U$ and the lemma is proved. Note that U is unique modulo multiplication on the left by an arbitrary real orthogonal matrix.

---

108 The $2n \times 2n$ matrix M_R is a real representation of the $n \times n$ complex matrix M.

109 Note that $(-\mathrm{Im}\, v, \mathrm{Re}\, v)$ corresponds to replacing v_k in Eq. (D.2.3) by iv_k. However, for $m < 0$ these solutions are not relevant for Takagi diagonalization (where the m_k are by definition non-negative). The case of $m = 0$ is considered in footnote 110.

110 For $m = 0$, the corresponding vectors $(\mathrm{Re}\, v, \mathrm{Im}\, v)$ and $(-\mathrm{Im}\, v, \mathrm{Re}\, v)$ are two linearly independent eigenvectors of M_R; but these yield only one independent Takagi vector v (since v and iv are linearly dependent).

111 This is in contrast to the singular value decomposition, where R can be determined from Eq. (D.1.6) modulo right multiplication by a [diagonal] unitary matrix in the [non-]degenerate subspace and L is then determined by Eq. (D.1.7) modulo multiplication on the right by Eq. (D.1.8).

Second Proof of the Takagi diagonalization. Starting from the singular value decomposition of M, there exist unitary matrices L and R such that $M = L^* M_D R^\dagger$, where M_D is the diagonal matrix of singular values. Since $M = M^\mathsf{T} = R^* M_D L^\dagger$, we have two different singular value decompositions for M. However, as noted below Eq. (D.1.6), R is unique modulo multiplication on the right by an arbitrary [diagonal] unitary matrix, V, within the [non-]degenerate subspace. Thus, it follows that a [diagonal] unitary matrix V exists such that $L = RV$. Moreover, $V = V^\mathsf{T}$. This is manifestly true within the non-degenerate subspace where V is diagonal. Within the degenerate subspace, M_D is proportional to the identity matrix so that $L^* R^\dagger = R^* L^\dagger$. Inserting $L = RV$ then yields $V^\mathsf{T} = V$. Using the lemma proved above, there exists a unitary matrix U such that $V = U^\mathsf{T} U$. That is,

$$L = RU^\mathsf{T} U, \tag{D.3.3}$$

for some unitary matrix U. Moreover, it is now straightforward to show that

$$M_D U^* = U^* M_D. \tag{D.3.4}$$

To see this, note that within the degenerate subspace, Eq. (D.3.4) is trivially true since M_D is proportional to the identity matrix. Within the non-degenerate subspace V is diagonal; hence we may choose $U = U^\mathsf{T} = V^{1/2}$, so that Eq. (D.3.4) is true since diagonal matrices commute. Using Eqs. (D.3.3) and (D.3.4), we can write the singular value decomposition of M as follows

$$M = L^* M_D R^\dagger = R^* U^\dagger U^* M_D R^\dagger = (RU^\mathsf{T})^* M_D U^* R^\dagger = \Omega^* M_D \Omega^\dagger, \tag{D.3.5}$$

where $\Omega \equiv RU^\mathsf{T}$ is a unitary matrix. Thus the existence of the Takagi diagonalization of an arbitrary complex symmetric matrix [Eq. (D.2.1)] is once again proved.

In the diagonalization of the two-component fermion mass matrix, M, the eigenvalues of $M^\dagger M$ typically fall into two classes—non-degenerate eigenvalues corresponding to neutral fermion mass eigenstates and degenerate pairs corresponding to charged (Dirac) mass eigenstates. In this case, the sector of the neutral fermions corresponds to a non-degenerate subspace of the space of fermion fields. Hence, in order to identify the neutral fermion mass eigenstates, it is sufficient to diagonalize $M^\dagger M$ with a unitary matrix R [as in Eq. (D.1.6)], and then adjust the overall phase of each column of R so that the resulting matrix Ω satisfies $\Omega^\mathsf{T} M \Omega = M_D$, where M_D is a diagonal matrix of the non-negative fermion masses. This last result is a consequence of Eqs. (D.3.3)–(D.3.5), where $\Omega = RV^{1/2}$ and V is a diagonal matrix of phases.

D.4. Reduction of a complex antisymmetric matrix to the real normal form

In the case of two-component fermions that transform under a pseudo-real representation of a compact Lie group [cf. Eq. (3.2.35)], the corresponding mass matrix is in general complex and antisymmetric. In this case, one needs the antisymmetric analogue of the Takagi diagonalization of a complex symmetric matrix [147].

Theorem. *For any complex [or real] antisymmetric $n \times n$ matrix M, there exists a unitary [or real orthogonal] matrix U such that:*

$$U^\mathsf{T} M U = N \equiv \mathrm{diag}\left\{ \begin{pmatrix} 0 & m_1 \\ -m_1 & 0 \end{pmatrix}, \begin{pmatrix} 0 & m_2 \\ -m_2 & 0 \end{pmatrix}, \ldots, \begin{pmatrix} 0 & m_p \\ -m_p & 0 \end{pmatrix}, \mathbb{O}_{n-2p} \right\}, \tag{D.4.1}$$

where N is written in block diagonal form with 2×2 matrices appearing along the diagonal, followed by an $(n-2p) \times (n-2p)$ block of zeros (denoted by $\mathbb{O}_{n-2p}$), and the m_j are real and positive. N is called the real normal form of an antisymmetric matrix [149,266,267].

Proof. A number of proofs can be found in the literature [148,149,266–268]. Here we provide a proof inspired by Ref. [266]. Following Appendix D.1, we first consider the eigenvalue equation for $M^\dagger M$:

$$M^\dagger M v_k = m_k^2 v_k, \quad m_k > 0, \quad \text{and} \quad M^\dagger M u_k = 0, \tag{D.4.2}$$

where we have distinguished the eigenvectors corresponding to positive eigenvalues and zero eigenvalues, respectively. The quantities m_k are the positive singular values of M. Noting that $u_k^\dagger M^\dagger M u_k = \langle M u_k \,|\, M u_k \rangle = 0$, it follows that

$$M u_k = 0, \tag{D.4.3}$$

so that the u_k are the eigenvectors corresponding to the zero eigenvalues of M. For each eigenvector of $M^\dagger M$ with $m_k \neq 0$, we define a new vector

$$w_k \equiv \frac{1}{m_k} M^* v_k^*. \tag{D.4.4}$$

It follows that $m_k^2 v_k = M^\dagger M v_k = m_k M^\dagger w_k^*$, which yields $M^\dagger w_k^* = m_k v_k$. Comparing with Eq. (D.1.4), we identify v_k and w_k as the right and left singular vectors, respectively, corresponding to the non-zero singular values of M. For any antisymmetric matrix, $M^\dagger = -M^*$. Hence,

$$M v_k = m_k w_k^*, \qquad M w_k = -m_k v_k^*, \tag{D.4.5}$$

and

$$M^\dagger M w_k = -m_k M^\dagger v_k^* = m_k M^* v_k^* = m_k^2 w_k, \quad m_k > 0. \tag{D.4.6}$$

That is, the w_k are also eigenvectors of $M^\dagger M$.

The key observation is that for fixed k the vectors v_k and w_k are orthogonal, since Eq. (D.4.5) implies that:

$$\langle w_k|v_k\rangle = \langle v_k|w_k\rangle^* = -\frac{1}{m_k^2}\langle Mw_k|Mv_k\rangle = -\frac{1}{m_k^2}\langle w_k|M^\dagger M v_k\rangle = -\langle w_k|v_k\rangle\,, \tag{D.4.7}$$

which yields $\langle w_k|v_k\rangle = 0$. Thus, if all the m_k are distinct, it follows that m_k^2 is a doubly degenerate eigenvalue of $M^\dagger M$, with corresponding linearly independent eigenvectors v_k and w_k, where $k = 1, 2, \ldots, p$ (and $p \leq \frac{1}{2}n$). The remaining zero eigenvalues are $(n-2p)$-fold degenerate, with corresponding eigenvectors u_k (for $k = 1, 2, \ldots, n-2p$). If some of the m_k are degenerate, these conclusions still apply. For example, suppose that $m_j = m_k$ for $j \neq k$, which means that m_k^2 is at least a three-fold degenerate eigenvalue of $M^\dagger M$. Then, there must exist an eigenvector v_j that is orthogonal to v_k and w_k such that $M^\dagger M v_j = m_k^2 v_j$. We now construct $w_j \equiv M^* v_j^*/m_k$ according to Eq. (D.4.4). According to Eq. (D.4.7), w_j is orthogonal to v_j. But, we still must show that w_j is also orthogonal to v_k and w_k. But this is straightforward:

$$\langle w_j|w_k\rangle = \langle w_k|w_j\rangle^* = \frac{1}{m_k^2}\langle Mv_k|Mv_j\rangle = \frac{1}{m_k^2}\langle v_k|M^\dagger M v_j\rangle = \langle v_k|v_j\rangle = 0, \tag{D.4.8}$$

$$\langle w_j|v_k\rangle = \langle v_k|w_j\rangle^* = -\frac{1}{m_k^2}\langle Mw_k|Mv_j\rangle = -\frac{1}{m_k^2}\langle w_k|M^\dagger M v_j\rangle = -\langle w_k|v_j\rangle = 0, \tag{D.4.9}$$

where we have used the assumed orthogonality of v_j with v_k and w_k, respectively. If follows that v_j, w_j, v_k and w_k are linearly independent eigenvectors corresponding to a four-fold degenerate eigenvalue m_k^2 of $M^\dagger M$. Additional degeneracies are treated in the same way.

Thus, the number of non-zero eigenvalues of $M^\dagger M$ must be an even number, denoted by $2p$ above. Moreover, one can always choose the complete set of eigenvectors $\{u_k, v_k, w_k\}$ of $M^\dagger M$ to be orthonormal. These orthonormal vectors can be used to construct a unitary matrix U with matrix elements:

$$\begin{aligned} &U_{\ell,2k-1} = (w_k)_\ell, \qquad U_{\ell,2k} = (v_k)_\ell, \quad k = 1, 2, \ldots, p, \\ &U_{\ell,k+2p} = (u_k)_\ell, \quad k = 1, 2, \ldots, n-2p, \end{aligned} \tag{D.4.10}$$

for $\ell = 1, 2, \ldots, n$, where e.g., $(v_k)_\ell$ is the ℓth component of the vector v_k with respect to the standard orthonormal basis. The orthonormality of $\{u_k, v_k, w_k\}$ implies that $(U^\dagger U)_{\ell k} = \delta_{\ell k}$ as required. Eqs. (D.4.3) and (D.4.5) are thus equivalent to the matrix equation $MU = U^* N$, which immediately yields Eq. (D.4.1), and the theorem is proven. If M is a real antisymmetric matrix, then all the eigenvectors of $M^\dagger M$ can be chosen to be real, in which case U is a real orthogonal matrix.

Finally, we address the non-uniqueness of the matrix U. For definiteness, we fix an ordering of the 2×2 blocks containing the m_k in the matrix N. In the subspace corresponding to a non-zero singular value of degeneracy d, U is unique up to multiplication on the right by a $2d \times 2d$ unitary matrix S that satisfies:

$$S^{\mathsf{T}} J S = J, \tag{D.4.11}$$

where the $2d \times 2d$ matrix J, defined by

$$J = \mathrm{diag}\left\{ \begin{pmatrix} 0 & 1 \\ -1 & 0 \end{pmatrix}, \begin{pmatrix} 0 & 1 \\ -1 & 0 \end{pmatrix}, \ldots, \begin{pmatrix} 0 & 1 \\ -1 & 0 \end{pmatrix} \right\}, \tag{D.4.12}$$

is a block diagonal matrix with d blocks of 2×2 matrices. A unitary matrix S that satisfies Eq. (D.4.11) is an element of the unitary symplectic group, $\mathrm{Sp}(d)$. If there are no degeneracies among the m_k, then $d = 1$. Identifying $\mathrm{Sp}(1) \cong \mathrm{SU}(2)$, it follows that within the subspace corresponding to a non-degenerate singular value, U is unique up to multiplication on the right by an arbitrary SU(2) matrix. Finally, in the subspace corresponding to the zero eigenvalues of M, U is unique up to multiplication on the right by an arbitrary unitary matrix.

Appendix E. Lie group theoretical techniques for gauge theories

E.1. Basic facts about Lie groups, Lie algebras and their representations

Consider a compact connected Lie Group G [269]. The most general form for G is a direct product of compact simple groups and U(1) groups. If no U(1) factors are present, then G is semisimple. For any $U \in G$,

$$U = \exp(-i\theta^a \boldsymbol{T^a}), \tag{E.1.1}$$

where the $\boldsymbol{T^a}$ are called the generators of G, and the θ^a are real numbers that parameterize the elements of G. The corresponding real Lie algebra $\mathfrak{g}$ consists of arbitrary real linear combinations of the generators, $\theta^a\boldsymbol{T^a}$. The Lie group generators $\boldsymbol{T^a}$ satisfy the commutation relations:

$$[\boldsymbol{T^a}, \boldsymbol{T^b}] = if_c^{ab}\boldsymbol{T^c}, \tag{E.1.2}$$

where the real structure constants f_c^{ab} define the compact Lie algebra. The generator indices run over $a, b, c = 1, 2, \ldots, d_G$, where d_G is the dimension of the Lie algebra. For compact Lie algebras, the Killing form $g^{ab} = \mathrm{Tr}(\boldsymbol{T^a}\boldsymbol{T^b})$ is positive definite, so one can always choose a basis for the Lie algebra in which $g^{ab} \propto \delta^{ab}$ (where the proportionality constant is a positive real number). With respect to this new basis, the structure constants $f^{abc} \equiv g^{ad}f_d^{bc}$ are totally antisymmetric with respect to the interchange of the indices a, b and c. Henceforth, we shall always assume that such a *preferred* basis of generators has been chosen.

The elements of the compact Lie group G act on a multiplet of fields that transform under some d_R-dimensional representation R of G. The group elements $U \in G$ are represented by $d_R \times d_R$ unitary matrices, $D_R(U) = \exp(-i\theta^a\boldsymbol{T_R^a})$, where the $\boldsymbol{T_R^a}$ are $d_R \times d_R$ hermitian matrices that satisfy Eq. (E.1.2) and thus provide a representation of the Lie group generators. For any representation R of a semisimple group, $\mathrm{Tr}\,\boldsymbol{T_R^a} = 0$ for all a. A representation R' is unitarily equivalent to R if there exists a fixed unitary matrix S such that $D_{R'}(U) = S^{-1}D_R(U)S$ for all $U \in G$. Similarly, the corresponding generators satisfy $\boldsymbol{T_{R'}^a} = S^{-1}\boldsymbol{T_R^a}S$ for all $a = 1, 2, \ldots, d_G$.

For compact semisimple Lie groups, two representations are noteworthy. If G is one of the classical groups, SU(N) [for $N \geq 2$], SO(N) [for $N \geq 3$] or Sp($N/2$) [the latter is defined by Eqs. (D.4.11) and (D.4.12) for even $N \geq 2$], then the $N \times N$ matrices that define these groups comprise the *fundamental (or defining) representation* F, with $d_F = N$. For example, the fundamental representation of SU(N) consists of $N \times N$ unitary matrices with determinant equal to one, and the corresponding generators comprise a suitably chosen basis for the $N \times N$ traceless hermitian matrices. Every Lie group G also possesses an *adjoint representation* A, with $d_A = d_G$. The matrix elements of the generators in the adjoint representation are given by[112]

$$(\boldsymbol{T_A^a})^{bc} = -if^{abc}. \tag{E.1.3}$$

Given the unitary representation matrices $D_R(U)$ of the representation R of G, the matrices $[D_R(U)]^*$ constitute the *conjugate* representation R^*. Equivalently, if the $\boldsymbol{T_R^a}$ comprise a representation of the Lie algebra $\mathfrak{g}$, then the $-(\boldsymbol{T_R^a})^* = -(\boldsymbol{T_R^a})^{\mathsf{T}}$ comprise a representation R^* of $\mathfrak{g}$ of the same dimension d_R. If R and R^* are unitarily equivalent representations, then we say that the representation R is *self-conjugate*. Otherwise, we say that the representation R is *complex*, or "strictly complex" in the language of Ref. [270]. However, the representation matrices $D_R(U)$ of a self-conjugate representation can also be complex. We can then define two classes of self-conjugate representations. If R and R^* are unitarily equivalent to a representation R' that satisfies the reality property $[D_{R'}(U)]^* = [D_{R'}(U)]$ for all $U \in G$ (equivalently, the matrices $i\boldsymbol{T_{R'}^a}$ are real for all a), then R is said to be *real*, or "strictly real" in the language of Ref. [270]. If R and R^* are unitarily equivalent representations, but neither is unitarily equivalent to a representation that satisfies the reality property above, then R is said to be *pseudo-real*.

Henceforth, we drop the adjective "strictly" and simply refer to real, pseudo-real and complex representations. Self-conjugate representations are either real or pseudo-real. An important theorem states that for self-conjugate representations, there exists a constant unitary matrix W such that [270]

$$[D_R(U)]^* = WD_R(U)W^{-1}, \quad \text{or equivalently, } (i\boldsymbol{T_R^a})^* = W(i\boldsymbol{T_R^a})W^{-1}, \tag{E.1.4}$$

where

$$WW^* = \mathbb{1}, \qquad W^{\mathsf{T}} = W, \qquad \text{for real representations,} \tag{E.1.5}$$

$$WW^* = -\mathbb{1}, \qquad W^{\mathsf{T}} = -W, \qquad \text{for pseudo-real representations,} \tag{E.1.6}$$

and $\mathbb{1}$ is the $d_R \times d_R$ identity matrix. Taking the determinant of Eq. (E.1.6), and using the fact that W is unitary (and hence invertible), it follows that $1 = (-1)^{d_R}$. Therefore, a pseudo-real representation must be even-dimensional.

If we redefine the basis for the Lie group generators by $\boldsymbol{T_R^a} \to V^{-1}\boldsymbol{T_R^a}V$, where V is unitary, then $W \to V^{\mathsf{T}}WV$. We can make use of this change of basis to transform W to a canonical form. Since W is unitary, its singular values (i.e. the positive square roots of the eigenvalues of $W^\dagger W$) are all equal to 1. Hence, in the two cases corresponding to $W^{\mathsf{T}} = \pm W$, respectively, Eqs. (D.2.1) and (D.4.1) yield the following canonical forms (for an appropriately chosen V),

$$W = \mathbb{1}, \quad \text{for a real representation } R, \text{ with } \varepsilon_\eta = +1, \tag{E.1.7}$$

$$W = J, \quad \text{for a pseudo-real representation } R, \text{ with } \varepsilon_\eta = -1, \tag{E.1.8}$$

where $J \equiv \mathrm{diag}\left\{\begin{pmatrix} 0 & 1 \\ -1 & 0 \end{pmatrix}, \begin{pmatrix} 0 & 1 \\ -1 & 0 \end{pmatrix}, \ldots, \begin{pmatrix} 0 & 1 \\ -1 & 0 \end{pmatrix}\right\}$ is a $d_R \times d_R$ matrix (and d_R is even).

[112] Since the f^{abc} are real, the $i\boldsymbol{T_A^a}$ are real antisymmetric matrices. The heights of the adjoint labels a, b and c are not significant, as they can be lowered by the inverse Killing form given by $g_{ab} \propto \delta_{ab}$ in the preferred basis.

There are many examples of complex, real and pseudo-real representations in mathematical physics. For example, the fundamental representation of SU(N) is complex for $N \geq 3$. The adjoint representation of any compact Lie group is real [cf. footnote 112]. The simplest example of a pseudo-real representation is the two-dimensional representation of SU(2),[113] where $\boldsymbol{T^a} = \frac{1}{2}\tau^a$ (and the τ^a are the usual Pauli matrices). More generally, the generators of a pseudo-real representation must satisfy

$$(i\boldsymbol{T^a_R})^* = C^{-1}(i\boldsymbol{T^a_R})C, \tag{E.1.9}$$

for some fixed unitary antisymmetric matrix C [previously denoted by W^{-1} in Eqs. (E.1.4) and (E.1.6)]. For the doublet representation of SU(2) just given, $C^{ab} = (i\tau^2)^{ab} \equiv \epsilon^{ab}$ is the familiar SU(2)-invariant tensor.

Finally, we note that for U(1), all irreducible representations are one-dimensional. The structure constants vanish and any d-dimensional representation of the U(1)-generator is given by the $d \times d$ identity matrix multiplied by the corresponding U(1)-charge. For a Lie group that is a direct product of a semisimple group and U(1) groups, $\mathrm{Tr}\,\boldsymbol{T^a_R}$ is non-zero when a corresponds to one of the U(1)-generators, unless the sum of the corresponding U(1)-charges of the states of the representation R vanishes.

E.2. The quadratic and cubic index and Casimir operator

In this section, we define the index and Casimir operator of a representation of a compact semisimple Lie algebra $\mathfrak{g}$. The *index* $I_2(R)$ of the representation R is defined by [269,271–273]

$$\mathrm{Tr}(\boldsymbol{T^a_R T^b_R}) = I_2(R)\delta^{ab}, \tag{E.2.1}$$

where $I_2(R)$ is a positive real number that depends on R. Once $I_2(R)$ is defined for one representation, its value is uniquely fixed for any other representation. In the case of a simple compact Lie algebra $\mathfrak{g}$, it is traditional to normalize the generators of the fundamental (or defining) representation F according to[114]

$$\mathrm{Tr}(\boldsymbol{T^a_F T^b_F}) = \tfrac{1}{2}\delta^{ab}. \tag{E.2.2}$$

If the representation R is reducible, it can be decomposed into the direct sum of irreducible representations, $R = \sum_k R_k$. In this case, the index of R is given by

$$I_2(R) = \sum_k I_2(R_k). \tag{E.2.3}$$

The index of a tensor product of two representations R_1 and R_2 is given by [271]

$$I_2(R_1 \otimes R_2) = d_{R_1} I_2(R_2) + d_{R_2} I_2(R_1). \tag{E.2.4}$$

Finally, we note that if R^* is the complex conjugate of the representation R, then

$$I_2(R^*) = I_2(R). \tag{E.2.5}$$

A Casimir operator of a Lie algebra $\mathfrak{g}$ is an operator that commutes with all the generators $\boldsymbol{T^a}$. If the representation of the $\boldsymbol{T^a}$ is *irreducible*, then Schur's lemma implies that the Casimir operator is a multiple of the identity. The proportionality constant depends on the representation R. The quadratic Casimir operator of an *irreducible* representation R is given by

$$(\boldsymbol{T^2_R})_i{}^j \equiv (\boldsymbol{T^a_R})_i{}^k (\boldsymbol{T^a_R})_k{}^j = C_R \delta_i{}^j, \tag{E.2.6}$$

where the sum over the repeated indices are implicit and $i, j, k = 1, 2 \ldots d_R$. A simple computation then yields the eigenvalue of the quadratic Casimir operator, C_R,

$$C_R = \frac{I_2(R) d_G}{d_R}. \tag{E.2.7}$$

For a simple Lie algebra (where the adjoint representation is irreducible), it immediately follows that $C_A = I_2(A)$. For a reducible representation, $\boldsymbol{T^2}$ is a block diagonal matrix consisting of $d_{R_k} \times d_{R_k}$ blocks given by $C_{R_k}\mathbb{1}$ for each irreducible component R_k of R.

The example of the simple Lie algebra $\mathfrak{su}(N)$ is well known. The dimension of this Lie algebra (equal to the number of generators) is given by $N^2 - 1$. As previously noted, $d_F = N$ and $I_2(F) = \frac{1}{2}$. It then follows that $C_F = (N^2 - 1)/(2N)$. One can also check that $C_A = I_2(A) = N$.

---

[113] No unitary matrix W exists such that the $Wi\tau^a W^{-1}$ are real for all $a = 1, 2, 3$. Thus, the two-dimensional representation of SU(2) is not real. However, $(i\tau^a)^* = (i\tau^2)(i\tau^a)(i\tau^2)^{-1}$ for $a = 1, 2, 3$, which proves that the two-dimensional representation of SU(2) is pseudo-real.

[114] In the literature, the index is often defined as the ratio $I_2(R)/I_2(F)$, where $I_2(F)$ is fixed by some convention. This has the advantage that the index of R is independent of the normalization convention of the generators. In this Appendix, we will simply refer to $I_2(R)$ as the index.

The Lie algebras $\mathfrak{su}(N)$ [$N \geq 3$] are the only simple Lie algebra that possesses a cubic Casimir operator. First, we define the symmetrized trace of three generators [273,274]:

$$D^{abc} \equiv \mathrm{Str}\,(\boldsymbol{T^a T^b T^c}) = \frac{1}{6}\mathrm{Tr}(\boldsymbol{T^a T^b T^c} + \text{perm.}), \tag{E.2.8}$$

where "perm." indicates five other terms obtained by permuting the indices a, b and c in all possible ways. Due to the properties of the trace, it follows that for a given representation R,

$$D^{abc}(R) = \tfrac{1}{2}\mathrm{Tr}\left[\{\boldsymbol{T^a_R}, \boldsymbol{T^b_R}\}\boldsymbol{T^c_R}\right]. \tag{E.2.9}$$

For the N-dimensional defining representation of $\mathfrak{su}(N)$, it is conventional to define

$$d^{abc} \equiv 2\mathrm{Tr}\left[\{\boldsymbol{T^a_F}, \boldsymbol{T^b_F}\}\boldsymbol{T^c_F}\right]. \tag{E.2.10}$$

One important property of the d^{abc} is [275,276]:

$$d^{abc}d^{abc} = \frac{(N^2-1)(N^2-4)}{N}. \tag{E.2.11}$$

In general, $D^{abc}(R)$ is proportional to d^{abc}. In particular, the *cubic index* $I_3(R)$ of a representation R is defined such that [273,275,277],

$$D^{abc}(R) = I_3(R)d^{abc}. \tag{E.2.12}$$

Having fixed $I_3(F) = \frac{1}{4}$, the cubic index is uniquely determined for all representations of $\mathfrak{su}(N)$ [275,277–279]. As in the case of the quadratic index $I_2(R)$, we have:

$$I_3(R) = \sum_k I_3(R_k), \tag{E.2.13}$$

for a reducible representation $R = \sum_k R_k$. The cubic index of a tensor product of two representations R_1 and R_2 is given by [277]

$$I_3(R_1 \otimes R_2) = d_{R_1} I_3(R_2) + d_{R_2} I_3(R_1). \tag{E.2.14}$$

If the generators of the representation R are $\boldsymbol{T^a_R}$, then the generators of the complex conjugate representation R^* are $-\boldsymbol{T^{a\top}_R}$. It then follows that

$$I_3(R^*) = -I_3(R). \tag{E.2.15}$$

In particular, the cubic index of a self-conjugate representation vanishes. Note that the converse is not true. That is, it is possible for the cubic index of a complex representation of $\mathfrak{su}(N)$ to vanish in special circumstances [279].

One can show that among the simple Lie groups, $D^{abc} = 0$ except for the case of SU(N), when $N \geq 3$ [275]. For any non-semisimple Lie group (i.e., a Lie group that is a direct product of simple Lie groups and at least one U(1) factor), D^{abc} is generally non-vanishing. For example, suppose that the $\boldsymbol{T^a_R}$ constitute an irreducible representation of the generators of $G\times$U(1), where G is a semisimple Lie group. Then the U(1) generator (which we denote by setting $\boldsymbol{a} = \boldsymbol{Q}$) is $\boldsymbol{T^Q_R} \equiv q\mathbb{1}$, where q is the corresponding U(1)-charge. It then follows that $D^{Qab} = qI_2(R)\delta^{ab}$. More generally, for a compact non-semisimple Lie group, D^{abc} can be non-zero when either one or three of its indices corresponds to a U(1) generator.

In the computation of the anomaly [cf. Section 6.26], the quantity $\mathrm{Tr}(\boldsymbol{T^a_R T^b_R T^c_R})$ appears. We can evaluate this trace using Eqs. (E.1.2) and (E.2.12):

$$\mathrm{Tr}(\boldsymbol{T^a_R T^b_R T^c_R}) = I_3(R)d^{abc} + \frac{i}{2}I_2(R)f^{abc}. \tag{E.2.16}$$

The cubic Casimir operator of an *irreducible* representation R is given by

$$(\boldsymbol{T^3_R})_i{}^j \equiv d^{abc}(\boldsymbol{T^a_R T^b_R T^c_R})_i{}^j = C_{3R}\delta_i{}^j. \tag{E.2.17}$$

Using Eqs. (E.2.11) and (E.2.12), we obtain a relation between the eigenvalue of the cubic Casimir operator, C_{3R} and the cubic index [275]:

$$C_{3R} = \frac{(N^2-1)(N^2-4)I_3(R)}{Nd_R}. \tag{E.2.18}$$

Again, we provide two examples. For the fundamental representation of $\mathfrak{su}(N)$, $I_3(F) = \frac{1}{4}$ and $C_{3F} = (N^2-1)(N^2-4)/(4N^2)$. For the adjoint representation, $I_3(A) = C_{3A} = 0$, since the adjoint representation is self-conjugate. A general formula for the eigenvalue of the cubic Casimir operator in an arbitrary $\mathfrak{su}(N)$ representation [or equivalently the cubic index $I_3(R)$, which is related to C_{3R} by Eq. (E.2.18)] can be found in Refs. [275,277–279].

Appendix F. Path integral treatment of two-component fermion propagators

In Section 4.2 we derived the two-component fermion propagators in momentum space, which are the Fourier transforms of the free-field expectation values of time-ordered products of two two-component fermion fields, for example,

$$\langle 0|\, T\xi_\alpha(x)\xi^\dagger_{\dot\beta}(y)\,|0\rangle_{\rm FT} \equiv \int \mathrm{d}^4w\, \langle 0|\, T\xi_\alpha(x)\xi^\dagger_{\dot\beta}(y)\,|0\rangle\, e^{ip\cdot w}, \qquad w \equiv x-y, \tag{F.1}$$

where the (translationally invariant) expectation values such as $\langle 0|\, T\xi_\alpha(x)\xi^\dagger_{\dot\beta}(y)\,|0\rangle$ are functions of the coordinate difference $w \equiv x-y$. In Section 4.2, the Fourier transforms of these quantities were computed by using the free-field expansion obtained from the canonical quantization procedure, and then evaluating the resulting spin sums. In this Appendix, we provide a derivation of the same result by employing path integral techniques. We follow the analysis given in Appendix C of Ref. [280] (with a few minor changes in notation). For a similar textbook treatment of two-component fermion propagators see for example Ref. [220]. For the analogous treatment of the four-component fermion propagator, see for example Ref. [114].

We first consider the action for a single massive neutral two-component fermion $\xi_\alpha(x)$, coupled to an anticommuting two-component fermionic source term $J_\alpha(x)$ [cf. Eq. (3.1.1)]:

$$S = \int \mathrm{d}^4x\,(\mathscr{L} + J\xi + \xi^\dagger J^\dagger) = \int \mathrm{d}^4x\left\{\tfrac{1}{2}\left[i\xi^\dagger\overline{\sigma}^\mu\partial_\mu\xi + i\xi\sigma^\mu\partial_\mu\xi^\dagger - m(\xi\xi + \xi^\dagger\xi^\dagger)\right] + J\xi + \xi^\dagger J^\dagger\right\}, \tag{F.2}$$

where we have split the kinetic energy term symmetrically into two terms. The generating functional is given by

$$W[J, J^\dagger] = N\int \mathscr{D}\xi\, \mathscr{D}\xi^\dagger\, e^{iS[\xi,\xi^\dagger JJ^\dagger]}, \tag{F.3}$$

where N is a normalization factor chosen such that $W[0,0] = 1$ and $\mathscr{D}\xi\,\mathscr{D}\xi^\dagger$ is the integration measure. It is convenient to Fourier transform the fields $\xi(x), \xi^\dagger(x)$ and sources $J(x), J^\dagger(x)$ in Eq. (F.3), and rewrite the action in terms of the corresponding Fourier coefficients $\widehat{\xi}(p), \widehat{\xi}^\dagger(p), \widehat{J}(p)$ and $\widehat{J}^\dagger(p)$:

$$\xi_\alpha(x) = \int \frac{\mathrm{d}^4p}{(2\pi)^4} e^{-ip\cdot x}\widehat{\xi}_\alpha(p), \qquad \xi^\dagger_{\dot\alpha}(x) = \int \frac{\mathrm{d}^4p}{(2\pi)^4} e^{ip\cdot x}\widehat{\xi}^\dagger_{\dot\alpha}(p), \tag{F.4}$$

$$J_\alpha(x) = \int \frac{\mathrm{d}^4p}{(2\pi)^4} e^{-ip\cdot x}\widehat{J}_\alpha(p), \qquad J^\dagger_{\dot\alpha}(x) = \int \frac{\mathrm{d}^4p}{(2\pi)^4} e^{ip\cdot x}\widehat{J}^\dagger_{\dot\alpha}(p). \tag{F.5}$$

Furthermore, we introduce the integral representation of the delta function:

$$\delta^{(4)}(x-x') = \int \frac{\mathrm{d}^4p}{(2\pi)^4} e^{-ip\cdot(x-x')}. \tag{F.6}$$

In order to rewrite Eq. (F.3) in a more convenient matrix form, we introduce the following definitions:

$$\Omega(p) \equiv \begin{pmatrix} \widehat{\xi}^{\dagger\dot\alpha}(-p) \\ \widehat{\xi}_\alpha(p)\end{pmatrix}, \qquad X(p) \equiv \begin{pmatrix} \widehat{J}_\alpha(p) \\ \widehat{J}^{\dagger\dot\alpha}(-p)\end{pmatrix}, \qquad \mathscr{M}(p) \equiv \begin{pmatrix} p\cdot\sigma_{\alpha\dot\beta} & -m\,\delta_\alpha{}^\beta \\ -m\,\delta^{\dot\alpha}{}_{\dot\beta} & p\cdot\overline{\sigma}^{\dot\alpha\beta}\end{pmatrix}. \tag{F.7}$$

Note that $\mathscr{M}$ is an hermitian matrix. We can then rewrite the action [Eq. (F.2)] in the following matrix form [after using Eqs. (2.59) and (2.60) to write the product of the spinor field and the source in a symmetrical fashion]:

$$S = \frac{1}{2}\int \frac{\mathrm{d}^4p}{(2\pi)^4}\left(\Omega^\dagger\mathscr{M}\Omega + \Omega^\dagger X + X^\dagger\Omega\right). \tag{F.8}$$

The linear term in the field Ω can be removed by a field redefinition

$$\Omega' = \Omega + \mathscr{M}^{-1}X. \tag{F.9}$$

In terms of Ω', the action now takes the convenient form:

$$S = \frac{1}{2}\int \frac{\mathrm{d}^4p}{(2\pi)^4}\left(\Omega'^\dagger\mathscr{M}\Omega' - X^\dagger\mathscr{M}^{-1}X\right), \tag{F.10}$$

where the inverse of the matrix $\mathscr{M}$ is given by

$$\mathscr{M}^{-1} = \frac{1}{p^2-m^2}\begin{pmatrix} p\cdot\overline{\sigma}^{\dot\alpha\beta} & m\,\delta^{\dot\alpha}{}_{\dot\beta} \\ m\,\delta_\alpha{}^\beta & p\cdot\sigma_{\alpha\dot\beta}\end{pmatrix}. \tag{F.11}$$

The Jacobian of the field transformation given in Eq. (F.9) is unity. Hence, one can insert the new action, Eq. (F.10), in the generating functional, Eq. (F.3) to obtain (after dropping the primes on the two-component fermion fields):

$$W[\widehat{J},\widehat{J}^\dagger] = N\int \mathcal{D}\xi\,\mathcal{D}\xi^\dagger \exp\left\{\frac{i}{2}\int\frac{\mathrm{d}^4p}{(2\pi)^4}\left(\Omega^\dagger\mathcal{M}\Omega - X^\dagger\mathcal{M}^{-1}X\right)\right\} \tag{F.12}$$

$$= N\left[\int \mathcal{D}\xi\,\mathcal{D}\xi^\dagger \exp\left\{\frac{i}{2}\Omega^\dagger\mathcal{M}\Omega\right\}\right]\exp\left\{-\frac{i}{2}\int\frac{\mathrm{d}^4p}{(2\pi)^4}X^\dagger\mathcal{M}^{-1}X\right\} \tag{F.13}$$

$$= \exp\left\{-\frac{i}{2}\int\frac{\mathrm{d}^4p}{(2\pi)^4}X^\dagger\mathcal{M}^{-1}X\right\}, \tag{F.14}$$

where we have defined the normalization constant N such that $W[0,0]=1$. Inserting the explicit forms for X and $\mathcal{M}$ into Eq. (F.14), we obtain

$$W[\widehat{J},\widehat{J}^\dagger] = \exp\Bigg\{-\frac{1}{2}\int\frac{\mathrm{d}^4p}{(2\pi)^4}\Bigg(\widehat{J}^\alpha(-p)\frac{ip\cdot\sigma_{\alpha\dot\beta}}{p^2-m^2}\widehat{J}^{\dagger\dot\beta}(-p)+\widehat{J}^\dagger_{\dot\alpha}(p)\frac{ip\cdot\overline{\sigma}^{\dot\alpha\beta}}{p^2-m^2}\widehat{J}_\beta(p)$$
$$+\widehat{J}^\alpha(-p)\frac{im\delta_\alpha{}^\beta}{p^2-m^2}\widehat{J}_\beta(p)+\widehat{J}^\dagger_{\dot\alpha}(p)\frac{im\delta^{\dot\alpha}{}_{\dot\beta}}{p^2-m^2}\widehat{J}^{\dagger\dot\beta}(-p)\Bigg)\Bigg\}. \tag{F.15}$$

Using Eq. (2.61), it is convenient to rewrite the first two terms of the integrand on the right-hand side of Eq. (F.15) in two different ways:

$$\frac{1}{2}\int\frac{\mathrm{d}^4p}{(2\pi)^4}\left[\widehat{J}^\alpha(-p)\frac{ip\cdot\sigma_{\alpha\dot\beta}}{p^2-m^2}\widehat{J}^{\dagger\dot\beta}(-p)+\widehat{J}^\dagger_{\dot\alpha}(p)\frac{ip\cdot\overline{\sigma}^{\dot\alpha\beta}}{p^2-m^2}\widehat{J}_\beta(p)\right]$$
$$=\int\frac{\mathrm{d}^4p}{(2\pi)^4}\widehat{J}^\alpha(-p)\frac{ip\cdot\sigma_{\alpha\dot\beta}}{p^2-m^2}\widehat{J}^{\dagger\dot\beta}(-p)=\int\frac{\mathrm{d}^4p}{(2\pi)^4}\widehat{J}^\dagger_{\dot\alpha}(p)\frac{ip\cdot\overline{\sigma}^{\dot\alpha\beta}}{p^2-m^2}\widehat{J}_\beta(p), \tag{F.16}$$

where we have changed integration variables from $p\to -p$ in relating the two terms above. The vacuum expectation value of the time-ordered product of two spinor fields in configuration space is obtained by taking two functional derivatives of the generating functional with respect to the sources J and $J^\dagger$ and then setting $J=J^\dagger=0$ at the end of the computation (e.g., see Ref. [114]). For example,

$$\left(-i\frac{\overrightarrow{\delta}}{\delta J^\alpha(x_1)}\right)W[J,J^\dagger]\left(-i\frac{\overleftarrow{\delta}}{\delta J^{\dagger\dot\beta}(x_2)}\right)\Bigg|_{J=J^\dagger=0} = N\int\mathcal{D}\xi\,\mathcal{D}\xi^\dagger\,\xi_\alpha(x_1)\xi^\dagger_{\dot\beta}(x_2)\exp\left(i\int\mathrm{d}^4x\,\mathscr{L}\right)$$
$$=\langle 0|T\xi_\alpha(x_1)\xi^\dagger_{\dot\beta}(x_2)|0\rangle, \tag{F.17}$$

where the functional derivatives act in the indicated direction (which ensures that no extra minus signs are generated due to the anticommutativity properties of the sources and their functional derivatives). To obtain the two-point functions involving the product of two spinor fields with different combinations of dotted and undotted spinors, it may be more convenient to write $J\xi=\xi J$ and/or $\xi^\dagger J^\dagger = J^\dagger\xi^\dagger$ in Eq. (F.3). One can then easily verify the following expressions for the four possible two-point functions:

$$\langle 0|T\xi_\alpha(x_1)\xi^\dagger_{\dot\beta}(x_2)|0\rangle = \left(-i\frac{\overrightarrow{\delta}}{\delta J^\alpha(x_1)}\right)W[J,J^\dagger]\left(-i\frac{\overleftarrow{\delta}}{\delta J^{\dagger\dot\beta}(x_2)}\right)\Bigg|_{J=J^\dagger=0}, \tag{F.18}$$

$$\langle 0|T\xi^{\dagger\dot\alpha}(x_1)\xi^\beta(x_2)|0\rangle = \left(-i\frac{\overrightarrow{\delta}}{\delta J^\dagger_{\dot\alpha}(x_1)}\right)W[J,J^\dagger]\left(-i\frac{\overleftarrow{\delta}}{\delta J_\beta(x_2)}\right)\Bigg|_{J=J^\dagger=0}, \tag{F.19}$$

$$\langle 0|T\xi^{\dagger\dot\alpha}(x_1)\xi^\dagger_{\dot\beta}(x_2)|0\rangle = \left(-i\frac{\overrightarrow{\delta}}{\delta J^\dagger_{\dot\alpha}(x_1)}\right)W[J,J^\dagger]\left(-i\frac{\overleftarrow{\delta}}{\delta J^{\dagger\dot\beta}(x_2)}\right)\Bigg|_{J=J^\dagger=0}, \tag{F.20}$$

$$\langle 0|T\xi_\alpha(x_1)\xi^\beta(x_2)|0\rangle = \left(-i\frac{\overrightarrow{\delta}}{\delta J^\alpha(x_1)}\right)W[J,J^\dagger]\left(-i\frac{\overleftarrow{\delta}}{\delta J_\beta(x_2)}\right)\Bigg|_{J=J^\dagger=0}. \tag{F.21}$$

As an example, we provide details for the evaluation of Eq. (F.18). Using Eqs. (F.15) and (F.16), we obtain:

$$\langle 0|T\xi_\alpha(x_1)\xi^\dagger_{\dot\beta}(x_2)|0\rangle = \frac{\overrightarrow{\delta}}{\delta J^\alpha(x_1)}\left(\int\frac{\mathrm{d}^4p}{(2\pi)^4}\widehat{J}^\alpha(-p)\frac{ip\cdot\sigma_{\alpha\dot\beta}}{p^2-m^2}\widehat{J}^{\dagger\dot\beta}(-p)\right)\frac{\overleftarrow{\delta}}{\delta J^{\dagger\dot\beta}(x_2)}. \tag{F.22}$$

The chain rule for functional differentiation and the inverse Fourier transforms of Eq. (F.5) yield:

$$\frac{\delta}{\delta J^\alpha(x_1)} = \int \mathrm{d}^4p_1\, \frac{\delta\widehat{J}^\beta(-p_1)}{\delta J^\alpha(x_1)}\frac{\delta}{\delta\widehat{J}^\beta(-p_1)} = \int \mathrm{d}^4p_1\, e^{-ip_1\cdot x_1}\frac{\delta}{\delta\widehat{J}^\alpha(-p_1)}, \tag{F.23}$$

$$\frac{\delta}{\delta J^{\dagger\dot\beta}(x_2)} = \int \mathrm{d}^4p_2\, \frac{\delta\widehat{J}^{\dagger\dot\alpha}(-p_2)}{\delta J^{\dagger\dot\beta}(x_2)}\frac{\delta}{\delta\widehat{J}^{\dagger\dot\alpha}(-p_2)} = \int \mathrm{d}^4p_2\, e^{ip_2\cdot x_2}\frac{\delta}{\delta\widehat{J}^{\dagger\dot\beta}(-p_2)}. \tag{F.24}$$

Applying Eqs. (F.23) and (F.24) to Eq. (F.22), we obtain:

$$\langle 0|T\xi_\alpha(x_1)\xi^\dagger_{\dot\beta}(x_2)|0\rangle = \int \frac{\mathrm{d}^4p}{(2\pi)^4}\, e^{-ip\cdot(x_1-x_2)}\frac{ip\cdot\sigma_{\alpha\dot\beta}}{p^2-m^2}, \tag{F.25}$$

which is equivalent to Eq. (4.2.1) of Section 4.2. With the same methods applied to Eqs. (F.19)–(F.21), one can easily reproduce the results of Eqs. (4.2.2)–(4.2.4).

We next consider the action for a single massive Dirac two-component fermion. We shall work in a basis of fields where the action, including external anticommuting sources, is given by

$$S[\chi,\chi^\dagger,\eta,\eta^\dagger,J_\chi,J_\chi^\dagger,J_\eta,J_\eta^\dagger] = \int d^4x\Big[i\chi^\dagger\overline{\sigma}^\mu\partial_\mu\chi + i\eta^\dagger\overline{\sigma}^\mu\partial_\mu\eta - m(\chi\eta+\chi^\dagger\eta^\dagger) + J_\chi\chi + \chi^\dagger J_\chi^\dagger + J_\eta\eta + \eta^\dagger J_\eta^\dagger\Big]. \tag{F.26}$$

Following the techniques employed above, we introduce Fourier coefficients for all the fields and sources and define

$$\Omega_c(p) \equiv \begin{pmatrix}\widehat{\eta}^{\dagger\dot\alpha}(-p)\\ \widehat{\chi}_\alpha(p)\end{pmatrix}, \qquad X_c(p) \equiv \begin{pmatrix}\widehat{J}_{\eta\alpha}(p)\\ \widehat{J}^{\dagger\dot\alpha}_\chi(-p)\end{pmatrix}. \tag{F.27}$$

The action functional, Eq. (F.26), can then rewritten in matrix form as before (but with no overall factor of 1/2):

$$S = \int \frac{\mathrm{d}^4p}{(2\pi)^4}\left(\Omega_c^\dagger\mathcal{M}\Omega_c + \Omega_c^\dagger X_c + X_c^\dagger\Omega_c\right), \tag{F.28}$$

where $\mathcal{M}$ is again given by Eq. (F.7). The remaining calculation proceeds as before with few modifications, and yields the Dirac two-component fermion free-field propagators given in Eqs. (4.2.7)–(4.2.10).

Appendix G. Correspondence to four-component spinor notation

G.1. Dirac gamma matrices and four-component spinors

In four-dimensional Minkowski space, four-component spinor notation employs four-component Dirac spinor fields and the 4×4 Dirac gamma matrices, whose defining property is:

$$\{\gamma^\mu,\gamma^\nu\} = 2g^{\mu\nu}\mathbb{1}, \tag{G.1.1}$$

where $\mathbb{1}$ is the 4×4 identity matrix.

The correspondence between the two-component spinor notation and the four-component Dirac spinor notation is most easily exhibited in the basis in which γ_5 is diagonal (this is called the *chiral* representation[115]). In 2×2 blocks, the gamma matrices are given by[116]:

$$\gamma^\mu \equiv \begin{pmatrix}0 & \sigma^\mu_{\alpha\dot\beta}\\ \overline{\sigma}^{\mu\,\dot\alpha\beta} & 0\end{pmatrix}, \qquad \gamma_5 \equiv i\gamma^0\gamma^1\gamma^2\gamma^3 = \begin{pmatrix}-\delta_\alpha{}^\beta & 0\\ 0 & \delta^{\dot\alpha}{}_{\dot\beta}\end{pmatrix}, \tag{G.1.2}$$

and the 4×4 identity matrix that appears in Eq. (G.1.1) can be written as:

$$\mathbb{1} = \begin{pmatrix}\delta_\alpha{}^\beta & 0\\ 0 & \delta^{\dot\alpha}{}_{\dot\beta}\end{pmatrix}. \tag{G.1.3}$$

In addition, we identify the generators of the Lorentz group in the $(\frac12,0)\oplus(0,\frac12)$ representation[117]:

$$\tfrac12\Sigma^{\mu\nu} \equiv \frac{i}{4}[\gamma^\mu,\gamma^\nu] = \begin{pmatrix}\sigma^{\mu\nu}{}_\alpha{}^\beta & 0\\ 0 & \overline{\sigma}^{\mu\nu\dot\alpha}{}_{\dot\beta}\end{pmatrix}, \tag{G.1.4}$$

115 For a review of other representations of the Dirac gamma matrices and their properties, see e.g. Refs. [281,282].

116 Employing the conventions for the sigma matrices described in Appendix A, it follows that the definition of γ^μ is independent of the choice of metric signature, whereas $\gamma_\mu \equiv g_{\mu\nu}\gamma^\nu$ changes sign under a reversal of the metric signature. In the metric signature convention with $g_{00}=+1$, our gamma matrix conventions follow those of Ref. [114], whereas in the convention with $g_{00}=-1$, our gamma matrix conventions follow those of Ref. [65].

117 In most textbooks, $\Sigma^{\mu\nu}$ is called $\sigma^{\mu\nu}$. Here, we use the former symbol so that there is no confusion with definition of $\sigma^{\mu\nu}{}_\alpha{}^\beta$ given in Eq. (2.70).

where $\Sigma^{\mu\nu}$ satisfies the duality relation,

$$\gamma_5 \Sigma^{\mu\nu} = \tfrac{1}{2} i \epsilon^{\mu\nu\rho\tau} \Sigma_{\rho\tau}. \tag{G.1.5}$$

A four-component *Dirac spinor* field, $\Psi(x)$, is made up of two mass-degenerate two-component spinor fields, $\chi_\alpha(x)$ and $\eta_\alpha(x)$, of opposite U(1)-charge as follows:

$$\Psi(x) \equiv \begin{pmatrix} \chi_\alpha(x) \\ \eta^{\dagger\dot\alpha}(x) \end{pmatrix}. \tag{G.1.6}$$

We next introduce the chiral projections operators,

$$P_L \equiv \tfrac{1}{2}(\mathbb{1} - \gamma_5) = \begin{pmatrix} \delta_\alpha{}^\beta & 0 \\ 0 & 0 \end{pmatrix}, \quad \text{and} \quad P_R \equiv \tfrac{1}{2}(\mathbb{1} + \gamma_5) = \begin{pmatrix} 0 & 0 \\ 0 & \delta^{\dot\alpha}{}_{\dot\beta} \end{pmatrix}, \tag{G.1.7}$$

and the (left- and right-handed) *Weyl spinor* fields, $\Psi_L(x)$ and $\Psi_R(x)$, which are defined by[118]:

$$\Psi_L(x) \equiv P_L \Psi(x) = \begin{pmatrix} \chi_\alpha(x) \\ 0 \end{pmatrix}, \qquad \Psi_R(x) \equiv P_R \Psi(x) = \begin{pmatrix} 0 \\ \eta^{\dagger\dot\alpha}(x) \end{pmatrix}. \tag{G.1.8}$$

Equivalently, one can define the Weyl spinors Ψ_L and Ψ_R as the four-component spinor eigenstates of γ_5 with corresponding eigenvalues -1 and $+1$, respectively (i.e., $\gamma_5 \Psi_{L,R} = \mp \Psi_{L,R}$).

The Dirac conjugate field $\overline{\Psi}(x)$ and the charge conjugate field $\Psi^C(x)$ are defined by:

$$\overline{\Psi}(x) \equiv \Psi^\dagger A = \left(\eta^\alpha(x),\, \chi^\dagger_{\dot\alpha}(x) \right), \tag{G.1.9}$$

$$\Psi^C(x) \equiv C \overline{\Psi}^{\mathsf{T}}(x) = \begin{pmatrix} \eta_\alpha(x) \\ \chi^{\dagger\dot\alpha}(x) \end{pmatrix}, \tag{G.1.10}$$

where the Dirac conjugation matrix A and the charge conjugation matrix C satisfy [283–285]:

$$A \gamma_\mu A^{-1} = \gamma_\mu^\dagger, \qquad C^{-1} \gamma_\mu C = -\gamma_\mu^{\mathsf{T}}. \tag{G.1.11}$$

It is convenient to introduce a notation for left- and right-handed charge-conjugated fields (which are also Weyl spinor fields) following the conventions of Refs. [67,286],[119]

$$\Psi_L^C(x) \equiv P_L \Psi^C(x) = C \overline{\Psi}_R^{\mathsf{T}}(x) = [\Psi_R(x)]^C, \tag{G.1.12}$$

$$\Psi_R^C(x) \equiv P_R \Psi^C(x) = C \overline{\Psi}_L^{\mathsf{T}}(x) = [\Psi_L(x)]^C. \tag{G.1.13}$$

To fix the properties of A and C, it is conventional to impose two additional conditions:

$$\Psi = A^{-1} \overline{\Psi}^\dagger, \qquad (\Psi^C)^C = \Psi. \tag{G.1.14}$$

The first of these conditions together with Eq. (G.1.9) is equivalent to the statement that $\overline{\Psi}\Psi$ is hermitian. The second condition corresponds to the statement that the (discrete) charge conjugation transformation applied twice is equal to the identity operator. Using Eqs. (G.1.11) and (G.1.14) and the defining property of the gamma matrices [Eq. (G.1.1)], one can show (independently of the gamma matrix representation) that the matrices A and C must satisfy:

$$A^\dagger = A, \qquad C^{\mathsf{T}} = -C, \qquad (AC)^{-1} = (AC)^*. \tag{G.1.15}$$

Following Ref. [135], it is convenient to introduce a matrix D such that

$$D \equiv C A^{\mathsf{T}}, \qquad D^{-1} \gamma_\mu D = -\gamma_\mu^*, \tag{G.1.16}$$

and $D^* D = D D^* = \mathbb{1}$. The charge-conjugated four-component spinor is then given by:

$$\Psi^C(x) \equiv D \Psi^*(x). \tag{G.1.17}$$

---

118 In the earlier literature, a different set of conventions for the sigma matrices in which the roles of σ and $\overline{\sigma}$ were reversed [e.g., as in Eqs. (A.11) and (A.12)] resulted in $\gamma_5 = \mathrm{diag}(\mathbb{1}_{2\times2}, -\mathbb{1}_{2\times2})$ in the chiral representation, which differs from our convention by an overall sign [cf. Eq. (G.1.2)]. As a result, in this latter convention, P_L [P_R] projects out the raised dotted [lowered undotted] two-component spinor field. This latter convention is still prevalent in the literature of the spinor helicity method (see footnote 156 in Appendix I.2).

119 The reader is warned that the opposite convention is often employed in the literature (e.g., see Ref. [287]) in which Ψ_L^C is a right-handed field and Ψ_R^C is a left-handed field.

A four-component *Majorana spinor* field, $\Psi_M(x)$, is defined by imposing the constraint $\Psi^C(x) = \Psi(x)$ on a four-component Dirac spinor, which sets $\eta = \chi$. That is, the *Majorana condition* is

$$\Psi_M(x) = D\Psi_M^*(x) = \begin{pmatrix} \chi_\alpha(x) \\ \chi^{\dagger\dot\alpha}(x) \end{pmatrix}. \tag{G.1.18}$$

For a review of the Majorana field and its properties, see e.g. Refs. [143,144].

For completeness, we also introduce a matrix B that satisfies [283–285,288]:

$$B \equiv -C^{-1}\gamma_5, \qquad B\gamma_\mu B^{-1} = \gamma_\mu^{\mathsf T}. \tag{G.1.19}$$

The matrix B arises in the study of time reversal invariance of the Dirac equation. In the chiral representation, A, B, C and D are explicitly given by

$$A = \begin{pmatrix} 0 & \delta^{\dot\alpha}{}_{\dot\beta} \\ \delta_\alpha{}^\beta & 0 \end{pmatrix}, \qquad C = \begin{pmatrix} \epsilon_{\alpha\beta} & 0 \\ 0 & \epsilon^{\dot\alpha\dot\beta} \end{pmatrix}, \tag{G.1.20}$$

$$B = \begin{pmatrix} \epsilon^{\alpha\beta} & 0 \\ 0 & -\epsilon_{\dot\alpha\dot\beta} \end{pmatrix}, \qquad D = \begin{pmatrix} 0 & \epsilon_{\alpha\beta} \\ \epsilon^{\dot\alpha\dot\beta} & 0 \end{pmatrix}. \tag{G.1.21}$$

Note the *numerical* equalities, $A = \gamma^0$, $B = \gamma^1\gamma^3$, $C = i\gamma^0\gamma^2$ and $D = -i\gamma^2$. However these identifications do not respect either the structure of the undotted and dotted spinor indices specified in Eqs. (G.1.20) and (G.1.21), or the four-component spinor index structure introduced below [cf. Eqs. (G.1.46) and (G.1.47)].[120] In translating between two-component and four-component spinor notation, Eqs. (G.1.20) and (G.1.21) should always be used. In practical four-component spinor calculations, there is often no harm in employing the numerical values for A, B, C and D.

Using Eqs. (G.1.11)–(G.1.19), the following results are easily derived:

$$A\Gamma A^{-1} = \eta_\Gamma^A \Gamma^\dagger, \qquad \eta_\Gamma^A = \begin{cases} +1, & \text{for } \Gamma = \mathbb{1},\ \gamma^\mu,\ \gamma^\mu\gamma_5,\ \Sigma^{\mu\nu}, \\ -1, & \text{for } \Gamma = \gamma_5,\ \Sigma^{\mu\nu}\gamma_5, \end{cases} \tag{G.1.22}$$

$$B\Gamma B^{-1} = \eta_\Gamma^B \Gamma^{\mathsf T}, \qquad \eta_\Gamma^B = \begin{cases} +1, & \text{for } \Gamma = \mathbb{1},\ \gamma_5,\ \gamma^\mu, \\ -1, & \text{for } \Gamma = \gamma^\mu\gamma_5,\ \Sigma^{\mu\nu},\ \Sigma^{\mu\nu}\gamma_5, \end{cases} \tag{G.1.23}$$

$$C^{-1}\Gamma C = \eta_\Gamma^C \Gamma^{\mathsf T}, \qquad \eta_\Gamma^C = \begin{cases} +1, & \text{for } \Gamma = \mathbb{1},\ \gamma_5,\ \gamma^\mu\gamma_5, \\ -1, & \text{for } \Gamma = \gamma^\mu,\ \Sigma^{\mu\nu},\ \Sigma^{\mu\nu}\gamma_5. \end{cases} \tag{G.1.24}$$

$$D^{-1}\Gamma D = \eta_\Gamma^D \Gamma^*, \qquad \eta_\Gamma^D = \begin{cases} +1, & \text{for } \Gamma = \mathbb{1},\ \gamma^\mu\gamma_5,\ \Sigma^{\mu\nu}\gamma_5, \\ -1, & \text{for } \Gamma = \gamma^\mu,\ \gamma_5,\ \Sigma^{\mu\nu}. \end{cases} \tag{G.1.25}$$

The Lorentz transformation properties of the four-component spinor field can be determined from those of the two-component spinor fields given in Section 2. The 4×4 representation matrices of the Lorentz group in the $(\frac{1}{2},0)\oplus(0,\frac{1}{2})$ representation are given by

$$\mathbb{M} = \begin{pmatrix} M & 0 \\ 0 & (M^{-1})^\dagger \end{pmatrix} = \exp\left(-\frac{i}{4}\theta_{\mu\nu}\Sigma^{\mu\nu}\right) \simeq \mathbb{1}_{4\times4} - \tfrac{1}{4}i\theta_{\mu\nu}\Sigma^{\mu\nu}, \tag{G.1.26}$$

where the infinitesimal forms of M and $(M^{-1})^\dagger$ are given in Eqs. (2.100) and (2.101). Two useful identities that follow from Eqs. (G.1.22), (G.1.24) and (G.1.26) are[121]:

$$A\,\mathbb{M}A^{-1} = (\mathbb{M}^{-1})^\dagger, \tag{G.1.27}$$

$$C^{-1}\mathbb{M}C = (\mathbb{M}^{-1})^{\mathsf T}. \tag{G.1.28}$$

The four-component Dirac or Majorana spinor, Ψ_a, is assigned a lowered spinor index a, and is defined in terms of two-component spinors by Eq. (G.1.6) or (G.1.18), respectively. Four-component spinor indices, which will be chosen in general from the beginning of the lower case Roman alphabet, $a, b, c, \ldots$, can assume integer values 1, 2, 3, 4. Under a Lorentz transformation, Ψ_a transforms as

$$\Psi_a \to \mathbb{M}_a{}^b\,\Psi_b. \tag{G.1.29}$$

---

120 When treated as ordinary 4×4 matrices A, B, C and D are unitary. But when written in 2×2 block form [noting that $\delta^{\dot\alpha}{}_{\dot\beta} = (\delta^\alpha{}_\beta)^*$ and $\epsilon^{\dot\alpha\dot\beta} \equiv (\epsilon^{\alpha\beta})^*$, as indicated below Eqs. (2.19) and (2.23)], the products $AA^\dagger$, $BB^\dagger$, $CC^\dagger$ and $DD^\dagger$ are not covariant with respect to the dotted and undotted two-component spinor indices. Similarly, these matrix products are not covariant with respect to the four-component spinor indices. In practice, only covariant combinations of A, B, C, D and the four-component spinor fields arise in typical calculations.

121 Note that Eq. (G.1.28) is a direct consequence of the identities in two-component spinor notation given in Eqs. (2.102) and (2.103).

In analogy with the conventions for two-component spinor indices, we sum implicitly over a pair of repeated indices consisting of a raised and a lowered spinor index. The transformation law for the Dirac conjugate spinor (often called the Dirac adjoint spinor), $\overline{\Psi} = \Psi^\dagger A$, is obtained from Eq. (G.1.29) after employing $A^\dagger = A$ and Eq. (G.1.27),

$$\overline{\Psi}^a \to \overline{\Psi}^b \, (\mathbb{M}^{-1})_b{}^a. \tag{G.1.30}$$

In particular, $\overline{\Psi}\Psi \equiv \overline{\Psi}^a \Psi_a$ is a Lorentz scalar, which justifies the assignment of a raised spinor index for the Dirac conjugate spinor $\overline{\Psi}^a$.

It is convenient to introduce *barred* four-component spinor indices [289] in the transformation laws of the hermitian-conjugated four-component spinors,[122]

$$\Psi^\dagger_{\bar{a}} \to \Psi^\dagger_{\bar{b}} \, (\mathbb{M}^\dagger)^{\bar{b}}{}_{\bar{a}}, \tag{G.1.31}$$

$$\overline{\Psi}^{\dagger\,\bar{a}} \to [(\mathbb{M}^{-1})^\dagger]^{\bar{a}}{}_{\bar{b}} \, \overline{\Psi}^{\dagger\,\bar{b}}, \tag{G.1.32}$$

where there is an implicit sum over the repeated lowered and raised barred spinor indices, and

$$\Psi^\dagger_{\bar{a}} \equiv (\Psi_a)^\dagger, \qquad \overline{\Psi}^{\dagger\,\bar{a}} \equiv (\overline{\Psi}^a)^\dagger. \tag{G.1.33}$$

The spinor index structure of the Dirac conjugation matrix A is then fixed by noting that the Dirac conjugate spinor, $\overline{\Psi}^b \equiv \Psi^\dagger_{\bar{a}} A^{\bar{a}b}$, has a raised unbarred spinor index, whereas the hermitian-conjugated spinor has a lowered barred spinor index.

The charge conjugation matrix can be used to raise and lower four-component spinor indices [289], which we shall employ in defining the spinors Ψ^a, $\Psi^{\dagger\,\bar{a}}$, $\overline{\Psi}_a$ and $\overline{\Psi}^\dagger_{\bar{a}}$, [123]

$$\Psi_a = C_{ab}\Psi^b, \qquad \Psi^a = (C^{-1})^{ab}\Psi_b, \tag{G.1.34}$$

$$\Psi^\dagger_{\bar{a}} = C_{\bar{a}\bar{b}}\Psi^{\dagger\,\bar{b}}, \qquad \Psi^{\dagger\,\bar{a}} = (C^{-1})^{\bar{a}\bar{b}}\Psi^\dagger_{\bar{b}}, \tag{G.1.35}$$

where

$$C_{\bar{a}\bar{b}} \equiv (C_{ab})^*, \qquad (C^{-1})^{\bar{a}\bar{b}} \equiv [(C^{-1})^{ab}]^*. \tag{G.1.36}$$

Eqs. (G.1.34) and (G.1.35) also apply to $\overline{\Psi}^a$, $\overline{\Psi}_a$ and their hermitian conjugates. In particular, one can identify the Dirac conjugate spinor with a lowered spinor index ($\overline{\Psi}_a$) as the charge-conjugated spinor, $\Psi^C \equiv C\overline{\Psi}^{\mathsf{T}}$, and the Dirac spinor with a raised spinor index (Ψ^a) as the Dirac conjugate of the charged-conjugated spinor, $\overline{\Psi^C} = -\Psi^{\mathsf{T}} C^{-1}$. That is,[124]

$$\Psi^C_a \equiv \overline{\Psi}_a = C_{ab}\overline{\Psi}^b, \qquad \overline{\Psi^C}^a = \Psi^a = (C^{-1})^{ab}\Psi_b. \tag{G.1.37}$$

The rules for raising and lowering spinor indices are consistent with the Lorentz transformation properties of Eqs. (G.1.29)–(G.1.32), as a consequence of Eq. (G.1.28). In particular, the condition for a self-conjugate four-component (Majorana) spinor, $\overline{\Psi}_a \equiv \Psi^C_a = \Psi_a$, is Lorentz covariant.

Using Eq. (G.1.15), (G.1.34), (G.1.35), and the definition of the Dirac conjugate spinor, it then follows that:

$$\overline{\Psi}_a = (A^{-1})_{a\bar{b}}\Psi^{\dagger\,\bar{b}}, \qquad \overline{\Psi}^a = \Psi^\dagger_{\bar{b}} A^{\bar{b}a}, \tag{G.1.38}$$

$$\Psi^\dagger_{\bar{a}} = \overline{\Psi}^b (A^{-1})_{b\bar{a}}, \qquad \Psi^{\dagger\,\bar{a}} = A^{\bar{a}b}\,\overline{\Psi}_b. \tag{G.1.39}$$

One can check that Eqs. (G.1.38) and (G.1.39) are consistent with the Lorentz transformation properties of Eqs. (G.1.29)–(G.1.32), as a consequence of Eq. (G.1.27).

In addition to the Lorentz scalar $\overline{\Psi}\Psi \equiv \overline{\Psi}^a\Psi_a$, one can construct two additional independent Lorentz scalar quantities,[125]

$$-\Psi^{\mathsf{T}} C^{-1}\,\Psi \equiv -\Psi_a (C^{-1})^{ab}\Psi_b = \Psi^a\Psi_a, \tag{G.1.40}$$

and its hermitian conjugate,

$$\overline{\Psi}\,C\,\overline{\Psi}^{\mathsf{T}} \equiv \overline{\Psi}^a C_{ab}\overline{\Psi}^b = \overline{\Psi}^a\overline{\Psi}_a = \Psi^\dagger_{\bar{a}}\Psi^{\dagger\,\bar{a}} = (\Psi^a\Psi_a)^\dagger, \tag{G.1.41}$$

122 Of course, Eqs. (G.1.29)–(G.1.32) can also be derived directly from the corresponding two-component spinor transformation laws of Section 2.

123 In contrast to the epsilon symbols of the two-component spinor formalism, here we prefer to explicitly exhibit the inverse symbols in $(C^{-1})^{ab}$ and $(C^{-1})^{\bar{a}\bar{b}}$ [cf. footnote 7].

124 For a Dirac spinor field defined in Eq. (G.1.6), $\overline{\Psi}_a(x) = \Psi^C_a(x)$ is given in terms of two-component spinors by Eq. (G.1.10), and $\Psi^a(x) = \overline{\Psi^C}^a(x) = \left(\chi^\alpha(x),\, \eta^\dagger_{\dot{\alpha}}(x)\right)$.

125 A fourth possible Lorentz scalar, $\Psi^a\overline{\Psi}_a = (C^{-1})^{ab}C_{ac}\Psi_b\overline{\Psi}^c = -\Psi_c\overline{\Psi}^c = \overline{\Psi}^c\Psi_c$, is not independent. Here, we have used $C^{\mathsf{T}} = -C$ and the anticommutativity of the spinors. Equivalently, $\overline{\Psi^C}\Psi^C = \overline{\Psi}\Psi$.

after using C^{-1} and C to raise and lower the appropriate spinor indices, respectively. The penultimate equality in Eq. (G.1.41) is a consequence of Eq. (G.1.39). The Lorentz invariance of $\overline{\Psi}^a\Psi_a$, $\Psi^a\Psi_a$ and $\Psi_{\bar{a}}^\dagger\Psi^{\dagger\,\bar{a}} = \overline{\Psi}^a\overline{\Psi}_a$ is manifest and demonstrates the power of the four-component spinor index notation developed above. After invoking Eq. (G.1.37), we note that [analogous to Eq. (2.36)] *descending* contracted unbarred spinor indices and *ascending* contracted barred spinor indices can be suppressed in spinor-index-contracted products. For example,

$$\overline{\Psi}^a\Psi_a \equiv \overline{\Psi}\Psi \qquad \Psi^a\Psi_a = \overline{\Psi^C}^a\Psi_a \equiv \overline{\Psi^C}\Psi \qquad \overline{\Psi}^a\overline{\Psi}_a = \overline{\Psi}^a\Psi_a^C \equiv \overline{\Psi}\Psi^C, \tag{G.1.42}$$

where the suppression of barred spinor indices is implicit in the definition of $\overline{\Psi}^b \equiv \Psi_{\bar{a}}^\dagger A^{\bar{a}b}$.

The charge-conjugated spinor can also be written as $\Psi_a^C \equiv D_a{}^{\bar{c}}\Psi_{\bar{c}}^\dagger$ [cf. Eq. (G.1.17)]. The spinor index structure of D (and its inverse) derives from:

$$D_a{}^{\bar{c}} \equiv C_{ab}(A^{\mathsf{T}})^{b\bar{c}} = C_{ab}A^{\bar{c}b}, \qquad (D^{-1})_{\bar{a}}{}^c \equiv (C^*A)_{\bar{a}}{}^c = C_{\bar{a}\bar{b}}A^{\bar{b}c}, \tag{G.1.43}$$

where we have used $D^{-1} = D^*$. Combining the results of Eqs. (G.1.34), (G.1.35), (G.1.38) and (G.1.39) then yields:

$$\overline{\Psi}_a = D_a{}^{\bar{c}}\,\Psi_{\bar{c}}^\dagger, \qquad \Psi_{\bar{a}}^\dagger = (D^{-1})_{\bar{a}}{}^c\,\overline{\Psi}_c, \tag{G.1.44}$$

$$\overline{\Psi}^a = -\Psi^{\dagger\,\bar{c}}(D^{-1})_{\bar{c}}{}^a, \qquad \Psi^{\dagger\,\bar{a}} = -\overline{\Psi}^c D_c{}^{\bar{a}}. \tag{G.1.45}$$

In summary, a four-component spinor Ψ_a and its charge-conjugated spinor Ψ_a^C possess a lowered unbarred spinor index, whereas the corresponding Dirac conjugates, $\overline{\Psi}^a$ and $\overline{\Psi^C}^a$, possess a raised unbarred spinor index. The corresponding hermitian-conjugated spinors exhibit barred spinor indices (with the height of each spinor index unchanged). Following Eqs. (G.1.34) and (G.1.35), one can also lower or raise a four-component unbarred or barred spinor index by multiplying by the appropriate matrix C, C^{-1}, C^* or $(C^{-1})^*$, respectively.

The identity matrix, the gamma matrices and their products are denoted collectively by Γ. The spinor index structure of these matrices and their inverses is given by:

$$\delta_a^b,\ \Gamma_a{}^b,\ (\Gamma^{-1})_a{}^b, \tag{G.1.46}$$

where the δ_a^b are the matrix elements of the identity matrix $\mathbb{1}$. In this case, the rows are labeled by the lowered index and the columns are labeled by the raised index. Note that the quantities $\overline{\Psi}^a\,\Gamma_a{}^b\,\Psi_b$, $\Psi^a\,\Gamma_a{}^b\,\Psi_b$, and $\overline{\Psi}^a\,\Gamma_a{}^b\,\overline{\Psi}^b$ transform as Lorentz tensors, whose rank is equal to the number of (suppressed) spacetime indices of Γ.

For the matrices A, B, C, D and their inverses, the spinor index structure is given by:

$$A^{\bar{a}b},\ (A^{-1})_{a\bar{b}},\ B^{ab},\ (B^{-1})_{ab},\ C_{ab},\ (C^{-1})^{ab},\ D_a{}^{\bar{b}},\ (D^{-1})_{\bar{a}}{}^b. \tag{G.1.47}$$

The corresponding complex-conjugated matrices exhibit the analogous spinor index structure with unbarred spinor indices changed to barred spinor indices and vice versa. Matrix transposition interchanges rows and columns. For example,

$$(\Gamma^{\mathsf{T}})^a{}_b \equiv \Gamma_b{}^a, \qquad (A^{\mathsf{T}})^{a\bar{b}} \equiv A^{\bar{b}a}, \qquad (C^{\mathsf{T}})_{ab} = C_{ba}, \qquad (D^{\mathsf{T}})^{\bar{a}}{}_b \equiv D_b{}^{\bar{a}}. \tag{G.1.48}$$

Hermitian conjugation is complex conjugation followed by matrix transposition. For example,

$$(\Gamma^\dagger)^{\bar{a}}{}_{\bar{b}} \equiv (\Gamma_b{}^a)^*, \qquad (A^\dagger)^{\bar{a}b} \equiv (A^{\bar{b}a})^*, \qquad (C^\dagger)_{\bar{a}\bar{b}} = (C_{ba})^*, \qquad (D^\dagger)^a{}_{\bar{b}} \equiv (D_b{}^{\bar{a}})^*. \tag{G.1.49}$$

Using the above results, it is straightforward to identify the four-component spinor index structure of Eqs. (G.1.1)–(G.1.28). For example, specifying the four-component spinor indices of Eq. (G.1.28) yields:

$$(C^{-1})^{ab}\mathbb{M}_b{}^cC_{cd} = [(\mathbb{M}^{-1})^{\mathsf{T}}]^a{}_d \equiv (\mathbb{M}^{-1})_d{}^a. \tag{G.1.50}$$

To complete the spinor index formalism, we introduce hybrid quantities L, $\overline{L}$, R and $\overline{R}$ that contain an unbarred four-component spinor index and a two-component undotted or dotted spinor index [290]:

$$L_\beta{}^b = (\mathbb{1}_{2\times2} \quad \mathbb{0}_{2\times2}), \qquad R^{\dot\beta\,b} = (\mathbb{0}_{2\times2} \quad \mathbb{1}_{2\times2}), \tag{G.1.51}$$

$$\overline{L}_b{}^\beta = \begin{pmatrix}\mathbb{1}_{2\times2}\\ \mathbb{0}_{2\times2}\end{pmatrix}, \qquad \overline{R}_{b\dot\beta} = \begin{pmatrix}\mathbb{0}_{2\times2}\\ \mathbb{1}_{2\times2}\end{pmatrix}. \tag{G.1.52}$$

These quantities satisfy:

$$\overline{L}_a{}^\alpha L_\alpha{}^b = (P_L)_a{}^b, \qquad L_\alpha{}^a\overline{L}_a{}^\beta = \delta_\alpha{}^\beta, \tag{G.1.53}$$

$$\overline{R}_{a\dot\alpha}R^{\dot\alpha\,b} = (P_R)_a{}^b, \qquad R^{\dot\alpha\,a}\overline{R}_{a\dot\beta} = \delta^{\dot\alpha}{}_{\dot\beta}, \tag{G.1.54}$$

where P_L and P_R are the chiral projection operators defined in Eq. (G.1.7). It then follows that:

$$L_\alpha{}^a(P_L)_a{}^b = L_\alpha{}^b, \qquad (P_L)_a{}^b\overline{L}_b{}^\beta = \overline{L}_a{}^\beta, \tag{G.1.55}$$

$$R^{\dot\alpha\, a}(P_R)_a{}^b = R^{\dot\alpha\, b}, \qquad (P_R)_a{}^b\overline{R}_{b\dot\beta} = \overline{R}_{a\dot\beta}. \tag{G.1.56}$$

The hybrid quantities L, $\overline{L}$, R and $\overline{R}$ connect objects with four-component and two-component spinor indices. For the Dirac spinor defined in Eq. (G.1.6), it follows that:

$$\chi_\alpha = L_\alpha{}^b\Psi_b, \qquad \eta^\alpha = \overline{\Psi}^b\,\overline{L}_b{}^\alpha, \tag{G.1.57}$$

$$\eta^{\dagger\dot\alpha} = R^{\dot\alpha\, b}\Psi_b, \qquad \chi^\dagger_{\dot\alpha} = \overline{\Psi}^b\,\overline{R}_{b\dot\alpha}. \tag{G.1.58}$$

The corresponding inverse relations are:

$$(P_L)_a{}^b\,\Psi_b = \overline{L}_a{}^\beta\chi_\beta, \qquad \overline{\Psi}^a(P_L)_a{}^b = \eta^\beta L_\beta{}^b, \tag{G.1.59}$$

$$(P_R)_a{}^b\,\Psi_b = \overline{R}_{a\dot\beta}\eta^{\dagger\dot\beta}, \qquad \overline{\Psi}^a(P_R)_a{}^b = \chi^\dagger_{\dot\beta}R^{\dot\beta\, b}. \tag{G.1.60}$$

One can use Eqs. (G.1.2), (G.1.4) and (G.1.20) to identify:

$$\sigma^\mu_{\alpha\dot\beta} = L_\alpha{}^a(\gamma^\mu)_a{}^b\overline{R}_{b\dot\beta}, \qquad \overline{\sigma}^{\mu\dot\alpha\beta} = R^{\dot\alpha\, a}(\gamma^\mu)_a{}^b\overline{L}_b{}^\beta, \tag{G.1.61}$$

$$\sigma^{\mu\nu}{}_\alpha{}^\beta = L_\alpha{}^a\left(\tfrac{1}{2}\Sigma^{\mu\nu}\right)_a{}^b\overline{L}_b{}^\beta, \qquad \overline{\sigma}^{\mu\nu\dot\alpha}{}_{\dot\beta} = R^{\dot\alpha\, a}\left(\tfrac{1}{2}\Sigma^{\mu\nu}\right)_a{}^b\overline{R}_{b\dot\beta}, \tag{G.1.62}$$

$$\delta_\alpha{}^\beta = -L_\alpha{}^a(\gamma_5)_a{}^b\overline{L}_b{}^\beta, \qquad \delta^{\dot\alpha}{}_{\dot\beta} = R^{\dot\alpha\, a}(\gamma_5)_a{}^b\overline{R}_{b\dot\beta}, \tag{G.1.63}$$

$$\epsilon_{\alpha\beta} = L_\alpha{}^a C_{ab}L_\beta{}^b, \qquad \epsilon^{\dot\alpha\dot\beta} = R^{\dot\alpha\, a}C_{ab}R^{\dot\beta\, b}, \tag{G.1.64}$$

$$\epsilon^{\alpha\beta} = \overline{L}_a{}^\alpha(C^{-1})^{ab}\overline{L}_b{}^\beta, \qquad \epsilon_{\dot\alpha\dot\beta} = \overline{R}_{a\dot\alpha}(C^{-1})^{ab}\overline{R}_{b\dot\beta}. \tag{G.1.65}$$

Inverting these results yields:

$$(\gamma^\mu P_L)_c{}^d = \overline{R}_{c\dot\alpha}\overline{\sigma}^{\mu\dot\alpha\beta}L_\beta{}^d, \qquad (\gamma^\mu P_R)_c{}^d = \overline{L}_c{}^\alpha\sigma^\mu_{\alpha\dot\beta}R^{\dot\beta d}, \tag{G.1.66}$$

$$\tfrac{1}{2}(\Sigma^{\mu\nu}P_L)_c{}^d = \overline{L}_c{}^\alpha\sigma^{\mu\nu}{}_\alpha{}^\beta L_\beta{}^d \qquad \tfrac{1}{2}(\Sigma^{\mu\nu}P_R)_c{}^d = \overline{R}_{c\dot\alpha}\overline{\sigma}^{\mu\nu\dot\alpha}{}_{\dot\beta}R^{\dot\beta d}, \tag{G.1.67}$$

$$(AP_L)_c{}^d = \overline{R}_c{}^\beta L_\beta{}^d, \qquad (AP_R)_c{}^d = \overline{L}_{c\dot\beta}R^{\dot\beta d}, \tag{G.1.68}$$

$$(P_LC)_{cd} = \epsilon_{\alpha\beta}\overline{L}_c{}^\alpha\overline{L}_d{}^\beta, \qquad (P_RC)_{cd} = \epsilon^{\dot\alpha\dot\beta}\overline{R}_{c\dot\alpha}\overline{R}_{d\dot\beta}, \tag{G.1.69}$$

$$(C^{-1}P_L)^{cd} = \epsilon^{\alpha\beta}L_\alpha{}^cL_\beta{}^d, \qquad (C^{-1}P_R)^{cd} = \epsilon_{\dot\alpha\dot\beta}R^{\dot\alpha c}R^{\dot\beta d}. \tag{G.1.70}$$

Likewise, one can introduce $L^\dagger$, $\overline{L}^\dagger$, $R^\dagger$ and $\overline{R}^\dagger$, which are hybrid quantities that contain a barred four-component spinor index and a two-component undotted or dotted spinor index:

$$(L^\dagger)^{\bar a}{}_{\dot\beta} \equiv (L_\beta{}^a)^*, \qquad (R^\dagger)^{\bar\alpha\beta} \equiv (R^{\dot\beta a})^*, \tag{G.1.71}$$

$$(\overline{L}^\dagger)^{\dot\beta}{}_{\bar a} \equiv (\overline{L}_a{}^\beta)^*, \qquad (\overline{R}^\dagger)_{\beta\bar a} \equiv (\overline{R}_{a\dot\beta})^*. \tag{G.1.72}$$

In particular, using Eqs. (G.1.59) and (G.1.60), one can relate the quantities L, $\overline{L}$, R and $\overline{R}$ and their hermitian conjugates:

$$(L^\dagger)^{\bar a}{}_{\dot\beta} = A^{\bar a b}\overline{R}_{b\dot\beta}, \qquad (R^\dagger)^{\bar\alpha\beta} = A^{\bar\alpha b}\overline{L}_b{}^\beta, \tag{G.1.73}$$

$$(\overline{L}^\dagger)^{\dot\beta}{}_{\bar a} = R^{\dot\beta b}(A^{-1})_{b\bar a}, \qquad (\overline{R}^\dagger)_{\beta\bar a} = L_\beta{}^b(A^{-1})_{b\bar a}, \tag{G.1.74}$$

after employing $AP_L = P_R^\dagger A$ [cf. Eq. (G.1.22)] and $A^\dagger = A$. The set of equations analogous to Eqs. (G.1.53)–(G.1.70) involving the corresponding hermitian-conjugated quantities can also be obtained. However, such formulae will rarely be needed in practice.

Eqs. (G.1.53)–(G.1.70) [and their hermitian conjugates] can be employed to translate any expression involving two-component spinors into the corresponding expression involving four-component spinors, and vice versa. With a little practice, both two-component and four-component spinor indices can be suppressed, which greatly simplifies the manipulation of the spinor quantities. In particular, by treating the four-component spinors Ψ_a and Ψ_a^C as column vectors and their hermitian (Dirac) conjugates $\Psi^\dagger_{\bar a}$ and $\Psi^{C\,\dagger}_{\bar a}$ ($\overline{\Psi}^a$ and $\overline{\Psi^C}^a$) as row vectors, all equations in the four-component spinor formalism have a natural interpretation as products of matrices and vectors. Henceforth, we shall suppress all four-component spinor indices.

Multiple species of fermions are indicated with a flavor index such as i and j. Dirac fermions are constructed from two-component fields of opposite charge, χ_i and η^i (hence the opposite flavor index heights). Thus, we establish the following conventions for the flavor indices of four-component Dirac fermions:

$$\Psi_i(x) \equiv \begin{pmatrix} \chi_{\alpha i}(x) \\ \eta_i^{\dagger\dot\alpha}(x) \end{pmatrix}, \qquad \overline{\Psi}^i(x) = \left(\eta^{\alpha i}(x),\, \chi^{\dagger\, i}_{\dot\alpha}(x)\right), \qquad \Psi^{C\, i}(x) \equiv \begin{pmatrix} \eta^{\ i}_\alpha(x) \\ \chi^{\dagger\dot\alpha i}(x) \end{pmatrix}. \tag{G.1.75}$$

Note that $\chi^{\dagger\, i} = (\chi_i)^\dagger$ and $\eta_i^\dagger \equiv (\eta^i)^\dagger$ following the conventions established in Section 3.2. Raised flavor indices can only be contracted with lowered flavor indices and vice versa. In contrast, Majorana fermions are neutral so that there is no a priori distinction between raised and lowered flavor indices. That is,

$$\Psi_{Mi}(x) = \Psi^{\ i}_M(x) = \Psi^C_{Mi}(x) = \Psi^{C\, i}(x) \equiv \begin{pmatrix} \xi_{\alpha i}(x) \\ \xi^{\dagger\dot\alpha i}(x) \end{pmatrix}, \qquad \overline{\Psi}_{Mi}(x) = \overline{\Psi}^{\ i}_M(x) \equiv \left(\xi_i^\alpha(x),\, \xi^{\dagger\, i}_{\dot\alpha}(x)\right). \tag{G.1.76}$$

In this case, the contraction of two repeated flavor indices is allowed in all cases, irrespective of the heights of the two indices. In the convention adopted in Section 3.2, in which all neutral left-handed $(\frac{1}{2}, 0)$ [right-handed $(0, \frac{1}{2})$] fermions have lowered [raised] flavor indices, the height of the flavor index of a four-component Majorana fermion field is meaningful when multiplied by a left-handed or right-handed projection operator. Thus, the height of the flavor index for Majorana fermions can be consistently chosen according to one of the following four cases:

$$P_L\Psi_{Mi}, \qquad \overline{\Psi}_{Mi}P_L, \qquad P_R\Psi^{\ i}_M, \qquad \overline{\Psi}^{\ i}_M P_R. \tag{G.1.77}$$

Bilinear covariants are quantities that are quadratic in the spinor fields and transform irreducibly as Lorentz tensors. We first construct a translation table between the two-component form and the four-component form for the bilinear covariants made up of a pair of Dirac fields. Using Eqs. (G.1.59) and (G.1.60) to convert the four-component spinor fields into the corresponding two-component spinor fields, and employing the appropriate identities involving products of the hybrid quantities L, $\bar L$, R and $\bar R$, the following results are then obtained:

$$\overline{\Psi}^i P_L\Psi_j = \eta^{\ i}\chi_j, \tag{G.1.78}$$

$$\overline{\Psi}^i P_R\Psi_j = \chi^{\dagger\, i}\eta_j^\dagger, \tag{G.1.79}$$

$$\overline{\Psi}^i \gamma^\mu P_L\Psi_j = \chi^{\dagger\, i}\overline{\sigma}^\mu\chi_j, \tag{G.1.80}$$

$$\overline{\Psi}^i \gamma^\mu P_R\Psi_j = \eta^{\ i}\sigma^\mu\eta_j^\dagger, \tag{G.1.81}$$

$$\overline{\Psi}^i \Sigma^{\mu\nu} P_L\Psi_j = 2\,\eta^{\ i}\sigma^{\mu\nu}\chi_j, \tag{G.1.82}$$

$$\overline{\Psi}^i \Sigma^{\mu\nu} P_R\Psi_j = 2\,\chi^{\dagger\, i}\overline{\sigma}^{\mu\nu}\eta_j^\dagger. \tag{G.1.83}$$

The first two results above follow immediately after using Eqs. (G.1.53) and (G.1.54), respectively, and the last four results are a consequence of Eqs. (G.1.61) and (G.1.62).

Eqs. (G.1.78)–(G.1.83) apply to both commuting and anticommuting fermion fields.[126] These results can then be used to express the standard four-component spinor bilinear covariants in terms of two-component spinor bilinears:

$$\overline{\Psi}^i\Psi_j = \eta^{\ i}\chi_j + \chi^{\dagger\, i}\eta_j^\dagger \tag{G.1.84}$$

$$\overline{\Psi}^i\gamma_5\Psi_j = -\eta^{\ i}\chi_j + \chi^{\dagger\, i}\eta_j^\dagger \tag{G.1.85}$$

$$\overline{\Psi}^i\gamma^\mu\Psi_j = \chi^{\dagger\, i}\overline{\sigma}^\mu\chi_j + \eta^{\ i}\sigma^\mu\eta_j^\dagger \tag{G.1.86}$$

$$\overline{\Psi}^i\gamma^\mu\gamma_5\Psi_j = -\chi^{\dagger\, i}\overline{\sigma}^\mu\chi_j + \eta^{\ i}\sigma^\mu\eta_j^\dagger \tag{G.1.87}$$

$$\overline{\Psi}^i\Sigma^{\mu\nu}\Psi_j = 2(\eta^{\ i}\sigma^{\mu\nu}\chi_j + \chi^{\dagger\, i}\overline{\sigma}^{\mu\nu}\eta_j^\dagger) \tag{G.1.88}$$

$$\overline{\Psi}^i\Sigma^{\mu\nu}\gamma_5\Psi_j = 2(-\eta^{\ i}\sigma^{\mu\nu}\chi_j + \chi^{\dagger\, i}\overline{\sigma}^{\mu\nu}\eta_j^\dagger). \tag{G.1.89}$$

[126] In the case of anticommuting spinors, it is often useful to apply Eq. (2.61) to Eqs. (G.1.81), (G.1.86) and (G.1.87) and rewrite $\eta^{\ i}\sigma^\mu\eta_j^\dagger = -\eta_j^\dagger\overline{\sigma}^\mu\eta^{\ i}$.

Additional identities can be derived that involve the charge-conjugated four-component Dirac fermion fields. As an example, we may use $C^{\mathsf{T}} = -C$ and $\overline{\Psi^C} = -\Psi^{\mathsf{T}} C^{-1}$ to prove that

$$\overline{\Psi_i^C}\,\Gamma\,\Psi^{Cj} = -(-1)^A \overline{\Psi}^j C\,\Gamma^{\mathsf{T}}\,C^{-1}\Psi_i = -(-1)^A \eta_\Gamma^C\,\overline{\Psi}^j\,\Gamma\,\Psi_i, \tag{G.1.90}$$

where the sign η_Γ^C is given in Eq. (G.1.24). The factor of $(-1)^A = \pm 1$ [for commuting/anticommuting fermion fields, respectively] arises at the second step above after reversing the order of the terms by matrix transposition. Identities involving just one charge-conjugated four-component field can also be easily obtained. For example, using Eqs. (G.1.57) and (G.1.70),

$$\overline{\Psi_i^C} P_L \Psi_j = -\Psi_i^{\mathsf{T}} C^{-1} P_L \Psi_j = -\Psi_{ai}\epsilon^{\alpha\beta} L_\alpha{}^a L_\beta{}^b \Psi_{bj} = -\epsilon^{\alpha\beta}\chi_{\alpha i}\chi_{\beta j} = \chi_i\chi_j. \tag{G.1.91}$$

In general, if one replaces Ψ_k with Ψ^{Ck} in Eqs. (G.1.78)–(G.1.89), then in the corresponding two-component expression one simply interchanges $\chi_k \leftrightarrow \eta^k$ and $\chi^{\dagger k} \leftrightarrow \eta_k^\dagger$.

Eqs. (G.1.78)–(G.1.89) also apply to four-component Majorana spinors, Ψ_{Mi}, by setting $\chi_i = \eta^i \equiv \xi_i$, and $\chi^{\dagger i} = \eta_i^\dagger \equiv \xi^{\dagger i}$. This implements the Majorana condition, $\Psi_{Mi} = D\Psi_{Mi}^*$, and imposes additional restrictions on the Majorana bilinear covariants. For example, Eqs. (G.1.24) and (G.1.90) imply that *anticommuting* Majorana four-component fermions satisfy[127]:

$$\overline{\Psi}_{Mi}\Psi_{Mj} = \overline{\Psi}_{Mj}\Psi_{Mi}, \tag{G.1.92}$$

$$\overline{\Psi}_{Mi}\gamma_5\Psi_{Mj} = \overline{\Psi}_{Mj}\gamma_5\Psi_{Mi}, \tag{G.1.93}$$

$$\overline{\Psi}_{Mi}\gamma^\mu\Psi_{Mj} = -\overline{\Psi}_{Mj}\gamma^\mu\Psi_{Mi}, \tag{G.1.94}$$

$$\overline{\Psi}_{Mi}\gamma^\mu\gamma_5\Psi_{Mj} = \overline{\Psi}_{Mj}\gamma^\mu\gamma_5\Psi_{Mi}, \tag{G.1.95}$$

$$\overline{\Psi}_{Mi}\Sigma^{\mu\nu}\Psi_{Mj} = -\overline{\Psi}_{Mj}\Sigma^{\mu\nu}\Psi_{Mi}, \tag{G.1.96}$$

$$\overline{\Psi}_{Mi}\Sigma^{\mu\nu}\gamma_5\Psi_{Mj} = -\overline{\Psi}_{Mj}\Sigma^{\mu\nu}\gamma_5\Psi_{Mi}. \tag{G.1.97}$$

By setting $i = j$, it follows that $\overline{\Psi}_M\gamma^\mu\Psi_M = \overline{\Psi}_M\Sigma^{\mu\nu}\Psi_M = \overline{\Psi}_M\Sigma^{\mu\nu}\gamma_5\Psi_M = 0$. One additional useful result is:

$$\overline{\Psi}_M^i\gamma^\mu P_L\Psi_{Mj} = -\overline{\Psi}_{Mj}\gamma^\mu P_R\Psi_M^i, \tag{G.1.98}$$

which follows immediately from Eqs. (G.1.94) and (G.1.95). Note that in Eq. (G.1.98), the heights of the flavor indices follow the convention established in Eq. (G.1.77).

In the four-component spinor formalism, Fierz identities (first introduced in Ref. [291]) consist of relations among products of two bilinear covariants, in which the fermion fields appear in two different orders. The corresponding two-component spinor Fierz identities are treated in detail in Appendix B.1. In principle, the latter can be converted into four-component spinor Fierz identities using the techniques developed in this appendix. However, it is easier to derive the four-component spinor Fierz identities directly using the properties of the gamma matrix algebra [281,288].

Instead of Eqs. (B.1.5)–(B.1.7), the equivalent identity relevant for four-component spinors is:

$$\delta_a^b\delta_c^d = \frac{1}{4}\left[\delta_a^d\delta_c^b + (\gamma_5)_a{}^d(\gamma_5)_c{}^b + (\gamma^\mu)_a{}^d(\gamma_\mu)_c{}^b - (\gamma^\mu\gamma_5)_a{}^d(\gamma_\mu\gamma_5)_c{}^b + \tfrac{1}{2}(\Sigma^{\mu\nu})_a{}^d(\Sigma_{\mu\nu})_c{}^b\right]. \tag{G.1.99}$$

This is the fundamental identity from which many other such identities can be derived (cf. the Appendix of Ref. [285]). One of many possible Fierz identities can be obtained by multiplying Eq. (G.1.99) by $\overline{\Psi}_1^a\Psi_{2b}\overline{\Psi}_3^c\Psi_{4d} = (-1)^A\,\overline{\Psi}_1^a\Psi_{4d}\overline{\Psi}_3^c\Psi_{2b}$, where $(-1)^A = +1$ [-1] for commuting [anticommuting] Dirac, Majorana or Weyl spinors. More generally [281,292,293],

$$(\overline{\Psi}_1\Gamma^{(k)I}\Psi_2)(\overline{\Psi}_3\Gamma_I^{(k)}\Psi_4) = (-1)^A\sum_{n=1}^{5} F^k{}_n\,(\overline{\Psi}_1\Gamma^{(n)J}\Psi_4)(\overline{\Psi}_3\Gamma_J^{(n)}\Psi_2), \tag{G.1.100}$$

where the sum is taken over the 4×4 matrices, $\Gamma^{(n)} \in \Gamma$, which have been ordered as follows,[128]

$$\Gamma = \{\mathbb{1},\ \gamma^\mu,\ \Sigma^{\mu\nu}(\mu<\nu),\ \gamma^\mu\gamma_5,\ \gamma_5\}, \tag{G.1.101}$$

I, J represent zero, one or two spacetime indices (sums over repeated I and J are implied), and

$$F = \frac{1}{4}\begin{pmatrix} 1 & 1 & \frac{1}{2} & -1 & 1 \\ 4 & -2 & 0 & -2 & -4 \\ 12 & 0 & -2 & 0 & 12 \\ -4 & -2 & 0 & -2 & 4 \\ 1 & -1 & \frac{1}{2} & 1 & 1 \end{pmatrix}. \tag{G.1.102}$$

127 Here, one is free to choose all flavor indices to be in the lowered position [cf. Eq. (G.1.76)].

128 The 16 matrices of Γ constitute a complete set that spans the sixteen-dimensional vector space of 4×4 matrices.

For example, taking $k = 1$ in Eq. (G.1.100) yields a result equivalent to Eq. (G.1.99):

$$(\overline{\Psi}_1\Psi_2)(\overline{\Psi}_3\Psi_4) = \tfrac{1}{4}(-1)^A\Big[(\overline{\Psi}_1\Psi_4)(\overline{\Psi}_3\Psi_2) + (\overline{\Psi}_1\gamma_5\Psi_4)(\overline{\Psi}_3\gamma_5\Psi_2) + (\overline{\Psi}_1\gamma^\mu\Psi_4)(\overline{\Psi}_3\gamma_\mu\Psi_2) - (\overline{\Psi}_1\gamma^\mu\gamma_5\Psi_4)(\overline{\Psi}_3\gamma_\mu\gamma_5\Psi_2) + \tfrac{1}{2}(\overline{\Psi}_1\Sigma^{\mu\nu}\Psi_4)(\overline{\Psi}_3\Sigma_{\mu\nu}\Psi_2)\Big]. \tag{G.1.103}$$

For a comprehensive treatment of all possible four-component spinor Fierz identities, see Ref. [294]. Simple derivations of generalized Fierz identities have also been given in Refs. [293,295]. A Mathematica package for performing Fierz transformations is available in Ref. [296].

G.2. Free-field four-component fermion Lagrangians

The free-field Lagrangian density in four-component spinor notation can be obtained from the corresponding two-component fermion Lagrangian by employing the relevant identities for the bilinear covariants given in Eqs. (G.1.78)–(G.1.89). First, consider a collection of free anticommuting four-component Majorana fields, $\Psi_{Mi} = \Psi_{Mi}^C$. The free-field Lagrangian (in terms of mass-eigenstate fields) may be obtained from Eq. (3.2.10) by converting to four-component spinor notation using Eqs. (G.1.84) and (G.1.86) with $\chi = \eta \equiv \xi$, which yields [3]:

$$\mathscr{L} = \tfrac{1}{2}i\overline{\Psi}_{Mi}\gamma^\mu\partial_\mu\Psi_{Mi} - \tfrac{1}{2}m_i\overline{\Psi}_{Mi}\Psi_{Mi}, \tag{G.2.1}$$

where the sum over i is implicit. The corresponding free-field equation for Ψ_{Mi} is the Dirac equation:

$$(i\gamma^\mu\partial_\mu - m)\Psi_{Mi} = 0. \tag{G.2.2}$$

For simplicity, we focus on a theory of a single four-component Majorana fermion field, $\Psi_M(x) = \Psi_M^C(x)$. One can rewrite the free-field Majorana fermion Lagrangian in terms of a single Weyl fermion, $\Psi_L(x) \equiv P_L\Psi(x)$, where $\Psi(x)$ is a four-component fermion field whose lower two components (in the chiral representation) are irrelevant for the present discussion. The Majorana and Weyl fields are related by:

$$\Psi_M(x) = \Psi_L(x) + \Psi_R^C(x), \tag{G.2.3}$$

where $\Psi_R^C(x)$ is defined in Eq. (G.1.13). The corresponding Dirac conjugate field is given by $\overline{\Psi}_M(x) = \overline{\Psi}_L(x) + \overline{\Psi_R^C}(x)$, where

$$\overline{\Psi}_L(x) \equiv [P_L\Psi(x)]^\dagger A = \overline{\Psi}(x)P_R, \tag{G.2.4}$$

$$\overline{\Psi_R^C}(x) \equiv \overline{\Psi^C}(x)P_L = -\Psi^{\mathsf{T}}(x)C^{-1}P_L = -\Psi_L^{\mathsf{T}}(x)C^{-1}. \tag{G.2.5}$$

Using the identity[129]:

$$\overline{\Psi_R^C}\gamma^\mu\partial_\mu\Psi_R^C = -\Psi^{\mathsf{T}}C^{-1}P_L\gamma^\mu\partial_\mu P_R C\overline{\Psi}^{\mathsf{T}} = \overline{\Psi}_L\gamma^\mu\partial_\mu\Psi_L + \text{ total divergence}, \tag{G.2.6}$$

the Lagrangian for a single Majorana field can be written in terms of a single Weyl field[130]:

$$\mathscr{L} = i\overline{\Psi}_L\gamma^\mu\partial_\mu\Psi_L + \tfrac{1}{2}m\left(\Psi_L^{\mathsf{T}}C^{-1}\Psi_L - \overline{\Psi}_L C\overline{\Psi}_L^{\mathsf{T}}\right). \tag{G.2.7}$$

The corresponding free-field equation is

$$i\gamma^\mu\partial_\mu\Psi_L = mC\overline{\Psi}_L^{\mathsf{T}}, \tag{G.2.8}$$

where we have used $(\overline{\Psi}_L C)^{\mathsf{T}} = -C\overline{\Psi}_L^{\mathsf{T}}$ and the anticommutativity of $\Psi_L, \overline{\Psi}_L$. The generalization of Eqs. (G.2.3)–(G.2.7) to the case of a multiplet of four-component Majorana fields is straightforward and is left as an exercise for the reader.

Of course, one could have chosen instead to rewrite the four-component Majorana fermion Lagrangian in terms of a single Weyl fermion, $\Psi_R(x) \equiv P_R\Psi(x)$, in which case the upper two components (in the chiral representation) of $\Psi(x)$ are not relevant. In this case, the Majorana and Weyl fields are related by[131]:

$$\Psi_M(x) = \Psi_R(x) + \Psi_L^C(x), \tag{G.2.9}$$

---

[129] In deriving Eq. (G.2.6), we have used Eq. (G.1.24) and the anticommutativity of the spinor fields. The total divergence can be dropped from the Lagrangian, as it does not contribute to the field equations.

[130] Using Eq. (G.1.15), it follows that $(\Psi^{\mathsf{T}}C^{-1}\Psi)^\dagger = -\overline{\Psi}A^{-1}C^{-1*}A^{-1*}\overline{\Psi}^{\mathsf{T}} = -\overline{\Psi}\,C\,\overline{\Psi}^{\mathsf{T}}$.

[131] If Ψ is an unconstrained four-component spinor, then Ψ_L and Ψ_R are independent Weyl fields, in which case $\Psi_L + \Psi_R^C$ and $\Psi_R + \Psi_L^C$ are independent self-conjugate fields.

where $\Psi_L^C(x)$ is defined in Eq. (G.1.12). The corresponding Dirac conjugate field is given by $\overline{\Psi}_M(x) = \overline{\Psi}_R(x) + \overline{\Psi_L^C}(x)$, where

$$\overline{\Psi}_R(x) \equiv [P_R\Psi(x)]^\dagger A = \overline{\Psi}(x)P_L, \tag{G.2.10}$$

$$\overline{\Psi_L^C}(x) \equiv \overline{\Psi^C}(x)P_R = -\Psi^{\mathsf{T}}(x)C^{-1}P_R = -\Psi_R^{\mathsf{T}}(x)C^{-1}. \tag{G.2.11}$$

The corresponding Weyl fermion Lagrangian is given by Eq. (G.2.7) with L replaced by R.

Thus, a Majorana fermion can be represented either by a four-component self-conjugate field $\Psi_M(x)$ or by a single Weyl field [either $\Psi_L(x)$ or $\Psi_R(x)$]. Both descriptions are unitarily equivalent [287,297]; i.e., one can construct a unitary similarity transformation that connects a Majorana field operator and a Weyl field operator (and vice versa). Of course, this is hardly a surprise in the two-component spinor formalism, where both the Majorana and Weyl forms of the Lagrangian correspond to the same field theory of a single two-component spinor field $\xi_\alpha(x)$.

For $m \neq 0$, the Weyl Lagrangian given by Eq. (G.2.7) possesses no global symmetry, and hence no conserved charge. In contrast, for $m = 0$ the Weyl Lagrangian exhibits a U(1) chiral symmetry. In a theory of massless neutrinos, the U(1) chiral charge of the neutrino is correlated with its lepton number L, and one is free to use either a Majorana or Weyl description. In the former, the neutrino is a neutral self-conjugate fermion, which is not an eigenstate of L. In the latter, $\Psi_L(x)$ corresponds to the left-handed neutrino and $\Psi_R^C(x)$ corresponds to the right-handed antineutrino, which are eigenstates of L with opposite sign lepton numbers. No experimental observable can distinguish between these two descriptions.

We now consider a collection of free anticommuting four-component Dirac fields, Ψ_i. The free-field Lagrangian (in terms of mass-eigenstate fields) may be obtained from Eq. (3.2.34) by converting to four-component spinor notation. We then obtain the standard textbook result:

$$\mathscr{L} = i\overline{\Psi}^i\gamma^\mu\partial_\mu\Psi_i - m_i\overline{\Psi}^i\Psi_i. \tag{G.2.12}$$

By writing $\Psi = \Psi_L + \Psi_R$, we see that the Lagrangian for a single Dirac field can be written in terms of two Weyl fields:

$$\mathscr{L} = i\overline{\Psi}_L\gamma^\mu\partial_\mu\Psi_L + i\overline{\Psi}_R\gamma^\mu\partial_\mu\Psi_R - m\left(\overline{\Psi}_L\Psi_R + \overline{\Psi}_R\Psi_L\right). \tag{G.2.13}$$

The corresponding free-field equations are:

$$i\gamma^\mu\partial_\mu\Psi_L = m\Psi_R, \qquad i\gamma^\mu\partial_\mu\Psi_R = m\Psi_L. \tag{G.2.14}$$

Summing these two equations yields the Dirac equation, $(i\gamma^\mu\partial_\mu - m)\Psi = 0$.

As a pedagogical example in which both Dirac and Majorana mass terms are present, we perform the diagonalization of the neutrino mass matrix in a one-generation seesaw model[132] using the four-component spinor formalism. Following Appendix A of Ref. [298], we first introduce a four-component anticommuting neutrino field ν_D, and the corresponding Weyl fields,

$$\nu_L \equiv P_L\nu_D, \qquad \nu_L^C \equiv P_L\nu_D^C, \qquad \nu_R \equiv P_R\nu_D, \quad \text{and} \quad \nu_R^C \equiv P_R\nu_D^C. \tag{G.2.15}$$

Note that Eqs. (G.1.12) and (G.2.5) imply that the anticommuting Weyl fermion fields satisfy:

$$\overline{\nu_R^C}\nu_L^C = \overline{\nu_R}\nu_L, \qquad \overline{\nu_L^C}\nu_R^C = \overline{\nu_L}\nu_R. \tag{G.2.16}$$

A Dirac mass term for the neutrinos in the one-generation seesaw model couples ν_L and ν_L^C (and by hermiticity of the Lagrangian, ν_R^C and ν_R), and can be written equivalently as:

$$m_D(\nu_L^{\mathsf{T}}C^{-1}\nu_L^C + \nu_R^{\mathsf{T}}C^{-1}\nu_R^C) = -m_D(\overline{\nu_R^C}\nu_L^C + \overline{\nu_L^C}\nu_R^C) = -m_D(\overline{\nu_R}\nu_L + \overline{\nu_L}\nu_R) = -m_D\overline{\nu}_D\nu_D, \tag{G.2.17}$$

after making use of Eq. (G.2.16). The Majorana mass term for the neutrinos in the one-generation seesaw model couples ν_L^C to itself (and by hermiticity of the Lagrangian, ν_R to itself), and can be written equivalently as:

$$\tfrac{1}{2}M(\nu_L^{C\,\mathsf{T}}C^{-1}\nu_L^C + \nu_R^{\mathsf{T}}C^{-1}\nu_R) = -\tfrac{1}{2}M(\overline{\nu_R}\nu_L^C + \overline{\nu_L^C}\nu_R). \tag{G.2.18}$$

We shall define the phases of the neutrino fields such that the parameters m_D and M are real and non-negative.

Thus, the mass terms of the one-generation neutrino seesaw Lagrangian, given in Eq. (J.2.18) in terms of two-component fermion fields, translates in four-component spinor notation to

$$\begin{aligned}\mathscr{L}_{\text{mass}} &= -\tfrac{1}{2}m_D(\overline{\nu_L}\nu_R + \overline{\nu_R}\nu_L + \overline{\nu_L^C}\nu_R^C + \overline{\nu_R^C}\nu_L^C) - \tfrac{1}{2}M(\overline{\nu_R}\nu_L^C + \overline{\nu_L^C}\nu_R)\\ &= -\tfrac{1}{2}\begin{pmatrix}\overline{\nu_R^C} & \overline{\nu_R}\end{pmatrix}\begin{pmatrix}0 & m_D\\ m_D & M\end{pmatrix}\begin{pmatrix}\nu_L\\ \nu_L^C\end{pmatrix} - \tfrac{1}{2}\begin{pmatrix}\overline{\nu_L} & \overline{\nu_L^C}\end{pmatrix}\begin{pmatrix}0 & m_D\\ m_D & M\end{pmatrix}\begin{pmatrix}\nu_R^C\\ \nu_R\end{pmatrix}\\ &= \tfrac{1}{2}\begin{pmatrix}\nu_L^{\mathsf{T}} & \nu_L^{C\,\mathsf{T}}\end{pmatrix}C^{-1}\begin{pmatrix}0 & m_D\\ m_D & M\end{pmatrix}\begin{pmatrix}\nu_L\\ \nu_L^C\end{pmatrix} + \text{h.c.},\end{aligned} \tag{G.2.19}$$

[132] In Appendix J.2, the seesaw model of neutrino masses is introduced using the two-component spinor formalism.

where we have used Eq. (G.2.16) to write the first line of Eq. (G.2.19) in a symmetrical fashion and Eqs. (G.1.12) and (G.2.5) to obtain the final form above. Note that if $M = 0$, then one can write $\mathscr{L}_{\rm mass} = -m_D \overline{\nu}_D \nu_D$ and identify ν_D as a four-component massive Dirac neutrino.

The Takagi diagonalization of the neutrino mass matrix yields two mass eigenstates, which we designate by ν_ℓ and ν_h, where ℓ and h stand for *light* and *heavy*, respectively. The mass-eigenstate Weyl neutrino fields are related to the interaction-eigenstate Weyl neutrino fields via

$$\begin{pmatrix} \nu_L \\ \nu_L^C \end{pmatrix} = \mathcal{U} \begin{pmatrix} P_L \nu_\ell \\ P_L \nu_h^C \end{pmatrix}, \tag{G.2.20}$$

where $\mathcal{U}$ is a 2×2 unitary matrix that is chosen such that

$$\mathcal{U}^{\rm T} \begin{pmatrix} 0 & m_D \\ m_D & M \end{pmatrix} \mathcal{U} = \begin{pmatrix} m_{\nu_\ell} & 0 \\ 0 & m_{\nu_h} \end{pmatrix}. \tag{G.2.21}$$

For $M \neq 0$, the neutrino mass eigenstates are *not* Dirac fermions. In the seesaw limit of $M \gg m_D$, the corresponding neutrino masses are $m_{\nu_\ell} \simeq m_D^2/M$ and $m_{\nu_h} \simeq M + m_D^2/M$, with $m_{\nu_\ell} \ll m_{\nu_h}$. In terms of the mass eigenstates, the neutrino mass Lagrangian is:

$$\mathscr{L}_{\rm mass} = \tfrac{1}{2}\left[m_{\nu_\ell} \nu_\ell^{\rm T} C^{-1} P_L \nu_\ell + m_{\nu_h} \nu_h^{C\,{\rm T}} C^{-1} P_L \nu_h^C \right] + {\rm h.c.}, \tag{G.2.22}$$

after using Eq. (G.1.24). We now define four-component self-conjugate Majorana neutrino fields, denoted by Ψ_ℓ and Ψ_h respectively, according to Eqs. (G.2.3) and (G.2.9),

$$\Psi_\ell \equiv P_L \nu_\ell + P_R\, C \overline{\nu}_\ell^{\rm T}, \qquad \overline{\Psi}_\ell \equiv \overline{\nu}_\ell P_R - \nu_\ell^{\rm T} C^{-1} P_L, \tag{G.2.23}$$

$$\Psi_h \equiv P_R \nu_h + P_L C \overline{\nu}_h^{\rm T}, \qquad \overline{\Psi}_h \equiv \overline{\nu}_h P_L - \nu_h^{\rm T} C^{-1} P_R. \tag{G.2.24}$$

Then, Eq. (G.2.22) reduces to the expected form:

$$\mathscr{L}_{\rm mass} = -\tfrac{1}{2}\left[m_{\nu_\ell} \overline{\Psi}_\ell \Psi_\ell + m_{\nu_h} \overline{\Psi}_h \Psi_h \right]. \tag{G.2.25}$$

A comparison with the analysis of the neutrino mass matrix given in Appendix J.2 exhibits the power and the simplicity of the two-component spinor formalism, as compared to the rather awkward four-component spinor analysis presented above.

G.3. Gamma matrices and spinors in spacetimes of diverse dimensions and signatures

The translation from two-component to four-component spinor notation given in Appendix G.1 is specific to $3+1$ spacetime dimensions. In $d = 4$ Euclidean space dimensions (independently of the choice of convention for the Minkowski metric), the Dirac gamma matrix algebra is defined by $\{\gamma_E^\mu, \gamma_E^\nu\} = 2\delta^{\mu\nu}\mathbb{1}$, where $\delta^{\mu\nu} \equiv {\rm diag}(1,1,1,1)$. Using Eqs. (A.23) and (G.1.2), the Euclidean gamma matrices (defined for $\mu, \nu = 1, \ldots, 4$) are hermitian and given by $\gamma_E^k \equiv -i\gamma^k$ ($k = 1,2,3$), $\gamma_E^4 \equiv \gamma^0$ and $\gamma_{5E} \equiv -\gamma_E^1\gamma_E^2\gamma_E^3\gamma_E^4 = \gamma_5$ (e.g., see Appendix A.1.2 of Ref. [299]).[133] The four-dimensional reducible (Dirac) spinor representation corresponds to the $(\frac{1}{2}, 0) \otimes (0, \frac{1}{2})$ representation of SO(4), although the $(\frac{1}{2}, 0)$ and $(0, \frac{1}{2})$ representations are independent pseudo-real representations of SO(4) not related by hermitian conjugation, as noted at the end of Section 2. A complete treatment of Euclidean two-component spinors can be found in Ref. [128].

The Euclidean space formalism for fermions is necessary for a rigorous definition of the path integral in quantum field theory [121,122]. Using the Euclidean Dirac gamma matrices introduced above, one can express the four-component Dirac Lagrangian directly in Euclidean space [220]. Carrying out the same procedure for the four-component Majorana Lagrangian is problematical. Because the $(\frac{1}{2}, 0)$ and $(0, \frac{1}{2})$ representations of SO(4) are not hermitian conjugates of each other, a self-conjugate Euclidean Majorana fermion does not exist. Nevertheless, it is possible to devise a continuous Wick rotation from Minkowski spacetime to Euclidean space for Dirac, Majorana and Weyl spinor fields and the gamma matrices. In particular, one can construct a non-hermitian Euclidean action for a single Majorana or Weyl field whose Green functions are related to the usual Minkowski space Green functions by analytic continuation and a Wick rotation of the spinor fields. Further details can be found in Refs. [126,127].[134]

The two-component spinor technology of this review is specifically designed to treat spinors in three space and one time dimension. In theories of d spacetime dimensions (where d is any positive integer), more general techniques are required.

---

133 One can also choose to define the Euclidean Dirac algebra by $\{\gamma_E^\mu, \gamma_E^\nu\} = -2\delta^{\mu\nu}\mathbb{1}$ (simply by multiplying all gamma matrices by a factor of i), in which case the Euclidean gamma matrices, $\gamma_E^k \equiv \gamma^k$ and $\gamma_E^4 \equiv i\gamma^0$ are anti-hermitian, and $\gamma_{5E} \equiv -\gamma_E^1\gamma_E^2\gamma_E^3\gamma_E^4 = \gamma_5$ is hermitian (e.g., see Ref. [300]). These conventions arise more naturally in the general treatment of gamma matrices in d spacetime dimensions as defined in Eq. (G.3.1). The corresponding Euclidean sigma matrices would then be defined as in footnote 88.

134 Previous attempts in the literature to define Euclidean Majorana field theories can be found in Ref. [125].

By considering spinors in this more general setting, one gains insight into the concepts of Majorana, Weyl and Dirac spinors and their distinguishing features.

The mathematics of spinors [130] in spacetimes of dimension $d = t + s$ (where t is the number of time dimensions and s is the number of space dimensions) is most easily treated by introducing higher-dimensional analogues of the gamma matrices, Γ^μ, which satisfy the Clifford algebra [90,91,131–136,140–142,289,301], [135]

$$\{\Gamma^\mu, \Gamma^\nu\} = 2\eta^{\mu\nu}\mathbb{1}, \qquad \eta^{\mu\nu} = \mathrm{diag}(\underbrace{+ + \cdots +}_{t}, \underbrace{- - \cdots -}_{s}), \tag{G.3.1}$$

where the identity matrix $\mathbb{1}$ and the Γ^μ are $2^{[d/2]} \times 2^{[d/2]}$ matrices, and $[d/2]$ is the integer part of $d/2$,

$$[d/2] \equiv \begin{cases} d/2, & \text{for } d \text{ even}, \\ (d-1)/2, & \text{for } d \text{ odd}. \end{cases} \tag{G.3.2}$$

The choice of (s, t) denotes the signature of the spacetime. One can choose $\Gamma^{\mu\,\dagger} = \Gamma^\mu$ for $\mu = 1, 2, \ldots, t$ and $\Gamma^{\mu\,\dagger} = -\Gamma^\mu$ for $\mu = t+1, t+2, \ldots, d$. We identify $\frac{1}{2}\Sigma^{\mu\nu} \equiv \frac{1}{4} i\,[\Gamma^\mu, \Gamma^\nu]$ as the generators of SO(s, t) in the spinor representation. Next, we introduce the $[d/2]$-component (complex) Dirac spinor Ψ and its Dirac conjugate $\overline{\Psi} \equiv \Psi^\dagger A$, where $A = \Gamma^1\Gamma^2\cdots\Gamma^t$ is a unitary matrix that satisfies[136]:

$$A\Gamma^\mu A^{-1} = (-1)^{t+1}\Gamma^{\mu\,\dagger}, \qquad A^\dagger = (-1)^{t(t-1)/2}A. \tag{G.3.3}$$

One can now build SO(s, t)-covariant bilinears, $\overline{\Psi}\Gamma\Psi$, where Γ is a product of gamma matrices. Biquadratic spinor Fierz identities involving quantities such as $(\overline{\Psi}_1\Gamma^I\Psi_2)(\overline{\Psi}_3\Gamma_I\Psi_4)$ can also be derived [302], where the $\Gamma^I = \left\{\mathbb{1}, \Gamma^\mu, \Gamma^{\mu\nu}\ (\mu < \nu), \Gamma^\mu\Gamma^\nu\Gamma^\lambda\ (\mu < \nu < \lambda), \ldots, \Gamma^1\Gamma^2\cdots\Gamma^{2[d/2]}\right\}$ are a complete set of $2^{2[d/2]}$ linearly independent matrices [which generalizes Eq. (G.1.101)].

If d is even, one can also introduce the d-dimensional analogue of γ_5 by defining[137]

$$\Gamma_{d+1} \equiv i^{(s-t)/2}\,\Gamma^1\Gamma^2\cdots\Gamma^d, \tag{G.3.4}$$

which is hermitian and satisfies $(\Gamma_{d+1})^2 = \mathbb{1}$ and $\{\Gamma^\mu, \Gamma_{d+1}\} = 0$. In the case of even-dimensional spacetimes, there are two possible choices for the charge-conjugated spinor Ψ^C,[138]

$$\Psi^C = B_\eta^{-1}\Psi^*, \quad \text{where } \eta = \pm 1, \tag{G.3.5}$$

and the B_η are unitary matrices that satisfy:

$$B_\eta\Gamma^\mu B_\eta^{-1} = \eta\Gamma^{\mu\,*}, \quad \eta = \pm 1. \tag{G.3.6}$$

For even d, a convenient choice is $B_+ = B_-\Gamma_{d+1}$ [135].

If d is odd with signature (s, t), then the $2^{(d-1)/2} \times 2^{(d-1)/2}$ gamma matrices Γ^μ $(\mu = 1, 2, \ldots, d)$ consist of $\left\{\Gamma^1, \Gamma^2, \ldots, \Gamma^{d-1}, \pm i\Gamma_{d+1}\right\}$ of the $(d-1)$-dimensional theory of signature $(s-1, t)$. By assumption, $\mu = d$ is a space index, so that $\Gamma^d \equiv \pm i\Gamma_{d+1}$ is anti-hermitian. In the case of odd d, only one sign choice for η, namely $\eta = (-1)^{(s-t+1)/2}$, is consistent with Eq. (G.3.6) as applied to Γ^d.[139] Consequently, only one definition of the charge-conjugated spinor is viable, namely $\Psi^C = B_-^{-1}\Psi^*$ for $s - t = 1, 5 \pmod 8$ and $\Psi^C = B_+^{-1}\Psi^*$ for $s - t = 3, 7 \pmod 8$.

One important property of the B_η is [131,134,140,141]:

$$B_\eta^* B_\eta = \varepsilon_\eta, \quad \varepsilon_\eta = \pm 1, \tag{G.3.7}$$

for $\eta = \pm 1$ in even-dimensional spacetimes and $\eta = (-1)^{(s-t+1)/2}$ in odd-dimensional spacetimes. In particular [134],[140]

$$\varepsilon_- = \begin{cases} +1, & \text{for } s - t = 0, 1, 2 \pmod 8, \\ -1, & \text{for } s - t = 4, 5, 6 \pmod 8, \end{cases} \qquad \varepsilon_+ = \begin{cases} +1, & \text{for } s - t = 0, 6, 7 \pmod 8, \\ -1, & \text{for } s - t = 2, 3, 4 \pmod 8. \end{cases} \tag{G.3.8}$$

---

135 This includes the Euclidean case [139] corresponding to $t = 0$ and $s = d$ [cf. footnote 133], and the Minkowski case corresponding to $t = 1$ and $s = d - 1$.

136 In d-dimensional Euclidean space (where $t = 0$), $\Gamma^{\mu\,\dagger} = -\Gamma^\mu$ for all $\mu = 1, 2, \ldots, d$. As a result, we may choose $A = \mathbb{1}$, in which case $\overline{\Psi} = \Psi^\dagger$.

137 For $t = 1$ and d even, one traditionally takes $\mu = 0, 1, 2, \ldots, d-1$ (where 0 is the time index), in which case, $\Gamma_{d+1} \equiv i^{(d-2)/2}\,\Gamma^0\Gamma^1\cdots\Gamma^{d-1}$.

138 In four-dimensional Minkowski spacetime, we identify $D = B_-^{-1}$ [cf. Eq. (G.1.17)] and $\gamma_5 D = B_+^{-1}$.

139 The two sign choices for Γ^d correspond to two inequivalent representations of the Clifford algebra [Eq. (G.3.1)] for d odd. Nevertheless, the corresponding $\Sigma^{\mu\nu}$ yield equivalent spinor representations of SO(s, t).

140 For d even, one can use $B_+ = B_-\Gamma_{d+1}$ and $B_\eta\Gamma_{d+1}B_\eta^{-1} = (-1)^{(s-t)/2}\Gamma_{d+1}^*$ to derive $\varepsilon_+ = (-1)^{(s-t)/2}\,\varepsilon_-$.

Using the charge-conjugated spinor defined in Eq. (G.3.5), one can define a self-conjugate spinor, $\Psi^C = \Psi$. Two cases arise depending on the sign of η [134,140–142],

$$\text{Majorana spinor:} \qquad \Psi = B_-^{-1}\Psi^*, \tag{G.3.9}$$

$$\text{pseudo-Majorana spinor:} \qquad \Psi = B_+^{-1}\Psi^*. \tag{G.3.10}$$

Due to the reality conditions [Eqs. (G.3.9) and (G.3.10)], the (pseudo-)Majorana spinor possesses $2^{[d/2]}$ real degrees of freedom. Using Eq. (G.3.7), one immediately sees that Eqs. (G.3.9) and (G.3.10) are respectively consistent if and only if $\varepsilon_\eta = +1$.[141] The possible existence of Majorana [pseudo-Majorana] spinors in d-dimensional spacetime depends on the choice of $s-t$ such that $\varepsilon_- = +1$ [$\varepsilon_+ = +1$]. Using Eq. (G.3.8), it follows that Majorana spinors can only exist in spacetimes where $s - t = 0, 1, 2 \pmod 8$, and pseudo-Majorana can only exist in spacetimes where $s - t = 0, 6, 7 \pmod 8$.[142] In particular, a Majorana spinor cannot exist in four-dimensional Euclidean space.

Given a choice of sign for $\eta = \pm 1$, one can define a corresponding charge conjugation matrix C_η, which is unitary and is defined by[143]

$$C_\eta \equiv B_\eta^{\mathsf{T}} A, \quad \text{where } C_\eta \Gamma^\mu C_\eta^{-1} = \eta(-1)^{t+1}\Gamma^{\mu\,\mathsf{T}}. \tag{G.3.11}$$

Eq. (G.3.5) then yields $\Psi^C = C_\eta^* \overline{\Psi}^{\mathsf{T}}$. The unitary matrices A, B_η and C_η satisfy the following useful identities[134,140]:

$$B_\eta^{\mathsf{T}} = \varepsilon_\eta B_\eta, \qquad C_\eta^{\mathsf{T}} = \varepsilon_\eta \eta^t (-1)^{t(t-1)/2} C_\eta, \qquad A^* B_\eta = \eta^t B_\eta A, \qquad A^{\mathsf{T}} C_\eta = \eta^t C_\eta A^{-1}. \tag{G.3.12}$$

In the case of even d, one can define left- and right-handed chiral projection operators:

$$P_L \equiv \tfrac{1}{2}(1 - \Gamma_{d+1}), \qquad P_R \equiv \tfrac{1}{2}(1 + \Gamma_{d+1}), \tag{G.3.13}$$

and introduce Weyl fermions, Ψ_L and Ψ_R, which satisfy $\Gamma_{d+1}\Psi_{R,L} = \pm\Psi_{R,L}$. Equivalently,

$$\Psi_L \equiv P_L \Psi, \qquad \Psi_R \equiv P_R \Psi, \tag{G.3.14}$$

so that Ψ_L (and likewise Ψ_R) possesses $2^{(d-2)/2}$ complex degrees of freedom. It is possible for a spinor to be simultaneously a (pseudo) Majorana and a Weyl spinor if the spinor and its charge conjugate have the same chirality, in which case $B_\eta \Gamma_{d+1} B_\eta^{-1} = \Gamma_{d+1}^*$ (for even d). The latter condition holds when $i^{s-t} = 1$ or equivalently $s - t = 0 \pmod 4$. Combining this requirement with the condition for the existence of a (pseudo) Majorana spinor, it follows that a (pseudo) Majorana–Weyl spinor, which possesses $2^{(d-2)/2}$ real degrees of freedom, can only exist in spacetimes where $s - t = 0 \pmod 8$. For further details, see Refs. [91,131–134,140–142,289].

As in Section 3.2, one can also consider a multiplet of fermions Ψ_i that transforms under a complex, real or pseudo-real representation R of the flavor group G as

$$\Psi_i \to (D_R)_i^{\ j}\Psi_j, \qquad D_R = \exp(-i\theta^a \boldsymbol{T_R^a}), \quad i, j = 1, 2, \ldots, d_R, \tag{G.3.15}$$

where D_R is unitary and the corresponding generators $\boldsymbol{T_R^a}$ are hermitian. The dimension of R is denoted by d_R, which must be even in the pseudo-real case. In both the real and pseudo-real cases, one can also impose a reality condition that generalizes the Majorana conditions of Eqs. (G.3.9) and (G.3.10),

$$(\Psi_i)^* \equiv \Psi^{*\,i} = W^{ij} B_\eta \Psi_j, \tag{G.3.16}$$

where W is a unitary matrix and B_η acts on the (suppressed) spinor indices of Ψ_j. Additional constraints on the form of W are obtained as follows. First, taking the complex conjugate of Eq. (G.3.16) and inserting the result back into the same equation, it follows that

$$W^* W = \varepsilon_\eta \mathbb{1}, \tag{G.3.17}$$

after making use of Eq. (G.3.7). Second, Eq. (G.3.16) must hold true if Ψ is replaced by $D_R\Psi$ on both sides of the equation, in order to be compatible with the flavor symmetry group transformation law [Eq. (G.3.15)]. This latter requirement combined with Eq. (G.3.17) yields:

$$D_R = \varepsilon_\eta W^* D_R^* W = W^{-1} D_R^* W. \tag{G.3.18}$$

---

141 If $\varepsilon_\eta = -1$ then one can introduce a generalized reality condition [cf. Eq. (G.3.16)], which constrains the structure of a multiplet of Dirac fermions that transforms under a pseudo-real representation of the flavor group. In this case, the corresponding (generalized) self-conjugate spinors are called symplectic (pseudo-)Majorana spinors, as discussed below Eq. (G.3.20).

142 As shown in Refs. [134,140], no SO(s, t)-invariant mass term is allowed for a pseudo-Majorana spinor.

143 In four-dimensional Minkowski spacetime, we identify $C = (C_-^{\mathsf{T}})^{-1} = C_-^*$ [cf. Eq. (G.1.10)] and $B = C_+$ [cf. Eq. (G.1.19)]. In this case, one cannot use C_+ to consistently define a self-conjugate spinor, as the corresponding $\varepsilon_+ = -1$.

Eq. (G.3.18) can be expressed in terms of the flavor group generators,

$$iT_R^a = W^{-1}(iT_R^a)^* W. \tag{G.3.19}$$

Comparing with Eqs. (E.1.4)–(E.1.6), we conclude that the unitary matrix W satisfies:

$$W = \varepsilon_\eta W^{\mathsf{T}}, \quad \varepsilon_\eta = \begin{cases} +1, & R \text{ is a real representation,} \\ -1, & R \text{ is a pseudo-real representation.} \end{cases} \tag{G.3.20}$$

When R is a real representation, $W = W^{\mathsf{T}}$, and a basis for the flavor group generators can be chosen such that $W = \mathbb{1}$ [cf. Eq. (E.1.7)], in which case D_R is a real orthogonal matrix. Since $\varepsilon_\eta = +1$, Eq. (G.3.16) yields (pseudo-)Majorana spinors (depending on the sign of η) as defined previously in Eqs. (G.3.9) and (G.3.10).

When R is a pseudo-real representation, $W = -W^{\mathsf{T}}$, and a basis for the flavor group generators can be chosen such that $W = J \equiv \text{diag}\left\{\begin{pmatrix} 0 & 1 \\ -1 & 0 \end{pmatrix}, \begin{pmatrix} 0 & 1 \\ -1 & 0 \end{pmatrix}, \ldots, \begin{pmatrix} 0 & 1 \\ -1 & 0 \end{pmatrix}\right\}$ is a $d_R \times d_R$ matrix, where d_R is even [cf. Eq. (E.1.8)]. In this case, $D_R^{\mathsf{T}} J D_R = J$, which implies that D_R is a unitary symplectic matrix [136]. Moreover, $\varepsilon_\eta = -1$, which was incompatible with the reality conditions of Eqs. (G.3.9) and (G.3.10), but is compatible with the generalized reality condition of Eq. (G.3.16).

Therefore, we define *symplectic* (pseudo-)Majorana spinors [134,136,137,142,289] to be spinors that transform as a pseudo-real representation under some flavor group and satisfy the generalized reality condition of Eq. (G.3.16), where W is a unitary antisymmetric matrix, depending on the choice of $\eta = \pm 1$ (with $\eta = -1$ yielding the "pseudo" designation). As suggested by Eqs. (3.2.35)–(3.2.40), $2d_R$ symplectic (pseudo-)Majorana spinors are equivalent to d_R Dirac fermions. The possible existence of symplectic (pseudo-)Majorana spinors in a d-dimensional spacetime is governed by Eq. (G.3.8). Requiring that $\varepsilon_\eta = -1$ implies that symplectic Majorana spinors exist in spacetimes where $s - t = 4, 5, 6 \pmod 8$, and symplectic pseudo-Majorana spinors exist in spacetimes where $s - t = 2, 3, 4 \pmod 8$. Using this nomenclature, the fermions described by the four-dimensional Minkowski space Lagrangian given in Eq. (3.2.35) are symplectic pseudo-Majorana spinors.

G.4. Four-component spinor wave functions

In four-dimensional Minkowski space, the free four-component Majorana field can be expanded in a Fourier series; each positive [negative] frequency mode is multiplied by a *commuting* spinor wave function $u(\vec{p}, s)$ [$v(\vec{p}, s)$] as in Eq. (3.2.11),[144]

$$\Psi_{Mi}(x) = \sum_s \int \frac{\mathrm{d}^3\vec{p}}{(2\pi)^{3/2}(2E_{i\boldsymbol{p}})^{1/2}} \left[u(\vec{p}, s)a_i(\vec{p}, s)e^{-ip\cdot x} + v(\vec{p}, s)a_i^\dagger(\vec{p}, s)e^{ip\cdot x}\right], \tag{G.4.1}$$

where $E_{i\boldsymbol{p}} \equiv (|\vec{p}|^2 + m_i^2)^{1/2}$, and the creation operators $a_i^\dagger$ and the annihilation operators a_i satisfy anticommutation relations:

$$\{a_i(\vec{p}, s), a_j^\dagger(\vec{p}\,', s')\} = \delta^3(\vec{p} - \vec{p}\,')\delta_{ss'}\delta_{ij}, \tag{G.4.2}$$

with all other anticommutation relations vanishing. We employ covariant normalization of the one-particle states given by Eq. (3.2.13). It then follows that

$$\langle 0|\, \Psi_M(x)\, \big|\vec{p}, s\big\rangle = u(\vec{p}, s)e^{-ip\cdot x}, \qquad \langle 0|\, \overline{\Psi}_M(x)\, \big|\vec{p}, s\big\rangle = \bar{v}(\vec{p}, s)e^{-ip\cdot x}, \tag{G.4.3}$$

$$\big\langle \vec{p}, s\big|\, \overline{\Psi}_M(x)\, |0\rangle = \bar{u}(\vec{p}, s)e^{ip\cdot x}, \qquad \big\langle \vec{p}, s\big|\, \Psi_M(x)\, |0\rangle = v(\vec{p}, s)e^{ip\cdot x}. \tag{G.4.4}$$

These results are the four-component spinor versions of Eqs. (3.1.7) and (3.1.8).

Likewise, the free Dirac field can be expanded in a Fourier series,

$$\Psi_i(x) = \sum_s \int \frac{\mathrm{d}^3\vec{p}}{(2\pi)^{3/2}(2E_{i\boldsymbol{p}})^{1/2}} \left[u(\vec{p}, s)a_i(\vec{p}, s)e^{-ip\cdot x} + v(\vec{p}, s)b_i^\dagger(\vec{p}, s)e^{ip\cdot x}\right], \tag{G.4.5}$$

where the creation operators $a_i^\dagger$ and $b_i^\dagger$ and the annihilation operators a_i and b_i satisfy anticommutation relations:

$$\{a_i(\vec{p}, s), a_j^\dagger(\vec{p}\,', s')\} = \delta^3(\vec{p} - \vec{p}\,')\delta_{ss'}\delta_{ij}, \tag{G.4.6}$$

$$\{b_i(\vec{p}, s), b_j^\dagger(\vec{p}\,', s')\} = \delta^3(\vec{p} - \vec{p}\,')\delta_{ss'}\delta_{ij}, \tag{G.4.7}$$

with all other anticommutation relations vanishing. We employ covariant normalization of the fermion (F) and antifermion ($\overline{F}$) one-particle states given by Eq. (3.2.22). It then follows that

$$\langle 0|\, \Psi(x)\, \big|\vec{p}, s; F\big\rangle = u(\vec{p}, s)e^{-ip\cdot x}, \qquad \langle 0|\, \overline{\Psi}(x)\, \big|\vec{p}, s; \overline{F}\big\rangle = \bar{v}(\vec{p}, s)e^{-ip\cdot x}, \tag{G.4.8}$$

$$\big\langle \vec{p}, s; F\big|\, \overline{\Psi}(x)\, |0\rangle = \bar{u}(\vec{p}, s)e^{ip\cdot x}, \qquad \big\langle \vec{p}, s; \overline{F}\big|\, \Psi(x)\, |0\rangle = v(\vec{p}, s)e^{ip\cdot x}, \tag{G.4.9}$$

144 Some subtleties arise in the choice of relative phases of the creation and annihilation operators, which are related to the C, CP and CPT transformation properties of the Majorana field. For further details, see Ref. [303].

and the four other single-particle matrix elements vanish. These results are the four-component spinor versions of Eqs. (3.2.23)–(3.2.26). The Fourier expansion of the charge-conjugated free Dirac field $\Psi_i^C(x) = C\overline{\Psi}_i^{\mathsf{T}}(x)$ is given by:

$$\Psi_i^C(x) = \sum_s \int \frac{\mathrm{d}^3\vec{\boldsymbol{p}}}{(2\pi)^{3/2}(2E_{i\boldsymbol{p}})^{1/2}} \left[u(\vec{\boldsymbol{p}},s)b_i(\vec{\boldsymbol{p}},s)e^{-ip\cdot x} + v(\vec{\boldsymbol{p}},s)a_i^\dagger(\vec{\boldsymbol{p}},s)e^{ip\cdot x}\right], \tag{G.4.10}$$

where we have used Eq. (G.4.13). That is, the charge conjugation transformation interchanges the annihilation and creation operators, $a_i \leftrightarrow b_i$ and $a_i^\dagger \leftrightarrow b_i^\dagger$. Thus, if $\Psi^C(x) = \Psi(x)$, then we must identify $a = b$ and $a^\dagger = b^\dagger$, corresponding to the free Majorana field given in Eq. (G.4.1).

The two-component spinor momentum space wave functions are related to the traditional four-component spinor wave functions according to:

$$u(\vec{\boldsymbol{p}},s) = \begin{pmatrix} x_\alpha(\vec{\boldsymbol{p}},s) \\ y^{\dagger\dot{\alpha}}(\vec{\boldsymbol{p}},s)\end{pmatrix}, \qquad \bar{u}(\vec{\boldsymbol{p}},s) = (y^\alpha(\vec{\boldsymbol{p}},s), x_{\dot{\alpha}}^\dagger(\vec{\boldsymbol{p}},s)), \tag{G.4.11}$$

$$v(\vec{\boldsymbol{p}},s) = \begin{pmatrix} y_\alpha(\vec{\boldsymbol{p}},s) \\ x^{\dagger\dot{\alpha}}(\vec{\boldsymbol{p}},s)\end{pmatrix}, \qquad \bar{v}(\vec{\boldsymbol{p}},s) = (x^\alpha(\vec{\boldsymbol{p}},s), y_{\dot{\alpha}}^\dagger(\vec{\boldsymbol{p}},s)), \tag{G.4.12}$$

where the u and v-spinors are related by

$$v(\vec{\boldsymbol{p}},s) = C\bar{u}(\vec{\boldsymbol{p}},s)^{\mathsf{T}}, \qquad u(\vec{\boldsymbol{p}},s) = C\bar{v}(\vec{\boldsymbol{p}},s)^{\mathsf{T}}, \tag{G.4.13}$$

$$\bar{v}(\vec{\boldsymbol{p}},s) = -u(\vec{\boldsymbol{p}},s)^{\mathsf{T}}C^{-1}, \qquad \bar{u}(\vec{\boldsymbol{p}},s) = -v(\vec{\boldsymbol{p}},s)^{\mathsf{T}}C^{-1}. \tag{G.4.14}$$

The spin quantum number takes on values $s = \pm\frac{1}{2}$, and refers either to the component of the spin as measured in the rest frame with respect to a fixed axis or to the helicity (as discussed in Section 3.1 and Appendix C). Note that the u and v-spinors also satisfy:

$$v(\vec{\boldsymbol{p}},s) = -2s\gamma_5 u(\vec{\boldsymbol{p}},-s), \qquad u(\vec{\boldsymbol{p}},s) = 2s\gamma_5 v(\vec{\boldsymbol{p}},-s), \tag{G.4.15}$$

which follows from Eq. (3.1.23). Explicit forms for the four-component spinor wave functions in the chiral representation can be obtained using Eqs. (3.1.19)–(3.1.22), where $\chi_s(\hat{\boldsymbol{s}})$ is given in Eq. (C.1.11). For helicity spinors, further simplifications result by employing Eqs. (C.3.4)–(C.3.7).

One can check that u and v satisfy the Dirac equations

$$(\not{p} - m)\, u(\vec{\boldsymbol{p}},s) = (\not{p} + m)\, v(\vec{\boldsymbol{p}},s) = 0, \tag{G.4.16}$$

$$\bar{u}(\vec{\boldsymbol{p}},s)\,(\not{p} - m) = \bar{v}(\vec{\boldsymbol{p}},s)\,(\not{p} + m) = 0, \tag{G.4.17}$$

corresponding to Eqs. (3.1.9)–(3.1.12), and

$$(2s\gamma_5 \not{S} - 1)\, u(\vec{\boldsymbol{p}},s) = (2s\gamma_5 \not{S} - 1)\, v(\vec{\boldsymbol{p}},s) = 0, \tag{G.4.18}$$

$$\bar{u}(\vec{\boldsymbol{p}},s)\,(2s\gamma_5 \not{S} - 1) = \bar{v}(\vec{\boldsymbol{p}},s)\,(2s\gamma_5 \not{S} - 1) = 0, \tag{G.4.19}$$

corresponding to Eqs. (3.1.24)–(3.1.27), where the spin vector S^μ is defined in Eq. (3.1.15).[145] For massive fermions, Eqs. (3.1.46)–(3.1.49) correspond to

$$u(\vec{\boldsymbol{p}},s)\bar{u}(\vec{\boldsymbol{p}},s) = \tfrac{1}{2}(1 + 2s\gamma_5 \not{S})\,(\not{p} + m), \tag{G.4.20}$$

$$v(\vec{\boldsymbol{p}},s)\bar{v}(\vec{\boldsymbol{p}},s) = \tfrac{1}{2}(1 + 2s\gamma_5 \not{S})\,(\not{p} - m). \tag{G.4.21}$$

To apply the above formulae to the massless case we must employ helicity states, where s is replaced by the helicity quantum number λ, and S^μ is defined by Eq. (3.1.16). In particular, in the $m \to 0$ limit, $S^\mu = p^\mu/m + \mathcal{O}(m/E)$. Inserting this result in Eqs. (G.4.18) and (G.4.19) and using the Dirac equations, it follows that the massless helicity spinors are eigenstates of γ_5,

$$\gamma_5 u(\vec{\boldsymbol{p}},\lambda) = 2\lambda u(\vec{\boldsymbol{p}},\lambda), \qquad \gamma_5 v(\vec{\boldsymbol{p}},\lambda) = -2\lambda v(\vec{\boldsymbol{p}},\lambda). \tag{G.4.22}$$

Combining these results with Eq. (G.4.15) [with s replaced by λ] yields:

$$v(p,\lambda) = -2\lambda\gamma_5 u(p,-\lambda) = u(p,-\lambda), \quad \lambda = \pm\tfrac{1}{2}, \tag{G.4.23}$$

and we see that the massless u and v spinors of opposite helicity are the same.

[145] We use the standard Feynman slash notation: $\not{p} \equiv \gamma_\mu p^\mu$ and $\not{S} \equiv \gamma_\mu S^\mu$.

Applying the above $m \to 0$ limiting procedure to Eqs. (G.4.20) and (G.4.21) and using the mass–shell condition ($\not{p}\not{p} = p^2 = m^2$), one obtains the massless helicity projection operators corresponding to Eqs. (3.1.54)–(3.1.57):

$$u(\vec{\boldsymbol{p}}, \lambda)\bar{u}(\vec{\boldsymbol{p}}, \lambda) = \tfrac{1}{2}(1 + 2\lambda\gamma_5)\not{p}, \tag{G.4.24}$$

$$v(\vec{\boldsymbol{p}}, \lambda)\bar{v}(\vec{\boldsymbol{p}}, \lambda) = \tfrac{1}{2}(1 - 2\lambda\gamma_5)\not{p}. \tag{G.4.25}$$

Summing over the spin degree of freedom, we obtain the spin-sum identities corresponding to Eqs. (3.1.58)–(3.1.61),

$$\sum_s u(\vec{\boldsymbol{p}}, s)\bar{u}(\vec{\boldsymbol{p}}, s) = \not{p} + m, \tag{G.4.26}$$

$$\sum_s v(\vec{\boldsymbol{p}}, s)\bar{v}(\vec{\boldsymbol{p}}, s) = \not{p} - m, \tag{G.4.27}$$

$$\sum_s u(\vec{\boldsymbol{p}}, s)v^{\mathsf{T}}(\vec{\boldsymbol{p}}, s) = (\not{p} + m)C^{\mathsf{T}}, \tag{G.4.28}$$

$$\sum_s \bar{u}^{\mathsf{T}}(\vec{\boldsymbol{p}}, s)\bar{v}(\vec{\boldsymbol{p}}, s) = C^{-1}(\not{p} - m), \tag{G.4.29}$$

$$\sum_s \bar{v}^{\mathsf{T}}(\vec{\boldsymbol{p}}, s)\bar{u}(\vec{\boldsymbol{p}}, s) = C^{-1}(\not{p} + m), \tag{G.4.30}$$

$$\sum_s v(\vec{\boldsymbol{p}}, s)u^{\mathsf{T}}(\vec{\boldsymbol{p}}, s) = (\not{p} - m)C^{\mathsf{T}}, \tag{G.4.31}$$

which are valid for both the massive case and the massless $m \to 0$ limit.

As previously noted, the results for the bilinear covariants obtained in Eqs. (G.1.78)–(G.1.89) can also be applied to expressions involving the commuting spinor wave functions. Various relations among the possible bilinear covariants can be established by using Eqs. (G.4.13) and (G.4.14). As an example, for $\Gamma = \mathbb{1}, \gamma_5, \gamma^\mu, \gamma^\mu\gamma_5, \Sigma^{\mu\nu}, \Sigma^{\mu\nu}\gamma_5$,

$$\bar{u}(\vec{\boldsymbol{p}}_1, s_1)\Gamma v(\vec{\boldsymbol{p}}_2, s_2) = -v(\vec{\boldsymbol{p}}_1, s_1)^{\mathsf{T}}C^{-1}\Gamma C\bar{u}(\vec{\boldsymbol{p}}_2, s_2)^{\mathsf{T}} = -\eta_\Gamma^C\bar{u}(\vec{\boldsymbol{p}}_2, s_2)\Gamma v(\vec{\boldsymbol{p}}_1, s_1), \tag{G.4.32}$$

$$\bar{u}(\vec{\boldsymbol{p}}_1, s_1)\Gamma u(\vec{\boldsymbol{p}}_2, s_2) = -v(\vec{\boldsymbol{p}}_1, s_1)^{\mathsf{T}}C^{-1}\Gamma C\bar{v}(\vec{\boldsymbol{p}}_2, s_2)^{\mathsf{T}} = -\eta_\Gamma^C\bar{v}(\vec{\boldsymbol{p}}_2, s_2)\Gamma v(\vec{\boldsymbol{p}}_1, s_1), \tag{G.4.33}$$

where the sign η_Γ^C [defined in Eq. (G.1.24)] arises after taking the transpose and applying Eq. (G.1.24). In particular, the (commuting) u and v spinors satisfy the following relations:

$$\bar{u}(\vec{\boldsymbol{p}}_1, s_1)P_L v(\vec{\boldsymbol{p}}_2, s_2) = -\bar{u}(\vec{\boldsymbol{p}}_2, s_2)P_L v(\vec{\boldsymbol{p}}_1, s_1), \tag{G.4.34}$$

$$\bar{u}(\vec{\boldsymbol{p}}_1, s_1)P_R v(\vec{\boldsymbol{p}}_2, s_2) = -\bar{u}(\vec{\boldsymbol{p}}_2, s_2)P_R v(\vec{\boldsymbol{p}}_1, s_1), \tag{G.4.35}$$

$$\bar{u}(\vec{\boldsymbol{p}}_1, s_1)\gamma^\mu P_L v(\vec{\boldsymbol{p}}_2, s_2) = \bar{u}(\vec{\boldsymbol{p}}_2, s_2)\gamma^\mu P_R v(\vec{\boldsymbol{p}}_1, s_1), \tag{G.4.36}$$

$$\bar{u}(\vec{\boldsymbol{p}}_1, s_1)\gamma^\mu P_R v(\vec{\boldsymbol{p}}_2, s_2) = \bar{u}(\vec{\boldsymbol{p}}_2, s_2)\gamma^\mu P_L v(\vec{\boldsymbol{p}}_1, s_1), \tag{G.4.37}$$

and four similar relations obtained by interchanging $v(\vec{\boldsymbol{p}}_2, s_2) \leftrightarrow u(\vec{\boldsymbol{p}}_2, s_2)$.

G.5. Feynman rules for four-component fermions

We now illustrate some basic applications of the above formalism. In particular, we shall establish a set of Feynman rules for four-component fermions that treat both Dirac and Majorana fermions on the same footing. These rules generalize the standard Feynman rules for four-component Dirac fermions found in most quantum field theory textbooks. Two advantages of the rules presented here are: (i) no factors of the charge conjugation matrix C are required for fermion interaction vertices and propagators, and (ii) the *relative* sign between different diagrams corresponding to the same physical process is simply determined. Our rules have been obtained by translating our two-component fermion Feynman rules into the four-component spinor language. The resulting Feynman rules for four-component Majorana fermions are equivalent to the set of rules independently obtained in Ref. [304] (see also Refs. [305,306]).

Consider first the Feynman rule for the four-component fermion propagator. Virtual Dirac fermion lines can either correspond to Ψ or Ψ^C. Here, there is no ambiguity in the propagator Feynman rule, since for free Dirac fermion fields,[146]

$$\langle 0|\, T[\Psi_a(x)\overline{\Psi}^b(y)]\,|0\rangle = \langle 0|\, T[\Psi_a^C(x)\overline{\Psi^C}^b(y)]\,|0\rangle\,, \tag{G.5.1}$$

so that the Feynman rules for the propagator of a Ψ and Ψ^C line, exhibited in Fig. G.5.1, are identical. The same rule also applies to a four-component Majorana fermion.

146 In deriving Eq. (G.5.1), we have used $\mathcal{C}\,\Psi_a\,\mathcal{C}^{-1} = \eta_c\Psi_a^C$ and $\mathcal{C}\,\overline{\Psi}^a\,\mathcal{C}^{-1} = \eta_c^*\,\overline{\Psi^C}^a$, where $\mathcal{C}$ is the charge conjugation *operator* that acts on the quantum Hilbert space and η_c is a convention-dependent phase factor [36,38]. Note that $\mathcal{C}$ is a unitary operator and $\mathcal{C}\,|0\rangle = |0\rangle$ in the free-field vacuum.

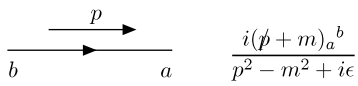

Fig. G.5.1. Feynman rule for the propagator of a four-component fermion with mass m. The same rule applies to a Majorana, Dirac and charge-conjugated Dirac fermion. The four-component spinor labels a and b are specified.

Using Eq. (G.1.2), the four-component fermion propagator Feynman rule can be expressed as a partitioned matrix of 2×2 blocks,

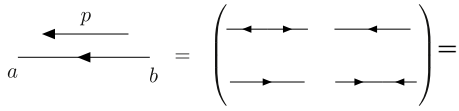

$$= \frac{i}{p^2-m^2+i\epsilon}\begin{pmatrix} m\,\delta_\alpha{}^\beta & p\cdot\sigma_{\alpha\dot\beta} \\ p\cdot\overline{\sigma}^{\dot\alpha\beta} & m\,\delta^{\dot\alpha}{}_{\dot\beta}\end{pmatrix}, \tag{G.5.2}$$

where a and b are four-component spinor indices. That is, Eq. (G.5.2) is a partitioned matrix whose blocks consist of two-component fermion propagators defined in Fig. 4.2.1, with the undotted and dotted α [β] indices on the left [right] and with the momentum flowing from right to left.

The derivation of the four-component Dirac fermion propagator is treated in most modern textbooks of quantum field theory (see, e.g., Ref. [114]). Here, we briefly sketch the path integral derivation of the four-component fermion propagator by exploiting the path integral treatment of the two-component fermion propagators outlined in Appendix F. Consider a single massive Dirac fermion $\Psi(x)$ coupled to an anticommuting four-component Dirac fermionic source term

$$J_\psi(x) \equiv \begin{pmatrix} J_{\eta\alpha}(x) \\ J^{\dagger\dot\alpha}_\chi(x)\end{pmatrix}. \tag{G.5.3}$$

The corresponding action [Eq. (F.2)] in four-component notation is given by

$$S = \int \mathrm{d}^4x\,(\mathscr{L} + \bar J_\psi\Psi + \overline{\Psi}J_\psi) = \int \mathrm{d}^4x\,\left[\overline{\Psi}(i\not{\partial}-m)\Psi + \bar J_\psi\Psi + \overline{\Psi}J_\psi\right]. \tag{G.5.4}$$

Introducing the momentum space Fourier coefficients:

$$\Psi(x) = \int \frac{d^4p}{(2\pi)^4}e^{-ip\cdot x}\widehat{\Psi}(p), \qquad J_\psi(x) = \int \frac{d^4p}{(2\pi)^4}e^{-ip\cdot x}\widehat{J}_\psi(p), \tag{G.5.5}$$

we can identify the following four-component quantities with matrices of two-component quantities given in Eqs. (F.7) and (F.27):

$$\widehat{\Psi}(p) = A^{-1}\Omega_c(p), \qquad \widehat{J}_\psi(p) = X_c(p), \qquad \not{p}-m = \mathcal{M}(p)A, \tag{G.5.6}$$

where A is the Dirac conjugation matrix defined in Eqs. (G.1.9) and (G.1.11). Using the results of Appendix F, one easily derives:

$$\langle 0|T(\Psi(x_1)\overline{\Psi}(x_2))|0\rangle = \left(-i\frac{\overrightarrow{\delta}}{\delta\bar J_\psi(x_1)}\right)W[J,\bar J]\left(-i\frac{\overleftarrow{\delta}}{\delta J_\psi(x_2)}\right)\Bigg|_{J_\psi=\bar J_\psi=0}, \tag{G.5.7}$$

where

$$W[J_\psi,\bar J_\psi] = \exp\left\{-i\int\frac{d^4p}{(2\pi)^4}\,\widehat{\bar J}_\psi(p)\frac{\not{p}+m}{p^2-m^2}\widehat{J}_\psi(p)\right\}. \tag{G.5.8}$$

Using the analogues of Eqs. (F.23) and (F.24), we end up with the expected result

$$\langle 0|T(\Psi(x_1)\overline{\Psi}(x_2))|0\rangle = \int\frac{d^4p}{(2\pi)^4}\,e^{-ip\cdot(x_1-x_2)}\,\frac{i(\not{p}+m)}{p^2-m^2}. \tag{G.5.9}$$

In principle, the analogous computation can be carried out for a single four-component Majorana fermion field $\Psi_M(x)$ coupled to a Majorana fermionic source, $J_\xi(x)$. The corresponding action is similar to that of Eq. (G.5.4), with an extra overall factor of $1/2$. However, in evaluating the functional derivative in Eq. (G.5.8), one must take into account that the Majorana fermionic source $J_\xi(x)$ satisfies $J^C_\xi \equiv C\bar J^{\mathsf{T}}_\xi = J_\xi$. Consequently, the functional derivative with respect to $\bar J_\xi$ is related to the corresponding functional derivative with respect to J_ξ. Hence, the calculation of Eq. (G.5.8) will yield two equal terms that will cancel the overall factor of $1/2$, resulting again in Eq. (G.5.9). Nevertheless, this computation is somewhat awkward using four-component spinor notation, in contrast to the straightforward calculation of Appendix F.

We next examine the various interactions involving four-component fermions. First, we consider the interactions of a neutral scalar ϕ or a gauge boson A^a_μ with a pair of Majorana fermions. To obtain the interactions of the four-component

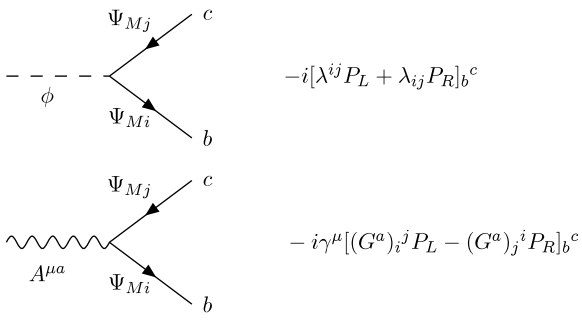

Fig. G.5.2. Feynman rules for neutral scalar and gauge boson interactions with a pair of four-component Majorana fermions (labeled by four-component spinor indices b and c). The G^a are defined in Eq. (4.3.16). The index a runs over the neutral (mass-eigenstate) gauge bosons.

fermion fields, we first identify the neutral two-component fermion mass-eigenstate neutral fields ξ_i. Using Eqs. (4.3.9) and (4.3.15), the interaction Lagrangian in two-component form is given by:

$$\mathscr{L}_{\rm int} = -\tfrac{1}{2}(\lambda^{ij}\xi_i\xi_j + \lambda_{ij}\xi^{\dagger i}\xi^{\dagger j})\phi - (G^a)_i{}^j\,\xi^{\dagger i}\overline{\sigma}^\mu\xi_j A^a_\mu, \tag{G.5.10}$$

where λ is a complex symmetric matrix with $\lambda^{ij} \equiv \lambda^*_{ij}$ [cf. Eq. (3.2.2)], the A^a_μ are the mass-eigenstate gauge fields, and the corresponding hermitian matrices G^a are defined in Eq. (4.3.16). It is now simple to convert this result into four-component notation:

$$\mathscr{L}_{\rm int} = -\tfrac{1}{2}(\lambda^{ij}\overline{\Psi}_{Mi}P_L\Psi_{Mj} + \lambda_{ij}\overline{\Psi}^i_M P_R\Psi^j_M)\phi - (G^a)_i{}^j\overline{\Psi}^i_M\gamma^\mu P_L\Psi_{Mj}A^a_\mu, \tag{G.5.11}$$

where the Ψ_{Mj} are a set of (neutral) Majorana four-component fermions. It is convenient to use Eq. (G.1.98) to rewrite the term proportional to $(G^a)_i{}^j$ in Eq. (G.5.11) as follows

$$\begin{aligned}(G^a)_i{}^j\overline{\Psi}^i_M\gamma^\mu P_L\Psi_{Mj} &= \tfrac{1}{2}(G^a)_i{}^j\left[\overline{\Psi}^i_M\gamma^\mu P_L\Psi_{Mj} - \overline{\Psi}_{Mj}\gamma^\mu P_R\Psi^i_M\right]\\ &= \tfrac{1}{2}\overline{\Psi}_{Mi}\gamma^\mu\left[(G^a)_i{}^j P_L - (G^a)_j{}^i P_R\right]\Psi_{Mj}.\end{aligned} \tag{G.5.12}$$

In the last step above, we have lowered the flavor indices of the four-component Majorana fermion fields, as the heights of these indices can be arbitrarily chosen [cf. Eq. (G.1.76)].

Using standard four-component spinor methods, the corresponding four-component spinor Feynman rules are displayed in Fig. G.5.2. A Majorana fermion is neutral under all conserved charges (and thus equal to its own antiparticle). Hence, an arrow on a Majorana fermion line simply reflects the structure of the interaction Lagrangian; i.e., $\overline{\Psi}_M$ [Ψ_M] is represented by an arrow pointing out of [into] the vertex. These arrows are then used for determining the placement of the u and v spinors in an invariant amplitude, according to the rules of Appendix G.6. In particular, the four-component spinor labels of Fig. G.5.2 indicate that one should traverse any continuous fermion line by moving antiparallel to the direction of the fermion arrows.

Next, we consider the interactions of a (possibly complex) scalar Φ or a gauge boson A^a_μ with a pair of Dirac fermions. The Dirac fermions are charged with respect to some global or local U(1) symmetry, which is assumed to be a symmetry of the Lagrangian. To obtain the interactions of the four-component fermion fields, we first identify the mass-degenerate oppositely charged pairs χ_j and η_j (with U(1)-charges q_j and $-q_j$, respectively) that combine to form the mass-eigenstate Dirac fermions. The scalar field Φ carries a U(1)-charge q_Φ. We also identify the gauge boson mass eigenstates of definite U(1)-charge by A^a_μ as described in Section 4.3 (cf. footnote 41). Using Eqs. (4.3.9) and (4.3.18), the interaction Lagrangian in two-component form is given by:

$$\mathscr{L}_{\rm int} = -\kappa^i{}_j\chi_i\eta^j\Phi - \kappa_i{}^j\chi^{\dagger i}\eta^\dagger_j\Phi^\dagger - \left[(G^a_L)_i{}^j\chi^{\dagger i}\overline{\sigma}^\mu\chi_j - (G^a_R)_j{}^i\eta^\dagger_i\overline{\sigma}^\mu\eta^j\right]A^a_\mu, \tag{G.5.13}$$

where $\kappa_i{}^j \equiv (\kappa^i{}_j)^*$ [cf. Eq. (3.2.28)] and κ is an arbitrary complex matrix coupling, subject to the conditions that $\kappa^i{}_j = 0$ unless $q_\Phi = q_j - q_i$. For the gauge boson couplings, we follow the notation of Eqs. (4.3.19) and (4.3.20). In particular, $A^a_\mu G^a_L$ and $A^a_\mu G^a_R$ are hermitian matrix-valued gauge fields, which when summed over a can contain both neutral and charged [with respect to U(1)] mass-eigenstate gauge boson fields. Converting to four-component notation yields:

$$\mathscr{L}_{\rm int} = -\kappa^i{}_j\overline{\Psi}^j P_L\Psi_i\Phi - \kappa_i{}^j\overline{\Psi}^i P_R\Psi_j\Phi^\dagger - \left[(G^a_L)_i{}^j\overline{\Psi}^i\gamma^\mu P_L\Psi_j + (G^a_R)_i{}^j\overline{\Psi}^i\gamma^\mu P_R\Psi_j\right]A^a_\mu, \tag{G.5.14}$$

where the Ψ_j are a set of Dirac four-component fermions. If Φ is a real (neutral) scalar field, then we shall write $\phi \equiv \Phi = \Phi^\dagger$. The corresponding four-component spinor Feynman rules are exhibited in Fig. G.5.3. The rules involving the charge-conjugated Dirac fields have been obtained by using Eq. (G.1.90). Note that the arrows on the charged scalar and Dirac fermion lines depict the flow of the conserved U(1)-charge.

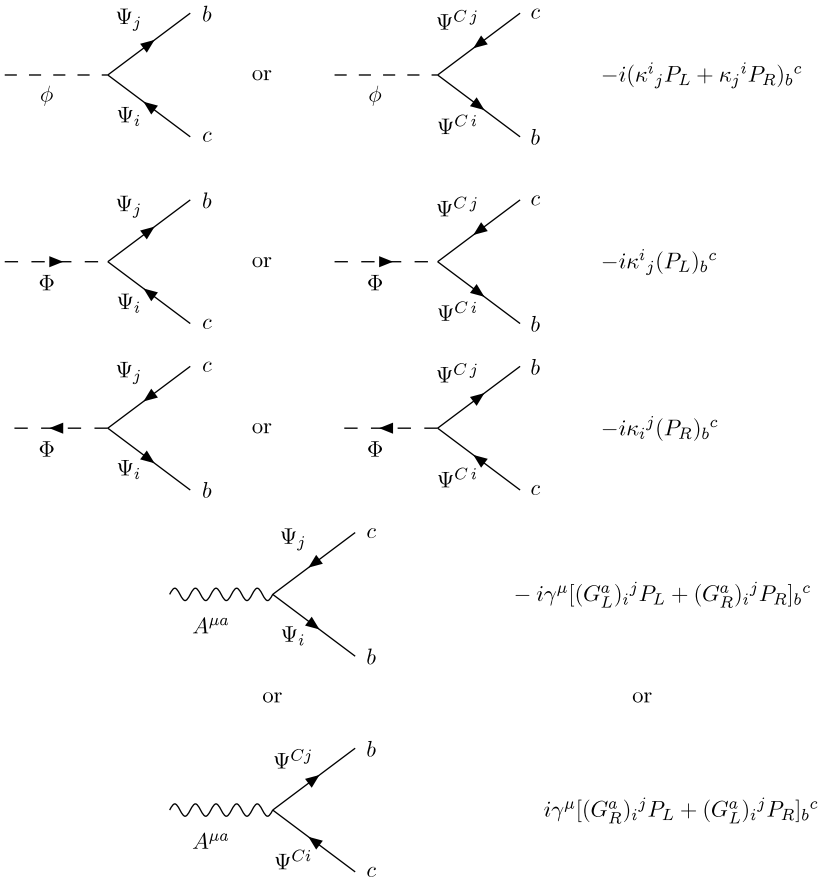

Fig. G.5.3. Feynman rules for neutral scalar (ϕ), charged scalar (Φ) and gauge boson ($A^{\mu a}$) interactions with a pair of four-component Dirac fermions (labeled by four-component spinor indices b and c). In each case, one has two choices for the corresponding Feynman rule: one involving Ψ and one involving the oppositely charged Ψ^C (with the arrows of the corresponding Ψ and Ψ^C lines pointing in opposite directions). The arrows indicate the direction of flow of the U(1)-charges of the Dirac fermion and charged scalar fields. The index a runs over both neutral and charged (mass-eigenstate) gauge bosons, consistent with charge conservation at the vertex.

Finally, we treat the interaction of a charged scalar boson Φ (with U(1)-charge q_Φ) or a charged vector boson W (with U(1)-charge q_W) with a fermion pair consisting of one Majorana and one Dirac fermion. We denote the neutral fermion mass-eigenstate fields by ξ_i and pairs of oppositely charged fermion mass-eigenstate fields by χ_j and η^j (with U(1)-charges q_j and $-q_j$, respectively). Using Eqs. (4.3.9) and (4.3.21), the interaction Lagrangian is given by:

$$\begin{aligned}\mathscr{L}_{\rm int} &= -\Phi[(\kappa_1)^i{}_j \xi_i \eta^j + (\kappa_2)_{ij}\xi^{\dagger i}\chi^{\dagger j}] - \Phi^\dagger[(\kappa_2)^{ij}\xi_i\chi_j + (\kappa_1)_i{}^j\xi_i^{\dagger i}\eta_j^\dagger] \\ &\quad - W_\mu[(G_1)_j{}^i\chi^{\dagger j}\overline{\sigma}^\mu\xi_i - (G_2)_{ij}\xi^{\dagger i}\overline{\sigma}^\mu\eta^j] - W_\mu^\dagger[(G_1)^j{}_i\xi^{\dagger i}\overline{\sigma}^\mu\chi_j - (G_2)^{ij}\eta_j^\dagger\overline{\sigma}^\mu\xi_i],\end{aligned} \tag{G.5.15}$$

where κ_1, κ_2, G_1, and G_2 are arbitrary complex coupling matrices, subject to the conditions that $(\kappa_1)^i{}_j = (\kappa_2)_{ij} = 0$ unless $q_\Phi = q_j$, and $(G_1)_j{}^i = (G_2)_{ij} = 0$ unless $q_W = q_j$. Converting to four-component spinor notation yields:

$$\mathscr{L}_{\rm int} = -\left[(\kappa_1)^i{}_j\overline{\Psi}^j P_L\Psi_{Mi} + (\kappa_2)_{ij}\overline{\Psi}^j P_R\Psi_M^i\right]\Phi - \left[(G_1)_j{}^i\overline{\Psi}^j\gamma^\mu P_L\Psi_{Mi} + (G_2)_{ij}\overline{\Psi}^j\gamma^\mu P_R\Psi_M^i\right]W_\mu + \text{h.c.} \tag{G.5.16}$$

The corresponding four-component spinor Feynman rules are exhibited in Fig. G.5.4.

There is an equivalent form for the interactions given by Eqs. (G.5.13) and (G.5.16) where $\mathscr{L}_{\rm int}$ is written in terms of charge-conjugated Dirac fields [after using Eq. (G.1.90)]. The Feynman rules involving Dirac fermions can take two possible forms, as shown in Figs. G.5.3 and G.5.4. As previously noted, the direction of an arrow on a Dirac fermion line indicates the direction of the fermion charge flow (whereas the arrow on the Majorana fermion line is unconnected to charge flow). However, we are free to choose either a Ψ or Ψ^C line to represent a Dirac fermion at any place in a given Feynman graph.[147] For any decay or scattering process, a suitable choice of either the Ψ-rule or the Ψ^C-rule at each vertex (the choice can

[147] Since the charge of Ψ^C is opposite in sign to the charge of Ψ, the corresponding arrow directions of the Ψ and Ψ^C lines must point in opposite directions.

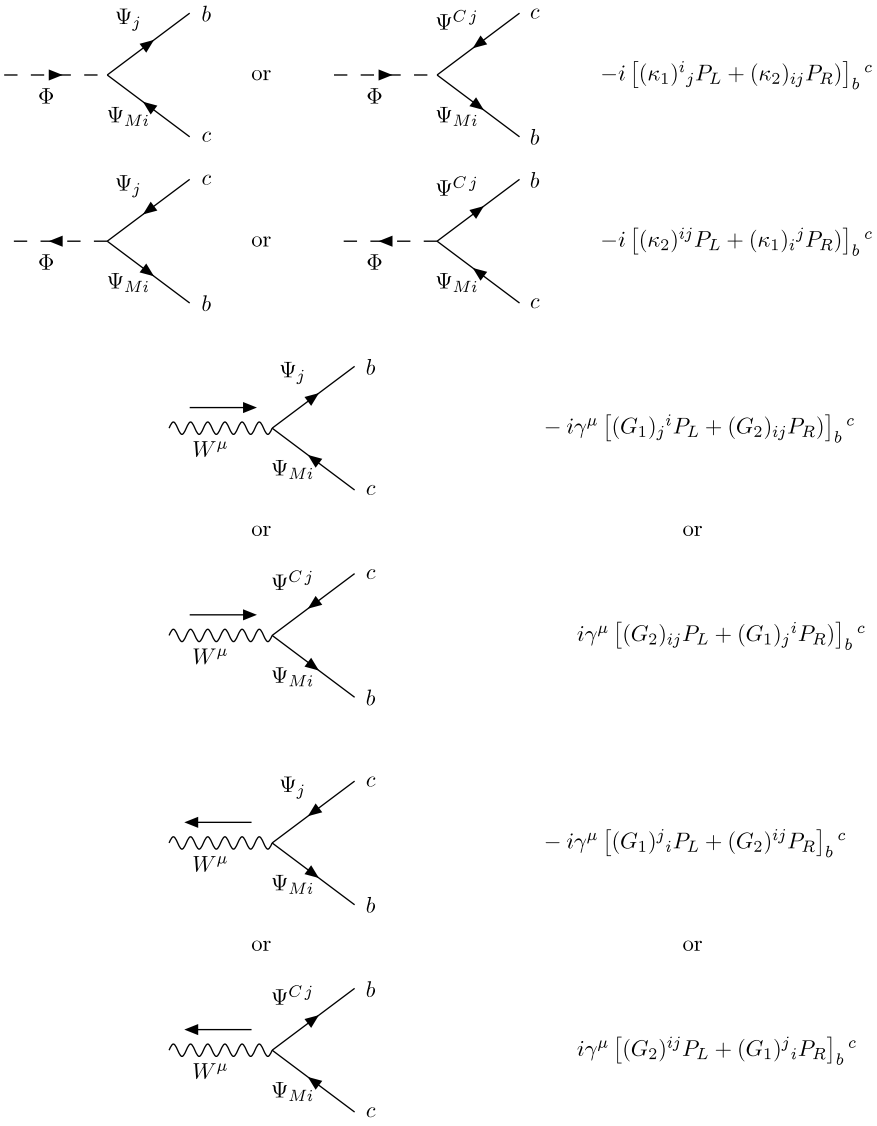

Fig. G.5.4. Feynman rules for charged scalar and vector boson interactions with a fermion pair consisting of one Majorana and one Dirac four-component fermion (labeled by four-component spinor indices b and c). In each case, one has two choices for the corresponding Feynman rule: one involving Ψ and one involving the oppositely charged Ψ^C (with the arrows of the Ψ and Ψ^C lines pointing in opposite directions). The arrows of the Dirac fermion and charged bosons indicate the direction of flow of the corresponding U(1)-charges. That is, the charge of the boson (either Φ or W above) must coincide with the charge of Ψ_j. The arrows of the Majorana fermions satisfy the requirement that the fermion line arrow directions flow continuously through the vertex.

be different at different vertices), will guarantee that the arrow directions on fermion lines flow continuously through the Feynman diagram. Then, to evaluate an invariant amplitude, one should traverse *any* continuous fermion line (either Ψ or Ψ^C) by moving antiparallel to the direction of the fermion arrows, as indicated by the order of the four-component spinor labels in the Feynman rules of Figs. G.5.3 and G.5.4. Examples will be provided in Appendix G.6.

G.6. Applications of four-component spinor Feynman rules

For a given process, there may be a number of distinct choices for the arrow directions on the Majorana fermion lines, which may depend on whether one represents a given Dirac fermion by Ψ or Ψ^C. However, different choices do *not* lead to independent Feynman diagrams.[148] When computing an invariant amplitude, one first writes down the relevant Feynman diagrams with no arrows on any Majorana fermion line. The number of distinct graphs contributing to the process is then determined. Finally, one makes some choice for how to distribute the arrows on the Majorana fermion lines and how to label

[148] In contrast, the two-component Feynman rules developed in Section 4 require that two vertices differing by the direction of the arrows on the two-component fermion lines must both be included in the calculation of the matrix element.

Dirac fermion lines (either as the field Ψ or its charge conjugate Ψ^C) in a manner consistent with the rules of Figs. G.5.2 and G.5.4. The end result for the invariant amplitude (apart from an overall unobservable phase) does not depend on the choices made for the direction of the fermion arrows.

Using the above procedure, the Feynman rules for the external fermion wave functions are the same for Dirac and Majorana fermions:

- $u(\vec{\boldsymbol{p}}, s)$: incoming Ψ [or Ψ^C] with momentum $\vec{\boldsymbol{p}}$ parallel to the arrow direction,
- $\bar{u}(\vec{\boldsymbol{p}}, s)$: outgoing Ψ [or Ψ^C] with momentum $\vec{\boldsymbol{p}}$ parallel to the arrow direction,
- $v(\vec{\boldsymbol{p}}, s)$: outgoing Ψ [or Ψ^C] with momentum $\vec{\boldsymbol{p}}$ antiparallel to the arrow direction,
- $\bar{v}(\vec{\boldsymbol{p}}, s)$: incoming Ψ [or Ψ^C] with momentum $\vec{\boldsymbol{p}}$ antiparallel to the arrow direction.

The proof that the above rules for external wave functions apply unambiguously to Majorana fermions is straightforward. Simply insert the plane wave expansion of the Majorana field given by Eq. (G.4.1) into Eq. (G.5.11), and evaluate matrix elements for, e.g., the decay of a scalar or vector particle into a pair of Majorana fermions.

We now reconsider the matrix elements for scalar and vector particle decays into fermion pairs and $2 \to 2$ elastic scattering of a fermion off a scalar and vector boson, respectively. We shall compute the matrix elements using the Feynman rules of Fig. G.5.2, and check that the results agree with the ones obtained by two-component methods in Section 4.5.

Consider first the decay of a neutral scalar boson ϕ into a pair of Majorana fermions, $\phi \to \Psi_{Mi}(\vec{\boldsymbol{p}}_1, s_1)\Psi_{Mj}(\vec{\boldsymbol{p}}_2, s_2)$, of flavor i and j, respectively. Here, $\Psi_{Mi}(\vec{\boldsymbol{p}}, s)$ denotes the one-particle state given by Eq. (3.2.13). The matrix element for the decay is given by

$$i\mathcal{M} = -i\bar{u}(\vec{\boldsymbol{p}}_1, s_1)(\lambda^{ij}P_L + \lambda_{ij}P_R)v(\vec{\boldsymbol{p}}_2, s_2). \tag{G.6.1}$$

One can easily check that this result matches with Eq. (4.5.2), which was derived using two-component spinor techniques. Note that if one had chosen to switch the two final states (equivalent to switching the directions of the Majorana fermion arrows), then the resulting matrix element would simply exhibit an overall sign change [due to the results of Eqs. (G.4.34) and (G.4.35)]. This overall sign change is a consequence of the Fermi–Dirac statistics, and corresponds to changing which order one uses to construct the two-particle final state.

Consider next the decay of a (neutral or charged) scalar boson Φ into a pair of Dirac fermions, $\Phi \to F_i(\vec{\boldsymbol{p}}_1, s_1)\overline{F}^j(\vec{\boldsymbol{p}}_2, s_2)$, where by $F(\vec{\boldsymbol{p}}, s)$ and $\overline{F}(\vec{\boldsymbol{p}}, s)$ we mean the one-particle states given by Eq. (3.2.22). The matrix element for the decay is given by

$$i\mathcal{M} = -i\bar{u}(\vec{\boldsymbol{p}}_1, s_1)(\kappa^j{}_i P_L + \kappa_i{}^j P_R)v(\vec{\boldsymbol{p}}_2, s_2), \tag{G.6.2}$$

which is equivalent to Eq. (4.5.5), which was derived using two-component spinor techniques.

For the decay of a neutral vector boson (denoted by A_μ) into a pair of Majorana fermions, $A_\mu \to \Psi_{Mi}(\vec{\boldsymbol{p}}_1, s_1)\Psi_{Mj}(\vec{\boldsymbol{p}}_2, s_2)$, we use the Feynman rules of Fig. G.5.2 to obtain:

$$i\mathcal{M} = -i\bar{u}(\vec{\boldsymbol{p}}_1, s_1)\gamma^\mu \left[G_i{}^j P_L - G_j{}^i P_R\right] v(\vec{\boldsymbol{p}}_2, s_2)\varepsilon_\mu, \tag{G.6.3}$$

The above result is equivalent to Eq. (4.5.8), which was derived using two-component spinor techniques. Again, we note that if one had chosen to switch the two final states (equivalent to switching the directions of the Majorana fermion arrows), then the resulting matrix element would simply exhibit an overall sign change [due to the results of Eqs. (G.4.36) and (G.4.37)].

For $i = j$, Eq. (G.6.3) simplifies to

$$i\mathcal{M} = iG\bar{u}(\vec{\boldsymbol{p}}_1, s_1)\gamma^\mu\gamma_5 v(\vec{\boldsymbol{p}}_2, s_2)\varepsilon_\mu, \tag{G.6.4}$$

where $G \equiv G_i{}^i$. The absence of a vector coupling of the vector boson to a pair of identical Majorana fermions is a consequence of the identity $\overline{\Psi}_M\gamma^\mu\Psi_M = 0$ noted below Eq. (G.1.97).

For the decay of a (neutral or charged) vector particle A_μ into a fermion pair consisting of a Dirac fermion and antifermion, $A_\mu \to F_i(\vec{\boldsymbol{p}}_1, s_1)\overline{F}^j(\vec{\boldsymbol{p}}_2, s_2)$, the matrix element is given by:

$$i\mathcal{M} = -i\bar{u}(\vec{\boldsymbol{p}}_1, s_1)\gamma^\mu \left[(G_L)_i{}^j P_L + (G_R)_i{}^j P_R\right] v(\vec{\boldsymbol{p}}_2, s_2)\varepsilon_\mu, \tag{G.6.5}$$

which matches the result of Eq. (4.5.12).

Finally, we consider the decay of a charged boson to a fermion pair consisting of one Dirac fermion and one Majorana fermion. Using the Feynman rules of Fig. G.5.4, we see that we have a choice of two rules for each decay process. As an example, consider the decay $W \to \Psi_{Mi}(\vec{\boldsymbol{p}}_1, s_1)F_j(\vec{\boldsymbol{p}}_2, s_2)$. If we apply the $W\Psi_M\Psi$ Feynman rule of Fig. G.5.4, we obtain:

$$i\mathcal{M} = -i\bar{u}(\vec{\boldsymbol{p}}_2, s_2)\left[(G_1)_j{}^i P_L + (G_2)_{ij}P_R\right] v(\vec{\boldsymbol{p}}_1, s_1). \tag{G.6.6}$$

If we apply the corresponding $W\Psi_M\Psi^C$ Feynman rule, we obtain the negative of Eq. (G.6.6) with $P_L \leftrightarrow P_R$ and $(\vec{\boldsymbol{p}}_1, s_1) \leftrightarrow (\vec{\boldsymbol{p}}_2, s_2)$. Using Eqs. (G.4.36) and (G.4.37), the resulting amplitude is the negative of Eq. (G.6.6), as expected since the order of the spinor wave functions in the two computations is reversed. A similar conclusion is obtained for the decay $\Phi \to \Psi_{Mi}F_j$.

Turning to the elastic scattering of a Majorana fermion and a neutral scalar, we shall examine two equivalent ways for computing the amplitude. Following the rules previously stated, there are two possible choices for the direction of arrows on the Majorana fermion lines. Thus, may evaluate either one of the following two diagrams:

plus a second set of diagrams (not shown) where the initial and final state scalars are crossed.

Evaluating the first diagram above, the matrix element for $\phi\Psi_M \to \phi\Psi_M$ is given by:

$$\begin{aligned} i\mathcal{M} &= \frac{-i}{s-m^2}\,\bar{u}(\vec{\boldsymbol{p}}_2,s_2)(\lambda P_L+\lambda^* P_R)(\not{p}+m)(\lambda P_L+\lambda^* P_R)u(\vec{\boldsymbol{p}}_1,s_1)+(\text{crossed}) \\ &= \frac{-i}{s-m^2}\,\bar{u}(\vec{\boldsymbol{p}}_2,s_2)\left[|\lambda|^2\not{p}+\left(\lambda^2 P_L+(\lambda^*)^2 P_R\right)m\right]u(\vec{\boldsymbol{p}}_1,s_1)+(\text{crossed}), \end{aligned} \tag{G.6.7}$$

where m is the Majorana fermion mass and $\sqrt{s}$ is the center-of-mass energy. Using Eqs. (G.1.2) and (G.4.11), one recovers the results of Eq. (4.5.13). Had we chosen to evaluate the second diagram instead, the resulting amplitude would have been given by:

$$i\mathcal{M} = \frac{-i}{s-m^2}\,\bar{v}(\vec{\boldsymbol{p}}_1,s_1)\left[-|\lambda|^2\not{p}+\left(\lambda^2 P_L+(\lambda^*)^2 P_R\right)m\right]v(\vec{\boldsymbol{p}}_2,s_2)+(\text{crossed}). \tag{G.6.8}$$

Using Eq. (G.4.33), it follow that:

$$\bar{v}(\vec{\boldsymbol{p}}_1,s_1)v(\vec{\boldsymbol{p}}_2,s_2) = -\bar{u}(\vec{\boldsymbol{p}}_2,s_2)u(\vec{\boldsymbol{p}}_1,s_1), \tag{G.6.9}$$

$$\bar{v}(\vec{\boldsymbol{p}}_1,s_1)\gamma^\mu v(\vec{\boldsymbol{p}}_2,s_2) = \bar{u}(\vec{\boldsymbol{p}}_2,s_2)\gamma^\mu u(\vec{\boldsymbol{p}}_1,s_1). \tag{G.6.10}$$

Consequently, the amplitude computed in Eq. (G.6.8) is just the negative of Eq. (G.6.7). This is expected, since the order of spinor wave functions in Eq. (G.6.8) is an odd permutation of the order of spinor wave functions in Eq. (G.6.7) [(12) and (21), respectively]. As in the two-component Feynman rules, the overall sign of the amplitude is arbitrary, but the relative signs of any pair of diagrams is unambiguous. This relative sign is positive [negative] if the permutation of the order of spinor wave functions of one diagram relative to the other diagram is even [odd].

Next, we consider the elastic scattering of a charged fermion and a neutral scalar. Again, we examine two equivalent ways for computing the amplitude. Following our rules, there are two possible choices for the directions of the fermion line arrows, depending on whether we represent the fermion by Ψ or Ψ^C. Thus, we may evaluate either one of the following two diagrams:

plus a second set of diagrams (not shown) where the initial and final state scalars are crossed. Evaluating the first diagram above, the matrix element for $\phi F \to \phi F$ is given by Eq. (G.6.7), with λ replaced by κ. Had we chose to evaluate the second diagram instead, the resulting amplitude would have been given by Eq. (G.6.8), with λ replaced by κ. Thus, the discussion above in the case of neutral fermion scattering processes also applies to charged fermion scattering processes.

In processes that only involve vertices with two Dirac fields, it is never necessary to use charge-conjugated Dirac fermion lines. In contrast, consider the following process that involves a vertex with one Dirac and one Majorana fermion. Specifically, we examine the scattering of a Dirac fermion and a charged scalar into its charge-conjugated final state, via the exchange of a Majorana fermion: $\Phi^\dagger F \to \Phi\overline{F}$. If one attempts to draw the relevant Feynman diagram employing Dirac fermion lines but with no charge-conjugated Dirac fermion lines, one finds that there is no possible choice of arrow direction for the Majorana fermion that is consistent with the vertex rules of Fig. G.5.4. The resolution is simple: one can choose the incoming line to be Ψ and the outgoing line to be Ψ^C or vice versa. Thus, the two possible choices are given by:

plus a second diagram in each case (not shown) in which the initial and final scalars are crossed. If we evaluate the first diagram, the resulting amplitude is given by:

$$
\begin{aligned}
i\mathcal{M} &= \frac{-i}{s-m^2}\,\bar{u}(\vec{\boldsymbol{p}}_2,s_2)(\kappa_2 P_L+\kappa_1^* P_R)(\not{p}+m)(\kappa_2 P_L+\kappa_1^* P_R)u(\vec{\boldsymbol{p}}_1,s_1)+(\text{crossed})\\
&= \frac{-i}{s-m^2}\,\bar{u}(\vec{\boldsymbol{p}}_2,s_2)\left[\kappa_1^*\kappa_2\not{p}+\left(\kappa_2^2 P_L+(\kappa_1^*)^2 P_R\right)m\right]u(\vec{\boldsymbol{p}}_1,s_1)+(\text{crossed}),
\end{aligned}
\tag{G.6.11}
$$

where m is the Majorana fermion mass. This result is equivalent to Eq. (4.5.17) obtained via the two-component spinor methods. Had we evaluated the second diagram, then one finds after using Eqs. (G.6.9) and (G.6.10) that the resulting amplitude is just the negative of Eq. (G.6.11), as expected. As before, the relative sign between diagrams for the same process is unambiguous.

In the literature, there are a number of alternative methods for dealing with scattering processes involving Majorana particles. For example, one can define a fermion number violating propagator for four-component fermions (see, *e.g.*, Ref. [7]). Using the methods of Ref. [7], factors of the charge conjugation matrix C appear both in fermion-number-violating propagators and vertices. However, all such factors of C eventually cancel out by the end of the computation of any S-matrix amplitude. Moreover, such methods often involve subtle choices of signs that require first-principles computations to verify. As previously noted, our four-component fermion diagrammatic techniques do not suffer from either of these complications.

In the case of elastic scattering of a Majorana fermion and a neutral vector boson, the two contributing diagrams include the following diagram:

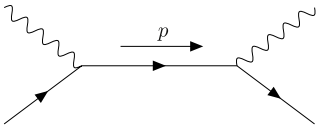

plus a second diagram (not shown) where the initial and final state vector bosons are crossed. Consider first the scattering of a neutral Majorana fermion of mass m. Using the Feynman rules of Fig. G.5.2, the Feynman rule for the $A_\mu\overline{\Psi}_M\Psi_M$ vertex is given by $iG\gamma^\mu\gamma_5$. Hence, the corresponding matrix element is given by

$$
i\mathcal{M} = \frac{-iG^2}{s-m^2}\,\bar{u}(\vec{\boldsymbol{p}}_2,s_2)\,\gamma\cdot\varepsilon_2^*\,(\not{p}-m)\,\gamma\cdot\varepsilon_1 u(\vec{\boldsymbol{p}}_1,s_1)+(\text{crossed}),
\tag{G.6.12}
$$

where we have used $\gamma^\nu\gamma_5(\not{p}+m)\gamma^\mu\gamma_5=\gamma^\nu(\not{p}-m)\gamma^\mu$. Using Eqs. (G.1.2) and (G.4.11), one easily recovers the results of Eq. (4.5.14).

The scattering of a Dirac fermion of mass m and a neutral vector boson can be similarly treated. The relevant Feynman graphs are the same as in the previous case, and the matrix element is given by

$$
\begin{aligned}
i\mathcal{M} &= \frac{-i}{s-m^2}\,\bar{u}(\vec{\boldsymbol{p}}_2,s_2)\,\gamma\cdot\varepsilon_2^*\,(G_L P_L+G_R P_R)(\not{p}+m)\,\gamma\cdot\varepsilon_1\,(G_L P_L+G_R P_R)u(\vec{\boldsymbol{p}}_1,s_1)+(\text{crossed})\\
&= \frac{-i}{s-m^2}\,\bar{u}(\vec{\boldsymbol{p}}_2,s_2)\,\gamma\cdot\varepsilon_2^*\left[(G_L^2 P_L+G_R^2 P_R)\not{p}+G_L G_R m\right]\,\gamma\cdot\varepsilon_1 u(\vec{\boldsymbol{p}}_1,s_1)+(\text{crossed}).
\end{aligned}
\tag{G.6.13}
$$

One can easily check that this result coincides with that of Eq. (4.5.18).

Finally, we examine the elastic scattering of two identical Majorana fermions via scalar exchange. The three contributing diagrams are:

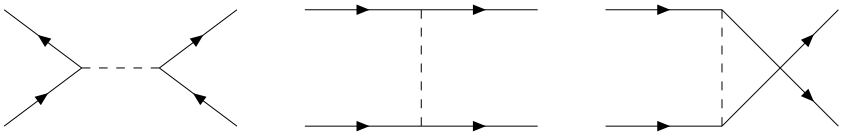

and the corresponding matrix element is given by

$$
\begin{aligned}
i\mathcal{M} &= \frac{-i}{s-m_\phi^2}\left[\bar{v}_1(\lambda P_L+\lambda^* P_R)u_2\,\bar{u}_3(\lambda P_L+\lambda^* P_R)v_4\right]+(-1)\frac{-i}{t-m_\phi^2}\left[\bar{u}_3(\lambda P_L+\lambda^* P_R)u_1\,\bar{u}_4(\lambda P_L+\lambda^* P_R)u_2\right]\\
&\quad+\frac{-i}{u-m_\phi^2}\left[\bar{u}_4(\lambda P_L+\lambda^* P_R)u_1\,\bar{u}_3(\lambda P_L+\lambda^* P_R)u_2\right],
\end{aligned}
\tag{G.6.14}
$$

where $u_i\equiv u(\vec{\boldsymbol{p}}_i,s_i)$, $v_j\equiv v(\vec{\boldsymbol{p}}_j,s_j)$ and m_ϕ is the exchanged scalar mass. The relative minus sign of the t-channel graph relative to the s and u-channel graphs is obtained by noting that 3142 [4132] is an odd [even] permutation of 1234. Using Eqs. (G.1.7), (G.4.11) and (G.4.12), one easily recovers the results of Eq. (4.5.19).

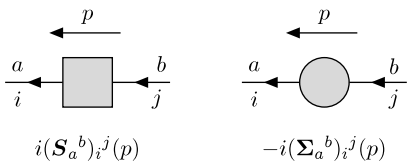

Fig. G.7.1. The full, loop-corrected propagator for four-component Dirac fermions, $i(\boldsymbol{S}_a{}^b)_i{}^j(p)$, is denoted by the shaded box, which represents the sum of all connected Feynman diagrams, with external legs included. The self-energy function for four-component Dirac fermions, $-i(\boldsymbol{\Sigma}_a{}^b)_i{}^j(p)$, is denoted by the shaded circle, which represents the sum of all one-particle irreducible, connected Feynman diagrams with the external legs amputated. In both cases, the four-momentum p flows from right to left.

G.7. Self-energy functions and pole masses for four-component fermions

In this section, we examine the self-energy functions and the pole masses for a set of four-component fermions. We first consider four-component Dirac fermion fields $\Psi_{\alpha i}$, where α is the four-component spinor index and i is the flavor index. The full, loop-corrected Feynman propagators with four-momentum p^μ are defined by the Fourier transforms [cf. footnote 35] of vacuum expectation values of time-ordered products of bilinears of the fully interacting four-component fermion fields:

$$\langle 0|\, T\Psi_{ai}(x)\overline{\Psi}^{bj}(y)\,|0\rangle_{\rm FT} = i(\boldsymbol{S}_a{}^b)_i{}^j(p), \tag{G.7.1}$$

with [307–314]

$$\boldsymbol{S}(p) \equiv \not{p}\left[P_L\boldsymbol{S}_{\boldsymbol{L}}^{\mathsf{T}}(p^2) + P_R\boldsymbol{S}_{\boldsymbol{R}}(p^2)\right] + P_L\overline{\boldsymbol{S}}_{\boldsymbol{D}}^{\mathsf{T}}(p^2) + P_R\boldsymbol{S}_{\boldsymbol{D}}(p^2), \tag{G.7.2}$$

where the four-component spinor indices α and β and the flavor indices i and j have been suppressed. As in Section 4.6, we shall organize the computation of the full propagator in terms of the 1PI self-energy function[310][149]:

$$\boldsymbol{\Sigma}(p) \equiv \not{p}\left[P_L\boldsymbol{\Sigma}_{\boldsymbol{L}}(p^2) + P_R\boldsymbol{\Sigma}_{\boldsymbol{R}}^{\mathsf{T}}(p^2)\right] + P_L\boldsymbol{\Sigma}_{\boldsymbol{D}}(p^2) + P_R\overline{\boldsymbol{\Sigma}}_{\boldsymbol{D}}^{\mathsf{T}}(p^2). \tag{G.7.3}$$

Diagrammatically, $i\boldsymbol{S}$ and $-i\boldsymbol{\Sigma}$ are shown in Fig. G.7.1.

The hermiticity of the effective action implies that $\boldsymbol{S}$ and $\boldsymbol{\Sigma}$ satisfy hermiticity conditions [299,315]

$$[\boldsymbol{S}^{\mathsf{T}}]^\star = A\boldsymbol{S}A^{-1}, \qquad [\boldsymbol{\Sigma}^{\mathsf{T}}]^\star = A\boldsymbol{\Sigma}A^{-1}, \tag{G.7.4}$$

where A is the Dirac conjugation matrix [$A = \gamma^0$ in the standard representations; see Eq. (G.1.20) and the text that follows] and the star symbol was defined in the paragraph below Eq. (4.6.6). Applying Eq. (G.7.4) to Eqs. (G.7.2) and (G.7.3) then yields the following conditions for the complex matrix functions:

$$[\boldsymbol{S}_{\boldsymbol{L}}^{\mathsf{T}}]^\star = \boldsymbol{S}_{\boldsymbol{L}}, \qquad [\boldsymbol{S}_{\boldsymbol{R}}^{\mathsf{T}}]^\star = \boldsymbol{S}_{\boldsymbol{R}}, \qquad \overline{\boldsymbol{S}}_{\boldsymbol{D}} = \boldsymbol{S}_{\boldsymbol{D}}^\star, \tag{G.7.5}$$

$$[\boldsymbol{\Sigma}_{\boldsymbol{L}}^{\mathsf{T}}]^\star = \boldsymbol{\Sigma}_{\boldsymbol{L}}, \qquad [\boldsymbol{\Sigma}_{\boldsymbol{R}}^{\mathsf{T}}]^\star = \boldsymbol{\Sigma}_{\boldsymbol{R}}, \qquad \overline{\boldsymbol{\Sigma}}_{\boldsymbol{D}} = \boldsymbol{\Sigma}_{\boldsymbol{D}}^\star. \tag{G.7.6}$$

Starting at tree level and comparing with Fig. G.5.1, the full propagator function is given by:

$$\boldsymbol{S}_i^j(p) = (\not{p} + m)\delta_i^j/(p^2 - m_i^2) + \ldots, \tag{G.7.7}$$

with no sum over i implied. The full loop-corrected propagator can be expressed diagrammatically in terms of the 1PI self-energy function:

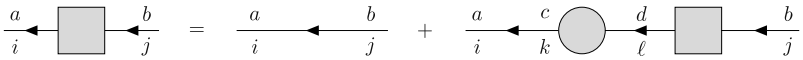

(G.7.8)

As in Section 4.6, the algebraic representation of Eq. (G.7.8) can be written as [cf. footnote 53]:

$$\boldsymbol{S} = \boldsymbol{T} + \boldsymbol{T}\boldsymbol{\Sigma}\boldsymbol{S} = (\boldsymbol{T}^{-1} - \boldsymbol{\Sigma})^{-1}, \tag{G.7.9}$$

where $\boldsymbol{T}_i^j \equiv (\not{p} + m)\delta_i^j/(p^2 - m_i^2)$ is the tree-level contribution to $\boldsymbol{S}$ given in Eq. (G.7.7). By writing the expressions for $\boldsymbol{S}$ and $\boldsymbol{\Sigma}$ given in Eqs. (G.7.2) and (G.7.3) and $\boldsymbol{T}$ in block matrix form using Eq. (G.1.2), one can verify that Eq. (G.7.9) is equivalent to Eq. (4.6.26). Consequently, the complex pole masses of the corresponding Dirac fermions are again determined from Eq. (4.6.31).

In the special case of a parity-conserving vectorlike theory of Dirac fermions (such as QED or QCD), the pseudoscalar and pseudovector parts of $\boldsymbol{S}(p)$ and $\boldsymbol{\Sigma}(p)$ must be absent. Thus, the following relations must hold among the loop-corrected

[149] Our notation in Eq. (G.7.3) differs from that of Ref. [310], as we employ $\boldsymbol{\Sigma}_{\boldsymbol{R}}^{\mathsf{T}}$ instead of $\boldsymbol{\Sigma}_{\boldsymbol{R}}$. Our motivation for this choice is that in the case of Majorana fermions [cf. Eq. (G.7.15)], we simply have $\boldsymbol{\Sigma}_{\boldsymbol{L}} = \boldsymbol{\Sigma}_{\boldsymbol{R}}$, without an extra transpose (or conjugation). We have also chosen to employ $\boldsymbol{S}_{\boldsymbol{L}}^{\mathsf{T}}$ in Eq. (G.7.2) for similar reasons.

propagator functions and self-energy functions, respectively:

$$\boldsymbol{S_R} = \boldsymbol{S_L}^{\mathsf{T}}, \qquad \boldsymbol{S_D} = [\boldsymbol{S_D}^{\mathsf{T}}]^\star, \tag{G.7.10}$$

$$\boldsymbol{\Sigma_L} = \boldsymbol{\Sigma_R}^{\mathsf{T}}, \qquad \boldsymbol{\Sigma_D} = [\boldsymbol{\Sigma_D}^{\mathsf{T}}]^\star, \tag{G.7.11}$$

in agreement with Eqs. (4.6.32) and (4.6.33).

In the case of a set of four-component Majorana fermion fields, we can still use the results of Eqs. (G.7.2)–(G.7.9). However, one obtains additional constraints on the full propagator and self-energy matrix functions due to the Majorana condition $\Psi_{Mi} = C\overline{\Psi}^{\mathsf{T}}_{Mi}$. Inserting this result into Eq. (G.7.1), and making use of the anticommutativity of the fermion fields, one easily derives:

$$\langle 0|\, T\Psi_{Mai}(x)\overline{\Psi}^{b}_{Mj}(y)\,|0\rangle_{\rm FT} = C_{ae}\,\langle 0|\, T\Psi_{Mdi}(x)\overline{\Psi}^{e}_{Mj}(y)\,|0\rangle_{\rm FT}\,(C^{-1})^{db}. \tag{G.7.12}$$

Consequently,

$$C\boldsymbol{S}^{\mathsf{T}}C^{-1} = \boldsymbol{S}, \qquad C\boldsymbol{\Sigma}^{\mathsf{T}}C^{-1} = \boldsymbol{\Sigma}. \tag{G.7.13}$$

Inserting the expressions for $\boldsymbol{S}$ and $\boldsymbol{\Sigma}$ [Eqs. (G.7.2) and (G.7.3)] and using the result of Eq. (G.1.90), it follows that:

$$\boldsymbol{S_L} = \boldsymbol{S_R}, \qquad \boldsymbol{S_D} = \boldsymbol{S_D}^{\mathsf{T}}, \qquad \overline{\boldsymbol{S}}_{\boldsymbol{D}} = \overline{\boldsymbol{S}}^{\mathsf{T}}, \tag{G.7.14}$$

$$\boldsymbol{\Sigma_L} = \boldsymbol{\Sigma_R}, \qquad \boldsymbol{\Sigma_D} = \boldsymbol{\Sigma_D}^{\mathsf{T}}, \qquad \overline{\boldsymbol{\Sigma}}_{\boldsymbol{D}} = \overline{\boldsymbol{\Sigma}}^{\mathsf{T}}_{\boldsymbol{D}}. \tag{G.7.15}$$

As expected, with these constraints the form of Eq. (4.6.26) matches precisely with the form of Eq. (4.6.16), corresponding to the equation for the full propagator functions for a theory of generic two-component fermion fields. In the notation of Section 4.6, we can therefore identify: $\boldsymbol{C} \equiv \boldsymbol{S_L} = \boldsymbol{S_R}$, $\boldsymbol{D} \equiv \boldsymbol{S_D}$, $\boldsymbol{\Xi} \equiv \boldsymbol{\Sigma_L} = \boldsymbol{\Sigma_R}$, and $\boldsymbol{\Omega} \equiv \boldsymbol{\Sigma_D}$.

Appendix H. Covariant spin operators and the Bouchiat–Michel formulae

Bouchiat and Michel derived a useful set of formulae [112] that generalize the spin projection operators used in four-component spinor computations. In this appendix, we establish the two-component analogues of the Bouchiat–Michel formulae, and demonstrate their equivalence to the corresponding four-component spinor formulae.

H.1. The covariant spin operators for a spin-1/2 fermion

Consider a massive spin-1/2 fermion of mass m and four-momentum p. We define a set of three four-vectors $S^{a\mu}$ ($a = 1, 2, 3$) such that the $S^{a\mu}$ and p^μ/m form an orthonormal set of four-vectors. In the rest frame of the fermion, where $p^\mu = (m; \vec{\boldsymbol{0}})$, we can define

$$S^{a\mu} \equiv (0; \hat{\boldsymbol{s}}^a), \quad a = 1, 2, 3, \tag{H.1.1}$$

where the unit vectors $\hat{\boldsymbol{s}}^a$ are a mutually orthonormal set of unit three-vectors that form a basis for a right-handed coordinate system. Explicit forms for the $\hat{\boldsymbol{s}}^a$ depend on the Euler angle γ used to define the spinor wave function $\chi_s(\hat{\boldsymbol{s}})$. Two common choices corresponding to $\gamma = -\phi$ and $\gamma = 0$ are given in Eqs. (C.1.39) and (C.1.40), respectively. Using Eq. (2.117), the three four-vectors $S^{a\mu}$, in a reference frame in which the four-momentum of the fermion is $p^\mu = (E; \vec{\boldsymbol{p}})$, are given by:

$$S^{a\mu} = \left(\frac{\vec{\boldsymbol{p}}\cdot\hat{\boldsymbol{s}}^{\boldsymbol{a}}}{m}; \hat{\boldsymbol{s}}^{\boldsymbol{a}} + \frac{(\vec{\boldsymbol{p}}\cdot\hat{\boldsymbol{s}}^{\boldsymbol{a}})\,\vec{\boldsymbol{p}}}{m(E+m)}\right), \quad a = 1, 2, 3. \tag{H.1.2}$$

As discussed in Appendix C, we identify $\hat{\boldsymbol{s}} = \hat{\boldsymbol{s}}^3$ as the quantization axis used in defining the third component of the spin of the fermion in its rest frame. It then follows that the spin four-vector, previously introduced in Eq. (3.1.15) is given by $S^\mu = S^{3\mu}$.

The orthonormal set of four four-vectors p^μ/m and the $S^{a\mu}$ satisfy the following Lorentz-covariant relations:

$$p\cdot S^a = 0, \tag{H.1.3}$$

$$S^a\cdot S^b = -\delta^{ab}, \tag{H.1.4}$$

$$\epsilon^{\mu\nu\lambda\sigma}p_\mu S^1_\nu S^2_\lambda S^3_\sigma = -m, \tag{H.1.5}$$

$$S^a_\mu S^b_\nu - S^a_\nu S^b_\mu = \epsilon^{abc}\epsilon_{\mu\nu\rho\sigma}S^{c\rho}\,\frac{p^\sigma}{m}, \tag{H.1.6}$$

$$S^a_\mu S^a_\nu = -g_{\mu\nu} + \frac{p_\mu p_\nu}{m^2}, \tag{H.1.7}$$

where the sum over the repeated indices is implicit. It is convenient to define a matrix-valued spin four-vector $\mathscr{S}^\mu$, whose matrix elements are given by:

$$\mathscr{S}^\mu_{ss'} \equiv S^{a\mu}\tau^a_{ss'}, \quad s, s' = \pm\tfrac{1}{2}, \tag{H.1.8}$$

where $\tau^a_{ss'}$ are the matrix elements of the Pauli matrices (see footnote 95). Then, we can rewrite Eqs. (H.1.4) and (H.1.6) as:

$$\tfrac{1}{3}\, g_{\mu\nu}\mathscr{S}^\mu\mathscr{S}^\nu = -\mathbb{1}_{2\times 2}, \tag{H.1.9}$$

$$\mathscr{S}^\mu\mathscr{S}^\nu - \mathscr{S}^\nu\mathscr{S}^\mu = \frac{2i}{m}\epsilon^{\mu\nu\rho\sigma}\mathscr{S}_\rho p_\sigma, \tag{H.1.10}$$

where the product $\mathscr{S}^\mu\mathscr{S}^\nu$ corresponds to ordinary 2×2 matrix multiplication. The $\mathscr{S}^\mu$ serve as covariant spin operators for a spin-1/2 fermion. In particular, in the rest frame, the $\frac{1}{2}\mathscr{S}^i$ satisfy the usual SU(2) commutation relations, with $(\frac{1}{2}\vec{\mathscr{S}})^2 = \frac{3}{4}$ as expected for a spin-1/2 particle.

It is often desirable to work with helicity states. In this case, we choose:

$$\hat{\boldsymbol{s}}^a = \hat{\boldsymbol{p}}^{\boldsymbol{a}}, \tag{H.1.11}$$

where the $\hat{\boldsymbol{p}}^{\boldsymbol{a}}$ are an orthonormal triad of unit three-vectors with $\hat{\boldsymbol{p}}^3 \equiv \hat{\boldsymbol{p}}$. Moreover, since $\hat{\boldsymbol{p}}^{\boldsymbol{a}}\cdot\hat{\boldsymbol{p}} = 0$ for $a \neq 3$, it follows that $S^{a\mu} = (0; \hat{\boldsymbol{p}}^{\boldsymbol{a}})$ for $a = 1, 2$ in all reference frames obtained from the rest frame by a boost in the $\hat{\boldsymbol{p}}$ direction. Hence, in a reference frame where $p^\mu = (E; \vec{\boldsymbol{p}})$, Eq. (H.1.2) yields,

$$S^{1\mu} = (0; \hat{\boldsymbol{p}}^1), \tag{H.1.12}$$

$$S^{2\mu} = (0; \hat{\boldsymbol{p}}^2), \tag{H.1.13}$$

$$S^{3\mu} = \left(\frac{|\vec{\boldsymbol{p}}|}{m}; \frac{E}{m}\hat{\boldsymbol{p}}\right), \tag{H.1.14}$$

in a coordinate system where $\hat{\boldsymbol{p}} = (\sin\theta\cos\phi, \sin\theta\sin\phi, \cos\theta)$. One can check that Eqs. (H.1.1)–(H.1.7) are also satisfied by the $S^{a\mu}$ defined in Eqs. (H.1.12)–(H.1.14).

As expected, $S^{3\mu}$ is the spin four-vector for helicity states obtained in Eq. (3.1.16). In the high energy limit ($E \gg m$),

$$mS^{a\mu} = p^\mu\,\delta^{a3} + \mathcal{O}(m). \tag{H.1.15}$$

Explicit forms for $\hat{\boldsymbol{p}}^1$ and $\hat{\boldsymbol{p}}^2$ are convention dependent and depend on the conventional choice of the Euler angle γ. For example, consider the quantities:

$$S^\mu_- \equiv \tfrac{1}{2}S^{a\mu}\tau^a_{\frac{1}{2},-\frac{1}{2}} = \tfrac{1}{2}(S^{1\mu} - iS^{2\mu}), \qquad S^\mu_+ \equiv \tfrac{1}{2}S^{a\mu}\tau^a_{-\frac{1}{2},\frac{1}{2}} = \tfrac{1}{2}(S^{1\mu} + iS^{2\mu}). \tag{H.1.16}$$

Using Eqs. (H.1.11)–(H.1.14) and employing Eq. (C.1.27) with $\mathcal{R}$ given by Eq. (C.1.4),

$$\sigma\cdot S_- = e^{i\gamma}\begin{pmatrix} \frac{1}{2}\sin\theta & e^{-i\phi}\sin^2\frac{\theta}{2} \\ -e^{i\phi}\cos^2\frac{\theta}{2} & -\frac{1}{2}\sin\theta \end{pmatrix}, \qquad \overline{\sigma}\cdot S_+ = e^{-i\gamma}\begin{pmatrix} \frac{1}{2}\sin\theta & -e^{-i\phi}\cos^2\frac{\theta}{2} \\ e^{i\phi}\sin^2\frac{\theta}{2} & -\frac{1}{2}\sin\theta \end{pmatrix}. \tag{H.1.17}$$

In the convention of Eq. (C.1.39) [Eq. (C.1.40)], we take $\gamma = -\phi$ [$\gamma = 0$], respectively.

H.2. Two-component spinor wave function relations

In Section 3.1, we wrote down explicit forms for the undotted spinor wave functions

$$x_\alpha(\vec{\boldsymbol{p}}, s) = \sqrt{p\cdot\sigma}\,\chi_s, \qquad x^\alpha(\vec{\boldsymbol{p}}, s) = -2s\chi^\dagger_{-s}\sqrt{p\cdot\overline{\sigma}}, \tag{H.2.1}$$

$$y_\alpha(\vec{\boldsymbol{p}}, s) = 2s\sqrt{p\cdot\sigma}\,\chi_{-s}, \qquad y^\alpha(\vec{\boldsymbol{p}}, s) = \chi_s^\dagger\sqrt{p\cdot\overline{\sigma}}, \tag{H.2.2}$$

and the dotted spinor wave functions

$$x^{\dagger\dot\alpha}(\vec{\boldsymbol{p}}, s) = -2s\sqrt{p\cdot\overline{\sigma}}\,\chi_{-s}, \qquad x^\dagger_{\dot\alpha}(\vec{\boldsymbol{p}}, s) = \chi_s^\dagger\sqrt{p\cdot\sigma}, \tag{H.2.3}$$

$$y^{\dagger\dot\alpha}(\vec{\boldsymbol{p}}, s) = \sqrt{p\cdot\overline{\sigma}}\,\chi_s, \qquad y^\dagger_{\dot\alpha}(\vec{\boldsymbol{p}}, s) = 2s\chi^\dagger_{-s}\sqrt{p\cdot\sigma}, \tag{H.2.4}$$

where $\sqrt{p\cdot\sigma}$ and $\sqrt{p\cdot\overline{\sigma}}$ are defined either by Eqs. (2.109) and (2.110) or by Eqs. (2.113) and (2.114), respectively (as mandated by the spinor index structure). As shown in Appendix C, the two-component spinors χ_s satisfy:

$$\tfrac{1}{2}\,\vec{\boldsymbol{\sigma}}\cdot\hat{\boldsymbol{s}}^{\boldsymbol{a}}\chi_{s'} = \tfrac{1}{2}\tau^a_{ss'}\chi_s, \qquad \chi_s^\dagger(\hat{\boldsymbol{s}})\chi_{s'}(\hat{\boldsymbol{s}}) = \delta_{ss'}, \quad s, s' = \pm\tfrac{1}{2}. \tag{H.2.5}$$

Next, we use Eqs. (2.118) and (2.119) to obtain:

$$\sqrt{p\cdot\sigma}\,S^a\cdot\overline{\sigma}\,\sqrt{p\cdot\sigma} = m\,\vec{\boldsymbol{\sigma}}\cdot\hat{\boldsymbol{s}}^{\boldsymbol{a}}, \tag{H.2.6}$$

$$\sqrt{p\cdot\overline{\sigma}}\,S^a\cdot\sigma\,\sqrt{p\cdot\overline{\sigma}} = -m\,\vec{\boldsymbol{\sigma}}\cdot\hat{\boldsymbol{s}}^{\boldsymbol{a}}, \tag{H.2.7}$$

which extends the results of Eqs. (3.1.17) and (3.1.18). As a result, we obtain a generalization of Eqs. (3.1.24)–(3.1.27):

$$(S^a\cdot\overline{\sigma})^{\dot\alpha\beta}x_\beta(\vec{\boldsymbol{p}},s') = \tau^a_{ss'}y^{\dagger\dot\alpha}(\vec{\boldsymbol{p}},s), \qquad (S^a\cdot\sigma)_{\alpha\dot\beta}y^{\dagger\dot\beta}(\vec{\boldsymbol{p}},s') = -\tau^a_{ss'}x_\alpha(\vec{\boldsymbol{p}},s), \tag{H.2.8}$$

$$(S^a\cdot\sigma)_{\alpha\dot\beta}x^{\dagger\dot\beta}(\vec{\boldsymbol{p}},s') = -\tau^a_{s's}y_\alpha(\vec{\boldsymbol{p}},s), \qquad (S^a\cdot\overline{\sigma})^{\dot\alpha\beta}y_\beta(\vec{\boldsymbol{p}},s') = \tau^a_{s's}x^{\dagger\dot\alpha}(\vec{\boldsymbol{p}},s), \tag{H.2.9}$$

$$x^\alpha(\vec{\boldsymbol{p}},s')(S^a\cdot\sigma)_{\alpha\dot\beta} = -\tau^a_{s's}y^\dagger_{\dot\beta}(\vec{\boldsymbol{p}},s), \qquad y^\dagger_{\dot\alpha}(\vec{\boldsymbol{p}},s')(S^a\cdot\overline{\sigma})^{\dot\alpha\beta} = \tau^a_{s's}x^\beta(\vec{\boldsymbol{p}},s), \tag{H.2.10}$$

$$x^\dagger_{\dot\alpha}(\vec{\boldsymbol{p}},s')(S^a\cdot\overline{\sigma})^{\dot\alpha\beta} = \tau^a_{ss'}y^\beta(\vec{\boldsymbol{p}},s), \qquad y^\alpha(\vec{\boldsymbol{p}},s')(S^a\cdot\sigma)_{\alpha\dot\beta} = -\tau^a_{ss'}x^\dagger_{\dot\beta}(\vec{\boldsymbol{p}},s), \tag{H.2.11}$$

where there are implicit sums over the repeated labels $s=\pm\frac{1}{2}$. As expected, the case of $a=3$ simply reproduces the results of Eqs. (3.1.24)–(3.1.27) obtained previously. The above equations also apply to helicity wave functions $x(\vec{\boldsymbol{p}},\lambda)$ and $y(\vec{\boldsymbol{p}},\lambda)$ by replacing s, s' with λ, λ' and defining the $S^{a\mu}$ by Eqs. (H.1.12)–(H.1.14).

The derivation of Eqs. (H.2.8)–(H.2.11) for arbitrary a closely follows the corresponding derivation for $a=3$ previously given. For example, using Eqs. (H.2.6) and (H.2.7) and the definitions for $x_\alpha(\vec{\boldsymbol{p}},s)$ and $y^{\dagger\dot\alpha}(\vec{\boldsymbol{p}},s)$, we find (suppressing spinor indices),

$$\sqrt{p\cdot\sigma}\,S^a\cdot\overline{\sigma}\,x(\vec{\boldsymbol{p}},s') = \sqrt{p\cdot\sigma}\,S^a\cdot\overline{\sigma}\,\sqrt{p\cdot\sigma}\,\chi_{s'} = m\vec{\boldsymbol{\sigma}}\cdot\hat{\boldsymbol{s}}^{\boldsymbol{a}}\,\chi_{s'} = m\tau^a_{ss'}\,\chi_s, \tag{H.2.12}$$

after using Eq. (H.2.5). Multiplying both sides of Eq. (H.2.12) by $\sqrt{p\cdot\overline{\sigma}}$, we end up with

$$S^a\cdot\overline{\sigma}\,x(\vec{\boldsymbol{p}},s') = \tau^a_{ss'}\sqrt{p\cdot\overline{\sigma}}\,\chi_s = \tau^a_{ss'}\,y^\dagger(\vec{\boldsymbol{p}},s). \tag{H.2.13}$$

Similarly,

$$S^a\cdot\sigma x^\dagger(\vec{\boldsymbol{p}},s') = 2s'\tau^a_{-s,-s'}\sqrt{p\cdot\sigma}\,\chi_{-s} = -\tau^a_{s's}\,y(\vec{\boldsymbol{p}},s), \tag{H.2.14}$$

where we have used:

$$4ss'\tau^a_{-s,-s'} = -\tau^a_{s's}, \quad \text{for } s,s' = \pm 1/2. \tag{H.2.15}$$

All the results of Eqs. (H.2.8)–(H.2.11) can be derived in this manner.

H.3. Two-component Bouchiat–Michel formulae

To establish the Bouchiat–Michel formulae, we begin with the following identity:

$$\tfrac{1}{2}(\delta_{ss'}+\vec{\boldsymbol{\sigma}}\cdot\hat{\boldsymbol{s}}^a\,\tau^a_{ss'})\sum_{t=\pm1/2}\chi_t\chi_t^\dagger = \chi_{s'}\chi_s^\dagger. \tag{H.3.1}$$

To verify Eq. (H.3.1), we used Eq. (H.2.5) to write $\vec{\boldsymbol{\sigma}}\cdot\hat{\boldsymbol{s}}^a\chi_t = \tau^a_{t't}\chi_{t'}$ and evaluated the product of two Pauli matrices:

$$\tau^a_{ss'}\tau^a_{t't} = 2\,\delta_{st}\delta_{s't'} - \delta_{ss'}\delta_{tt'}. \tag{H.3.2}$$

We then use Eq. (H.2.6) and the completeness relation given in Eq. (C.1.21) to rewrite Eq. (H.3.1) in terms of $\mathscr{S}^\mu_{ss'}$ defined in Eq. (H.1.8),

$$\chi_{s'}\chi_s^\dagger = \tfrac{1}{2}\left(\delta_{ss'}+\frac{1}{m}\sqrt{p\cdot\sigma}\,\mathscr{S}_{ss'}\cdot\overline{\sigma}\,\sqrt{p\cdot\sigma}\right). \tag{H.3.3}$$

Hence, with both spinor indices in the lowered position,

$$\begin{aligned} x(\vec{\boldsymbol{p}},s')x^\dagger(\vec{\boldsymbol{p}},s) &= \sqrt{p\cdot\sigma}\,\chi_{s'}\chi_s^\dagger\,\sqrt{p\cdot\sigma} \\ &= \tfrac{1}{2}\sqrt{p\cdot\sigma}\left[\delta_{ss'}+\frac{1}{m}\sqrt{p\cdot\sigma}\,\mathscr{S}_{ss'}\cdot\overline{\sigma}\,\sqrt{p\cdot\sigma}\right]\sqrt{p\cdot\sigma} \\ &= \tfrac{1}{2}\left[p\cdot\sigma\,\delta_{ss'}+\frac{1}{m}\,p\cdot\sigma\,\mathscr{S}_{ss'}\cdot\overline{\sigma}\,p\cdot\sigma\right] \\ &= \tfrac{1}{2}\,(p\cdot\sigma\,\delta_{ss'} - m\mathscr{S}_{ss'}\cdot\sigma)\,. \end{aligned} \tag{H.3.4}$$

In the final step of Eq. (H.3.4), we simplified the product of three dot products by noting that $p \cdot S^a = 0$ implies that $\mathscr{S}_{ss'} \cdot \overline{\sigma}\; p \cdot \sigma = -p \cdot \overline{\sigma}\; \mathscr{S}_{ss'} \cdot \sigma$. Eq. (H.3.4) is the two-component version of one of the Bouchiat–Michel formulae. We list below a complete set of Bouchiat–Michel formulae, which can be derived by similar techniques:

$$x_\alpha(\vec{\boldsymbol{p}}, s')x^\dagger_{\dot\beta}(\vec{\boldsymbol{p}}, s) = \tfrac{1}{2}(p\,\delta_{ss'} - m\mathscr{S}_{ss'}) \cdot \sigma_{\alpha\dot\beta}, \tag{H.3.5}$$

$$y^{\dagger\dot\alpha}(\vec{\boldsymbol{p}}, s')y^\beta(\vec{\boldsymbol{p}}, s) = \tfrac{1}{2}(p\,\delta_{ss'} + m\mathscr{S}_{ss'}) \cdot \overline{\sigma}^{\dot\alpha\beta}, \tag{H.3.6}$$

$$x_\alpha(\vec{\boldsymbol{p}}, s')y^\beta(\vec{\boldsymbol{p}}, s) = \tfrac{1}{2}\left[m\delta_{ss'}\delta_\alpha{}^\beta - [(\sigma \cdot \mathscr{S}_{ss'})\,(\overline{\sigma} \cdot p)]_\alpha{}^\beta\right], \tag{H.3.7}$$

$$y^{\dagger\dot\alpha}(\vec{\boldsymbol{p}}, s')x^\dagger_{\dot\beta}(\vec{\boldsymbol{p}}, s) = \tfrac{1}{2}\left[m\delta_{ss'}\delta^{\dot\alpha}{}_{\dot\beta} + [(\overline{\sigma} \cdot \mathscr{S}_{ss'})\,(\sigma \cdot p)]^{\dot\alpha}{}_{\dot\beta}\right]. \tag{H.3.8}$$

If we set $s = s'$, we recover Eqs. (3.1.46)–(3.1.49) as expected. The Bouchiat–Michel formulae can also be verified directly by using the explicit forms for the two-component spinor wave functions [Eq. (C.1.11)] and the $\mathscr{S}^\mu_{ss'}$ [defined in Eq. (H.1.8)]. The latter depends on the explicit form of the $\hat{\boldsymbol{s}}^{\boldsymbol{a}}$ via Eq. (H.1.2).

An equivalent set of Bouchiat–Michel formulae can be obtained by raising and/or lowering the appropriate free spinor indices using Eqs. (2.31) and (2.78):

$$x^{\dagger\dot\alpha}(\vec{\boldsymbol{p}}, s')x^\beta(\vec{\boldsymbol{p}}, s) = \tfrac{1}{2}(p\,\delta_{s's} - m\mathscr{S}_{s's}) \cdot \overline{\sigma}^{\dot\alpha\beta}, \tag{H.3.9}$$

$$y_\alpha(\vec{\boldsymbol{p}}, s')y^\dagger_{\dot\beta}(\vec{\boldsymbol{p}}, s) = \tfrac{1}{2}(p\,\delta_{s's} + m\mathscr{S}_{s's}) \cdot \sigma_{\alpha\dot\beta}, \tag{H.3.10}$$

$$y_\alpha(\vec{\boldsymbol{p}}, s')x^\beta(\vec{\boldsymbol{p}}, s) = -\tfrac{1}{2}\left[m\delta_{s's}\delta_\alpha{}^\beta + [(\sigma \cdot \mathscr{S}_{s's})\,(\overline{\sigma} \cdot p)]_\alpha{}^\beta\right], \tag{H.3.11}$$

$$x^{\dagger\dot\alpha}(\vec{\boldsymbol{p}}, s')y^\dagger_{\dot\beta}(\vec{\boldsymbol{p}}, s) = -\tfrac{1}{2}\left[m\delta_{s's}\delta^{\dot\alpha}{}_{\dot\beta} - [(\overline{\sigma} \cdot \mathscr{S}_{s's})\,(\sigma \cdot p)]^{\dot\alpha}{}_{\dot\beta}\right]. \tag{H.3.12}$$

In this derivation, the spin labels in Eqs. (H.3.9)–(H.3.12) are reversed relative to those in Eqs. (H.3.5)–(H.3.8) due to Eq. (H.2.15). Eight additional relations of the Bouchiat–Michel type can be obtained by replacing one x-spinor with a y-spinor (or vice versa). Recalling that the x and y spinors are related by [cf. Eq. (3.1.23)],

$$y(\vec{\boldsymbol{p}}, s) = 2sx(\vec{\boldsymbol{p}}, -s), \qquad y^\dagger(\vec{\boldsymbol{p}}, s) = 2sx^\dagger(\vec{\boldsymbol{p}}, -s), \tag{H.3.13}$$

all possible spinor bilinears can be obtained from Eqs. (H.3.5)–(H.3.12).

Note that Eqs. (H.3.5)–(H.3.12) also apply to helicity spinor wave functions $x(\vec{\boldsymbol{p}}, \lambda)$ and $y(\vec{\boldsymbol{p}}, \lambda)$ after replacing s, s' with λ, λ' and using the $S^{a\mu}$ as defined in Eqs. (H.1.12)–(H.1.14). Strictly speaking, all results involving the spinor wave functions obtained up to this point apply in the case of a massive spin-1/2 fermion. If we take the massless limit, then the four-vector $S^{3\mu}$ does not exist, as its definition depends on the existence of a rest frame. (In contrast, the four-vectors $S^{1\mu}$ and $S^{2\mu}$ do exist in the massless limit.) Nevertheless, massless helicity spinor wave functions are well defined; explicit forms can be found in Eqs. (3.1.37)–(3.1.40). Using these forms, one can derive the Bouchiat–Michel formulae for a massless spin-1/2 fermion:

$$x_\alpha(\vec{\boldsymbol{p}}, \lambda')x^\dagger_{\dot\beta}(\vec{\boldsymbol{p}}, \lambda) = \left(\tfrac{1}{2} - \lambda\right)\,\delta_{\lambda\lambda'}\,p \cdot \sigma_{\alpha\dot\beta}, \tag{H.3.14}$$

$$y^{\dagger\dot\alpha}(\vec{\boldsymbol{p}}, \lambda')y^\beta(\vec{\boldsymbol{p}}, \lambda) = \left(\tfrac{1}{2} + \lambda\right)\,\delta_{\lambda\lambda'}\,p \cdot \overline{\sigma}^{\dot\alpha\beta}, \tag{H.3.15}$$

$$x_\alpha(\vec{\boldsymbol{p}}, \lambda')y^\beta(\vec{\boldsymbol{p}}, \lambda) = -\left(\tfrac{1}{2} - \lambda'\right)\left(\tfrac{1}{2} + \lambda\right)[(\sigma \cdot S_-)(\overline{\sigma} \cdot p)]_\alpha{}^\beta, \tag{H.3.16}$$

$$y^{\dagger\dot\alpha}(\vec{\boldsymbol{p}}, \lambda')x^\dagger_{\dot\beta}(\vec{\boldsymbol{p}}, \lambda) = \left(\tfrac{1}{2} + \lambda'\right)\left(\tfrac{1}{2} - \lambda\right)[(\overline{\sigma} \cdot S_+)(\sigma \cdot p)]^{\dot\alpha}{}_{\dot\beta}, \tag{H.3.17}$$

where S^μ_- and S^μ_+ are defined in Eq. (H.1.16). The equivalent set of Bouchiat–Michel formulae, obtained by raising and/or lowering the appropriate free spinor indices, is given by:

$$x^{\dagger\dot\alpha}(\vec{\boldsymbol{p}}, \lambda')x^\beta(\vec{\boldsymbol{p}}, \lambda) = \left(\tfrac{1}{2} - \lambda\right)\,\delta_{\lambda\lambda'}\,p \cdot \overline{\sigma}^{\dot\alpha\beta}, \tag{H.3.18}$$

$$y_\alpha(\vec{\boldsymbol{p}}, \lambda')y^\dagger_{\dot\beta}(\vec{\boldsymbol{p}}, \lambda) = \left(\tfrac{1}{2} + \lambda\right)\,\delta_{\lambda\lambda'}\,p \cdot \sigma_{\alpha\dot\beta}, \tag{H.3.19}$$

$$y_\alpha(\vec{\boldsymbol{p}}, \lambda')x^\beta(\vec{\boldsymbol{p}}, \lambda) = -\left(\tfrac{1}{2} + \lambda'\right)\left(\tfrac{1}{2} - \lambda\right)[(\sigma \cdot S_-)(\overline{\sigma} \cdot p)]_\alpha{}^\beta, \tag{H.3.20}$$

$$x^{\dagger\dot\alpha}(\vec{\boldsymbol{p}}, \lambda')y^\dagger_{\dot\beta}(\vec{\boldsymbol{p}}, \lambda) = \left(\tfrac{1}{2} - \lambda'\right)\left(\tfrac{1}{2} + \lambda\right)[(\overline{\sigma} \cdot S_+)(\sigma \cdot p)]^{\dot\alpha}{}_{\dot\beta}. \tag{H.3.21}$$

Eight additional relations of the Bouchiat–Michel type can be obtained by replacing one x-spinor with a y-spinor (or vice versa), using the results of Eq. (H.3.13). As a check, one can verify that the above results follow from Eqs. (H.3.5)–(H.3.12) by replacing s with λ, setting $mS^{a\mu} = p^\mu \delta^{a3}$, applying the mass–shell condition ($p^2 = m^2$), and taking the $m \to 0$ limit at the end of the computation.

We now demonstrate how to use the Bouchiat–Michel formulae to evaluate helicity amplitudes involving two equal mass spin-1/2 fermions. A typical amplitude involving a fermion–antifermion pair, evaluated in the center-of-mass frame of the pair has the generic structure:

$$z(\vec{\boldsymbol{p}}, \lambda)\, \Gamma\, z'(-\vec{\boldsymbol{p}}, \lambda'), \tag{H.3.22}$$

where z is one of the two-component spinor wave functions x, $x^\dagger$, y, or $y^\dagger$, and Γ is a 2×2 matrix (in spinor space) that is either the identity matrix, or is made up of alternating products of σ and $\overline{\sigma}$. As an illustration, we evaluate:

$$x^\dagger_{\dot\alpha}(\vec{\boldsymbol{p}}, \lambda)\, \Gamma^{\dot\alpha\beta}\, y_\beta(-\vec{\boldsymbol{p}}, \lambda') = 2\lambda'\, \Gamma^{\dot\alpha\beta}\, x_\beta(-\vec{\boldsymbol{p}}, -\lambda') x^\dagger_{\dot\alpha}(\vec{\boldsymbol{p}}, \lambda) = 2\lambda'\, \xi_{\lambda'}(\hat{\boldsymbol{p}})\ \Gamma^{\dot\alpha\beta} \sigma^0_{\beta\dot\beta}\, y^{\dagger\dot\beta}(\vec{\boldsymbol{p}}, \lambda') x^\dagger_{\dot\alpha}(\vec{\boldsymbol{p}}, \lambda), \tag{H.3.23}$$

where $\xi_{\lambda'}(\hat{\boldsymbol{p}})$ is defined in Eq. (C.3.15), and we have used Eqs. (C.3.20) and (3.1.23). We can now employ the Bouchiat–Michel formula to convert the above result into a trace. By a similar computation, all expressions of the form of Eq. (H.3.22) can be expressed as a trace:

$$x^\dagger_{\dot\alpha}(\vec{\boldsymbol{p}}, \lambda)\, \Gamma^{\dot\alpha\beta}\, y_\beta(-\vec{\boldsymbol{p}}, \lambda') = \lambda'\, \xi_{\lambda'}(\hat{\boldsymbol{p}})\ \mathrm{Tr}\left[\Gamma\, \sigma^0 (m\delta_{\lambda\lambda'} + \overline{\sigma} \cdot \mathscr{S}_{\lambda\lambda'}\, \sigma \cdot p)\right], \tag{H.3.24}$$

$$y^\alpha(\vec{\boldsymbol{p}}, \lambda)\, \Gamma_{\alpha\dot\beta}\, x^{\dagger\dot\beta}(-\vec{\boldsymbol{p}}, \lambda') = -\lambda'\, \xi_{\lambda'}(\hat{\boldsymbol{p}})\ \mathrm{Tr}\left[\Gamma\, \overline{\sigma}^0 (m\delta_{\lambda\lambda'} - \sigma \cdot \mathscr{S}_{\lambda\lambda'}\, \overline{\sigma} \cdot p)\right], \tag{H.3.25}$$

$$y^\alpha(\vec{\boldsymbol{p}}, \lambda)\, \Gamma_\alpha{}^\beta\, y_\beta(-\vec{\boldsymbol{p}}, \lambda') = \lambda'\, \xi_{\lambda'}(\hat{\boldsymbol{p}})\ \mathrm{Tr}\left[\Gamma\, \sigma^0 (\overline{\sigma} \cdot p\, \delta_{\lambda\lambda'} + m\overline{\sigma} \cdot \mathscr{S}_{\lambda\lambda'})\right], \tag{H.3.26}$$

$$x^\dagger_{\dot\alpha}(\vec{\boldsymbol{p}}, \lambda)\, \Gamma^{\dot\alpha}{}_{\dot\beta}\, x^{\dagger\dot\beta}(-\vec{\boldsymbol{p}}, \lambda') = -\lambda'\, \xi_{\lambda'}(\hat{\boldsymbol{p}})\ \mathrm{Tr}\left[\Gamma\, \overline{\sigma}^0 (\sigma \cdot p\, \delta_{\lambda\lambda'} - m\sigma \cdot \mathscr{S}_{\lambda\lambda'})\right], \tag{H.3.27}$$

after making use of Eqs. (H.3.5) and (H.3.8). Similarly, there are four additional results that make use of Eqs. (H.3.9) and (H.3.12):

$$y^\dagger_{\dot\alpha}(\vec{\boldsymbol{p}}, \lambda)\, \Gamma^{\dot\alpha\beta}\, x_\beta(-\vec{\boldsymbol{p}}, \lambda') = \lambda'\, \xi_{-\lambda'}(\hat{\boldsymbol{p}})\ \mathrm{Tr}\left[\Gamma\, \sigma^0 (m\delta_{\lambda'\lambda} - \overline{\sigma} \cdot \mathscr{S}_{\lambda'\lambda}\, \sigma \cdot p)\right], \tag{H.3.28}$$

$$x^\alpha(\vec{\boldsymbol{p}}, \lambda)\, \Gamma_{\alpha\dot\beta}\, y^{\dagger\dot\beta}(-\vec{\boldsymbol{p}}, \lambda') = -\lambda'\, \xi_{-\lambda'}(\hat{\boldsymbol{p}})\ \mathrm{Tr}\left[\Gamma\, \overline{\sigma}^0 (m\delta_{\lambda'\lambda} + \sigma \cdot \mathscr{S}_{\lambda'\lambda}\, \overline{\sigma} \cdot p)\right], \tag{H.3.29}$$

$$x^\alpha(\vec{\boldsymbol{p}}, \lambda)\, \Gamma_\alpha{}^\beta\, x_\beta(-\vec{\boldsymbol{p}}, \lambda') = -\lambda'\, \xi_{-\lambda'}(\hat{\boldsymbol{p}})\ \mathrm{Tr}\left[\Gamma\, \sigma^0 (\overline{\sigma} \cdot p\, \delta_{\lambda'\lambda} - m\overline{\sigma} \cdot \mathscr{S}_{\lambda'\lambda})\right], \tag{H.3.30}$$

$$y^\dagger_{\dot\alpha}(\vec{\boldsymbol{p}}, \lambda)\, \Gamma^{\dot\alpha}{}_{\dot\beta}\, y^{\dagger\dot\beta}(-\vec{\boldsymbol{p}}, \lambda') = \lambda'\, \xi_{-\lambda'}(\hat{\boldsymbol{p}})\ \mathrm{Tr}\left[\Gamma\, \overline{\sigma}^0 (\sigma \cdot p\, \delta_{\lambda'\lambda} + m\sigma \cdot \mathscr{S}_{\lambda'\lambda})\right]. \tag{H.3.31}$$

For amplitudes involving equal mass fermions (or equal mass antifermions), other combinations of spinor bilinears appear in which one x-spinor above is replaced by a y-spinor or vice versa. These amplitudes can be reduced to one of the eight listed above by using Eq. (3.1.23).

In the massless limit, one can again put $mS^{a\mu} = p^\mu \delta^{a3}$, set $p^2 = m^2$ and take $m \to 0$ at the end of the computation. Alternatively, one can repeat the derivation of Eqs. (H.3.24)–(H.3.31) using the results of Eqs. (H.3.14) and (H.3.21). For completeness, we record the end result here.

$$x^\dagger_{\dot\alpha}(\vec{\boldsymbol{p}}, \lambda)\, \Gamma^{\dot\alpha\beta}\, y_\beta(-\vec{\boldsymbol{p}}, \lambda') = \left(\tfrac{1}{2} + \lambda'\right)\left(\tfrac{1}{2} - \lambda\right)\ \xi_{\lambda'}(\hat{\boldsymbol{p}})\, \mathrm{Tr}(\Gamma\, \sigma^0 \overline{\sigma} \cdot S_-\, \sigma \cdot p), \tag{H.3.32}$$

$$y^\alpha(\vec{\boldsymbol{p}}, \lambda)\, \Gamma_{\alpha\dot\beta}\, x^{\dagger\dot\beta}(-\vec{\boldsymbol{p}}, \lambda') = -\left(\tfrac{1}{2} - \lambda'\right)\left(\tfrac{1}{2} + \lambda\right)\ \xi_{\lambda'}(\hat{\boldsymbol{p}})\, \mathrm{Tr}(\Gamma\, \overline{\sigma}^0 \sigma \cdot S_-\, \overline{\sigma} \cdot p), \tag{H.3.33}$$

$$y^\alpha(\vec{\boldsymbol{p}}, \lambda)\, \Gamma_\alpha{}^\beta\, y_\beta(-\vec{\boldsymbol{p}}, \lambda') = \left(\tfrac{1}{2} + \lambda\right)\ \delta_{\lambda\lambda'}\, \xi_{\lambda'}(\hat{\boldsymbol{p}})\, \mathrm{Tr}(\Gamma\, \sigma^0\, \overline{\sigma} \cdot p), \tag{H.3.34}$$

$$x^\dagger_{\dot\alpha}(\vec{\boldsymbol{p}}, \lambda)\, \Gamma^{\dot\alpha}{}_{\dot\beta}\, x^{\dagger\dot\beta}(-\vec{\boldsymbol{p}}, \lambda') = \left(\tfrac{1}{2} - \lambda\right)\ \delta_{\lambda\lambda'}\, \xi_{\lambda'}(\hat{\boldsymbol{p}})\, \mathrm{Tr}(\Gamma\, \overline{\sigma}^0\, \sigma \cdot p). \tag{H.3.35}$$

The equivalent set of formulae, obtained by raising and/or lowering the appropriate free spinor indices as before, is given by:

$$y^\dagger_{\dot\alpha}(\vec{\boldsymbol{p}}, \lambda)\, \Gamma^{\dot\alpha\beta}\, x_\beta(-\vec{\boldsymbol{p}}, \lambda') = \left(\tfrac{1}{2} - \lambda'\right)\left(\tfrac{1}{2} + \lambda\right)\ \xi_{-\lambda'}(\hat{\boldsymbol{p}})\, \mathrm{Tr}(\Gamma\, \sigma^0 \overline{\sigma} \cdot S_+\, \sigma \cdot p), \tag{H.3.36}$$

$$x^\alpha(\vec{\boldsymbol{p}}, \lambda)\, \Gamma_{\alpha\dot\beta}\, y^{\dagger\dot\beta}(-\vec{\boldsymbol{p}}, \lambda') = -\left(\tfrac{1}{2} + \lambda'\right)\left(\tfrac{1}{2} - \lambda\right)\ \xi_{-\lambda'}(\hat{\boldsymbol{p}})\, \mathrm{Tr}(\Gamma\, \overline{\sigma}^0 \sigma \cdot S_+\, \overline{\sigma} \cdot p), \tag{H.3.37}$$

$$x^\alpha(\vec{\boldsymbol{p}}, \lambda)\, \Gamma_\alpha{}^\beta\, x_\beta(-\vec{\boldsymbol{p}}, \lambda') = \left(\tfrac{1}{2} - \lambda\right)\ \delta_{\lambda\lambda'}\, \xi_{-\lambda'}(\hat{\boldsymbol{p}})\, \mathrm{Tr}(\Gamma\, \sigma^0\, \overline{\sigma} \cdot p), \tag{H.3.38}$$

$$y^\dagger_{\dot\alpha}(\vec{\boldsymbol{p}}, \lambda)\, \Gamma^{\dot\alpha}{}_{\dot\beta}\, y^{\dagger\dot\beta}(-\vec{\boldsymbol{p}}, \lambda') = \left(\tfrac{1}{2} + \lambda\right)\ \delta_{\lambda\lambda'}\, \xi_{-\lambda'}(\hat{\boldsymbol{p}})\, \mathrm{Tr}(\Gamma\, \overline{\sigma}^0\, \sigma \cdot p). \tag{H.3.39}$$

The traces are easily evaluated using the results of Appendix B. Here, we apply the above results to the amplitude for the decay $Z^0 \to f\bar{f}$ [see Section 6.2]. The corresponding center-of-mass frame helicity amplitude is a linear combination of Eqs. (H.3.24) and (H.3.25) with $\Gamma = \overline{\sigma}$ and $\Gamma = \sigma$, respectively. Evaluating the corresponding terms, we find for $\Gamma = \overline{\sigma}$,

$$x^\dagger(\vec{\boldsymbol{p}},\lambda)\overline{\sigma}^\mu y(-\vec{\boldsymbol{p}},\lambda') = 2\lambda'\,\xi_{\lambda'}(\hat{\boldsymbol{p}})\,\left[mg^{\mu 0}\delta_{\lambda\lambda'} + p^\mu \mathscr{S}^0_{\lambda\lambda'} - p^0\mathscr{S}^\mu_{\lambda\lambda'} - 2m(\mathscr{S}^\mu\mathscr{S}^0 - \mathscr{S}^0\mathscr{S}^\mu)_{\lambda\lambda'}\right], \tag{H.3.40}$$

where we have used Eq. (H.1.10) to replace the term with the Levi-Civita tensor. Similarly, we calculate for $\Gamma = \sigma$,

$$y(\vec{\boldsymbol{p}},\lambda)\sigma^\mu x^\dagger(-\vec{\boldsymbol{p}},\lambda') = 2\lambda'\,\xi_{\lambda'}(\hat{\boldsymbol{p}})\,\left[-mg^{\mu 0}\delta_{\lambda\lambda'} + p^\mu \mathscr{S}^0_{\lambda\lambda'} - p^0\mathscr{S}^\mu_{\lambda\lambda'} + 2m(\mathscr{S}^\mu\mathscr{S}^0 - \mathscr{S}^0\mathscr{S}^\mu)_{\lambda\lambda'}\right]. \tag{H.3.41}$$

Eqs. (H.3.40) and (H.3.41) provide explicit forms for the $Z^0 \to f\bar{f}$ decay helicity amplitudes defined in Eqs. (6.2.3) and (6.2.4).

The above method is not applicable if the two fermions have unequal mass. In order to compute the helicity amplitudes of the form given by Eq. (H.3.22) for unequal masses, a generalization of the above techniques is required. Some methods for four-component spinor wave functions have been proposed in Ref. [316]. We leave it as an exercise for the reader to translate these techniques so that they are applicable to helicity amplitudes expressed in terms of two-component spinor wave functions. An alternative approach, which is applicable to the computation of helicity amplitudes for processes involving multi-fermion final states of arbitrary mass, is reviewed in Appendix I.1.

H.4. Four-component Bouchiat–Michel formulae

Using the results of Appendix G, the translation of the results of Appendix H.3 into four-component spinor notation is straightforward. First, we consider a massive spin-1/2 fermion. Eqs. (H.2.8)–(H.2.11) yield [285]:

$$\gamma_5 \not{S}^a\, u(\vec{\boldsymbol{p}},s') = \tau^a_{ss'}\, u(\vec{\boldsymbol{p}},s), \qquad \gamma_5 \not{S}^a\, v(\vec{\boldsymbol{p}},s') = \tau^a_{s's}\, v(\vec{\boldsymbol{p}},s), \tag{H.4.1}$$

$$\bar{u}(\vec{\boldsymbol{p}},s')\,\gamma_5 \not{S}^a = \tau^a_{ss'}\,\bar{u}(\vec{\boldsymbol{p}},s), \qquad \bar{v}(\vec{\boldsymbol{p}},s')\,\gamma_5 \not{S}^a = \tau^a_{s's}\,\bar{v}(\vec{\boldsymbol{p}},s). \tag{H.4.2}$$

In the case of $a = 3$, Eqs. (H.4.1) and (H.4.2) reduce to those of Eqs. (G.4.18) and (G.4.19).

The four-component Bouchiat–Michel formulae [112,316,317] can be obtained from Eqs. (H.3.5)–(H.3.12):

$$u(\vec{\boldsymbol{p}},s')\bar{u}(\vec{\boldsymbol{p}},s) = \tfrac{1}{2}\left[\delta_{ss'} + \gamma_5\gamma_\mu \mathscr{S}^\mu_{ss'}\right](\not{p} + m), \tag{H.4.3}$$

$$v(\vec{\boldsymbol{p}},s')\bar{v}(\vec{\boldsymbol{p}},s) = \tfrac{1}{2}\left[\delta_{s's} + \gamma_5\gamma_\mu \mathscr{S}^\mu_{s's}\right](\not{p} - m), \tag{H.4.4}$$

where $\mathscr{S}^\mu_{ss'} \equiv S^{a\mu}\tau^a_{ss'}$. As expected, the above results for $s = s'$ correspond to the spin projection operators given in Eqs. (G.4.20) and (G.4.21). Related formulae involving products of u and v-spinors can be obtained by using [cf. Eq. (G.4.15)]:

$$v(\vec{\boldsymbol{p}},s) = -2s\gamma_5 u(\vec{\boldsymbol{p}},-s), \qquad u(\vec{\boldsymbol{p}},s) = 2s\gamma_5 v(\vec{\boldsymbol{p}},-s). \tag{H.4.5}$$

Eqs. (H.4.1)–(G.4.15) also apply to helicity u and v-spinors, after replacing s, s' with λ, λ' and using the S^a as defined in Eq. (H.1.14). The four-component versions of Eqs. (C.3.20)–(C.3.23) yield:

$$u(-\boldsymbol{p},-\lambda) = \xi_\lambda(\hat{\boldsymbol{p}})\,\gamma^0\,u(\boldsymbol{p},\lambda), \qquad v(-\boldsymbol{p},-\lambda) = \xi_\lambda(\hat{\boldsymbol{p}})\,\gamma^0\,v(\boldsymbol{p},\lambda), \tag{H.4.6}$$

$$\bar{u}(-\boldsymbol{p},-\lambda) = \bar{u}(\boldsymbol{p},\lambda)\,\gamma^0\,\xi_{-\lambda}(\hat{\boldsymbol{p}}), \qquad \bar{v}(-\boldsymbol{p},-\lambda) = \bar{v}(\boldsymbol{p},\lambda)\,\gamma^0\,\xi_\lambda(\hat{\boldsymbol{p}}), \tag{H.4.7}$$

where the phase $\xi_\lambda(\hat{\boldsymbol{p}})$ was defined in Eq. (C.3.12). In order to consider the massless limit, one must employ helicity spinors, as discussed in Appendix H.3. For $a = 1, 2$, Eqs. (H.4.1) and (H.4.2) apply in the $m \to 0$ limit as written. The corresponding massless limit for the case of $a = 3$ is smooth and results in Eq. (G.4.22). Similarly, the massless limit of the Bouchiat–Michel formulae for helicity spinors can be obtained by setting $mS^{a\mu} = p^\mu\,\delta^{a3}$, applying the mass–shell condition ($p^2 = m^2$), and taking the $m \to 0$ limit at the end of the computation. The end result is given by

$$u(p,\lambda')\bar{u}(p,\lambda) = \tfrac{1}{2}(1 + 2\lambda\gamma_5)\,\not{p}\delta_{\lambda\lambda'} + \tfrac{1}{2}\gamma_5[\,\not{S}^1\tau^1_{\lambda\lambda'} + \not{S}^2\tau^2_{\lambda\lambda'}]\,\not{p}, \tag{H.4.8}$$

$$v(p,\lambda')\bar{v}(p,\lambda) = \tfrac{1}{2}(1 - 2\lambda\gamma_5)\,\not{p}\delta_{\lambda'\lambda} + \tfrac{1}{2}\gamma_5[\,\not{S}^1\tau^1_{\lambda'\lambda} + \not{S}^2\tau^2_{\lambda'\lambda}]\,\not{p}. \tag{H.4.9}$$

As expected, when $\lambda = \lambda'$, we recover the helicity projection operators for massless spin-1/2 particles given in Eqs. (G.4.24) and (G.4.25).

As before, we can use the Bouchiat–Michel formulae to evaluate helicity amplitudes involving two equal mass spin-1/2 fermions. A typical amplitude involving a fermion–antifermion pair, evaluated in the center-of-mass frame of the pair, has the generic structure:

$$\overline{w}(\vec{\boldsymbol{p}},\lambda)\,\Gamma\,w'(-\vec{\boldsymbol{p}},\lambda'), \tag{H.4.10}$$

where w is either a u or v spinor, w' is respectively either a v or u spinor, and Γ is a product of Dirac gamma matrices. For example,

$$\bar{u}(\vec{\boldsymbol{p}},\lambda)\,\Gamma\,v(-\vec{\boldsymbol{p}},\lambda') = -2\lambda'\bar{u}(\vec{\boldsymbol{p}},\lambda)\,\Gamma\,\gamma_5\,u(-\vec{\boldsymbol{p}},-\lambda') = -2\lambda'\,\xi_{\lambda'}(\hat{\boldsymbol{p}})\,\bar{u}(\vec{\boldsymbol{p}},\lambda)\,\Gamma\,\gamma_5\,\gamma^0\,u(\vec{\boldsymbol{p}},\lambda'), \tag{H.4.11}$$

where we have used the results of Eqs. (G.4.15) and (H.4.6). We can now employ the Bouchiat–Michel formula to convert the above result into a trace. By a similar computation, all expressions of the form of Eq. (H.4.10) can be expressed as a trace:

$$\bar{u}(\vec{\boldsymbol{p}},\lambda)\,\Gamma\,v(-\vec{\boldsymbol{p}},\lambda') = -\lambda'\,\xi_{\lambda'}(\hat{\boldsymbol{p}})\,\mathrm{Tr}\left[\Gamma\gamma_5\gamma^0(\delta_{\lambda\lambda'}+\gamma_5\gamma_\mu\mathscr{S}^\mu_{\lambda\lambda'})(\not{p}+m)\right], \tag{H.4.12}$$

$$\bar{v}(\vec{\boldsymbol{p}},\lambda)\,\Gamma\,u(-\vec{\boldsymbol{p}},\lambda') = \lambda'\,\xi_{-\lambda'}(\hat{\boldsymbol{p}})\,\mathrm{Tr}\left[\Gamma\gamma_5\gamma^0(\delta_{\lambda'\lambda}+\gamma_5\gamma_\mu\mathscr{S}^\mu_{\lambda'\lambda})(\not{p}-m)\right]. \tag{H.4.13}$$

These results are the four-component analogues of Eqs. (H.3.24)–(H.3.27) and Eqs. (H.3.28)–(H.3.31), respectively. For amplitudes that involve a pair of equal mass fermions [or equal mass antifermions], w and w' in Eq. (H.4.10) are both u-spinors [or v-spinors]. Using Eq. (G.4.15), these amplitudes can then be evaluated using the results of Eqs. (H.4.12) and (H.4.13) above.

In the massless limit, one can again put $mS^{a\mu} = p^\mu\delta^{a3}$, set $p^2 = m^2$ and take $m \to 0$ at the end of the computation. Alternatively, one can repeat the derivation of Eqs. (H.4.12)–(H.4.13) using the results of Eqs. (H.4.8) and (H.4.9). For completeness, we record the end result here.

$$\bar{u}(\vec{\boldsymbol{p}},\lambda)\,\Gamma\,v(-\vec{\boldsymbol{p}},\lambda') = \xi_{\lambda'}(\hat{\boldsymbol{p}})\left\{\tfrac{1}{2}\delta_{\lambda\lambda'}\,\mathrm{Tr}[\Gamma\gamma^0(1+2\lambda\gamma_5)\,\not{p}] + \lambda'\,\mathrm{Tr}[\Gamma\gamma^0(\not{S}^1\tau^1_{\lambda\lambda'}+\not{S}^2\tau^2_{\lambda\lambda'})\,\not{p}]\right\}, \tag{H.4.14}$$

$$\bar{v}(\vec{\boldsymbol{p}},\lambda)\,\Gamma\,u(-\vec{\boldsymbol{p}},\lambda') = \xi_{-\lambda'}(\hat{\boldsymbol{p}})\left\{\tfrac{1}{2}\delta_{\lambda'\lambda}\,\mathrm{Tr}[\Gamma\gamma^0(1-2\lambda\gamma_5)\,\not{p}] - \lambda'\,\mathrm{Tr}[\Gamma\gamma^0(\not{S}^1\tau^1_{\lambda'\lambda}+\not{S}^2\tau^2_{\lambda'\lambda})\,\not{p}]\right\}. \tag{H.4.15}$$

As an example, we consider once again the decay $Z^0 \to f\bar{f}$. The decay amplitude is equal to Eq. (H.4.12), where Γ is a linear combination of $\frac{1}{2}\gamma^\mu(1-\gamma_5)$ and $\frac{1}{2}\gamma^\mu(1+\gamma_5)$. Evaluating the corresponding traces yields:

$$\bar{u}(\vec{\boldsymbol{p}},\lambda)\,\tfrac{1}{2}\gamma^\mu(1-\gamma_5)\,v(-\vec{\boldsymbol{p}},\lambda') = 2\lambda'\,\xi_{\lambda'}(\hat{\boldsymbol{p}})\,\left[mg^{\mu0}\delta_{\lambda\lambda'}+p^\mu\mathscr{S}^0_{\lambda\lambda'}-p^0\mathscr{S}^\mu_{\lambda\lambda'}+i\epsilon^{0\mu\nu\rho}(\mathscr{S}_{\lambda\lambda'})_\nu p_\rho\right], \tag{H.4.16}$$

$$\bar{u}(\vec{\boldsymbol{p}},\lambda)\,\tfrac{1}{2}\gamma^\mu(1+\gamma_5)\,v(-\vec{\boldsymbol{p}},\lambda') = 2\lambda'\,\xi_{\lambda'}(\hat{\boldsymbol{p}})\,\left[-mg^{\mu0}\delta_{\lambda\lambda'}+p^\mu\mathscr{S}^0_{\lambda\lambda'}-p^0\mathscr{S}^\mu_{\lambda\lambda'}-i\epsilon^{0\mu\nu\rho}(\mathscr{S}_{\lambda\lambda'})_\nu p_\rho\right]. \tag{H.4.17}$$

Using Eq. (H.1.10), we see that Eqs. (H.4.16) and (H.4.17) reproduce exactly the results of Eqs. (H.3.40) and (H.3.41), respectively.

Finally, we note that if the two fermions do not have the same mass, then the method presented above is not applicable. However, generalizations of the above method exist in the literature that can be employed to evaluate helicity amplitudes of the form of Eq. (H.4.10) for unequal mass fermions; see, e.g., Ref. [316]. An alternative approach due to Hagiwara and Zeppenfeld [105] is reviewed in Appendix I.1.

Appendix I. Helicity amplitudes and the spinor helicity method

In Appendix H, we showed how to use the Bouchiat–Michel formulae (with versions applicable to both two-component and four-component spinor wave functions) to construct helicity amplitudes for processes with two initial state and two final state equal mass fermions (or a fermion–antifermion pair) in the center-of-mass frame of the two fermions. For practical applications, it is important to extend these techniques to allow for final states with an arbitrary number of particles. The techniques should be powerful enough to allow for pairs of fermions of unequal mass, and both massless and massive spin-1 particles. Ideally, these techniques should produce simple analytic results (when possible) and yield efficient numerical algorithms for the evaluation of the helicity amplitudes.

I.1. The helicity amplitude technique of Hagiwara and Zeppenfeld

One method for computing helicity amplitudes for multi-particle final states that is easily amenable to numerical analysis was developed by Hagiwara and Zeppenfeld (HZ) [105]. The HZ formalism was subsequently employed in Refs. [318,319] in developing a fast numerical algorithm for the computation of multi-parton processes. In this section, we demonstrate how our two-component formalism (denoted by DHM) can be connected to theirs. In particular, we present a translation between the two formalisms in Table I.1.1.

After removing the propagator factors, an arbitrary tree amplitude with external fermions can be expressed in terms of a four-component fermion string

$$\overline{\Psi}_i P_\tau\ \not{a}_1\ \not{a}_2\ldots\not{a}_n\Psi_j, \quad \tau = \pm1, \tag{I.1.1}$$

where Ψ_j is a four-component spinor wave function $u(p_j,\lambda_j)$ or $v(p_j,-\lambda_j)$,[150] and $P_\pm = \frac{1}{2}(1\pm\gamma_5)$ are the chiral projection operators. Furthermore, $\not{a}_k \equiv \gamma_\mu a_k^\mu$ where a_k represents an arbitrary Lorentz four-vector, which can be a four-momentum p_k^μ, a vector boson wave function $\epsilon^\mu(p_k,\lambda_k)$, an axial vector (e.g., $\epsilon^{\mu\nu\rho\sigma}p_{k\nu}p_{m\rho}p_{n\sigma}$) or another fermion string with uncontracted Lorentz indices (e.g., $\overline{\Psi}_m\gamma^\mu\Psi_n$).

[150] HZ defines $v(p,\lambda) = C\bar{u}^{\mathsf{T}}(p,\lambda)$, where $C = i\gamma^2\gamma^0$, which differs by an overall minus sign from the conventions employed in this review [cf. Eq. (G.1.20)]. In this section, we will modify the HZ results in order to be consistent with our sign convention.

Table I.1.1
Translation between our notation (denoted by DHM) and the notation of Hagiwara and Zeppenfeld (HZ) [105]. The sign convention governing the definition of $v(p,\lambda)_\pm$ is opposite to that of HZ (cf. footnote 150).

DHM Formalism	HZ Formalism
$x_\alpha(p,\lambda)$	$u(p,\lambda)_-$
$x^\alpha(p,\lambda)$	$v^\dagger(p,\lambda)_+$
$x^{\dagger\dot\alpha}(p,\lambda)$	$v(p,\lambda)_+$
$x^\dagger_{\dot\alpha}(p,\lambda)$	$u^\dagger(p,\lambda)_-$
$y_\alpha(p,\lambda)$	$v(p,\lambda)_-$
$y^\alpha(p,\lambda)$	$u^\dagger(p,\lambda)_+$
$y^{\dagger\dot\alpha}(p,\lambda)$	$u(p,\lambda)_+$
$y^\dagger_{\dot\alpha}(p,\lambda)$	$v^\dagger(p,\lambda)_-$
$p\cdot\sigma$	$(\not{p})_+$
$p\cdot\overline{\sigma}$	$(\not{p})_-$
σ^μ	σ^μ_+
$\overline{\sigma}^\mu$	σ^μ_-
P_R	P_+
P_L	P_-
$\lambda=\pm\frac{1}{2}$	$\lambda=\pm1$
$\chi_\lambda(-\hat{\boldsymbol{z}})$	$-\chi_\lambda(-\hat{\boldsymbol{z}})$

In order to rewrite the fermion string, Eq. (I.1.1), in terms of two-component spinors, HZ decomposes the four-component spinors as follows:

$$\Psi_j\equiv\begin{pmatrix}(\psi_j)_-\\(\psi_j)_+\end{pmatrix},\qquad u(p_j,\lambda_j)\equiv\begin{pmatrix}u(p_j,\lambda_j)_-\\u(p_j,\lambda_j)_+\end{pmatrix},\qquad v(p_j,\lambda_j)\equiv\begin{pmatrix}v(p_j,\lambda_j)_-\\v(p_j,\lambda_j)_+\end{pmatrix}. \tag{I.1.2}$$

Comparing with Eqs. (G.4.11) and (G.4.12), the corresponding expressions in our notation are given in Table I.1.1. Note that $\lambda=\pm1$ in the notation of HZ, whereas in our notation (which we follow below) $\lambda=\pm\frac{1}{2}$.

The four-component fermion string is then replaced by the two-component fermion string:

$$\overline{\Psi}_i P_\tau\ \not{a}_1\not{a}_2\ldots\not{a}_n\Psi_j=(\psi_i)^\dagger_\tau(\not{a}_1)_\tau(\not{a}_2)_{-\tau}\ldots(\not{a}_n)_{-\delta_n\tau}(\psi_j)_{-\delta_n\tau},\quad \tau=\pm1,\quad \text{where } \delta_n\equiv(-1)^n. \tag{I.1.3}$$

In the notation of HZ,

$$(\not{a})_\pm=a_\mu\sigma^\mu_\pm, \tag{I.1.4}$$

where $\sigma^\mu_+\equiv\sigma^\mu$ and $\sigma^\mu_-\equiv\overline{\sigma}^\mu$. In Eq. (I.1.3), the helicity labels are suppressed; more explicitly,

$$(\psi_k)_\tau\equiv\psi_k(p_k,\lambda_k)_\tau=u(p_k,\lambda_k)_\tau\quad\text{or}\quad v(p_k,-\lambda_k)_\tau. \tag{I.1.5}$$

This convention of HZ (note the $-\lambda_k$ argument of v) allows one to write simple generic formulae in terms of $(\psi)_\pm$ that are applicable to both $u_\pm$ and $v_\pm$.

Using the results of Table I.1.1, one can verify that Eq. (I.1.3) is covariant with respect to dotted and undotted indices. That is, the sign τ of $\psi_i^\dagger$ must match the sign of the first σ-matrix in the string $(\not{a}_1)_\tau(\not{a}_2)_{-\tau}\ldots(\not{a}_n)_{-\delta_n\tau}$. The signs of the sigma matrices within this string alternate (either $+-+-\cdots$ or $-+-+\cdots$ in the case of $\tau=+1$ or -1, respectively). Finally, the sign of the last σ-matrix in the string [which must be equal to $-\delta_n\tau$ in light of the previous statement] must match the sign of ψ_j as indicated.

As noted above, it is possible that one of the $(\not{a}_i)_\tau$ could be of the form σ^μ_τ multiplied by another fermion string with a free μ-index. One can uncouple the two fermion strings by employing the Fierz identities given by Eqs. (2.67)–(2.69). For example,

$$\begin{aligned}&[(u_1)^\dagger_-(\not{a}_1)_-\sigma^\mu_+(\not{a}_2)_-(u_2)_-][(u_3)^\dagger_-(\not{a}_3)_-\sigma_{+\mu}(\not{a}_4)_-(u_4)_-]\\&\quad=[(u_1)^\dagger_-(\not{a}_1)_-(\not{a}_3)_+(v_3)_+][(v_4)^\dagger_+(\not{a}_4)_+(\not{a}_2)_-(u_2)_-],\end{aligned} \tag{I.1.6}$$

which is easily derived after translating to the DHM notation.[151] As a result, the helicity tree amplitude for any process can be expressed as the product of *uncoupled* strings of two-component fermion spinors

$$\mathrm{FS}=(\psi_i)^\dagger_\tau(\not{a}_1)_\tau(\not{a}_2)_{-\tau}\ldots(\not{a}_n)_{-\delta_n\tau}(\psi_j)_{-\delta_n\tau}. \tag{I.1.7}$$

[151] Here, we differ from HZ, who employ a Fierz identity that is not covariant with respect to the dotted and undotted indices [note the comment below Eq. (2.54)]. Thus, Eq. (I.1.6) differs from the result obtained in Eq. (3.17b) of HZ.

To evaluate the fermion string FS, we employ the explicit forms for the two-component helicity spinor wave functions given in Eqs. (C.3.4)–(C.3.7), which can be rewritten as

$$\psi(p_k,\lambda_k)_\tau = C_k\,\omega_{\tau\lambda_k}(\vec{\boldsymbol{p}})\,\chi_{\lambda_k}(\hat{\boldsymbol{p}}_{\boldsymbol{k}}), \tag{I.1.8}$$

where, following the convention of Eq. (I.1.5),

$$C_k = \begin{cases} 1 & \text{for } (\psi_k)_\tau = u(p_k,\lambda_k)_\tau, \\ 2\lambda_k\tau & \text{for } (\psi_k)_\tau = v(p_k,-\lambda_k)_\tau, \end{cases} \qquad \tau=\pm1, \qquad \lambda_k=\pm1/2, \tag{I.1.9}$$

and $\omega_\lambda(\vec{\boldsymbol{p}}) \equiv (E+2\lambda|\vec{\boldsymbol{p}}|)^{1/2}$ for $\lambda=\pm1/2$. Hence, the fermion string [Eq. (I.1.7)] is given by [105]

$$\mathrm{FS} = C_i\,C_j\,\omega_{\tau\lambda_i}(\vec{\boldsymbol{p}}_{\boldsymbol{i}})\,\omega_{-\delta_n\tau\lambda_j}(\vec{\boldsymbol{p}}_{\boldsymbol{j}})\,S(p_i,a_1,a_2,\ldots,a_n,p_j)^\tau_{\lambda_i\lambda_j}, \tag{I.1.10}$$

where the function S is defined as

$$S(p_i,a_1,a_2,\ldots,a_n,p_j)^\tau_{\lambda_i\lambda_j} \equiv \chi^\dagger_{\lambda_i}(\hat{\boldsymbol{p}}_{\boldsymbol{i}})\left[\prod_{k=1}^{n}(\not{a}_k)_{-\delta_k\tau}\right]\chi_{\lambda_j}(\hat{\boldsymbol{p}}_{\boldsymbol{j}}), \tag{I.1.11}$$

where $\delta_k \equiv (-1)^k$. In the absence of the $\not{a}_{\pm\tau}$ factors, we define

$$S(p_i,p_j)_{\lambda_i\lambda_j} \equiv T(\hat{\boldsymbol{p}}_{\boldsymbol{i}},\hat{\boldsymbol{p}}_{\boldsymbol{j}})_{2\lambda_i,2\lambda_j} = \chi^\dagger_{\lambda_i}(\hat{\boldsymbol{p}}_{\boldsymbol{i}})\chi_{\lambda_j}(\hat{\boldsymbol{p}}_{\boldsymbol{j}}), \tag{I.1.12}$$

where the $T(\hat{\boldsymbol{p}}_{\boldsymbol{i}},\hat{\boldsymbol{p}}_{\boldsymbol{j}})_{2\lambda_i,2\lambda_j}$ are proportional to the (massless) spinorial products introduced by Kleiss [98] [cf. Eqs. (I.2.22) and (I.2.23)].

To evaluate S, we assume that the four-vectors a_k^μ are real.[152] Then, we may employ the following identity[153]:

$$(\not{a})_\tau = \sum_{\tau'=\pm}\left[a^0-\tau'\tau|\vec{\boldsymbol{a}}|\right]\chi_{\tau'/2}(\hat{\boldsymbol{a}})\chi^\dagger_{\tau'/2}(\hat{\boldsymbol{a}}), \tag{I.1.13}$$

where $\chi_{\tau'/2}(\hat{\boldsymbol{a}})$ is a two-component helicity spinor with three-momentum $\vec{\boldsymbol{a}}$. Using Eq. (I.1.13) in Eq. (I.1.11), we end up with the desired expression:

$$\begin{aligned} S(p_i,a_1,a_2,\ldots,a_n,p_j)^\tau_{\lambda_i\lambda_j} = {} & \left[\prod_{k=1}^{n}\sum_{\tau_k=\pm}\left[a_k^0+\tau_k\delta_k\tau|\vec{\boldsymbol{a}}_{\boldsymbol{k}}|\right]\right]T(\hat{\boldsymbol{p}}_i,\hat{\boldsymbol{a}}_1)_{2\lambda_i,\tau_1}T(\hat{\boldsymbol{a}}_1,\hat{\boldsymbol{a}}_2)_{\tau_1\tau_2} \\ & \times\ \ldots T(\hat{\boldsymbol{a}}_{n-1},\hat{\boldsymbol{a}}_n)_{\tau_{n-1}\tau_n}T(\hat{\boldsymbol{a}}_n,\hat{\boldsymbol{p}}_j)_{\tau_n,2\lambda_j}. \end{aligned} \tag{I.1.14}$$

All that remains is to evaluate the spinorial product $T(\hat{\boldsymbol{a}},\hat{\boldsymbol{b}})_{\tau_a\,\tau_b}$ ($\tau_a,\ \tau_b\ =\ \pm1$) for arbitrary unit three-vectors $\hat{\boldsymbol{a}}$ and $\hat{\boldsymbol{b}}$. Two properties of the spinorial product $T(\hat{\boldsymbol{a}},\hat{\boldsymbol{b}})_{\tau_a,\tau_b}$ are noteworthy. First, as this product is a scalar, it follows that $T(\hat{\boldsymbol{a}},\hat{\boldsymbol{b}})^*_{\tau_a,\tau_b} = T(\hat{\boldsymbol{a}},\hat{\boldsymbol{b}})^\dagger_{\tau_a,\tau_b}$. Hence, Eq. (I.1.12) implies that

$$T(\hat{\boldsymbol{a}},\hat{\boldsymbol{b}})_{\tau_a\,\tau_b} = T(\hat{\boldsymbol{b}},\hat{\boldsymbol{a}})^*_{\tau_b\,\tau_a}. \tag{I.1.15}$$

Second, we use Eq. (C.1.8) to write:

$$\begin{aligned} T(\hat{\boldsymbol{a}},\hat{\boldsymbol{b}})_{\tau_a\,\tau_b} = {} & \chi^\dagger_{\tau_a/2}(\hat{\boldsymbol{z}})\ \exp(i\gamma_a\sigma^3/2)\ \exp(i\theta_a\sigma^2/2)\ \exp(i\phi_a\sigma^3/2) \\ & \times\ \exp(-i\phi_b\sigma^3/2)\ \exp(-i\theta_b\sigma^2/2)\ \exp(-i\gamma_b\sigma^3/2)\ \chi_{\tau_b/2}(\hat{\boldsymbol{z}}). \end{aligned} \tag{I.1.16}$$

Complex conjugating this result, and using the fact that $\chi(\hat{\boldsymbol{z}})$, σ^1 and σ^3 are real and σ^2 is pure imaginary,

$$\begin{aligned} T(\hat{\boldsymbol{a}},\hat{\boldsymbol{b}})^*_{\tau_a\,\tau_b} = {} & \tau_a\tau_b\,\chi^\dagger_{-\tau_a/2}(\hat{\boldsymbol{z}})\,\sigma^2\ \exp(-i\gamma_a\sigma^3/2)\ \exp(i\theta_a\sigma^2/2)\ \exp(-i\phi_a\sigma^3/2) \\ & \times\ \exp(i\phi_b\sigma^3/2)\ \exp(-i\theta_b\sigma^2/2)\ \exp(i\gamma_b\sigma^3/2)\,\sigma^2\,\chi_{-\tau_b/2}(\hat{\boldsymbol{z}}), \end{aligned} \tag{I.1.17}$$

after using Eq. (C.1.22). Since σ^2 anticommutes with σ^3, we end up with:

$$\begin{aligned} T(\hat{\boldsymbol{a}},\hat{\boldsymbol{b}})^*_{\tau_a\,\tau_b} = {} & \tau_a\tau_b\,\chi^\dagger_{-\tau_a/2}(\hat{\boldsymbol{z}})\ \exp(i\gamma_a\sigma^3/2)\ \exp(i\theta_a\sigma^2/2)\ \exp(i\phi_a\sigma^3/2) \\ & \times\ \exp(-i\phi_b\sigma^3/2)\ \exp(-i\theta_b\sigma^2/2)\ \exp(-i\gamma_b\sigma^3/2)\ \chi_{-\tau_b/2}(\hat{\boldsymbol{z}}) \\ = {} & \tau_a\tau_b\,T(\hat{\boldsymbol{a}},\hat{\boldsymbol{b}})_{-\tau_a,-\tau_b}. \end{aligned} \tag{I.1.18}$$

152 In the case of complex a^μ, one should decompose a^μ into its real and imaginary parts and evaluate separately the real and imaginary parts of S.

153 To obtain Eq. (I.1.13), we make use of Eq. (3.1.43) applied to helicity spinors: $\chi_\lambda\chi^\dagger_\lambda = \frac{1}{2}(1+2\lambda\vec{\boldsymbol{\sigma}}\cdot\hat{\boldsymbol{p}})$.

Since $\tau_a, \tau_b = \pm 1$, it follows that

$$T(\hat{\boldsymbol{a}}, \hat{\boldsymbol{b}})_{-\tau_a,-\tau_b} = \tau_a\, \tau_b\, T(\hat{\boldsymbol{a}}, \hat{\boldsymbol{b}})^*_{\tau_a\, \tau_b}. \tag{I.1.19}$$

Using Eqs. (I.1.15) and (I.1.19), it is sufficient to give explicit forms for only two of the spinorial products [99,105]. Eq. (I.1.16) yields:

$$T(\hat{\boldsymbol{a}}, \hat{\boldsymbol{b}})_{++} = e^{i(\phi_a-\phi_b+\gamma_a-\gamma_b)/2} \cos\frac{\theta_a}{2}\cos\frac{\theta_b}{2} + e^{-i(\phi_a-\phi_b-\gamma_a+\gamma_b)/2} \sin\frac{\theta_a}{2}\sin\frac{\theta_b}{2}, \tag{I.1.20}$$

$$T(\hat{\boldsymbol{a}}, \hat{\boldsymbol{b}})_{-+} = e^{-i(\phi_a-\phi_b+\gamma_a+\gamma_b)/2} \cos\frac{\theta_a}{2}\sin\frac{\theta_b}{2} - e^{i(\phi_a-\phi_b-\gamma_a-\gamma_b)/2} \sin\frac{\theta_a}{2}\cos\frac{\theta_b}{2}, \tag{I.1.21}$$

where (θ_p, ϕ_p) are the polar and azimuthal angles of $\hat{\boldsymbol{p}}$ (for $\hat{\boldsymbol{p}} = \hat{\boldsymbol{a}}$ and $\hat{\boldsymbol{b}}$, respectively). In the case where $\hat{\boldsymbol{a}}$ and/or $\hat{\boldsymbol{b}}$ are parallel to the negative z-axis, we employ the convention of Eq. (C.1.7) and choose the corresponding azimuthal angle equal to π.[154] Note that HZ employ a convention for their spinor wave functions [cf. Eq. (C.1.8)] in which $\gamma = -\phi$, although the convention in which $\gamma = 0$ yields a slightly more symmetrical form for the spinorial products.

Eqs. (I.1.7), (I.1.10) and (I.1.11) can be written in a form that is reminiscent of the results obtained in Appendix H.3. For example, using Eqs. (C.3.4)–(C.3.7),

$$x^\dagger_{\dot\alpha}(\vec{\boldsymbol{p}}, \lambda)\, \Gamma^{\dot\alpha\beta}\, y_\beta(\vec{\boldsymbol{p}}', -\lambda') = -2\lambda' \omega_{-\lambda}(\vec{\boldsymbol{p}})\omega_{-\lambda'}(\vec{\boldsymbol{p}}')\chi^\dagger_\lambda(\hat{\boldsymbol{p}})\Gamma\chi_{\lambda'}(\hat{\boldsymbol{p}}'), \tag{I.1.22}$$

$$y^\alpha(\vec{\boldsymbol{p}}, \lambda)\, \Gamma_{\alpha\dot\beta}\, x^{\dagger\dot\beta}(\vec{\boldsymbol{p}}', -\lambda') = 2\lambda' \omega_{\lambda}(\vec{\boldsymbol{p}})\omega_{\lambda'}(\vec{\boldsymbol{p}}')\chi^\dagger_\lambda(\hat{\boldsymbol{p}})\Gamma\chi_{\lambda'}(\hat{\boldsymbol{p}}'), \tag{I.1.23}$$

$$y^\alpha(\vec{\boldsymbol{p}}, \lambda)\, \Gamma_\alpha{}^\beta\, y_\beta(\vec{\boldsymbol{p}}', -\lambda') = -2\lambda' \omega_{\lambda}(\vec{\boldsymbol{p}})\omega_{-\lambda'}(\vec{\boldsymbol{p}}')\chi^\dagger_\lambda(\hat{\boldsymbol{p}})\Gamma\chi_{\lambda'}(\hat{\boldsymbol{p}}'), \tag{I.1.24}$$

$$x^\dagger_{\dot\alpha}(\vec{\boldsymbol{p}}, \lambda)\, \Gamma^{\dot\alpha}{}_{\dot\beta}\, x^{\dagger\dot\beta}(\vec{\boldsymbol{p}}', -\lambda') = 2\lambda' \omega_{-\lambda}(\vec{\boldsymbol{p}})\omega_{\lambda'}(\vec{\boldsymbol{p}}')\chi^\dagger_\lambda(\hat{\boldsymbol{p}})\Gamma\chi_{\lambda'}(\hat{\boldsymbol{p}}'), \tag{I.1.25}$$

where Γ is a product of alternating σ and $\overline{\sigma}$ matrices. The spinor index structure determines the identity of the first and last matrix (e.g., $\Gamma^{\dot\alpha}{}_{\dot\beta}$ indicates a string of matrices that begins with a $\overline{\sigma}$ and ends with a σ, etc.). By suitable interchanges of x and y, twelve additional equations of similar type may be written. Note that $\chi^\dagger_\lambda \Gamma \chi_{\lambda'}$ [appearing on the right-hand side of Eqs. (I.1.22)–(I.1.25)] corresponds precisely to the $S(p, a_1, a_2, \ldots, a_n, p')^\tau_{\lambda\lambda'}$ of Eq. (I.1.11), where the four possible (τ, δ_n) combinations are in one-to-one correspondence with the four possible spinor index structures of Γ. If $\vec{\boldsymbol{p}}' = -\vec{\boldsymbol{p}}$, then one should recover Eqs. (H.3.24)–(H.3.27). Thus, the HZ method provides a powerful generalization of the helicity amplitude methods derived in Appendix H.3.

I.2. The spinor helicity method

In many practical calculations, the masses of the fermions can be neglected. In this case the computation of multi-particle helicity amplitudes simplifies considerably. In this section, we give a brief introduction to the spinor helicity method; for a review, see Refs. [320,321]. The spinor helicity method is a powerful technique for computing helicity amplitudes for multi-particle processes involving massless spin-1/2 and spin-1 particles. Although initially applied to tree-level processes, more general techniques have also been developed that are applicable to one-loop (and multiloop) diagrams [322]. Rules for computing dimensionally regularized amplitudes within the framework of the spinor helicity method have been given by Ref. [323]. The spinor helicity techniques are ideal for QCD where light quark masses can almost always be neglected. Generalizations of these methods that incorporate massive spin-1/2 and spin-1 particles exist, although they tend to be quite cumbersome [324,325]. A Mathematica implementation of the spinor helicity formalism can be found in Ref. [326]. In this section, we restrict the discussion to the massless case.

The spinor helicity technique described below is based on a formalism developed by Xu et al. [101] (denoted henceforth by XZC), which is a modification of techniques established by the CALKUL collaboration [327]. The XZC formalism (which was also independently developed in Refs. [99,328]) is based on the four-component spinor formalism. Using Eq. (G.4.23), XZC introduce a very useful notation for massless spinors

$$|p\pm\rangle \equiv u\left(p, \pm\tfrac{1}{2}\right) = v\left(p, \mp\tfrac{1}{2}\right), \tag{I.2.1}$$

$$\langle p\pm| \equiv \bar{u}\left(p, \pm\tfrac{1}{2}\right) = \bar{v}\left(p, \mp\tfrac{1}{2}\right). \tag{I.2.2}$$

Using these spinor wave functions, they define two non-trivial (massless) spinor products (which are equivalent to the spinorial products introduced by Kleiss [98])[155]:

$$\langle p\, q\rangle \equiv \langle p - |q+\rangle = \bar{u}\left(p, -\tfrac{1}{2}\right)\, u\left(q, +\tfrac{1}{2}\right), \tag{I.2.3}$$

$$[p\, q] \equiv \langle p + |q-\rangle = \bar{u}\left(p, +\tfrac{1}{2}\right)\, u\left(q, -\tfrac{1}{2}\right). \tag{I.2.4}$$

154 This convention yields a value of $\chi_\lambda(-\hat{\boldsymbol{z}})$ that is opposite in sign to the convention adopted by HZ.

155 Note that $\langle p - |q-\rangle = \langle p + |q+\rangle = 0$ due to $P_L P_R = P_R P_L = 0$.

The $\pm$ notation specified by the bra and ket indicates the chirality (i.e. the eigenvalue of γ_5) of the corresponding four-component spinor [cf. Eq. (G.4.22)].

However, the two-component spinor formalism is especially economical in the case of massless spin-1/2 fermions. Hence, we shall reformulate the XZC approach using two-component spinor notation. First, we consider the explicit forms for the two-component helicity spinor wave functions [given by Eqs. (3.1.37)–(3.1.40)] in the massless limit:

$$x_\alpha\left(\vec{\boldsymbol{p}},-\tfrac{1}{2}\right)=y_\alpha\left(\vec{\boldsymbol{p}},\tfrac{1}{2}\right)=(2E)^{1/2}\,\chi_{-1/2}(\hat{\boldsymbol{p}}),\qquad x^\alpha\left(\vec{\boldsymbol{p}},-\tfrac{1}{2}\right)=y^\alpha\left(\vec{\boldsymbol{p}},\tfrac{1}{2}\right)=(2E)^{1/2}\,\chi^\dagger_{1/2}(\hat{\boldsymbol{p}}), \tag{I.2.5}$$

$$x^{\dagger\dot\alpha}\left(\vec{\boldsymbol{p}},-\tfrac{1}{2}\right)=y^{\dagger\dot\alpha}\left(\vec{\boldsymbol{p}},\tfrac{1}{2}\right)=(2E)^{1/2}\,\chi_{1/2}(\hat{\boldsymbol{p}}),\qquad x^\dagger_{\dot\alpha}\left(\vec{\boldsymbol{p}},-\tfrac{1}{2}\right)=y^\dagger_{\dot\alpha}\left(\vec{\boldsymbol{p}},\tfrac{1}{2}\right)=(2E)^{1/2}\,\chi^\dagger_{-1/2}(\hat{\boldsymbol{p}}), \tag{I.2.6}$$

where $E=|\vec{\boldsymbol{p}}|$. For all other choices of helicities, the corresponding helicity spinor wave functions vanish. Hence, we define[156]:

$$|p+\rangle=y^{\dagger\dot\alpha}\left(\vec{\boldsymbol{p}},\tfrac{1}{2}\right)=x^{\dagger\dot\alpha}\left(\vec{\boldsymbol{p}},-\tfrac{1}{2}\right),\qquad \langle p+|=y^\alpha\left(\vec{\boldsymbol{p}},\tfrac{1}{2}\right)=x^\alpha\left(\vec{\boldsymbol{p}},-\tfrac{1}{2}\right), \tag{I.2.7}$$

$$|p-\rangle=x_\alpha\left(\vec{\boldsymbol{p}},-\tfrac{1}{2}\right)=y_\alpha\left(\vec{\boldsymbol{p}},\tfrac{1}{2}\right),\qquad \langle p-|=x^\dagger_{\dot\alpha}\left(\vec{\boldsymbol{p}},-\tfrac{1}{2}\right)=y^\dagger_{\dot\alpha}\left(\vec{\boldsymbol{p}},\tfrac{1}{2}\right). \tag{I.2.8}$$

The $|p\pm\rangle$ and $\langle p\pm|$ satisfy the massless Dirac equation [cf. Eqs. (3.1.9)–(3.1.12)]:

$$p\cdot\sigma_\pm\,|p\pm\rangle=0,\qquad \langle p\pm|\,p\cdot\sigma_\pm=0, \tag{I.2.9}$$

where $\sigma_+\equiv\sigma$ and $\sigma_-\equiv\overline{\sigma}$ as indicated in Table I.1.1. The above and the following equations should each be read as two separate equations corresponding to the upper and lower set of signs, respectively. The following properties are also noteworthy:

$$|p\pm\rangle\,\langle p\pm|=p\cdot\sigma_\mp, \tag{I.2.10}$$

$$\langle p\pm|\,\sigma^\mu_\pm\,|p\pm\rangle=2p^\mu, \tag{I.2.11}$$

$$\langle p\pm|q\mp\rangle=-\langle q\pm|p\mp\rangle, \tag{I.2.12}$$

$$\langle p+|\,\sigma^\mu_+\,|q+\rangle=\langle q-|\,\sigma^\mu_-\,|p-\rangle, \tag{I.2.13}$$

$$\langle p\pm|\,\sigma^\mu_\pm\sigma^\nu_\mp\,|q\mp\rangle=-\langle q\pm|\,\sigma^\nu_\pm\sigma^\mu_\mp\,|p\mp\rangle. \tag{I.2.14}$$

Note that Eqs. (I.2.9)–(I.2.14) are covariant with respect to the undotted and dotted spinor indices. Eqs. (I.2.10) and (I.2.11) follow from Eqs. (3.1.54) and (3.1.55). For example,

$$\langle p+|\,\sigma^\mu_+\,|p+\rangle=y^\alpha\left(\vec{\boldsymbol{p}},\tfrac{1}{2}\right)\sigma^\mu_{\alpha\dot\beta}\,y^{\dagger\dot\beta}\left(\vec{\boldsymbol{p}},\tfrac{1}{2}\right)=\sigma^\mu_{\alpha\dot\beta}\,y^{\dagger\dot\beta}\left(\vec{\boldsymbol{p}},\tfrac{1}{2}\right)y^\alpha\left(\vec{\boldsymbol{p}},\tfrac{1}{2}\right)=\mathrm{Tr}\,(\sigma^\mu p\cdot\overline{\sigma})=2p^\mu, \tag{I.2.15}$$

and similarly for $\langle p-|\,\sigma^\mu_-\,|p-\rangle$. Eqs. (I.2.12)–(I.2.14) follow immediately from Eqs. (2.59)–(2.63). Eqs. (I.2.13) and (I.2.14) generalize easily to the case of a product of an even and odd number of $\sigma/\overline{\sigma}$ matrices. For any positive integer n,

$$\langle p+|\,\sigma^{\mu_1}_+\sigma^{\mu_2}_-\cdots\sigma^{\mu_{2n-1}}_+\,|q+\rangle=\langle q-|\,\sigma^{\mu_{2n-1}}_-\cdots\sigma^{\mu_2}_+\sigma^{\mu_1}_-\,|p-\rangle, \tag{I.2.16}$$

$$\langle p\pm|\,\sigma^{\mu_1}_\pm\sigma^{\mu_2}_\mp\cdots\sigma^{\mu_{2n}}_\mp\,|q\mp\rangle=-\langle q\pm|\,\sigma^{\mu_{2n}}_\pm\cdots\sigma^{\mu_2}_\pm\sigma^{\mu_1}_\mp\,|p\mp\rangle. \tag{I.2.17}$$

Spinor products can be formed from the bras and kets in the usual way and satisfy:

$$\langle p\pm|q\mp\rangle^*=\langle q\mp|p\pm\rangle, \tag{I.2.18}$$

$$\left\langle p\pm|\sigma^\mu_\pm|q\pm\right\rangle^*=\left\langle q\pm|\sigma^\mu_\pm|p\pm\right\rangle, \tag{I.2.19}$$

where we have used the fact that the $\sigma^\mu_\pm$ are hermitian. Covariance with respect to the undotted and dotted spinors allows only two possible spinor products[157]:

$$\langle p\,q\rangle\equiv\langle p-|q+\rangle=x^\dagger\left(\vec{\boldsymbol{p}},-\tfrac{1}{2}\right)y^\dagger\left(\vec{\boldsymbol{q}},\tfrac{1}{2}\right), \tag{I.2.20}$$

$$[p\,q]\equiv\langle p+|q-\rangle=y\left(\vec{\boldsymbol{p}},\tfrac{1}{2}\right)x\left(\vec{\boldsymbol{q}},-\tfrac{1}{2}\right). \tag{I.2.21}$$

156 The association of undotted and dotted indices in Eqs. (I.2.7) and (I.2.8) is a consequence of our convention for the Dirac gamma matrices given in Appendix G [cf. Eq. (G.1.2)]. Note that in this convention, the left-handed [right-handed] projection operator P_L [P_R] projects out the lowered undotted [raised dotted] index components of the four-component spinor [cf. Eq. (G.1.6)]. However, the reader is warned that in the literature on the spinor helicity method, one almost always finds $|p+\rangle$ associated with a lowered undotted index and $|p-\rangle$ associated with an upper dotted index. This is due to a different convention for the sigma matrices, such as the Wess and Bagger definition given in Eqs. (A.11) and (A.12). Numerically, this is equivalent to a convention for the Dirac gamma matrices in which σ^μ and $\overline{\sigma}^\mu$ are interchanged in Eq. (G.1.2), resulting in an overall change of sign in the matrix representation of γ_5. As a result, in this latter convention the lowered undotted [raised dotted] index components are associated with positive [negative] chirality. For an historical perspective, see the discussion following Eq. (A.12).

157 Since we wish to preserve the definition of the spinor products given in Eq. (I.2.3), $\langle p\,q\rangle$ is a sum over dotted indices and $[p\,q]$ is a sum over undotted indices in our two-component spinor conventions. This is to be contrasted with most of the literature on the spinor helicity method, in which $\langle p\,q\rangle$ is written as a sum over undotted indices and $[p\,q]$ as a sum over dotted indices. The origin of this difference is explained in footnote 156.

In particular, the products $\langle p+|q+\rangle$ and $\langle p-|q-\rangle$ never arise in a computation using two-component spinor notation. In terms of the spinorial products defined in Eq. (I.1.12),

$$\langle p\,q\rangle \equiv \langle p-|q+\rangle = (2E_p)^{1/2}(2E_q)^{1/2}T(\hat{\boldsymbol{p}},\hat{\boldsymbol{q}})_{-+}, \tag{I.2.22}$$

$$[p\,q] \equiv \langle p+|q-\rangle = (2E_p)^{1/2}(2E_q)^{1/2}T(\hat{\boldsymbol{p}},\hat{\boldsymbol{q}})_{+-}, \tag{I.2.23}$$

where $E_p = |\vec{\boldsymbol{p}}|$ and $E_q = |\vec{\boldsymbol{q}}|$. Explicit forms for $T(\hat{\boldsymbol{p}},\hat{\boldsymbol{q}})_{-+}$ and $T(\hat{\boldsymbol{p}},\hat{\boldsymbol{q}})_{+-} = -T(\hat{\boldsymbol{p}},\hat{\boldsymbol{q}})^*_{-+}$ can be obtained from Eq. (I.1.21). Using Eqs. (I.1.15) and (I.1.19) [or equivalently, using Eqs. (I.2.12) and (I.2.18)], the spinor products satisfy the following relations:

$$\langle p\,q\rangle = -\langle q\,p\rangle\,, \tag{I.2.24}$$

$$[p\,q] = -[q\,p], \tag{I.2.25}$$

$$\langle p\,q\rangle^* = -[p\,q]. \tag{I.2.26}$$

One immediate consequence of the above results is:

$$\langle p\,p\rangle = \langle p-|p+\rangle = 0, \tag{I.2.27}$$

$$[p\,p] = \langle p+|p-\rangle = 0. \tag{I.2.28}$$

We next compute the absolute square of the spinor product:

$$\begin{aligned} |\langle p\,q\rangle|^2 &= x^\dagger_{\dot\alpha}\left(\vec{\boldsymbol{p}},-\tfrac{1}{2}\right)\, y^{\dagger\dot\alpha}\left(\vec{\boldsymbol{q}},\tfrac{1}{2}\right)\, x_\alpha\left(\vec{\boldsymbol{p}},-\tfrac{1}{2}\right)\, y^\alpha\left(\vec{\boldsymbol{q}},\tfrac{1}{2}\right) = x_\alpha\left(\vec{\boldsymbol{p}},-\tfrac{1}{2}\right)\, x^\dagger_{\dot\alpha}\left(\vec{\boldsymbol{p}},-\tfrac{1}{2}\right)\, y^{\dagger\dot\alpha}\left(\vec{\boldsymbol{q}},\tfrac{1}{2}\right)\, y^\alpha\left(\vec{\boldsymbol{q}},\tfrac{1}{2}\right) \\ &= p\cdot\sigma_{\alpha\dot\alpha}\,q\cdot\overline{\sigma}^{\dot\alpha\alpha} = p_\mu q_\nu\,\mathrm{Tr}(\sigma^\mu\overline{\sigma}^\nu) = 2p\cdot q. \end{aligned} \tag{I.2.29}$$

Using this result and Eq. (I.2.26) yields

$$|\langle p\,q\rangle|^2 = |[p\,q]|^2 = 2p\cdot q, \tag{I.2.30}$$

which indicates that the spinor products are roughly the square roots of the corresponding dot products. One other noteworthy relation is:

$$\begin{aligned} \langle p_1\,p_2\rangle\,[p_2\,p_3]\,\langle p_3\,p_4\rangle\,[p_4\,p_1] &= \mathrm{Tr}\,(\sigma\cdot p_1\,\overline{\sigma}\cdot p_2\,\sigma\cdot p_3\,\overline{\sigma}\cdot p_4) \\ &= 2(g_{\mu\nu}g_{\rho\kappa} - g_{\mu\rho}g_{\nu\kappa} + g_{\mu\kappa}g_{\nu\rho} + i\epsilon_{\mu\nu\rho\kappa})p_1^\mu p_2^\nu p_3^\rho p_4^\kappa, \end{aligned} \tag{I.2.31}$$

where the trace has been evaluated using Eq. (B.2.26). Note that the first line of Eq. (I.2.31) immediately follows from Eqs. (3.1.54) and (3.1.55) after plugging in the definition of the spinor products.

In Appendix I.1, we showed that a fermion string can be expressed in terms of products of the spinorial products T [cf. Eq. (I.1.14)]. When applied to massless spinors, Eq. (I.2.30) indicates that the square of the helicity amplitude of a multi-fermion scattering process can be expressed in terms of products of dot products of pairs of fermion momenta. If more than one diagram contributes to a helicity amplitude, then it is often possible to combine the contributions after a rearrangement of momenta via the Fierz identities. Using Eqs. (2.65)–(2.69), it follows that:

$$\langle p_1\,p_2\rangle\,\langle p_3\,p_4\rangle = \langle p_1\,p_3\rangle\,\langle p_2\,p_4\rangle + \langle p_1\,p_4\rangle\,\langle p_3\,p_2\rangle\,, \tag{I.2.32}$$

$$[p_1\,p_2]\,[p_3\,p_4] = [p_1\,p_3]\,[p_2\,p_4] + [p_1\,p_4]\,[p_3\,p_2], \tag{I.2.33}$$

$$\langle p_1+|\sigma^\mu_+|p_2+\rangle\langle p_3+|\sigma_{+\mu}|p_4+\rangle = 2\,[p_1\,p_3]\,\langle p_4\,p_2\rangle\,, \tag{I.2.34}$$

$$\langle p_1-|\sigma^\mu_-|\,p_2-\rangle\langle p_3-|\sigma_{-\mu}|p_4-\rangle = 2\,\langle p_1\,p_3\rangle\,[p_4\,p_2], \tag{I.2.35}$$

$$\langle p_1+|\sigma^\mu_+|p_2+\rangle\langle p_3-|\sigma_{-\mu}|p_4-\rangle = 2\,[p_1\,p_4]\,\langle p_3\,p_2\rangle\,. \tag{I.2.36}$$

Eqs. (I.2.32) and (I.2.33) are often called the Schouten identities, as they follow from Eq. (2.26).

It is desirable to extend the spinor helicity formalism to multi-particle processes involving massless fermions and massless spin-1 bosons. In particular, XZC developed a simple technique for expressing the squares of the corresponding helicity amplitudes in terms of ratios of products of dot products. Their trick was to introduce a convenient expression for the massless spin-1 polarization vector in terms of products of massless spin-1/2 spinor wave functions. Before exhibiting their result, we provide a brief review of spin-1 polarization vectors in the helicity basis.

We first consider a massless spin-1 particle moving in the z-direction with four-momentum $k^\mu = E(1;0,0,1)$. The textbook expression for the helicity ±1 polarization vectors of a massless spin-1 boson is given by [254–256,329]:

$$\varepsilon^\mu(\hat{\boldsymbol{z}},\pm1) = \frac{1}{\sqrt{2}}\,(0;\mp1,-i,0)\,. \tag{I.2.37}$$

Note that the $\varepsilon^\mu(\hat{\boldsymbol{z}},\lambda)$ are normalized eigenvectors of the spin-1 operator $\vec{\boldsymbol{\mathcal{S}}}\cdot\hat{\boldsymbol{z}}$,

$$(\vec{\boldsymbol{\mathcal{S}}}\cdot\hat{\boldsymbol{z}})^\mu{}_\nu\,\varepsilon^\nu(\hat{\boldsymbol{z}},\lambda) = \lambda\,\varepsilon^\mu(\hat{\boldsymbol{z}},\lambda), \tag{I.2.38}$$

where $\mathcal{S}^i \equiv \frac{1}{2}\epsilon^{ijk}\mathcal{S}_{jk}$, and the matrix elements of the 4×4 matrices $\mathcal{S}_{jk}$ are given by Eq. (2.9).

If we transform $\varepsilon^\mu(\hat{\boldsymbol{z}},\lambda)$ by employing a three-dimensional rotation $\mathcal{R}$ such that $\hat{\boldsymbol{k}} = \mathcal{R}\,\hat{\boldsymbol{z}}$, then we can obtain the polarization vector for a massless spin-1 boson of energy E moving in the direction $\hat{\boldsymbol{k}} = (\sin\theta\cos\phi, \sin\theta\sin\phi, \cos\theta)$. That is,

$$\varepsilon^\mu(\hat{\boldsymbol{k}},\lambda) = \Lambda^\mu{}_\nu(\phi,\theta,\gamma)\,\varepsilon^\nu(\hat{\boldsymbol{z}},\lambda), \tag{I.2.39}$$

where

$$\Lambda^0{}_0 = 1, \qquad \Lambda^i{}_0 = \Lambda^0{}_i = 0, \quad \text{and} \quad \Lambda^i{}_j = \mathcal{R}^{ij}(\phi,\theta,\gamma), \tag{I.2.40}$$

and $\mathcal{R}(\phi,\theta,\gamma)$ is the rotation matrix introduced in Eq. (C.1.4). A simple computation yields:

$$\varepsilon^\mu(\hat{\boldsymbol{k}},\pm1) = \frac{1}{\sqrt{2}}\,e^{\mp i\gamma}\,(0; \mp\cos\theta\cos\phi + i\sin\phi, \mp\cos\theta\sin\phi - i\cos\phi, \pm\sin\theta)\,. \tag{I.2.41}$$

Note that $\varepsilon^\mu(\hat{\boldsymbol{k}},\pm1)$ depends only on the direction of $\vec{\boldsymbol{k}}$ and not on its magnitude $E = |\vec{\boldsymbol{k}}|$. One can easily check that the $\varepsilon^\mu(\hat{\boldsymbol{k}},\pm1)$ are normalized eigenstates of $\vec{\boldsymbol{s}}\cdot\hat{\boldsymbol{k}}$ with corresponding eigenvalues ±1.

Similar to the corresponding discussion in Appendix C for the spin-1/2 spinor wave functions, the Euler angle γ is arbitrary. In the literature, one typically finds conventions where $\gamma = -\phi$ [36,254,255] or $\gamma = 0$ [256], and we will consider both possibilities below.

Although we will not need it here, the expressions given by Eqs. (I.2.37) and (I.2.41) also apply in the case of a massive spin-1 particle. In addition, there is a helicity $\lambda = 0$ polarization vector which depends on the magnitude of the momentum as well as its direction:

$$\varepsilon^\mu(|\vec{\boldsymbol{k}}|\hat{\boldsymbol{z}},0) = (|\vec{\boldsymbol{k}}|/m; 0, 0, E/m), \tag{I.2.42}$$

where $E = (|\vec{\boldsymbol{k}}|^2 + m^2)^{1/2}$. One can use Eq. (I.2.39) to obtain the helicity zero polarization vector for a massive spin-1 particle moving in an arbitrary direction

$$\varepsilon^\mu(\vec{\boldsymbol{k}},0) = \frac{1}{m}\left(|\vec{\boldsymbol{k}}|; E\sin\theta\cos\phi, E\sin\theta\sin\phi, E\cos\theta\right). \tag{I.2.43}$$

Note that both the massless and massive spin-1 polarization vectors satisfy[158]:

$$\epsilon^\mu(k,\lambda)^* = (-1)^\lambda\epsilon^\mu(k,-\lambda). \tag{I.2.44}$$

One can check that the $\epsilon^\mu(k,\lambda)$ also satisfies the standard conditions for a valid polarization four-vector:

$$k\cdot\epsilon(k,\lambda) = 0, \qquad \epsilon(k,\lambda)\cdot\epsilon(k,\lambda')^* = -\delta_{\lambda\lambda'}. \tag{I.2.45}$$

If the spin-1 boson three-momentum is $-\vec{\boldsymbol{k}}$, then its polarization vector can be obtained from Eqs. (I.2.41) and (I.2.43) by taking $\theta \to \pi - \theta$ and $\phi \to \phi + \pi$. It can also be derived from Eqs. (I.2.39) and (I.2.40) by making use of the spin-1 analogue of Eq. (C.3.9),

$$\mathcal{R}(\phi+\pi, \pi-\theta, \gamma(-\hat{\boldsymbol{k}})) = \mathcal{R}(\phi,\theta,\gamma(\hat{\boldsymbol{k}}))\,R(\hat{\boldsymbol{z}}, -\gamma(\hat{\boldsymbol{k}}) - \gamma(-\hat{\boldsymbol{k}}))\,R(\hat{\boldsymbol{x}},\pi), \tag{I.2.46}$$

where we have exhibited the possible dependence of γ on the direction of $\hat{\boldsymbol{k}}$, and R is the rotation matrix given by Eq. (C.1.5). Introducing the notation $\varepsilon^\mu \equiv (\varepsilon^0; \hat{\boldsymbol{\varepsilon}})$, and noting the relations:

$$R(\hat{\boldsymbol{x}},\pi)\hat{\boldsymbol{\varepsilon}}(\hat{\boldsymbol{z}},\lambda) = -\hat{\boldsymbol{\varepsilon}}(\hat{\boldsymbol{z}},-\lambda), \tag{I.2.47}$$

$$R(\hat{\boldsymbol{z}},\beta)\hat{\boldsymbol{\varepsilon}}(\hat{\boldsymbol{z}},\lambda) = e^{-i\lambda\beta}\,\hat{\boldsymbol{\varepsilon}}(\hat{\boldsymbol{z}},\lambda), \tag{I.2.48}$$

it follows that:

$$\varepsilon^\mu(-\vec{\boldsymbol{k}},\lambda) = -g_{\mu\mu}\,\xi_{-\lambda}(\hat{\boldsymbol{k}})\,\varepsilon^\mu(\vec{\boldsymbol{k}},-\lambda), \qquad \lambda = 0,\pm1, \tag{I.2.49}$$

where there is no sum over the repeated index μ, and

$$\xi_\lambda(\hat{\boldsymbol{k}}) = -e^{i\lambda[\gamma(\hat{\boldsymbol{k}})+\gamma(-\hat{\boldsymbol{k}})]}, \quad \lambda = 0,\pm1. \tag{I.2.50}$$

158 Some authors introduce polarization vectors where the sign factor $(-1)^\lambda$ in Eq. (I.2.44) is omitted. One motivation for Eq. (I.2.44) is to maintain consistency with the Condon–Shortley phase conventions [330] for the eigenfunctions of the spin angular momentum operators $\vec{\boldsymbol{S}}^2$ and S_z (for spin-1 particles). In particular, note the relation $\hat{\boldsymbol{r}}\cdot\hat{\boldsymbol{\varepsilon}}^\mu(\hat{\boldsymbol{z}},\pm1) = (4\pi/3)^{1/2}Y_{1,\pm1}(\theta,\phi)$ between the polarization three-vector and the $\ell = 1$ spherical harmonics without any additional sign factors.

Note that for $\lambda = \pm 1$, the phase factor $\xi_\lambda(\hat{\boldsymbol{k}})$ depends on the convention for the definition of the Euler angle γ used to define the spin-1 polarization vector. As an example, corresponding to the two conventional choices for γ,

$$\xi_\lambda(\hat{\boldsymbol{k}}) = \begin{cases} (-1)^{1-\lambda} e^{-2i\lambda\phi} & \text{for } \gamma(\hat{\boldsymbol{k}}) = -\phi,\ \gamma(-\hat{\boldsymbol{k}}) = -\pi + \phi, \\ -1 & \text{for } \gamma(\hat{\boldsymbol{k}}) = \gamma(-\hat{\boldsymbol{k}}) = 0. \end{cases} \tag{I.2.51}$$

To motivate the XZC form for the massless spin-1 polarization vectors, we first introduce a four-vector

$$\widetilde{k}^\mu \equiv E(1; -\hat{\boldsymbol{k}}), \tag{I.2.52}$$

corresponding to the four-momentum $k^\mu = E(1; \hat{\boldsymbol{k}})$ of the massless spin-1 boson. A straightforward calculation then shows that

$$\epsilon^\mu(k, \pm 1) = \frac{1}{\sqrt{2}} \frac{\langle k \mp | \sigma_\mp^\mu | \widetilde{k} \mp \rangle}{\langle k \pm | \widetilde{k} \mp \rangle} \tag{I.2.53}$$

precisely reproduces the result of Eq. (I.2.41), where the massless spinor wave functions are defined according to Eq. (C.1.8). Eq. (I.2.53) is somewhat inconvenient because the four-vector $\widetilde{k}$ cannot be covariantly defined in terms of k. XZC finessed this problem by introducing a "reference" four-vector p (in practical computations, p is taken to be another four-momentum vector in the scattering process of interest), with the properties that $p^2 = 0$ and $p \cdot k \neq 0$. The XZC spin-1 polarization vectors are given by [cf. Eq. (2.33)][159]

$$\epsilon^\mu(k, \pm 1) = \frac{1}{\sqrt{2}} \frac{\langle k \mp | \sigma_\mp^\mu | p \mp \rangle}{\langle k \pm | p \mp \rangle}. \tag{I.2.54}$$

One can immediately check that $\epsilon^\mu(k, \lambda)$ so defined satisfy the standard conditions for a valid polarization four-vector given in Eq. (I.2.45) and the phase convention of Eq. (I.2.44). The representation of the massless spin-1 polarization vector in terms of spinor products [Eqs. (I.2.53) and (I.2.54)] is an application of the spinor calculus that was first developed by van der Waerden [1].

The significance of the reference four-vector p can be discerned from the property that if a different reference momentum is chosen then ϵ^μ is shifted by a factor proportional to k^μ. Explicitly, if $\varepsilon^\mu(k, p, \lambda)$ is a polarization vector with reference momentum p, then[160]

$$\varepsilon^\mu(k, q, \pm 1) = \varepsilon^\mu(k, p, \pm 1) + \frac{\sqrt{2}\,\langle q \pm | p \mp \rangle}{\langle k \pm | q \mp \rangle\, \langle k \pm | p \mp \rangle}\, k^\mu. \tag{I.2.55}$$

In particular, if we choose $q = \widetilde{k}$, we see that the difference of the XZC spin-1 polarization vector and the polarization vector given by Eq. (I.2.41) is proportional to k^μ. This shift of the reference momentum from p to q in the XZC definition of the polarization vector does not affect Eq. (I.2.45) since $k^2 = 0$ for massless spin-1 particles. Moreover, this shift does not affect the final result for any observable (in particular the sum of amplitudes of any gauge invariant set of Feynman diagrams remains unchanged). Thus, the presence of the arbitrary four-vector p just reflects the gauge invariance of the theory of massless spin-1 particles.

We can also verify that $\epsilon^\mu(k, p, \lambda)$ defined in Eq. (I.2.54) behaves as expected under rotations. Using Eq. (C.1.8), massless spinors transform as:

$$|k\pm\rangle \longrightarrow \mathcal{D}(\phi, \theta, \gamma)\, |k\pm\rangle\,, \qquad \langle k\pm| \longrightarrow \langle k\pm|\, [\mathcal{D}(\phi, \theta, \gamma)]^{-1}, \tag{I.2.56}$$

under a rotation specified by the Euler angles ϕ, θ and γ. We shall rotate the spin-1 polarization vectors by rotating both $\vec{\boldsymbol{k}}$ and the reference momentum $\vec{\boldsymbol{p}}$ simultaneously (since one is always free to shift the reference vector with no physical consequence). Using Eq. (C.1.33), it follows that:

$$[\mathcal{D}(\phi, \theta, \gamma)]^{-1}\, \sigma_\pm^\mu\, \mathcal{D}(\phi, \theta, \gamma) = \Lambda^\mu{}_\nu \sigma_\pm^\nu, \tag{I.2.57}$$

where $\Lambda^\mu{}_\nu$ is specified by Eq. (I.2.40). Indeed, if we simultaneously rotate both k and p via $k^\mu \to \Lambda^\mu{}_\nu k^\nu$ and $p^\mu \to \Lambda^\mu{}_\nu p^\nu$, then

$$\varepsilon^\mu(k, p, \lambda) \longrightarrow \Lambda^\mu{}_\nu\, \varepsilon^\mu(k, p, \lambda), \tag{I.2.58}$$

[159] In the literature on the spinor helicity method, the spin-1 polarization vector ε is employed in Feynman diagram computations for an *outgoing* final state boson, in contrast to the standard conventions of most quantum field theory textbooks. In this review, we subscribe to the latter [as indicated at the end of Section 4.1]. Hence, to be consistent with our conventions above for the spin-1 polarization vector, we have taken the complex conjugate of the original definition of the XZC spin-1 polarization vectors. In addition, we have removed an overall $\pm$ sign in order to conform to Eq. (I.2.44) [cf. footnote 158].

[160] To derive Eq. (I.2.55), evaluate $\varepsilon^\mu(k, q, \lambda) - \varepsilon^\mu(k, p, \lambda)$, and simplify the resulting expression using Eqs. (I.2.10), (I.2.13) and (I.2.14).

as expected. By a similar computation, one can check that under $\vec{k} \to -\vec{k}$ and $\vec{p} \to -\vec{p}$, Eq. (I.2.49) is satisfied.[161] In terms of the $\lambda_{\pm 1/2}$ defined in Eq. (C.3.12), we find

$$\xi_\lambda(\vec{k}) = -\left(\frac{\xi_{-\lambda/2}(\vec{k})}{\xi_{\lambda/2}(\vec{k})}\right)^* = \left[\xi_{\lambda/2}(\vec{k})\right]^2, \quad \lambda = \pm 1, \tag{I.2.59}$$

which agrees with Eq. (I.2.50).

The following additional properties of $\epsilon^\mu(k, p, \lambda)$ defined in Eq. (I.2.54) are noteworthy:

$$p \cdot \epsilon(k, p, \lambda) = 0, \tag{I.2.60}$$

$$\sum_{\lambda=\pm 1} \epsilon_\mu(k, p, \lambda)\epsilon_\nu(k, p, \lambda)^* = -g_{\mu\nu} + \frac{p_\mu k_\nu + p_\nu k_\mu}{p \cdot k}. \tag{I.2.61}$$

For example, to prove Eq. (I.2.61), we use Eqs. (I.2.18) and (I.2.19), and simplify the resulting expression with the help of Eqs. (I.2.10) and (I.2.16), which yields:

$$\sum_{\lambda=\pm 1} \epsilon_\mu(k, p, \lambda)\epsilon_\nu(k, p, \lambda)^* = \frac{\langle k+|\,(\sigma_\mu p \cdot \overline{\sigma}\sigma_\nu + \sigma_\nu p \cdot \overline{\sigma}\sigma_\mu)\,|k+\rangle}{2\,\langle k+|\,p \cdot \sigma\,|k+\rangle}. \tag{I.2.62}$$

Using Eq. (B.2.17) to simplify the product of three $\sigma/\overline{\sigma}$ matrices, and employing Eq. (I.2.11) then yields Eq. (I.2.61).

Finally, using the Fierz identities given in Eqs. (B.1.5)–(B.1.7), one derives from Eq. (I.2.54) that

$$\sigma_\pm \cdot \epsilon(k, \pm 1) = \frac{\sqrt{2}\,|p\mp\rangle\,\langle k\mp|}{\langle k \pm |p\mp\rangle}, \qquad \sigma_\pm \cdot \epsilon(k, \pm 1)^* = \frac{\sqrt{2}\,|k\mp\rangle\,\langle p\mp|}{\langle p \mp |k\pm\rangle}, \tag{I.2.63}$$

$$\sigma_\mp \cdot \epsilon(k, \pm 1) = \frac{\sqrt{2}\,|k\pm\rangle\,\langle p\pm|}{\langle k \pm |p\mp\rangle}, \qquad \sigma_\mp \cdot \epsilon(k, \pm 1)^* = \frac{\sqrt{2}\,|p\pm\rangle\,\langle k\pm|}{\langle p \mp |k\pm\rangle}. \tag{I.2.64}$$

Note that each equation in Eqs. (I.2.63) and (I.2.64) represents two separate equations, corresponding to the upper and lower signs in each equation, respectively.

It should now be clear how to convert the square of a helicity amplitude for a multi-particle process involving massless spin-1/2 and massless spin-1 particles into a ratio of products of dot products of momenta. By writing all massless spin-1 polarization vectors in the form of Eq. (I.2.54) and using the properties given above, the helicity amplitudes can easily be expressed as a ratio of two quantities, each of which is a product of spinor products. Squaring the corresponding amplitude then yields a ratio of products of dot products of four-momenta. A following simple example will demonstrate the technique.

Consider Compton scattering in QED, $e^-(\vec{p}_1, \lambda_1)\gamma(\vec{k}_1, \lambda_1') \to e^-(\vec{p}_2, \lambda_2)\gamma(\vec{k}_2, \lambda_2')$, in the limit of massless electrons. The amplitude for this process is given by Eq. (4.5.18) with $m = 0$ and $G_L = G_R = -e$. Writing out the "crossed" term explicitly, and noting that for massless particles, $s \equiv (p_1 + k_1)^2 = 2p_1 \cdot k_1$ and $u \equiv (p_1 - k_2)^2 = -2p_1 \cdot k_2$,

$$\begin{aligned} i\mathcal{M} = {} & \frac{-ie^2}{2p_1 \cdot k_1}\left\{x^\dagger(\vec{p}_2, \lambda_2)\,\overline{\sigma} \cdot \varepsilon_2^*\,\sigma \cdot (p_1 + k_1)\,\overline{\sigma} \cdot \varepsilon_1\,x(\vec{p}_1, \lambda_1) + y(\vec{p}_2, \lambda_2)\,\sigma \cdot \varepsilon_2^*\,\overline{\sigma} \cdot (p_1 + k_1)\,\sigma \cdot \varepsilon_1 y^\dagger(\vec{p}_1, \lambda_1)\right\} \\ & + \frac{ie^2}{2p_1 \cdot k_2}\left\{x^\dagger(\vec{p}_2, \lambda_2)\,\overline{\sigma} \cdot \varepsilon_1\,\sigma \cdot (p_1 - k_2)\,\overline{\sigma} \cdot \varepsilon_2^*\,x(\vec{p}_1, \lambda_1) + y(\vec{p}_2, \lambda_2)\,\sigma \cdot \varepsilon_1\,\overline{\sigma} \cdot (p_1 - k_2)\,\sigma \cdot \varepsilon_2^* y^\dagger(\vec{p}_1, \lambda_1)\right\}. \end{aligned} \tag{I.2.65}$$

The results of Eqs. (3.1.37)–(3.1.40) imply that the helicity amplitudes with $\lambda_1 \neq \lambda_2$ vanish. Using Eqs. (I.2.7) and (I.2.8), we identify:

$$\begin{aligned} i\mathcal{M}\left(\lambda_1 = \lambda_2 = \tfrac{1}{2}\right) &= \frac{-ie^2}{2p_1 \cdot k_1}\left\langle p_2 + |\sigma_+ \cdot \varepsilon_2^*\,\sigma_- \cdot (p_1 + k_1)\,\sigma_+ \cdot \varepsilon_1 |p_1 +\right\rangle \\ &\quad + \frac{ie^2}{2p_1 \cdot k_2}\left\langle p_2 + |\sigma_+ \cdot \varepsilon_1\,\sigma_- \cdot (p_1 - k_2)\,\sigma_+ \cdot \varepsilon_2^* |p_1 +\right\rangle, \end{aligned} \tag{I.2.66}$$

$$\begin{aligned} i\mathcal{M}\left(\lambda_1 = \lambda_2 = -\tfrac{1}{2}\right) &= \frac{-ie^2}{2p_1 \cdot k_1}\left\langle p_2 - |\sigma_- \cdot \varepsilon_2^*\,\sigma_+ \cdot (p_1 + k_1)\,\sigma_- \cdot \varepsilon_1 |p_1 -\right\rangle \\ &\quad + \frac{ie^2}{2p_1 \cdot k_2}\left\langle p_2 - |\sigma_- \cdot \varepsilon_1\,\sigma_+ \cdot (p_1 - k_2)\,\sigma_- \cdot \varepsilon_2^* |p_1 -\right\rangle. \end{aligned} \tag{I.2.67}$$

[161] Here, we have used Eqs. (B.2.16) and (B.2.17) to write $\sigma_\pm^0\sigma_\mp^\mu\sigma_\pm^0 = -\sigma_\pm^\mu + 2g^{\mu 0}\sigma_\pm^0 = g^{\mu\mu}\sigma_\pm^\mu$ (no sum over μ).

Further simplification ensues when we apply the results of Eqs. (I.2.63) and (I.2.64). To use these results, we must select a reference momentum p, which can be any lightlike four-vector that is not parallel to the corresponding photon polarization vector. One is free to choose a different reference momentum for each photon polarization vector. Moreover, when computing two different helicity amplitudes (each of which are gauge invariant quantities), one may select a different reference momentum for the *same* photon polarization vector in the two computations. The decision on which reference momenta to choose is somewhat of an art; experience will teach you which choices lead to the most simplification in a given calculation.

We shall consider two possible choices for the reference momenta for ε_1 and ε_2, which we denote as $p^{(1)}$ and $p^{(2)}$, respectively:

1. $p^{(1)} = p_1$ and $p^{(2)} = p_2$,
2. $p^{(1)} = p_2$ and $p^{(2)} = p_1$.

With either choice, it is straightforward to show that $\mathcal{M}(\lambda_1 = \lambda_2 = \pm\frac{1}{2})$ vanish unless the photon helicities are equal, i.e. $\lambda_1' = \lambda_2'$. This leaves only four possible non-vanishing helicity amplitudes.

For the case of $\lambda_1 = \lambda_2 = \pm\frac{1}{2}$ and $\lambda_1' = \lambda_2' = \pm 1$ (i.e., $\lambda_1\lambda_1' > 0$), we choose reference momenta $p^{(1)} = p_2$ and $p^{(2)} = p_1$. Then, the second term vanishes on the right-hand side of Eqs. (I.2.66) and (I.2.67), respectively. Making use of Eqs. (I.2.10), (I.2.63) and (I.2.64), we find

$$i\mathcal{M}\left(\lambda_1 = \lambda_2 = \tfrac{1}{2}, \lambda_1' = \lambda_2' = 1\right) = \frac{-ie^2}{p_1\cdot k_1}\frac{\langle p_2+|k_2-\rangle\ \langle p_1-|k_1+\rangle\ \langle k_1+|p_2-\rangle\ \langle k_1-|p_1+\rangle}{\langle p_1-|k_2+\rangle\ \langle k_1+|p_2-\rangle}$$
$$= \frac{-ie^2}{p_1\cdot k_1}\frac{\langle p_1\,k_1\rangle\,\langle k_1\,p_1\rangle\,[p_2\,k_2]}{\langle p_1\,k_2\rangle}. \tag{I.2.68}$$

Using Eqs. (I.2.24) and (I.2.30) to write the dot product in terms of spinor products, we obtain:

$$i\mathcal{M}\left(\lambda_1 = \lambda_2 = \tfrac{1}{2}, \lambda_1' = \lambda_2' = 1\right) = 2ie^2\frac{\langle p_1\,k_1\rangle}{\langle p_1\,k_1\rangle^*}\frac{[p_2\,k_2]}{\langle p_1\,k_2\rangle}. \tag{I.2.69}$$

A similar computation yields

$$i\mathcal{M}\left(\lambda_1 = \lambda_2 = -\tfrac{1}{2}, \lambda_1' = \lambda_2' = -1\right) = 2ie^2\frac{[p_1\,k_1]}{[p_1\,k_1]^*}\frac{\langle p_2\,k_2\rangle}{[p_1\,k_2]}. \tag{I.2.70}$$

For the case of $\lambda_1 = \lambda_2 = \pm\frac{1}{2}$ and $\lambda_1' = \lambda_2' = \mp 1$ (i.e., $\lambda_1\lambda_1' < 0$), we choose reference momenta $p^{(1)} = p_1$ and $p^{(2)} = p_2$. Then, the first term vanishes on the right-hand side of Eqs. (I.2.69) and (I.2.70), respectively. A similar calculation to the one given above yields:

$$i\mathcal{M}\left(\lambda_1 = \lambda_2 = -\tfrac{1}{2}, \lambda_1' = \lambda_2' = 1\right) = 2ie^2\frac{[p_1\,k_2]}{[p_1\,k_2]^*}\frac{\langle p_2\,k_1\rangle}{[p_1\,k_1]}, \tag{I.2.71}$$

$$i\mathcal{M}\left(\lambda_1 = \lambda_2 = \tfrac{1}{2}, \lambda_1' = \lambda_2' = -1\right) = 2ie^2\frac{\langle p_1\,k_2\rangle}{\langle p_1\,k_2\rangle^*}\frac{[p_2\,k_1]}{\langle p_1\,k_1\rangle}. \tag{I.2.72}$$

Note that each pair of helicity amplitudes above is simply related:

$$\mathcal{M}_{\lambda_1,\lambda_1';\lambda_2,\lambda_2'}(s,\theta,\phi)^* = \mathcal{M}_{-\lambda_1,-\lambda_1';-\lambda_2,-\lambda_2'}(s,\theta,\phi), \tag{I.2.73}$$

which is a consequence of rotational and parity invariance (as shown below). Thus in this example, we only need to evaluate two non-zero helicity amplitudes. It is clear that we have simplified the computation enormously by our choice of reference momenta. With a less judicious choice, the calculation is significantly more tedious, although gauge invariance guarantees that one must arrive at the same result for the helicity amplitudes quoted above.

One can easily evaluate the spinor products above in the center-of-mass system. Writing $p_1^\mu = E(1;\hat{\boldsymbol{z}})$, $k_1^\mu = E(1;-\hat{\boldsymbol{z}})$, $p_2^\mu = E(1;\hat{\boldsymbol{p}}_{\rm CM})$ and $k_2^\mu = E(1;-\hat{\boldsymbol{p}}_{\rm CM})$, and using the results of Eqs. (I.1.21) and (I.2.22), we obtain:

$$\langle p_1\,k_1\rangle = 2E\xi_{-1/2}(\hat{\boldsymbol{z}}), \qquad \langle p_1\,k_2\rangle = 2Ee^{i[\phi+\gamma(\hat{\boldsymbol{p}}_{\rm CM})]/2}\xi_{-1/2}(\hat{\boldsymbol{p}}_{\rm CM})\cos(\theta/2), \tag{I.2.74}$$

$$\langle p_2\,k_2\rangle = 2E\xi_{-1/2}(\hat{\boldsymbol{p}}_{\rm CM}), \qquad \langle p_2\,k_1\rangle = 2Ee^{-i[\phi+\gamma(\hat{\boldsymbol{p}}_{\rm CM})]/2}\xi_{-1/2}(\hat{\boldsymbol{z}})\cos(\theta/2), \tag{I.2.75}$$

where θ and ϕ are the polar and azimuthal angles of $\hat{\boldsymbol{p}}_{\rm CM}$. Phase factors involving $\xi_{-1/2}$ arise from the use of Eqs. (C.3.11) and (C.3.12). For example, corresponding to the two conventional choices for γ, we use Eq. (C.3.15) to obtain

$$\xi_{-1/2}(\hat{\boldsymbol{z}}) = \begin{cases} -1 & \text{for } \gamma(\hat{\boldsymbol{z}}) = 0,\ \gamma(-\hat{\boldsymbol{z}}) = -\pi, \\ i & \text{for } \gamma(\hat{\boldsymbol{z}}) = \gamma(-\hat{\boldsymbol{z}}) = 0, \end{cases} \tag{I.2.76}$$

$$\xi_{-1/2}(\hat{\boldsymbol{p}}_{\rm CM}) = \begin{cases} -e^{i\phi} & \text{for } \gamma(\hat{\boldsymbol{p}}) = -\phi,\ \gamma(-\hat{\boldsymbol{p}}) = -\pi+\phi \\ i & \text{for } \gamma(\hat{\boldsymbol{p}}) = \gamma(-\hat{\boldsymbol{p}}) = 0. \end{cases} \tag{I.2.77}$$

All other relevant spinor products can be found using Eqs. (I.2.24)–(I.2.26).

It is always possible to define the plane of the scattering process to be the x–z plane, in which case $\phi = 0$ and all the spinor products in Eqs. (I.2.74) and (I.2.75) are manifestly real. Nevertheless, by keeping the explicit ϕ-dependence, one maintains a useful check of the calculation. Inserting the explicit forms for the spinor products into Eqs. (I.2.69)–(I.2.72), we confirm that the ϕ-dependence of the helicity amplitudes is given by [256,331]:

$$\mathcal{M}_{\lambda_1,\lambda_1';\lambda_2,\lambda_2'}(s,\theta,\phi) = \begin{cases} e^{i(\lambda_1-\lambda_1'-\lambda_2-\lambda_2')\phi}\mathcal{M}_{\lambda_1,\lambda_1';\lambda_2,\lambda_2'}(s,\theta), & \text{for } \gamma(\hat{\boldsymbol{p}}_{\rm CM}) = -\phi, \text{ and } \gamma(-\hat{\boldsymbol{p}}_{\rm CM}) = -\pi+\phi, \\ e^{i(\lambda_1-\lambda_1')\phi}\mathcal{M}_{\lambda_1,\lambda_1';\lambda_2,\lambda_2'}(s,\theta), & \text{for } \gamma(\hat{\boldsymbol{p}}_{\rm CM}) = \gamma(-\hat{\boldsymbol{p}}_{\rm CM}) = 0, \end{cases} \tag{I.2.78}$$

as a consequence of rotational invariance [257].[162] The remaining θ-dependent amplitudes are easily evaluated and are in agreement with the results of Refs. [256,332]. Note that parity invariance implies that Eqs. (I.2.69)–(I.2.72) must satisfy [256,257,332]

$$\mathcal{M}_{\lambda_1,\lambda_1';\lambda_2,\lambda_2'}(s,\theta) = \mathcal{M}_{-\lambda_1,-\lambda_1';-\lambda_2,-\lambda_2'}(s,\theta). \tag{I.2.79}$$

Indeed, in our computation above, Eq. (I.2.73) is satisfied, which is consistent with Eq. (I.2.79) in light of Eq. (I.2.78).

To compute the unpolarized cross-section for Compton scattering, one must sum the absolute squares of the helicity amplitudes and divide by 4 to average over the initial helicities. Since quantities such as $\langle p_1\, k_1\rangle \,/\, \langle p_1\, k_1\rangle^*$ are pure phases, one immediately obtains:

$$\left|\mathcal{M}\left(\lambda_1=\lambda_2=\tfrac{1}{2},\lambda_1'=\lambda_2'=1\right)\right|^2 = \left|\mathcal{M}\left(\lambda_1=\lambda_2=-\tfrac{1}{2},\lambda_1'=\lambda_2'=-1\right)\right|^2 = 4e^4\frac{p_1\cdot k_1}{p_1\cdot k_2}, \tag{I.2.80}$$

$$\left|\mathcal{M}\left(\lambda_1=\lambda_2=-\tfrac{1}{2},\lambda_1'=\lambda_2'=1\right)\right|^2 = \left|\mathcal{M}\left(\lambda_1=\lambda_2=\tfrac{1}{2},\lambda_1'=\lambda_2'=-1\right)\right|^2 = 4e^4\frac{p_1\cdot k_2}{p_1\cdot k_1}, \tag{I.2.81}$$

after employing Eq. (I.2.30) and noting that $p_1\cdot k_1 = p_2\cdot k_2$ and $p_1\cdot k_2 = p_2\cdot k_1$ (which follow from four-momentum conservation, $p_1+k_1 = p_2+k_2$, for the scattering of massless particles). Thus,

$$\tfrac{1}{4}\sum_{\rm spins}|\mathcal{M}|^2 = 2e^4\left(\frac{p_1\cdot k_1}{p_1\cdot k_2}+\frac{p_1\cdot k_2}{p_1\cdot k_1}\right), \tag{I.2.82}$$

which coincides with the well-known result quoted in Ref. [114].

Appendix J. The Standard Model and its seesaw extension

In the Standard Model, three generations of quarks and leptons are described by the two-component fermion fields listed in Table J.1, where Y is the weak hypercharge, T_3 is the third component of the weak isospin, and $Q = T_3 + Y$ is the electric charge. After $\mathrm{SU}(2)_L \times \mathrm{U}(1)_Y$ breaking, the quark and lepton fields gain mass in such a way that the above two-component fields combine to make up four-component Dirac fermions:

$$U_i = \begin{pmatrix} u_i \\ \bar{u}^{\dagger i}\end{pmatrix}, \qquad D_i = \begin{pmatrix} d_i \\ \bar{d}^{\dagger i}\end{pmatrix}, \qquad L_i = \begin{pmatrix} \ell_i \\ \bar{\ell}^{\dagger i}\end{pmatrix}, \tag{J.1}$$

while the neutrinos ν_i remain massless. The extension of the Standard Model to include neutrino masses will be treated in Appendix J.2.

Here, we follow the convention for particle symbols established in Table 5.1. Note that u, $\bar{u}$, d, $\bar{d}$, ℓ and $\bar{\ell}$ are two-component fields, whereas the usual four-component quark and charged lepton fields are denoted by capital letters U, D and E. Consider a generic four-component field expressed in terms of the corresponding two-component fields:

$$F = \begin{pmatrix} f \\ \bar{f}^{\dagger}\end{pmatrix}. \tag{J.2}$$

The electroweak quantum numbers of f are denoted by T_3^f, Y_f and Q_f, whereas the corresponding quantum numbers for $\bar{f}$ are $T_3^{\bar{f}} = 0$ and $Q_{\bar{f}} = Y_{\bar{f}} = -Q_f$. Thus we have the correspondence to our general notation [Eq. (G.1.6)]

$$f \longleftrightarrow \chi, \qquad \bar{f} \longleftrightarrow \eta. \tag{J.3}$$

We can then immediately translate the couplings given in the general case in Fig. 4.3.3 to the Standard Model.

[162] In the first case, where $\gamma(\hat{\boldsymbol{p}}_{\rm CM}) = -\phi$ and $\gamma(-\hat{\boldsymbol{p}}_{\rm CM}) = -\pi+\phi$, the sign of λ_2' in the ϕ-dependent phase factor of Eq. (I.2.78) is opposite to the one given in Ref. [257], due to the Jacob–Wick second-particle convention, which we do not employ here. Since $\lambda_1 = \lambda_2$ and $\lambda_1' = \lambda_2'$, the latter would imply that the ϕ-dependent phase cancels exactly if the Jacob–Wick second-particle convention is used. This is easily checked by putting $\gamma(\hat{\boldsymbol{p}}_{\rm CM}) = -\phi$ and $\xi_\lambda = 1$ in Eqs. (I.2.74) and (I.2.75), in which case all the spinor products are real.

Table J.1
Fermions of the Standard Model (following the naming conventions of Table 5.1) and their SU(3) × SU(2)$_L$ × U(1)$_Y$ quantum numbers. The generation indices run over $i = 1, 2, 3$. Color indices for the quarks are suppressed. The bars on the two-component antifermion fields are part of their names, and do not denote some form of complex conjugation.

Two-component fermion fields	SU(3)	SU(2)$_L$	Y	T_3	$Q = T_3 + Y$
$\boldsymbol{Q}_i \equiv \begin{pmatrix} u_i \\ d_i \end{pmatrix}$	triplet	doublet	$\frac{1}{6}$	$\frac{1}{2}$	$\frac{2}{3}$
	triplet		$\frac{1}{6}$	$-\frac{1}{2}$	$-\frac{1}{3}$
$\bar{u}^i$	anti-triplet	singlet	$-\frac{2}{3}$	0	$-\frac{2}{3}$
$\bar{d}^i$	anti-triplet	singlet	$\frac{1}{3}$	0	$\frac{1}{3}$
$\boldsymbol{L}_i \equiv \begin{pmatrix} \nu_i \\ \ell_i \end{pmatrix}$	singlet	doublet	$-\frac{1}{2}$	$\frac{1}{2}$	0
	singlet		$-\frac{1}{2}$	$-\frac{1}{2}$	-1
$\bar{\ell}^i$	singlet	singlet	1	0	1

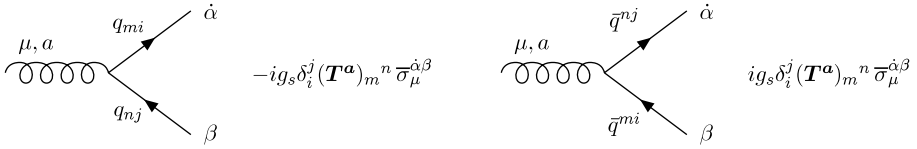

Fig. J.1.1. Fermionic Feynman rules for QCD that involve the gluon, with $q = u, d, c, s, t, b$. Lowered (raised) indices m, n correspond to the fundamental (anti-fundamental) representation of $SU(3)_c$. The gluon interactions are flavor-diagonal (where i, j are flavor indices). For each rule, a corresponding one with lowered spinor indices is obtained by $\overline{\sigma}_\mu^{\dot{\alpha}\beta} \to -\sigma_{\mu\beta\dot{\alpha}}$.

J.1. Standard Model fermion interaction vertices

The QCD color interactions of the quarks are governed by the following interaction Lagrangian:

$$\mathscr{L}_{\rm int} = -g_s A_a^\mu q^{\dagger mi}\,\overline{\sigma}_\mu (\boldsymbol{T}^a)_m{}^n q_{ni} + g_s A_a^\mu \bar{q}^\dagger_{ni}\,\overline{\sigma}_\mu (\boldsymbol{T}^a)_m{}^n \bar{q}^{mi}, \tag{J.1.1}$$

summed over the generations i, where q is a (mass-eigenstate) quark field, m and n are SU(3) color triplet indices, A_a^μ is the gluon field (with the corresponding gluons denoted by g_a), and $\boldsymbol{T}^a$ are the color generators in the triplet representation of SU(3). The corresponding Feynman rules are given in Fig. J.1.1.

Next, we write out the Feynman rules for the electroweak interactions of quarks and leptons. Using Eqs. (4.3.11) and (4.3.12), the interactions of the gauge bosons and quarks are given by:

$$\begin{aligned}\mathscr{L}_{\rm int} = &-\frac{g}{\sqrt{2}}\left[(\hat{u}^{\dagger i}\overline{\sigma}^\mu \hat{d}_i + \hat{\nu}^{\dagger i}\overline{\sigma}^\mu \hat{\ell}_i)W_\mu^+ + (\hat{d}^{\dagger i}\overline{\sigma}^\mu \hat{u}_i + \hat{\ell}^{\dagger i}\overline{\sigma}^\mu \hat{\nu}_i)W_\mu^-\right] \\ &-\frac{g}{c_W}\sum_{f=u,d,\nu,\ell}\left\{(T_3^f - s_W^2 Q_f)\hat{f}^{\dagger i}\overline{\sigma}^\mu \hat{f}_i + s_W^2 Q_f \hat{\bar{f}}^{\dagger i}\overline{\sigma}^\mu \hat{\bar{f}}_i\right\} Z_\mu - e\sum_{f=u,d,\ell} Q^f(\hat{f}^{\dagger i}\overline{\sigma}^\mu \hat{f}_i - \hat{\bar{f}}^{\dagger i}\overline{\sigma}^\mu \hat{\bar{f}}_i)A_\mu,\end{aligned} \tag{J.1.2}$$

where $s_W \equiv \sin\theta_W$, $c_W \equiv \cos\theta_W$, the hatted symbols indicate fermion interaction eigenstates and i labels the generations. Following the discussion of Section 3.2, we must convert from fermion interaction eigenstates to mass eigenstates. In order to accomplish this step, we must first identify the quark and lepton mass matrices. In the electroweak theory, the fermion mass matrices originate from the fermion–Higgs Yukawa interactions.

The Higgs field of the Standard Model is a complex SU(2)$_L$ doublet of hypercharge $Y = \frac{1}{2}$,

$$\boldsymbol{\Phi}_a \equiv \begin{pmatrix} \Phi^+ \\ \Phi^0 \end{pmatrix}, \tag{J.1.3}$$

where the SU(2)$_L$ index $a = 1, 2$ is defined such that $\boldsymbol{\Phi}_1 \equiv \Phi^+$ and $\boldsymbol{\Phi}_2 \equiv \Phi^0$. Here, the superscripts + and 0 refer to the electric charge of the Higgs field, $Q = T_3 + Y$, with $Y = \frac{1}{2}$ and $T_3 = \pm\frac{1}{2}$. Since $\boldsymbol{\Phi}_a$ is complex, we can also introduce the complex conjugate Higgs doublet field with hypercharge $Y = -\frac{1}{2}$,

$$\boldsymbol{\Phi}^{\dagger a} \equiv \left(\Phi^-, (\Phi^0)^\dagger\right), \tag{J.1.4}$$

where $\Phi^- \equiv (\Phi^+)^\dagger$. The SU(2)$_L$ × U(1)$_Y$ gauge invariant Yukawa interactions of the quarks and leptons with the Higgs field are then given by:

$$\mathscr{L}_{\rm Y} = \epsilon^{ab}(\boldsymbol{Y}_u)^i{}_j \boldsymbol{\Phi}_a \hat{\boldsymbol{Q}}_{bi}\bar{u}^j - (\boldsymbol{Y}_d)^i{}_j \boldsymbol{\Phi}^{\dagger a}\hat{\boldsymbol{Q}}_{ai}\hat{\bar{d}}^j - (\boldsymbol{Y}_\ell)^i{}_j \boldsymbol{\Phi}^{\dagger a}\hat{\boldsymbol{L}}_{ai}\hat{\bar{\ell}}^j + \text{h.c.} \tag{J.1.5}$$

where ϵ^{ab} is the antisymmetric invariant tensor of $SU(2)_L$, defined such that $\epsilon^{12} = -\epsilon^{21} = +1$. Using the definitions of the $SU(2)_L$ doublet quark and lepton fields given in Table J.1, one can rewrite Eq. (J.1.5) more explicitly as:

$$-\mathscr{L}_Y = (\boldsymbol{Y}_u)^i{}_j \left[\Phi^0 \hat{u}_i \hat{\bar{u}}^j - \Phi^+ \hat{d}_i \hat{\bar{u}}^j\right] + (\boldsymbol{Y}_d)^i{}_j \left[\Phi^- \hat{u}_i \hat{\bar{d}}^j + \Phi^{0*} \hat{d}_i \hat{\bar{d}}^j\right] + (\boldsymbol{Y}_\ell)^i{}_j \left[\Phi^- \hat{\nu}_i \hat{\bar{\ell}}^j + \Phi^{0*} \hat{\ell}_i \hat{\bar{\ell}}^j\right] + \text{h.c.} \tag{J.1.6}$$

The Higgs fields can be written in terms of the physical Higgs scalar h_{SM} and Nambu–Goldstone bosons G^0, $G^\pm$ as

$$\Phi^0 = v + \frac{1}{\sqrt{2}}(h_{SM} + iG^0), \tag{J.1.7}$$

$$\Phi^+ = G^+ = (\Phi^-)^\dagger = (G^-)^\dagger. \tag{J.1.8}$$

where $v = \sqrt{2} m_W/g \simeq 174$ GeV. In the unitary gauge appropriate for tree-level calculations, the Nambu–Goldstone bosons become infinitely heavy and decouple. We identify the quark and lepton mass matrices by setting $\Phi^0 = v$ and $\Phi^+ = \Phi^- = 0$ in Eq. (J.1.6):

$$(\boldsymbol{M}_u)^i{}_j = v(\boldsymbol{Y}_u)^i{}_j, \qquad (\boldsymbol{M}_d)^i{}_j = v(\boldsymbol{Y}_d)^i{}_j, \qquad (\boldsymbol{M}_\ell)^i{}_j = v(\boldsymbol{Y}_\ell)^i{}_j. \tag{J.1.9}$$

The neutrinos remain massless. An extension of the Standard Model that incorporates massive neutrinos is treated in Appendix J.2.

To diagonalize the quark and lepton mass matrices, we introduce four unitary matrices for the quark mass diagonalization, L_u, L_d, R_u and R_d, and two unitary matrices for the lepton mass diagonalization, L_ℓ and R_ℓ [cf. Eq. (3.2.31)] such that

$$\hat{u}_i = (L_u)_i{}^j u_j, \qquad \hat{d}_i = (L_d)_i{}^j d_j, \qquad \hat{\bar{u}}^i = (R_u)^i{}_j \bar{u}^j, \qquad \hat{\bar{d}}^i = (R_d)^i{}_j \bar{d}^j, \tag{J.1.10}$$

$$\hat{\ell}_i = (L_\ell)_i{}^j \ell_j, \qquad \hat{\bar{\ell}}^i = (R_\ell)^i{}_j \bar{\ell}^j, \tag{J.1.11}$$

where the unhatted fields u, d, $\bar{u}$ and $\bar{d}$ are the corresponding quark mass eigenstates and ν, ℓ and $\bar{\ell}$ are the corresponding lepton mass eigenstates. The fermion mass diagonalization procedure consists of the singular value decomposition of the quark and lepton mass matrices:

$$L_u^\dagger \boldsymbol{M}_u R_u = \text{diag}(m_u, m_c, m_t), \tag{J.1.12}$$

$$L_d^\dagger \boldsymbol{M}_d R_d = \text{diag}(m_d, m_s, m_b), \tag{J.1.13}$$

$$L_\ell^\dagger \boldsymbol{M}_\ell R_\ell = \text{diag}(m_e, m_\mu, m_\tau), \tag{J.1.14}$$

where the diagonalized masses are real and non-negative (cf. Appendix D.1). Since the neutrinos are massless, we are free to define the physical neutrino fields, ν_i, as the weak SU(2) partners of the corresponding charged lepton mass-eigenstate fields. That is,

$$\hat{\nu}_i = (L_\ell)_i{}^j \nu_j. \tag{J.1.15}$$

We can now write out the couplings of the mass-eigenstate quarks and leptons to the gauge bosons and Higgs bosons. Consider first the charged current interactions of the quarks and leptons. Using Eq. (J.1.10), it follows that $\hat{u}^{\dagger i} \overline{\sigma}^\mu \hat{d}_i = \boldsymbol{K}_i{}^j u^{\dagger i} \overline{\sigma}^\mu d_j$, where

$$\boldsymbol{K} = L_u^\dagger L_d \tag{J.1.16}$$

is the unitary Cabibbo–Kobayashi–Maskawa (CKM) matrix [333].[163] Due to Eq. (J.1.15), the corresponding leptonic CKM matrix is the unit matrix. Hence, the charged current interactions take the form

$$\mathscr{L}_{\text{int}} = -\frac{g}{\sqrt{2}} \left[\boldsymbol{K}_i{}^j u^{\dagger i} \overline{\sigma}^\mu d_j W_\mu^+ + (\boldsymbol{K}^\dagger)_i{}^j d^{\dagger i} \overline{\sigma}^\mu u_j W_\mu^- + \nu^{\dagger i} \overline{\sigma}^\mu \ell_i W_\mu^+ + \ell^{\dagger i} \overline{\sigma}^\mu \nu_i W_\mu^-\right], \tag{J.1.17}$$

where $[\boldsymbol{K}^\dagger]_i{}^j \equiv [\boldsymbol{K}_j{}^i]^*$. Note that in the Standard Model, $\bar{u}$, $\bar{d}$ and $\bar{\ell}$ do not couple to the $W^\pm$.

To obtain the neutral current interactions, we insert Eqs. (J.1.10)–(J.1.15) into Eq. (J.1.2). All factors of the *unitary* matrices L_f and R_f ($f = u, d, \ell$) cancel out, and the resulting interactions are flavor-diagonal. That is, we may simply remove the hats from the quark and lepton fields that couple to the Z and photon fields in Eq. (J.1.2). This is the well-known Glashow–Iliopoulos–Maiani (GIM) mechanism for the flavor-conserving neutral currents [335].[164]

163 The CKM matrix elements V_{ij} as defined in Ref. [334] are related by, for example, $V_{tb} = \boldsymbol{K}_3{}^3$ and $V_{us} = \boldsymbol{K}_1{}^2$.

164 This also provides the justification for employing mass-eigenstate quark fields in the QCD interaction Lagrangian in Eq. (J.1.1).

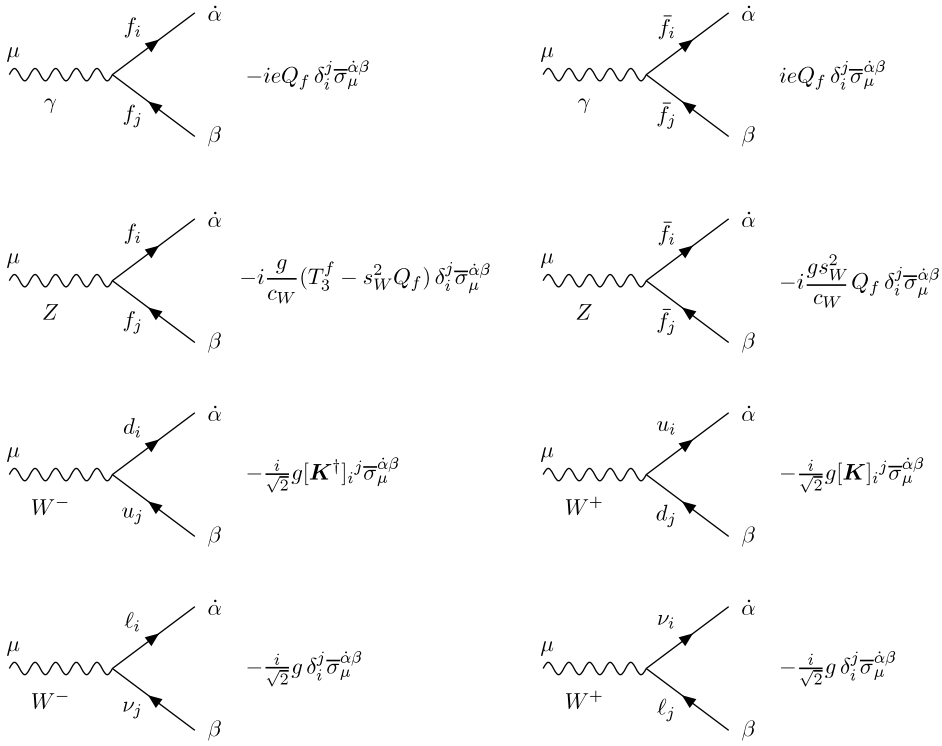

Fig. J.1.2. Feynman rules for the two-component fermion interactions with electroweak gauge bosons in the Standard Model. The couplings of the fermions to γ and Z are flavor-diagonal. In all couplings, i and j label the fermion generations; an upper [lowered] flavor index in the corresponding Feynman rule is associated with a fermion line that points into [out from] the vertex. For the $W^\pm$ bosons, the charge indicated is flowing into the vertex. The electric charge is denoted by Q_f (in units of $e>0$), with $Q_e=-1$ for the electron. $T_3^f=1/2$ for $f=u,\nu$, and $T_3^f=-1/2$ for $f=d,\ell$. The CKM mixing matrix is denoted by $\boldsymbol{K}$, and $s_W\equiv\sin\theta_W$, $c_W\equiv\cos\theta_W$ and $e\equiv g\sin\theta_W$. For each rule, a corresponding one with lowered spinor indices is obtained by $\overline\sigma_\mu^{\dot\alpha\beta}\to-\sigma_{\mu\beta\dot\alpha}$.

The Feynman rules for the interactions of the quarks and leptons with the charged and neutral gauge bosons are exhibited in Fig. J.1.2. For each of the rules of Fig. J.1.2, we have chosen to employ $\overline\sigma_\mu^{\dot\alpha\beta}$. If the indices are lowered one should take $\overline\sigma_\mu^{\dot\alpha\beta}\to-\sigma_{\mu\beta\dot\alpha}$.

Finally, we exhibit the interactions of the quark and lepton mass eigenstates with the Higgs fields. The diagonalization of the fermion mass matrices is equivalent to the diagonalization of the Yukawa couplings [cf. Eqs. (J.1.9) and (J.1.12)–(J.1.14)]. Thus, we define[165]

$$Y_{fi}=m_{fi}/v,\qquad f=u,d,\ell, \tag{J.1.18}$$

where i labels the fermion generation. It is convenient to rewrite Eqs. (J.1.12)–(J.1.14) as follows:

$$(L_f)_k{}^j(\boldsymbol{Y}_f)^k{}_m(R_f)^m{}_i=Y_{fi}\delta_i^j,\qquad f=u,d,\ell, \tag{J.1.19}$$

with no sum over the repeated index i. Using the unitarity of L_f ($f=u,d$), Eq. (J.1.19) is equivalent to the following convenient form:

$$(\boldsymbol{Y}_fR_f)^k{}_i=Y_{fi}(L_f^\dagger)_i{}^k. \tag{J.1.20}$$

Inserting Eqs. (J.1.10), (J.1.15) and (J.1.19) into Eq. (J.1.6), the resulting Higgs–fermion Lagrangian is flavor-diagonal:

$$\mathscr{L}_{\rm int}=-\frac{1}{\sqrt2}h_{\rm SM}\left[Y_{ui}u_i\bar u^i+Y_{di}d_i\bar d^i+Y_{\ell i}\ell_i\bar\ell^i\right]+\text{h.c.} \tag{J.1.21}$$

The corresponding Feynman rules for the Higgs–fermion interaction are shown in Fig. J.1.3.

In the case of more general covariant gauge-fixing (e.g., the 't Hooft–Feynman gauge or Landau gauge), the Goldstone bosons appear explicitly in internal lines of Feynman diagrams. The Feynman rules for G^0–fermion interactions are flavor-diagonal, whereas the corresponding rules for $G^\pm$ exhibit flavor-changing interactions that depend on the CKM matrix

165 Boldfaced symbols are used for the non-diagonal Yukawa matrices, while non-boldfaced symbols are used for the diagonalized Yukawa couplings.

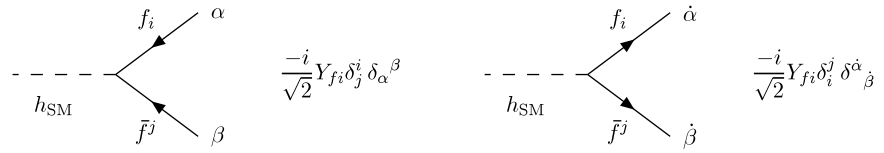

Fig. J.1.3. Feynman rules for the Standard Model Higgs boson interactions with fermions, where $Y_{fi} \equiv m_{fi}/v$, and i, j label the generations.

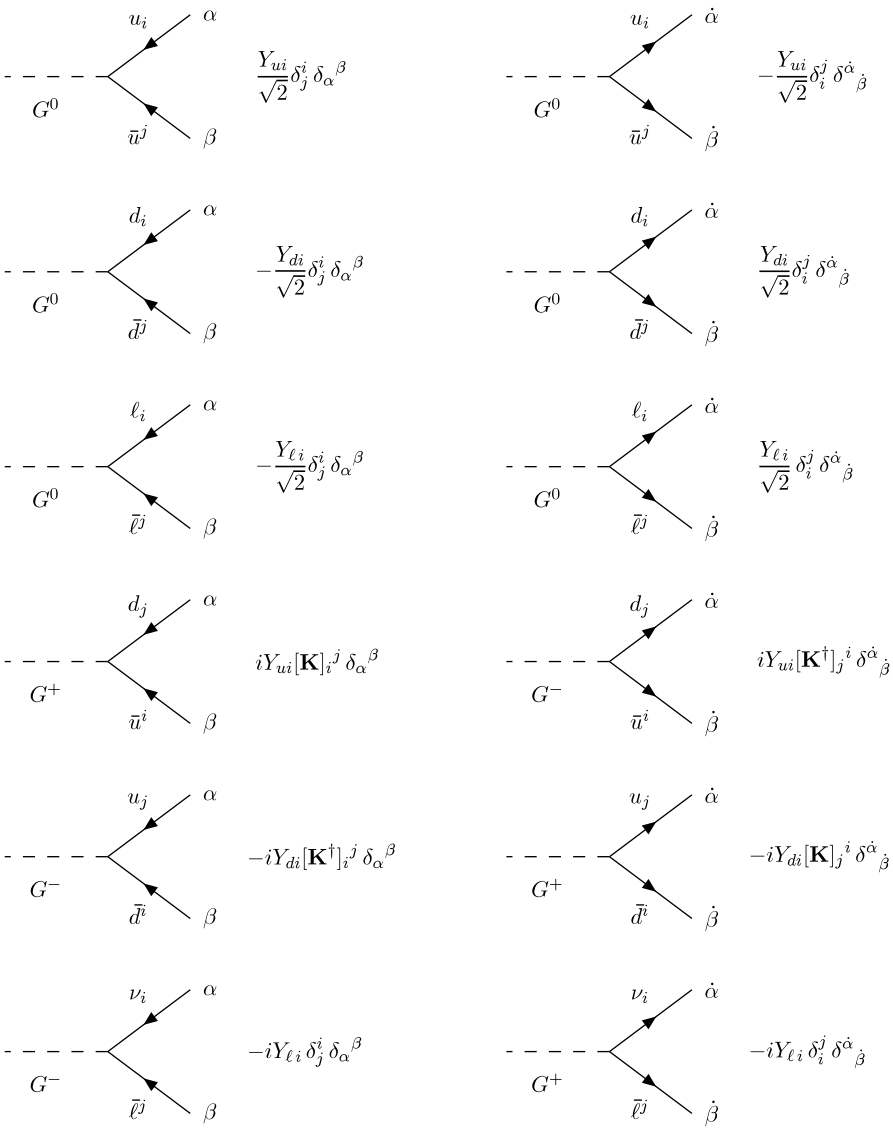

Fig. J.1.4. Feynman rules for the Standard Model Nambu–Goldstone boson interactions with quarks and leptons, where $Y_{fi} \equiv m_{fi}/v$, and i, j label the generations.

elements, as shown in Fig. J.1.4. In the derivation of the couplings of the Nambu–Goldstone bosons to the fermion mass eigenstates [cf. Eqs. (J.1.6)–(J.1.8)], the following quantities appear:

$$(L_d)_k{}^j(\boldsymbol{Y}_u)^k{}_m(R_u)^m{}_i = Y_{ui}(L_d)_k{}^j(L_u^\dagger)_i{}^k = Y_{ui}(L_u^\dagger L_d)_i{}^j = [\boldsymbol{K}]_i{}^j Y_{ui}, \tag{J.1.22}$$

$$(L_u)_k{}^j(\boldsymbol{Y}_d)^k{}_m(R_d)^m{}_i = Y_{di}(L_u)_k{}^j(L_d^\dagger)_i{}^k = Y_{di}(L_d^\dagger L_u)_i{}^j = [\boldsymbol{K}^\dagger]_i{}^j Y_{di}, \tag{J.1.23}$$

with no sum over the repeated index i. The CKM matrix, $\boldsymbol{K}$, appears by virtue of Eqs. (J.1.16) and (J.1.20). Hence, the interaction Lagrangian for the coupling of the Nambu–Goldstone bosons to the fermion mass eigenstates is given by:

$$\mathscr{L}_{\rm int} = Y_{ui}[\boldsymbol{K}]_i^{\ j} d_j \bar{u}^i G^+ - Y_{di}[\boldsymbol{K}^\dagger]_i^{\ j} u_j \bar{d}^i G^- - Y_{\ell i}\nu_i \bar{\ell}^i G^- + \frac{i}{\sqrt{2}}\left[Y_{di} d_i \bar{d}^i - Y_{ui} u_i \bar{u}^i + Y_{\ell\, i}\ell_i \bar{\ell}^i\right] G^0 + \text{h.c.}, \tag{J.1.24}$$

which yields the diagrammatic Feynman rules shown in Fig. J.1.4.

J.2. Incorporating massive neutrinos into the Standard Model

To accommodate massive neutrinos, we must slightly extend the Standard Model [336]. The simplest approach is to introduce an SU(2)×U(1) gauge invariant dimension-five operator [337],

$$\begin{aligned}\mathscr{L}_5 &= -\frac{\hat{\boldsymbol{F}}^{ij}}{2\Lambda}(\epsilon^{ab}\boldsymbol{\Phi}_a \hat{\boldsymbol{L}}_{bi})(\epsilon^{cd}\boldsymbol{\Phi}_c \hat{\boldsymbol{L}}_{dj}) + \text{h.c.}\\ &= -\frac{\hat{\boldsymbol{F}}^{ij}}{2\Lambda}(\Phi^0\hat{\nu}_i - \Phi^+\hat{\ell}_i)(\Phi^0\hat{\nu}_j - \Phi^+\hat{\ell}_j) + \text{h.c.},\end{aligned} \tag{J.2.1}$$

where $\hat{\boldsymbol{F}}^{ij}$ are generalized Yukawa couplings, the hatted fields indicate two-component fermion interaction eigenstates (with spinor indices suppressed), and i,j label the three generations. After electroweak symmetry breaking, the neutral component of the doublet Higgs field acquires a vacuum expectation value, and a Majorana mass matrix for the neutrinos is generated.

The diagonalization of the charged lepton mass matrix is unmodified from the treatment given in Appendix J.1, where the unhatted mass-eigenstate charged lepton fields are given by Eq. (J.1.11), and L_ℓ and R_ℓ satisfy Eq. (J.1.14). However, the unhatted neutrino field introduced in Eq. (J.1.15) is *not* a neutrino mass-eigenstate field when the effect of the dimension-five Lagrangian, Eq. (J.2.1), is taken into account. To avoid confusion, we replace the unhatted neutrino fields of Eq. (J.1.15) with new neutrino fields $\check{\nu}_j$. That is, we define

$$\hat{\nu}_i = (L_\ell)_i^{\ j}\check{\nu}_j. \tag{J.2.2}$$

We then rewrite Eq. (J.2.1) in terms of the charged lepton mass-eigenstate field and the new neutrino field defined by Eq. (J.2.2):

$$\mathscr{L}_5 = -\frac{\boldsymbol{F}^{ij}}{2\Lambda}(\Phi^0\check{\nu}_i - \Phi^+\ell_i)(\Phi^0\check{\nu}_j - \Phi^+\ell_j) + \text{h.c.}, \tag{J.2.3}$$

where $\boldsymbol{F} \equiv L_\ell^{\rm T}\hat{\boldsymbol{F}}L_\ell$. Setting $\Phi^0 = v$ and $\Phi^+ = \Phi^- = 0$, we identify the 3×3 complex symmetric effective light neutrino mass matrix, $\boldsymbol{M}_{\nu_\ell}$, by

$$-\mathscr{L}_{m_\nu} = \tfrac{1}{2}(\boldsymbol{M}_{\nu_\ell})^{ij}\check{\nu}_i\check{\nu}_j + \text{h.c.}, \tag{J.2.4}$$

where

$$\boldsymbol{M}_{\nu_\ell} = \frac{v^2}{\Lambda}\boldsymbol{F}. \tag{J.2.5}$$

Current bounds on light neutrino masses suggest that $v^2/\Lambda \lesssim 1$ eV, or $\Lambda \gtrsim 10^{13}$ GeV [334,338].

The physical neutrino mass-eigenstate fields can be identified by introducing the unitary Maki–Nakagawa–Sakata (MNS) matrix, $\boldsymbol{U}_{\rm MNS}$, such that [339],[166]

$$(\check{\nu}_\ell)_i = (\boldsymbol{U}_{\rm MNS})_i^{\ j}(\nu_\ell)_j, \tag{J.2.6}$$

where the unhatted $(\nu_\ell)_j$ fields [$j = 1,2,3$] denote the physical (mass-eigenstate) Majorana neutrino fields. $\boldsymbol{U}_{\rm MNS}$ is determined by the Takagi diagonalization of $\boldsymbol{M}_{\nu_\ell}$ [cf. Appendix D.2]:

$$\boldsymbol{U}_{\rm MNS}^{\rm T}\boldsymbol{M}_{\nu_\ell}\boldsymbol{U}_{\rm MNS} = \text{diag}(m_{\nu_\ell 1}, m_{\nu_\ell 2}, m_{\nu_\ell 3}), \tag{J.2.7}$$

where the $m_{\nu_\ell j}$ are the (real non-negative) masses of the physical neutrinos.

The interaction Lagrangian of the neutrino mass eigenstates can now be determined. The charged current neutrino interactions are given by [cf. Eq. (J.1.17)]:

$$\begin{aligned}\mathscr{L}_{\rm int} &= -\frac{g}{\sqrt{2}}\left[\check{\nu}^{\dagger i}\overline{\sigma}^\mu \ell_i W_\mu^+ + \ell^{\dagger i}\overline{\sigma}^\mu\check{\nu}_i W_\mu^-\right]\\ &= -\frac{g}{\sqrt{2}}\left[(\boldsymbol{U}_{\rm MNS}^\dagger)_j^{\ i}\nu_\ell^{\dagger j}\overline{\sigma}^\mu\ell_i W_\mu^+ + (\boldsymbol{U}_{\rm MNS})_i^{\ j}\ell^{\dagger i}\overline{\sigma}^\mu\nu_{\ell j}W_\mu^-\right],\end{aligned} \tag{J.2.8}$$

166 In the literature, the MNS matrix is often defined such that $\boldsymbol{U}_{\rm MNS}^*$ (and *not* $\boldsymbol{U}_{\rm MNS}$) appears in Eq. (J.2.6).

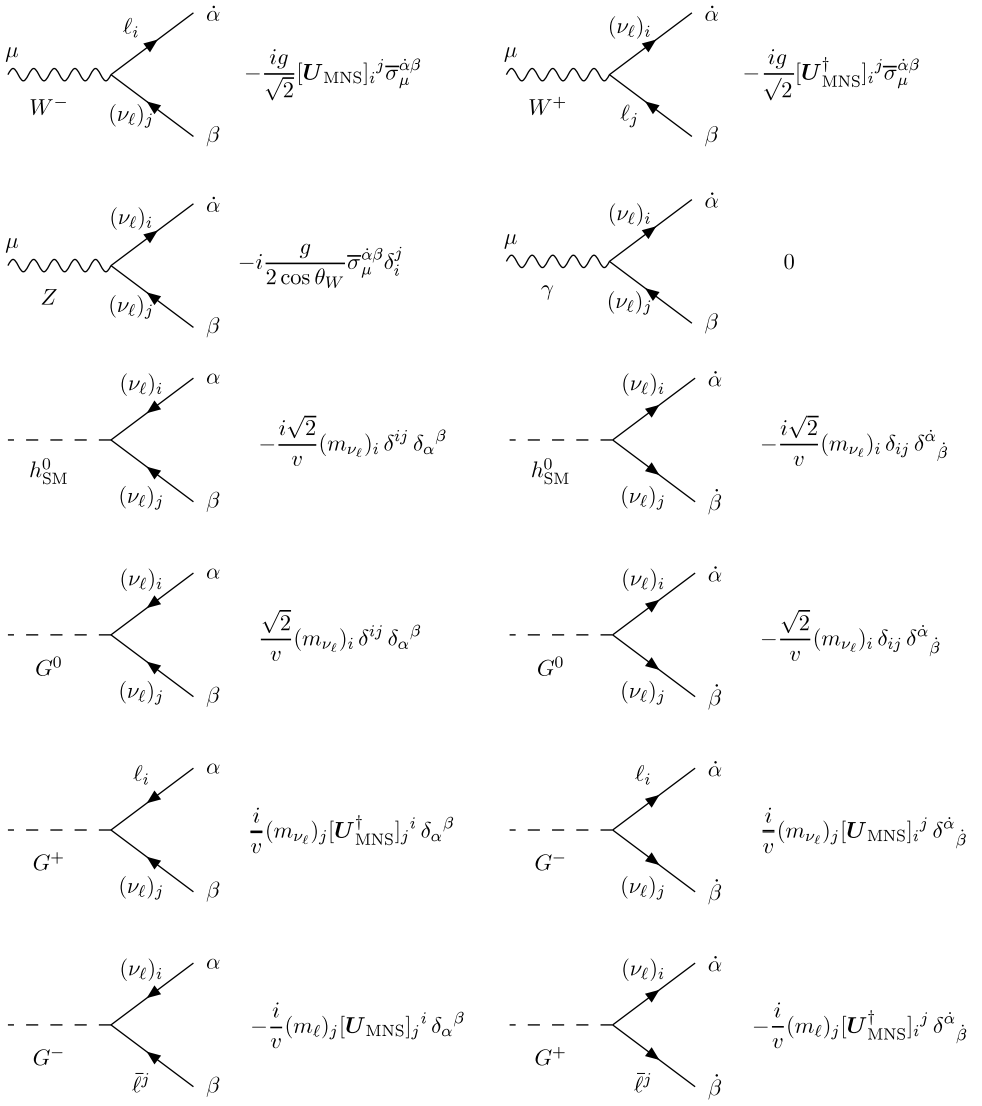

Fig. J.2.1. Feynman rules for the interactions of the two-component light neutrino (ν_ℓ) with electroweak gauge bosons, the Standard Model Higgs boson and the Nambu–Goldstone bosons, where i, j label the generation. For the $W^\pm$ bosons and $G^\pm$ scalars, the charge indicated is flowing into the vertex. The MNS mixing matrix is denoted by $\boldsymbol{U}_{\rm MNS}$. For the rules involving $W^\pm$ and Z bosons, a corresponding one with lowered spinor indices is obtained by $\overline{\sigma}_\mu^{\dot\alpha\beta} \to -\sigma_{\mu\beta\dot\alpha}$. In the $h^0_{\rm SM}$ and G^0 interactions, a factor of 2 is included to account for the identical neutrinos.

where we have used Eq. (J.2.6) to express the interaction Lagrangian in terms of the neutrino mass-eigenstate fields. The neutral current neutrino interactions are flavor-diagonal (which follows from the unitarity of $U_{\rm MNS}$), and are thus equivalent to those of the Standard Model. Finally, the couplings of the neutrinos to the Higgs and Nambu–Goldstone fields arise from Eq. (J.2.3) and from the term in Eq. (J.1.6) proportional to $\boldsymbol{Y}_\ell$. Neglecting terms of $\mathcal{O}(m_\nu^2/v^2)$, one obtains:

$$\begin{aligned}\mathscr{L}_{\rm int} &= \frac{1}{v}\sum_{i,j}\Big[(m_{\nu_\ell})_j(\boldsymbol{U}^\dagger_{\rm MNS})_j{}^i(\nu_\ell)_j\,\ell_i\,G^+ - (m_\ell)_i(\boldsymbol{U}_{\rm MNS})_i{}^j(\nu_\ell)_j\,\bar\ell^i\,G^- + \text{h.c.}\Big]\\ &\quad - \frac{1}{\sqrt{2}v}\sum_j(m_{\nu_\ell})_j\left[(\nu_\ell)_j(\nu_\ell)_j(h_{\rm SM}+iG^0) + \text{h.c.}\right].\end{aligned} \tag{J.2.9}$$

The Feynman rules for the interactions of the neutrino with the electroweak gauge bosons, the Higgs boson and the Nambu–Goldstone bosons are exhibited in Fig. J.2.1.

The dimension-five Lagrangian, Eq. (J.2.1), is generated by new physics beyond the Standard Model at the scale Λ. A possible realization of Eq. (J.2.1) is the seesaw mechanism, which was independently discovered on a number of occasions [4]. In the seesaw extension of the Standard Model [5], one introduces the SU(3)×SU(2)×U(1) gauge singlet two-component neutrino fields $\bar\nu^I$ ($I = 1, 2, \ldots, n$) and writes down the most general renormalizable couplings of the $\bar\nu^I$ to the

Standard Model fields:

$$\mathscr{L}_{\text{seesaw}} = \epsilon^{ab}(\hat{\boldsymbol{Y}}_\nu)^i{}_J \boldsymbol{\Phi}_a \hat{\boldsymbol{L}}_{bi} \hat{\bar{\nu}}^J - \tfrac{1}{2}\hat{\boldsymbol{M}}_{IJ}\hat{\bar{\nu}}^I\hat{\bar{\nu}}^J + \text{h.c.}, \tag{J.2.10}$$

where the Yukawa coupling proportional to $\hat{\boldsymbol{Y}}_\nu$ is the leptonic analogue of the Higgs–quark Yukawa coupling proportional to $\hat{\boldsymbol{Y}}_u$ [cf. Eq. (J.1.5)]. In Eq. (J.2.10), we have distinguished the flavor labels of three generations of Standard Model neutrino and charged lepton fields (denoted by lower case Roman letters $i, j, \ldots$) and the flavor labels of singlet neutrino fields (denoted by upper case Roman letters $I, J, \ldots$). Note that $\hat{\boldsymbol{Y}}_\nu$ is a $3 \times n$ matrix and $\hat{\boldsymbol{M}}$ is an $n \times n$ matrix, where n is the number of singlet neutrino flavors. In general, we shall not specify the value of n, which may differ from the number of Standard Model lepton generations.

If $\Lambda \equiv \|\hat{\boldsymbol{M}}\| \gg v$,[167] then a dimension-five operator of the form given by Eq. (J.2.1) is generated in the effective theory at energy scales below Λ. In this limit, we may neglect the kinetic energy term of the gauge singlet neutrino fields. Using the Lagrange field equations, we may solve for $\hat{\bar{\nu}}^I$. Inserting the solution back into Eq. (J.2.10) then yields Eq. (J.2.1), with $\hat{\boldsymbol{F}}/\Lambda$ given by

$$\hat{\boldsymbol{F}}^{ij}/\Lambda = -(\hat{\boldsymbol{Y}}_\nu)^i{}_K(\hat{\boldsymbol{Y}}_\nu)^j{}_N(\hat{\boldsymbol{M}}^{-1})^{KN}. \tag{J.2.11}$$

Using the definition of the $\text{SU}(2)_L$ doublet lepton field given in Table J.1, one can rewrite Eq. (J.2.10) more explicitly as:

$$\mathscr{L}_{\text{seesaw}} = -(\hat{\boldsymbol{Y}}_\nu)^i{}_J\left[\Phi^0\hat{\nu}_i\hat{\bar{\nu}}^J - \Phi^+\hat{\ell}_i\hat{\bar{\nu}}^J\right] - \tfrac{1}{2}\hat{\boldsymbol{M}}_{IJ}\hat{\bar{\nu}}^I\hat{\bar{\nu}}^J + \text{h.c.} \tag{J.2.12}$$

To analyze the physical consequences of the seesaw Lagrangian, we first express Eq. (J.2.12) in terms of the unhatted mass-eigenstate charged lepton fields [cf. Eq. (J.1.11)], and the light neutrino fields $\breve{\nu}_i$ introduced in Eq. (J.2.2). It is also convenient to introduce new gauge singlet neutrino fields $\breve{\bar{\nu}}^J$ by defining

$$\hat{\bar{\nu}}^I = N^I{}_J\breve{\bar{\nu}}^J, \tag{J.2.13}$$

where N is the unitary matrix that Takagi diagonalizes the complex symmetric matrix $\hat{\boldsymbol{M}}$. That is,

$$\boldsymbol{M} \equiv N^{\mathsf{T}}\hat{\boldsymbol{M}}N = \text{diag}(M_1, M_2, \ldots, M_n), \tag{J.2.14}$$

where the M_I are the singular values of $\hat{\boldsymbol{M}}$ (i.e., the non-negative square roots of the eigenvalues of $\hat{\boldsymbol{M}}^\dagger\hat{\boldsymbol{M}}$). In terms of the mass-eigenstate charged lepton fields ℓ_i and the neutrino fields $\breve{\nu}_i$ and $\breve{\bar{\nu}}^I$, the seesaw Lagrangian [Eq. (J.2.12)] is then given by:

$$\mathscr{L}_{\text{seesaw}} = -(\boldsymbol{Y}_\nu)^i{}_J\left[\Phi^0\breve{\nu}_i\breve{\bar{\nu}}^J - \Phi^+\ell_i\breve{\bar{\nu}}^J\right] - \tfrac{1}{2}\boldsymbol{M}_{IJ}\breve{\bar{\nu}}^I\breve{\bar{\nu}}^J + \text{h.c.}, \tag{J.2.15}$$

where

$$\boldsymbol{Y}_\nu \equiv L_\ell^{\mathsf{T}}\hat{\boldsymbol{Y}}_\nu N. \tag{J.2.16}$$

As above, in the limit of $\Lambda \equiv \|\hat{\boldsymbol{M}}\| = \|\boldsymbol{M}\| \gg v$, it is also possible to directly generate the effective dimension-five operator [Eq. (J.2.3)] in terms of the mass-eigenstate charged lepton fields and the new neutrino fields $\breve{\nu}_j$. We then identify the corresponding coefficient, $\boldsymbol{F}/\Lambda$, as

$$\boldsymbol{F}^{ij}/\Lambda = -(\boldsymbol{Y}_\nu)^i{}_K(\boldsymbol{Y}_\nu)^j{}_N(\boldsymbol{M}^{-1})^{KN}. \tag{J.2.17}$$

Recalling that $\boldsymbol{F} = L_\ell^{\mathsf{T}}\hat{\boldsymbol{F}}L_\ell$, one can check that Eq. (J.2.17) indeed follows from Eqs. (J.2.11), (J.2.14) and (J.2.16).

To identify the neutrino mass matrix, we set $\Phi^0 = v$ and $\Phi^+ = \Phi^- = 0$ in Eq. (J.2.15):

$$-\mathscr{L}_{m_\nu} = \tfrac{1}{2}\begin{pmatrix}\breve{\nu}_i & \breve{\bar{\nu}}^J\end{pmatrix}\mathcal{M}_\nu\begin{pmatrix}\breve{\nu}_k \\ \breve{\bar{\nu}}^M\end{pmatrix} + \text{h.c.} \tag{J.2.18}$$

The neutrino mass matrix $\mathcal{M}_\nu$ is a $(3+n) \times (3+n)$ complex symmetric matrix given in block form by:

$$\mathcal{M}_\nu \equiv \begin{pmatrix}\mathbb{O} & \boldsymbol{M_D} \\ \boldsymbol{M_D}^{\mathsf{T}} & \boldsymbol{M}\end{pmatrix}, \tag{J.2.19}$$

where $\mathbb{O}$ is the 3×3 zero matrix, $\boldsymbol{M}$ is the diagonal matrix defined in Eq. (J.2.14) and $\boldsymbol{M_D}$ is a $3 \times n$ complex matrix (called the Dirac neutrino mass matrix),

$$(\boldsymbol{M_D})^i{}_j \equiv v(\boldsymbol{Y}_\nu)^i{}_j. \tag{J.2.20}$$

[167] The Euclidean matrix norm is defined by $\|A\| \equiv \left[\text{Tr}(A^\dagger A)\right]^{1/2} = \left[\sum_{i,j}|a_{ij}|^2\right]^{1/2}$, for a matrix A whose matrix elements are given by a_{ij}.

Note that if $n = 3$ and $\boldsymbol{M} = \mathbb{O}$, then $\boldsymbol{M_D}$ is a 3×3 matrix that is simply the leptonic analogue of the up-type quark mass matrix $\boldsymbol{M}_u$. In this case, we would perform a singular value decomposition of $\boldsymbol{M_D}$ and identify the unhatted neutrino mass-eigenstate fields, which can be assembled into three generations of four-component Dirac neutrinos,

$$N_i = \begin{pmatrix} \nu_i \\ \bar{\nu}^{\dagger i} \end{pmatrix}, \quad i = 1, 2, 3. \tag{J.2.21}$$

In the seesaw model (with n not specified), we assume that $\|\boldsymbol{M}\| \gg \|\boldsymbol{M_D}\|$. In this case, the neutrino mass matrix can be perturbatively Takagi block diagonalized as follows [280,298,340]. Introduce the $(3+n) \times (3+n)$ (approximate) unitary matrix:

$$\mathcal{U} = \begin{pmatrix} \mathbb{1}_{3\times 3} - \frac{1}{2}\boldsymbol{M_D^*}\boldsymbol{M}^{-2}\boldsymbol{M_D^{\mathsf{T}}} & \boldsymbol{M_D^*}\boldsymbol{M}^{-1} \\ -\boldsymbol{M}^{-1}\boldsymbol{M_D^{\mathsf{T}}} & \mathbb{1}_{n\times n} - \frac{1}{2}\boldsymbol{M}^{-1}\boldsymbol{M_D^{\mathsf{T}}}\boldsymbol{M_D^*}\boldsymbol{M}^{-1} \end{pmatrix}, \tag{J.2.22}$$

where $\mathbb{1}$ is the identity matrix (whose dimension is explicitly specified above). We define transformed [light (ℓ) and heavy (h)] neutrino states $(\breve{\nu}_\ell)_i$ and $(\breve{\breve{\nu}}_h)^j$ by:

$$\begin{pmatrix} \breve{\nu}_i \\ \breve{\breve{\nu}}^J \end{pmatrix} = \mathcal{U} \begin{pmatrix} (\breve{\nu}_\ell)_k \\ (\breve{\breve{\nu}}_h)^M \end{pmatrix}. \tag{J.2.23}$$

By straightforward matrix multiplication, one can verify that to second order accuracy in perturbation theory,

$$\mathcal{U}^{\mathsf{T}}\mathcal{M}_\nu\,\mathcal{U} \simeq \begin{pmatrix} -\boldsymbol{M_D}\boldsymbol{M}^{-1}\boldsymbol{M_D^{\mathsf{T}}} & \mathbb{O} \\ \mathbb{O}^{\mathsf{T}} & \boldsymbol{M} + \frac{1}{2}(\boldsymbol{M}^{-1}\boldsymbol{M_D^\dagger}\boldsymbol{M_D} + \boldsymbol{M_D^{\mathsf{T}}}\boldsymbol{M_D^*}\boldsymbol{M}^{-1}) \end{pmatrix}, \tag{J.2.24}$$

where $\mathbb{O}$ is the $3 \times n$ zero matrix.

We now can identify an effective 3×3 complex symmetric mass matrix $\boldsymbol{M}_{\nu_\ell}$ for the three light neutrinos as the upper left-hand block of Eq. (J.2.24),

$$\boldsymbol{M}_{\nu_\ell} \simeq -\boldsymbol{M_D}\boldsymbol{M}^{-1}\boldsymbol{M_D^{\mathsf{T}}}, \tag{J.2.25}$$

where corrections of $\mathcal{O}(v^4/\Lambda^3)$ have been neglected. Using Eqs. (J.2.17) and (J.2.20), we see that the light neutrino mass matrix obtained in Eq. (J.2.5) has been correctly reproduced to leading order in v^2/Λ^2.

The physical light neutrino mass-eigenstate fields and their masses are identified by Eqs. (J.2.6) and (J.2.7). At energy scales below the heavy neutrino mass scale, $\Lambda \equiv \|\boldsymbol{M}\|$, and we can set $\breve{\breve{\nu}}_h = 0$. Neglecting corrections of $\mathcal{O}(v^2/\Lambda^2)$, Eqs. (J.2.20)–(J.2.25) imply that[168]

$$\breve{\nu}_i \simeq (\boldsymbol{U}_{\rm MNS})_i{}^j(\nu_\ell)_j, \tag{J.2.26}$$

$$(\boldsymbol{Y}_\nu)^i{}_J\,\breve{\breve{\nu}}^J \simeq \frac{1}{v}(\boldsymbol{M}_{\nu_\ell}\boldsymbol{U}_{\rm MNS})^{ik}(\nu_\ell)_k = \frac{1}{v}\sum_k (\boldsymbol{U}^\dagger_{\rm MNS})_k{}^i\,(m_{\nu_\ell})_k(\nu_\ell)_k, \tag{J.2.27}$$

where in the last step above we have used Eq. (J.2.7) and $(\boldsymbol{U}^\dagger_{\rm MNS})_j{}^i \equiv [(\boldsymbol{U}_{\rm MNS})_i^j]^*$. Using Eqs. (J.2.26) and (J.2.27) to express the seesaw Lagrangian in terms of the light neutrino mass-eigenstate fields, one can verify that the resulting interactions of the light neutrinos (and charged leptons) to gauge bosons, the Higgs boson and the Nambu–Goldstone bosons reproduce the results of Eqs. (J.2.8) and (J.2.9) at leading order in v^2/Λ^2.

For completeness, we examine the effective $n \times n$ complex symmetric mass matrix of the heavy neutrino states, $\boldsymbol{M}_{\nu_h}$, which is identified as the lower right-hand block in Eq. (J.2.24),

$$\boldsymbol{M}_{\nu_h} \simeq \boldsymbol{M} + \tfrac{1}{2}(\boldsymbol{M}^{-1}\boldsymbol{M_D^\dagger}\boldsymbol{M_D} + \boldsymbol{M_D^{\mathsf{T}}}\boldsymbol{M_D^*}\boldsymbol{M}^{-1}). \tag{J.2.28}$$

Although $\boldsymbol{M}$ is diagonal by definition [cf. Eq. (J.2.14)], the right-hand side of Eq. (J.2.28) is no longer diagonal due to the second order perturbative correction. However, we do not have to perform another Takagi diagonalization, since the off-diagonal elements of the lower right-hand block only affect the physical (diagonal) masses at higher order in perturbation theory. Thus, we identify the physical heavy neutrino mass eigenstates to leading order by the unhatted fields,

$$\bar{\nu}_h^J \simeq \breve{\breve{\nu}}_h^J, \tag{J.2.29}$$

---

168 Strictly speaking, Eq. (J.2.27) should be written as:

$$(\boldsymbol{Y}_\nu)^i{}_J\,\breve{\breve{\nu}}^J \simeq \frac{1}{v}\sum_{k,n}(\boldsymbol{U}^\dagger_{\rm MNS})_n{}^i\,\delta^{nk}(m_{\nu_\ell})_k(\nu_\ell)_k,$$

to maintain covariance in the flavor indices.

with masses

$$m_{\nu_{hJ}} \simeq M_J \left(1 + \frac{1}{M_J^2} \sum_i |(\boldsymbol{M_D})^i{}_J|^2\right), \tag{J.2.30}$$

where the M_J are the diagonal elements of $\boldsymbol{M}$ (and no sum over the repeated index J is implied). That is, the masses of the heavy neutrinos are simply given by $m_{\nu_{hJ}} \simeq M_J$, up to corrections that are of the same order as the light neutrino masses.

The interactions of the heavy neutrinos can be likewise obtained. The only unsuppressed interactions are heavy neutrino couplings to the Higgs boson and Nambu–Goldstone bosons that are proportional to the Dirac neutrino mass matrix,

$$\mathscr{L}_{\rm int} = -\frac{1}{\sqrt{2}v}(\boldsymbol{U}^{\rm T}_{\rm MNS}\boldsymbol{M_D})^k{}_J \bar{\nu}^J_h(\nu_\ell)_k(h^0_{\rm SM} + iG^0) + \frac{1}{v}(\boldsymbol{M_D})^i{}_J \ell_i \bar{\nu}^J_h G^+ + \text{h.c.} \tag{J.2.31}$$

All other couplings of the heavy neutrinos to the $W^\pm$ and Z bosons (and additional contributions to the couplings of the heavy neutrinos to the Higgs boson and Nambu–Goldstone bosons) are suppressed by (at least) a factor of $\mathcal{O}(v/\Lambda)$.

Appendix K. MSSM fermion interaction vertices

In this section, we provide the Feynman rules for the MSSM interaction vertices. To complete the tabulation of all MSSM Feynman rules, one requires the rules for the purely bosonic interactions of the MSSM. These can be found in Refs. [341,342].

K.1. Higgs–fermion interaction vertices in the MSSM

The MSSM Higgs sector is a two Higgs doublet model containing eight real scalar degrees of freedom: one complex $Y = -\frac{1}{2}$ doublet, $\boldsymbol{H_d} = (H^0_d, H^-_d)$ and one complex $Y = +\frac{1}{2}$ doublet, $\boldsymbol{H_u} = (H^+_u, H^0_u)$. The notation reflects the form of the MSSM Higgs sector coupling to fermions:

$$\mathscr{L}_{\rm Y} = \epsilon^{ab}\left[(\boldsymbol{Y}_u)^i{}_j(\boldsymbol{H_u})_a\hat{\boldsymbol{Q}}_{bi}\hat{\bar{u}}^j - (\boldsymbol{Y}_d)^i{}_j(\boldsymbol{H_d})_a\hat{\boldsymbol{Q}}_{bi}\hat{\bar{d}}^j - (\boldsymbol{Y}_\ell)^i{}_j(\boldsymbol{H_d})_a\hat{\boldsymbol{L}}_{bi}\hat{\bar{\ell}}^j\right] + \text{h.c.}, \tag{K.1.1}$$

where the hatted fields are interaction-eigenstate quark and lepton fields (with generation labels i and j), a and b are $\mathrm{SU}(2)_L$ indices and the invariant $\mathrm{SU}(2)_L$ tensor ϵ^{ab} is defined below Eq. (J.1.5). That is, the neutral Higgs fields H^0_d [H^0_u] couple exclusively to down-type [up-type] fermion pairs, respectively. In the supersymmetric model, both hypercharge $Y = -\frac{1}{2}$ and $Y = +\frac{1}{2}$ complex Higgs doublets are required in order that the theory (which now contains the corresponding higgsino superpartners) remain anomaly free. The supersymmetric structure of the theory forbids the coupling of $\boldsymbol{H^\dagger_u}$ to $\hat{\bar{d}}^j$ and $\hat{\bar{\ell}}^j$ or the coupling of $\boldsymbol{H^\dagger_d}$ to $\hat{\bar{u}}^j$, as such couplings would not be holomorphic. Consequently, (at least) two Higgs doublets are required in the MSSM to generate mass for both "up"-type and "down"-type quarks and charged leptons [170,343,344].

To find the couplings of the Higgs fields, we expand them around the neutral Higgs field vacuum expectation values $v_d \equiv \langle H^0_d\rangle$ and $v_u \equiv \langle H^0_u\rangle$. Depending on the application, these may be chosen to be the minimum of the tree-level scalar potential, or of the full loop-corrected effective potential, or just left arbitrary. It is always possible to choose the phases of the Higgs fields such that v_u and v_d are real and positive. We then define

$$\beta \equiv \tan^{-1}\left(\frac{v_u}{v_d}\right), \quad 0 \le \beta \le \frac{\pi}{2}. \tag{K.1.2}$$

The one potentially complex squared-mass parameter that appears in the tree-level MSSM Higgs scalar potential is necessarily real in the convention where the vacuum expectation values of the neutral Higgs fields are real and positive.[169] Consequently, the tree-level MSSM Higgs sector conserves CP, which implies that the neutral Higgs mass eigenstates possess definite CP quantum numbers.[170] Spontaneous electroweak symmetry breaking results in three Goldstone bosons $G^\pm$, G^0 (the neutral Goldstone boson is a CP-odd scalar field), which are absorbed and become the longitudinal components of the $W^\pm$ and Z. The remaining five physical Higgs particles consist of a charged Higgs pair $H^\pm$, one CP-odd scalar A^0, and two CP-even scalars h^0 and H^0.

169 The coefficients of the quartic terms of the tree-level MSSM Higgs potential are related to the electroweak gauge couplings and are manifestly real, independently of the convention for the phases of the Higgs fields.

170 When one-loop corrections are taken into account, new MSSM phases can enter in the loops that cannot be removed. In this case, the physical neutral Higgs states can be mixtures of CP-even and CP-odd scalar states [345].

It is convenient to define $H_u^- \equiv (H_u^+)^\dagger$ and $H_d^+ \equiv (H_d^-)^\dagger$. One can then parameterize the mixing angles between Higgs gauge eigenstates and mass eigenstates by writing:

$$H_u^0 = v_u + \frac{1}{\sqrt{2}} \sum_{\phi^0} k_{u\phi^0} \phi^0, \qquad H_u^\pm = \sum_{\phi^\pm} k_{u\phi^\pm} \phi^\pm, \tag{K.1.3}$$

$$H_d^0 = v_d + \frac{1}{\sqrt{2}} \sum_{\phi^0} k_{d\phi^0} \phi^0, \qquad H_d^\pm = \sum_{\phi^\pm} k_{d\phi^\pm} \phi^\pm. \tag{K.1.4}$$

For $\phi^\pm = (H^\pm, G^\pm)$,[171]

$$k_{u\phi^\pm} = (\cos\beta_\pm, \sin\beta_\pm), \tag{K.1.5}$$

$$k_{d\phi^\pm} = (\sin\beta_\pm, -\cos\beta_\pm), \tag{K.1.6}$$

and for $\phi^0 = (h^0, H^0, A^0, G^0)$,

$$k_{u\phi^0} = (\cos\alpha, \sin\alpha, i\cos\beta_0, i\sin\beta_0), \tag{K.1.7}$$

$$k_{d\phi^0} = (-\sin\alpha, \cos\alpha, i\sin\beta_0, -i\cos\beta_0), \tag{K.1.8}$$

where the mixing angle α parameterizes the orthogonal matrix that diagonalizes the 2×2 CP-even Higgs squared-mass matrix $\mathcal{M}_0^2$ [defined in Eq. (K.1.11) below].

In Eqs. (K.1.3) and (K.1.4), the normalization of the vacuum expectation values is

$$v_d^2 + v_u^2 = 2m_W^2/g^2 \simeq (174\ \text{GeV})^2, \tag{K.1.9}$$

if one chooses v_u, v_d to be near the true minimum of the Higgs effective potential. Note that in the special case that v_u and v_d are at the minimum of the *tree-level* potential, the mixing angles $\beta_\pm$ in the charged Higgs sector and β_0 in the CP-odd neutral Higgs sectors coincide such that $\beta_\pm = \beta_0 = \beta$, where β is defined in Eq. (K.1.2). However, if one expands around a more general choice of v_u, v_d, including for example the minimum of the full effective potential, then the tree-level mixing angles β_0 and $\beta_\pm$ are distinct from each other and from β. (Depending on the choice of renormalization scale for a particular calculation, the tree-level potential in the MSSM may have a very different minimum from the true minimum of the full effective potential, or may not have a proper minimum at all.) Therefore, we do not assume anything specific about v_u and v_d except that they are real and positive by convention.

All MSSM Higgs boson masses and the mixing angle α are determined at tree level by two Higgs sector parameters, usually taken to be the ratio of the tree-level vacuum expectation values, $\tan\beta = v_u/v_d$, and the mass of the CP-odd Higgs scalar, m_A [170,344]. The tree-level value of the squared mass of the charged Higgs boson is given by

$$m_{H^\pm}^2 = m_A^2 + m_W^2. \tag{K.1.10}$$

The CP-even Higgs bosons h^0 and H^0 are eigenstates of the tree-level squared-mass matrix,

$$\mathcal{M}_0^2 = \begin{pmatrix} m_A^2 \sin^2\beta + m_Z^2 \cos^2\beta & -(m_A^2 + m_Z^2)\sin\beta\cos\beta \\ -(m_A^2 + m_Z^2)\sin\beta\cos\beta & m_A^2\cos^2\beta + m_Z^2\sin^2\beta \end{pmatrix}. \tag{K.1.11}$$

The eigenvalues of $\mathcal{M}_0^2$ are the tree-level squared masses of the two CP-even Higgs scalars,

$$m_{H,h}^2 = \tfrac{1}{2}\left(m_A^2 + m_Z^2 \pm \sqrt{(m_A^2 + m_Z^2)^2 - 4m_Z^2 m_A^2 \cos^2 2\beta} \right), \tag{K.1.12}$$

with $m_h \le m_H$. The angle α of the orthogonal matrix that diagonalizes $\mathcal{M}_0^2$ is given by [346]:

$$\sin 2\alpha = -\sin 2\beta \left(\frac{m_A^2 + m_Z^2}{m_H^2 - m_h^2} \right), \qquad \cos 2\alpha = -\cos 2\beta \left(\frac{m_A^2 - m_Z^2}{m_H^2 - m_h^2} \right). \tag{K.1.13}$$

Since $\sin 2\alpha \le 0$, the tree-level value of α is restricted to lie in the range $-\pi/2 \le \alpha \le 0$.

Radiative corrections can have a significant impact on the tree-level Higgs masses and mixing angle α [345,347]. For example, the tree-level bound $m_h \le m_Z |\cos 2\beta| \le m_Z$ [which follows from Eq. (K.1.12)] is significantly modified by an incomplete cancellation of top quark and top squark loop corrections. Including the latter implies that $m_h \lesssim 135$ GeV [348], which (in contrast to the tree-level prediction) is not experimentally excluded.

171 Note that $\phi^- \equiv (\phi^+)^\dagger$. Since the $k_{f\phi^\pm}$ (for $f = u, d$) are real quantities, we adopt the notation in which $k_{f\phi^+} = k_{f\phi^-} \equiv k_{\phi^\pm}$ and $\beta_+ = \beta_- \equiv \beta_\pm$.

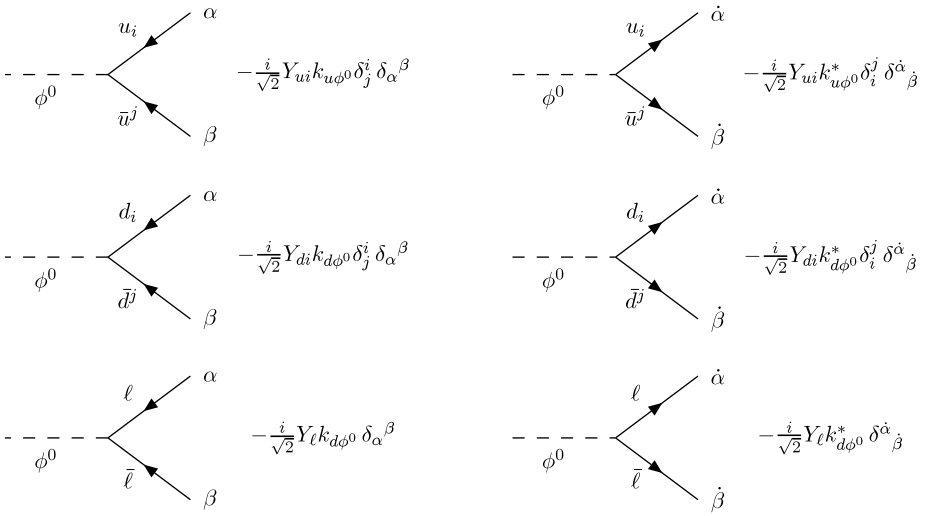

Fig. K.1.1. Feynman rules for the interactions of neutral Higgs bosons $\phi^0 = (h^0, H^0, A^0, G^0)$ with fermion–antifermion pairs in the MSSM. The repeated index j is not summed.

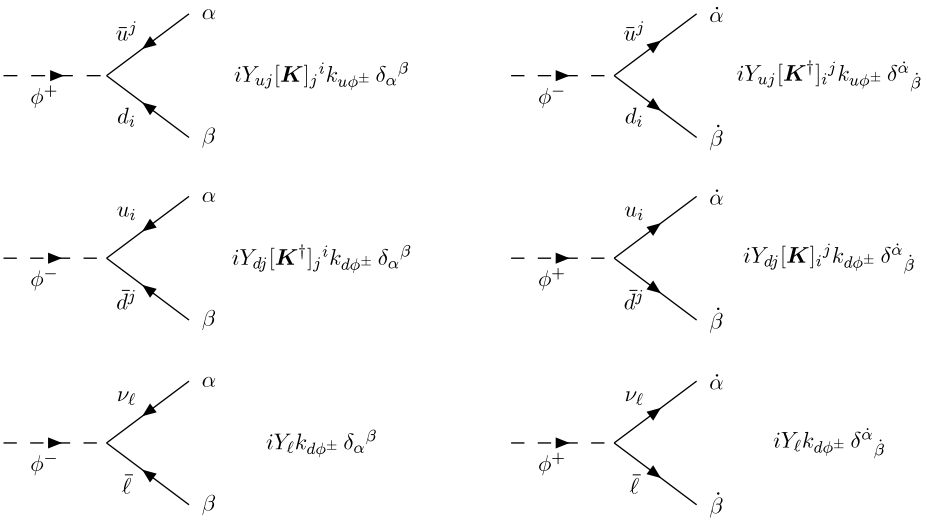

Fig. K.1.2. Feynman rules for the interactions of charged Higgs bosons $\phi^\pm = (H^\pm, G^\pm)$ with fermion–antifermion pairs in the MSSM.

The Higgs–fermion Yukawa couplings in the gauge-interaction basis are given by Eq. (K.1.1). Explicitly,

$$-\mathscr{L}_Y = (\mathbf{Y}_u)^i{}_j\left[\hat{u}_i\hat{\bar{u}}^j H_u^0 - \hat{d}_i\hat{\bar{u}}^j H_u^+\right] + (\mathbf{Y}_d)^i{}_j\left[\hat{d}_i\hat{\bar{d}}^j H_d^0 - \hat{u}_i\hat{\bar{d}}^j H_d^-\right] + (\mathbf{Y}_\ell)^i{}_j\left[\hat{\ell}_i\hat{\bar{\ell}}^j H_d^0 - \hat{\nu}_i\hat{\bar{\ell}}^j H_d^-\right] + \text{h.c.} \tag{K.1.14}$$

We use Eqs. (K.1.3) and (K.1.4) to express the interaction-eigenstate Higgs fields in terms of the physical Higgs fields and Goldstone fields. We can identify the quark and lepton mass matrices simply by setting $H_u^0 = v_u$, $H_d^0 = v_d$ and $H_u^+ = H_d^- = 0$ in Eq. (K.1.14),

$$(\boldsymbol{M}_u)^i{}_j = v_u(\mathbf{Y}_u)^i{}_j, \qquad (\boldsymbol{M}_d)^i{}_j = v_d(\mathbf{Y}_d)^i{}_j, \qquad (\boldsymbol{M}_\ell)^i{}_j = v_d(\mathbf{Y}_\ell)^i{}_j. \tag{K.1.15}$$

We then use Eqs. (J.1.10) and (J.1.11) to express the interaction-eigenstate quark and lepton fields in terms of the corresponding mass-eigenstate fields. Eqs. (J.1.12) and (J.1.14) ensure that the fermion mass matrices are diagonal (with real non-negative elements) in the fermion mass-eigenstate basis. In this basis, the resulting neutral Higgs–fermion interactions are diagonal. Here, the diagonalized Higgs–fermion Yukawa coupling matrices appear:

$$\text{diag}(Y_{u1}, Y_{u2}, Y_{u3}) \equiv \text{diag}(Y_u, Y_c, Y_t) = L_u^{\mathsf{T}}\mathbf{Y}_u R_u, \tag{K.1.16}$$

$$\text{diag}(Y_{d1}, Y_{d2}, Y_{d3}) \equiv \text{diag}(Y_d, Y_s, Y_b) = L_d^{\mathsf{T}}\mathbf{Y}_d R_d, \tag{K.1.17}$$

$$\text{diag}(Y_{\ell1}, Y_{\ell2}, Y_{\ell3}) \equiv \text{diag}(Y_e, Y_\mu, Y_\tau) = L_\ell^{\mathsf{T}}\mathbf{Y}_\ell R_\ell. \tag{K.1.18}$$

The diagonalized Yukawa couplings are related to the corresponding fermion masses by

$$Y_{ui} = m_{u_i}/v_u, \qquad Y_{di} = m_{d_i}/v_d, \qquad Y_{\ell i} = m_{\ell_i}/v_d. \tag{K.1.19}$$

We have used the same symbol for the Yukawa couplings in the MSSM as we did for the Standard Model Yukawa couplings in Appendix J.1. However, it is important to note that the MSSM Yukawa couplings are normalized differently because of the presence of two neutral Higgs field vacuum expectation values. Using a superscript SM to denote the Standard Model Yukawa couplings of Appendix J.1, the MSSM Yukawa couplings defined here are related by:

$$Y_{ui} = Y_{ui}^{\rm SM}/\sin\beta, \qquad Y_{di} = Y_{di}^{\rm SM}/\cos\beta, \qquad Y_{\ell i} = Y_{\ell i}^{\rm SM}/\cos\beta. \tag{K.1.20}$$

The interactions of the neutral Higgs and Goldstone scalars $\phi^0 = (h^0, H^0, A^0, G^0)$ with Standard Model fermions are given in Fig. K.1.1. Note that the rules involving undotted spinor indices are proportional to either couplings $k_{d\phi^0}$ and $k_{u\phi^0}$, whereas the rules involving dotted spinor indices are proportional to the corresponding complex-conjugated couplings. For the CP-even scalars, h^0 and H^0, the corresponding couplings are real. Hence, starting with the rule for the coupling of the CP-even neutral scalars to fermions with undotted indices, one obtains the corresponding rule for the coupling to fermions with dotted indices (with the direction of the arrows reversed) by taking $\delta_\alpha{}^\beta \to \delta^{\dot\alpha}{}_{\dot\beta}$. In contrast, for the CP-odd scalars, A^0 and G^0, the corresponding couplings $k_{d\phi^0}$ and $k_{u\phi^0}$ are purely imaginary. Therefore, starting with the rule for the coupling of the CP-odd neutral scalars to fermions with undotted indices, one obtains the corresponding rule for the coupling to fermions with dotted indices (with the direction of the arrows reversed) by taking $\delta_\alpha{}^\beta \to -\delta^{\dot\alpha}{}_{\dot\beta}$. The latter minus sign is a signal that A^0 and G^0 are CP-odd scalars. In particular, due to the fact that the Feynman rules for A^0 and G^0 arise from a term in $\mathscr{L}_{\rm int}$ proportional to $i\,{\rm Im}\,H^0$, the latter i flips sign when the rule is conjugated resulting in the extra minus sign noted above. As an additional consequence, since the Feynman rules are obtained from $i\mathscr{L}_{\rm int}$, the overall A^0 and G^0 rules are real.

The couplings of the charged Higgs and Goldstone bosons to quark–antiquark pairs are not flavor-diagonal and involve the CKM matrix $\boldsymbol{K}$. Starting with Eq. (K.1.14), and changing to the mass-eigenstate basis as before, we make use of Eqs. (J.1.22) and (J.1.23) to obtain

$$\begin{aligned}\mathscr{L}_{\rm int} &= Y_{ui}[\boldsymbol{K}]_i{}^j d_j \bar u^i H^+ \cos\beta_\pm + Y_{di}[\boldsymbol{K}^\dagger]_i{}^j u_j \bar d^i H^- \sin\beta_\pm + Y_{\ell i}\nu_i \bar\ell^i H^- \sin\beta_\pm \\ &\quad + Y_{ui}[\boldsymbol{K}]_i{}^j d_j \bar u^i G^+ \sin\beta_\pm - Y_{di}[\boldsymbol{K}^\dagger]_i{}^j u_j \bar d^i G^- \cos\beta_\pm - Y_{\ell i}\nu_i \bar\ell^i G^- \cos\beta_\pm + {\rm h.c.}\end{aligned} \tag{K.1.21}$$

The resulting charged scalar Feynman rules of the MSSM are given in Fig. K.1.2. Note that when Eq. (K.1.20) is taken into account, the fermion couplings to the neutral and charged Goldstone bosons are equivalent to those of the Standard Model [cf. Eq. (J.1.24)] if we choose $\beta_0 = \beta_\pm = \beta$.

K.2. Gauge-interaction vertices for neutralinos and charginos

Following Eqs. (C83) and (C88) of Ref. [7], we define:

$$O^L_{ij} = -\frac{1}{\sqrt{2}} N_{i4} V^*_{j2} + N_{i2} V^*_{j1}, \tag{K.2.1}$$

$$O^R_{ij} = \frac{1}{\sqrt{2}} N^*_{i3} U_{j2} + N^*_{i2} U_{j1}, \tag{K.2.2}$$

$$O'^L_{ij} = -V_{i1} V^*_{j1} - \tfrac{1}{2} V_{i2} V^*_{j2} + \delta_{ij} s_W^2, \tag{K.2.3}$$

$$O'^R_{ij} = -U^*_{i1} U_{j1} - \tfrac{1}{2} U^*_{i2} U_{j2} + \delta_{ij} s_W^2, \tag{K.2.4}$$

$$O''^L_{ij} = -O''^R_{ji} = \tfrac{1}{2}(N_{i4} N^*_{j4} - N_{i3} N^*_{j3}), \tag{K.2.5}$$

where $s_W \equiv \sin\theta_W$. Here U and V are the unitary matrices that diagonalize the chargino mass matrix via the singular value decomposition:

$$U^* M_{\psi^\pm} V^{-1} = {\rm diag}(m_{\tilde C_1}, m_{\tilde C_2}), \tag{K.2.6}$$

with

$$M_{\psi^\pm} = \begin{pmatrix} M_2 & g v_u \\ g v_d & \mu \end{pmatrix}. \tag{K.2.7}$$

Similarly, N is a unitary matrix that Takagi diagonalizes the neutralino mass matrix,

$$N^* M_{\psi^0} N^{-1} = {\rm diag}(m_{\tilde N_1}, m_{\tilde N_2}, m_{\tilde N_3}, m_{\tilde N_4}), \tag{K.2.8}$$

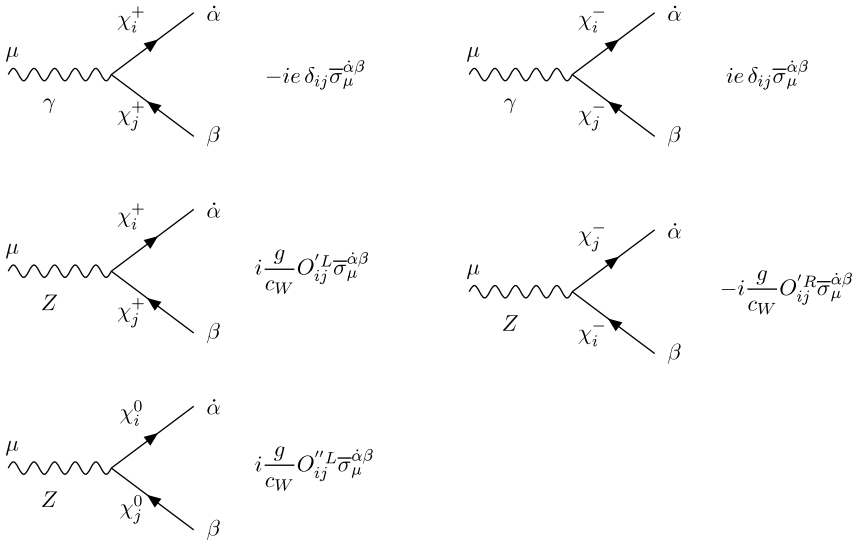

Fig. K.2.1. Feynman rules for the chargino and neutralino interactions with neutral gauge bosons. The coupling matrices are defined in Eqs. (K.2.3)–(K.2.5) and $c_W \equiv \cos\theta_W$. For each rule, a corresponding one with lowered spinor indices is obtained by $\overline{\sigma}_\mu^{\dot\alpha\beta} \to -\sigma_{\mu\beta\dot\alpha}$.

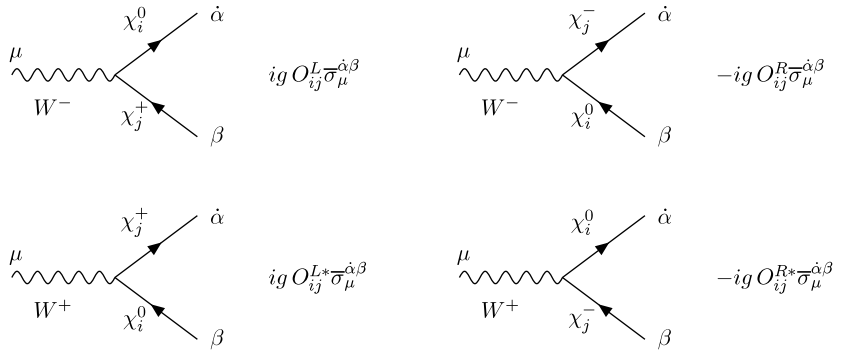

Fig. K.2.2. Feynman rules for the chargino and neutralino interactions with $W^\pm$ gauge bosons. The charge indicated on the W boson is flowing into the vertex in each case. The coupling matrices are defined in Eqs. (K.2.1) and (K.2.2). For each rule, a corresponding one with lowered spinor indices is obtained by $\overline{\sigma}_\mu^{\dot\alpha\beta} \to -\sigma_{\mu\beta\dot\alpha}$.

with

$$M_{\psi^0} = \begin{pmatrix} M_1 & 0 & -g' v_d/\sqrt{2} & g' v_u/\sqrt{2} \\ 0 & M_2 & g v_d/\sqrt{2} & -g v_u/\sqrt{2} \\ -g' v_d/\sqrt{2} & g v_d/\sqrt{2} & 0 & -\mu \\ g' v_u/\sqrt{2} & -g v_u/\sqrt{2} & -\mu & 0 \end{pmatrix}. \tag{K.2.9}$$

As noted above Eq. (K.1.2), we work in a convention in which v_u and v_d are real and positive. The gaugino mass parameters M_1, M_2 and the higgsino mass parameter μ are potentially complex.

We now list the gauge boson interactions with the neutralinos and charginos in the form of Feynman rules. Here, we make use of the results presented in Figs. 4.3.2–4.3.4. The Feynman rules for Z and γ interactions with charginos and neutralinos are given in Fig. K.2.1 and the corresponding rules for $W^\pm$ interactions are given in Fig. K.2.2. For each of these rules, one has a version with lowered spinor indices by replacing $\overline{\sigma}_\mu^{\dot\alpha\beta} \to -\sigma_{\mu\beta\dot\alpha}$. We label fermion lines with the symbols of the two-component fermion fields as given in Table 5.1. The $Z\widetilde{N}_i\widetilde{N}_j$ interaction vertex also subsumes the O''^R_{ij} interaction found in four-component Majorana Feynman rules as in Ref. [7], due to the result of Eq. (G.1.98) and the relation $O''^R_{ij} = -O''^L_{ji}$ of Eq. (K.2.5).

The chargino sector is CP-conserving if $\mathrm{Im}(M_2\mu^*) = 0$. In this case, the chargino fields can be rephased such that M_2 and μ are real, and the chargino mixing matrices U and V can be chosen to be real orthogonal. In particular, the couplings O'^L

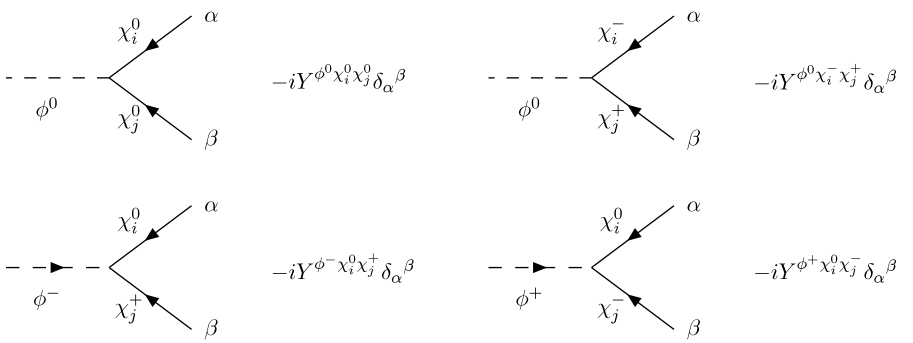

Fig. K.3.1. Feynman rules for the interactions of neutral Higgs bosons $\phi^0 = (h^0, H^0, A^0, G^0)$ with neutralino pairs and chargino pairs, respectively, and the interaction of charged Higgs bosons $\phi^\pm = (H^\pm, G^\pm)$ with chargino–neutralino pairs. For each rule, there is a corresponding one with all arrows reversed, undotted indices changed to dotted indices with the opposite height, and the Y coupling (without the explicit $-i$) replaced by its complex conjugate.

and O'^R are manifestly real. Likewise, the neutralino sector is CP-conserving if $\mathrm{Im}(M_1\mu^*) = \mathrm{Im}(M_2\mu^*) = \mathrm{Im}(M_1 M_2^*) = 0$.[172] In this case, the neutralino fields can be rephased such that M_1, M_2 and μ are all real, and the neutralino mixing matrix can be chosen [cf. Eqs. (D.2.4) and (D.2.5)] such that [170]:

$$N_{ij} = \varepsilon_i^{1/2} Z_{ij}, \quad \text{no sum over } i, \tag{K.2.10}$$

where Z is a real orthogonal matrix, and ε_i is the sign (either ± 1) of the ith eigenvalue of the real symmetric neutralino mass matrix, M_{ψ^0}. That is, the ith row of N is purely real [imaginary] if $\varepsilon_i = +1$ [-1]. In particular, the matrix element O''^L_{ij} is purely real [imaginary] if $\varepsilon_i\varepsilon_j = +1$ [-1]. More generally, the neutralino and chargino interactions with the electroweak gauge bosons are CP-conserving if the corresponding Feynman rules for the interaction vertices are either purely real or purely imaginary.

In the CP-violating case, the matrices U and V cannot be chosen to be real orthogonal, and N cannot be written in the form of Eq. (K.2.10).[173] Nevertheless, the diagonal couplings O'^L_{ii}, O'^R_{ii} and O''^L_{ii} are manifestly real. This indicates that the diagonal $Z^0\widetilde{C}_i^+\widetilde{C}_i^-$ and $Z^0\widetilde{N}_i\widetilde{N}_i$ couplings are CP-conserving at tree level, even in the presence of a CP-violating chargino and neutralino sector. Similarly, the diagonal $\gamma\widetilde{C}_i^+\widetilde{C}_i^-$ couplings are CP-conserving, whereas the off-diagonal $\gamma\widetilde{C}_i^\pm\widetilde{C}_j^\mp$ couplings ($i \neq j$) vanish at tree level, as expected from gauge invariance.

K.3. Higgs interactions with charginos and neutralinos

The couplings of chargino and neutralino mass eigenstates to the Higgs mass eigenstates can be written, in terms of the Higgs mixing parameters of Eqs. (K.1.7) and (K.1.8) and the neutralino and chargino mixing matrices of Appendix K.2, as [170]:

$$Y^{\phi^0\chi_i^0\chi_j^0} = \frac{1}{2}(k^*_{d\phi^0}N^*_{i3} - k^*_{u\phi^0}N^*_{i4})(gN^*_{j2} - g'N^*_{j1}) + (i \leftrightarrow j), \tag{K.3.1}$$

$$Y^{\phi^0\chi_i^-\chi_j^+} = \frac{g}{\sqrt{2}}(k^*_{u\phi^0}U^*_{i1}V^*_{j2} + k^*_{d\phi^0}U^*_{i2}V^*_{j1}), \tag{K.3.2}$$

$$Y^{\phi^+\chi_i^0\chi_j^-} = k_{d\phi^\pm}\left[g\left(N^*_{i3}U^*_{j1} - \frac{1}{\sqrt{2}}N^*_{i2}U^*_{j2}\right) - \frac{g'}{\sqrt{2}}N^*_{i1}U^*_{j2}\right], \tag{K.3.3}$$

$$Y^{\phi^-\chi_i^0\chi_j^+} = k_{u\phi^\pm}\left[g\left(N^*_{i4}V^*_{j1} + \frac{1}{\sqrt{2}}N^*_{i2}V^*_{j2}\right) + \frac{g'}{\sqrt{2}}N^*_{i1}V^*_{j2}\right], \tag{K.3.4}$$

for $\phi^0 = h^0, H^0, A^0, G^0$ and $\phi^\pm = H^\pm, G^\pm$. We exhibit the Higgs boson and Goldstone boson interactions with the neutralinos and charginos in Fig. K.3.1. For each of the Feynman rules in Fig. K.3.1, one can reverse all arrows by taking $\delta_\alpha{}^\beta \to \delta^{\dot\alpha}{}_{\dot\beta}$ and complex conjugating the corresponding coupling (but not the overall factor of $-i$).

Goldstone bosons may appear as internal lines in of Feynman graphs that are evaluated in the 't Hooft–Feynman gauge. The propagation of a Goldstone boson yields a result that is identical to the propagation of the corresponding longitudinal gauge boson in the unitary gauge. It is thus convenient to express the Goldstone boson couplings to the neutralinos and

172 If all three of the potentially complex parameters M_1, M_2 and μ are non-zero, then only two of the three conditions for a CP-conserving neutralino sector are independent, since the third condition follows automatically from the first two conditions.

173 Since M_{ψ^0} is in general a *complex* symmetric matrix, its eigenvalues are not necessarily all real. In particular, if the ith eigenvalue is not real, then there is no longer any meaning to the sign ε_i.

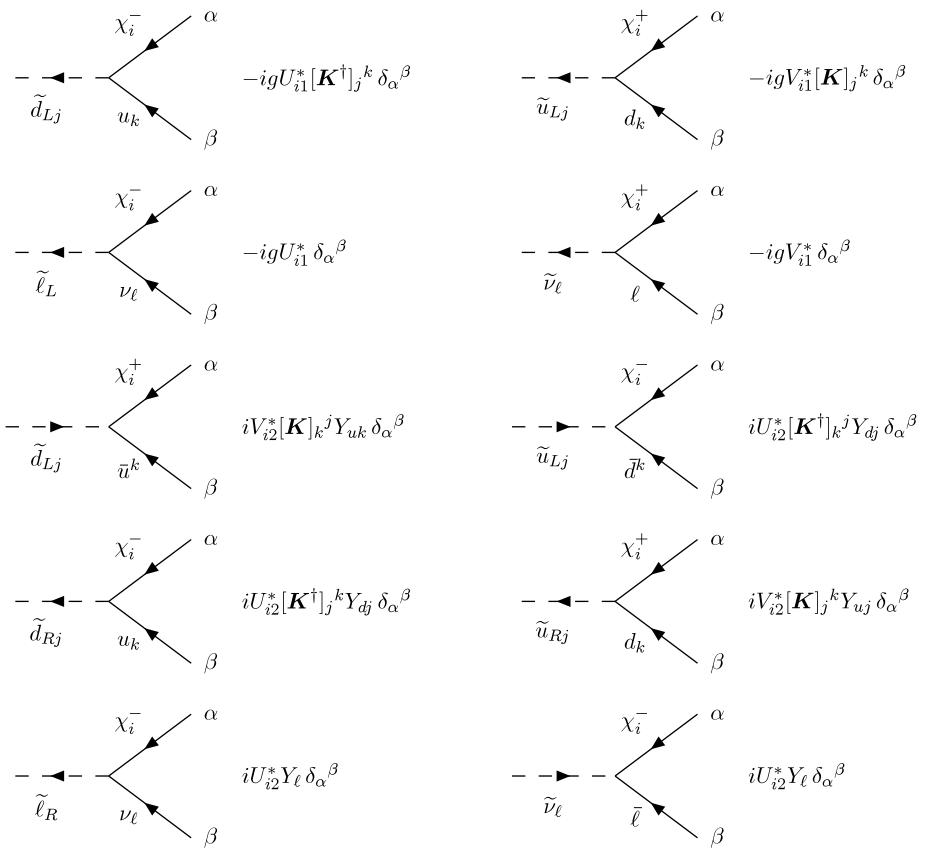

Fig. K.4.1. Feynman rules for the interactions of charginos with fermion/sfermion pairs in the MSSM. The fermions are taken to be in a mass-eigenstate basis, and the sfermions are in a basis whose elements are the supersymmetric partners of them. For each rule, there is a corresponding one with all arrows reversed, undotted indices changed to dotted indices with the opposite height, and the coupling (without the explicit i) replaced by its complex conjugate. Note that chargino interaction vertices involving $\widetilde{u}\widetilde{d}_R$ and $\widetilde{d}\widetilde{u}_R$ do not occur in the MSSM. An alternative version of these rules, for the case that mixing is allowed only among third-family sfermions, is given in Fig. K.4.3.

charginos in terms of the corresponding gauge boson couplings. To accomplish this, we first record a number of identities among the neutralino and chargino mixing matrices. First, we use Eqs. (K.2.6) and (K.2.7) to derive:

$$M_2U_{i1}^* + g v_d U_{i2}^* = m_{\widetilde{C}_i} V_{i1}, \qquad g v_u U_{i1}^* + \mu U_{i2}^* = m_{\widetilde{C}_i} V_{i2}, \tag{K.3.5}$$

$$M_2V_{i1}^* + g v_u V_{i2}^* = m_{\widetilde{C}_i} U_{i1}, \qquad g v_d V_{i1}^* + \mu V_{i2}^* = m_{\widetilde{C}_i} U_{i2}. \tag{K.3.6}$$

Next, we use Eqs. (K.2.8) and (K.2.9) to derive:

$$m_{\widetilde{N}_i} N_{i4} = \sum_{j=1}^{4} N_{ij}^* (M_{\psi^0})_{j4} = \frac{v_u}{\sqrt{2}} \left(g' N_{i1}^* - g N_{i2}^*\right) - \mu N_{i3}^*, \tag{K.3.7}$$

$$m_{\widetilde{N}_i} N_{i3} = \sum_{j=1}^{4} N_{ij}^* (M_{\psi^0})_{j3} = -\frac{v_d}{\sqrt{2}} \left(g' N_{i1}^* - g N_{i2}^*\right) - \mu N_{i4}^*, \tag{K.3.8}$$

$$m_{\widetilde{N}_i} N_{i2} = \sum_{j=1}^{4} N_{ij}^* (M_{\psi^0})_{j2} = N_{i2}^* M_2 + \frac{g}{\sqrt{2}} \left(v_d N_{i3}^* - v_u N_{i4}^*\right). \tag{K.3.9}$$

By a judicious combination of the above identities, μ and M_2 can be eliminated. One can then rewrite the Goldstone boson couplings of Eqs. (K.3.1)–(K.3.4) in terms of the gauge boson couplings $O^{L,R}$, $O'^{L,R}$ and $O''^{L,R}$ defined in Eqs. (K.2.1)–(K.2.5). It

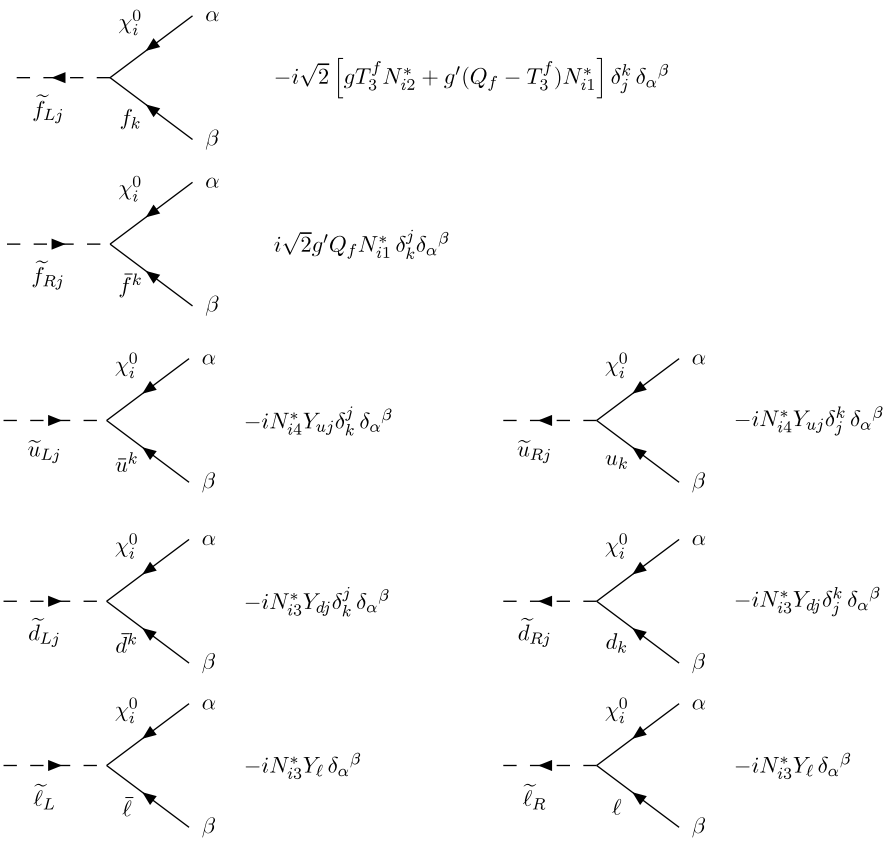

Fig. K.4.2. Feynman rules for the interactions of neutralinos with fermion/sfermion pairs in the MSSM. The fermions are taken to be in a mass-eigenstate basis, and the sfermions are in a basis whose elements are the supersymmetric partners of them. For each rule, there is a corresponding one with all arrows reversed, undotted indices changed to dotted indices with the opposite height, and the coupling (without the explicit i) replaced by its complex conjugate. An alternative version of these rules, for the case that mixing is allowed only among third-family sfermions, is given in Fig. K.4.4.

then follows that:

$$iY^{G^0\chi_i^0\chi_j^0} = \frac{\sqrt{2}}{v}\left(m_{\widetilde{N}_i}O''^L_{ij} - m_{\widetilde{N}_j}O''^R_{ij}\right), \tag{K.3.10}$$

$$iY^{G^0\chi_i^-\chi_j^+} = \frac{\sqrt{2}}{v}\left(m_{\widetilde{C}_i}O'^L_{ij} - m_{\widetilde{C}_j}O'^R_{ij}\right), \tag{K.3.11}$$

$$Y^{G^+\chi_i^0\chi_j^-} = \frac{\sqrt{2}}{v}\left(m_{\widetilde{C}_j}O^{L*}_{ij} - m_{\widetilde{N}_i}O^{R*}_{ij}\right), \tag{K.3.12}$$

$$Y^{G^-\chi_i^0\chi_j^+} = -\frac{\sqrt{2}}{v}\left(m_{\widetilde{N}_i}O^L_{ij} - m_{\widetilde{C}_j}O^R_{ij}\right). \tag{K.3.13}$$

Note that by using $O''^R_{ij} = -O''^L_{ji}$, it follows from Eq. (K.3.10) that $iY^{G^0\chi_i^0\chi_j^0}$ is symmetric under the interchange of i and j, as expected.

In general, for a CP-violating chargino and neutralino sector, the couplings $Y^{\phi^0\chi_i^0\chi_i^0}$ and $Y^{\phi^0\chi_i^+\chi_i^-}$ for $\phi^0 = h^0, H^0, A^0$ are neither purely real nor purely imaginary. That is, the diagonal neutralino and chargino couplings to the physical neutral Higgs bosons are generically CP-violating. However for $\phi^0 = G^0$, the diagonal neutralino and chargino couplings to the neutral Goldstone boson (when multiplied by i) are manifestly real. In particular, Eqs. (K.3.10) and (K.3.11) yield:

$$iY^{G^0\chi_i^0\chi_i^0} = \frac{2\sqrt{2}m_{\widetilde{N}_i}}{v}O''^L_{ii} = \frac{\sqrt{2}\,m_{\widetilde{N}_i}}{v}\left[|N_{i4}|^2 - |N_{i3}|^2\right], \tag{K.3.14}$$

$$iY^{G^0\chi_i^-\chi_i^+} = \frac{\sqrt{2}\,m_{\widetilde{C}_i}}{v}(O'^L_{ii} - O'^R_{ii}) = \frac{m_{\widetilde{C}_i}}{\sqrt{2}\,v}\left[|V_{i2}|^2 - |U_{i2}|^2\right], \tag{K.3.15}$$

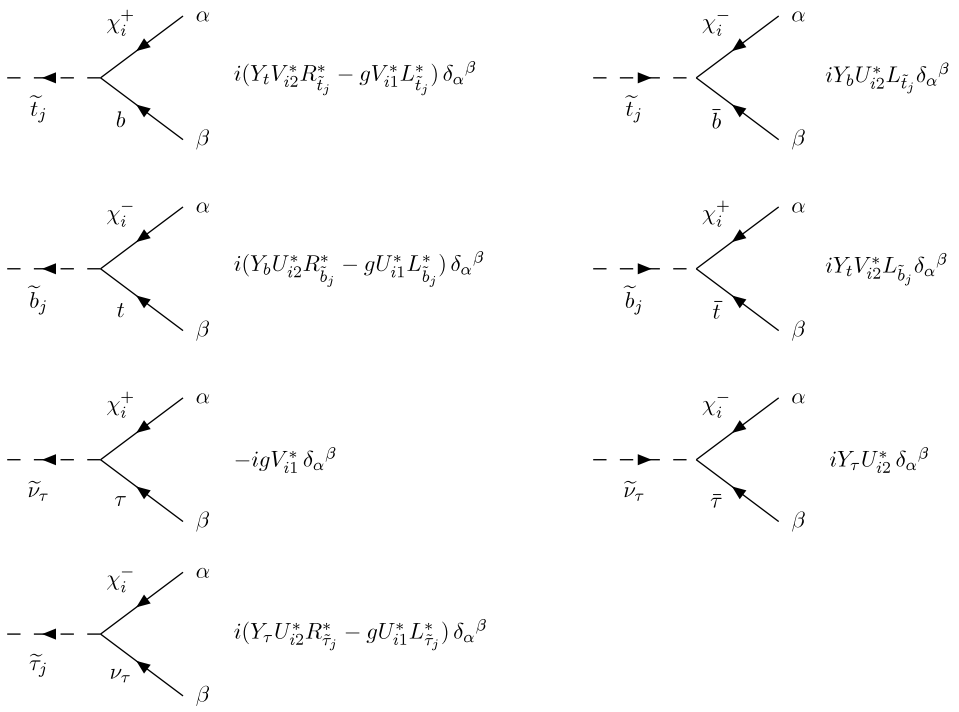

Fig. K.4.3. Feynman rules for the interactions of charginos with third-family fermion/sfermion pairs in the MSSM. The fermions are taken to be in a mass-eigenstate basis. CKM mixing is neglected, and the sfermions are assumed to only mix within the third family. The corresponding rules for the first and second families with the approximation of no mixing and vanishing fermion masses can be obtained from these by setting $Y_f = 0$ and $L_{\tilde{f}_2} = R_{\tilde{f}_1} = 1$ and $L_{\tilde{f}_1} = R_{\tilde{f}_2} = 0$ (so that $\widetilde{f}_1 = \widetilde{f}_R$ and $\widetilde{f}_2 = \widetilde{f}_L$). For each rule, there is a corresponding one with all arrows reversed, undotted indices changed to dotted indices with the opposite height, and the coupling (without the explicit i) replaced by its complex conjugate.

where the unitarity of U and V has been used to obtain the final expression in Eq. (K.3.15). It follows that the diagonal neutralino and chargino couplings to the neutral Goldstone boson are CP-conserving. This result is not surprising, as the corresponding diagonal tree-level couplings of the (longitudinal) Z^0 boson are always CP-conserving as noted at the end of Appendix K.2.

K.4. Chargino and neutralino interactions with fermions and sfermions

In the MSSM, the scalar partners of the two-component fields q and $\bar{q}^\dagger$ are the squarks, denoted by $\widetilde{q}_L$ and $\widetilde{q}_R$, respectively. In our notation, $\widetilde{q}_L^*$ and $\widetilde{q}_R^*$ denote both the complex conjugate fields and the names of the corresponding anti-squarks. Thus $u, \widetilde{u}_L$ and $\widetilde{u}_R$ all have electric charges $+2/3$, whereas $\bar{u}, \widetilde{u}_L^*$ and $\widetilde{u}_R^*$ all have electric charges $-2/3$. Likewise, the scalar partners of the two-component fields ℓ and $\bar{\ell}^\dagger$ are the charged sleptons, denoted by $\widetilde{\ell}_L$ and $\widetilde{\ell}_R$, respectively, with $\ell = e, \mu, \tau$. The sneutrino, $\widetilde{\nu}$ is the superpartner of the neutrino. There is no $\widetilde{\nu}_R$, since there is no $\bar{\nu}$ in the theory.[174]

The Feynman rules for the chargino–quark–squark interactions are given in Fig. K.4.1, and the rules for the neutralino–quark–squark interactions are given in Fig. K.4.2. Here we have taken the quark and lepton two-component fields to be in a mass-eigenstate basis, and the squark and slepton field basis consists of the superpartners of these fields, as described above. Therefore, in practical applications, one must include unitary rotation matrix elements relating the squarks and sleptons as given to the mass eigenstates, which can be different.

In principle, all sfermions with a given electric charge can mix with each other. However, there is a popular, and perhaps phenomenologically and theoretically favored, approximation in which only the sfermions of the third family have significant mixing. For $f = t, b, \tau$, one can then write the relationship between the gauge eigenstates $\tilde{f}_L, \tilde{f}_R$ and the mass eigenstates $\tilde{f}_1, \tilde{f}_2$ as [349]

$$\begin{pmatrix} \tilde{f}_R \\ \tilde{f}_L \end{pmatrix} = X_{\tilde{f}} \begin{pmatrix} \tilde{f}_1 \\ \tilde{f}_2 \end{pmatrix}, \qquad X_{\tilde{f}} \equiv \begin{pmatrix} R_{\tilde{f}_1} & R_{\tilde{f}_2} \\ L_{\tilde{f}_1} & L_{\tilde{f}_2} \end{pmatrix}, \tag{K.4.1}$$

174 It is possible to construct a seesaw-extended MSSM that would be the minimal supersymmetric extension of the seesaw-extended Standard Model described in Appendix J.2. In the seesaw-extended MSSM, both $\bar{\nu}$ and its supersymmetric partner $\widetilde{\nu}_R$ exist. For further details on the sneutrino sector of the seesaw-extended MSSM, see Ref. [298].

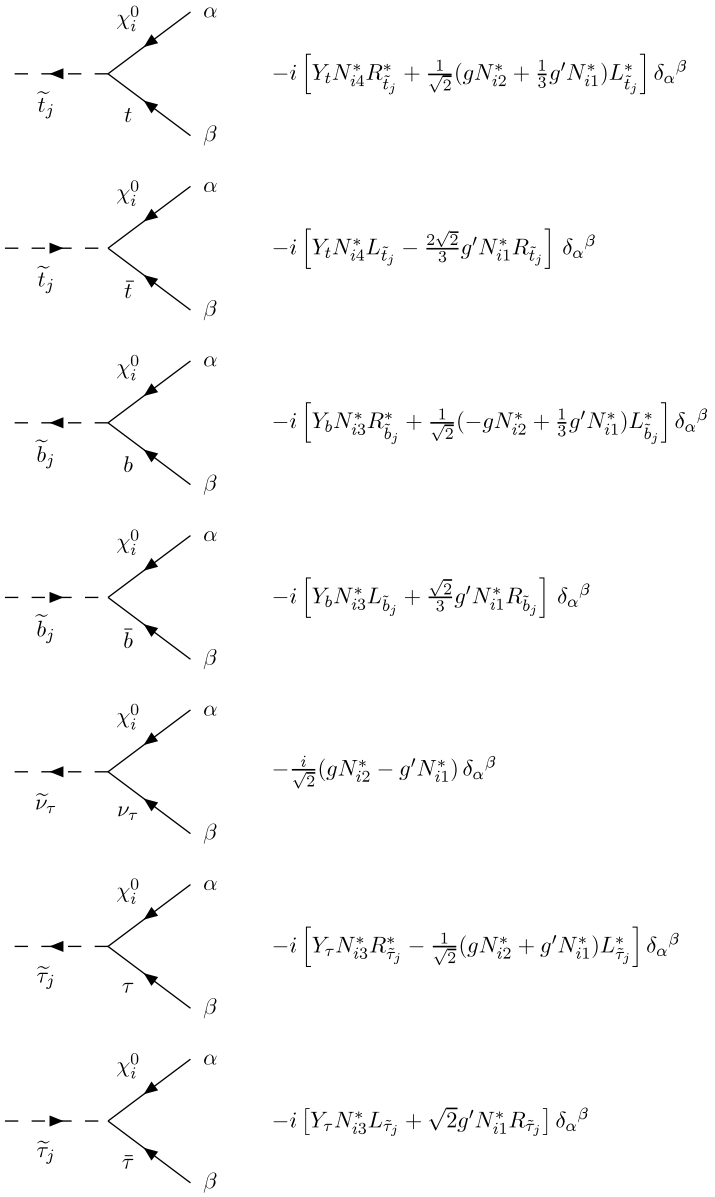

Fig. K.4.4. Feynman rules for the interactions of neutralinos with third-family fermion/sfermion pairs in the MSSM. The comments of the caption of Fig. K.4.3 also apply here.

where X is a 2×2 unitary matrix. Then one can choose $R_{\tilde{f}_1} = L_{\tilde{f}_2}^* = c_{\tilde{f}}$, and $L_{\tilde{f}_1} = -R_{\tilde{f}_2}^* = s_{\tilde{f}}$ with

$$|c_{\tilde{f}}|^2 + |s_{\tilde{f}}|^2 = 1. \tag{K.4.2}$$

If there is no CP violation, then $c_{\tilde{f}}$ and $s_{\tilde{f}}$ can be taken real, and they are the cosine and sine of a sfermion mixing angle.[175] For the other charged sfermions ($\widetilde{f} = \widetilde{u}, \widetilde{d}, \widetilde{c}, \widetilde{s}, \widetilde{e}, \widetilde{\mu}$), one can use the same notation, and approximate $L_{\tilde{f}_2} = R_{\tilde{f}_1} = 1$ and $L_{\tilde{f}_1} = R_{\tilde{f}_2} = 0$. The resulting Feynman rules for squarks and sleptons that mix within each generation are shown in Figs. K.4.3 and K.4.4.

For each Feynman rule in Figs. K.4.1–K.4.4, one can reverse all arrows by taking $\delta_\alpha{}^\beta \to \delta^{\dot{\alpha}}{}_{\dot{\beta}}$ and complex conjugating the corresponding rule (but leaving the explicit factor of i intact).

175 Our convention for $c_{\tilde{f}}, s_{\tilde{f}}$ has the property that for zero mixing angle, $\widetilde{f}_1 = \widetilde{f}_R$ and $\widetilde{f}_2 = \widetilde{f}_L$. The conventions most commonly found in the literature unfortunately do not have this nice property.

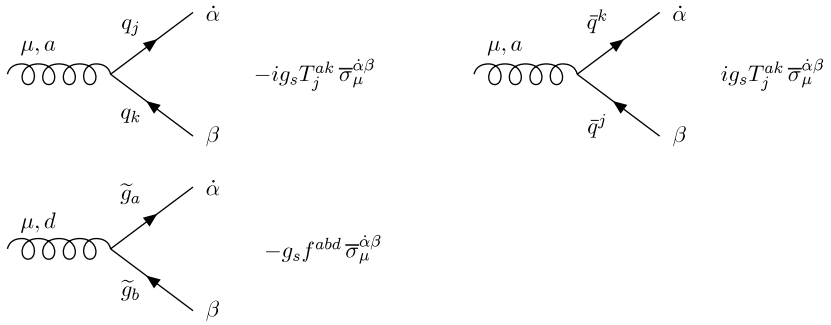

Fig. K.5.1. Fermionic Feynman rules for SUSY-QCD that involve the gluon, with $q = u, d, c, s, t, b$. Lowered (raised) indices j, k correspond to the fundamental (anti-fundamental) representation of $SU(3)_c$. For each rule, a corresponding one with lowered spinor indices is obtained by $\overline\sigma_\mu^{\dot\alpha\beta} \to -\sigma_{\mu\beta\dot\alpha}$.

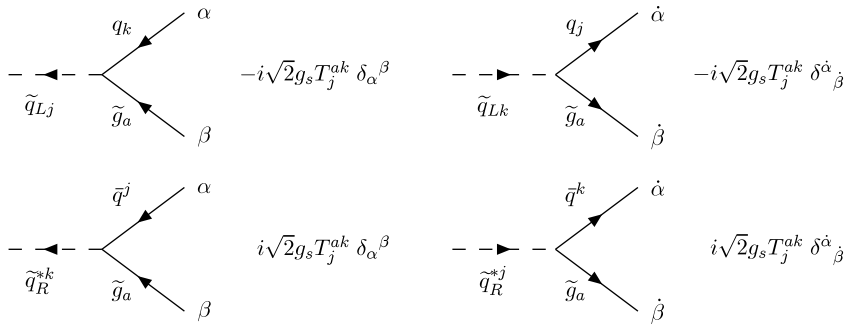

Fig. K.5.2. Fermionic Feynman rules for SUSY-QCD that involve the squarks, in a basis corresponding to the quark mass eigenstates $q = u, d, c, s, t, b$. Lowered (raised) indices j, k correspond to the fundamental (anti-fundamental) representation of $SU(3)_c$, and the index a labels the adjoint representation carried by the gluino. The spinor index heights can be exchanged in each case, by replacing $\delta_\alpha{}^\beta \to \delta_\beta{}^\alpha$ or $\delta^{\dot\alpha}{}_{\dot\beta} \to \delta^{\dot\beta}{}_{\dot\alpha}$. For an alternative set of rules, incorporating $\widetilde q_L$–$\widetilde q_R$ mixing, see Fig. K.5.3.

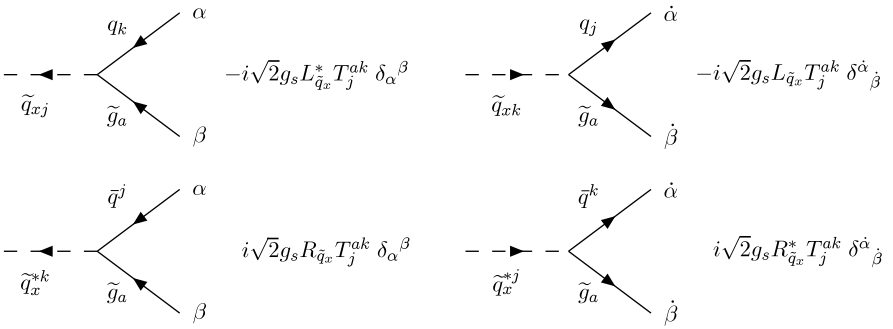

Fig. K.5.3. Fermionic Feynman rules for SUSY-QCD that involve the squarks in the mass-eigenstate basis labeled by $x = 1, 2$ and $q = u, d, c, s, t, b$, in the approximation where mixing is allowed only within a given flavor (typically, for the third family only), as in Eq. (K.4.1). Lowered (raised) indices j, k correspond to the fundamental (anti-fundamental) representation of $SU(3)_c$, and the index a labels the adjoint representation carried by the gluino. The spinor index heights can be exchanged in each case, by replacing $\delta_\alpha{}^\beta \to \delta_\beta{}^\alpha$ or $\delta^{\dot\alpha}{}_{\dot\beta} \to \delta^{\dot\beta}{}_{\dot\alpha}$.

K.5. SUSY-QCD Feynman rules

In supersymmetric (SUSY) QCD, the Lagrangian governing the gluon interactions with colored fermions (gluinos and quarks) in two-component spinor notation, which derives from the covariant derivatives in the kinetic terms, is given by

$$\mathscr{L}_{\rm int} = ig_s f^{abd}\,(\tilde g_a^\dagger\,\overline\sigma_\mu\,\tilde g_b) A_d^\mu - g_s T_j^{ak} \sum_q \left[q^{\dagger j}\overline\sigma_\mu q_k - \bar q_k^\dagger \overline\sigma_\mu \bar q^j\right] A_a^\mu. \tag{K.5.1}$$

Here g_s is the strong coupling constant, $a, b, d = 1, 2, \ldots, 8$ are $SU(3)_c$ adjoint representation indices, and f^{abd} are the $SU(3)$ structure constants. Raised (lowered) indices $j, k = 1, 2, 3$ are color indices in the fundamental (anti-fundamental) representation. We have denoted the two-component gluino field by $\widetilde g_a$ as in Table 5.1 and the gluon field by A_a^μ. The sum $\sum_q$ is over the six flavors $q = u, d, s, c, b, t$ (in either the mass-eigenstate or electroweak gauge-eigenstate basis). The

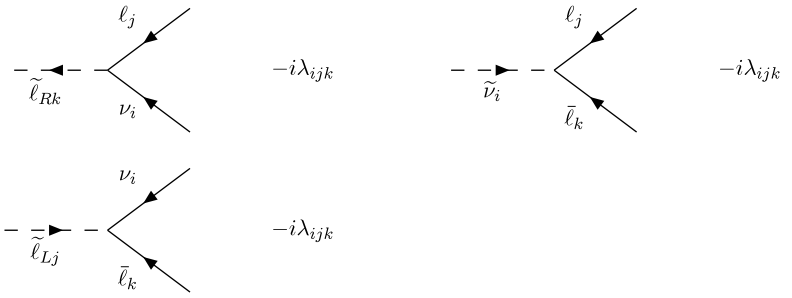

Fig. L.1. Feynman rules for the Yukawa couplings of two-component fermions due to the supersymmetric, R-parity-violating Yukawa Lagrangian $\mathscr{L}_{L\bar{L}\bar{E}}$ [cf. Eq. (L.1)]. For each diagram, there is another with all arrows reversed and $\lambda_{ijk} \to \lambda^*_{ijk}$.

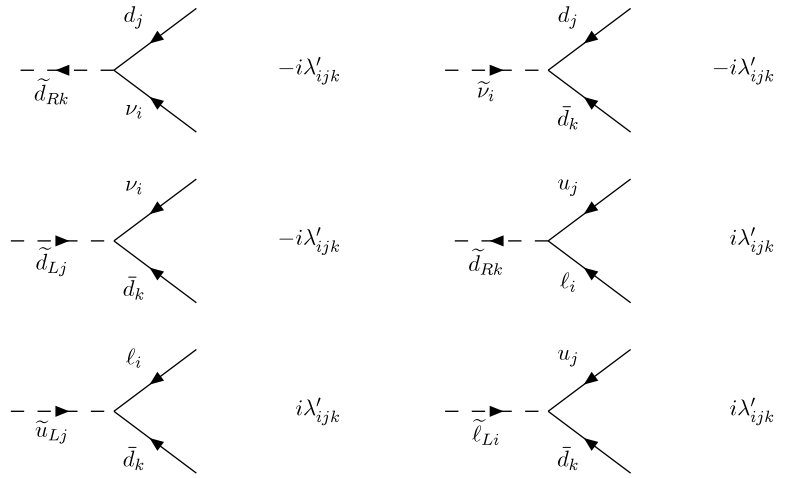

Fig. L.2. Feynman rules for the Yukawa couplings of two-component fermions for the supersymmetric, R-parity-violating Yukawa Lagrangian $\mathscr{L}_{LQ\bar{d}}$ [cf. Eq. (L.2)]. For each diagram, there is another with all arrows reversed and $\lambda'_{ijk} \to \lambda'^*_{ijk}$.

Fig. L.3. Feynman rules for the Yukawa couplings of two-component fermions due to the supersymmetric, R-parity-violating Yukawa Lagrangian $\mathscr{L}_{\bar{U}\bar{D}\bar{D}}$ [cf. Eq. (L.3)]. For each diagram, there is another with all arrows reversed and $\lambda''_{ijk} \to \lambda''^*_{ijk}$.

corresponding Feynman rules are shown in Fig. K.5.1. The gluino–squark–quark Lagrangian is given by:

$$\mathscr{L}_{\rm int} = -\sqrt{2} g_s T^{ak}_j \sum_q \left[\tilde{g}_a q_k \, \tilde{q}^{*j}_L + \tilde{g}^\dagger_a q^{\dagger j} \, \tilde{q}_{Lk} - \tilde{g}_a \bar{q}^j \, \tilde{q}_{Rk} - \tilde{g}^\dagger_a \bar{q}^\dagger_k \, \tilde{q}^{*j}_R \right], \tag{K.5.2}$$

where the squark fields are taken to be in the same basis as the quarks. The Feynman rules resulting from these Lagrangian terms are shown in Fig. K.5.2.

For practical applications, one typically takes the quark fields as the familiar mass eigenstates, and then performs a unitary rotation on the squarks in the corresponding basis to obtain their mass-eigenstate basis. In the approximation described at the end of Appendix K.4 [cf. Eqs. (K.4.1) and (K.4.2) and the accompanying text], one obtains the Feynman rules of Fig. K.5.3, as an alternative to those of Fig. K.5.2.

Appendix L. Trilinear *R*-parity-violating Yukawa interactions

In the MSSM, a multiplicative R-parity invariance is imposed, where $R = (-1)^{3(B-L)+2S}$ for a particle of baryon number B, lepton number L and spin S [350]. Equivalently, R-parity can be defined to be an additive quantum number modulo 2, where $R = +1$ corresponds to an even R-parity and $R = -1$ corresponds to an odd R-parity. In particular, all the ordinary Standard Model particles are R parity even, whereas the corresponding supersymmetric partners are R parity odd. In the

R-parity-violating extension of the MSSM (denoted below as RPV-MSSM), new interactions are allowed that violate R-parity. Such interactions necessarily violate the $B-L$ global symmetry. R-parity-violating interactions can significantly alter the phenomenology at colliders (see for example [205,208]), especially as the lightest supersymmetric particle (LSP) is no longer stable [209,351]. Moreover, the LSP need not be restricted to the lightest neutralino (or perhaps the sneutrino) as in the MSSM, but can be any supersymmetric particle [204].

In this appendix, we focus on new trilinear supersymmetric Yukawa interactions that can appear in an RPV-MSSM [351–354]:

$$\mathscr{L}_{LL\bar{e}} = -\tfrac{1}{2}\lambda_{ijk}\left(\widetilde{\ell}^{*}_{Rk}\nu_i\ell_j + \widetilde{\nu}_i\ell_j\bar{\ell}_k + \widetilde{\ell}_{Lj}\bar{\ell}_k\nu_i - \widetilde{\ell}^{*}_{Rk}\ell_i\nu_j - \widetilde{\nu}_j\bar{\ell}_k\ell_i - \widetilde{\ell}_{Li}\nu_j\bar{\ell}_k\right) + \text{h.c.}, \tag{L.1}$$

$$\mathscr{L}_{LQ\bar{d}} = -\lambda'_{ijk}\left(\widetilde{d}^{*}_{Rk}\nu_i d_j + \widetilde{\nu}_i d_j\bar{d}_k + \widetilde{d}_{Lj}\bar{d}_k\nu_i - \widetilde{d}^{*}_{Rk}\ell_i u_j - \widetilde{u}_{Lj}\bar{d}_k\ell_i - \widetilde{\ell}_{Li}u_j\bar{d}_k\right) + \text{h.c.}, \tag{L.2}$$

$$\mathscr{L}_{\bar{u}\bar{d}\bar{d}} = -\tfrac{1}{2}\lambda''_{ijk}\epsilon_{pqr}\left[\widetilde{u}^{p*}_{Ri}\bar{d}^{q}_{j}\bar{d}^{r}_{k} + \widetilde{d}^{q*}_{Rj}\bar{u}^{p}_{i}\bar{d}^{r}_{k} + \widetilde{d}^{r*}_{Rk}\bar{u}^{p}_{i}\bar{d}^{q}_{j}\right] + \text{h.c.}, \tag{L.3}$$

where repeated indices are summed over[176]. In Eqs. (L.1)–(L.3), λ_{ijk}, λ'_{ijk}, λ''_{ijk} are dimensionless coupling constants, i, j, k are generation indices, and p, q, $r = 1, 2, 3$ are color $SU(3)$ indices, respectively. The couplings proportional to λ and λ' violate L and conserve B, whereas the couplings proportional to λ'' violate B and conserve L. Various phenomenological constraints on these couplings are summarized in Ref. [354].

In addition to λ_{ijk}, λ'_{ijk}, λ''_{ijk}, the Lagrangian of the RPV-MSSM contains one additional supersymmetric L-violating mass parameter, κ_i, which leads to slepton–Higgs mixing and lepton–higgsino mixing. Finally, supersymmetry-breaking R-parity-violating parameters would also contribute to slepton–Higgs mixing and yields new trilinear scalar interactions. These effects modify the Feynman rules of Appendix K through additional mixing matrices, which we do not include here (for further details, see e.g. Ref. [199]).

Recently, the two-component fermion Feynman rules for the neutral fermions have been given in Refs. [280,355]. Using Eq. (4.3.2) and Fig. 4.3.1 we can now directly determine the corresponding Feynman rules. These are given in Figs. L.1–L.3. The same Lagrangian for the Yukawa interactions is given in terms of four-component fermions in Refs. [206,207]. Two sample computations that make use of these rules are presented in Sections 6.20 and 6.21.

References

[1] B.L. van der Waerden, Nachrichten Akad. Wiss. Göttingen, Math. Physik. Kl. (1929) 100.
[2] P.A.M. Dirac, Proc. R. Soc. (A) 117 (1928) 610; 118 (1928) 351.
[3] E. Majorana, Nuovo Cim. 14 (1937) 171.
[4] P. Minkowski, Phys. Lett. B67 (1977) 421;
M. Gell-Mann, P. Ramond, R. Slansky, in: D. Freedman, P. van Nieuwenhuizen (Eds.), Supergravity, North-Holland Publishing Company, Amsterdam, 1979, p. 315;
T. Yanagida, in: O. Sawada, A. Sugamoto (Eds.), Proceedings of the Workshop on Unified Theory and Baryon Number in the Universe, KEK, Tsukuba, Japan, 1979, p. 95;
R.N. Mohapatra, G. Senjanovic, Phys. Rev. Lett. 44 (1980) 912. Phys. Rev. D23 (1981) 165.
[5] J. Schechter, J.W.F. Valle, Phys. Rev. D 22 (1980) 2227, D25 (1982) 774.
[6] H.P. Nilles, Phys. Rep. 110 (1984) 1.
[7] H.E. Haber, G.L. Kane, Phys. Rep. 117 (1985) 75.
[8] S.P. Martin, A Supersymmetry Primer, in: G.L. Kane (Ed.), Perspectives on Supersymmetry II, World Scientific, Singapore, 2010, pp. 1–153. arXiv:hep-ph/9709356v5. Note that the sign conventions for the σ and $\overline{\sigma}$ matrices employed in the present review are the same as in version 5 of the Primer (but different from those used in earlier versions). For the latest version and errata, see http://zippy.physics.niu.edu/primer.html.
[9] D.J.H. Chung, L.L. Everett, G.L. Kane, S.F. King, J.D. Lykken, L.T. Wang, Phys. Rep. 407 (2005) 1. hep-ph/0312378.
[10] H.E. Haber, Supersymmetry, Part 1 (Theory), in C. Amsler et al. [Particle Data Group Collaboration], Review of Particle Physics, Phys. Lett. B667 (2008) 1211.
[11] E. Cartan, Bull. Math. France 41 (1913) 53.
[12] E. Cartan, Theory of Spinors, Hermann, Paris, 1966, The first edition of this book appeared in 1937.
[13] E. Scholz, Historia Math. 33 (2006) 440.
[14] H. Weyl, Gruppentheorie und Quantenmechanik, S. Hirzel Verlag, Leipzig, 1928, The English translation of this book is, The theory of groups and quantum mechanics, translated from the 2nd revised German edition by H.P. Robertson (Dover Publications, New York, 1949.).
[15] H. Weyl, Z. Phys. 56 (1929) 330; Acad. Sci. USA 15 (1929) 323.
[16] O. Laporte, G.E. Uhlenbeck, Phys. Rev. 37 (1931) 1380.
[17] L. Infeld, B.L. van der Waerden, Sitz.-Ber. Preuss. Akad. d. Wiss., Physik.-Math. Kl. 9 (1933) 380.
[18] B.L. van der Waerden, Group Theory and Quantum Mechanics, Springer-Verlag, Heidelberg, 1974, The original version of this book was published in German in 1932.
[19] W.L. Bade, H. Jehle, Rev. Modern Phys. 25 (1953) 714.
[20] F. Cap, Fortsch. Phys. 2 (1954) 207.
[21] P.G. Bergmann, Phys. Rev. 107 (1957) 624.
[22] R. Penrose, Ann. Physics 10 (1960) 171;
E. Newman, R. Penrose, J. Math. Phys. 3 (1962) 566; 4 (1963) 998 (erratum).
[23] P.A.E. Pirani, in: S. Deser, K.W. Ford (Eds.), Lectures on General Relativity, in: Proceedings of the 1964 Brandeis Summer Institute in Theoretical Physics, vol. 1, Prentice Hall, Inc, Englewood Cliffs, NJ, 1965, pp. 249–373.
[24] F. Cap, W. Majerotto, W. Raab, P. Unteregger, Fortsch. Phys. 14 (1966) 205.

[176] The extra factors of $\frac{1}{2}$ in Eqs. (L.1) and (L.3) have been chosen for convenience, due to the antisymmetry properties of the corresponding couplings: $\lambda_{ijk} = -\lambda_{jik}$, $\lambda''_{ijk} = -\lambda''_{ikj}$.

[25] R. Penrose, Acta Phys. Polon. B30 (1999) 2979.
[26] D. Canarutto, Int. J. Geom. Meth. Mod. Phys. 4 (2007) 1005.
[27] W.C. Parke, H. Jehle, in: W.E. Brittin, A.O. Barut (Eds.), Lectures in Theoretical Physics, Volume VII A—Lorentz Group, in: Proceedings of the Summer Institute for Theoretical Physics, University of Colorado, Boulder, CO, 1964, University of Colorado Press, Boulder, CO, 1965, pp. 297–386.
[28] E.M. Corson, Introduction to Tensors, Spinors and Relativistic Wave Equations, Blackie and Son, London, 1953.
[29] H. Umezawa, Quantum Field Theory, North-Holland Publishing Company, Amsterdam, 1956.
[30] J. Rzewuski, Field Theory Volume 1: Classical Theory, PWN-Polish Scientific Publishers, Warsaw, 1958, published in Great Britain by Iliffe Books Ltd., London, 1967.
[31] P. Roman, Theory of Elementary Particles, North-Holland Publishing Company, Amsterdam, 1960.
[32] I.M. Gel'fand, R.A. Milnos, Z. Ya Shapiro, Representations of the Rotation and Lorentz Groups and their Applications, The Macmillan Company, New York, 1963.
[33] J. Aharoni, The Special Theory of Relativity, 2nd ed., Oxford University Press, London, UK, 1965.
[34] A.O. Barut, The Theory of the Scattering Matrix for the Interactions of Fundamental Particles, The Macmillan Company, New York, 1967.
[35] V.B. Berestetskii, E.M. Lifshitz, L.P. Pitaevskii, Relativistic Quantum Theory, Pergammon Press, Oxford, UK, 1971.
[36] P.A. Carruthers, Spin and Isospin in Particle Physics, Gordon and Breach Science Publishers, New York, 1971.
[37] C.W. Misner, K.S. Thorne, J.A. Wheeler, Gravitation, W.H. Freeman and Company, San Francisco, CA, 1973.
[38] Yu.V. Novozhilov, Introduction to Elementary Particle Theory, Pergammon Press, Oxford, UK, 1975.
[39] V.B. Berestetskii, E.M. Lifshitz, L.P. Pitaevskii, Quantum Electrodynamics, Pergammon Press, Oxford, UK, 1980.
[40] A.O. Barut, Electrodynamics and Classical Theory of Fields and Particles, Dover Publications, Inc, New York, NY, 1980.
[41] F. Scheck, Leptons, Hadrons and Nuclei, North-Holland Physics Publishing, Amsterdam, 1983. The revised version of this book appears under a different title, Electromagnetism and Strong Interactions: An Introduction to Theoretical Particle Physics, 2nd ed., Springer-Verlag, Berlin, 1996
[42] R. Penrose, W. Rindler, Spinors and Space-Time, volume 1: Two-Spinor Calculus and Relativistic Fields, Cambridge University Press, Cambridge, UK, 1984.
[43] R.M. Wald, General Relativity, University of Chicago Press, Chicago, IL, 1984.
[44] W.-K. Tung, Group Theory in Physics, World Scientific, Singapore, 1985.
[45] K.N. Srinivasa Rao, The Rotation and Lorentz Groups and their Representations for Physicists, Wiley Eastern Limited, New Delhi, 1988.
[46] J. Stewart, Advanced General Relativity, Cambridge University Press, Cambridge, UK, 1991.
[47] G.L. Naber, The Geometry of Minkowski Spacetime: An Introduction to the Mathematics of the Special Theory of Relativity, Springer-Verlag, New York, 1992.
[48] L.H. Ryder, Quantum Field Theory, 2nd ed., Cambridge University Press, Cambridge, UK, 1996.
[49] R. Ticciati, Quantum Field Theory for Mathematicians, Cambridge University Press, Cambridge, UK, 1999.
[50] W. Siegel, Fields, arXiv:hep-th/9912205.
[51] J. Hladik, Spinors in Physics, Springer-Verlag, New York, 1999.
[52] M. Carmeli, S. Malin, Theory of Spinors: An Introduction, World Scientific, Singapore, 2000.
[53] M. Carmeli, Group Theory and General Relativity: Representations of the Lorentz Group and their Applications to the Gravitational Field, Imperial College Press, London, UK, 2000.
[54] R.F. Streater, A.S. Wightman, PCT, Spin and Statistics, and All That, Princeton University Press, Princeton, NJ, 2000.
[55] S. Pokorski, Gauge Field Theories, 2nd ed., Cambridge University Press, Cambridge, UK, 2000.
[56] R.U. Sexl, H.K. Urbantke, Relativity, Groups, Particles: Special Relativity and Relativistic Symmetry in Field and Particle Physics, Springer-Verlag, Vienna, 2001.
[57] M. Carmeli, Classical Fields: General Relativity and Gauge Theory, World Scientific, Singapore, 2001.
[58] A.I. Akhiezer, S.V. Peletminsky, Fields and Fundamental Interactions, Taylor & Francis, London, 2002.
[59] M. Blagojević, Gravitation and Gauge Symmetries, Institute of Physics Publishing, Bristol, UK, 2002.
[60] P. O'Donnell, Introduction to 2-Spinors in General Relativity, World Scientific, Singapore, 2003.
[61] T. Morii, C.S. Lim, S.N. Mukherjee, The Physics of the Standard Model and Beyond, World Scientific, Singapore, 2004.
[62] H. Stephani, Relativity: An Introduction to Special and General Relativity, 3rd ed., Cambridge University Press, Cambridge, UK, 2004.
[63] H. Saller, Operational Quantum Theory II: Relativistic Structures, Springer-Verlag, New York, 2006.
[64] J. Plebański, A. Krasiński, An Introduction to General Relativity and Cosmology, Cambridge University Press, Cambridge, UK, 2006.
[65] M. Srednicki, Quantum Field Theory, Cambridge University Press, Cambridge, UK, 2007.
[66] T. Banks, Modern Quantum Field Theory: A Concise Introduction, Cambridge University Press, Cambridge, UK, 2008.
[67] P. Langacker, The Standard Model and Beyond, CRC Press, Taylor & Francis Group, Boca Raton, FL, 2010.
[68] J. Wess, J. Bagger, Supersymmetry and Supergravity, Princeton University Press, Princeton, NJ, 1992.
[69] S.J. Gates Jr., M.T. Grisaru, M. Roček, W. Siegel, Superspace or One Thousand and One Lessons in Supersymmetry, Benjamin/Cummins Publishing Company, Reading, MA, 1983. Also available at arXiv:hep-th/0108200.
[70] G.G. Ross, Grand Unified Theories, Westview Press, Boulder, CO, 1985.
[71] M.F. Sohnius, Phys. Rep. 128 (1985) 39.
[72] P.P. Srivastava, Supersymmetry, Superfields and Supergravity: an introduction, Adam Hilger, Bristol, UK, 1986.
[73] O. Piguet, K. Sibold, Renormalized Supersymmetry, Birkhäuser, Boston, MA, 1986.
[74] H.J.W. Müller-Kirsten, A. Wiedemann, Supersymmetry: An Introduction with Conceptual and Calculational Details, World Scientific, Singapore, 1987. The revised version of this book appears under a different title, Introduction to Supersymmetry, 2nd ed., World Scientific, Singapore, 2010
[75] J.-P. Derendinger, Lecture notes on globally supersymmetric theories in four and two dimensions, in: E.N. Argyres, N. Tracas, G. Zoupanos (Eds.), Proceedings of the Hellenic School of Particle Physics, Corfu, Greece, September 1989, World Scientific, Singapore, 1990, pp. 111–243. Also available at http://www.derendinger.itp.unibe.ch.
[76] P. West, Introduction to Supersymmetry and Supergravity, extended 2nd ed., World Scientific, Singapore, 1990.
[77] D. Bailin, A. Love, Supersymmetric Gauge Field Theory and String Theory, Institute of Physics Publishing, Bristol, UK, 1994.
[78] I.L. Buchbinder, S.M. Kuzenko, Ideas and Methods of Supersymmetry and Supergravity or a Walk through Superspace, revised ed., Institute of Physics Publishing, Bristol, UK, 1995.
[79] J.D. Lykken, Introduction to supersymmetry, in: C. Efthimiou, B. Greene. (Eds.), Fields, Strings and Duality, in: Proceedings of the 1996 Theoretical Advanced Summer Institute, TASI-96, Boulder, CO, World Scientific, Singapore, 1997, pp. 85–153.
[80] S.K. Soni, S. Singh, Supersymmetry: Basics and Concepts, Narosa Publishing House, New Delhi, 2000.
[81] A.S. Galperin, E.A. Ivanov, V.I. Ogievetsky, E.S. Sokatchev, Harmonic Superspace, Cambridge University Press, Cambridge, UK, 2001.
[82] A. Bilal, Introduction to supersymmetry, expanded notes of lectures given at the Summer School GIF 2000, hep-th/0101055.
[83] J.M. Figueroa-O'Farrill, BUSSTEPP lectures on supersymmetry, hep-th/0109172.
[84] R.N. Mohapatra, Unification and Supersymmetry: The Frontiers of Quark-Lepton Physics, 3rd ed., Springer-Verlag, New York, 2003.
[85] M. Drees, R.M. Godbole, P. Roy, Theory and Phenomenology of Sparticles, World Scientific, Singapore, 2004.
[86] I.J.R. Aitchison, Supersymmetry in Particle Physics: An Elementary Introduction, Cambridge University Press, Cambridge, UK, 2007, A preliminary version of this book is available at arXiv:hep-ph/0505105.
[87] P. Binétruy, Supersymmetry: Theory, Experiment and Cosmology, Oxford University Press, Oxford, UK, 2006.
[88] J. Terning, Modern Supersymmetry, Oxford Science Publications, Oxford, UK, 2006.
[89] M. Dine, Supersymmetry and String Theory, Cambridge University Press, Cambridge, UK, 2007.
[90] P. Budinich, A. Trautman, The Spinorial Chessboard, Springer-Verlag, Berlin, 1988.

[91] I.M. Benn, R.W. Tucker, An Introduction to Spinors and Geometry with Applications in Physics, Adam Hilger, Bristol, UK, 1987.
[92] D.J. Hurley, M.A. Vandyck, Geometry, Spinors and Applications, Praxis Publishing Ltd, Chichester, UK, 2000.
[93] J.D. Bjorken, M.C. Chen, Phys. Rev. 154 (1966) 1335.
[94] G.R. Henry, Phys. Rev. 154 (1967) 1534.
[95] H.W. Fearing, R.R. Silbar, Phys. Rev. D6 (1972) 471.
[96] J.O. Eeg, J. Math. Phys. 21 (1980) 170.
[97] G. Passarino, Phys. Rev. D28 (1983) 2867; Nuclear Phys. B237 (1984) 249.
[98] R. Kleiss, Nuclear Phys. B241 (1984) 61.
[99] R. Kleiss, W.J. Stirling, Nuclear Phys. B262 (1985) 235.
[100] A. Ballestrero, E. Maina, Phys. Lett. B350 (1995) 225, hep-ph/9403244.
[101] Z. Xu, D.-H. Zhang, L. Chang, Tsinghua University preprints TUTP-84/3 (1984), TUTP-84/4 (1985); TUTP-84/5a (1985), Nuclear Phys. B291 (1987) 392.
[102] G. Chalmers, W. Siegel, Phys. Rev. D59 (1999) 045012, hep-ph/9708251 and 045013 hep-ph/9801220.
[103] G.R. Farrar, F. Neri, Phys. Lett. B130 (1983) 109; B152 (1985) 443 (erratum).
[104] A. Kersch, F. Scheck, Nuclear Phys. B263 (1986) 475.
[105] K. Hagiwara, D. Zeppenfeld, Nuclear Phys. B274 (1986) 1.
[106] F.A. Berends, W. Giele, Nuclear Phys. B294 (1987) 700;
F.A. Berends, W.T. Giele, H. Kuijf, Nuclear Phys. B321 (1989) 39.
[107] W.T. Giele, Properties and calculations of multi parton processes, Ph.D. Thesis, University of Leiden, 1989.
[108] S. Dittmaier, Gauge boson production in electron–photon collisions, Ph.D. Thesis, RX-1526, University of Würzburg, 1993.
[109] S. Dittmaier, Phys. Rev. D 59 (1999) 016007. hep-ph/9805445.
[110] T. Hahn, Nuclear Phys. B Proc. Suppl. 116 (2003) 363. hep-ph/0210220 ; and in the Proceedings of the 2005 International Linear Collider Workshop (LCWS 2005), Stanford, California, 18–22 March 2005, paper 0604. hep-ph/0506201.
[111] T. Takagi, Japan J. Math. 1 (1925) 83.
[112] C. Bouchiat, L. Michel, Nuclear Phys. 5 (1958) 416;
L. Michel, Suppl. Nuovo Cim. 14 (1959) 95.
[113] The LaTeX source file for this paper is available from H.K. Dreiner, H.E. Haber, S.P. Martin, arXiv:0812.1594 [hep-ph], at http://arxiv.org/abs/0812.1594.
[114] M. Peskin, D. Schroeder, Introduction to Quantum Field Theory, Westview Press, Boulder, CO, 1995.
[115] E. Massa, Nuovo Cim. B 9 (1972) 41.
[116] V. Bargmann, Sitz.-Ber. Preuss. Akad. Wiss., Physik.-Math. Kl. (1932) 346;
W. Pauli, Annalen Phys. 18 (1933) 305; 18, (1933), 337;
W. Kofink, Math. Z. 51 (1949) 702.
[117] Q. Duret, B. Machet, Annals of Physics (2010) in press (doi:10.1016/j.aop.2010.05.016), arXiv:0809.0431 [hep-ph].
[118] For a review and a guide to the literature, see e.g. D.J. Gross, R.D. Pisarski, L.G. Yaffe, Rev. Mod. Phys. 53 (1981) 43;
A.I. Vainshtein, V.I. Zakharov, V.A. Novikov, M.A. Shifman, Sov. Phys. Usp. 25 (1982) 195 [Usp. Fiz. Nauk 136 (1982) 553];
T. Schafer, E.V. Shuryak, Rev. Mod. Phys. 70 (1998) 323. hep-ph/9610451;
D. Diakonov, Prog. Part. Nucl. Phys. 51 (2003) 173. hep-ph/0212026.
[119] N. Dorey, T.J. Hollowood, V.V. Khoze, M.P. Mattis, Phys. Rep. 371 (2002) 231. hep-th/0206063.
[120] S. Vandoren, P. van Nieuwenhuizen, Lectures on instantons, arXiv:0802.1862 [hep-th].
[121] J. Zinn-Justin, Quantum Field Theory and Critical Phenomena, 4th ed., Oxford University Press, Oxford, UK, 2002.
[122] K. Fujikawa, H. Suzuki, Path Integrals and Quantum Anomalies, Oxford University Press, Oxford, UK, 2004.
[123] G.C. Wick, Phys. Rev. 80 (1950) 268.
[124] G.'t Hooft, M.J.G. Veltman, Nuclear Phys. B44 (1972) 189;
C.G. Bollini, J.J. Giambiagi, Nuovo Cim. B12 (1972) 20;
J.F. Ashmore, Nuovo Cim. Lett. 4 (1972) 289; Commun. Math. Phys. 29 (1973) 177;
G.M. Cicuta, E. Montaldi, Nuovo Cim. Lett. 4 (1972);
For a nice review, see e.g. G. Leibbrandt, Rev. Mod. Phys. 47 (1975) 849;
R. Delbourgo, Rept. Prog. Phys. 39 (1976) 345.
[125] K. Osterwalder, R. Schrader, Phys. Rev. Lett. 29 (1972) 1423; Helv. Phys. Acta 46 (1973) 277;
J. Frohlich, K. Osterwalder, Helv. Phys. Acta 47 (781) (1975);
B. Zumino, Phys. Lett. 69B (1977) 369;
H. Nicolai, Nuclear Phys. B140 (1978) 294;
J. Kupsch, W.D. Thacker, Fortsch. Phys. 38 (1990) 35.
[126] M.R. Mehta, Phys. Rev. Lett. 65 (1990) 1983; 66 (1991) 522 (erratum); Mod. Phys. Lett. A6 (1991) 2811; Phys. Lett. B274 (1992) 53.
[127] P. van Nieuwenhuizen, A. Waldron, Phys. Lett. B389 (1996) 29. hep-th/9608174;
A. Waldron, Phys. Lett. B433 (1998) 369. hep-th/9702057;
A.J. Mountain, The JHEP Proceedings of the TMR Meeting on Quantum Aspects of Gauge Theories, Supersymmetry and Unification, Paris, France, 1–7 September 1999.
[128] D.G.C. McKeon, T.N. Sherry, Annals Phys. 288 (2001) 2.
[129] J. Lukierski, A. Nowicki, J. Math. Phys. 25 (1984) 2545;
T. Hatanaka, S.V. Ketov, Nuclear Phys. B794 (2008) 495. arXiv:0707.4218 [hep-th].
[130] R. Brauer, H. Weyl, Amer. J. Math. 57 (1935) 425.
[131] F. Gliozzi, J. Scherk, D.I. Olive, Nuclear Phys. B122 (1977) 253;
J. Scherk, Recent Developments in Gravitation, in: M. Lévy, S. Deser (Eds.), Proceedings of the NATO Advanced Study Institute, Cargèse 1978, Plenum Press, New York, 1979, pp. 479–517.
[132] P. Van Nieuwenhuizen, Six lectures at the Trieste 1981 summer school on supergravity, in: S. Ferrara, J.G. Taylor (Eds.), Supergravity'81, Proceedings of the 1st School on Supergravity, International Centre for Theoretical Physics, Trieste, Italy, 22 April–6 May 1981, Cambridge University Press, Cambridge, UK, 1982, pp. 151–196;
See also Appendix A of P. Van Nieuwenhuizen, Phys. Rep. 68 (1981) 189.
[133] R. Coquereaux, Phys. Lett. 115 (1982) 389;
A. Trautman, G. Furlan (Eds.), Spinors, reflections and clifford algebras: a review, in: Spinors in Physics and Geometry (Proceedings of the Conference on Spinors in Physics and Geometry, 11–13 Sep 1986, Trieste, Italy), World Scientific, Singapore, 1988, pp. 135–190;
Clifford algebras, spinors and fundamental interactions: Twenty years after, arXiv:math-ph/0509040.
[134] T. Kugo, P.K. Townsend, Nuclear Phys. B221 (1983) 357.
[135] See Appendix A.7 of Ref. [71].
[136] P. Van Nieuwenhuizen, An introduction to simple supergravity and the Kaluza-Klein program, in: B.S. DeWitt, R. Stora (Eds.), Relativity, Groups and Topology II (Proceedings of the Les Houches École d'Été de Physique Théorique, Session XL, 27 June–4 August, 1983), North-Holland Publishing Company, Amsterdam, 1984, pp. 823–932.
[137] G. Chapline, R. Slansky, Nuclear Phys. B209 (1982) 461;
C. Wetterich, Nucl. Phys. B211 (1983) 177; B222 (1983) 20; B234 (1984) 413.

[138] R. Finkelstein, M. Villasante, Phys. Rev. D31 (1985) 425.
[139] J. Kupsch, W.D. Thacker, Fortsch. Phys. 38 (1990) 35.
[140] M.A. De Andrade, Mod. Phys. Lett. A10 (1995) 961. hep-th/9411155;
M.A. De Andrade, F. Toppan, Mod. Phys. Lett. A14 (1999) 1797. hep-th/9904134.
[141] Y. Tanii, Introduction to supergravities in diverse dimensions, arXiv:hep-th/9802138.
[142] A. Van Proeyen, Tools for supersymmetry, lectures in the spring school, in: Quantum Field Theory, Supersymmetry and Superstrings, (Călimăneşti, Romania, April 1988) arXiv:hep-th/9910030;
J.M. Figueroa-O'Farrill, Majorana Spinors, Available from http://www.maths.ed.ac.uk/~jmf/Teaching/Notes.html.
[143] K.M. Case, Phys. Rev. 107 (1957) 307.
[144] A. Aste, arXiv:0806.1690 [hep-th].
[145] P. Cvitanović, Group Theory: Birdtracks, Lie's, and Exceptional Groups, Princeton University Press, Princeton, NJ, 2008.
[146] See e.g. H. Georgi, Annual Rev. Nucl. Part. Sci. 43 (1993) 209;
T. Mannel, Effective Field Theories, in: Springer Tracts in Modern Physics, vol. 203, Springer-Verlag, Berlin, 2004.
[147] R.A. Horn, C.R. Johnson, Matrix Analysis, Cambridge University Press, Cambridge, UK, 1990.
[148] O. Napoly, Phys. Lett. 106B (1981) 125.
[149] B. Zumino, J. Math. Phys. 3 (1962) 1055.
[150] J. Schechter, J.W.F. Valle, Phys. Rev. D24 (1981) 1883; D25 (1982) 283 (erratum).
[151] See, e.g. T.-P. Cheng, L.-F. Li, Gauge Theory of Elementary Particle Physics, Oxford University Press, Oxford, UK, 1984;
D. Bailin, A. Love, Introduction to Gauge Field Theory, revised ed., Institute of Physics Publishing, Bristol, UK, 1993.
[152] L. Bergstrom, P. Ullio, J.H. Buckley, Astropart. Phys. 9 (1998) 137. astro-ph/9712318.
[153] P. Gondolo, G. Gelmini, Nuclear Phys. B360 (1991) 145.
[154] P. Ullio, L. Bergstrom, J. Edsjo, C.G. Lacey, Phys. Rev. D66 (2002) 123502. astro-ph/0207125.
[155] E.W. Kolb, M.S. Turner, The Early Universe, Westview Press, Boulder, CO, 1994.
[156] See e.g. M. Maggiore, A Modern Introduction to Quantum Field Theory, Oxford University Press, Oxford, UK, 2005, pp. 167–170.
[157] J.J. Sakurai, Advanced Quantum Mechanics, Addison-Wesley Publishing Company, Reading, MA, 1967.
[158] C.P. Frahm, Am. J. Phys. 51 (1983) 826.
[159] D.S. Bernstein, Matrix Mathematics: Theory, Facts, and Formulas, 2nd ed., Princeton University Press, Princeton, NJ, 2009.
[160] H.J. Bhabha, Proc. Roy. Soc. London A 154 (1935) 195.
[161] S. Weinberg, Phys. Rev. Lett. 19 (1967) 1264.
[162] M. Kobayashi, T. Maskawa, Prog. Theor. Phys. 49 (1973) 652;
N. Cabibbo, Phys. Rev. Lett. 10 (1963) 531.
[163] K. Byckling, K. Kajantie, Particle Kinematics, John Wiley & Sons, Ltd, London, 1973.
[164] V.D. Barger, R.J.N. Phillips, Collider Physics, Westview Press, Boulder, CO, 1996.
[165] L.B. Okun, Leptons and Quarks, North-Holland Publishing Company, Amsterdam, 1982.
[166] This was first calculated for electrons in L. Resnick, M.K. Sundaresan, P.J.S. Watson, Phys. Rev. D8 (1973) 172.
[167] J.F. Gunion, H.E. Haber, G. Kane, S. Dawson, The Higgs Hunter's Guide, Westview Press, Boulder, CO, 2000.
[168] D.A. Dicus, S. Nandi, X. Tata, Phys. Lett. B129 (1983) 451; B145 (1984) 448 (erratum).
[169] J.F. Gunion, H.E. Haber, Phys. Rev. D37 (1988) 2515.
[170] J.F. Gunion, H.E. Haber, Nuclear Phys. B272 (1986) 1; B402 (1993) 567 (erratum).
[171] W.Y. Keung, L. Littenberg, Phys. Rev. D28 (1983) 1067.
[172] A. Denner, S. Dittmaier, Nucl. Phys. B Proc. Suppl. 160 (2006) 22. hep-ph/0605312.
[173] A. Denner, S. Dittmaier, M. Roth, D. Wackeroth, Nuclear Phys. B560 (1999) 33. hep-ph/9904472;
A. Denner, S. Dittmaier, M. Roth, L.H. Wieders, Nuclear Phys. B724 (2005) 247. hep-ph/0505042.
[174] R.M. Barnett, K.S. Lackner, H.E. Haber, Phys. Rev. Lett. 51 (1983) 176; Phys. Rev. D29 (1984) 1381.
[175] A. Bartl, H. Fraas, W. Majerotto, Nuclear Phys. B278 (1986) 1.
[176] J.R. Ellis, J.M. Frere, J.S. Hagelin, G.L. Kane, S.T. Petcov, Phys. Lett. B132 (1983) 436;
E. Reya, Phys. Lett. B133 (1983) 245;
P. Chiappetta, J. Soffer, P. Taxil, F.M. Renard, P. Sorba, Nuclear Phys. B262 (1985) 495; B279 (1987) 824 (erratum).
[177] S. Dawson, E. Eichten, C. Quigg, Phys. Rev. D31 (1985) 1581.
[178] H. Goldberg, Phys. Rev. Lett. 50 (1983) 1419.
[179] J.R. Ellis, J.S. Hagelin, D.V. Nanopoulos, K.A. Olive, M. Srednicki, Nuclear Phys. B238 (1984) 453.
[180] K. Griest, Phys. Rev. Lett. 61 (1988) 666; Phys. Rev. D38 (1988) 2357; D39 (1989) 3802 (erratum).
[181] G. Jungman, M. Kamionkowski, K. Griest, Phys. Rep. 267 (1996) 195. hep-ph/9506380.
[182] A. Bottino, F. Donato, N. Fornengo, S. Scopel, Phys. Rev. D68 (2003) 043506. hep-ph/0304080;
G. Belanger, F. Boudjema, A. Cottrant, A. Pukhov, S. Rosier-Lees, J. High Energy Phys. 0403 (2004) 012. hep-ph/0310037.
[183] H.K. Dreiner, S. Heinemeyer, O. Kittel, U. Langenfeld, A.M. Weber, G. Weiglein, Eur. Phys. J. C62 (2009) 547. arXiv:0901.3485 [hep-ph].
[184] A.J. Tylka, Phys. Rev. Lett. 63 (1989) 840; 63 (1989) 1658 (erratum);
M. Kamionkowski, M.S. Turner, Phys. Rev. D43 (1991) 1774;
E.A. Baltz, J. Edsjo, Phys. Rev. D59 (1998) 023511. astro-ph/9808243;
D. Hooper, J. Silk, Phys. Rev. D71 (2005) 083503. hep-ph/0409104;
S. Profumo, P. Ullio, JCAP 0407 (2004) 006. hep-ph/0406018.
[185] W.H. Press, D.N. Spergel, Astrophys. J. 296 (1985) 679;
J.R. Ellis, R.A. Flores, S. Ritz, Phys. Lett. B 198 (1987) 393;
A. Gould, Astrophys. J. 321 (1987) 560;
S. Ritz, D. Seckel, Nuclear Phys. B304 (1988) 877;
M. Kamionkowski, Phys. Rev. D44 (1991) 3021;
M. Ackermann, et al., AMANDA Collaboration, Astropart. Phys. 24 (2006) 459. astro-ph/0508518.
[186] L. Bergstrom, J. Edsjo, M. Kamionkowski, Astropart. Phys. 7 (1997) 147. astro-ph/9702037.
[187] A. Bartl, H. Fraas, W. Majerotto, Z. Phys. C30 (1986) 441.
[188] D.A. Dicus, S. Nandi, W.W. Repko, X. Tata, Phys. Rev. Lett. 51 (1983) 1030; 51 (1983) 1813 (erratum);
P. Chiappetta, J. Soffer, P. Taxil, F.M. Renard, P. Sorba, Nuclear Phys. B262 (1985) 495; B279 (1987) 824 (erratum).
[189] S.Y. Choi, A. Djouadi, H.K. Dreiner, J. Kalinowski, P.M. Zerwas, Eur. Phys. J. C7 (1999) 123. hep-ph/9806279.
[190] W. Beenakker, M. Klasen, M. Kramer, T. Plehn, M. Spira, P.M. Zerwas, Phys. Rev. Lett. 83 (1999) 3780. hep-ph/9906298.
[191] H. Baer, K. Hagiwara, X. Tata, Phys. Rev. D35 (1987) 1598.
[192] S. Dimopoulos, M. Dine, S. Raby, S.D. Thomas, Phys. Rev. Lett. 76 (1996) 3494. hep-ph/9601367.
[193] G.F. Giudice, R. Rattazzi, Phys. Rep. 322 (1999) 419. hep-ph/9801271.
[194] S. Ambrosanio, G.D. Kribs, S.P. Martin, Nuclear Phys. B516 (1998) 55. hep-ph/9710217.
[195] P. Fayet, Phys. Lett. 70B (1977) 461; 86B (1979) 272;
R. Casalbuoni, S. De Curtis, D. Dominici, F. Feruglio, R. Gatto, Phys. Lett. B215 (1988) 313; Phys. Rev. D39 (1989) 2281.

[196] N. Cabibbo, G.R. Farrar, L. Maiani, Phys. Lett. 105B (1981) 155;
D.R. Stump, M. Wiest, C.P. Yuan, Phys. Rev. D54 (1996) 1936. hep-ph/9601362;
S. Ambrosanio, G.L. Kane, G.D. Kribs, S.P. Martin, S. Mrenna, Phys. Rev. Lett. 76 (1996) 3498. hep-ph/9602239; Phys. Rev. D54 (1996) 5395. hep-ph/9605398.
[197] R. Cutler, D.W. Sivers, Phys. Rev. D17 (1978) 196.
[198] P.R. Harrison, C.H. Llewellyn Smith, Nuclear Phys. B213 (1983) 223; B223 (1983) 542 (erratum).
[199] B.C. Allanach, A. Dedes, H.K. Dreiner, Phys. Rev. D69 (2004) 115002. hep-ph/0309196.
[200] B.C. Allanach, M.A. Bernhardt, H.K. Dreiner, C.H. Kom, P. Richardson, Phys. Rev. D75 (2007) 035002. hep-ph/0609263;
H.K. Dreiner, S. Grab, M.K. Trenkel, Phys. Rev. D79 (2009) 016002; D79 (2009) 019902 (erratum). arXiv:0808.3079 [hep-ph].
[201] S. Dimopoulos, L.J. Hall, Phys. Lett. B207 (1988) 210;
J. Erler, J.L. Feng, N. Polonsky, Phys. Rev. Lett. 78 (1997) 3063. hep-ph/9612397;
H.K. Dreiner, P. Richardson, M.H. Seymour, Phys. Rev. D63 (2001) 055008. hep-ph/0007228.
[202] H.K. Dreiner, S. Grab, M. Kramer, M.K. Trenkel, Phys. Rev. D75 (2007) 035003. hep-ph/0611195.
[203] M.A. Bernhardt, S.P. Das, H.K. Dreiner, S. Grab, Phys. Rev. D79 (2009) 035003. arXiv:0810.3423 [hep-ph].
[204] H.K. Dreiner, S. Grab, Phys. Lett. B679 (2009) 45. arXiv:0811.0200 [hep-ph].
[205] S. Dimopoulos, R. Esmailzadeh, L.J. Hall, G.D. Starkman, Phys. Rev. D41 (1990) 2099.
[206] H.K. Dreiner, P. Richardson, M.H. Seymour, J. High Energy Phys. 0004 (2000) 008. hep-ph/9912407.
[207] P. Richardson, Simulations of *R*-parity violating SUSY models, Ph.D. Thesis, Oxford University, 2000. hep-ph/0101105.
[208] H.K. Dreiner, G.G. Ross, Nuclear Phys. B365 (1991) 597.
[209] S. Dawson, Nuclear Phys. B261 (1985) 297.
[210] B.C. Allanach, H.K. Dreiner, P. Morawitz, M.D. Williams, Phys. Lett. B420 (1998) 307. hep-ph/9708495;
H. Baer, C. Kao, X. Tata, Phys. Rev. D51 (1995) 2180. hep-ph/9410283;
M. Hirsch, A. Vicente, W. Porod, Phys. Rev. D77 (2008) 075005. arXiv:0802.2896 [hep-ph].
[211] E.A. Baltz, P. Gondolo, Phys. Rev. D57 (1998) 2969. hep-ph/9709445.
[212] J. Butterworth, H.K. Dreiner, Nuclear Phys. B397 (1993) 3. hep-ph/9211204;
H.K. Dreiner, M. Guchait, D.P. Roy, Phys. Rev. D49 (1994) 3270. hep-ph/9310291;
H.K. Dreiner, P. Morawitz, Nuclear Phys. B428 (1994) 31; B574 (2000) 874 (erratum). hep-ph/9405253.
[213] Y. Nambu, G. Jona-Lasinio, Phys. Rev. 122 (1961) 345; 124 (1961) 246.
[214] Y. Nambu, New trends in strong coupling gauge theories, in: M. Bando, T. Muta, K. Yamawaki (Eds.), Proceedings of the 1988 International Workshop, Nagoya, Japan, 24–27 August 1988, World Scientific, Singapore, 1989, pp. 3–11.
[215] V.A. Miransky, M. Tanabashi, K. Yamawaki, Mod. Phys. Lett. A4 (1989) 1043; Phys. Lett. B221 (1989) 177;
W.J. Marciano, Phys. Rev. Lett. 62 (1989) 2793; Phys. Rev. D41 (1990) 219.
[216] W.A. Bardeen, C.T. Hill, M. Lindner, Phys. Rev. D41 (1990) 1647.
[217] D.E. Clague, G.G. Ross, Nuclear Phys. B364 (1991) 43.
[218] C.T. Hill, Phys. Lett. B266 (1991) 419.
[219] C.T. Hill, E.H. Simmons, Phys. Rep. 381 (2003) 235; 390 (2004) 553 (erratum). hep-ph/0203079.
[220] P. Ramond, Field Theory: A Modern Primer, 2nd ed., Westview Press, Boulder, CO, 1997.
[221] G.'t Hooft, M.J.G. Veltman, Nuclear Phys. B153 (1979) 365;
G. Passarino, M.J.G. Veltman, Nuclear Phys. B160 (1979) 151.
[222] W.A. Bardeen, A.J. Buras, D.W. Duke, T. Muta, Phys. Rev. D18 (1978) 3998.
[223] W. Siegel, Phys. Lett. 84B (1979) 193;
D.M. Capper, D.R.T. Jones, P. van Nieuwenhuizen, Nuclear Phys. B167 (1980) 479.
[224] R. Hempfling, B.A. Kniehl, Phys. Rev. D51 (1995) 1386. hep-ph/9408313.
[225] R. Tarrach, Nuclear Phys. B183 (1981) 384.
[226] S.P. Martin, M.T. Vaughn, Phys. Lett. B318 (1993) 331. hep-ph/9308222;
The gauge boson loop part of the 1-loop gaugino pole mass can be found in Y. Yamada, Phys. Lett. B316 (1993) 109. hep-ph/9307217.
[227] D.M. Pierce, A. Papadopoulos, Nuclear Phys. B430 (1994) 278. hep-ph/9403240;
D.M. Pierce, J.A. Bagger, K.T. Matchev, R.-J. Zhang, Nuclear Phys. B491 (1997) 3. hep-ph/9606211.
[228] S. Weinberg, The Quantum Theory of Fields, Vol. 2: Modern Applications, Cambridge University Press, Cambridge, UK, 1996.
[229] C.T. Hill, Lecture notes for massless spinor and massive spinor triangle diagrams, FERMILAB-Pub-TM/2341-T (2006) hep-th/0601155.
[230] For a review and a guide to the literature, see J. Novotny, Czech. J. Phys. 44 (1994) 633.
[231] F. Jegerlehner, Eur. Phys. J. C18 (2001) 673. hep-th/0005255.
[232] R. Jackiw, in: S.B. Trieman, R. Jackiw, B. Zumino, E. Witten (Eds.), Current Algebra and Anomalies, World Scientific, Singapore, 1985, pp. 81–210;
J.C. Taylor, Gauge Theories of Weak Interactions, Cambridge University Press, Cambridge, UK, 1976, p. 106.
[233] V. Elias, G. McKeon, R.B. Mann, Phys. Rev. D28 (1983) 1978; Can. J. Phys. 63 (1985) 1498.
[234] R.A. Bertlmann, Anomalies in Quantum Field Theory, Oxford University Press, Oxford, UK, 2000.
[235] A. Bilal, Lectures on Anomalies, arXiv:0802.0634 [hep-th].
[236] R.E. Pugh, Can. J. Phys. 47 (1969) 1263.
[237] J.M. Jauch, F. Rohrlich, The Theory of Photons and Electrons, 2nd expanded ed., Springer-Verlag, New York, 1976.
[238] S.L. Adler, Phys. Rev. 177 (1969) 2426.
[239] K. Huang, Quarks, Leptons and Gauge Fields, 2nd ed., World Scientific, Singapore, 1992.
[240] G. 't Hooft, Phys. Rev. Lett. 37 (1976) 8.
[241] See, e.g. J.A. Harvey, C.T. Hill, R.J. Hill, Phys. Rev. D77 (2008) 085017. arXiv:0712.1230 [hep-th].
[242] V. Parameswaran Nair, Quantum Field Theory: A Modern Perspective, Springer Science, New York, 2005.
[243] H. Lütkepohl, Handbook of Matrices, John Wiley & Sons Ltd., Chichester, UK, 1996.
[244] W.A. Bardeen, Phys. Rev. 184 (1969) 1848.
[245] Y. Makeenko, Methods of Contemporary Gauge Theory, Cambridge University Press, Cambridge, UK, 2002.
[246] I. Montvay, G. Münster, Quantum Fields on a Lattice, Cambridge University Press, Cambridge, UK, 1994.
[247] V. Rubakov, Classical Theory of Gauge Fields, Princeton University Press, Princeton, NJ, 2002.
[248] G. 't Hooft, Phys. Rev. D14 (1976) 3432; D18 (1978) 2199 (erratum).
[249] W. Siegel, Phys. Lett. 94B (1980) 37.
[250] L.V. Avdeev, Theor. Math. Phys. 58 (1984) 203;
L.V. Avdeev, A.A. Vladimirov, Nuclear Phys. B219 (1983) 262.
[251] M. Blatter, Helv. Phys. Acta 65 (1992) 1011.
[252] See e.g. M.S. Chanowitz, M. Furman, I. Hinchliffe, Nuclear Phys. B159 (1979) 225 and references therein.
[253] M.E. Rose, Elementary Theory of Angular Momentum, John Wiley, New York, 1957.
[254] P.R. Auvil, J.J. Brehm, Phys. Rev. 145 (1966) 1152.
[255] P. Carruthers, Phys. Rev. 152 (1966) 1345; J. Math. Phys. 9 (1968) 1835.
[256] E. Leader, Spin in Particle Physics, Cambridge University Press, Cambridge, UK, 2001.
[257] M. Jacob, G.C. Wick, Ann. Physics(NY) 7 (1959) 404; reprinted in Ann. Physics 281 (2000) 774.

[258] R.A. Horn, C.R. Johnson, Topics in Matrix Analysis, Cambridge University Press, Cambridge, UK, 1991.
[259] L. Autonne, Sur les matrices hypohermitiennes et sur les matrices unitaire, Annales de l'Université de Lyon, Nouvelle Série I, Fasc. 38 (1915) 1–77.
[260] R.N. Mohapatra, P.B. Pal, Massive Neutrinos in Physics and Astrophysics, 3rd ed., World Scientific, Singapore, 2004.
[261] A. Bunse–Gerstner, W.B. Gragg, J. Comput. Appl. Math. 21 (1988) 41;
W. Xu, S. Qiao, SIAM J. Matrix Anal. Appl. 30 (2008) 142.
[262] S.Y. Choi, M. Drees, (unpublished). This proof was inspired by the diagonalization algorithm for hermitian matrices in W.H. Williams, B.P. Flannery, S.A. Teukolsky and W.T. Vetterling, Numerical Recipes in Fortran 77, second ed., Cambridge University Press, Cambridge, UK, 1992, Section 11.4 [Available at: http://www.nrbook.com/a/bookfpdf.php]. A similar method of proof is outlined in Ref. [147], Section 4.4, problem 2 (pp. 212–213) and Section 4.6, problem 15 (p. 254).
[263] S.Y. Choi, H.E. Haber, J. Kalinowski, P.M. Zerwas, Nuclear Phys. B778 (2007) 85. hep-ph/0612218.
[264] T. Hahn, Routines for the diagonalization of complex matrices, arXiv:physics/0607103. The software for the Takagi diagonalization of complex matrices can be obtained from http://www.feynarts.de/diag/.
[265] F.T. Luk, S. Qiao, in: F.T. Luk (Ed.), Advanced Signal Processing Algorithms, Architectures, and Implementations XI, in: Proc. SPIE, vol. 4474, 2001, p. 254;
X. Wang, S. Qiao, in: H.R. Arabnia (Ed.), Proceedings of the 2002 International Conference on Parallel and Distributed Processing Techniques and Applications, PDPTA'02, Las Vegas, Nevada, June 2002, vol. I, CSREA Press, 2002, pp. 206–212.
[266] H.G. Becker, Lett. Nuovo Cim. 8 (1973) 185.
[267] W.H. Greub, Linear Algebra, 4th ed., Springer-Verlag, New York, 1981, pp. 230–231.
[268] L.F. Li, Phys. Rev. D9 (1974) 1723.
[269] See, e.g. R. Gilmore, Lie Groups, Lie Algebras and Some of Their Applications, Wiley & Sons, New York, 1974.
[270] L. O'Raifeartaigh, Group Structure of Gauge Theories, Cambridge University Press, Cambridge, UK, 1986.
[271] E.B. Dynkin, Am. Math. Trans. 6 (1957) 111.
[272] W.G. McKay, J. Patera, Tables of Dimensions, Indices and Branching Rules for Representations of Simple Lie Algebras, Dekker, New York, 1981.
[273] T. van Ritbergen, A.N. Schellekens, J.A.M. Vermaseren, Int. J. Mod. Phys. A14 (1999) 41. hep-ph/9802376.
[274] A.J. Mountain, J. Math. Phys. 39 (1998) 5601;
A.J. Macfarlane, H. Pfeiffer, J. Math. Phys. 41 (2000) 3192;
J.A. de Azcárraga, A.J. Macfarlane, A.J. Mountain, J.C. Perez, Bueno, Nuclear Phys. B510 (1998) 657.
[275] S. Okubo, Phys. Rev. D16 (1977) 3528.
[276] A. Sudbury, J. Phys. A23 (1990) L705.
[277] J. Banks, H. Georgi, Phys. Rev. D14 (1976) 1159.
[278] J. Patera, R.T. Sharp, J. Math. Phys. 22 (1981) 2352.
[279] A. Baha Balantekin, J. Math. Phys. 23 (1982) 486.
[280] A. Dedes, S. Rimmer, J. Rosiek, J. High Energy Phys. 0608 (2006) 005. hep-ph/0603225.
[281] R.H. Good, Rev. Modern Phys. 27 (1955) 187.
[282] J. Uschersohn, Dirac, Weyl, Majorana . . .: a review, preprint LYCEN/8213, 1982.
[283] See Appendix A2-2 of Ref. [237].
[284] P. Longe, Physica 32 (1966) 603.
[285] D. Bailin, Weak Interactions, 2nd ed., Adam Hilger, Bristol, UK, 1982.
[286] P. Langacker, Phys. Rep. 72 (1981) 185;
J.D. Vergados, Phys. Rep. 133 (1986) 1.
[287] M. Fukugita, T. Yanagida, Physics of Neutrinos and Applications to Astrophysics, Springer-Verlag, Berlin, 2003.
[288] W. Pauli, Ann. Inst. Henri Poincaré 6 (1936) 109.
[289] F. Brandt, preprint ITP-UH-19/09, arXiv:0911.2118 [hep-th].
[290] N. Setzer, ν seesaw uses: UV insensitive supersymmetry breaking without tachyons, Ph. D. Thesis, University of Maryland, 2008.
[291] M. Fierz, Z. Phys. 104 (1937) 553.
[292] E. De Vries, A.J. Van Zanten, Comm. Math. Phys. 17 (1970) 322.
[293] J.F. Nieves, P.B. Pal, Amer. J. Phys. 72 (2004) 1100. hep-ph/0306087.
[294] Y. Takahashi, J. Math. Phys. 24 (1983) 1783; The Fierz identities, in: H. Ezawa, S. Kamefuchi (Eds.), Progress in Quantum Field Theory, North-Holland Publishing Company, Amsterdam, 1986, pp. 121–132.
[295] C.C. Nishi, Amer. J. Phys. 73 (2005) 1160. hep-ph/0412245.
[296] U. Gran, arXiv:hep-th/0105086.
[297] Some of the earliest works that address the equivalence of massless Majorana and Weyl fermions can be found in J. Serpe, Physica 18 (1952) 295;
J.A. McLennan Jr., Phys. Rev. 106 (1957) 821;
L.A. Radicati, B. Touschek, Nuovo Cim. 5 (1957) 1693;
W. Pauli, Nuovo Cim. 6 (1957) 204;
F. Gürsey, Nuovo Cim. 7 (1958) 411.
[298] A. Dedes, H.E. Haber, J. Rosiek, J. High Energy Phys. 0711 (2007) 059. arXiv:0707.3718 [hep-ph].
[299] M. Bohm, A. Denner, H. Joos, Gauge Theories of the Strong and Electroweak Interaction, Teubner, Stuttgart, Germany, 2001.
[300] See e.g., p. 150 of Ref. [122] or p. 250 of Ref. [234].
[301] H.W. Braden, J. Math. Phys. 26 (1985) 613.
[302] K.M. Case, Phys. Rev. 97 (1955) 810;
H.W. Braden, J. Phys. A: Math. Gen. 17 (1984) 2927.
[303] B. Kayser, Phys. Rev. D30 (1984) 1023.
[304] A. Denner, H. Eck, O. Hahn, J. Kublbeck, Phys. Lett. B291 (1992) 278; Nuclear Phys. B387 (1992) 467.
[305] E.I. Gates, K.L. Kowalski, Phys. Rev. D37 (1988) 938.
[306] R. Kleiss, I. Malamos, G. van den Oord, Eur. Phys. J. C64 (2009) 387. arXiv:0906.3388 [hep-ph].
[307] J.F. Donoghue, Phys. Rev. D19 (1979) 2772.
[308] M. Capdequi Peyranere, M. Talon, Nuovo Cim. A75 (1983) 205.
[309] A. Denner, T. Sack, Nuclear Phys. B347 (1990) 203;
A. Denner, Fortsch. Phys. 41 (1993) 307.
[310] B.A. Kniehl, A. Pilaftsis, Nuclear Phys. B474 (1996) 286. hep-ph/9601390;
A. Pilaftsis, Phys. Rev. D65 (2002) 115013. hep-ph/0203210.
[311] D.M. Pierce, Renormalization of supersymmetric theories, in: J.A. Bagger (Ed.), Supersymmetry, Supergravity and Supercolliders, Proceedings of the Theoretical Advanced Study Institute in Elementary Particle Physics, TASI 97, Boulder, CO, 1–27 June 1997, World Scientific, Singapore, 1999, pp. 343–389. hep-ph/9805497.
[312] S. Kiyoura, M.M. Nojiri, D.M. Pierce, Y. Yamada, Phys. Rev. D58 (1998) 075002. hep-ph/9803210.
[313] P. Gambino, P.A. Grassi, Phys. Rev. D62 (2000) 076002. hep-ph/9907254.

[314] A.O. Bouzas, Eur. Phys. J. C20 (2001) 239; C27 (2003) 623 (erratum). hep-ph/0101101;
Y. Yamada, Phys. Rev. D64 (2001) 036008. hep-ph/0103046;
D. Espriu, J. Manzano, P. Talavera, Phys. Rev. D66 (2002) 076002. hep-ph/0204085;
Y. Zhou, J. Phys. G29 (2003) 1031. hep-ph/0301090; Mod. Phys. Lett. A21 (2006) 2763. hep-ph/0502186;
Y. Liao, Phys. Rev. D69 (2004) 016001. hep-ph/0309034.
[315] K.I. Aoki, Z. Hioki, M. Konuma, R. Kawabe, T. Muta, Progr. Theoret. Phys. Suppl. 73 (1982) 1;
M. Bohm, H. Spiesberger, W. Hollik, Fortsch. Phys. 34 (1986) 687.
[316] R. Vega, J. Wudka, Phys. Rev. D53 (1996) 5286; D56 (1997) 6037 (erratum). hep-ph/9511318.
[317] H.E. Haber, Spin formalism and applications to new physics searches, in: Proceedings of the 21st SLAC Summer Institute on Particle Physics: Spin Structure in High Energy Processes, SLAC, Stanford, CA, 26 July–6 August 1993, pp. 231–272 hep-ph/9405376.
[318] K. Hagiwara, D. Zeppenfeld, Nuclear Phys. B313 (1989) 560.
[319] H. Murayama, I. Watanabe, K. Hagiwara, HELAS: HELicity amplitude subroutines for Feynman diagram evaluations, preprint KEK-91-11, 1992.
[320] R. Gastmans, T.T. Wu, The Ubiquitous Photon: Helicity Method for QED and QCD, Oxford University Press, Oxford, UK, 1990.
[321] M.L. Mangano, S.J. Parke, Phys. Rep. 200 (1991) 301. hep-th/0509223;
L.J. Dixon, QCD and beyond, in: D.E. Soper (Ed.), Proceedings of the Theoretical Advanced Study Institute in Elementary Particle Physics, TASI 95, Boulder, CO, 4–30 June 1995, World Scientific, Singapore, 1996, pp. 539–584. hep-ph/9601359.
[322] C.S. Lam, Can. J. Phys. 72 (1994) 415. hep-ph/9308289;
Z. Bern, L.J. Dixon, D.A. Kosower, Ann. Rev. Nucl. Part. Sci. 46 (1996) 109. hep-ph/9602280; Ann. Phys. 322 (2007) 1587. arXiv:0704.2798 [hep-ph].
[323] D.A. Kosower, Phys. Lett. B254 (1991) 439.
[324] F.A. Berends, P.H. Daverveldt, R. Kleiss, Nuclear Phys. B253 (1985) 441;
R. Kleiss, W.J. Stirling, Phys. Lett. B179 (1986) 159;
C. Mana, M. Martinez, Nuclear Phys. B287 (1987) 601;
V.V. Andreev, Phys. Rev. D62 (2000) 014029. hep-ph/0101140.
[325] C. Schwinn, S. Weinzierl, J. High Energy Phys. 0505 (2005) 006. hep-th/0503015; J. High Energy Phys. 0704 (2007) 072. hep-ph/0703021;
G. Rodrigo, J. High Energy Phys. 0509 (2005) 079. hep-ph/0508138;
A. Hall, Phys. Rev. D77 (2008) 025011. arXiv:0710.1300 [hep-ph].
[326] D. Maitre, P. Mastrolia, Comput. Phys. Commun. 179 (2008) 501. arXiv:0710.5559 [hep-ph].
[327] P. de Causmaecker, R. Gastmans, W. Troost, T.T. Wu, Phys. Lett. B105 (1981) 215; Nuclear Phys. B206 (1982) 53;
D. Danckaert, P. De Causmaecker, R. Gastmans, W. Troost, T.T. Wu, Phys. Lett. B114 (1982) 203;
F.A. Berends, P. de Causmaecker, R. Gastmans, R. Kleiss, W. Troost, T.T. Wu, Nuclear Phys. B206 (1982) 61; B239 (1984) 382; B239 (1984) 395; B264 (1986) 243; B264 (1986) 265.
[328] J.F. Gunion, Z. Kunszt, Phys. Lett. B161 (1985) 333.
[329] H. Pilkuhn, The Interactions of Hadrons, North-Holland Publishing Company, Amsterdam, 1967.
[330] A.R. Edmonds, Angular Momentum in Quantum Mechanics, Princeton University Press, Princeton, NJ, 1974.
[331] T.B. Anders, A.O. Barut, W. Jachmann, Internat. J. Modern Phys. A6 (1991) 4223.
[332] M. Anselmino, F. Caruso, U. Piovano, Helicity Formalism and Spin Effects, preprint CBPF-NF-045-90, 1990.
[333] N. Cabibbo, Phys. Rev. Lett. 10 (1963) 531;
M. Kobayashi, T. Maskawa, Progr. Theoret. Phys. 49 (1973) 652.
[334] C. Amsler, et al., [Particle Data Group Collaboration], Review of particle physics, Phys. Lett. B667 (2008) 1 and 2009 partial update for the 2010 edition.
[335] S.L. Glashow, J. Iliopoulos, L. Maiani, Phys. Rev. D2 (1970) 1285.
[336] For a review of the theory of massive neutrinos, see e.g. S.M. Bilenky, S.T. Petcov, Rev. Modern Phys. 59 (1987) 671; 60 (1988) 575 (erratum); 61 (1989) 169 (erratum);
S.M. Bilenky, C. Giunti, W. Grimus, Prog. Part. Nuclear Phys. 43 (1999) 1. hep-ph/9812360.
[337] S. Weinberg, Phys. Rev. Lett. 43 (1979) 1566; Phys. Rev. D22 (1980) 1694;
F. Maltoni, J.M. Niczyporuk, S. Willenbrock, Phys. Rev. Lett. 86 (2001) 212. hep-ph/0006358;
K.S. Babu, C.N. Leung, Nuclear Phys. B619 (2001) 667. hep-ph/0106054;
A. Broncano, M.B. Gavela, E.E. Jenkins, Nuclear Phys. B672 (2003) 163. hep-ph/0307058.
[338] A. Strumia, F. Vissani, Neutrino masses and mixings and . . ., hep-ph/0606054;
M.C. Gonzalez-Garcia, M. Maltoni, Phys. Rep. 460 (2008) 1. arXiv:0704.1800 [hep-ph];
H. Nunokawa, S.J. Parke, J.W.F. Valle, Prog. Part. Nuclear Phys. 60 (2008) 338. arXiv:0710.0554 [hep-ph].
[339] Z. Maki, M. Nakagawa, S. Sakata, Progr. Theoret. Phys. 28 (1962) 870;
B. Pontecorvo, Sov. Phys. JETP 26 (1968) 984. [Zh. Eksp. Teor. Fiz. 53 (1967) 1717].
[340] E. Arganda, M.J. Herrero, Phys. Rev. D73 (2006) 055003. hep-ph/0510405.
[341] J. Rosiek, Phys. Rev. D41 (1990) 3464. arXiv:hep-ph/9511250 (erratum). The most recent version of this collection of MSSM Feynman rules can be found at http://www.fuw.edu.pl/~rosiek/physics/prd41.html.
[342] M. Kuroda, arXiv:hep-ph/9902340, 1999.
[343] P. Fayet, Nuclear Phys. B78 (1974) 14; B90 (1975) 104.
[344] K. Inoue, A. Kakuto, H. Komatsu, S. Takeshita, Progr. Theoret. Phys. 68 (1982) 927; 70 (1983) 330 (erratum) 71 (1984) 413;
R. Flores, M. Sher, Ann. Phys. (NY) 148 (1983) 95.
[345] For a review and a comprehensive guide to the original literature, see M. Carena, H.E. Haber, Prog. Part. Nuclear Phys. 50 (2003) 63. hep-ph/0208209.
[346] J.F. Gunion, H.E. Haber, Nuclear Phys. B278 (1986) 449; B402 (1993) 569 (erratum).
[347] H.E. Haber, R. Hempfling, Phys. Rev. Lett. 66 (1991) 1815;
Y. Okada, M. Yamaguchi, T. Yanagida, Progr. Theoret. Phys. 85 (1991) 1;
J.R. Ellis, G. Ridolfi, F. Zwirner, Phys. Lett. B257 (1991) 83.
[348] G. Degrassi, S. Heinemeyer, W. Hollik, P. Slavich, G. Weiglein, Eur. Phys. J. C28 (2003) 133. hep-ph/0212020;
B.C. Allanach, A. Djouadi, J.L. Kneur, W. Porod, P. Slavich, J. High Energy Phys. 0409 (2004) 044. hep-ph/0406166;
S.P. Martin, Phys. Rev. D75 (2007) 055005. hep-ph/0701051.
[349] J.R. Ellis, S. Rudaz, Phys. Lett. B128 (1983) 248;
F. Browning, D. Chang, W.Y. Keung, Phys. Rev. D64 (2001) 015010. hep-ph/0012258;
A. Bartl, S. Hesselbach, K. Hidaka, T. Kernreiter, W. Porod, Phys. Lett. B573 (2003) 153. hep-ph/0307317; Phys. Rev. D70 (2004) 035003. hep-ph/0311338.
[350] P. Fayet, Phys. Lett. 69B (1977) 489.
[351] L.J. Hall, M. Suzuki, Nuclear Phys. B231 (1984) 419.
[352] S. Weinberg, Phys. Rev. D26 (1982) 287;
N. Sakai, T. Yanagida, Nuclear Phys. B197 (1982) 533.
[353] J.R. Ellis, G. Gelmini, C. Jarlskog, G.G. Ross, J.W.F. Valle, Phys. Lett. B150 (1985) 142.
[354] H.K. Dreiner, in: G.L. Kane (Ed.), Perspectives on Supersymmetry, World Scientific, Singapore, 1998, pp. 462–479. hep-ph/9707435;
M. Chemtob, Prog. Part. Nuclear Phys. 54 (2005) 71. hep-ph/0406029;
R. Barbier, et al., Phys. Rep. 420 (2005) 1. hep-ph/0406039.
[355] A. Dedes, S. Rimmer, J. Rosiek, M. Schmidt-Sommerfeld, Phys. Lett. B627 (2005) 161. hep-ph/0506209.